Before discussing oscillatory shear in greater detail, we consider the Kinematics of simple shear. Simple shear is the flow and deformation induced when material is confined between parallel plates moving laterally with constant separation, h. This is illustrated in Figure 9.

The equation of motion in rectangular coordinates for simple shear gives:

$$\phi \frac{\delta v_1}{\delta t} = -\frac{\delta p}{\delta x_1} - \frac{\delta \sigma_{12}}{\delta x_2} + \phi g \sin \theta , \qquad (39)$$

where ϕ is the fluid density, g is the acceleration due to gravity and θ is the angle between the plates and the horizontal. By inspection, we see that for horizontal plates, where there is no pressure drop in the x_1 direction, σ_{12} is everywhere constant at steady state.

The equation of energy for simple shear gives:

$$\phi C_v \frac{\delta T}{\delta t} = -\frac{\delta q_2}{\delta x_2} + \sigma_{12} \dot{\gamma} . \qquad (40)$$

Unlike the stress tensor which is uniquely defined, we have seen that there is more than one way to describe deformation. The Finger strain and Cauchy strain provide different ways of looking at simple shear.

A SLIDING PLATE MELT RHEOMETER INCORPORATING A SHEAR STRESS TRANSDUCER

by

A. Jeffrey Giacomin, P.Eng

A thesis submitted

to the Faculty of Graduate Studies and Research

in partial fulfillment of the

requirements for the degree of

DOCTOR OF PHILOSOPHY

Department of Chemical Engineering

at

McGill University

Montreal, Canada

June, 1987

ISBN 0-315-44471-1

A SLIDING PLATE MELT RHEOMETER INCORPORATING A SHEAR STRESS TRANSDUCER

For Marie, for everything.

ABSTRACT

In currently used shear rheometers, shear stress is inferred from a measurement of either total force or total torque. These methods are subject to experimental errors due to uncontrolled flow at the sample boundaries. Such errors can be avoided by measuring the shear stress locally, in the region of controllable flow, using a shear stress transducer. A new sliding plate rheometer for molten plastics has been developed to incorporate a recently developed shear stress transducer. The rheometer operates at temperatures up to 250°C. Static and dynamic calibrations showed that the shear stress transducer sensitivity is stable and that its frequency response is suitable for the study of molten plastics This rheometer was equipped with a computer controlled servo-hydraulic linear actuator, which provided wide flexibility in shear history selection Digital data acquisition and signal processing enabled the use of the discrete Fourier transform for nonlinear viscoelastic property determination. Important differences were observed between the locally measured shear stress and values inferred from total force in both large amplitude oscillatory shear and in reciprocating exponential shear tests. For these property measurements, free boundary errors can dominate the dynamics of total force measurements.

RESUME

Le principe d'opération selon fonctionnent les rhéomètres, comprend généralement l'inférence de la contrainte de cisaillement d'une mesure totale soit du torque en instrument employant les écoulement rotationels, ou bien de la force en ceux utilisant les écoulement rectilinéaires. Ces méthodes sont sujets aux erreurs expérimentales provenant des écoulements non-controllables aux frontières des échantillons. On peut circomvenir de tels erreurs en mesurant la contrainte de cisaillement localement dans la région d'ecoulement controllable avec un capteur de contrainte de cisaillement. Un nouveau rhéomètre, type plaque-glissante pour les plastiques à l'état fondu, était développé incorporant un nouveau capteur de contrainte de cisaillement tolèrant les températures élevées, dit 250°C. Les étallonnages statiques et dynamiques ont démontré que la sensitivitée du capteur est stable et sa réponse dynamique permet la charactérisation rhéologique des plastiques à l'état fondu. L'obtention des données et leurs conditionnement par méthodes numériques a permis l'utilization des transformes discrètes de Fourier pour la détermination des propriétées viscoélastiques nonlinéaires. En cisaillement oscillatoire et en cisaillement exponentielle alternative, des différences importantes furent observer entre la contrainte de cisaillement mesurée avec le nouveau capteur et la valeur correspondante déduit de la force totale. Pour la mesures de tels propriétés viscoelastiques, les erreurs de bout et de bord peuvent gouverner la force totale.

ACKNOWLEDGEMENTS

I should like to acknowledge Professor Dealy for his careful planning, sustained encouragement, patient guidance and dedicated teaching. The environment for engineering research which Professor Dealy has established is a pleasure to work in. His entertaining, thought-provoking course lectures in "Rheology of Liquids" and "Fluid Mechanics" contributed significantly to my development as an engineer. Special acknowledgement is given for his meticulous work in revising and ameliorating this document.

Friends often served as sounding boards for new ideas during this work. Specifically, interesting discussions with Turgut Mutel produced the idea to compare the total stress with the locally measured shear stress for the new rheometer. The help of Tony Samurkas and Shailesh Doshi in trouble-shooting software is greatly appreciated. My gratitude is also extended to Navnit Patel who trained me on the oscilloscope and provided his data acquisition program for preliminary work with the IBM personal computer. Lively lunch-table discussions with Dan Cusson, Regis Lamontagne, Qun Geng and Burke Nelson were also of great value. Greg Soo's help in perfecting required electronic circuitry is appreciated. Ed Chu's help with the color photography of the rheometer is greatly appreciated. To Jean-François Chamblain I extend my gratitude for his many encouraging suggestions, and especially for his advice on personal computing. Acknowledgement is also extended to Toby Thomas for his advice on printing and for proofreading this text.

The importance of the departmental machine shop to the present research cannot be overstated. Mr. Herb Alexander's machining experience and craftsmanship were indispensable technical resources in fabricating the new rheometer His patient lessons on machining are greatly appreciated. Hat's off to shop supervisor Mr Andy Krish for a well run machine shop

Important contributions to the rheometer development program from the folks at the MTS Systems Corporation are gratefully acknowledged. Their excellent equipment and technical advice, kindly provided by Dr. Pat Cain and Mr Bob Proehl, were invaluable resources Special thanks is extended to Dr Cain for encouraging me to employ the discrete Fourier transform and for patiently explaining how it is used for materials testing. This idea played a key role in shaping this research. Thanks also goes to Messrs. Milan Sebek and Bob Brosch also of MTS for administering the MTS support. The technical advice of Mr. Curtis Kissinger of MTI Instruments, Inc. is also recognized His recommendation of capacitance proximetry for the new transducer was invaluable

The inspiration of my former colleagues at Du Pont Canada cannot go unmentioned For their vital roles in fostering my passion for plastics research, Bernie Kershaw, Peter Kelly, Mahender Khurana, Dr. Dave Axelson and Dr. Brian Smith are warmly recognized. Special thanks to the late Kalev Pugi, who convinced me to pursue a higher degree in chemical engineering. He is sorely missed. The financial support of the Research Division of Du Pont Canada is also gratefully acknowledged.

Several fruitful discussions on viscoelastic theory with Dr. Daniel De Kee of the University of Windsor are also gratefully recognized. His lectures on rheology inspired me to pursue a career in plastics engineering. Dr. Pierre Carreau of Ecole Polytechnique is also recognized for his interesting course "Rhéologie des Polymères"

Departmental storekeeper Mr. Jean Dumont's resourcefulness, dedication and indefatigable good humor is gratefully acknowledged Mr Henry Lim of the Physical Sciences and Engineering Library is thankfully commended for his resourcefulness in tracking down key bibliographic information

I hold fond memories of the affection shown to me by the close friends which I have had the good fortune of making during my stay at McGill. Special thanks is extended to Suna and Osman Polat for their selfless companionship

I owe my faith in myself to my parents, Louis and Barbara Giacomin. Happily, their positive influence on me lasted well beyond my formative years. Their unconditional support and interested encouragement were invaluable

Last but not least, I acknowledge Marie, my wife and best friend, whose generous encouragement and selfless patience sustained me throughout this research. Her sacrifices contributed enormously to the successful completion of this research.

CONTENTS

LIST OF TABLES

LIST OF FIGURES

NOMENCLATURE

The Society of Rheology has established a convenient standard nomenclature for viscoelastic properties of liquids and the present document conforms to this standard.[1,2,3,*]

$(\delta_1)_n$	phase angle of nth harmonic of N_1
ϵ	fractional error
η	second order damping factor
η''	elastic component of complex viscosity
η'	viscous component of complex viscosity
η^*	complex viscosity
η_o	limiting low-shear viscosity
α	surface tension
β	radian angle of shear
σ	shear stress
σ_{ij}	extra stress tensor
σ_n	amplitude of nth harmonic of shear stress
σ_o	overall amplitude of shear stress
μ	viscosity
γ	shear strain
γ_o	shear strain amplitude
θ	relaxation time variable
θ_{3dB}	first order time constant
δ	lateral beam deflection
$\delta/\delta t$	Jaumann derivative
δ_e	phase error
δ_n	phase angle of nth harmonic of shear stress
ϕ	density
a	thermal diffusivity
A	attenuation
A^T	transpose of matrix A
A_{eff}	effective area of piston
C_p	heat capacity at constant pressure
C_v	heat capacity at constant volume
D	actuator displacement
D_e	dielectric constant
E	Young's modulus
f	frequency, Hz
F	force
f_m	actuator resonant frequency
f_n	nth mode resonant frequency
f_o	fundamental frequency
G	modulus in shear

*The ASTM D4065-82 standard does exist for properties of solid plastics, but it pertains only to oscillatory properties.

g	acceleration due to gravity
G''	loss modulus
G'	storage modulus
G^*	dynamic or complex modulus
g_c	32.17 lb-ft/lbm-s^2
h	sample thickness
I	moment of inertia
$Im[x]$	imaginary part of complex number x
k	instrument heat-up constant
k	fluid thermal conductivity
L	roller bearing longevity
L	sample length
m_{Ma}	mass of moving assembly
n	any integer
N_1	first normal stress difference
N_2	second normal stress difference
P	hydraulic fluid pressure drop
P_{mean}	average power of viscous dissipation evaluated n cycles
q_I	transducer input signal
q_i	heat flux in ith direction
q_O	transducer output signal
R	ratio of minor to major axes for an ellipse
R	length to thickness ratio
Re	Reynolds number
$Re[x]$	real part of complex number x
s	$t-t'$
t	current time
T	absolute temperature
t'	time from current time
u	velocity
U	amplitude of plate velocity
v	volume
V	plate velocity
v_s	shear wave velocity
ω	angular frequency, rad/sec
W	work done with respect to reference time
W_c	work done in one full cycle
ω_r	cantilever lateral-mode resonant frequencies
W_s	stored energy
X	unaccomplished temperature difference
$X(f)$	Fourier transform of x(t)
x_1	coordinate for axis in shear direction
x_2	coordinate for axis normal to shear plane
x_2	coordinate for axis in shear plane orthogonal to x_1
x_i	ith axis coordinate
$\dot{\gamma}$	shear rate
$\underline{P}$	position vector
$\underline{\Delta}$	rate of deformation tensor

$\underline{\Gamma}$	any indifferent strain tensor
$\underline{C}$	Cauchy tensor
$\underline{J}$	Cauchy strain
$\underline{H}$	Finger strain
$\underline{F}$	deformation gradient tensor
$\underline{Q}$	rate of rotation tensor
$\underline{W}$	vorticity tensor
$\underline{\sigma}$	extra stress tensor
$\underline{T}$	total stress tensor
$\underline{\delta}$	unit tensor

$\underline{\Gamma}$	any indifferent strain tensor
$\underline{C}$	Cauchy tensor
$\underline{J}$	Cauchy strain
$\underline{H}$	Finger strain
$\underline{F}$	deformation gradient tensor
$\underline{Q}$	rate of rotation tensor
$\underline{W}$	vorticity tensor
$\underline{\sigma}$	extra stress tensor
$\underline{T}$	total stress tensor
$\underline{\delta}$	unit tensor

I INTRODUCTION

A. Viscoelasticity of Molten Plastics

Viscoelastic behavior is usually classified as either linear or nonlinear. For molten plastics, nonlinear behavior usually arises when the melt is rapidly subjected to large deformations. Where such high rates of strain are imposed in a well-defined, time unsteady flow, the components of the deforming stress describe nonlinear viscoelastic functions. When the strains or strain rates are kept small, these components describe linear viscoelastic properties. Since the cost effective mass production of plastic products inevitably involves time unsteady flows at high strain rates, one expects that the properties governing processability will depend on the nonlinear viscoelastic properties of the melt.

1. What are Rheological Properties?

The formal mathematical definition of the deforming stress, called the extra stress tensor, is

$$\underline{\underline{\sigma}} = \begin{bmatrix} \sigma_{11} & \sigma_{12} & \sigma_{13} \\ \sigma_{21} & \sigma_{22} & \sigma_{23} \\ \sigma_{31} & \sigma_{32} & \sigma_{33} \end{bmatrix} . \qquad (1)$$

The indices of the scalar components specify the directions of the stress components and the face of a fluid element on which they act. The components of this tensor having like indices are called normal stresses. Those having unlike indices are called shear stresses. For incompressible fluids any nonzero shear stress can cause deformation, but only a difference in the normal stress components can cause deformation.

Hence, the extra stress tensor is the difference between the total stress, T_{ij}, and an unspecified isotropic stress, $\pi\delta_{ij}$ Thus, $\sigma_{ij} = T_{ij} - \pi\delta_{ij}$, where δ_{ij} is the unit tensor[4] and the extra stress is the anisotropic contribution to the total stress.

Melt compressibility can affect rheological properties, especially when high pressures are encountered in processing. But the experimental rheologist using simple shear takes his samples to be incompressible since simple shear is isochoric by definition. This means that there is no rheological cause for volume changes in samples. It has recently been confirmed experimentally that molten plastics in simple shear do indeed maintain constant volume.[5]

The stress at a point is given by the tensor with components σ_{ij} representing the force per unit area acting in the j direction on the fluid surface of constant i by the fluid in the region greater than i.*

Since there are three normal stresses, there are but two independent normal stress differences, $\sigma_{11}-\sigma_{22}$ and $\sigma_{22}-\sigma_{33}$.

The cause of the extra stress is the deformation, which is itself a tensor-valued quantity However, unlike the extra stress tensor which is uniquely defined, there is more than one way to define a deformation tensor. The different ways of defining the deformation are considered in the separate section on nonlinear viscoelastic theory. For the purposes of introduction, suffice it to say that the strain can also be completely described in terms of tensors

To know what rheological properties are, one must first understand what a property is A material property is a relation between two causally related variables. For instance, for a simple rubbery material in static simple shear, the shear stress is proportional to the shear strain.

$$\sigma_{12} = G\,\gamma_{12} \tag{2}$$

The rheological property of the rubber is given in terms of the effect of the shear strain on the shear stress. It is incidental that the

*The phrase "by the fluid in the region of greater i" establishes a sign convention for stress mathematical equation for this relation is known, and that it is summarized by a simple proportionality with constant, G. By definition, the material property is the relationship between σ_{12} and γ_{12}, it is not to be confused with the modulus in shear, G, which is simply a constant in an equation proposed to summarize the latter relationship. When there is no equation known to describe such relations, the material properties can only be presented as plots of experimental data, such as σ_{12} versus γ_{12}. The independent variable for reporting such properties is, by convention, taken to be the variable that was controlled experimentally.

Hence, rheological properties describe the effect that a prescribed deformation history has on the shear stresses and the normal stress differences Alternatively, a rheological property may be expressed as the effect on deformation of a prescribed stress history.

Rheological properties are often reported as dimensional ratios. Viscosity, for instance, is the ratio of shear stress to shear rate in steady shear. Additionally, the stress growth coefficient is a viscoelastic property defined as the ratio of shear stress to shear rate under suddenly applied steady shear. The use of such ratios originates in Newtonian fluid mechanics where the viscosity is part of a unified theory. Despite their common usage in the literature, these ratios make it difficult to see what effect strain has on stress since they confound the two Instead of confounding dependent variables with independent ones, the writer has chosen to simply use shear stress and normal stress differences for reporting viscoelastic properties.

2. Why is Melt Viscoelasticity Important?

Plastics are an industrially important subclass of polymers, which are long chain molecules. Plastics are widely used because they are easily formed and have useful solid state properties such as strength and toughness. Where an efficient way of converting them can be devised, the mass production of plastic products can be lucrative indeed. The ease with which a particular plastic can be processed into a specific premium quality product is called processability. Since the cost effective mass production of plastic products usually requires processing in the molten state, plastics processability depends, in large part, on melt flow properties

An important and difficult problem facing plastics engineers is the systematic, quantitative prediction of processability from rheological properties The present section aims to introduce (1) what rheological properties are, (2) which ones are expected to govern plastics processability, (3) how they can be measured and (4) how the new rheometer permits their measurement .

Rheology is the study of the flow and deformation of matter. To induce flow and deformation in polymeric liquids one must subject them to a deforming stress. If the flow is time steady, it is called viscometric. Hence, the shear stress and normal stress differences for steady simple shear are called the viscometric functions. Viscoelastic properties are, by definition, time dependent quantities which distinguishes them from the viscometric functions.*

Most plastics processing operations involve time unsteady flow fields. So, the deforming stress to which a molten plastic is subjected in a processing operation varies with time. Entering the mold in an injection molding operation, for example, the fluid element is suddenly subjected to a high shear rate for a short period of time as it is forced through a narrow gate Here the fluid elements will experience a transient sequence of deformations until solidification. Film blowing, blow molding and extrusion are also examples of plastics processes which involve fast, transient deformation histories. Clearly, the rheological properties associated with time unsteady flows, the nonlinear viscoelastic properties, are likely to govern plastics processability

3. <u>How are Viscoelastic Properties Used?</u>

Firstly, those developing new plastics materials need to be able to distinguish resins that process well from those that do not. The rheological characterization of novel plastics produced in the laboratory or on a pilot plant scale is currently limited to viscometric and linear or slightly nonlinear viscoelastic property measurements. Where the processabilities of the resins under development are governed by their

---

*Parenthetically, some authors refer to normal stress differences in steady shear as viscoelastic properties since fluids which exhibit normal stress differences usually exhibit viscoelasticity.

nonlinear viscoelastic properties one must currently test the resins under process conditions on industrial scale equipment. Since industrial scale tests generally require large quantities of resin, resin selection for scale-up must necessarily be made with little information about the processabilities of the chosen resins.[6] As a result, good resins can be passed over and resins that are less than adequate can end up in the marketplace.

A history of the advent of linear low density polyethylenes is a good example of such a problem. When films were first blown at commercial rates, from linear low density polyethylene, differences in processability between the linear lows and their long-chain branched competitive counterparts came as a surprise. These differences in processability included a surface roughness limitation that did not emerge until the new film resins were processed at commercial rates[7] Furthermore, the power required to process linear lows was much higher than was expected from past experience with long-chain branched resins. One can speculate that a comparison of the nonlinear viscoelastic properties of the linear lows with their long-chain branched predecessors might have signaled these differences in processability before scale-up

Furthermore, it is not uncommon for resins manufactured to meet given conventional rheological specifications, such as viscosity, to exhibit distinctly different processabilities in the field. Hence, incentives for the development of experimental techniques for measuring nonlinear viscoelastic properties exist wherever one must control product processability. Horror stories about particular lots of resin, manufactured according to a strict set of established specifications, yet intermittently rejected by converters as impossible to process are well known to resin manufacturers.[8] Since certain aspects of processability are expected to depend critically on certain nonlinear viscoelastic properties, the want of practicable means of monitoring such properties represents a significant problem for plastics manufacturers and processors alike.[9]

Analytical chemists use viscoelastic properties as a sensitive probe of molecular structure. For instance, linear viscoelastic properties of molten plastics have been correlated with molecular weight distribution[10,11,12,13,14,15,16,17] Furthermore, effects of long-chain branching and molecular weight distribution on nonlinear viscoelastic properties of polybutadiene solutions have been measured.[18,19] Hence, once necessary correlations are established, some features of molecular structure can be inferred from viscoelastic properties. This is helpful, because viscoelastic properties are easier to obtain than results from some chemical analyses such as size exclusion chromatography. Furthermore, rheological properties are sometimes better able to detect slight differences in the high molecular weight fractions of polydisperse samples.[20]

Nonlinear viscoelastic property measurements on molten plastics are also used to test theories of flow behavior. The development of constitutive equations has long suffered from a paucity of experimental data to test predictions. It will be seen that, in principle, such equations can provide the framework for a fundamental understanding of the flow behavior of polymeric liquids. Despite an ocean of such theoretical work, witness the many books and technical journals dedicated, to theoretical rheology, the successful application of such sophisticated approaches to practical engineering problems has been limited. To the writer's knowledge, few useful quantitative predictions of molten plastic processability have been achieved. This want of good quantitative predictive models for plastics processability is partly because model constants are estimated from experimental flows that do not approach the flows encountered in the commercial process. Be this as it may, recent work has shown considerable promise in qualitatively predicting processability in, for instance, injection molding processes, from such equations [21]

Finally, it has not escaped the author's attention that the incentives for measuring nonlinear viscoelastic properties extend well beyond the already vast field of plastics engineering. The need for nonlinear viscoelastic information has been documented for many other materials including food,[22,23,24,25] pharmaceuticals,[26] biofluids such as blood and synovial fluids,[27,28,29] and filled elastomers[30] to name a few. It will be seen that such previous work has suggested several interesting methods of representing nonlinear viscoelastic data.

4. What is Rheometry?

The art of measuring rheological properties is called rheometry. From our definition of a rheological property it follows that rheometry is the experimental study of relations between deforming stresses and deformations. Theoretical rheology is confined to the study of mathematical equations proposed to summarize, explain and predict the effects observed in experimental rheology.

The art of measuring viscosity is called viscometry. The term rheometry, on the other hand, includes the arts of measuring both viscometric and viscoelastic properties.

To understand the role that the shear stress transducer plays amongst established experimental techniques, consider the following outline of the state of the art in rheometry. A comprehensive review of this state of the art has been provided by Dealy.[31,32]

To determine the viscometric functions it is necessary to measure the shear stress and the two normal stress differences in a time steady shear flow. For the measurement of the shear stress over a wide range of shear rates, several commercial instruments are available. These instruments permit the measurement of shear stress in well defined viscometric flows over a wide range of shear rates. The capillary viscometer is one example of such an instrument. In contrast, the state of the art in normal stress difference measurement is not so well developed. For example, the technique of normal thrust measurement in the cone-plate geometry, although popular, restricts accurate normal stress difference measurement to a low range of shear rates. Similarly, birefringence techniques employing the stress optical relation are limited to low shear rates, because this relation can only be validated with normal stress difference measurements made on the cone-plate rheometer.* For molten plastics, this range of shear rates lies well below those commonly associated with most aspects of melt processing. More recent efforts to extend the range of shear rates for measuring normal stress differences in viscometric flows remain highly controversial.[33] Lodge's pressure hole error technique and Han's exit and entrance pressure loss technique are two examples of such controversial methods.[34]

In the broader field of rheometry, the use of homogeneous flow fields simplifies enormously the determination of viscoelastic properties, especially the measurement of nonlinear ones. In nonhomogeneous flows such nonlinear properties must either be inferred from the rates of change of the observables of nonhomogeneous flows or deduced from observables after dubious assumptions are made about the nature of the fluid under study. It is instructive to review work done with rheometers using homogeneous flow fields, such as those in cone-plate and sliding plate designs. Additionally, sliding cylinder and concentric cylinder geometries can approach flow-field homogeneity.

Though their detailed review is left for a later section, a common theme in these conventional approaches is that they depend on the inference of shear stress from either total force or total torque measurements. However, free boundary effects can jeopardize the homogeneity of the flow

*Obviously, this method can only be applied to materials that exhibit birefringence at the shear rates under study.

field and introduce experimental error in such measurements. Additionally, torsional flows are subject to the destabilizing influence of centripetal acceleration, which can also disturb flow-field homogeneity. To circumvent these causes of flow-field inhomogeneity, a shear stress transducer, incorporated in a sliding plate rheometer, can be used for measuring the nonlinear viscoelastic properties of molten plastics. This method has the unique advantage of measuring shear stress locally in the region of controllable flow

B. Experimental Methods in Nonlinear Viscoelasticity

Previous work on the measurement of nonlinear viscoelastic properties of molten plastics can be subdivided into six categories according to rheometer geometry. Though these techniques have previously been reviewed,[35] their merits for the study of nonlinear viscoelasticity are compared below The eccentric rotating disk geometry has also been used to measure limits of linear viscoelasticity but not for nonlinear viscoelastic property measurements per se.[36,37,38,39]

The advantages of using homogeneous flow fields are recurring themes in the literature on previous measurements of nonlinear viscoelastic properties.

1. Need for Flow-Field Homogeneity

A field of flow is homogeneous when the deformation of the fluid is the same at every point in the flow field. Hence both strain, however it is defined, and strain history are the same at all points in the fluid. Now viscoelastic properties are, by definition, time dependent ones. Otherwise stated, the stress state of each fluid element depends intimately on the strain history of that fluid element. So when a flow field is nonhomogeneous, as is true for torsional flow between parallel disks, the strain history and the stress state vary from point to point. Hence, viscoelastic properties, and particularly the nonlinear viscoelastic properties, cannot be obtained from rheometers that use nonhomogeneous flow fields without using tedious iterative techniques.[40,41,42,43,44] Hence, where a broad spectrum of nonlinear viscoelastic properties are under study, rheometers must make use of homogeneous flow fields.

Parenthetically, such an emphasis on homogeneous flow fields, or flows with constant strain history, is not generally found in conventional texts on rheometry.[45,46] Moreover, this emphasis on homogeneous flow fields has recently been criticized,[47,48] while others extol the special virtues of flow-field homogeneity for nonlinear viscoelastic property measurement.[49,50,51,52,53] The reason for this controversy is that conventional texts focus on viscometric functions and linear viscoelastic properties, for which flow-field homogeneity is not essential. In contrast, texts emphasizing nonlinear properties focus on homogeneous flow fields.

Finally, nonhomogeneous flow fields can cause a polydisperse polymer to partially fractionate by causing low molecular weight material migration toward high shear rate regions. For instance, this has been observed for polymer solutions in parallel disk flow.[54]

2. Cone-Plate Flow

Cone-plate flow is the most widely used flow geometry for the study of nonlinear viscoelasticity in polymeric liquids. MacSporran and Spiers,[55,56] for instance, recently reported the use of a Weissenberg rheogoniometer for the characterization of polymer solutions under large amplitude oscillatory shear with the cone-plate geometry. Such torsional flows are known to be subject to the destabilizing influence of centripetal accelerations In low viscosity fluids, these effects cause secondary flows that cause sample outflow. This limits the shear rates and shear strain amplitudes that can be studied using cone-plate flow. The importance of these inertial effects has been reviewed by Dealy,[57] and Walters [58,59] Such secondary flows, by definition, destroy the homogeneity of the flow field, which prevents the measurement of rheological properties.

For higher viscosity liquids an additional limitation results from the normal stress differences that arise when viscoelastic fluids are sheared. This effect results in an uncontrolled distortion of the free surface at the outer edge of the sample.[60,61] This limiting effect has been shown for example, to become acute when concentrated polymer solutions and melts undergo large amplitude oscillatory shear deformation.[62,63]

For solids another interesting phenomenon, called edge fracture, arises where the shear stress to which the sample is subjected is raised to such a level that highly localized deformation leading to fracture is favoured over homogeneous deformation. In contrast to the aforementioned phenomena, fracture is distinguished by the creation of topologically distinct surfaces.[64] Furthermore, when fracture occurs at the shearing boundary it is called adhesive failure. Adhesive failure has been observed for molten plastics in sliding plate rheometers.[65]

3. Parallel-Disk Flow

The flow between rotating parallel disks has also been used extensively for the measurement of viscometric and linear viscoelastic properties in polymeric liquids. Although the sources of error for such experiments are the same as those listed for cone and plate flow, the severity with which the effects of inertia and normal stress difference destabilize the flow between parallel rotating disks is much reduced. This geometry has also been used, on occasion, as a means of studying nonlinear viscoelasticity.[66] However, the flow field for this geometry is highly nonhomogeneous, so the interpretation of torque in terms of well defined rheological properties is difficult.

Two recent attempts have been made to infer nonlinear viscoelastic properties from parallel disk experiments for the special case of oscillatory shear. The amplitudes of these experiments are called large but the strain for the parallel disk geometry really varies from zero at the center to a maximum at the edge. The mathematics required to extract stress responses, be they harmonic or anharmonic,* to large amplitude oscillatory shear, from the observed torque in such tests, has recently been worked out [67,68] The results have been corroborated by cone and plate data for a polymer solution. However, the mathematics for the method are tedious, and the need to corroborate the parallel disk result with the homogeneous flow result seems unavoidable.

A less general scheme for extracting well defined nonlinear viscoelastic oscillatory shear properties from the torque output for parallel disk flow has been reported. Working equations have been provided for the superposed flows of large amplitude oscillatory shear and steady shear, both when the stress is harmonic and when it is not.[69,70] The calculations assume a specific constitutive relation, from which equations are derived relating the time dependent observables, torque and thrust, to the time dependent properties, shear stress and first normal stress difference This method was recently extended to the inference of stress growth at start-up and of stress relaxation after cessation of steady shear [71,72] Only the shear stress was determined with these techniques and

*The term harmonic means shaped like a sinusoid. Strictly speaking, the term anharmonic means not shaped like a sinusoid, which would include noise, subharmonics and higher harmonics. In the present context, we are referring to stress responses containing higher harmonics only.

it was successfully corroborated by cone and plate flow data for two polymer solutions. Be this as it may, such calculations are tedious and, should the particular constitutive equation not hold, what might be done is unclear. Furthermore, the assumption of a particular constitutive equation seems unnecessary in the light of the general method reviewed above. Additionally, the need for corroboration by cone and plate flow experiments limits the usefulness of such a technique.

Finally, a rheometer using parallel disk flow and incorporating a shear stress transducer to minimize problems of flow field inhomogeneity has recently been developed [73,74,75] A shear stress transducer has been specially designed for in-line rheometry of molten plastics.

The parallel disk approach to studying nonlinear viscoelasticity with oscillatory shear has not been attempted for molten plastics These parallel-disk flow examples do, however, illustrate just how much trouble one must go to in order to extract a single meaningful nonlinear viscoelastic property from the observables associated with nonhomogeneous flow fields.

4. Concentric Cylinder Rheometry

Some of the most successful attempts to study nonlinear viscoelasticity in molten plastics employed concentric cylinder rheometers.* Such a

*Not to be confused with sliding cylinder rheometers discussed in the next section.

rheometer was developed by Petersen, Tee and Dealy for the study of the response of molten plastics to large amplitude oscillatory shear.[76,77,78] Although several plastics were studied, a tedious sample insertion technique requiring the premolding of samples was needed. Additionally, maintaining concentricity proved difficult, since gaps as small as .25 mm were required, and long term dimensional instability of the steel cylinders at elevated temperatures caused unacceptable eccentricity. Melt outflow from the gap was a serious problem This phenomenon, termed the "Weissenberg effect", is a result of the influence of normal stress differences at the free boundary Finally, the rheometer made use of an electromechanical drive system limiting its use to steady shear and steady oscillatory shear Despite these limitations, this work provided a benchmark for future work in the area

Maxwell used a concentric cylinder rheometer to study the liquid-liquid transition in nonlinear viscoelastic properties for molten polystyrene.[79,80] A commercial version of this instrument has also been developed[81] Others have used concentric cylinder rheometers at room temperature to measure nonlinear viscoelastic properties of polymer solutions, melts and suspensions in large amplitude oscillatory shear in both harmonic and anharmonic regimes.[82,83,84]

5. Sliding Cylinder Flow

Sliding cylinder rheometers have been used for the study of nonlinear viscoelasticity in polymeric liquids. Strictly speaking, such flows are nonhomogeneous, but they can be made nearly homogeneous. McCarthy[85] reports a successful series of characterizations of molten plastics in large amplitude oscillatory shear comprising both harmonic and anharmonic regimes. This method is distinguished by its special sample loading technique, in which the sample is extruded into the annular gap. Without such a technique, sliding cylinder rheometers are hard to load, since annular gaps are hard to get at Special precautions must be taken when filling the annular gap, since polymeric liquids, and especially polymer melts, are notorious for their propensity to entrain air bubbles when poured. McCarthy employed an MTS servohydraulic drive system to obtain a sinusoidal displacement of the inner cylinder. The technique achieved satisfactory temperature control, but the sample loading technique subjected the sample to the extrusion loading shear history which, one might speculate, could be a source of error for melts, which take their time relaxing. Furthermore, flow-field inhomogeneity is not discussed by McCarthy

Sliding cylinder rheometers have also been used to study nonlinear viscoelasticity in bread dough using oscillatory shear.[86,87] Flow-field homogeneity was a serious problem with such measurements, and a clever experimental method has been proposed to circumvent this problem.[88,89,90,91,92] The method has been validated for harmonic responses only and entails the plotting of the logarithms of apparent storage and loss moduli versus gap size. For bread dough, the logarithm of such apparent moduli was linear with gap size for small gaps. Extrapolation to zero gap was used to obtain moduli which are taken as nonlinear viscoelastic properties. Such moduli are both strain amplitude and frequency dependent and that, in principle, this method could be extended to include higher harmonics, which are usually observed for molten plastics The method proved highly successful for the study of bread doughs since, unlike polymer melts, no anharmonic regime was observed for the systems studied [93] Hibberd et al recently chose to use the sliding plate instead of the sliding cylinder geometry for their studies of nonlinear viscoelasticity [94,95]

In contrast, in an ongoing effort at the University of California at Berkeley researchists opted for the sliding cylinder over the sliding plate approach in a study of nonlinear viscoelasticity in polymer solutions, and the two methods were compared.[96,97,98] Firstly, a bubble free sample loading technique was developed for the sliding cylinder rheometer, which had previously been used to load a sliding plate rheometer [99] Secondly, signal noise in the load cell output was lower for the sliding cylinder rheometer than for the sliding plate rheometer. This noise in the sliding plate rheometer output signal is due to friction in the precision guide rods used to maintain parallelism. Thirdly, the sliding cylinder rheometer, by virtue of its geometry, is subject to end effects only, whereas the sliding plate rheometer is subject to both edge and end effects However, the definitive test for end effects in the sliding cylinder rheometer, the sample size sensitivity experiment, has not been carried out Furthermore, some theoretical predictions have been made for the errors caused by end effects in sliding plate fixtures. Until sample size sensitivity studies are carried out, the relative merits of sliding cylinder rheometry and sliding plate rheometry concerning free boundary effects will remain an open question. Finally, a broad spectrum of nonlinear viscoelastic properties were measured for the polymer solutions studied in this work, including large amplitude oscillatory shear tests, stress growth experiments and stress relaxation after steady shear. The instrument was equipped with a programmable MTS servohydraulic drive system permitting great flexibility in flow pattern selection.

Maxwell used a sliding cylinder rheometer for characterizing molten plastics using nonlinear stress relaxation following imposition of a sudden strain, and subsequent strain recovery.[100,101,102] Liquid-liquid transitions were documented for such nonlinear viscoelastic properties for both polystyrene and poly(methyl methacrylate).

Neither Tsai and Soong, nor Maxwell (1984) report gap sensitivity studies such as those reported by Hibberd et al [103,104,105,106,107] Flow fields are tacitly assumed to be nearly homogeneous.

A concentric cylinder rheometer was recently developed in which the inner cylinder can both translate and rotate so that shear in two orthogonal directions can be studied.[108]

6. Classical Uses of Sliding Plate Flow

Sliding plate rheometers can be categorized into two subclasses, single sample sheating fixtures and sandwich type shearing fixtures. The single sample shearing fixture requires that the moving plate be connected to the stationary plate through precision linear bearings. This allows parallelism to be maintained to the close tolerance of the linear bearings. Where the shear stress under study is inferred from a total force measurement, friction in the bearings causes error. Where frictional forces are erratic, stress response signals are noisy. Sandwich type sliding plate rheometers, on the other hand, usually make use of two stationary plates and one moving plate, between which two identical samples are inserted The requirement that the sample thicknesses be the same arises because there are no bearings guiding the plates. Such a design circumvents bearing friction in single sample devices, but adequate parallelism requires that both samples be positioned exactly opposite one another and that they have identical dimensions.

Classical sliding plate rheometers are either strain-controlled or stress-controlled. Most use a controlled deformation with a load cell to measure the total shearing force on the stationary plate. The shear stress is then inferred from the total force by dividing it by the apparent contact area. Conversely, some control the stress using weights and pulleys and measure the resulting total strain.

Sliding plate rheometers are sometimes used to study nonlinear viscoelasticity but errors arise from edge and end effects since, in classical instruments, the shear stress is inferred from the total force. End effects do not arise in concentric cylinder rotational rheometers since annular samples, being continuous in the plane of shear, have no ends.

Nonetheless, the destabilizing influence of centripetal acceleration and the Weissenberg effect do distort the sample edges and limit the use of rotational rheometers such as the concentric cylinder devices to shear rates well below the shear rates incurred in most plastics manufacturing processes. Hence, there has been a recent renewal of interest in sliding plate rheometry.[109,110]

Stress controlled sliding plate rheometers have been used to measure the nonlinear properties of molten plastics.[111] Recently, for instance, a sophisticated creepmeter was used to study nonlinear creep and stress relaxation following cessation of steady shear in molten plastics.[112] This creepmeter is of the sandwich type Another sandwich rheometer has been used where the middle plate is fixed and the outer plates are rigidly connected to a moving cage [113,114] This creepmeter was specifically designed to study molten plastics at shear stresses approaching those occurring in actual processing operations. Although errors due to instrument vibration existed, high and low density polyethylenes were characterized in highly nonlinear creep and relaxation following steady shear at 100 s^{-1}. Despite the limitations involved in inferring shear stress from total force, these results remain a benchmark for the characterization of molten plastics in the nonlinear viscoelastic regime.

Recently, Meissner and coworkers extended the use of sliding plates to incluae shearing in two directions.[115,116,117] This was done with two linear ıctuators mounted orthogonally on the moving plate. Components of the shear stress were measured separately using two load cells which restricts the use of the instrument to low shear rates. Although this rheometer permits the directional dependence of nonlinear viscoelastic properties to be measured, it has only been used at room temperature.

By measuring the optical transmittance in the x_3 direction in a sliding plate rheometer, the 1,2 component of the birefringence tensor can be measured.[118,119,120,121,122,123,124] Where the stress optical law is valid this allows one to measure shear stress in dynamic tests. The advantage of the method is its superb dynamic response since data acquisition is entirely optical and electronic However, since birefringence is multivalued with transmittance, the inference of shear stress from transmittance is complicated It is restricted to transparent materials which are highly birefringent, and end effects restrict its use to small strain experiments.

Sliding glass plates can be used to measure birefringence and shear stress simultaneously in molten plastics[125,126] and in polymer solutions.[127] Information about the first and second normal stress differences can be gleaned from such measurements with some degree of approximation.[128]

At room temperature, sliding plate rheometers have been used for studying nonlinear viscoelasticity in polymer melts,[129,130,131,132] soaps,[133] filled polymers,[134] filled elastomers[135,136] and rubber.[137]

Although some workers have tried to correct for free boundary errors,[138,139] most have decided to live with them.*

Sliding plate rheometers of the sandwich type have also been used for measuring the nonlinear viscoelastic properties of foods.[140,141,142] After much experience with sliding cylinder rheometry, Hibberd and Parker [143,144,145] recently opted for a sliding plate rheometer of the single sample variety to measure nonlinear creep and stress relaxation following cessation of steady shear in bread doughs.

Finally, workers at the University of California at Berkeley[146,147,148,149] recently used a sandwich type sliding plate rheometer for the study of nonlinear viscoelasticity in polymer solutions Properties measured included stress growth, stress relaxation after cessation of steady shear, interrupted shear and large amplitude oscillatory shear in start-up and in harmonic and anharmonic regimes, stress relaxation following large amplitude oscillatory shear, stress growth superposed on stress relaxation after large amplitude oscillatory shear, small amplitude oscillatory shear superposed on stress growth, and exponential shearing. This flexibility in the choice of flows was permitted by the programmable MTS servohydraulic drive system. Although this unit was of the sandwich variety, it required the use of precision guide rods to maintain parallelism. Friction in the bearing resulted in a noisy stress signal which limited the work to flows having shear rates less

---

*See section on free boundary errors for further detail.

than 5 s^{-1}. The work remains a benchmark for future work in nonlinear viscoelasticity because of its great flexibility in choice of flows.

7. Free-Boundary Errors

Developing a sliding plate rheometer of the single sample variety, Philippoff[150] observed:

> "that simple shear cannot be realized in the shearing of a cube by moving two parallel sides in opposite directions ... this is caused by the boundary conditions of the experiment which require freedom from stress at the geometrical limits of the sample"

Yet few have tried to measure the free boundary effects in classical sliding plate rheometers.

Uncontrolled flow can occur near free boundaries simply because the shape of the free boundaries is not controlled. In theoretical predictions for deviations from simple shear near the free boundary, the periphery is usually assumed to be at ambient conditions and stress-free. However, other boundary conditions have been posited for the periphery of a viscoelastic liquid in simple shear.[151,152,153]

Although the present discussion limits itself to sliding plate flow, free boundary errors occur in other rheometrical flows too. Such errors can be important since the stress acting near the rim contributes most to the total torque which is measured. For example, using local pressure transducers for viscoelastic fluids in steady cone-plate flow, gauge pressure was shown to decrease with radial position.[154,155,156,157]

We distinguish two kinds of free-boundary error. Firstly, there are uncontrollable flows induced by the stress-free condition at the leading and trailing ends of the sample in simple shear. Secondly, edge effects are uncontrollable flow induced by the stress-free condition on the sides of the sample. For circular samples these effects are not separable. Moreover, the bulging which occurs at the edges of rectangular samples has been attributed to the interaction between edge and end effects.[158,159]

a. End Effects

Neglecting edge effects, Read[160] calculated the free boundary errors for rectangular rubber samples subjected to small shear strain in a sliding plate rheometer. The analysis pertains to linear elastic and viscoelastic solids. The upper and lower bounds for the strain energy of the deformation, distorted from true simple shear, were approximated numerically. This thermodynamic analysis applies to large apparent shear strains under static or dynamic conditions and indicates that the apparent shear stress, σ_a, will be lower than the true shear stress, σ. The fractional error, $\epsilon = \sigma_a/\sigma - 1$, incurred when shear stress is inferred from total force, is negative and proportional to the sample's length to thickness ratio, R, and ϵ decreases with increasing Poisson ratio. Read's results, replotted in Figure 7, show that for R=10 and a Poisson ratio of ½, the free boundary error envelope ranges from -1.6 to -2.7%.

Parenthetically, this work summarizes a larger study[161] which is unfortunately no longer on record.[162,163,164,*] The larger study is reported to have included estimates of free boundary errors in oscillatory shear, showing that the flow field inhomogeneity induces additional damping to appear for viscoelastic solids.

A theory for static deformation has also been proposed[165] and used[166,167] which estimates ϵ for linear elastic materials by superposing the nonideal bending deformation permitted by the free boundary with the ideal simple shearing deformation. This simple analysis concludes that:

$$\epsilon = 3/(3+1/R^2) \tag{3}$$

and applies to small γ. Figures 3 and 4 show the comparison of Read's thermodynamic theory with this elastic theory. Figure 3 shows that for $R \geq 2$, the simple elastic theory predicts much lower errors than the thermodynamic envelope. Despite the discrepancies, we conclude that significant negative free boundary error is predicted by theory for simple elastic and viscoelastic solids.

More recently, Gent[168] observed that the shear stress distribution across a square rubber sample with a diameter to thickness ratio of 8.6 and under shear is nonhomogeneous due to free boundary effects, even for small shear strains. This observation, replotted in Figure 2, was made by

---

*Note that Read's analysis concerns end effects, not edge effects, despite its title which refers to end effects as edge effects.

measuring the interfacial shear stress locally at different positions in a sample under a static shear strain. Figure 2 shows, for a sample with half length .112 m and R = 8.6, the shear stress is nearly homogeneous in the middle of the sample only. The local shear stress measured close to the ends at the rubber-plate interface, is well above zero.

Significantly, Roscoe and coworkers at Cambridge University incorporated an array of local shear stress transducers into a simple shear fixture designed for soils.[169,170] Marked stress inhomogeneities were observed at the ends of the soil samples Additionally, sophisticated radiography revealed the corresponding strain inhomogeneities.[171,172] Furthermore, several attempts have been made to model end effects in soils.[173,174,175,176] Stress and strain inhomogeneities caused by end effects can be pronounced for soils in simple shear. Indeed, some workers have designed mechanical constraints for sample boundaries in an attempt to minimize free boundary effects. These curious devices move with the free boundary, confining it to the desired deformation They have been used for both rectangular[177,178] and circular samples.[179]

Andrade[180] observed spectacular end and edge effects in large samples of gelatine-glycerine jelly in a sliding plate fixture. Large time dependent deviations from the desired simple shearing deformation were found. Similar observations have also been made on plasticene, in simple shear.[181]

Researchers at the University of Tennessee[182,183] found that end effects in a sliding plate rheometer posed a serious problem, and drastic measures were taken to correct for them. Nonlinear viscoelastic properties of elastomers in creep, stress growth and stress relaxation after cessation of steady shear were measured. The correction used the arbitrary subtraction of the exposed area of the shearing plates from the original sample area. This practice cannot be used to get fundamental quantities. In earlier work the same group used a sandwich shear fixture for the study of nonlinear viscoelasticity in elastomers and their compounds,[184,185] but in this case the subtraction of exposed area was not made.

Some have argued that end effects are negligible for polymer solutions. For instance, the group at Berkeley successively carried out stress growth and relaxation experiments with different starting plate positions on the same sample[186] Reproducibility of the stress traces for these tests indicated that free boundary effects were indeed negligible for stress growth experiments done with total shear strains of 48 and shear rates of 4 8 s^{-1} This finding contrasts sharply with what has been said about free boundary effects. It is surprising since at this strain, for the sample thickness of 1.32 mm and length of 34 cm, the area of exposed plate is 32% of the sample's initial contact area. Sample size sensitivity experiments were not carried out for the polymer solutions studied. Although free boundary effects were small in low shear rate tests on polymer solutions, the importance of such effects for molten plastics remains an open question.

Tanner has noted that simple shear is the flow which ideally governs the performance of straight slider bearings.[187] However, end effects in slider bearings can affect sliding bearing capacity. Using a boundary element computation, Tanner computed the shape of the trailing edge for a model viscoelastic liquid in steady simple shear.[188,189] It was concluded that an accurate condition for the boundary at the free ends is $\Delta P = b + \frac{1}{2} N_1$ for simple shear, where ΔP is the gauge pressure sensed in the region of controllable flow and b is the offset caused by the flows near the free-end. The boundary element computation predicts that $b = 3/2$.

Interestingly, the gauge pressure was measured for a polystyrene solution in steady shear using two flush-mounted transducers in the region of controllable flow.[190] The gauge pressure was indeed linear with $\frac{1}{2} N_1$. However, a significant difference in offset was discovered for steady shear tests done in forward and backward directions where, $b = 1.2$ and $b = 0.8$ respectively. This discrepancy in b was partially explained as a hydrodynamic effect of uncontrolled deviations from simple shear at the free ends. This is one reason that gauge pressure in sliding plate rheometers cannot be used to measure first normal stress difference.[191,192,193]

Finally, Laun and Meissner have computed the effect of surface tension at the leading and trailing bounds of a rectangular sample in simple shear where new surface must be generated during simple shear.[194] From this thermodynamic analysis, the additional total force due to surface tension effects is the following simple function of shear strain:

$$\Delta F = 2 \alpha W \gamma / \sqrt{(1 + \gamma^2)} \tag{4}$$

For instance, Figure 5 shows that the effect of surface tension for rectangular molten HDPE samples at $T = 150^{\circ}C$ which are 5 and 10 cm wide. Thus ΔF rises sharply with shear strain, levelling off near $\gamma = 3$ at:

$$\Delta F_{max} = 2 \alpha W \quad (5)$$

Figure 6 shows the ΔF_{max} for the 5 cm HDPE sample as a function of sample width. This error is not time dependent, so ΔF persists until γ is returned to zero This analysis assumes that the boundary behaves ideally. Since the stress free condition at the boundary permits nonideal flow, (4) and (5) cannot be used for accurate correction of total force measurements for surface tension errors. This error obviously becomes important when the ratio of ΔF to the total measured force is significant.

b. Edge Effects

Joseph has shown that the edges of a rectangular sample in oscillatory shear are subject to a distortion which is analogous to the Weissenberg effect observed on edges of samples in oscillatory shear in concentric cylinder rheometers.[195,196] Edge distortion, caused by the first normal stress difference, is composed of average and oscillating components of deviation from the desired straight boundary. The magnitude of the overall edge distortion can be deduced from $G'(\omega)$, $G''(\omega)$ and $N_2(\omega)$. In principle, a design estimate for the required sample width for a particular gap can be obtained However, the solution is a complicated one, and in general, the first normal stress coefficient is not known in oscillatory shear. Remarkably, predicted distortions are not symmetric about the sample midplane. Hence, just as the Weissenberg effect depends on which cylinder is rotated, the shape of edge distortion depends on which plate is oscillated Also, for model viscoelastic fluids, no edge distortion is predicted in steady simple shear However, Joseph assumes no variation in the x_1 direction restricting his analysis to a sample of infinite length This precludes interactions between end and edge effects which are expected to cause bulging at the edges when $|N_1|>|N_2|$ [197,198]

C. Local Shear Stress Transducers

A transducer is a device that converts one physical quantity into another, observable quantity. A shear stress transducer is simply a device that makes shear stress observable The physical quantity is called the measurand or input, and the observable quantity is called the transducer response or output Most authors further restrict the definition of transducer to include only those with the measurand linearly related to the observable, since measurement systems require simplicity to be useful.*

Few local shear stress transducers have been developed [199,200] Since local shear stress transducers have never been sold commercially, textbooks on mechanical measurements do not usually mention such sensors. Previous

*A further distinction is usually made between active and passive transducers. Active transducers use an external source of power, and passive transducers do not Most of the shear stress transducers reviewed here are active transducers work on shear stress transducers is scant, aimed at static not dynamic measurement and was not done at high temperature.

There are two types of mechanism used to measure local shear stress. Firstly, one can measure the stress on a moving wall element, called the active face, by connecting it directly to a force transducer. Alternately, one can measure the deflection of a beam, usually a cantilever, that itself supports the active face. The second approach requires a proximeter which distinguishes it from the first approach employing load cells which normally incorporate strain gauges or piezoelectric sensing elements. Moving wall element methods are popular for studying gases and Newtonian liquids,[201] whereas beam deflection methods are popular for studying solids.*

Furthermore, there are two ways of implementing these mechanisms. Either the deflection is measured directly or, in sophisticated designs, the restoring force required to keep the active face stationary is applied and measured. These are called the positive deflection and null balance methods, respectively. Positive deflection is a simpler method than null balance since no motor is needed for restoring a null active face position. Using identical proximeters, transducers based on null balances generally give better resolution and sensitivity than those based on positive

---

*Moving wall element methods are sometimes called floating head methods, especially when wall element motion is confined to translation without rotation.

deflection. However, unless deflection itself causes damping,* deflection methods give better dynamic response than null methods. Specifically, if a servo system is used, the phase lag of the motor is added to that of the deflection meter.[202]

1. Transducers for Newtonian Liquids and Gases

The earliest transducers, developed by Froude and Kempf,[203] were used to measure shear stress locally on objects in flowing water.[204,205] Here moving wall elements were used with null balances using strong electromagnets to apply and measure the restoring force Magnetic field strength was adjusted manually to null the balance, hence, only time steady measurements were possible Similar devices were used on surfaces in steady air flows.[206,207,208,209,210] In the late fifties, acceleration insensitive versions of such transducers were mounted on Viking rocket ships to measure local shear stress during ascending flight.[211,212] Recently, a linear servo motor was used to null a local skin friction balance automatically.[213,214] The null position in the balance can easily be changed to center the active face or to check its sensitivity to eccentricity

Electromagnetic coils have also been used in local shear stress transducers for measuring the stresses acting on the hull of a ship as it passes through ice.[215] Either stiff metal springs or hard rubber bars are

*With transducers for molten plastics, movement of the active face causes damping.

used to join the active face to the housing, and these can be sealed hermetically.

The positive deflection method, using a linear variable differential transformer, has also been used with moving wall elements on flat surfaces in air flows. These sophisticated designs ensured absolute flushness by using four flexing leaf spring supports permitting the moving wall element to translate without rotating.[216,217] Others have used ball thrust bearings for the same purpose in a shear stress transducer with biaxial capabilities for studying hot gas flows.[218]

Finally, housings for these sensors often incorporate viscous dampers such as air bearings[219] or silicone oil dashpots[220,221] to eliminate errors due to equipment vibration

2. Transducers for Soils and Rubbers

Previous work in shear stress transduction focusses on shear and normal stress measurements in soils. Longstanding, ongoing research at the University of Cambridge has led to the development of several shear stress transducers for the static measurement of shear and normal stress in soils. Bransby[222] has provided a detailed review of this research before 1973. The first of these transducers used foil-type electric resistance strain gauges mounted on four steel columns which support the transducer's square active face.[223,224] These strain gauges were configured in a three bridge circuit, and shear and normal stresses were measured. A rigid design was used so that at full load of 25 psi shear stress, lateral deflection of the active face reached only .001 inches.

Later designs at Cambridge were based on the bending of beams rather than by the compression of columns.[225] These transducers were used for monitoring shear stresses in granular solids.[226,227] Rugged versions of these transducers have also been used to study soils in the field.[228,229,230] The Cambridge transducers have only been used at room temperature.[231] Waterproof[232] versions of these transducers were incorporated into simple shear fixtures to measure the mechanical properties of sand[233,234,235] and soft clays[236] Finally, an array of such transducers incorporated in a simple shear fixture has been used to study the importance of end and edge effects in soils.[237]

Shear and normal stress transducers employing single cantilever beams have also been used for studying soils. Here the active face of the transducer is secured to the end of, and perpendicular to, the thin deflecting beam. For instance, two force transducers, incorporating unbonded strain gauges, were used to measure normal and shear stress by attaching them directly, respectively, to the fixed end and side of the cantilever.[238,239] Also, a two-beam design with two full strain gauge bridges which permit acceleration compensation with biaxial shear capability has also been used to measure local shear stresses dynamically in soils.[240]

A shear and normal stress transducer using strain gauges fixed directly to a single stiff cantilever was incorporated in a shearing fixture[241] and used for the determination of stress distributions in compressed rubber samples in shear.* Similarly, strain gauges mounted directly on a stiff beam have been used in a transducer for soils at high earth pressures.[242,243] A rubber gasket was inserted between the sensing face and beam housing to eliminate soil influx to the gap which would prevent beam deflection The flexibility of the rubber minimized impedance of beam deflection. A similar approach has been used to eliminate polymer influx into the gap for a shear stress transducer to be used in an in-line rheometer for molten plastics.[244,245]

Broersma reviewed a patented transducer design which supports the cantilever with four perpendicular flexible members.[246,247] Strain gauges sense deflection in these cross-beams to transduce pressure and shear stress simultaneously.

A different approach has been used extensively for shear stress measurements in soils at the Czechoslovak Academy of Science.[248,249] Here, the active face was secured to a steel ring with strain gauges on the ring's inner and outer sides.[250,251,252,253,254] Several transducers were used by this group including one with a curved active face for measuring time steady stresses of granular materials flowing in cylindrical bins.

*Results of this work are discussed in the section on free boundary error.

Others were used to measure static shear and normal stresses acting on the floor beneath piles of granular solid.

3. Tactile Sensing and Shear Stress Transducers

Human skin, especially at the fingertips, has the well developed capability of sensing shear stress. For years, experts in robotics have tried to emulate this capability with miniature sensors, but they are still a long way from approaching the quality of shear stress transduction provided in human hands [255]

Hands transduce shear stress using a sensitive array of nerve endings in the fingertips which convert both shear and normal stress simultaneously to electrical impulses. Theses impulses quickly relay the stress measurements to the brain. The transduction is fast enough to form part of a sophisticated closed loop control system that can sense and react to slight changes in shear stress. Consider the man who falls asleep in bed when holding a cigarette. As the grip is inadvertently loosened, the cigarette will start to slip across the surfaces of the fingers. The slight fluctuations in shear and normal stresses caused by the sliding cigarette are sensed, messages are dispatched to, interpreted and processed by the brain, the hand is caused to tighten, and ideally, the man is awakened. Human tactile sensing can transduce shear stress quickly so the measurand can be controlled. Observe that the man exerts just enough force on the cigarette* to keep it from dropping, but not enough to crush it.

Shear stress transducers using strain gauges have recently been incorporated into robotic hands used in general purpose manufacturing robots.[256]

4. Shear Stress Transducers for Polymer Melts

From the review on sliding plate rheometers it can be seen that the use of simple shear simplifies the relation between force and shear stress. However, it can also be seen to be limited to use at small strains by end and edge effects.

Now with molten plastics, it was argued that rheological properties incorporating fast transient deformations are the ones most likely to correlate with processability. In the study of fast transient responses it is important that the observable quantity be simply related to the primary physical quantity, here the shear stress. Where such simple relations cannot be established, iterative calculations and many experiments are required to extract a single nonlinear viscoelastic property. This was seen to be true where large amplitude oscillatory shear properties are extracted from parallel disk flow data for instance. Furthermore, even where the tedium of such approaches can be tolerated, corroboration of the

*The shear stress exerted by 1 cm^2 of skin surface required to support a 1 gram cigarette is 98 Pa or .014 psi.

results with those of less complicated experiments is desired. If the errors associated with end or edge effects could be circumvented, a sliding plate rheometer could be constructed wherein nonlinear viscoelastic properties of molten plastics could be determined reliably and conveniently.

None of the shear stress transducers reviewed above have been used for dynamic measurement. In a rheometer, it is critical that the transducer track the shear stress accurately as a function of time, since viscoelasticity implies time dependence Recent progress at McGill University included the development of a prototype shear stress transducer for molten polymers.[257,258,259,260,261]

All sliding plate rheometers reviewed above require that the shear stress be inferred from a measurement of total force. Soong and Dealy proposed that the shear stress be measured locally in the region of controllable flow, away from the free boundary of the sample under study, so that the free boundaries errors might be circumvented.[262,263] They incorporated a shear stress transducer into a single-sample, sliding plate rheometer which they used to measure nonlinear viscoelastic properties of polyisobutylene at room temperature.[264] Stress growth, stress relaxation following cessation of steady shear and interrupted shear experiments were performed. An electromechanical drive system was used which limited flexibility in property selection. This rheometer is the precursor to the device developed for the present work, which is a sliding plate rheometer for molten plastics incorporating a shear stress transducer.

Initial designs for a transducer included the use of thin flexible cantilever beams of rectangular cross-section with a square active face fastened to the beam's free end. Foil-type piezoresistive strain gauges were mounted directly on the flexing beam. The design allows the melt under study to penetrate the gap between the active face and housing. The transducer could be used to measure melt viscosity. However, it had poor transient response in stress relaxation following steady shear when compared with measurements made on a mechanical spectrometer using a cone-plate fixture.

To improve the transient response, a second design used a stiffer cantilever whose diameter was only slightly smaller than that of the active face. Unfortunately, strain gauges were insensitive to the diminished strains in the thicker beam, and a new approach was sought.

The insertion of a piezoelectric crystal in the flexing member was considered, so that with suitable charge amplification, the desired linear voltage output could be obtained.[265-266] Although such an approach remains attractive, another equally attractive technique was pursued because it involved a simple change to the prototype.

A sensitive optical method was chosen to measure cantilever displacement in the stiff beam transducer mentioned above.[267] This combination permitted the measurement of nonlinear stress growth, stress relaxation following steady shear and interrupted shear properties of polyisobutylene melts. Attempts to measure shear stress in large amplitude oscillatory shearing were also made but an error was made in recording the data. The proximeter employed fiber optics to measure the displacement of the cantilever at a point several centimeters from the active face. The method provides sufficient sensitivity, although drift in sensitivity, noise, baseline drift and an inconvenient calibration method compromised the quality of the data. Since fiber optic displacement probes are not readily available for high temperature service,[268] a new displacement measurement technique was sought by the writer in designing a transducer for molten plastics.

D. General Objectives

The single most important objective of the present research was the development of a shear stress transducer for the rheological characterization of molten plastics. The transducer is incorporated in a sliding plate rheometer designed for use at temperatures up to 250°C. The sliding plate design was chosen to take advantage of the simplicity of planar Couette flow and to avoid errors due to centripetal acceleration and edge failure incurred with rotational flow geometries.

The second principal objective of the present research was to evaluate the rheometer's suitability for the measurement of nonlinear viscoelastic properties of molten plastics. A broad selection of shearing patterns are permitted by using a servohydraulic actuator to drive the rheometer. Quantitative evaluation of the rheometer for such measurements is difficult since most of these properties cannot be measured by any other means. Furthermore, those nonlinear viscoelastic properties that can be measured by other means can be obtained only with great difficulty. A new dynamic calibration method has been designed to permit an evaluation of the new instrument for a wide range of property measurements.

II. THEORY OF VISCOELASTICITY

A. How is Theory Useful for Rheometer Development?

The purpose of this research was to develop a new rheometer. Several theorists have tried to predict the sorts of properties that the new rheometer is designed to measure. Some of their theories suggest ways of analyzing nonlinear viscoelastic properties which is helpful for rheometer development. This is important in the present context since the properties measured on the new rheometer cannot be measured any other way. Whereas dynamic calibration, described in a later section, helps us to pinpoint errors in the new measurements, the present review of theory tells us what results are physically admissible.

There are, of course, several other uses for nonlinear viscoelastic theory. Firstly, such models can be used to simulate polymer manufacturing processes. For instance, the Leonov model, based on nonequilibrium thermodynamics, has been used to model the injection molding process.[269] Secondly, nonlinear viscoelastic models, if sufficiently general, provide a unified basis for summarizing and comparing nonlinear viscoelastic properties. Thirdly, molecular models can help explain which aspects of molecular structure determine nonlinear viscoelasticity and therefore processability for some materials. Model parameters can then be correlated with processability and molecular structure. The scope of the present review of viscoelastic theory is strictly delimited to what is useful for rheometer development.

B. What is a Theory of Viscoelasticity?

Viscoelasticity is the relationship of the extra stress tensor to the strain tensor. A viscoelastic theory is simply a mathematical expression which approximates such a relationship. The quest for such theories presumes that such equations exist. These equations are called constitutive equations, and in material science there are no existence theorems. The most general form for a viscoelastic theory is:

$$\underline{\sigma}(t) = f\,\{\underline{\Gamma}(t)\}\,, \tag{6}$$

where f is any function, Γ represents any material frame indifferent deformation tensor, and where the stress and deformation tensors are time dependent.

For prescribed transient deformation patterns, the deforming stress is also time dependent. Hence, viscoelastic properties are defined as the time dependent stress caused by a prescribed, time dependent, deformation. Thus, (6) gives a general mathematical description for viscoelastic properties.* However, there is no unifying theory that allows the extra

*Inversely, one can define viscoelasticity as the relationship of the strain tensor to a prescribed transient deforming stress. Those working with controlled stress instruments prefer this point of view.

stress tensor to be explicitly written as a function, f, of an indifferent strain tensor. This is why nonlinear rheological properties are defined by a prescribed transient deformation and its time dependent stress response.

C. Symmetry of the Stress Tensor

A torque balance on a differential rectangular fluid element subject to neither internal moments nor couple stresses proves that $\sigma_{ij} = \sigma_{ji}$, and so the extra stress tensor is symmetric. The premises of (1) no internal moments and (2) no couple stresses are important constitutive assumptions.[*,270,271]

Angular acceleration of the differential fluid element makes no contribution to the force or torque since differential elements have no mass. A torque balance on a finite fluid element must, however, include terms for its angular acceleration.

Now the assumption of no internal moments is a reasonable one since internal moments, or body couples, require action at a distance on the fluid element. Body couples are important when a magnetic fluid encounters a magnetic field. So the assumption of no body couples seems reasonable for molten plastics which are, in general, either nonmagnetic or not subjected to magnetic fields.

---

*This pair of assumptions is variously called Cauchy's second law, the Cauchy stress principle, the complimentary shear stress condition, the principle of local action or the principle of local equilibrium.

The assumption of no stress couples, on the other hand, may or may not be correct.[272] Furthermore, Tanner recently pointed out that the important consequence of the constitutive assumption, the symmetry of the stress tensor, has not as yet been verified experimentally.[273]

The potential significance of stress couples and angular acceleration in sliding plate rheometry is treated in the next chapter.

D. Why Use Tensors?

In the introductory chapter we noticed that since the stress tensor is symmetric, and since only shear stresses and normal stress differences are deforming stresses, the stress state at a point in a fluid is described by the five independent quantities. shear stresses σ_{12}, σ_{13}, σ_{23} and normal stress differences $\sigma_{11}-\sigma_{22}$ and $\sigma_{22}-\sigma_{33}$.

The uninitiated will wonder why he must still write constitutive equations in terms of tensors, which have nine components, when only five components are required. Early work carried out when few measurements of viscoelastic properties were available, established a branch of mathematics called rational mechanics. In rational mechanics, the most plausible suppositions were made about the nature of a fluid, and their mathematical consequences were studied. Supposing that the fluid is a continuum led to the single most important contribution of rational mechanics to viscoelastic theory, the principle of material frame indifference.*

This principle simply states that the stress and strain tensors should be unchanged by a change of reference frame. This assertion has obvious meaning but far reaching consequences. The principle is simply saying that one's prediction about fluid flow should not be changed by one's point of view ... the fluid ought to be, after all, indifferent to the observer's reference frame

A change of reference frame may be time dependent and may involve any combination of translation, rotation or time shift. Mathematically, a change of the reference frame is described by an orthogonal tensor.** This tensor is called the rate of rotation tensor and is defined by

$$\underline{P}_1^* - \underline{P}_2^* = \underline{Q}(t) \cdot (\underline{P}_1 - \underline{P}_2) \; , \tag{7}$$

where $\underline{P}_i$ represent position vectors of material points in different reference frames. Tensors can be indifferent, which is why we like to use tensors to describe the states of stress and strain. Finally, the result we glean from rational mechanics is that for $\underline{A}$ to be indifferent it must have the following property:

---

*Also called the principle of material objectivity.

**Recall that an orthogonal tensor is one whose inverse is equal to its transpose.

$$\underline{A}^{*} = \underline{Q}(t) \cdot \underline{A} \cdot \underline{Q}^{T}(t) \ . \tag{8}$$

For constitutive equations we require both the extra stress and the strain to be frame indifferent. This is why tensors are used to formulate constitutive equations.

Finally, some indifferent nonlinear viscoelastic models can be written using 5x1 matrices for the extra stress and deformation rate.[274]

E. Deformation Tensors

We are now ready to tackle the important problem of defining frame indifferent tensors to describe deformation. Our special interest here is to formulate the general tensors for simple shear in the upcoming section.

Consider Figure 9 illustrating two material points at different times in a homogeneous flow field with position vectors $\underline{P}_1(t)$, $\underline{P}_2(t)$, $\underline{P}_1(t_o)$ and $\underline{P}_2(t_o)$, where t_o is a reference time. We now construct a deformation gradient tensor by considering, one by one, the effect that a differential change in one component of the reference position vector has on the positions of the material points at time t:

$$F_{ij} = dP_i(t)/dP_j(t_o) \ . \tag{9}$$

This tensor is not indifferent, but it is used to construct indifferent deformation tensors.

For instance, the Cauchy deformation tensor* is the following simple function of F_{ij}:

$$\underline{C} = \underline{F}^T \cdot \underline{F} \tag{10}$$

and it can be shown that this tensor is material frame indifferent and that it becomes the unit tensor** when the material is in its reference state.

$$\underline{C}(t_o) = \underline{1} \ . \tag{11}$$

Since the Cauchy tensor explicitly involves the distances between material points it is commonly called a measure of stretching. This does not imply however, that it does not describe shearing deformation, for (10) completely describes any deformation.

Another way of looking at deformation is provided by the inverse of the Cauchy tensor, called the Finger strain tensor which is also material frame indifferent. It can be shown that the area of a surface of a fluid element, da, at time t is the following simple function of the Finger tensor and the area of the same surface at the reference time t_o:

---

*Sometimes called the right Cauchy-Green tensor.

** $1_{ij} = 1$ for $i=j$, $1_{ij} = 0$ for $i \neq j$.

$$[da(t)]^2 = [da(t_o)] \cdot \underline{C}^{-1} \cdot [da(t)] \ . \tag{12}$$

The Finger tensor relates material surface areas of a fluid element at time t to those of the same element at time t_o.

Because it is sometimes convenient to use a measure of deformation which is zero when the material is in its reference configuration, two more material frame indifferent deformation tensors can be defined:

$$\underline{J} = \underline{C} - \underline{1} \tag{13}$$

and

$$\underline{H} = \underline{C}^{-1} - \underline{1} \tag{14}$$

These are called the ~~Cauchy~~ strain and the Finger strain respectively.*
The upcoming discussion on simple shear will focus on these two tensors.

Additionally, the fractional change in volume is:[275]

$$\Delta v = \frac{\sqrt{(\det J(t))} - \sqrt{(\det J(t_o)}}{\sqrt{(\det \underline{J}(t_o)}} , \tag{15}$$

and for an incompressible fluid $\Delta v = 0$.

*Beware of confusion between Finger and Cauchy strains, and the separate and distinct Finger and Cauchy tensors. The Finger and Cauchy strains are tensors too.

F. The Rate of Deformation Tensor

A rate of deformation tensor can be defined as the time derivative of the Cauchy tensor but such a tensor is not indifferent. To obtain an indifferent rate of deformation tensor we require a time coordinate transformation. Specifically, the reference time must be taken as the current time t. Hence, the material objective rate of deformation tensor is the time derivative of the Cauchy tensor if and only if the reference time t_o is taken to be the current time t. This is written as:

$$\underset{\sim}{\Delta} = \frac{d}{dt}\left[\underset{\sim}{C}\right]\bigg|_{t_o=t} \tag{16}$$

Time derivatives of indifferent tensors are not necessarily indifferent. Specifically, the time derivatives of the rate of deformation tensor are not indifferent. However, when special types of derivative operate on an indifferent tensor, the result can be made to be indifferent.

For instance, the Jaumann derivative is defined as:

$$\frac{\delta \underset{\sim}{\alpha}}{\delta t} = \frac{D\underset{\sim}{\alpha}}{Dt} - \underset{\sim}{W}\cdot\underset{\sim}{\alpha} + \underset{\sim}{\alpha}\cdot\underset{\sim}{W} , \tag{17}$$

where the vorticity tensor, $W_{ij} = \frac{1}{2}(\nabla \underline{v} - \nabla \underline{v}^T)$, and D/Dt is the substantial derivative which is:

$$D/Dt = d/dt + (\underline{v} \cdot \nabla) \quad . \tag{18}$$

Another important material indifferent derivative, called the contravariant convected derivative, is:

$$\frac{\delta \underline{\alpha}}{\delta t} = \frac{D\underline{\alpha}}{Dt} - \nabla \underline{v} \cdot \underline{\alpha} - \underline{\alpha} \cdot \nabla \underline{v}^T \quad . \tag{19}$$

Many viscoelastic theories for liquids are written in terms of the rate of deformation tensor and its indifferent derivatives rather than deformation tensors. In contrast to deformation, which can be described by several indifferent tensors, the deformation rate is uniquely defined by (16) For instance, the Jaumann derivatives of the Cauchy and Finger strains both give the tensor in (16) when the reference time is taken to be the current time t. Constitutive equations for liquids can use uniquely defined tensors which is not true for solids.

The relation between the rate of deformation tensor and the deformation gradient tensor is:

$$\underline{\Delta} = \dot{\underline{F}}^T \cdot \underline{F} + \underline{F}^T \cdot \dot{\underline{F}} \quad . \tag{20}$$

where the reference time used to construct the rate of deformation tensor must be taken as the current time.

G. What Distinguishes Liquids From Solids?

The need for the time coordinate transformation underscores a fundamental difference between solids and liquids. The reason liquids can be effectively modelled without reference to a fixed reference time is because, unlike solids, the stress state of liquids depends prominently on the recent past, nominally on the distant past and negligibly on the very distant past. Otherwise stated, stress in liquids depends on its deformation rate history rather than the deformation history as is true for solids. This underscores the more basic difference which is the existence of a unique reference configuration for solids, and the absence of same for liquids.

Experimentally, we distinguish liquids from solids by observing the stress after a long time in the absence of deformation. Without changing shape, liquids cannot support a deforming stress indefinitely. For liquids at rest:

$$\lim_{t \to \infty} \underline{\sigma}(t) = \underline{0} \quad . \tag{21}$$

the deforming stresses vanish whereas for solids the extra stress depends on the strain relative to a unique reference configuration.

For example, a simple constitutive equation for a simple rubber is,

$$\underline{\sigma} = G\,\underline{J} \; , \tag{22}$$

where G is the shear modulus and where the Cauchy strain is relative to a fixed reference time taken when the material is unstressed. Comparing this with the well known constitutive equation for a Newtonian fluid:

$$\underline{\sigma} = \eta\,\underline{\Delta} \; , \tag{23}$$

where η is the familiar Newtonian viscosity, and the rate of deformation tensor is relative to the current time t. For both the simple rubber and the Newtonian fluid, the rheological properties are completely described by equations containing single constants, G and η respectively. The limit in (21) goes to the zero tensor for the Newtonian liquid. For the simple rubber, the same limit gives a stress tensor proportional to the Cauchy strain. This illustratos the fundamental difference between a liquid and a solid It also explains why those modelling liquid-like viscoelastic materials conventionally write their equations in terms of the deformation rate tensor and invariants of the extra stress tensor. In contrast, theories of solid viscoelasticity are normally written in terms of the indifferent deformation tensors.

Finally, viscoelastic theory describes materials that can be caused to behave in a manner intermediate to the Newtonian and simple rubber extremes. We call the constitutive equations for Newtonian liquids and simple rubbers unifying theories for two reasons. Firstly, because they accurately approximate a wide range of real materials. Secondly, these theories can be used to predict the stress response to any deformation. We shall see that, in this sense, no unifying theory has as yet been proposed for viscoelastic media. The linear viscoelastic theory does, however, approximate a broad range of real materials over a narrow range of deformations

H. Linear Viscoelastic Behavior

Linear viscoelasticity is the kind of behavior commonly exhibited by viscoelastic materials when strains or strain rates are small. The theory that explains the phenomenon of linear viscoelasticity is a powerful one. In this section, this important theory is reviewed.

For instance, in classical stress relaxation, where strain amplitude is small, the shear stress at time t is linear with strain amplitude, and for liquids, is proportional to the strain amplitude. The shear modulus, $G = \sigma/\gamma_0$, is independent of strain amplitude and for solids is:

$$G(t) = \sigma(t)/\gamma_0 + G_\infty , \tag{24}$$

27or, for liquids, it is:

$$G(t) = \sigma(t)/\gamma_o \tag{25}$$

Similarly, this kind of time dependency is found in oscillatory shear where

$$\gamma = \gamma_o \cos \omega t \tag{26}$$

and

$$\dot{\gamma} = \gamma_o \omega \sin \omega t$$

$$= \dot{\gamma}_o \sin \omega t \tag{27}$$

Here, where strain or strain rate amplitude is small, the shear stress is also harmonic and its amplitude is proportional to strain amplitude. Hence,

$$\sigma(t) = \sigma_o \cos [\omega t + \delta(\omega)] \tag{28}$$

where $\delta(\omega)$ and σ_o are independent of γ_o. An expression analogous to (25) gives the absolute magnitude of the complex modulus:

$$|G^*(\omega)| = \sigma_o(\omega)/\gamma_o \tag{29}$$

Consider the oscillatory shear test results for molten polypropylene at 250°C reported by Mutel and Kamal.[276] These data, replotted in Figures 7a and 7b, present a good example of linear viscoelastic behavior of a molten plastic which is observed with currently available rotational rheometers. Figure 7a shows the linear proportionality observed between the stress and the strain amplitudes in oscillatory shear, whereas Figure 7b shows that the phase angle is essentially independent of shear strain amplitude. These are the defining criteria for linear viscoelastic behavior in oscillatory shear. There are, of course, many other experimental manifestations of linear viscoelasticity.

I. Theory of Linear Viscoelasticity

We call linear viscoelasticity a phenomenon because it is known through observation. It is not a logical necessity that liquids behave this way at small strains The Boltzmann superposition principle was devised to unify this behavior into one simple but powerful theory.[277]

This principle states that when the stress or the strain histories of linear viscoelastic experiments are superposed, the resulting strain or stress response is the linear sum of, respectively, the stress or strain responses for the component tests. This principle can be written:

$$\sigma(t) = \sum_{n} G(t-t^{n}) \quad \Delta \gamma_n \tag{30}$$

When a strain or stress history can be represented as an infinite sum of superposed linear viscoelastic tests, applying the principle permits one to integrate over past time to obtain respectively the stress or strain response. For instance, for the shear stress:[278]

$$\sigma(t) = \int_0^\infty G(s)\,\dot{\gamma}(t-s)\,ds + G_\infty ,\tag{31}$$

which is simply a corollary of the Boltzmann superposition principle. For liquids, $G_\infty = 0$. The linear viscoelastic theory for a liquid is obtained when this corollary is written for the extra stress and rate of deformation tensors.

$$\underline{\sigma}(t) = \int_0^\infty G(s)\,\underline{\Delta}(t-s)\,ds .\tag{32}$$

Hence, linear viscoelastic theory hypothesizes that for any viscoelastic fluid, where the strain or strain rate is small, the stress tensor is the integral, over past time, of the relaxation modulus multiplied by the rate of deformation tensor. The strength of this theory is that it unifies the rheological properties of many fluids for low strains and strain rates. For example, in steady simple shear a constant viscosity is predicted to be the integral of the relaxation modulus over past time:

$$\eta_0 = \int_0^\infty G(s)\,ds \tag{33}$$

This viscosity is equal to the limiting low shear viscosity exhibited by many fluids in steady simple shear. The constant viscosity is also related to the material function, $G'(\omega)$, for oscillatory shear by:

$$\eta_0 = \frac{2}{\pi} \int_0^{\infty} \frac{G'(\omega)}{\omega^2} \, d\omega \, . \tag{34}$$

Relations for the material functions of linear viscoelasticity involve integrals over infinite intervals of time or frequency.

To carry out these integrations, the material functions of linear viscoelasticity are commonly rewritten in terms of the linear relaxation spectrum, $H(\theta)$. This spectrum is defined by:

$$G(t) = \int_{-\infty}^{\infty} H(\theta) \exp[-t/\theta] \, d(\ln \theta) \, , \tag{35}$$

where H and θ have units of stress and time. This provides one way of comparing the results of tests which used different strain histories. Alternately, any two linear viscoelastic properties can be written as explicit functions of one another. These relations can provide better bases for such comparisons since the approximations and extrapolations required to evaluate the integral in (35) introduce unnecessary uncertainty in data manipulations.

The linear viscoelastic theory requires that the function G(t) be determined empirically. Some empirical correlations have been proposed which allow one to infer G(t) from molecular structure. In the absence of such correlations, or the molecular weight distribution, the relaxation modulus must be measured for all experimentally important times.

J. Problems with Linear Viscoelastic Theory

The linear viscoelastic theory is not material indifferent because integrals of indifferent tensors are not indifferent. It seems paradoxical that our most useful theory of viscoelasticity, the one that unifies the most rheological properties, contradicts rational mechanics. This is a theoretical limitation.

The main practical limitation of linear viscoelastic theory is its restriction to small strains. Moreover, the theory provides no indication of the magnitude of strain at which deviations from linearity will occur. There are many practical implications of this weakness. Firstly, this strain limit varies from material to material. Secondly, this strain limit varies depending on test conditions. In oscillatory shear, at low frequency, the upper limit decreases with increasing frequency. Thirdly, the upper limit varies from one type of test to the next. For instance, one cannot deduce the limits of linear viscoelasticity for oscillatory shear from those observed in classical stress relaxation experiments. Finally, the limits of linear viscoelasticity depend on how one defines the limit. In practice, one can define such a limit in terms of a percentage deviation from linearity[279] with a statistical confidence level. The problem with this approach is that the value of the upper limit will depend on the precision of the instrument and the number of replicates taken to establish the limit.*

Oscillatory shear test results obtained using a sliding cylinder rheometer for bread dough at room temperature have been reported[280] and are replotted in Figures 8a through 8e. Figure 8a shows the effect of shear strain amplitude on shear stress amplitude Figure 8b shows that when the abscissa is expanded there is nonlinearity for bread dough at minute shear strains. Figures 7a and 8a show opposite extremes. The polypropylene melt of Figure 7a is shown to be linear for shear strains up to 9%. For the bread dough, nonlinearity well above experimental imprecision is observed even for the lowest of shear strains. One can still define the limits of $G^*(\omega)$ and $\delta(\omega)$ as $\gamma \to 0$ but these can only be measured by extrapolation to zero strain amplitude for the bread dough.

To refer to these limits as linear viscoelastic properties when no linearity is observed implies a fallacy. For materials like the bread dough these limits should properly be called simply the low strain limits of viscoelasticity.

---

*Conversely, the percentage deviation definition works well for evaluating limits to linear viscoelasticity predicted by nonlinear theories since such predictions contain no scatter.

Furthermore, fluids such as molten plastics with broad molecular weight distributions do not exhibit the predicted constant viscosity at the lowest shear rates attainable experimentally. It has been argued that this is due to experimental inadequacies and that all viscoelastic fluids will behave linearly, in this regard, if only a low enough shear rate test could be devised for them.[281] This hypothesis is not testable.

Linear viscoelastic theory predicts zero normal stress differences, ~~which is not the case~~ for many fluids. For instance, for a simple rubber the first normal stress difference is proportional to the square of shear strain:[282]

$$N_1 = G\,\gamma^2, \tag{36}$$

This effect is a second order one and the ratio of the first normal stress difference to the shear stress for a simple rubber equals the shear strain.

$$N_1/\sigma = \gamma \tag{37}$$

Similarly, for polymer solutions in small amplitude oscillatory shear the amplitude of the second harmonic of first normal stress difference is proportional to γ^2 for a fixed frequency.[283] Indeed for certain polyethylene melts, the first normal stress difference reportedly exceeds the shear stress by several times in stress growth and in steady shear.[284,285] Material indifferent nonlinear theories for viscoelastic fluids undergoing small amplitude oscillatory shear usually predict a significant first normal stress difference.[286,287]

Furthermore, for molten plastics such as polyethylene and polystyrene the birefringence, Δn_{13}, usually taken to be proportional to N_1+N_2,* is linearly related to the shear stress.[288] Hence, although linear viscoelasticity is a commonly observed phenomenon, the theory of linear viscoelasticity normally used to explain the phenomenon, can only approximate it.

It has also been argued that linear viscoelastic theory is only meant to apply to infinitesimal strains or strain rates.[289] This hypothesis is not testable since infinitesimal strains cannot be studied in anything but thought experiments. A variant of this hypothesis, is that the linear theory only unifies the limits of viscoelasticity at small strain.

$$\lim_{\underline{\underline{\gamma}}\to 0} \underline{\sigma}(t) = \int_0^\infty G(s)\ \underline{\Delta}(t-s)\, ds . \tag{38}$$

This reasonable hypothesis is used as a basis for most theories of nonlinear viscoelasticity but the strength of the theory is that it does

---

*This assumption, called the stress optical law, has its own exceptions. For instance, some Newtonian fluids exhibit 1,3 birefringence in simple shear where $N_1 = N_2 = 0$.

explain behavior in flows of finite, albeit low, strain amplitude for many fluids.

Still others argue that as strain approaches zero, viscoelastic behavior must approach linearity, but this assertion is difficult to test. Moreover, the theory of linear viscoelasticity, even in its weakest form of (38) is but a hypothesis after all, it is not a logical necessity.

K. What are Nonlinear Viscoelastic Properties?

Viscoelastic nonlinearity is defined by default, behavior not described by (32) is nonlinear. There are an infinite number of time dependent shearing patterns that can be defined. The strain patterns prescribed for linear properties can also define nonlinear viscoelastic properties. To define a viscoelastic property is, after all, simply to prescribe a shearing pattern and to define the variables to be used in presenting the results In sharp contrast to the case of linear viscoelastic properties, there is no unifying theory for nonlinear viscoelastic properties. The nonlinear viscoelastic properties of a fluid are those that the linear theory cannot unify. Consequently, a nonlinear viscoelastic property is not deducible from other viscoelastic properties. Each viscoelastic property taken outside the linear regime, provides a separate and distinct piece of rheological information about the fluid.

In Chapter 1 we saw that a constitutive equation can be written with either the extra stress tensor or the strain tensor as the dependent variable. So there are two kinds of properties that one can measure. The stress can be controlled and the resultant strain can be measured. Or the strain can be controlled and the resultant stress measured. On some rheometers equipped with computer controlled drive systems, both types of test can be performed. The present work includes strain controlled tests only.

L. Cyclic and Noncyclic Properties

Nonlinear viscoelastic properties can be cyclic or noncyclic. The most commonly studied viscoelastic property is the shear stress response to harmonic strain in simple shear. All the other properties that are commonly studied are noncyclic ones. Stress relaxation following steady shear is a noncyclic test. Extensional properties of liquids are always noncyclic since the free flowing liquid will buckle if the flow field is reversed. Conversely, harmonic oscillation in extension is the most commonly studied viscoelastic property of solids.[290] Cyclic properties can further be classified into steady and unsteady subclasses. Shear stress response to oscillatory shear started from the unstressed state is an unsteady cyclic property. If the stress response stabilizes, then the property is a steady cyclic one. "Steady cyclic" does not mean time steady, since the stress is changing during cyclic testing. Steady cyclic simply means that a standing wave with time steady phase shift is obtained.

Many noncyclic tests focus on material behavior in transitions from the equilibrium state to stressed states. Tests like stress growth, classical stress relaxation and exponential shearing are examples of such tests. Other noncyclic tests probe the melt behavior when it is far from the equilibrium state. Double step stress relaxation, strain rate reduction and interrupted shear tests are examples of such tests. Of course, since any shearing pattern can be reversed, one can define cyclic properties for all the traditional noncyclic tests. A triangular strain wave, for instance, is a reciprocating stress growth test.

M. Why Focus on Steady Oscillatory Shear?

We begin by confining the discussion of nonlinear theory to theories which can be used for large amplitude oscillatory shear. We do this for several reasons. Firstly, since there are an infinite number of separate and distinct properties that one can define, any discussion on nonlinear theory must confine itself to some finite set of properties. Secondly, the most common linear viscoelastic property measurement reported is oscillatory shear. Additionally, oscillatory shear is an intrinsically interesting flow since it combines flow reversal, large strain amplitudes and large strain rates into a single frequency test. Furthermore, this is the test most commonly used for development of finite strain rheometers. This is the case because, it will be seen, it is particularly handy for debugging hardware problems encountered during rheometer development and for evaluating the rheometer.

N. What is Simple Shear?

Before discussing oscillatory shear in greater detail, we consider the kinematics of simple shear. Simple shear is the flow and deformation induced when material is confined between parallel plates moving laterally with constant separation, h. This is illustrated in Figure 9.

The equation of motion in rectangular coordinates for simple shear gives:

$$\phi \frac{\delta v_1}{\delta t} = -\frac{\delta p}{\delta x_1} - \frac{\delta \sigma_{12}}{\delta x_2} + \phi g \sin \theta , \tag{39}$$

where ϕ is the fluid density, g is the acceleration due to gravity and θ is the angle between the plates and the horizontal. By inspection, we see that for horizontal plates, where there is no pressure drop in the x_1 direction, σ_{12} is everywhere constant at steady state

The equation of energy for simple shear gives:

$$\phi C_v \frac{\delta T}{\delta t} = -\frac{\delta q_2}{\delta x_2} + \sigma_{12} \dot{\gamma} . \tag{40}$$

Unlike the stress tensor which is uniquely defined, we have seen that there is more than one way to describe deformation. The Finger strain and Cauchy strain provide different ways of looking at simple shear.

To derive these tensors for a specific flow, we begin by constructing the deformation gradient tensor This is accomplished using (9) and by defining a scalar called shear strain, γ, which is simply the plate displacement per unit sample thickness relative to some reference time t_o * The result is:

$$\underline{F} = \begin{bmatrix} 1 & \gamma & 0 \\ 0 & 1 & 0 \\ 0 & 0 & 1 \end{bmatrix} \tag{41}$$

This is called a relative tensor since it is defined with respect to a reference time This tensor is not indifferent, but according to (9) and (10) the Cauchy strain and the Finger strain, which are indifferent strain tensors, are constructed from the deformation gradient tensor using (10), (13) and (14) Figure 9 shows that γ is also the tangent of the angle, β, formed between two position vectors in the 1,2 plane at time t and at time t_o.

For simple shear the Cauchy strain is.

$$\underline{J} = \begin{bmatrix} 0 & \gamma & 0 \\ \gamma & \gamma^2 & 0 \\ 0 & 0 & 0 \end{bmatrix} \tag{42}$$

*This is illustrated in Figure 9.

and the Finger strain is:

$$\underline{H} = \begin{bmatrix} \gamma^2 & -\gamma & 0 \\ -\gamma & 0 & 0 \\ 0 & 0 & 0 \end{bmatrix} . \tag{43}$$

These are important tensors for they describe completely the deformation which one hopes to generate in sliding plate rheometers

There is a positive diagonal component of the deformation, which reflects the fact that in simple shear the x_1 component of the vector between any two material points is changing. This is important because it can be used to explain the normal stress differences that are observed in simple shear. In fact, theories of viscoelasticity that use deformation tensors relative to a fixed reference time ascribe the first normal stress difference to this diagonal component. For instance, for a simple rubber $N_1 = G\gamma^2$ * Hence, when the reference time is taken as a fixed time we see that, for a rubber in simple shear, the cause of the first normal stress difference is the nonzero diagonal component of the deformation tensor.

Additionally, the nonzero diagonal components of the deformation tensors are the square of the 1,2 component. Note that $J_{12} = J_{21}$ and that $H_{12} = H_{21}$, so the strain is symmetric. In fact, these tensors are symmetric for any deformation.

---

*This is why the first normal stress difference is sometimes called an elastic property.

Consider the rate of deformation tensor, which is simply the time derivative of the Finger strain relative to the current time t:

$$\underline{\Delta} = \begin{bmatrix} 0 & \dot{\gamma} & 0 \\ \dot{\gamma} & 0 & 0 \\ 0 & 0 & 0 \end{bmatrix} . \tag{44}$$

There are no nonzero diagonal components of the rate of deformation tensor The Jaumann derivative of the rate of deformation tensor, which has nonzero diagonal components, is.*

$$\frac{\delta}{\delta t} \underline{\Delta} = \begin{bmatrix} -\dot{\gamma}^2 & 0 & 0 \\ 0 & \dot{\gamma}^2 & 0 \\ 0 & 0 & 0 \end{bmatrix} . \tag{45}$$

Hence, when the current time is chosen as the reference time we see that it is the diagonal components of the derivative of the rate of deformation tensor which cause the normal stress differences.

---

*For simple shear the vorticity tensor is:

$$W = \begin{bmatrix} 0 & \frac{1}{2}\dot{\gamma} & 0 \\ -\frac{1}{2}\dot{\gamma} & 0 & 0 \\ 0 & 0 & 0 \end{bmatrix} . \tag{46}$$

Finally, (15) implies that for simple shear the determinant of the Cauchy strain is identically zero for all times. Hence, simple shear is an isochoric flow meaning that constant volume is maintained. Hence, fluid compressibility will not affect rheological properties measured in simple shear.

<u>O. What is Oscillatory Shear?</u>

The shear strain, γ_{12} or simply γ, is defined relative to a fixed reference time. In strain controlled oscillatory shear, the reference time is conventionally taken at strain zero, which is true when $\omega t_o = 2\pi n$, where n is any integer. For a cosinusoidal strain,*

$$\gamma = \gamma_o \cos \omega t \ , \tag{47}$$

$$\begin{aligned} \gamma &= -\gamma_o \omega \sin \omega t \\ &= -\gamma_o \sin \omega t \ , \end{aligned} \tag{48}$$

$$\begin{aligned} \gamma^2 &= \gamma_o^2 \cos^2 \omega t \\ &= \tfrac{1}{2} \gamma_o^2 (1+\cos 2\omega t) \end{aligned}$$

and (49)

*The author chooses the cosinusoid for these examples for consistency with later discussion of the discrete Fourier transforms which is conventionally cosine based.

$$\gamma^2 = \gamma_o^2 \sin^2 \omega t$$
$$= \tfrac{1}{2} \gamma_o^2 (1-\cos 2\omega t). \qquad (50)$$

For a fixed reference time, the Cauchy strain for oscillatory shear is

$$\underline{J} = \begin{bmatrix} 0 & \gamma_o \cos \omega t & 0 \\ \gamma_o \cos \omega t & \tfrac{1}{2} \gamma_o^2 (1+\cos 2\omega t) & 0 \\ 0 & 0 & 0 \end{bmatrix} \qquad (51)$$

Examining this tensor we see that in oscillatory shear, when the moving plate oscillates with frequency ω, the 1,2 and 2,1 components of Cauchy strain are stimulated at exactly the frequency of the moving plate. On the other hand, the nonzero diagonal component of the Cauchy strain is stimulated with exactly twice the frequency of the oscillating plate. Furthermore, the amplitude of the diagonal stimulus is half the square of the amplitudes of the 1,2 and 2,1 component stimuli. Hence for $\gamma_o>2$, the diagonal stimulus is greater than the nondiagonal stimulus. The obvious implication of this, for the simple rubber, is that $N_1>\sigma_{12}$ when $\gamma_o>1$. This is important, because for small amplitude experiments one normally considers the first normal stress difference to be zero, as this is the case in the theory of linear viscoelasticity. However, for large amplitude oscillatory shear tests we see that the first normal stress difference can be high and it can even exceed the shear stress. This underscores one fundamental difference between small and large amplitude tests, for it is only in a large amplitude experiment that the diagonal components are stimulated significantly relative to the nondiagonal components.

The rate of deformation tensor relative to the current time t is.

$$\underset{\sim}{\Delta} = \begin{bmatrix} 0 & -\gamma_0 \sin \omega t & 0 \\ -\gamma_0 \sin \omega t & 0 & 0 \\ 0 & 0 & 0 \end{bmatrix} \tag{52}$$

which is simply the history of the rate of deformation Recall, that for a Newtonian fluid, the extra stress tensor depends on the rate of deformation tensor only Hence, since the diagonal components of the rate of deformation tensor are zero, Newtonian liquids in simple shear have zero normal stress differences

For oscillatory shear, the Finger strain is:

$$\underset{\sim}{H} = \begin{bmatrix} \frac{1}{2}\gamma_0^2(1+\cos 2\omega t) & -\gamma_0 \cos \omega t & 0 \\ -\gamma_0 \cos \omega t & 0 & 0 \\ 0 & 0 & 0 \end{bmatrix} \tag{53}$$

for a fixed reference time The Jaumann derivative of the rate of deformation tensor is:

$$\frac{\delta}{\delta t}\;\underline{\Delta} = \begin{bmatrix} -\tfrac{1}{2}\gamma_o^2\,(1-\cos 2\omega t) & 0 & 0 \\ 0 & \tfrac{1}{2}\gamma_o^2\,(1-\cos 2\omega t) & 0 \\ 0 & 0 & 0 \end{bmatrix} \tag{54}$$

P. Shape of Standing Stress Wave

Since there is no unifying theory of viscoelasticity, there are few logical necessities that apply to the stress response of a prescribed deformation. From experience with problems of forced vibrations, of which oscillatory shear is a special case, we can obtain rules for physical plausibility by induction for the stress response of a polymeric liquid to oscillatory shear

When a mechanical system is subjected to a forced oscillatory vibration, we generally observe that the force response becomes a standing wave. Furthermore, when an electrical system is subjected to an oscillating current, the voltage response normally becomes a standing wave. Finally, when polymeric liquids are subjected to oscillatory shear they normally respond with standing stress waves. Our reason for expecting standing waves for the stress response in oscillatory shear is inductive. Liquids that do not generate standing waves in oscillatory shear are called thixotropic.[291]

When a standing wave is obtained, the stress response can be written as a sum of harmonically related cosinusoids:*

$$\sigma(\omega t) = \sum_{n=0}^{\infty} \{\sigma_n \cos(n\omega t+\delta_n) + \sigma_{1/n}\cos(\omega t/n+\delta_{1/n})\}, \ n=0,1,2,\ldots \quad (55)$$

The $n\omega$ terms are called the principal harmonics whereas the 1/n terms are called the subharmonics. Furthermore, when n is even or odd these terms are qualified as even or odd.

In electrical systems subharmonics are commonly observed. In mechanical systems, however, subharmonics are rare. For instance, where little damping exists, mechanical systems can exhibit subharmonic responses to sinusoidal forcing functions.[292] Furthermore, subharmonics are never reported for liquids. Hence, we can further induce that only the principal harmonics are physically plausible and (55) simplifies to

$$\sigma(\omega t) = \sum_{n=0}^{\infty} \sigma_n \cos(n\omega t+\delta_n) \ , \ n=0,1,2,3,\ldots \quad (56)$$

Finally, from experience with polymeric liquids one can argue inductively that a standing shear stress wave can be composed of odd harmonics only.

---

*The use of cosines instead of sines runs against the rheological literature and its established conventions. However, it is consistent with conventions established for the discrete Fourier transform which is used extensively in the later chapters.

This implies that the standing wave will fold back on itself when shifted by π radians and folded along the abscissa.

The stress response can be plotted on a loop against either the shear strain or the shear rate. When the stress is composed of odd harmonics only, we observe that the stress-positive half of such loops coincides with the stress-negative part when the loop is folded successively about the abscissa and the ordinate This property is:*

$$\sigma(\omega t) = -\sigma(\omega t \pm n\pi) \quad , \; n=1,3,5, \tag{57}$$

By inductive reasoning we conclude that for polymeric liquids the standing shear stress wave will be represented by**

$$\sigma_{12}(\omega t) = \sum_{n=0}^{\infty} (\sigma_{12})_n \cos[n\omega t+(\delta_{12})_n] \quad , \; n=1,3,5,\ldots \tag{58}$$

Note that (57) and (58) imply each other

The property of twofold symmetry for the loop can also be represented as follows:[293]

$$\sigma(\gamma) = -\sigma(-\gamma), \tag{59}$$

---

*Sometimes called skew symmetry or alternance.

**One reasons inductively when one infers a general rule from a set of observations.

which states formally that stress is an odd function of strain.[294] Similarly:

$$\sigma(\gamma) = -\sigma(-\gamma), \tag{60}$$

and so, the stress is an odd function of shear rate.

Consider, for example, the special case of small amplitude oscillatory shear Eliminating ωt from $\sigma = \sigma_0 \cos(\omega t)$ and $\gamma = \gamma_0 \sin(\omega t+\delta)$ gives $\sigma(\gamma)$ implicitly as.[295]

$$(\sigma/\sigma_0)^2 + (\gamma/\gamma_0)^2 = \sin^2\delta + 2\,(\sigma/\sigma_0)\,(\gamma/\gamma_0)\cos\delta. \tag{61}$$

By inspection, the shear stress is seen to be an odd function of shear strain For large amplitude oscillatory shear, where higher odd harmonics of stress arise an analytical solution for $\sigma(\gamma)$ cannot be obtained. The twofold symmetry of such loops can be shown numerically.

Relations (57)-(60), which give the physically plausible shape for the shear stress wave, were obtained by induction. The reader should remember that the general rules that we hold to be valid for the shapes of stress waves in polymeric liquids are induced from past experience, which has mostly been limited to small amplitude oscillatory shear tests. One must take care not to discard results in the regions of nonlinear viscoelasticity because they do not obey rules induced from experience with small strain tests. It is conceivable that by applying large amplitude deformations, polymeric liquids can violate the above general rules governing the shape of the stress wave.

Furthermore, the reason that polymeric liquids respond with twofold symmetric shear stress waves to oscillatory shear is that most liquids at rest have no preferred orientation.[296] The property of preferred orientation at equilibrium is called material anisotropy,* relations (57)-(60) pertain to isotropic materials only In contrast, a liquid filled with oriented fibers will retain a preferred orientation so long as the fibers stay oriented. Similarly, solids such as wood can respond to oscillatory shear with even harmonics since their microstructure is oriented to begin with. Also, some solid polymers in oscillatory uniaxial extension exhibit even harmonics of tensile stress.[297,298] Moreover, liquids which exhibit a yield stress in suddenly imposed steady shear, are seen to produce even harmonics of shear stress in large amplitude oscillatory shear.[299,300,301]

Although most viscoelastic theories for polymeric liquids in oscillatory shear cannot explain even harmonics of shear stress,[302,303,304,305,306,307,308] some theories do predict them.[309] However, since most viscoelastic materials studied in oscillatory shear do not exhibit even harmonics of shear stress,[310,311,312,313,314,315,316,317,318] many attribute such observations

*Not to be confused with reversible anisotropy which can be induced by flow and which spontaneously fades when the fluid is ~~at~~ rest.

to experimental error.[319,320,321] In particular, studies of the parallel superposition of steady shear with oscillatory shear imply that a slight drift in imposed shear strain can cause significant even harmonics in shear stress.[322,323] Hence, although it is not impossible for a liquid to respond with even shear stress harmonics, it is unlikely for neat melts. The absence of even harmonics is not, a logical necessity as is sometimes suggested.[324,325,326]

Similarly, the physically plausible shape of the first normal stress difference in oscillatory shear is given by:[327,328]

$$N_1(\omega t) = \sum_{n=0}^{\infty} (N_1)_n \cos[n\omega t+(\delta_1)_n] \ , \ n=0,2,4,\ldots \ , \qquad (62)$$

but this induction is based on few observations, since dynamic measurement of the first normal stress difference is difficult.[329,330,331,332,333,334] Finally, one could postulate a similar shape for the second normal stress difference, but it has never been measured in oscillatory shear. Christiansen and Miller have suggested that their specially designed cone-plate rheometer could be used for this purpose.[335,336]

O. Thermodynamics of Oscillatory Shear

In upcoming discussions on fluid inertia we shall see that, from a thermodynamic perspective, there are two fundamental causes for deforming stress. For a deforming stress to exist, energy must either have been stored relative to a reference state or energy must be being dissipated.*

The dissipation of energy is generally accomplished by an increase in temperature. We shall see that in a well designed rheometer the increase in temperature occurs in the surroundings and only minimally in the deforming sample.

The storage of energy, on the other hand, is accomplished by any of several reversible changes on the molecular scale. In crystalline solids, for instance, slight changes in the proximities of atoms in a lattice explain the large stresses associated with small deformations. Larger deformations result in irreversible dislocations in the crystal structure[337] For solid plastics, large deformations result in irreversible changes in molecular structure and even localized deformations such as shear banding and fracture. In polymeric liquids, the storage of energy can occur by orienting molecular chains which in turn results in a decrease in entropy and therefore temperature. In contrast, for rubbers, the highly ordered crosslinked network increases its entropy upon deformation which causes its temperature to increase.[338,339] But in viscoelastic liquids there is a mixture of mechanisms causing the stress. Furthermore, there is no experimental way of identifying the specific molecular origins of stress in polymeric liquids.

---

*In fact, the units of stress are generally given in terms of force per unit area, momentum per unit area per unit time, or energy per unit volume in the fields of rheology, transport phenomena and thermodynamics respectively. These dimensions are interchangeable.

There is no way of separating, at any instant, the part of the stress due to viscous dissipation and from that due to stored energy. However, when a standing wave is obtained, cyclic tests do allow one to distinguish lost work from stored energy over one full cycle.

Work is done when force causes mass to be displaced, and in simple shear, it is the force due to the 2,1 component of stress causes fluid displacement in the x_1 direction[340,*] Hence, the work done on the fluid between times t_1 and t_2 is.

$$W = \int_{\gamma(t_1)}^{\gamma(t_2)} \sigma \, d\gamma \quad (63)$$

For instance, for the simple rubber, choosing the reference time, $t_1 = 0$ when $\gamma = 0$ gives:

$$W = \tfrac{1}{2} G\gamma^2 \quad (64)$$

For a simple rubber in oscillatory shear:

$$W = G\,(\gamma_o^2 \cos^2 \omega t) \quad (65)$$

---

*Note that the 1,2 contributes no work since there is no fluid displacement in the x_2 direction. The uninitiated may expect a contribution to work from the σ_{11} term, however, to get work from N_1 or N_2, one must have compression or extension in the x_1, x_2 or x_3 directions. Remember, there is a σ_{11} term even in the Newtonian case, but no work due to it.

which gives the cyclic integral of zero when evaluated at $\omega t = 2\pi$. All the work done on the solid is returned to the surroundings in each cycle.

The other interesting extreme is the Newtonian fluid whose shear stress lags the shear strain by $\pi/2$.* Thus the work done with respect to the reference time, taken as zero when $\gamma = 0$, is:

$$W = \int_{0}^{\gamma} \sigma_{12}\, d\gamma = \int_{0}^{\omega t} \sigma_o \cos(\omega t + \tfrac{1}{2}\pi)\ \gamma_o \cos(\omega t)\ d(\omega t) \tag{66}$$

and the cyclic integral, obtained by evaluating (66) at $\omega t = 2\pi$, gives.

$$W_c = \pi\ \gamma_o\ \sigma_o\ , \tag{67}$$

where W_c is the work done on the fluid evaluated over one full cycle.

For the stress response of a viscoelastic fluid, where a standing wave is obtained with shape given by (57)-(60), the integral in (63) evaluated over one full cycle becomes:

$$W_c = \pi\ \gamma_o\ \sigma_1\ \sin(\delta_1)\ . \tag{68}$$

---

*The stress lags the imposed strain when $\delta > 0$. A negative phase lag is called a phase lead.

Only the amplitude and the phase angle of the first harmonic contribute lost work.

R. Plausible Phase Angles

The second law of thermodynamics requires that the total work done on the fluid be positive. Hence, over one full cycle work must be lost by the fluid to the surroundings. Thus,

$$(\sigma)_1 \sin(\delta_1) \geq 0 \tag{69}$$

is the second law of thermodynamics for a fluid with a time steady temperature profile in oscillatory shear,* it implies:**

$$0 \leq \delta \leq \pi \tag{70}$$

---

*For the simple rubber, $\delta=0$ and $W_c=0$. For the Newtonian fluid, $\delta=\frac{1}{2}\pi$ and $W_c=\pi\sigma_0\gamma_0$.

**This restriction implies that shear stress rotates in a clockwise direction when it is plotted on a loop against shear strain. It rotates in a counterclockwise direction when plotted against shear rate. Obviously, if $\delta=\pi$ then a negative shear modulus is obtained which is physically meaningless. Hence, this restriction is necessary but not sufficient.

For the special case of a linear viscoelastic fluid, where the stress is composed of only one harmonic, (70) is written:

$$\sigma_o \sin \delta \geq 0 \tag{71}$$

For the linear viscoelastic fluid, the average power of the viscous dissipation by integrating $\sigma \cdot \gamma$ over one full cycle

$$P_{mean} = \tfrac{1}{2}\pi\omega\, \sigma_i \gamma_o \sin \delta_i \tag{72}$$

Further, for the ith harmonic, the stored energy is.

$$W_s = \int_0^{\omega t} \sigma_i \, d(\gamma/\omega) = -\sigma_i \gamma_o \int_0^{\omega t} \cos(\omega t + \delta_i) \cos \omega t \, d(\omega t)$$

$$= -\tfrac{1}{4}\, \sigma_i \gamma_o \left[-2\,\omega t \cos \delta_i - \sin \delta_i + \sin(2\omega t + \delta_i)\right] . \tag{73}$$

Evaluating this at $\omega t = 2\pi$ gives the work stored and recovered in one full cycle:

$$W_s = \pi\, \sigma_i \gamma_o \cos \delta_i \tag{74}$$

and the average power of this elastic storage is

$$P_{smean} = \tfrac{1}{2}\pi\omega\, \sigma_i \gamma_o \cos \delta_i . \tag{75}$$

Since the work stored must be positive, a second restriction on δ_1 is obtained:*

$$-\tfrac{1}{2}\pi \le \delta \le \tfrac{1}{2}\pi \tag{76}$$

Now combining (70) and (76) shows that the phase angle for the first harmonic must lie in the first quadrant:

$$0 \le \delta \le \tfrac{1}{2}\pi \tag{77}$$

This is the thermodynamic requirement for the first harmonic. For the linear viscoelastic case, it is consistent with what we expect intuitively, that δ should lie between its Newtonian and simple rubber extremes.

S. Nonlinear Behavior in Oscillatory Shear

For oscillatory shear, linear viscoelastic behavior implies that: (1) the shear stress amplitude be linear with, and proportional to, the shear strain amplitude and (2) the loss angle is dependent on frequency only. There are many ways that materials can deviate from linear behavior.

1 The shear stress wave can contain higher harmonics.

---

*Obviously, for $-\tfrac{1}{2}\pi$ δ 0, the average power of the stored energy would be negative, which implies that the fluid is an active system, or that the fluid has an external source of power.

2. The phase angles of each harmonic can depend on strain amplitude

3 The amplitudes of each harmonic can depend on strain amplitude.

As was explained in the introduction, one commonly observes higher harmonics in large amplitude oscillatory shear experiments.* However, all combinations of these three cases are possible and have been observed experimentally Consider the following combinations which have been reported

Using a concentric cylinder rheometer, Vinogradov et al document strain amplitude dependence of both phase angle and stress amplitude without higher harmonics for a polyisobutylene melt in large amplitude oscillatory shear [341]

Consider the behavior of a molten linear low-density polyethylene subjected to oscillatory shear in a cone-plate rheometer. Figures 10 and 11 show that phase angle depends on strain amplitude when the stress and strain amplitudes remain proportional for shear strains less than .8.** Similar results were obtained by Hoffman for a polypropylene melt for shear strains below unity [342] These data are plotted in Figures 12a and 12b. Recall that for the bread dough, shown in Figure 8a and 8c, the phase angle

---

*See Section I. B.

**These data kindly supplied by Mr. Tony Samurkas, Dept. Chemical Engineering, McGill University.

increased with shear strain where the shear stress was nonlinear with shear strain.

III. THEORETICAL ASPECTS OF SLIDING PLATE RHEOMETRY

A. Basic Concepts

1. Determinism

When a rheologist sets out to measure material properties, he normally presumes that he is measuring a deterministic quantity. He expects that all distribution in the measured values is due to experimental scatter. The cause of the variability is assumed to be either differences between samples or variations in the way the test is performed. In contrast, the materials scientist interprets distribution in measured values not only as experimental scatter but also as an integral part of the material behavior. For example, Kausch attributes the variance in strength of solid plastics to cumulative uncertainty brought on by the large number of molecular processes activated by applied stress.[343,344] Although this manner of thinking is ordinarily only associated with solids, we note a strong similarity between the behavior of solids and liquids in simple shear. For instance, melts tend to fracture or slip when caused to deform in highly nonlinear viscoelastic regimes in sliding plate rheometers.[345,346] This is similar to the fracture and shear banding* observed for solid plastics in simple shear.[347,348,349] Hence, an increase in variability can be expected for viscoelastic properties measured near the point of melt fracture.

---

*For solids in simple shear, sometimes the shearing deformations localizes in a narrow band instead of being uniformly distributed through the sample. This is the shear analogy to the more widely known tensile necking instability.

Furthermore, in cyclic tests one expects increased variability between cycles as the point of melt fracture is approached. Hence, viscoelastic properties might be better described by distributions instead of single values as the point of melt fracture is approached.

2. Local Equilibrium

In an earlier section we used the principle of local equilibrium to show that the extra stress tensor is symmetric. However, there are three limitations on this conclusion. Firstly, we noted that it applied strictly to differential elements. For finite material elements, the stresses cause moments which can, in principle, cause the complimentary shear stresses on the finite element to be unequal Secondly, since finite material elements have mass, their angular acceleration can contribute to the torque balance. Thirdly, the separate and distinct restriction for the principle of local equilibrium was that neither body couples, nor stress couples exist on the faces of the material element. In fact, several theories of viscoelasticity have been advanced which include the possibility of an asymmetric stress tensor.[350,351,352,353] The mathematics associated with such theories are formidable as both an extra stress tensor and a stress-couple tensor are required to describe the stress state.* Such theories have however been useful in explaining the viscoelastic behavior of materials containing preferred orientation such as liquid crystalline polymers.[354] The symmetry of the extra stress tensor has never been

*Evidently, no simplifications can be made from symmetry considerations.

verified experimentally.[355] Furthermore, in principle, the action of a stress-couple on the end of the cantilever beam in a shear stress transducer would cause an error in shear stress measurement.[356] For soils in simple shear, stress-couples commonly arise. The error caused in the shear stress measurement is called load eccentricity and special transducers have been designed to measure it.[357] Perhaps a transducer for fluids could be designed, on this basis, to measure shear stress and stress-couple simultaneously.

3. Incompressibility and Thermal Expansivity

Strictly speaking, molten plastics are not incompressible. However, for the purposes of the rheologist they can usually be assumed to be nearly so. In particular, for the case of simple shear we note that the surface area of a fluid element in the 1,2 plane is constant with shear strain. Hence, even for a compressible material we expect the sample volume to be constant in simple shear, if the material can be made to deform in simple shear. Therefore, simple shear is a flow of constant volume or an isochoric flow.

Be this as it may, isochoric processes are not necessarily isothermal. Furthermore, polymeric liquids can expand with temperature. In principle, viscous heat dissipation or a change in entropy will affect sample temperature and cause a deviation from simple shear due to thermal expansion.

For a polymeric liquid we expect system entropy to change in shear due to the contending effects of molecular orientation and network deformation. Further, an increase in temperature due to viscous dissipation can cause thermal expansion.

Bruker and Lodge measured the change in volume due to simple shear of a molten plastic using a specially designed cone-plate rheometer called a rheodilatometer.[358] They found that no change in sample volume could be detected for a low-density polyethylene melt.

B. Laminar Deviations from Simple Shear

Causes of deviations in fluid velocity from the desired simple shear distribution are causes for concern for the designer of sliding plate rheometers. The present section is aimed at meeting the needs of the designer with a selection of handy solutions for deviations in fluid velocity These are useful to the designer because, for instance, they tell him how thin a sample thickness should be used to minimize each type of error Complete certainty in determining the required sample thickness is only possible when the fluid rheology is known, which is a rare luxury.

The designer of sliding plate rheometers would like an expression for deviation in fluid velocity for each cause. Furthermore, the designer would like solutions for such deviations for the most important causes. Despite a rich literature on deviations from simple shear, the writer is not aware of solutions for any such combinations.

1. Viscous Heating

In addition to the small deviation from simple shear due to fluid thermal expansivity, the deviation caused by the temperature gradient can also be important. This is because the rheological properties are themselves temperature dependent, so by a process called thermal feedback temperature gradients can significantly affect fluid velocity. For rheometer design, the temperature rise is important not just because rheological properties depend on temperature, but also because temperature rise can affect fluid velocity. When the fluid is not viscoelastic and an analytical form for its temperature sensitivity is known, analytical solutions for the velocity are obtained. These allow determination of maximum usable shear rates on a sliding plate rheometer in specific sorts of test. Analytical solutions for steady simple shear, for oscillatory shear, and for the unsteady states following their respective sudden impositions, are reviewed below. These unsteady state solutions are particulary helpful when used to design short tests to capture transient properties which incorporate high shear rates before error due to viscous heating becomes important. Conspicuous by its absence in the literature is the solution for the effect of viscous heating on the velocity of viscoelastic fluids in steady simple shear tests.

Witness that, with only two exceptions, the boundary condition used for the following error analyses of viscous heating is either (1) adiabatic, $dT/dx_2 \rightarrow 0$, or (2) isothermal. Also, solutions derived for two isothermal boundaries can easily be adapted* for the combination of an adiabatic with an isothermal boundary since from symmetry the adiabatic condition, $dT/dx_2 = 0$, exists at the centerline for simple shear.[359] But Powell and Middleman have pointed out that real boundaries absorb heat from the sample and that the thermal response of the walls can significantly affect sample temperature.

a. Steady Simple Shear

Theories for the effect of viscous heating on fluid velocity in steady simple shear tests have been widely published for temperature sensitive fluids, both Newtonian,[360,361,362,363,364,365,366,367,368,369,370,371] and non-Newtonian.[372,373,374,375] In the absence of an analytical expression for viscosity-temperature dependence, a graphical method can be used to determine temperature rise, shear stress and fluid velocity in steady simple shear tests for Newtonian fluids.[376]

Consider the temperature dependent power-law fluid, described by:

$$\sigma = \mu_o \exp(-\alpha T) \dot{\gamma}^n . \tag{78}$$

The energy equation, solved for isothermal walls of equal temperature, gives the steady state temperature distribution:[377,378]

---

*By replacing h with ½h in equal isothermal wall solutions, the combined adiabatic and isothermal boundary solution is obtained.

$$\exp \frac{\alpha \Delta T}{n} = \frac{\alpha C_1^2 k}{2n\sigma} \left[\frac{\mu_o}{\sigma}\right]^{1/n} \operatorname{sech}^2 \left[\frac{\alpha C_1}{2n} (x_2 - \tfrac{1}{2}h)\right] , \tag{79}$$

where C_1 is defined implicitly in:

$$1 = \frac{\alpha C_1^2 k}{2n\sigma} \left[\frac{\mu_o}{\sigma}\right]^{1/n} \operatorname{sech}^2 \left[\frac{\alpha C_1}{4n}\right] , \tag{80}$$

ΔT is the difference between fluid and wall temperatures, k is fluid thermal conductivity, x_2 is distance from the centerline, and h is the plate separation. Recall that the shear stress, σ, is constant for steady simple shear.

Hence, the maximum temperature difference in the fluid is:

$$\Delta T_{max} = \frac{n}{\alpha} \ln \left[\frac{\alpha C_1^2 k}{2n\sigma} \left[\frac{\mu_o}{\sigma}\right]^{1/n} \right] , \tag{81}$$

Consequently, the fluid velocity deviates from the desired $u = Ux_2/h$ where

U is the plate velocity. The thermally altered velocity field is.

$$u = \tfrac{1}{2}U + \left[C_1 k/\sigma\right] \tanh \left[\frac{\alpha C_1}{2n} (x_2 - \tfrac{1}{2}h)\right] \tag{82}$$

Hence, the shear rate is.

$$\gamma = \frac{\alpha k C_1}{2n\sigma} \operatorname{sech}^2\left[\frac{\alpha C_1}{2n} (x_2 - \tfrac{1}{2}h)\right] \tag{83}$$

and the fractional deviation in shear rate from simple shear, $\epsilon_v = h\gamma/U - 1$, is:

$$\epsilon_v = \frac{\alpha k C_1 h}{2n\sigma U} \operatorname{sech}^2\left[\frac{\alpha C_1}{2n} (x_2 - \tfrac{1}{2}h)\right] - 1 \tag{84}$$

and thermal runaway* is predicted when:**

$$h \geq 4.7988n/\alpha C_1 \tag{85}$$

or, for the special case of the Newtonian fluid,[379] when:

$$h \geq 4.7988/\alpha C_1 \tag{86}$$

---

*The condition of an unbounded temperature increase.

**This constraint is more commonly stated as a maximum value of shear stress. Since the shear stress is a dependent variable, the design constraint placed on the gap is handier for design purposes.

and (80) simplifies to:

$$1 = \frac{\alpha C_1^2 k \mu_o}{2\sigma^2} \operatorname{sech}^2 \tfrac{1}{2}\alpha C_1 \qquad (87)$$

For Newtonian and power-law fluids, C_1 is double valued. This shows that there are two values of apparent shear rate which can cause the same shear stress.

Solutions for many other analytical forms of temperature dependence for Newtonian[380,381,382,383] and non-Newtonian[384,385,386] fluids in steady simple shear have been reported including a further refinement for temperature sensitive thermal conductivity.[387] For all these predictions for fluid velocity, the double valued shear rate is predicted. Furthermore, using a concentric cylinder rheometer, Sukanek and Lawrence confirmed this double valued shear rate experimentally for a polychlorinated biphenyl, a temperature sensitive Newtonian fluid.[388]

<u>b. After Imposition of Steady Simple Shear</u>

The energy equation has been solved for the thermal development of a temperature-sensitive Newtonian fluid described by:

$$\sigma = \mu_o \exp(-\alpha T). \tag{88}$$

after start-up of steady simple shear with both boundaries isothermal.[389] The key result, obtained using an analog computer, is that the temperature rises without bound when:

$$h > 3.52\ k\mu_o/\alpha\sigma^2. \tag{89}$$

This approximate formula is easier to use than the simultaneous equations, (80) and (85), obtained for thermal runaway in the analytical steady state solution. Furthermore, for subcritical values of h the steady state temperature deviates from its initial isothermal condition by roughly 5% when:

$$t \approx .0075\ C_p h^2/k\ . \tag{90}$$

Additionally, for supercritical values of h the temperature rises without bound, and specifically, when.

$$h > \left[\frac{40\ k\ \mu_o}{\alpha\ \sigma^2}\right]^{1/2}, \tag{91}$$

the mathematically trivial case for both boundaries adiabatic is recovered:*

*An approximate formula for the elapsed time when the condition of two adiabatic boundaries is approached is also given in this section.

$$\Delta T = T - T_o = \frac{\mu_o \exp(-\alpha T)\ t\ \dot{\gamma}^2}{C_p}, \tag{92}$$

describing a sample of uniform temperature T rising linearly with time.*
Here, the thermal response of the boundary is simply modelled by diffusion about a plane source.[390,391] The temperature rise at the walls is.[392]

$$T - T_o = \frac{h}{2a\sqrt{\pi}} \int_o^t \sigma(\theta)\gamma(\theta)\ (t-\theta)^{-\frac{1}{2}} \exp\left[\frac{-x^2}{4\ a^2(t-\theta)}\right] d\theta \tag{93}$$

For the temperature sensitive fluid, $\sigma\gamma = \mu_o\gamma^2 \exp(-\alpha T)$, so (93) must be evaluated numerically For the temperature insensitive fluid the solution is

$$T - T_o = \frac{h\mu\gamma^2}{2a\sqrt{\pi}} \int_o^t (t-\theta)^{-\frac{1}{2}} \exp\left[\frac{-x^2}{4\ a^2(t-\theta)}\right] d\theta\ . \tag{94}$$

where $\frac{1}{2}h\mu\gamma^2$ is the constant heat flux at each wall The exact solution for the rise in plate surface temperature is.[393]

---

*Thus, for the temperature insensitive Newtonian fluid, $\alpha = 0$, and,

$$\Delta T = \mu\gamma^2 t/C_p$$

$$T_s - T_o = .565 \frac{h\mu\gamma^2 \sqrt{(at)}}{k}, \tag{95}$$

a helpful relation for experimental design. Recall that this expression applies strictly to temperature-insensitive Newtonian fluids. Conditions (89) and (90) are satisfied for all temperature-insensitive Newtonian fluids.

Instead of using isothermal or adiabatic boundaries, the importance of the thermal response of the metal walls was also assessed for the unsteady state after start-up of steady shear for temperature-insensitive Newtonian fluids [394] Taking one boundary as isothermal and assuming that the steady state velocity profile, $u = Ux_2/h$, is achieved immediately in comparison with the time required for thermal equilibrium, a complete solution, albeit complicated, is obtained. However, for the special case when both $(k_b/k_f)/\sqrt{(\alpha_b/\alpha_f)}$ and $(hk_b)/Ck_f > 1$

$$t_{.05} = \frac{h\,k_w}{20\,C\,k_f} \tag{96}$$

and

$$t_{.95} = \frac{3\,h\,k_w}{C\,k_f}, \tag{97}$$

where t_x represent times for a rise in dimensionless wall temperature, such that:

$$x = \frac{T_w - T_o}{T_{wa} - T_o} . \tag{98}$$

T_w refers to the absorbing boundary, T_{wa} is the steady state of this same boundary when adiabatic, C is the plate thickness, and k_b and k_f are the boundary and fluid thermal conductivities respectively. Since both $(k_b/k_f)/\sqrt{(\alpha_b/\alpha_f)}$ and $(hk_b)/Ck_f > 1$ are satisfied for rheometers for molten plastics, both are useful for rheometer desfgn.[395]

Note that (96) and (97) account for the thermal response of only one boundary, assuming the other to be isothermal, whereas (95) accounts for the thermal response of both boundaries Powell and Middleman provide a formula for the time elapsed, θ_{95}, when the centerline temperature reaches 95% of the value, given by (95), for two adiabatic boundaries[396] Hence, this formula is the necessary condition for (95)

$$\theta = 2.9 \frac{(\rho C_p)_b C}{(\rho C_p)_f h} \tag{99}$$

Still more refined design calculations can be made for non-Newtonian fluids of arbitrary temperature sensitivity and incorporating the thermal response of the walls using numerical methods.[397,398]

<u>c. Steady Oscillatory Shear</u>

The effect of viscous heating on temperature sensitive viscoelastic fluids in steady oscillatory shear,[399] and in the unsteady state after start-up of oscillatory shear, have been examined for selected boundary conditions.[400,401,402,403,404,405] However, no account has been made for the thermal response of the boundary

The energy equation can also be solved for the case of the linear viscoelastic fluid where the time average rate of dissipation, obtained using (72), is[406]

$$D = \tfrac{1}{2}\omega\sigma_o\gamma_o \sin\delta \tag{100}$$

Combining the energy equation with Fourier's law gives

$$\rho C_p \frac{dT}{dt} = k\frac{d^2T}{dy^2} + \sigma\dot{\gamma} \tag{101}$$

For $t >> 2\pi/\omega$, $\sigma\dot{\gamma} \approx D$. For a sinusoidal strain:

$$\rho C_p \frac{dT}{dt} = k\frac{d^2T}{dy^2} + \tfrac{1}{2}\omega\sigma_o\gamma_o \sin\delta \tag{102}$$

For a nonlinear viscoelastic response σ_o is the amplitude of the first harmonic of the stress and δ is its phase lag. Hence, the rheometer design relations apply equally to nonlinear or linear viscoelastic regimes. For simplicity, consider the case of one boundary adiabatic with temperature T_a and one isothermal with temperature T_o. Assuming the following temperature dependencies for viscoelastic properties:[407]

$$G'(\omega,\gamma_o,\theta) = \frac{\omega^{n} \exp(-a\theta)}{(1+\beta^2)\, k_1}, \tag{103}$$

and

$$G''(\omega,\gamma_o,\theta) = \frac{\beta^2 \omega^{n} \exp(-a\theta)}{(1+\beta^2)\, k_2} \tag{104}$$

where $\beta = \tan\delta$, $\theta = (T-T_a)/(T_o-T_a)$ and $\theta_1 = (T_1-T_a)/(T_o-T_a)$ is the dimensionless temperature rise at the adiabatic boundary. Also,

$$G'(\omega,\gamma_o) = (\sigma_o/\gamma_o)\cos\delta \tag{105}$$

and

$$G''(\omega,\gamma_o) = (\sigma_o/\gamma_o)\sin\delta, \tag{106}$$

where σ_o is the fundamental of the stress wave and δ is its phase lag for anharmonic responses.

Introducing the dimensionless quantities $\epsilon = x/h$, $\Phi = a\theta$, $\eta = kt/C_p h^2$ and $g = \frac{1}{2}\sigma_o^2\omega^{1-n}h^2ak_2/k$ obtains.

$$d^2\Phi/d\epsilon^2 = (d\Phi/d\eta) - g \exp(\Phi) \ , \tag{107}$$

where g is a dimensionless steady shear stress amplitude. Steady and unsteady solutions for the adiabatic boundary ($d^2\Phi/d\epsilon^2 = 0$) can be derived. The steady state solution, implicit in Φ_1, is:

$$\exp\left[\frac{(\Phi_1 - \Phi)}{2}\right] = \cosh\left[\left[\tfrac{1}{2} g \exp(\Phi_1)\right]^{\frac{1}{2}} (1-\eta)\right] \ , \tag{108}$$

in which one boundary is adiabatic ($d\Phi/d\eta = 0$ at $\eta = 1$) and the other is isothermal ($\Phi = 0$ at $\eta = 0$) The unsteady solution with the adiabatic wall is

$$g = 2 \exp(-\Phi_1) \{\ln [\exp(\tfrac{1}{2}\Phi_1) + \exp \sqrt{(\Phi_1 - 1)}]\}^2 \ . \tag{109}$$

Defining a dimensionless shear strain amplitude, $\Gamma = \frac{1}{2} \gamma_o{}^2 \omega^{1+n} h^2 a k_2/k$, and solving for steady state with mixed adiabatic and isothermal boundaries gives the reduced adiabatic wall temperature rise:

$$\Phi_1 = \ln (\Gamma + 1), \tag{110}$$

a handy estimate of temperature rise due to steady oscillatory shear. Further, one can solve for $g(\Gamma)$:

$$g = [2/(\Gamma+1)]\ (\ln [\sqrt{(\Gamma+1)} + \sqrt{\Gamma}])^2 \ . \tag{111}$$

Figure 13, a plot of g against Γ, shows that g goes through a maximum of $g = .88$ at $\Gamma = 2$. Hence, the condition for thermal runaway, $g > .88$, is obtained. Furthermore, for all values of $g < .88$ the dimensionless shear strain is double valued. This behavior seems similar to the double valued shear rate obtained in the steady simple shear analyses given above. However, the important difference here is that one cannot determine the deviation in shear rate analytically

By inspection of (107), the case for both boundaries adiabatic is obtained for the reduced time:

$$\eta = \frac{1}{g} \int_0^{\Phi} \frac{d\Phi}{\exp(\Phi)} \tag{112}$$

Noting that this integral diverges to ∞ for finite reduced time, $\eta = 1/g$, one obtains the time for thermal runaway in oscillatory shear.

$$t = C_p h^2/gk \tag{113}$$

Other forms of temperature sensitivity have been examined for steady oscillatory shear behavior.[408,409,410,411] Handy constraints, analogous to (113) are obtained for the test time at thermal runaway. When the temperature dependence of the first harmonic has the assumed form, (113) can be used for the case of a nonlinear viscoelastic fluid.

d. Random Shear

Deviations from simple shear due to viscous effects have also been determined for the test condition where shear strain is a random function of time.[412] These can be used to assess the effect of background mechanical noise in the shear strain on the thermal profile of the sample.

For stationary random background noise, with a stress spectrum of uniform amplitude between ω_1 and ω_2, and with zero amplitude for $\omega<\omega_1$ and $\omega>\omega_2$, the steady dimensionless mean square shear stress, g_r, is:

$$g_r = \frac{\langle\sigma^2\rangle\, \omega^{1-n}\, h^2 a k}{k} \left[\frac{1}{2-n}\right] \left[\frac{\omega_2}{\omega}\right]^{1-n} \left[\frac{1-(\omega_1/\omega_2)^{2-n}}{1-(\omega_1/\omega_2)}\right], \qquad (114)$$

in which case, time to thermal runaway with both boundaries adiabatic becomes: $t_r = C_p h^2/g_r k$.

2. Fluid Inertia

Fluid inertia is simply the attenuation and delay in fluid motion resulting from fluid acceleration or deceleration. It can cause important deviations from simple shear for all tests other than steady simple shear, which involves no fluid acceleration.* Hence, high plate acceleration causes large deviations from simple shear. Specifically, experiments involving sudden changes in strain or shear rate suffer large inertial deviations from simple shear.** Furthermore, viscoelasticity can make these hard to minimize and difficult to correct.[413]

Errors due to fluid inertia are not easily predicted. Theories for such predictions begin with a model for the transmission of stress from the moving plate into the fluid These models are invariably based on theories of wave propagation. We shall see that for a velocity wave propagating in a Newtonian fluid, the resulting vorticity*** and shear stress waves can be predicted. However, several different approaches have been tried for viscoelastic fluids in simple shear. The propagation of waves of vorticity can be used as a basis for models of fluid inertial effects. This allows the consequent inhomogeneity in the shear stress to be predicted. Finally, the propagation of shear stress waves can be taken as the cause of momentum transport, which permits consequent errors in vorticity to be estimated. For instance, for perfect simple shear we often assume that shear stress is transmitted instantaneously to all points in the fluid, which implies that there are no errors due to fluid inertia.

---

*Variously called the effect of stress or shear wave propagation or reflection.

**These evidently include classical stress relaxation, stress growth, strain rate reduction and sudden cessation of steady shear.

***Recall that for simple shear, the vorticity tensor is proportional to the shear rate.

a. Stress Growth

(1) Newtonian Fluid

A series solution of the equation of motion gives the velocity profile in a Newtonian fluid during sudden imposition of steady simple shear.* The velocity is:[414,415]

$$u = U\left[1 - x_2/h\right] - \frac{2U}{\pi}\left[\sum_{n=1}^{\infty}\frac{1}{n}\exp-(n\pi/h)^2\mu t/\phi \, \sin\left[n\pi x_2/h\right]\right], \qquad (115)$$

or alternatively,[416]

$$u = U\sum_{n=0}^{\infty}\left[\operatorname{erfc}\frac{nh+\tfrac{1}{2}x_2}{\sqrt{(\mu t/\phi)}} - \operatorname{erfc}\frac{(n+1)h+\tfrac{1}{2}x_2}{\sqrt{(\mu t/\phi)}}\right]. \qquad (116)$$

These expressions make no allowance for deviations caused by thermal feedback Using (115) Batchelor gives a handy dimensionless plot of x_2/h against u/U for various values of $\mu t/\phi h^2$. It shows that the velocity profile deviates significantly from simple shear when:

$$\mu t/\phi h^2 < 4. \qquad (117)$$

---

*Sometimes called Stokes' first problem.

For those designing rheometers, an even handier relation can be obtained by differentiating (116) to obtain the shear rate profile:

$$\frac{du}{dt} = \frac{U}{\sqrt{\pi}\,\sqrt{(\mu t+\phi)}} \sum_{n=0}^{\infty} \left[\exp \frac{-[(n+1)h+\frac{1}{2}x\ ]^2}{\mu t+\phi} - \exp \frac{-[nh+\frac{1}{2}x\ ]^2}{\mu t+\phi} \right], \tag{118}$$

which can be used to calculate the fractional deviation in shear rate, $h\dot{\gamma}/U - 1$, due to fluid inertia in stress growth experiments. Furthermore, the stress profile across the fluid sample is simply $\mu(du/dt)$.

<u>(2) Viscoelastic Fluid</u>

It has been pointed out that since stress growth contains an impulse in plate acceleration, errors due to fluid inertia can be large. For example, fluid inertia can even cause overshoot in shear stress for stress growth for linear viscoelastic materials [417] This is important since overshoot is usually interpreted exclusively as a nonlinear viscoelastic property without considering fluid inertia. Although theoretical solutions exist for inertial errors in model viscoelastic fluids, these are rarely used for error correction since the constitutive equation must be known before measurement, a rare luxury in practice.[418,419,420]

Theories based on the reflection and propagation of a velocity wave give markedly different predictions from the Newtonian ones.[421,422]

Specifically, velocity overshoot, asymmetry about the midplane in the unsteady velocity field, and secondary overshoots in the shear stress at the walls are predicted These errors are difficult to correct. For some model viscoelastic fluids, significant deviations from simple shear are predicted when $\mu t/\phi h^2 < 58$ * Some of these remarkable predictions have recently been confirmed experimentally for collagen solutions by measuring the 1,2 component of the birefringence in a concentric cylinder rheometer [423]

b Oscillatory Shear

(1) Newtonian Fluid

For a Newtonian fluid following sudden imposition of sinusoidal shear the velocity profile is [424]

*Require 14.5 times longer than for Newtonian fluid. See equation (47).

$$u = UA \sin(\omega t + \Phi) - \frac{2\pi\mu U}{\phi}\left[\sum_{k=1}^{\infty} \frac{\phi^2 k (-1)^k \omega h^2}{\mu^2 (k\pi)^4 - (\omega h)^2} \sin\frac{k\pi x}{h} \exp -(\mu k\pi/h\phi)^2 t\right], \qquad (119)$$

with

$$A = \frac{\cosh 2(\omega\mu/2\phi)^{1/2} x - \cos 2(\omega\mu/2\phi)^{1/2} x}{\cosh 2(\omega\mu/2\phi)^{1/2} h - \cos 2(\omega\mu/2\phi)^{1/2} h} \qquad (120)$$

and

$$\Phi = \arg\left[\frac{\sinh(\omega\mu/2\phi)^{1/2}(1+i)}{\sinh(\omega\mu/2\phi)^{1/2}(1-i)}\right] \qquad (121)^{*}$$

The exponential term, $\exp -(\mu k\pi/h\phi)^2 t$, provides the following estimate of the cycle number, N, to begin data collection when performing an oscillatory shear test

---

*arg(x) = Re(x)/Im(x).

$$N = \frac{\omega \ln X}{-2\pi \ (\mu k\pi/h\phi)^2} , \tag{122}$$

where X can be taken as .02 to insure complete decay. Furthermore, this exponential term becomes unity in steady oscillatory shear giving the fully developed velocity profile:

$$u = UA \sin (\omega t + \Phi) , \tag{123}$$

which has been rewritten ~~as~~:[25]

$$u = U \exp \left[-(\omega\phi/2\mu)^{\frac{1}{2}} x_2 \right] \cdot \cos \left[\omega t - (\omega\phi/2\mu)^{\frac{1}{2}} x_2 \right] \tag{124}$$

Hence, this velocity profile is often interpreted as a damped shear wave* of wavelength $2\pi\sqrt{(2\mu/\phi\omega)}$ propagating in the x_2 direction with phase velocity $\sqrt{(2\omega\mu/\phi)}$. If steady oscillatory shear is achieved the phase lag between the actual and desired fluid velocities is $-\sqrt{(\omega\phi/2\mu)}\ x_2$, and the attenuation factor for the shear wave amplitude is $\exp(-\sqrt{(\omega\phi/2\mu)}\ x_2)$. Hence, phase lag is proportional to the distance from the oscillating surface, whereas the attenuation of the shear wave causes its amplitude to decay exponentially with distance.

<u>(2) Viscoelastic Medium</u>

*Also called a transverse wave.

For the viscoelastic medium in oscillatory shear the general solution for the effects of fluid inertia in steady oscillatory shear are obtained by solving the equation based on the propagation of a velocity wave.[426,427,428,429,430,431] Consider a fluid confined by two parallel plates, one stationary and one moving with velocity $U = U_o \sin(\omega t)$. The solution for the fluid velocity corrected for fluid inertia is.

$$u(x_2) = U_o\,[\sin(\Gamma x_2)/\sin(\Gamma h)]\,\exp(i\omega t), \tag{125}$$

and the shear rate profile is

$$\gamma = -U_o \sqrt{(\alpha^2+\beta^2)} \left[\frac{\cosh(2\alpha x_2) + \cos(2\beta x_2)}{\cosh(2\alpha h) + \cos(2\beta h)} \right] \cos(\omega t + \Phi) \;. \tag{126}$$

where

$$\Phi = -\Phi_1 + \Phi_2 + \Phi_3 \tag{127}$$

and

$$\Phi_1 = \arctan(\alpha/\beta) \tag{128}$$

$$\Phi_2 = \arctan[\tan(\beta x_2)\tanh(\alpha x_2)] \;. \tag{129}$$

$$\Phi_3 = \arctan[\tanh(\alpha h)/\tan(\beta h)] \;. \tag{130}$$

and

$$\alpha = \omega \sqrt{(\phi/G^*)}\,\sin(\delta/2) \;. \tag{131}$$

$$\beta = \omega \sqrt{(\phi/G^*)}\,\cos(\delta/2) \;. \tag{132}$$

Hence, the fractional deviation of shear rate amplitude from simple shear, ϵ_1, is:

$$\epsilon_i = \frac{\beta h \sqrt{[(\alpha/h)^2+1]} \sqrt{(\cosh(2\alpha x_2) + \cos(2\beta x_2))}}{\sqrt{(\cosh(2\alpha h) - \cos(2\beta h))}} , \tag{133}$$

Important design results are (1) for $\epsilon_i < .01$ and phase error less than 1°, $L_s \leq 20$ h and (2) steady state is reached when $t > 4h/v_s$. Nomographs, helpful for determining $\epsilon_i(x_2)$, are provided by Schrag.[432] Also, Darby gives explicit rheometer design constraints for some special cases of (133).[433,434]

Note that $\beta = 2\pi/L_s = \omega/v_s$, where L_s is the shear wavelength and v_s is the shear wave propagation velocity. Since G^* and δ are functions of frequency, it follows that shear wave propagation wavelength and velocity are also functions of frequency This effect has been demonstrated in viscoelastic clays.[435]

c. Sample Resonant Frequencies

The set of resonant frequencies for a slab vibrating in the nth mode in simple shear is:[436]

$$f_n = n v_s/2h , \tag{134}$$

where v_s is the shear wave velocity and h is the sample thickness. Experimental errors may arise when the shear wave has one or more component frequencies near any of the resonant frequencies.

3. Gravity Flow in Narrow Slit

To the casual observer it often seems impractical to have a sliding plate rheometer mounted vertically. In fact, for a particular sample thickness there is a minimum viscosity required to prevent significant outflow from the shear fixture. Neglecting end effects, the flowrate of a Newtonian fluid in a narrow slit caused by self-weight is[437]

$$Q = \rho g h^3 w / 12\eta \tag{135}$$

and the maximum fluid velocity is

$$u_{max} = (\rho g h^2 / 8\eta) \tag{136}$$

Of course, when a fluid is sufficiently viscous the downward flow due to self-weight will be eliminated by the opposing effect of surface tension. The effect of gravity flow on thick asphalt samples in a sliding plate rheometer has been photographed by Weinberg[438]. In general, for a sample 0.05 inches thick, polymer solutions with viscosities as low as 10^4 Pa-sec exhibit no measurable gravity flow[439,440].

4. Plate-Polymer Interactions

It is clearly advantageous to minimize sample thickness. However, Burton et al. found in their steady shear study of high molecular weight polystyrene melts using a parallel disk rotational rheometer that at sufficiently small gaps, the apparent shear stress decreased as the gap was further decreased at a fixed shear rate.[441] They attributed this to the atypical behavior of the polymer molecules in contact with the disk surface This suggests that there is a lower limit for the gap for high molecular weight polymeric liquids.[442,443]

C. Non-laminar Deviations from Simple Shear

To the writer's knowledge, with the obvious exception of free boundary effects, non-laminar flow has not been observed in sliding plate rheometers Such effects are, however, observed in most other rheometers, including those using rectilinear flow fields like capillary viscometers.

Recall that for all the deviations from simple shear reviewed in the preceding section, we have tacitly assumed flow to be an orderly sliding of virtually rigid adjacent lamina, with no interlaminar fluid exchange. However, for real materials in simple shear there turn out to be several potential causes for fluid exchange in the x_2 direction. Since such non-laminar behavior is often predicted from theory for simple shear, such theories are reviewed here. When all aforementioned causes are eliminated, non-laminar flow can explain anomalies obtained in sliding plate experiments.

Intuitively, we expect true simple shear to be more stable that its rotational approximations commonly used for rheometers, since it is free of the destabilizing effect of centripetal acceleration that dominates non-laminar behavior observed in such instruments. For instance, for concentric cylinder rheometers a transition from laminar to non-laminar flow occurs. For small gaps, the corresponding transition Reynolds number, $Re = \phi\langle v\rangle h/\mu$, is a simple function of the ratio between the inner and outer diameters:[444,445]

$$Re = \frac{41.3}{\left[1 - \frac{R_i}{R_o}\right]} \tag{137}$$

Here, as the gap size decreases, planar Couette flow is approached and (137) predicts perfectly laminar flow This is one reason planar Couette flow is preferred over flows generated in rotational instruments However, in principle, causes for non-laminar flow for true simple shear do exist, but they are different from those dominating (137) So, the prediction of infinite transition Reynolds number for sliding plate flow obtained from (137) must be taken with a grain of salt.

When laminar flow is disturbed, the disturbance can be amplified or attenuated. Flows that encourage amplification are called unstable, and it will be seen that certain laminar deviations from simple shear have been shown theoretically to permit disturbances to amplify.* These theories

---

*Flow stability is not to be confused with mathematical instability observed when certain constitutive equations are evaluated in simple shear at high Weissenberg number. [Phan-Thien, N., "Cone-and-plate flow of the Oldroyd-B fluid is unstable", J. Non-Newt. Fluid Mech., 17, 37-44 (1985).].

consider infinitesimal or finite disturbances in both shear rate and temperature.

Gill has proven that a necessary condition for non-laminar flow is the existence of a local extremum in vorticity.[446] Recall that vorticity is the tensor $W_{ij} = \frac{1}{2}(\nabla \underline{v} - \nabla \underline{v}^T)$.* For simple shear the vorticity tensor is.

$$\underline{\underline{W}} = \gamma \begin{bmatrix} 0 & -1 & 0 \\ 1 & 0 & 0 \\ 0 & 0 & 0 \end{bmatrix} \qquad (138)$$

Perfect simple shear contains no local extrema in vorticity and is, in principle, laminar for all shear rates. This not true for the rotational flows commonly used for rheometry

1. Free Boundary Effects

The importance of the free boundary is discussed in detail in the introductory chapter since these causes for deviation in simple shear are a raison d'étre for the development of rheometers with shear stress transducers.

2. Temperature Gradients

---

*Not to be confused with the vector $\nabla \underline{v}$ also sometimes called vorticity.

Deviations from simple shear caused by viscous effects in temperature sensitive fluids contain shear rate extrema, and hence, can be non-laminar. Where fluid inertia is negligible, the flow of temperature insensitive Newtonian liquids becomes perfectly laminar following any disturbance.[447,448,449,450,451,452,453,454]

We have seen that the laminar deviation from steady simple shear obtained for temperature sensitive Newtonian and non-Newtonian fluids can involve local extrema in the shear rate Furthermore, we saw that the shear stress could be double valued in shear rate. It has been shown that both values can be unstable and potentially non-laminar[455,456] Moreover, transition Reynolds numbers, Re, for the potential onset of non-laminar flow are complicated functions of the Brinkman number, Br, and the viscosity-temperature coefficient, α. Sukanek et al. published handy graphs for α(Re,Br) that can be used for the design of steady shear experiments[457]

3. Vorticity Propagation

Stability theories can be developed using vorticity wave propagation as the mechanism of stress transmission. Using such a model, for experiments involving impulses such as classical stress relaxation it can be shown that, in principle, discontinuities in the velocity profile can exist for both Newtonian and model viscoelastic fluids.[458,459,460] Furthermore, a thermodynamic argument predicts instability when the velocity at the boundary is higher than the shear wave velocity in the fluid.[461] Recall that for a viscoelastic medium the wave velocity is a strong function of frequency.

4. Melt Fracture

It has been mentioned that localized deformation is sometimes observed in the simple shearing of solids, particularly solid plastics.* In principle, for simple shear of solids, fracture may occur in either of the shearing or tearing modes[462] For simple shear, a shearing mode fracture occurs when new surface is swept out by a line segment oriented in x_3 direction which propagates in x_1 direction. Tearing mode fracture occurs when initiated at a line segment in the x_1 direction propagates in the x_2 direction ** For the cone-plate fixture theories for melt fracture it is usually tacitly assumed that fracture occurs in the tearing mode.[463] For the case of simple shear, however, visual observations show melt fracture in the shearing mode.[464]

Clearly the propagation of a fracture through the sample represents a major deviation from simple shear. In cyclic tests the shearing mode fracture will show twofold asymmetry on the stress versus strain loop if the crack front approaches the shear stress transducer. However, since the

---

*See section on determinism.

**Note that these are model fractures which occur exactly as described in linear elastic materials. For the case of a fracture propagating through a melt at high shear rate, the fracture might only be approximated by these modes The combination of both modes at once is also possible.

tearing mode fracture can approach the transducer from the side, it may or may not show up as twofold asymmetry in the loop for a cyclic test.

5. Shear-Induced Crystallization

It is well known that partial crystallization of a polymer melt can be caused in simple shear. This occurs at temperatures above the polymer's equilibrium melting point. Shear-induced crystallization, has been observed in molten isotactic polystyrene in steady simple shear in sliding plate rheometers[465,466] Under these circumstances, small crystals begin to grow throughout the sample. The resulting flow will deviate from simple shear since the phase change involves contraction. Furthermore, crystals whose size becomes significant relative to the sample thickness will cause significant deviations from simple shear.

D. Principles of Dynamic Measurement

Rheometers are normally calibrated using static methods. Rotational instruments, for instance, are calibrated by plotting static torque applied to the torque transducer against observed change in voltage output.

Consider a zero order transducer for which voltage output is linear with applied torque:[467]

$$V = kT + b \ . \qquad (139)$$

Offset, b, is usually set as close as possible to zero with an adjustable voltage subtractor circuit. Furthermore, a variable gain amplifier can be used to vary k. This is both necessary and sufficient for measuring viscosity.

However, when a time dependent torque is applied to the transducer, the voltage output deviates from the simple proportionality $V = kT$. The nature of the deviation will depend on the dynamic characteristics of the transducer, which can be obtained by dynamic calibration.

For example, consider a sinusoidal torque, $T = T_o \sin(\omega t)$ applied to a torque transducer. The dynamic characteristics of the transducer cause the measured voltage to be attenuated and phase shifted, so that:

$$V = AkT_o \sin(\omega t + \delta_e) \quad , \tag{140}$$

where attenuation, A, and phase lag, δ_e, are generally functions of frequency.

Traditionally, the dynamic response of a rheometer is evaluated by comparing dynamic measurements with those of other instruments, and especially with those of more widely used instruments.[468] This procedure tacitly assumes that the measurements of the other instruments are error free. However, if these are not error free then agreement between instruments only shows that both are equally inaccurate. Furthermore, when instruments can be calibrated dynamically the question of agreement between them becomes academic.

Specifications for the dynamic response of the stress transducers are not supplied with most commercial rheometers. Furthermore, the writer is not aware of any dynamic calibration of commercial rheometers. This seems remarkable since the principles of dynamic measurement are usually outlined in texts on measurement systems.[469] Hence, dynamic errors are generally neglected in rheological measurements on commercial instruments *

Using analog circuitry, it is possible to adjust the phase response of the strain transducer to match that of the torque transducer. Some rotational instruments are calibrated dynamically in precisely this way.[470] The limitations with this approach are that it corrects phase error only, not attenuation, and that it applies strictly only to oscillatory shear testing. Hence, if the transducer phase error is a function of frequency, then such an adjustment must be made separately for each test frequency.**

1. Dynamic Response of Transducers

---

*The user almost universally takes it for granted that the manufacturer knows what he is doing. Perhaps he is not "neglectful" so much as "overly trusting".

**Transducer dynamic error is not to be confused with imperfections in the shear strain caused by the dynamic limitations of the rheometer drive system. For cyclic tests, such imperfections can be allowed for by use of frequency modulation.

The dynamic response of transducers is usually modelled by the nth order differential equation:[471]

$$\sum_{i=n}^{0} a_i \left[\frac{d^i q_O}{dt^i}\right] = bq_I \quad (141)$$

where q_O and q_I are the measurand and the observable output respectively. Handy analytical solutions for frequency response of first and second order systems are discussed below.

a. First Order Responses

Sometimes the transducer response can be summed up with a single number, θ, called the transducer time constant. If so, then its response is called first order and the phase error is:

$$e(\omega) = \arctan(-\omega\theta) \quad (142)$$

and the attenuation* is:

$$A(\omega) = 1/\sqrt{(\omega^2\theta^2+1)} \quad (143)$$

---

*See equation (140).

Furthermore, the response of a first order instrument is normally specified in terms of the frequency of which $\theta = \pi/2$, where the decibel value of the attenuation is -3. The time constant, θ, is simply related to this frequency

$$\theta = 1/\omega_{3dB} \tag{144}$$

Resonance is observed at the 3dB frequency. Since $\tan \delta(\omega) = -\omega\theta$, a plot of $\tan \delta(\omega)$ versus ω gives θ directly as its slope. Note that θ is easily deduced from the response of the transducer to many other types of time dependent input[472,473,474].

Furthermore, for J first order elements in series

$$A(\omega) = \prod_{i=1}^{J} \frac{1}{\left[\omega_i^2 \theta_i^2 + 1\right]^{1/2}} \tag{145}$$

and

$$\delta(\omega) = \sum_{j=1}^{J} \arctan(-\omega\theta_j) \tag{146}$$

b. Second Order Responses

Second order instruments are described by the resonant frequency, ω_n, and the damping factor, η. These cause phase error

$$\delta_e = \arctan[2\eta/(\omega/\omega_n - \omega_n/\omega)] \tag{147}$$

and attenuation:

$$A(\omega) = 1/\sqrt{\{ [1-(\omega/\omega_n)^2]^2 + 4\eta^2\omega^2/\omega_n^2 \}} \quad (148)$$

Mechanical resonance is observed when $\eta < 1$. Note that η and ω_n can also be deduced from the transducer's response to other controlled dynamic force applied laterally to the shear stress transducer cantilever.[475,476]

c. Higher Order Responses

Although analytical solutions can be obtained for higher order instruments, it is easier to obtain $A(\omega)$ and $\delta_e(\omega)$ empirically. This is done by dynamic calibration using a controlled, time dependent transducer inputs at appropriate frequencies.

2. Phase Correction

There are three approaches to correcting for the dynamic error of a transducer. Firstly, phase error can be neglected altogether which is commonly done. This confounds the response of the transducer with that of the material. Secondly, when an analytical expression for the transducer response is known, then an analytical expression for $\delta_e(\omega)$ can be derived. Thirdly, the $\delta_e(\omega)$ can be determined experimentally for all ω. Whether the analytical solution is known or not, the most efficient way to error correct is to decompose the actual transducer output into amplitude and phase spectra, $A(\omega)$ and $\delta_e(\omega)$ respectively, and subtract $\delta_e(\omega)$ from each component of the measured phase spectrum. This method is applicable to both cyclic and noncyclic material responses.[477] The correction for attenuation can be made by multiplying each component of the measured amplitude spectrum by $1/A(\omega)$.*

Since waveforms can be approximated as a sum of harmonics, knowledge of $A(\omega)$ and $\delta_e(\omega)$ for the transducer permits complete correction for both attenuation and phase in the frequency domain. The corrected phase angle is obtained by subtracting δ_e from the measured phase angle. The precision of such corrections is deducible from the statistical confidence on each value of $A(\omega)$ and $\delta(\omega)$.

*In rheological measurements, attenuation is usually much less important than phase error.

IV. RHEOMETER DESIGN

A. Brief Chronology of New Rheometer Development

1 Preliminary investigations were carried out on the room temperature prototype originally developed by Soong[478,479,480] using analog signal recording and processing methods described by Tee and Dealy.[481,482] This early work produced a better proximeter for the shear stress transducer that was suitable for high temperatures, an improved calibration method especially well suited to high temperature work, and design concepts for the new rheometer[483]

2 A new rheometer for molten plastics was designed and assembled.

3 The electromechanical drive system of the room temperature prototype was replaced by the MTS servohydraulic actuator for the new rheometer. Initially, an IBM personal computer was used for data acquisition[484] and control of the linear actuator was accomplished by adjusting front panel switches.

4 Finally, a highly integrated microcomputer system was added for programmable linear actuation and digital data acquisition and processing. The microcomputer system included a high speed programmable function generator with high speed digital data acquisition. Figure 141 shows the

input-output media including the keyboard, the dot-matrix printer, and the pen plotter for high-speed, hard-copy graphics.

B. Design of the New Rheometer

An exploded isometric view, drawn to scale, of the shear fixture for the new rheometer is shown in Figure 14 Reduced versions of the dimensioned drawings used for its construction are presented in Figures 15 and 16 Figure 14 shows how the precision linear bearing table is configured within the frame-work of a solid steel housing The housing is sturdy, although its design incorporates holes for better heat transfer and it has been made as slim as possible to reduce thermal mass without compromising structural rigidity. Vertical grooves in the moving plate promote convective heat transfer to maximize temperature uniformity in the shear fixture The stationary plate is secured to the left side panels, brass shims inserted between these members determine the sample thickness The stationary plate is hinged to the left side panel with three triple action hinges, not shown The rheometer is vertically mounted on an MTS servohydraulic drive system and is completely enclosed in a retrofitted Fisher oven shown in Figure 16. A reduced version of the engineering drawing used for fabrication of the shear stress transducer is found in Figure 17. Several photographs are included showing the rheometer in use

The rheometer design is the result of several competing performance criteria. Mechanical considerations include the selection of the correct plate length and sample thicknesses to accommodate large shear strains and to minimize errors due to fluid and moving plate inertia. Bearing parallelism and preload, and plate surface texture are also important design considerations.

Thermal criteria for design include the minimization of sample temperature nonuniformities due to viscous heat dissipation and other factors Several previously reported layouts for sliding plate rheometers or viscometers were considered when designing the new system, and these are mentioned below The design for the new rheometer has been summarized in a recent paper [485]

C. Detailed Design Considerations

Important choices made leading up to the final design of the new sliding plate rheometer are explained here It is hoped that this section will help those designing their own sliding plate rheometers.

1. Desired Amplitudes and Frequencies

The designer must first decide what variety of tests will be required of the rheometer. If one needs oscillatory shear tests only, one can save considerable expense on the linear actuator. One may, for instance, opt for an open-loop electrohydraulic actuator as was used by Soong.[486] However, if a broader range of tests is to be used then a closed loop servohydraulic system should be considered.[487] Where a programmable shear strain history is desired, a computer controlled servo-hydraulic linear actuator must be considered.[488,489] Whether the rheometer is to be used for other strain-histories or not, oscillatory test data can be used as the basis for rheometer design.

As a rule of thumb, a rheometer for measuring nonlinear viscoelastic properties of molten plastics should be capable of (1) shear strains of 50 and (2) test frequencies between 1 and 100 Hz Of course, melt fracture will govern the maximum allowable shear strain at a given frequency and temperature, for a particular material

2. Actuator Performance

Sliding plate rheometers demand some form of linear actuation Performance characteristics for linear actuators are normally given graphically as a plot of displacement amplitude versus frequency for sinusoidal displacements This performance will depend on applied load Figure 18 shows the no-load and 20,000 lb_f load amplitude performance curves for the MTS servohydraulic linear actuation system used in this research * When shearing viscoelastic fluids during rheological testing, we expect the actuator to be operating near the no-load condition. For frequencies up to 100 Hz, the maximum amplitude of a sinusoidal displacement that can be achieved without significant distortion is.**

---

*This systems comprises an MTS series 244 actuator with an MTS model 252.23 servovalve Data for this system kindly supplied by Mr R. Proehl, MTS Systems Corp , Minneapolis, Minn.

**Deduced from the linear portion of Figure 18.

$$D_{max} = \tfrac{1}{2} f_{max}^{-1.023} , \quad .2 \le f \le 100 \text{ Hz} . \tag{149}$$

Note that (149) gives the limit for no distortion in a sinusoidal motion. For sinusoidal testing this is both necessary and sufficient. The six inch upper limit in Figure 18 is determined by the barrel length, whereas the lower limits are dictated by pump performance characteristics.

For nonsinusoidal waveforms both amplitude and relative phase content are important For example, for a square wave we require that each of the Fourier components be of a certain amplitude and of a certain phase relative to one another The maximum amplitude obtainable for nonsinusoidal waveforms can be estimated using $\tfrac{1}{2}f$ in (149), where f is the frequency of the fundamental. In general, this estimate can be realized when the gain of the servocontrol loop is set to its optimal level for each test.

a. Technical Data on the Actuator

Table 1 gives technical specifications for the MTS series 244 actuator.

Table 1: Actuator Specifications Pertaining to Figure 18

Piston Area, sq.in.	7.57
Stroke, in.	6.00
Hydraulic cushion, in	0.3
Rod diameter, in	2.75
Pump flow, gpm	6.0
Pump pressure, psi	3000
Hydraulic fluid bulk modulus, kpsi	17.5
Accumulator size, U.S. gal	0.12

Figure 19 is a photograph of the piston, servovalve and accumulator assembly These components were mounted vertically under the sliding plate rheometer Figure 20 shows the 6 gpm hydraulic pump, floor mounted beside the piston

3. Plate Design

a. Plate Shape

Although most sliding plate rheometers have been used with rectangular samples, other sample shapes are easily accommodated. For instance, circular samples have been used in single sample instruments.[490,491] When the shear stress is measured locally, rectangular plates are preferred since rectangular sample shapes accommodate a given maximum shear strain with minimum sample size.

b. Plate Size

Traditional sliding plate rheometers were designed so that the plate displacement, D_{max}, was much smaller than the sample length, L, to minimize end effects. Also the width to thickness ratio, W/h, had to be kept as high as possible to minimize edge effects. Hence, the aspect ratios D_{max}/L and W/h had to be high enough to eliminate sample size sensitivity. For a rheometer incorporating a shear stress transducer however, the relevant aspect ratio is simply the maximum plate displacement over the distance between the transducer and the nearest sample end. For a sample mounted with the transducer at its center, this distance is $\frac{1}{2}(L-D_T)$, where D_T is the diameter of the transducer active face. Hence, the relevant design ratio is $D_{max}/(L-D_T)$ This aspect ratio must be large enough so that at the peak shear strain the trailing boundary is not approached by the shear stress transducer. As we saw from theoretical predictions of end effects, just how large this aspect ratio must be depends on sample properties. Hence, the following criterion is suggested for sliding plate rheometer design:

$$D_{max}/(L-D_T) < \Phi_c. \qquad (150)$$

If the shear stress transducer is mounted near the end of the sample then the related criterion is simply:

$$D_{max}/d_{min} < \Phi_c, \qquad (151)$$

where d_{min} is the distance from the transducer's active face to the sample's nearest end. For molten polystyrene in large amplitude oscillatory shear a value of $\Phi_c \approx 1/5$ was measured. For a desired peak strain, γ_o, this implies that $d_{min} > 5h\gamma_o$. This is discussed under results.

c. Surface Texture

The surface texture of the shearing plates is important for two reasons Firstly, the roughness height and flaw size of the shearing surfaces in contact with the fluid acting on the shear stress transducer should be much smaller than the sample thickness Obviously, there is no need to improve plate flatness much below the parallelism tolerance of the linear bearing motion. For the linear bearing table used here, parallelism is below 0 2 μm/cm of plate travel [492]

Secondly, the macroscopic surface texture of the shearing plates is known to play a role in controlling stick-slip phenomena[493,494,495] and can influence melt fracture in sliding plate rheometers.[496] In fact, knurled surfaces can improve cohesion in sliding plate rheometers for molten polymers.[497,498] The role of roughness height, waviness, flaw size and lay of the plate surfaces, or that of the active face of the shear stress transducer, in initiating melt fracture, is not known.

Using a grinder equipped with a magnetic chuck, the surfaces of the plates for the new rheometer were ground to a roughness height of 0.0001 inches

4. Plate Inertia

For tests such as step strain, where high plate acceleration is required, the mass of the moving plate/piston assembly, roughly 58 lb, becomes important The mass of the MTS Model 204 actuator piston alone, Ma, is roughly 45 lb Actuator response time for tests incorporating impulses can be estimated, assuming constant acceleration, for the maximum hydraulic pressure, P

For a stress growth experiment, the time to reach steady velocity is

$$t = \frac{m_{ma} V}{P A_{eff} g_c} \qquad (152)$$

and for classical stress relaxation, the time to jump to the new position is:

$$t = \left[\frac{2 D_{max} m_{ma}}{P A_{eff}} \right]^{1/2} , \qquad (153)$$

where A_{eff} is the piston effective area, m_{ma} is the mass of moving assembly, D_{max} is the desired displacement and V is the desired velocity.

Hence, a 100 sec^{-1} stress growth test using a sample thickness of 1 mm will require roughly 0.02 ms for the piston to come up to speed, P = 4000 psi, A_{eff} = 7.35 sq. in. and m_{Ma} = 55 lb.[499] This estimate neglects the force of friction acting on the piston.

5. Fluid Inertia and Viscous Dissipation

Constraints on gap spacing due to fluid inertia and viscous heat dissipation have already been discussed. For the study of molten plastics, a series of shims were fabricated permitting sample thicknesses between 1/20 to 1/2 mm to be used. This was considered more than adequate for the measurement of nonlinear viscoelastic properties.

6. Linear Bearing Table

a. Parallelism of Plates

The quality of a sliding plate rheometer depends on its ability to subject fluids to planar Couette flow, hence parallelism is important. In a sliding plate fixture for shearing solid polymers at room temperature, a SCHNEEBERGER linear bearing table had previously been successfully used.[500,501] Linear bearings of this type meet a parallelism tolerance of 0.2 μm/cm of travel.[502] This permits tests on samples as thin as 0.3 mm with an error in parallelism of less than 0.1% for a shear strain of thirty.[503] A nickel plated steel linear bearing table, model NK6-260, fabricated at the SCHNEEBERGER plant in Switzerland, was used in this work.

b. Importance of Bearing Preload

The parallelism tolerance of 0.2 μm/cm of travel will be met if, and only if, the bearing preload is not exceeded by ancillary loads arising during testing Such loads will include the torque on the plates due to a lever action of the shear force at the wall about the center of mass of each plate Should the normal stresses arising from such a torque exceed the bearing preload, the plates may tend to misalign Additionally, the normal thrust resulting from shear induced normal stress differences in the sample can also cause the plates to separate should it cause the bearing preload to be exceeded It was found that the preload could be adjusted to finger tightness with an allen key at room temperature 504

c. Bearing Installation and Maintenance

Only a light silicone based oil should be used on the linear bearings since they are inside the environmental chamber. Bearings are generally shipped well-oiled with an organic lubricant.* Such lubricants tend to carbonize upon heating, which causes bearings to seize immediately. New bearings for use at high temperature should be dismantled and cleaned thoroughly before installation. An overnight soaking in bubbling

*Sometimes this lubricant is merely residual machining oil leftover from fabrication.

turpentine suffices to completely remove this organic lubricant.* Only a thin silicone based lubricant should be used on bearings utilized at high temperature.**

d. Bearing Table Longevity

The longevity in kilometers, L, of the roller bearings can be estimated from the dynamic load carrying capacity, C, the dynamic loading in service, P, the service temperature, T, and the statistical probability of failure, p, using the following relation:[505]

$$L = 250\ a\ (fC/P)^{[10/3]} \qquad (154)$$

where C = 5200 N for the model NK6-260 table, factor "a" accounts for failure probability and f accounts for temperature sensitivity. Selected values for a(p) and f(T) are listed below.

*Once seized the bearings must be dismantled and cleaned. The sodium hydroxide aerosol, sold under the trade name Easy-Off, can be used to remove carbonized lubricant from bearing components. Again, clean thoroughly before reassembling for even dust particles deteriorate parallelism.

**Grease, including noncarbonizing grease, is also to be avoided as it instantly causes bearing seizure.

p, %	90	95	96	97	98	99
a	1.	.62	.53	.44	.33	.21

T, °C	150	200	250	300
f	1.0	.90	.75	.60

Operating at capacity the parallelism tolerance for the model NK6-260 table operating at 200°C will be maintained for total displacement of 37 Km with 99% certainty Hence the bearings will tolerate 123,000 cycles of total travel under these conditions. Finally, when the service life is reached a new pair of rollers and guides should be installed.

7. Effect of Thermal Expansion

When a shear fixture expands and contracts with temperature some uncertainty can arise in the sample geometry. In cone-plate rheometers the cone-plate spacing is made adjustable to compensate for thermal expansion. A different cone position adjustment is required for each new test temperature In principle, shim thickness will change with temperature. However, a stress analysis on the sliding plate rheometer shows that the fractional variation in shim thickness, ϵ, due to thermal expansion is.

$$\epsilon = \alpha \ \Delta T , \qquad (155)$$

for a change in test temperature, ΔT, where α is the lineal thermal expansion coefficient. For metals α is so small that ϵ is less than ½% for a 300°C temperature change.

8. Good Safety Practices

The new rheometer should be treated with the same degree of caution afforded any powerful hydraulic equipment Hands should be kept free of moving parts when the hydraulic pump is on.

The rheometer operator should protect his arms from burns using well insulated, elbow-length gloves. In addition, standard laboratory safety practices, including the wearing of safety glasses, safety shoes and a laboratory coat are recommended.

9. Assembly, Loading and Cleaning

Laun has described a way of loading a sandwich type sliding plate rheometer.[506] Plastic plaques are loaded when the shear fixture is held in a horizontal position. The shear fixture is mounted vertically and heated. This design was easy to clean because the shear fixture could be removed from the heating chamber. The disadvantage of this approach is that considerable time is lost in cooling, disassembling, reassembling and reheating the shear fixture for each new sample. It will be seen that this time detracts from the useful life of the sample, as some molten plastics degrade within 20 minutes when exposed to air.

Conventional rotational instruments use a light shear fixture to minimize heat-up and cool-down times. They also incorporate nitrogen blanketing to increase the useful life of plastics samples. Despite these drawbacks, such instruments still take up to 30 minutes for thermal equilibration following sample insertion. Furthermore, nitrogen blanketing can significantly increase the operating cost of the rheometer.

To eliminate these drawbacks, McCarthy designed a self-charging sliding cylinder rheometer for molten plastics.[507] Samples are removed by purging the shear fixture with the next test material. This design circumvents time lost due to heating and cooling by operating continuously in the heat-soaked condition

The new rheometer design takes a different approach to minimizing time lost for sample insertion A rugged shear fixture with large thermal mass is used so that time lost waiting for thermal equilibration is minimal. Furthermore, an inconspicuous advantage of using local shear stress transduction is that it circumvents problems of oxidative degradation, and solvent gain or loss, when they are confined to the sample edges for a long time [508,509]. This increases the useful life of many plastics samples and obviates the need for nitrogen blanketing.

<u>a. How to Clean the New Rheometer</u>

Plastic samples can be scraped from the stainless steel surfaces using brass tools. If a new sample is to be inserted, this can be done without cooling the rheometer. The fan should be off when the oven is open to minimize heat loss and for operator comfort. Moreover, plastic samples are usually easier to remove when in the molten state. Hence, a thorough clean-up before each shut-down is advised.

A common complaint with rheometers for molten plastics is the difficulty in cleaning the metal surfaces of the shear fixture after a hard brown and black film of carbonized plastic builds up on them. It was found that this film can be easily removed from stainless steel surfaces by applying a commercial sodium hydroxide aerosol sold under the trade name "Easy-Off" and shown in Figure 135.* The efficacy of such cleaning materials has recently been evaluated for several commercial products for removing baked-on grime from household ovens [510] In general, two applications at twenty minute intervals provide clean surfaces with little aggravation. This cleaning procedure is illustrated in Figures 21 to 23. A final scraping with brass implements may still be required on persistent spots. Figure 24 shows the active face of the shear stress transducer being scraped clean.

b. How to Load the New Rheometer

---

*A word for the wise about Easy-Off. This product is sold in several fragrant formulations which give one a false sense of security. Although the manufacturer recommends that it be used in household ovens at 100°C, the writer observed that nasty vapours were liberated when applied to hot metal surfaces.

Once the rheometer is cleaned, a shim of desired thickness should be installed and the rheometer brought back to its equilibrium temperature. Shim installation is illustrated in Figure 25. The rectangular shim shape that allows the shim to be anchored at the top of the shearing box.* If the rheometer is not at the desired temperature the oven is closed and the fan is activated until thermal equilibrium is reached. During this period the stationary plate can be positioned away from the moving plate to maximize heat transfer area. Once the desired temperature is reached, a static calibration can be performed before sample insertion.

Once the calibration is complete, the prepared sample, usually a rectangular plaque, is carefully placed on the stationary plate centered around the active face of the shear stress transducer. This procedure should be carried out with the oven fan off. As a rule, prepared plaques ought to be at least 20% thicker than the shim thickness in use. The plastics samples conveniently stick to the hot plate. Figure 26 illustrates the sample insertion procedure. Air pockets are to be avoided and, on one side, these can be carefully pressed out by pushing outwardly on the melting sample. The stationary plate is then swung into place and securely fastened up against the shims. Air pockets on the outer side are minimized with the squeezing action due to the oversized samples. In general these do not pose a serious problem. They can be easily detected as they produce unusually high loop-to-loop variability in cyclic tests.

---

*This turns out to be a handy safety feature for when samples are removed loose hot shims may unexpectedly fall from the oven creating a burn hazard for the operator.

When voids are present, a new sample must be inserted. The plate can be positioned with one hand under the shear stress transducer and the other on the plate handle. This maneuver is illustrated in Figure 27. The stationary plate is then tightly set against the shims with tightening bolts, which are seated in the rheometer side panels and which pass through holes in the shims. This part of the procedure fixes the sample thickness and is illustrated in Figure 28. Squeezing flow is caused between the plates during insertion. This ensures good contact between the sample and the moving plate.

Next the oven fan should be reactivated. Once thermal equilibrium is reached, the operator can set up test programs from the computer terminal. After the test is completed, the sample can be scraped out and a dynamic calibration can be performed. The oven can be left on continuously, but samples should be thoroughly scraped from the plates. However, the shear stress transducer should not be left in the oven for extended periods when there is polymer around the cantilever, as polymer tends to carbonize after several hours. During continuous operation, it is good practice to remove the shear stress transducer for cleaning once per day and to keep it outside the oven when not in use.

c. Tips on Proper Assembly

With few exceptions large torques are not required for proper assembly and disassembly of the rheometer. This is particularly true of the shear stress transducer which can usually be assembled and disassembled with light implements and finger tightness. Undue tightness during assembly and disassembly almost always produces a damaged thread. A trip to the machine shop is advised to repair the thread before worse damage results.

Bolts used at high temperature tend to stick and seize. This problem can be eliminated by applying an anti-seizing compound, specified for high temperatures, to the threads of all threaded parts during assembly. A product sold under the commercial name NEVER-SEEZ and shown in Figure 135 was used effectively for this purpose.[*,511]

10. Temperature Control

More than forty papers describing sliding plate viscometers and rheometers used at high temperature were found and reviewed. These instrument designs can be classified in three groups. In the first group the shear fixture is enclosed in an environmental chamber. In the second category heaters are in direct contact with the plates. The third category is a two-pronged approach, combining an environmental chamber with directly applied heat.

a. Environmental Chambers

The most widely used design for high temperature work is the environmental chamber. By enclosing the shear fixture in a thermostated

---

*Under no circumstances should this grease come in contact with the bearings, for it will cause them to seize immediately.

chamber, the sample's temperature can be as uniform as the chamber. Heat loss through drive shafts extending outside the chamber can cause the steady state sample temperature to be lower than that of the environmental chamber. This is the case with rotational instruments using small shear fixtures.

The most common type of environmental chamber used with sliding plate viscometers or rheometers is the thermostated, insulated, free convection air oven[512,513,514,515,516,517,518,519,520,521,522] This type of chamber has also been used for low temperature sliding plate rheometry.[523] In these systems the uniformity of the sample temperature depends on natural convection. Free convection water baths have also been used with sliding plate rheometers for high temperature work.[524,525] In fact, an ASTM standard for sliding plate viscometry specifies a water bath for elevated temperature work.[526]

Forced convection air boxes are used in some commercial sliding plate rheometers.[527,528] The need for forced convection is due to a combination of low thermal mass of the shear fixture and significant heat loss through the shear fixture mounts, which extend outside the oven. Sample temperature perturbations caused by conduction losses can be significant for shear fixtures of low thermal mass. On the other hand, fixtures of high thermal mass will respond more slowly to changes in bath temperature and can take too much time for thermal equilibration when natural convection alone is relied upon. For instance, a sliding plate fixture weighing 150 pounds required about four hours to reach equilibrium. This complicated chamber enclosed the sliding plates in an air box which was itself immersed in a constant temperature oil bath.[529,530]

b. Direct Heat

Few designs place heaters in direct contact with the sliding plates. Some ink viscometers maintain sample temperature by circulating water through channels bored in the shearing plates.[531,532] In a sandwich type creep rheometer, the outer plates were fixed directly to the thick walls of the electrically heated chamber.[533] The advantage of applying heat directly to the plates is that the rheometer can be brought up to temperature faster than in systems relying on natural convection.

One disadvantage of direct heat is that the higher heat transfer rates to the rheometer can induce high temperature gradients in the shear fixture If the resulting thermal stresses are high enough, plastic strain can result leaving the shear fixture permanently warped. Tee and Dealy (1974) encountered this problem with their oil-jacketed concentric cylinder rheometer.[534]

Another disadvantage of direct heat application is difficulty in obtaining a uniform sample temperature. For example, the ink viscometers mentioned above can allow temperature variations within the ink depending on its proximity to the heating channels. On the other hand, resistance heaters in direct contact with the plates can apply heat uniformly across the sample surface such that heat losses at the sample's edges can cause temperature gradients within the sample.

McCarthy's self-charging rheometer overcame the disadvantages of direct heating by combining high conductivity metal with a low thermal mass fixture.[535]

c. Combining Chambers with Direct Heat

The combination of direct heated plates in an environmental chamber combines the advantages of low heat-up time and good sample temperature uniformity. For instance, Humphreys and Stone submerged a watertight environmental chamber for a sliding plate viscometer in a thermostated bath.[536] A small electrical heater, located under the moving plate, enabled the sample to be brought rapidly up to the experimental temperature. The risk of plate warpage, of course, exists whenever high heat transfer rates are employed.

d. Heating the New Rheometer

Two deep-well, J-type, glass jacketed wire thermocouple junctions were seated in the stationary plate, and one was seated near the geometric center of the moving plate. This thermocouple was used in the temperature control loop with a Thermoelectric Model 204 bandwidth proportional controller, which is visible in Figure 32. A Fluke multi-probe digital indicator was used for temperature display. Three independent measures of sample temperature were made using thermocouples in both plates. When all three temperatures agree within ½°C, the sample is judged to be at thermal equilibrium. Room temperature, oven air temperature, and the temperature of the MTS crosshead near the load cell were also monitored.

Two measures of oven performance are pertinent to rheometers for molten plastics. One of them is the time required to bring the shear fixture to thermal equilibrium from room temperature. A more important measure of oven performance is the time required to bring the system back to equilibrium after an excursion in temperature such as that observed during sample insertion.

(1) Oven Heat-Up Performance

Figure 29 shows a typical heat up curve for the new rheometer. These data are taken for heat-up from room temperature to setpoint temperatures of 28°C to 180°C respectively. The stationary plate of the rheometer is suspended away from the moving plate to increase the heat transfer surface. Furthermore, an additional 1 inch layer of fiberglass insulation was added to the walls of the Fisher oven to decrease heat losses. The moving plate reaches thermal equilibrium 2 hours after start-up, and the air temperature reaches a maximum value of about 210°C. This time can seem annoyingly long, but it can be circumvented by (1) running the oven continuously or (2) using an automatic timer to activate the oven well before work time.*

Interestingly, the time required for thermal equilibrium is comparable to that required for the much smaller commercial rotational instruments which, by virtue of their low thermal masses, allow temperature fluctuations to persist for a long time.[537]

(2) Oven Excursion Performance

The oven performance data collected for oven heat-up and used for Figure 29 can be generalized to predict oven performance under any transient condition of practical importance. Newton's law of cooling is.[538]

$$dT_p/dt = k\ (T_a - T_p)\ , \tag{156}$$

where T_p is the plate temperature, T_a is the air temperature and k is an instrument constant. Now dT_p/dt can be estimated from experimental data using the method of Whitaker and Pigford which is briefly described in the chapter on results.[539] Results are listed in Table 2 and plotted in Figure 30.

---

*The author prefers the first choice since it eliminates thermal cycling of the linear bearings which, in principle, may bend under thermal stresses arising primarily during heat-up. In practice, no such distortions were observed.

Table 2: Approximation of Heat-Up Rate

Time, h	T_p, °C	dT_p/dT, C°/h
0	27.7	
.167	34.2	-
.333	48.2	87.7
.500	66.8	105.
.667	84.5	112.
.833	104.	111.
1.00	[illegible]3.	108.
1.17	140.	99.4
1.33	156.	88.3
1.50	170.	64.2
1.67	181.	31.3
1.83	181.	3.91
2.00	177.	-11.1
2.17	175.	-6.70
2.33	174.	.559
2.50	177.	-
2.67	177.	-

The plot shows dT_p/dt to be proportional to (T_a-T_p). A least squares regression of (dT_p/dt) versus (T_a-T_p) gives the value of the proportionality constant, $k = 1.91°C/h$. Hence, for practical purposes the drop in plate temperature during sample insertion can be estimated by evaluating (156) for the case when T_a drops abruptly to room temperature, T_r, starting from thermal equilibrium, T_{eq}.*

$$dT_p/dt = k\,(T_a-T_r) \tag{157}$$

*Of course the temperature in the oven actually stays considerably warmer than this so our subsequent estimates for effect of insertion time will be conservative.

The solution is:

$$(T-T_r)/(T_{eq}-T_r) = \exp(-kt) \tag{158}$$

This gives an estimate of the deviation in plate temperature from thermal equilibrium caused by sample insertion. Defining the final temperature, T_f, at insertion time, t_i, and one obtains:

$$T_f = T_r - (T_r-T_{eq}) \exp(-kt_i) \tag{159}$$

Because the rheometer has large thermal mass and is heat-soaked we can assume that the oven air temperature jumps back to the setpoint quickly and one obtains

$$(T-T_{eq})/(T_f-T_{eq}) = \exp(-kt) \tag{160}$$

We know this result is valid because it agrees with experimental observations. Combining (159) and (160) gives the desired expression for unaccomplished temperature difference from the desired equilibrium temperature.

$$X = (T-T_{eq})/(T_r-T_{eq}) = [1-\exp(-kt_i)] \exp(-kt) \tag{161}$$

Using $k = 1.91°C/h$, obtained above, a series of plots are given in Figure 31 showing the effect of insertion time on equilibrium recovery. For a sample insertion time of 2 minutes, a typical value, the elapsed time required for plate temperature to recover to within 5% of equilibrium is 8 minutes. It was observed that the actual time required for the plate temperature to return to the setpoint after insertion is roughly equal to double the insertion time. This is why a large thermal mass is highly desirable for a rheometer designed for quick sample insertion, operating continuously in the heat soaked condition.

11. Materials of Construction

Stainless steel, although expensive, is the material of choice for rheometers for molten plastics. Specifically, any of the 400 series of stainless steels are magnetic and can be firmly secured with a magnetic chuck for drilling and grinding. This property permits accurate fabrication, because parts are deformed when they are secured mechanically.[540] The result is that roughness heights of 1/10,000th of an inch, without flaws, can be obtained on a grinder equipped with a magnetic chuck. This is why the 400 series stainless steels are commonly selected for fabrication of plastics process equipment.[541] The 420 stainless steel was annealed but not heat treated. Perry and Chilton list the properties of this material.[542]

Furthermore, the entire rheometer, including the shear stress transducer, was fabricated from the 420 series stainless steel. This eliminated the possibility of thermal stresses due to joining of materials of different lineal expansion coefficient. The linear bearing table is made of nickel plated carbon steel, since this item is not currently available in stainless steel.

D. Actuator Control and Data Acquisition

As mentioned in the chronology, the author successively employed three different systems for controlling plate motion.

1. Electromechanical Actuation

Preliminary work, done on the room temperature prototype, used a closed loop speed-controlled electromechanical drive system described elsewhere.[543] The drawbacks to this approach to actuator control are three-fold. Firstly, it limits shear history selection to steady shear and steady oscillatory shear. Secondly, the power surge that occurs at start-up causes the first few cycles to be at higher frequencies than the setpoint frequency. For high frequency measurements this can cause melt fracture. This problem can be partially avoided by gently moving up to the setpoint frequency with the speed selector but this strategy subjects the sample to several cycles, which increases likelihood of melt fracture. Thirdly, changing the displacement amplitude is tedious because it is achieved by adjusting the eccentricity of the rotating disks.

The main advantage of open-loop control electromechanical drive is low cost. Upgrading to position controlled closed loop electromechanical actuation is more expensive than the servohydraulic approach for systems of comparable dynamic performance.

2. Servohydraulic Actuation

The prefix servo- denotes closed loop control. A servohydraulic drive system engages the high pressure drop in a flowing hydraulic fluid to generate precisely controlled motion. The control system consists of a linear variable displacement transducer, LVDT, a servo controller, a function generator, and a servovalve driver. The LVDT monitors actuator piston position and conveys this to the servo controller. The function generator computes the desired position, which is also conveyed to the controller The controller monitors the difference between the command and actual piston position signals. This difference is, in turn, transmitted to the servovalve driver In layman's terms, the function generator tells you where the piston ought to be, the LVDT tells you where the piston is, and the controller measures the difference. Finally, the loop is closed when the servovalve driver responds to the error signal by proportioning oil flow in either chamber of the piston reservoirs. The system gain is adjustable so that system response characteristics can be tuned for peak dynamic performance This is particularly useful for tests involving fast transients. The error signal, accessible from the front panel, gives the operator a real time measure of accuracy for the piston motion.

Such servohydraulic systems are routinely used in force controlled experiments on solid samples. This option could in principle be used for shear stress controlled experiments on viscoelastic fluids such as creep, using the new sliding plate rheometer. In practice however, the range of stress-controlled experiments that can be performed will be limited to low rates of change of stress and to low stresses. This is expected because the system gain will depend on the fluid properties. A previous attempt to use a sliding plate rheometer for force controlled experiments with a servohydraulic actuator was unsuccessful.[544] With specially designed electronic circuitry, however, capability for stress-controlled testing could be developed for the new rheometer.

An important application for servohydraulic drive systems is for solids testing where precise motions are needed to determine solid-state properties Furthermore, servohydraulic drive systems are highly desirable for the study of nonlinear viscoelasticity in solids where large motions under high loads are required. Because it is the fast transient properties that are of interest to plastics engineers, one needs to move one part of the shearing fixture quickly and precisely. Hence, servohydraulic drive systems, long-since used for sophisticated solids characterization, are well suited to driving rheometers.

There are several reports of servohydraulic drive systems being combined with rheometers for the successful measurement of nonlinear viscoelastic properties of polymeric liquids. In the review of sliding cylinder rheometry, it was seen that an MTS servohydraulic drive system has been used for large amplitude oscillatory shear.[545] Also, the group at the University of California at Berkeley have combined an MTS servohydraulic drive system with a programmable function generator, providing great flexibility in flow definition.[546,547,548] A broad spectrum of nonlinear viscoelastic properties were measured in both sliding plate and sliding cylinder instruments.[549]

A detailed discussion of servohydraulics is clearly beyond the scope of this work Standard texts can be consulted on servohydraulic systems for this purpose Suffice it to say that the programmability of such systems makes them extremely flexible, and that the physical limitations of the particular system used herein can be estimated from Figure 18.

The MTS servohydraulic actuator can be controlled in either analog or digital mode.

a. Analog Control

In the analog mode, a shear history can be selected using front panel switches Here the selection is limited to square, triangular and harmonic waveforms.

(1) The MTS Harmonic Waveform

Most rheometers use the simple sinusoid for oscillatory shear testing: $\gamma(t) = \gamma_0 \sin \omega t$. Instead of a sinusoid, in MTS equipment the harmonic function used for oscillatory shear is:

$$\gamma(t) = \gamma_o + \gamma_o \sin (\omega t - \tfrac{1}{2}\pi). \tag{162}$$

This is a sinusoid that has been translated along the ordinate by γ_o and phase shifted by $-\pi/2$. Note that (162) has two equivalent forms:

$$\gamma(t) = \gamma_o (1 + \cos \omega t) \tag{163}$$

$$= 2 \gamma_o \cos^2(\tfrac{1}{2}\omega t) \tag{164}$$

where $2\gamma_o$ is called the double amplitude of shear strain.

b. Servocontrol Hardware

In addition to the components of the servocontrol system described in the last section, which are based primarily on analog electronics, a microcomputer based control system was added to the servohydraulic hardware. This was done to help with instrument development and to make the selection of shear history more flexible. This control system is integrated with the data acquisition hardware and software described below.

The dynamic capabilities of the instrument are those shown in Figure 18, these are valid for both the analog and digital modes of instrument operation. However, whereas the analog mode provides a limited number of user selectable flows, the microcomputer based systems allow one to design tests arbitrarily.

(1) Actuator Resonant Frequency

The hydraulic fluid column that generates the piston motion has a resonant frequency of its own. In general, this frequency is:

$$f_c = 2000 \sqrt{(A/wL_s)} \ , \tag{165}$$

where A is the piston effective area in sq.in., w is the weight of the piston/moving plate assembly in lb_f, L_s is the stroke length in inches, and f_c is in Hz.[550] Hence, for the model 204 actuator a resonant frequency of 300 Hz is predicted. Obviously, components of frequency spectra that are near 300 Hz should be avoided.

c. Servocontrol Software

All the communication required between the operator and the instrument is carried out by running compiled MTS BASIC programs. The data acquisition and servocontrol systems form one integrated package. A complete description of this package is contained in the MTS BASIC user manuals. Users of MTS systems may find useful the subroutines included in the programs given below. Suffice it to say that the sliding plate can be caused to move in a programmed fashion with specially designed statements incorporated into the MTS BASIC language.

3. Data Acquisition

a. Measurement Hardware

Before installing the digital data acquisition system, two other modes of data acquisition were tried. In preliminary work analog devices were used to record shear stress and strain in oscillatory shear tests. These were recorded as loops, by making polaroid photographs of the display of a storage oscilloscope set to operate in X-Y mode. Analog methods, previously described by Tee,[551] were also used to generate a signal proportional to the shear rate so that stress-strain rate loops could be recorded in real time.

These analog acquisition methods were later replaced by a digital storage scope* interfaced with an IBM personal computer. This method was particularly helpful for tests requiring very high speed data acquisition, such as the free beam mechanical damping factor measurements discussed in the section on shear stress transducer design. The software used to transfer data from the Tektronix digital storage scope to the personal computer has been described by Patel.[552] For all rheological testing, data acquisition was accomplished using the integrated data acquisition boards installed in the MTS servohydraulic system.

(1) Digital Versus Analog Methods

*The time constant for this scope is roughly 1.4 ps.

A comparison of the pros and cons of each approach to data acquisition is in order. Using analog methods it was difficult to obtain an oscillograph because much time was lost trying to center the loop on the analog scope before a photograph could be taken. However, analog methods provide the experimenter with an immediate picture of the state of his sample This can be an invaluable guide to the instrument developer who wishes to detect the source of problems with the rheometer. For instance, the onset of melt fracture can be detected at a glance by observing the scope output.

This being said, the best long term record of experimental work is provided through digital recordings. For instance, the importance of a design change in the rheometer can be quantitatively recorded for future reference. The comparison of oscillographs is a tedious process, which does not lend itself to efficient communications between coworkers. Hence, the process of instrument development was greatly accelerated by the addition of digital methods.

Finally, it will be seen that the addition of the PDP-11 data acquisition system, which permits high speed discrete Fourier transforms of collected data, greatly accelerated the development program.

b. Measurement Software

The integrated digital data acquisition package for the rheometer uses the RT-11 operating system,* which supports the MTS BASIC language.** This computer language is designed expressly for the materials scientist and will particularly benefit those needing flexibility in flow history selection.[553,554] The language includes statements that activate the built-in acquisition boards, allowing simultaneous four-channel sampling at rates up to 1000 Hz.

E. How to Design a Shear Stress Transducer

1. Operating Principle

The transducer, designed especially for measuring shear stress in molten plastics, is an active, positive-displacement probe, which is flush-mounted in the stationary plate of the rheometer. The shear stress acting on the free end of the beam causes lateral beam deflection which, when the transducer is properly designed, is proportional to the shear stress. To obtain a good dynamic response, the free end deflection must be much smaller than the gap between the active face and the housing. Beam length and diameter can be varied to allow for different ranges of shear stress from a single transducer. The lower limit for the shear stress range is dictated by the proximeter noise level.

2. Dynamic Beam Deflection Measurement

---

*A product of the Digital Equipment Corp.

**A product of the MTS Systems Corp.

As was seen in the general review of shear stress transducers, there is more than one way to convert a shear stress to an output voltage. Although the method of measuring beam deflection was pursued in the present work, other methods that appear equally promising for high temperature work were also considered These include mounting a small piezoelectric load cell[555] or a piezoelectric accelerometer on the cantilever.[556]

a. Proximeter Noise Level

The two most important criteria for proximeter selection are heat resistance and background noise level.* With a maximum free end deflection of 4 mil, we require a measuring range of about 1 mil at the proximeter, normally at the cantilever midpoint. With this displacement magnitude one requires a noise level of about .001 mil so that displacements can be clearly measured Several commercial proximeter systems were considered including those based on inductance, eddy current, magnetic reluctance and capacitance.[557,558] However, despite being available in heat resistant configurations, neither inductance, nor eddy current, nor magnetic reluctance based systems met the noise requirement.

It will be seen that the dynamic response of the transducer is largely determined by the effect of the squeezing flow of the polymer that surrounds the free end of the beam. When the beam deflects, this polymer

*By noise we mean the root mean square value of all spurious components. Hence, it may be broadband or otherwise.

is stretched, sheared or squeezed depending its position around the free end. Soong has given a first approximation to the effect of squeezing on the transducer response for a power-law fluid.[559] It was assumed that of the three modes, squeezing caused the most damping, so only this mode was analyzed. The dynamic response of the transducer improves with increasing beam stiffness, which is limited by the proximeter resolution.

b. Heat resistance

Since the rheometer is enclosed in an oven, the method of local shear stress transduction must perform well at high temperature. Piezoelectric accelerometers and load cells, optical and capacitance proximeters can all, in principle, meet the noise level requirement with sufficient heat resistance.[560,561] However, the capacitance systems are commercially available and can be used at temperatures up to 600°F.[562]

c. Optical Probes

The optical probe used in preliminary work on the room temperature prototype has transmitting and receiving fiber bundles.[563,564] When the end of the fiber bundle is near the reflective surface, transmitting fibers project light onto the mirrored cantilever surface, and receiving fibers return reflected light to a photosensor. Receiver illumination and instrument output are linear with proximity over a limited range, and the dynamic response of such systems is extremely good.[565,566] A model KD-100 Fotonic Sensor system, manufactured by MECHANICAL TECHNOLOGY INC. was used with a hemispherical probe configuration.* The fiber bundles are embedded in a polymer matrix that is not heat resistant. In principle, a heat resistant epoxy can be substituted for the usual polymer matrix, but such methods remain developmental.[567]

d. Capacitance Proximetry

The use of capacitance displacement measurement is advised for high temperature shear stress transducer applications.** Its time response is adequate for measuring nonlinear viscoelastic properties, it is a proven off-the-shelf technique, and it has been used successfully at 600°F.[568] This method is insensitive to temperature because the dielectric constant of air is sensibly constant over a wide temperature range.[569]

There are several capacitance proximeter systems sold commercially. Their calibrations may or may not depend on offset distance, an important practical consideration.

(1) Offset Dependent Calibrations

The offset distance, also called stand-off distance, is the separation between the capacitance probe and the target surface with the target

---

*Early work found little success with the model KD-45, a first generation Fotonic sensor, where calibration drift and background noise made its use difficult.

**The advice of Mr. Curtis Kissinger, Applications Engineer, MECHANICAL TECHNOLOGY INC., Latham N.Y. is gratefully acknowledged.

surface in the undeflected position. Some instruments require recalibration whenever the offset distance is changed. The advantage of such systems is that the probe range also changes with offset. Hence, these systems have a continuously adjustable noise level and measurement range with a single probe. The disadvantage of such systems is that they require recalibration with even a slight change in offset distance.

In one such circuit the measured capacitance modulates the circuit's electrical resonant frequency. A frequency-to-voltage converter, coupled with a linearizing circuit, allows accurate proximetry with an excellent dynamic response.[570,571] Unfortunately, the linearizing adjustments are also offset-dependent, which requires frequent, time-consuming recalibration.* Frequency modulation based systems have excellent frequency response and low noise levels, but available commercial models are susceptible to baseline drift caused by stray capacitances. Probes for such systems must be fabricated for individual applications as they are not currently sold commercially.

Another offset-dependent system uses a DC voltage across the gap for polarization. The gap forms part of a DC circuit, that provide a voltage proportional to displacement. Again, the sensitivity of the probe depends on offset, and this requires recalibration with every change in offset.[572,573,574,575]

---

*Note that with a digital approach to data collection, the problem of linearizing can be eliminated by performing it later during data processing. Hence, a voltage versus offset curve could be used to obviate the need for recalibration with such systems.

(2) Offset Independent Calibrations

Several systems have been used that provide offset independent sensitivity. Such systems do not require recalibration after a change in offset, which saves considerable operating time. Offset independence is achieved using a guard field around the active face of the capacitance probe.[576,577] The guard field keeps the electrical field linear at the active face so that the capacitance has its theoretical value:

$$C = D_e\, A/D\ , \tag{166}$$

where D_e is the dielectric constant of air, A is the effective area, and D is the distance between the probe and target surface. This guard sheath extends all the way back to the amplifier* providing a shield against stray capacitance effects.[578,579,580,581,582,583,584] An amplitude modulated circuit is used along with a subtractor circuit to remove offset voltage so that D is proportional to instrument output over a wide range of offset positions.[585,586,587] The sensitivity of such a system is changed by using probes with different effective areas.

The specific system used herein is sold under the commercial name Accumeasure-1000.**,*** The system's front panel is shown in Figure 32.

*See probe to cable connection in Figure 140.

**A product of MTI Instruments Inc., Latham, N.Y.

Two probes were used, models ASP-5HT and ASP-1HT, which have ranges of 1 and 5 mil respectively. These probes incorporate a special heat resistant epoxy used for the electrode-guard ring spacer.[588] This ring of epoxy is visible around the small circular active area at the probe tip. Figure 33 shows the tapered probe tip, also visible in Figure 34. This configuration is used for probes with ranges under 5 mil, because probe positioning is difficult when the probe is not tapered.[589,*] The method of adjustment of the probe stand off distance is illustrated in Figure 139.

e. Optics Versus Capacitance

Preliminary work permitted a direct comparison of a capacitance proximeter with the previously used optical sensor at room temperature. The results of this comparison are shown in Figure 35 for a static calibration sequence. A dimensioned drawing of the capacitance probe mounting fixture designed especially for this test is shown in Figure 36. Both probes were mounted opposite one another for the comparison. Here, a non-tapered model ASP-2 capacitance probe is compared with the optical probe described above.

Lower noise levels detected with the capacitance probe. Furthermore, the optical method suffered from an annoying drift in both baseline and

---

***The manufacturer's specification for the frequency response of the Accumeasure system is 5 kHz at -3dB. This gives a time constant of 3.2 x 10^{-5} sec.

*As of 1987, all commercial probes are supplied with tapered tips.

sensitivity, which required that recalibration be performed even between measurements. Furthermore, for the capacitance system, no measurable drift in capacitance probe sensitivity or baseline was observed over the trial period of two weeks.

3. Cantilever Design

The design of a cantilever for the shear stress transducer seems simple at first glance A good working beam however is designed around several contending criteria. These are explained below.

a. Beam Stiffness

(1) Lateral

The most important equation for cantilever design is the relation giving the lateral deflection caused by a lateral force, P This is the basis for the operation of the transducer. Here, the lateral deflection, δ, is taken in the 1 direction and the beam axis is in the 2 direction. Letting x_2 be the distance from the beam's fixed end, a force balance on the beam gives:[590]

$$\delta = Px_2^2\ (3a-x_2)/6EI, \qquad 0<x_2<a \tag{167}$$

and

$$\delta = Px_2^2\,(3x_2-a)/6EI, \qquad a<x_2<L\ , \tag{168}$$

where P is the lateral load applied at $x_2=a$, E is the tensile modulus, L is the beam length, and I is the moment of inertia. For a beam of circular cross-section the moment of inertia about x_1 is $I=\pi D^4/64$ The new calibration procedure, described in the next chapter, makes use of (167) and (168) However, the working transducer has the applied load at $x_2=L$ so that

$$\delta = Px_2^2(3L-x_2)/6EI\ , \tag{169}$$

gives the deflection caused by the shear stress acting at the free end. Note that (169) summarizes the operating principle of the shear stress transducer Potential causes for deviation from this ideal deflection are discussed below

A rule of thumb for transducer design is to limit the free end deflection to one half the gap between the housing and the beam at the free end For an 8 mil gap, a tolerance acceptable to the machinist, free end deflection is limited to 4 mil With the beam length chosen to be 7 cm and the free end area chosen as 1 sq cm., a design plot of beam diameter versus shear stress range can be constructed Shown in Figure 37, different beam diameters can then be chosen for the desired shear stress ranges. Three beams were fabricated for the new shear stress transducer, with ranges of 1.2, .6 and .1 MPa

(2) Longitudinal

The normal stress differences arising in viscoelastic materials in simple shear can cause deviations from (169) if longitudinal stiffness is sufficiently low. When there is no lateral force on the beam, there will be no lateral deflection caused by a normal thrust acting on the beam's free end. However, when the beam is laterally deflected, an additional deflection is caused by normal thrust.

A first approximation to the additional deflection caused by the normal force, N, is:[591]

$$\delta_e = Nx_2/EA \tag{170}$$

and the fractional error induced by this deflection is:

$$\epsilon = 1 - (1+K)^2 \, (1-Kx_2/(3L-x_2)) \, , \tag{171}$$

for $|P|>0$ where,

$$K = N/EA. \tag{172}$$

Hence, the case when P=0 is a singularity and the fractional error caused by the normal load is independent of P for all other loads. Evaluating (171) at $x_2=\frac{1}{2}L$ gives:

$$\epsilon_{\frac{1}{2}} = -1.8\,K - 0.6\,K^{2} + 0.2\,K^{3} \,. \qquad (173a)$$

Figures 38a-38c can be used for graphical estimation of this error when the displacement probe is at the beam midpoint.

Recall that (170) is only an estimate of the normal thrust error. A more complicated analytical solution for the case of combined lateral and normal loads at the cantilever's free end is:[592,593,594]

$$\delta = PL^{3}/3EI\,[1 + .4Q + (17Q^{2}/105)] \text{ for } Q < .53 \,, \qquad (173b)$$

where $Q = NL^2/EI$. This is useful for checking the accuracy of (170).

(3) Torsional

As was discussed under basic concepts, fluids are assumed to exhibit no stress couples. For fluids that do exhibit stress couples,[595] an additional deflection will result from the moment, M, acting on the cantilever's free end.

The moment, M, causes lateral deflection, δ, and, in the absence of other loads:[596]

$$\delta = Mx_2^{2}/2EI \,. \qquad (174)$$

The case of combined lateral load with free end moment has not been studied. Perhaps (174) could be used as the basis for a special transducer for verifying the assumed absence of stress couples.

b. Nonuniform Beams

Beam stiffness depends primarily on the stiffness near the fixed end. Hence, much machining time can be saved by simply varying the thickness of the top half of the beam for varying shear stress range. This is especially true for thin beams, which have a strong tendency to buckle on the lathe. The shapes of the three beams used for the new transducer can be seen in Figure 34. Of course, when the bottom half of the cantilever is thick, it is slightly softer than the straight beam predictions of (167)-(169). The lateral deflection of the top section for the lateral force, P, acting at the free end is:

$$\delta = PL_1^3/3EI_1 + PL_2L_1^2/2EI_1, \qquad x_2 = L_1. \tag{175}$$

Also, the lateral deflection at the free end for a lateral force acting at L_1 is:

$$\delta = PL_2^3/3EI_2 + P/EI_1\ (L_1^3/3 + L_2L_1^2 + L_2^2L_1/2),\ x_2 = L_1+L_2\ , \tag{176}$$

where L_1 is the length of the beam's top section and L_2 is the length its lower section. Only the diameter of the top half of the beam need be changed to alter transducer sensitivity. The deflection given by (176) cannot exceed the gap between the housing and the beam's free end, which is 8 mil.

c. Calibration Stiffness

If the proximeter is located near $x_2 = L_1$, where the top and bottom sections meet, then the deflection at the proximeter is given by (175). Furthermore, if the calibration hook is located opposite the proximeter, then the deflection caused by the calibration weight, P_{cal}, is:

$$\delta_{cal} = P_{cal}L_1^3/3EI_1. \tag{177}$$

Setting (175) equal to (177) relates the calibration weight to the free end force that would cause an equal deflection. Hence, the ratio of equivalent shear stress to the calibration weight, σ_{eq}/P_{cal}, is:

$$\sigma_{eq}/P_{cal} = 2A_{af}/(1 + 3L_2/L_1)\ , \tag{178}$$

where A_{af} is the area of the transducer's active face. This is the working relation for transducer calibration. Hence, so long as the proximeter is located at the shoulder between top and bottom sections, at $x_2 = L_1$, the relation between equivalent shear stress and calibration weight is a simple one For a circular beam:

$$\sigma_{eq}/P_{cal} = 8/[\pi D_{af} (1 + 3L_2/L_1)] \ , \tag{179}$$

where D_{af} is the active face diameter

d. Resonant Frequencies

Resonant frequencies in mechanical systems pose a theoretical limit on the frequency content of their forced motion. The classic examples of parts shattering and bridges collapsing come to mind For shear stress transducer cantilevers, however, the squeezing flow at the free end adds enough viscous damping to eliminate beam resonant frequency effects, which are clearly observable on a dry transducer Measurements above or below these resonant frequencies are equally feasible. It is only when a frequency component approaches a resonant frequency that a theoretical problem arises Although measurements near the resonant frequency of the cantilever and its nearest subharmonics are to be avoided, in practice, transducer errors rarely arise from such effects.

(1) Lateral

A cantilever can resonate laterally at several frequencies. In fact, in principle, there is an infinite set of lateral frequencies for lateral resonance. An accurate estimate of these frequencies is:

$$\omega_r = p^2 \sqrt{(EI/A\phi)} \,, \tag{180}$$

where p is an element of the set of positive roots of[597,598]

$$\cosh pL \cos pL = -1 \tag{181}$$

The first seven lateral modes for beam resonance are pL = 1 6, 4.7, 7.8, 11 0, 14 1 and 17 3 A design plot is easily constructed with ω_r for a particular beam length versus the diameter of the straight beam. Figures 39a-39b are plots used in the design of the new transducer It includes the first four modes of lateral resonance Note that (180) is approximate and its accuracy has been demonstrated using a more accurate numerical analysis[599]

(a) Experimental Determination

The first lateral mode resonant frequency of the transducer cantilever is readily measured with a time domain sampling of beam deflection with the beam in free oscillation. This is best accomplished using a digital oscilloscope in triggering mode for displacement measurement. Free oscillation is easily induced by suddenly releasing an applied load from the transducer calibration hook.* For an initial displacement d_i, an underdamped second order system will respond with an oscillation of decreasing amplitude according to:

$$d/Kd_i = -\exp(-\eta\omega_n t)/\sqrt{(1-\eta^2)} \quad \sin[\sqrt{(1-\eta^2)}\,\omega_n t + \phi] + 1 , \tag{182}$$

where

$$\phi = \arcsin \sqrt{(1-\eta^2)} . \tag{183}$$

From (182) it can be shown that a plot of the logarithm of half-wave rectified (HWR) displacement against time will be a straight line of slope $-\eta\omega_n$. Figure 40a is a typical displacement response to the step input showing damped free oscillation. Figure 40b shows that by expanding the time scale the mode 1 resonant frequency can be measured. The log plot of HWR displacement, shown in Figure 40c, is linear so the clean transducer has second order frequency response.

The mode 1 prediction, provided by (180) is 1510 Hz, which agrees well with the beam #1 determination. Also, the resonant frequencies for nonuniform beams are more difficult to predict from first principles.

---

*Very sudden release can be achieved by snipping a piece of fishing line supporting the weight suspended from the calibration hook.

Table 3. Beam Resonant Frequency Determinations

Beam #	L, cm	L_1, cm	ω_n, Hz	η
1	7.00	L	1440	00175
2	7 00	3 50	730	.00172
3	7 00	3.50	46	00127

Figure 48 shows the second order phase errors calculated for beams #1 and #2 Figure 49 shows the second order phase error curve calculated for beam #3 For beam #3 the resonant frequency of the beam appears in the expected measurement range for the rheometer Beam #3 cannot be used for measurements with frequencies harmonically related to 46 Hz

(2) Longitudinal

A cantilever can also resonate longitudinally. In principle, this could be caused by the oscillating component of normal thrust due to the first normal stress difference The infinite set of longitudinal resonant frequencies for a cantilever is[600]

$$\omega_n = m\sqrt{(Eg/\phi)}/2L, \quad m=1,3,5,. \tag{184}$$

where ϕ is beam density, g is the acceleration due to gravity, E is Young's modulus and L is beam length. For the beams used for shear stress transducers, these resonant frequencies are usually much higher than those for transverse mode resonance. For instance, for beam #1, (184) predicts a mode 1 longitudinal resonance at 5800 Hz.

e. Configuration of Free End

In addition to increasing beam stiffness, a further improvement can be made to the dynamic response of a shear stress transducer by sharpening the edge at the free end of the beam [601] This minimizes the squeezing flow in the polymer in the beam/housing gap. This improvement can be large for soft beams, but is less important for stiffer systems. The sharpened edge is visible on the three beams shown in Figure 34. The concentricity of the free-end in the circular orifice in the housing is maintained by an alignment pin which fits tightly in a circular hole drilled through the threads on the fixed end of the cantilever. Views of the fixed and free ends of the cantilever are shown in Figures 136 and 138 for the assembled transducer.

f. Buckling Criterion

When working with thin beams, one must also guard against buckling. A cantilever will buckle when the normal force on the beam exceeds.[602]

$$P_{cr} = \tfrac{1}{4}\pi^2 EI/L^2 \qquad (185)$$

For the beams used in the new shear stress transducer P_{cr} is never exceeded.

4. New Method of Static Calibration

Shear stress transducer calibration is not to be confused with proximeter calibration. Proximeter calibration is the measurement of signal output per unit cantilever displacement. Shear stress transducer calibration is signal output per unit shear stress acting on the active face. Methods previously reported for shear stress transducers calibration are all static calibration techniques. They include introducing a known deflection to the beam by suspending weights from, and orthogonal to, the active face.[603,604,605,606] There are two main drawbacks to this approach. Firstly, one must bond a hook to the active face. This takes considerable time and can be accomplished neither at high temperature nor with a sample in the rheometer. Although the method does permit calibration of the shear stress transducer, it is inconvenient and time consuming. Secondly, obtaining good bonding to the active face is difficult.

An equally tedious technique for calibrating the shear stress transducer would be using a fluid of known viscosity. This method must ultimately be used but is not useful for day to day calibration checks.

A new calibration method was devised that permits the calibration of the shear stress transducer in seconds with or without the sample in place and at the temperature under study. The benefits of such a technique are significant since most rheometers, including cone-plate rheometers, require the calibration of the stress cell with the sample removed from the unit and the fixture at room temperature. Such an approach does not permit quick checks of the calibration, say between tests on the same sample, and requires that one assume that the calibration observed with the fixture at room temperature is the same as that at the test temperature. When the transducer is itself temperature sensitive, this assumption is unsatisfactory.

Figure 41 shows the threaded end of a special hook which is passed through a port in the housing and threaded in a small hole in the cantilever. Such a modification allows weights to be hung directly from the cantilever beam with or without the sample in place and at the temperature of interest. Furthermore, the linearity of the calibration can also be quickly checked by sequentially hanging a series of different weights on the beam and plotting transducer output versus equivalent shear stress. Figure 42 shows the dead-pan assembly that extends below the oven so that the lead weights can easily be added from outside the oven. When the rheometer is suspended from a load cell, the load cell can be calibrated simultaneously. Finally, since the method is readily amenable to automation, the rheometer can, in principle, be made self-calibrating.

5. Techniques for Dynamic Calibration

The importance of dynamic calibration has been discussed under principles of dynamic measurement. Dynamic calibration of the shear stress transducer is accomplished by applying a known dynamic transverse load to the beam and recording the transducer response. When an oscillating force is used, the frequency response of the transducer is the phase lag and attenuation observed for each frequency. The stress amplitude dependence of the transducer's dynamic response can also be measured in this way by varying force amplitude. For dynamic calibration one needs a dynamic force source.

The MTS piston, otherwise unused during calibration procedures, is potentially a good dynamic force source. Specifically, a spring can be coupled between the transducer calibration hook and the piston. A special coupling, shown in Figure 137, was fabricated to fasten the spring to the piston and to align it with a small hole in the oven bottom. When the spring is properly selected, the piston motion causes a lateral force on the cantilever equal to the product of the spring constant and spring extension The piston displacement should be large relative to the induced cantilever deflection

Resonant frequencies of the spring make spring selection difficult, but when a good combination of spring and cantilever are found, good clean dynamic calibrations can be carried out. These tests can be carried out with molten plastic in the gap at the active face of the cantilever. The transducer response in the actual test condition can therefore be measured. Polymer must not contact the moving plate during dynamic calibration.

F. Total Force Measurement

The single most important result of this research is the experimental comparison of total force with local shear stress. It is this comparison that establishes the importance of the free boundary errors, the primary raison d'être for the development of the shear stress transducer.

The rheometer was suspended from an MTS load cell* positioned on the top side of the oven.[607] A long connecting rod was coupled to the center of the load cell, so that the coupling for the moving plate was aligned with the piston. There are three important sources of error associated with the load cell. Firstly, load cell compliance causes the stationary rheometer assembly to move. The resulting inertial forces subtract from the force the cell is intended to measure. Secondly, this motion causes a slight error in the shear strain measured by the LVDT. Thirdly, bearing friction causes noise in the load cell output, a problem typically encountered with traditional sliding plate rheometers.

1. Load Cell Compliance

The force exerted by the fluid on the stationary plate, F, is.

$$F = F_m + F_i, \tag{186}$$

---

*Model No. 661.19B-02.

where F_m is the measured force and F_i is the inertial force. Hence, the fractional error in the measured load is $\epsilon = F_i/F$.

a. Sinusoidal Load

Consider a cosinusoidal component of force exerted by the fluid on the stationary plate.

$$F = F_o \cos \omega t \ . \tag{187}$$

The inertial force is

$$F_i = -m\ dv/dt = -m\ d^2p/dt^2 \ , \tag{188}$$

where v is velocity of the stationary plate assembly, p is its position and m is its mass. Furthermore,

$$p = KF \ , \tag{189}$$

where K is the load cell compliance, the deflection per unit applied force. Hence,

$$F_i = -Km\ d^2F/dt^2 = Km\omega^2 F_o \cos \omega t \ . \tag{190}$$

The fractional error in measured load is:

$$\epsilon = Km\omega^2 \quad . \tag{191}$$

For the new rheometer the stationary assembly weighs roughly 35 Kg and for the MTS load cell, K = .005 mm/kN. For the new rheometer,

$$\epsilon = (209\mu sec \cdot \omega)^2 \quad . \tag{192}$$

A 100 Hz component of force will be attenuated by 2% and, when there is no mechanical damping in the load cell, compliance causes no phase error in measured load.

Furthermore, from (189) we see that the displacement of the stationary plate is.

$$d = d_o \cos \omega t = KF_o \cos \omega t \quad . \tag{193}$$

When d is significant relative to D, an error results in the imposed shear strain, since it is inferred from the position of the moving piston recorded with the LVDT. For a cosinusoidal displacement of the moving piston:

$$D = D_o \cos (\omega t - \delta) \quad . \tag{194}$$

The relative plate displacement is:

$$D\text{-}d = D_o \cos (\omega t - \delta) - KF_o \cos \omega t \quad , \tag{195}$$

which reduces to:

$$D-d = \alpha \cos(\omega t-\beta) \;, \tag{196}$$

where

$$\alpha = \sqrt{(D_o \cos \delta - KF_o)^2 + D_o \sin^2\delta} \tag{197}$$

and

$$\beta = -\arctan\left[\frac{\tan \delta}{1 - \dfrac{KF_o}{D_o \cos \delta}}\right] . \tag{198}$$

Hence, load cell compliance causes errors in both the amplitude and phase of imposed strain. By inspecting (197) and (198) we see that these errors become unimportant when $KF_o \ll D_o \cos \delta$. This provides a handy criterion for compliance error but correction for this error is nontrivial.[608] Compliance phase error becomes important as δ approaches $\pi/2$, which is the case for Newtonian fluids. When the force contains higher harmonics, the imposed shear strain will also contain spurious higher harmonics.

Fortunately, force amplitudes observed for molten plastics in the new rheometer are generally below 100 N, so compliance error does not affect imposed strain amplitude in most tests. Furthermore, since phase lags approaching $\pi/2$ are rarely observed for molten plastics compliance phase error is negligible for most tests performed on the new rheometer.

2. Bearing Friction

Although bearing friction has traditionally been a problem in load cell based sliding plate systems, the SCHNEEBERGER linear bearing table produces little friction. Bearing friction for a prescribed plate displacement can be measured with no sample in the rheometer. For instance, an amplitude spectrum of the load due to friction during an oscillatory plate displacement is shown in Figure 43 Several harmonics of the driving frequency, 1 Hz in this case, can be distinguished. The force of friction is usually below .5 N, which is normally negligible This is a large improvement over what has been previously reported. This serendipitous result permits an excellent comparison of shear stress apparent from the total force with that measured with the shear stress transducer.

V. ANALYZING OSCILLATORY SHEAR TEST RESULTS

Deciding how best to analyze nonlinear viscoelastic properties is not an easy task. Although many methods have been used to analyze nonlinear viscoelastic property measurements, only a few methods are for analyzing large deviations from linearity such as those which the new rheometer is intended to measure. It is argued here that the best method for analyzing viscoelastic properties is the use of the discrete Fourier transform (DFT).

A. Spectral Analysis and the DFT

Volumes can be written on uses for discrete Fourier transforms[609,610] and a complete discussion of this subject is well beyond the scope of the present work. The uninitiated are encouraged to consult the recent text by Ramirez (1985) which explains how to use the DFT with a minimum of mathematical drudgery.[611,612]

1. What is a Frequency Spectrum?

Nonperiodic functions can be approximated with Fourier series:

$$x(t) = \lim_{\Delta f \to 0} \sum_{n=-\infty}^{\infty} X(nf_o) \exp (j2\pi nf_o t) \Delta f \ . \tag{199}$$

where $X(nf_o)$ represents the frequency spectrum of $x(t)$. Each element of $X(nf_o)$ is called a spectral component or spectral line. Obviously, from (199), the frequency spectrum of a nonperiodic function consists of an infinite set of spectral lines. Furthermore, $X(nf_o)$ can be resolved into real and imaginary parts

$$X(nf_o) = \text{Re}\ [X(nf_o)] + j\ \text{Im}\ [X(nf_o)] \tag{200}$$

and from these parts the amplitude and phase spectra can be computed.

$$A(nf_o) = \left[(\text{Re}[X(nf_o)])^2 + (\text{Im}[X(nf_o)])^2\right] \tag{201}$$

and

$$\delta(nf_o) = \arctan \{\text{Im}[X(nf_o)]/\text{Re}[X(nf_o)]\} \tag{202}$$

These frequency spectra are important experimental tools. They allow time domain results to be analyzed in the frequency domain, in terms of their spectral components.

When an analytical expression for $x(t)$ is known, an analytical expression for $X(nf_o)$ can often be obtained by carrying out the integration:

$$X(f) = \int_{-\infty}^{\infty} x(t) \exp(-j\, 2\pi f t)\, dt\ , \tag{203}$$

where $j = \sqrt{-1}$, f is the frequency, and X is a continuous function of f. X(f) is called the frequency spectrum of x(t). The integral in (203) is called the Fourier transform of the continuous function x(t) and

$$\int_{-\infty}^{\infty} |x(t)|dt < \infty\ , \tag{204}$$

is one condition for the existence of X(f).

There is no analytical expression for the Fourier transform of a periodic function. Furthermore, the Fourier transform is only useful for frequency domain analysis when an analytical expression for x(t) is known. Viscoelastic property measurements are normally obtained as time series rather than analytical expressions.

2. What is a Time Series?

Experimental data can be collected either continuously, or as a set of discrete values. So far, we have talked about the continuous function x(t) Chart recorders and analog storage oscilloscopes are devices that collect data continuously. Digital data acquisition, on the other hand, involves collection of a discrete set of values. When collected sequentially at equal time intervals, Δt, the time series can be represented as $x(n\Delta t)$. In layman's terms, a time series is a set of observations recorded at different times.

Whether collected continuously or discretely with time, experimental data are normally analyzed as time series. For example, chart records can be reduced to time series by reading values of the measurand corresponding to positions on the chart coinciding with prescribed times.

3. Spectral Analysis of Periodic Functions

We have seen that the Fourier transform of a periodic function does not exist. Periodic functions can, however, be represented as sums of discrete harmonically related components called a Fourier series.[613]

$$x(t) = 1/T \sum_{n=-\infty}^{\infty} X(nf_o) \exp(j2\pi nf_o t) \quad (205)$$

Each element of the set $X(nf_o)$ is called a spectral component of $x(t)$. When an analytical expression for $x(t)$ is known, $X(nf_o)$ can be deduced analytically using:

$$X(nf_o) = 1/T \int_{-\frac{1}{2}T}^{\frac{1}{2}T} x(t) \exp(-j2\pi nf_o t)\, dt \qquad (206)$$

Note that (206) can only be used to analyze a time series when the analytical expression, x(t), is known.

Equation (205) is the exponential or rectangular form for the Fourier series. This equation can also be written in polar form as a sum of cosinusoids:

$$x(t) = \sum_{n=-\infty}^{\infty} x_n \cos(2\pi nf_o t + \delta_n) \qquad (207)$$

Hence, in layman's terms, a Fourier series is simply the sum of harmonically related cosinusoids that best approximates a time series.

a. Spectral Analysis in Frequency Domain

An alternate approach to the determination of $X(nf_o)$ is the use of the discrete Fourier transform (DFT), which is defined by:

$$X_d(nf_o) = 1/N \sum_{n=0}^{N-1} x(n) \left[\frac{\cos 2\pi nf_o}{N} \right] - j\, x(n) \left[\frac{\sin 2\pi nf_o}{N} \right] \qquad (208)$$

This is easily evaluated using a computer. However, the number of floating point operations required to obtain X_d is roughly N^2.[614] Hence, for large N the computing time required to calculate the DFT can be prohibitive.

The main advantages of time series analysis over the DFT approach are that (1) an analytical expression for the frequency spectrum can be obtained once x(t) is known and, (2) the elements of the time series need not be equidistant in time. The main disadvantages of time series analysis are (1) that a proper analytical expression for x(t) must be chosen a priori and (2) that when x(t) contains several parameters, the statistical fit of x(t) with $x(n\Delta t)$ is a lengthy computation.[615]

<u>(1) Fourier Transforms Add Linearly</u>

The addition of components in the time domain, sometimes called parallel superposition, is the same as the addition of the rectangular forms for these components in the frequency domain, if and only if component spectra have a common time base. Given two time series having common time bases x(t) and y(t) having DFT's X(f) and Y(f) respectively, x(t)+y(t) transforms to X(t)+Y(t). This is useful for property measurement because undesired components may be easily removed from a spectrum when clearly resolved and identified.[616]

(2) Time Shifting is Frequency Modulation

When $x(t)$ becomes $x(t-T)$ we say that x has been time-shifted by T. If $x(t)$ transforms to $X(f)$, then the exponential form for the transform of $x(t-T)$ is $X(f) \exp(-j2\pi fT)$. In other words, when $x(t)$ becomes $x(t-T)$, $\delta(f)$ becomes $\delta(f)+2\pi fT$. This is used for signal conditioning when a baseline is taken prior to measurement so that its phase spectrum is known relative to that of the measurement. The baseline spectrum can be subtracted from the measured spectrum if and only if both time series have the same time base. Spectra computed for time series with different time bases must be properly frequency modulated before they can be subtracted from one another

Hence, when the phase contents of the baseline error components are known, the phase contents of desired components at the same frequency can be obtained by adding $2\pi fT$ to $\delta(f)$, where T is the interval between when the first elements of the baseline and the measurement time series were collected.[617]

b. The Fast Fourier Transform Approximation

The fast Fourier transform (FFT) is a type of algorithm specially designed to closely approximate the DFT using only $N \log_2 N$ floating point operations.[618] This algorithm makes it possible to evaluate the DFT of large time series. There are many commercial versions of this special type of algorithm. These packages usually require that the time series be equidistant in time and often require that the total number of points in the time series be 2 raised to an integer exponent, m.

Modern signal averaging instruments that are dedicated to digital frequency analysis normally incorporate hardware with digital FFT-based programs. Such an approach has occasionally been used for the harmonic analysis of shear stress waves for viscoelastic liquids in oscillatory shear.[619,620]

c. Software for Spectral Analysis

Since program size determines the space occupied in random access memory (RAM), one likes to keep programs as small as possible. Hence, it is desirable to keep analysis software separate from test software. In the section on rheometer design, the test programs for oscillatory shear and exponential shear were described. These programs generate data files in a standardized five column format. These columns are (1) command shear strain, (2) load in newtons, (3) shear stress in MPa, (4) shear strain and (5) time in seconds. The standardized file format permits archival data to be used and reused with new data analysis programs. This makes it easy to analyze old data using new analysis programs.

The spectral analysis program for the shear stress resulting from oscillatory shear is listed in Appendix 3. Similar programs for shear strain and load are easily obtained by. (1) using the appropriate column in the standardized data file as the time series and (2) renaming appropriate axis labels in the graphics subroutines.

Extensive use of subroutines has been made so that the program skeleton is contained in the first page of the listing. Students of MTSBASIC should be able to follow the program with a minimum of difficulty. Recall that the frequency matching subroutine used at the time of data collection ensures that the data will be suitable for spectral analysis.*

Operations required before the FFT statement include (1) removing the DC offset and (2) scaling the time series from the recorded floating point values to integer values spanning $\pm\ 2^{16}/2$ or ± 32767. A corresponding unscaling operation is required after performing the FFT to return to the same engineering units as the original time series. The engineering units of the Fourier transform, $X(nf_o)$, are the same as those of the time series, $x(n\Delta t)$

<u>(1) Frequency Matching</u>

To obtain an accurate frequency spectrum with the desired frequency range and resolution care must be taken in choosing the sampling rate and

---

*See section on frequency matching.

size of the time series. The process of suiting the time series to the Fourier transform is called frequency matching and a subroutine for this purpose is included in the test program listed in Appendix 1.

For an oscillatory shear test of frequency f_o we expect the shear stress response to be a standing wave with spectral lines at odd integer multiple frequencies of the shear strain, nf_o. The expected frequencies for spectral components are nf_o. A potential problem with the DFT is that, if there are spectral lines in the material response between adjacent DFT components, these can have incorrect amplitudes or, when frequency resolution is poor, they may not show up in the DFT. Hence, it is desirable to have spectral lines located precisely at the principal harmonics of the test frequency. However, the sampling rates available on a digital data acquisition system are not continuously variable. Therefore, the sampling rate must be chosen from the discrete set of available acquisition frequencies *

(a) Select desired test frequency, f_D.

The test frequency should be chosen to avoid foreseeable error components including the principal harmonics of 60 Hz and the mechanical resonant frequencies of the rheometer.

(b) Decide how many higher harmonics are needed, H.

---

*The highest sampling rate provided for by the digital acquisition system used in this research is 1000 Hz.

For large amplitude oscillatory shear a value between 8 and 10 is recommended For small amplitude oscillatory shear a smaller number can be used.

(c) Compute desired Nyquist frequency, $N_{QD} = 3Hf_D/2$.

Note the safety factor of 3/2 here. Slight computational inaccuracies can arise in the upper third of the FFT, hence, the desired Nyquist frequency is somewhat higher than the theoretical value.[621] It is advisable to draw a vertical line on frequency spectra to mark the upper third of the spectrum.

(d) Select total number of points, N.

Here the total number of points is chosen such that the computer memory is not exceeded and so that a practicable computation time will result.

(e) Compute desired sampling interval: $\Delta t_D = 1/2N_{QD}$.

Here the desired time between samplings is calculated. The reciprocal of this value is the desired sampling rate.

(f) Chose available clock speed, Δt, nearest Δt_D.

On a digital data acquisition system one must chose from a set of discrete sampling rates. When the desired sampling interval is not available, as is generally the case, then the value of Δt which is nearest but not greater than Δt_D is chosen.

(g) Compute Nyquist frequency, $N_Q = 1/2\Delta t$.

This new Nyquist frequency is greater than or equal to the value specified in Step 4.

(h) Compute required test period: $T = N\Delta t$.

The required test period is then calculated. This does not imply when the test period should be started which varies with test conditions and material. Data should not be sampled from the initial transient. Sampling should begin after a predetermined time has elapsed to ensure generation of the standing shear stress wave. When to start the test is determined from experience.

(i) Compute frequency resolution, $\Delta f = 1/N\Delta t$.

If this frequency resolution is less than desired, select a higher value of N and start again at Step #4.

If a test result is to be closely scrutinized, fine resolution is desired. However, if one decides to neglect all frequencies except the principal harmonics, one can save computation time by using $\Delta f = f_o$.

(j) Compute upper limit for test frequency.

The maximum allowable test frequency which can provide a frequency-matched frequency spectrum is $f_{max} = 2N_Q/3H$. The adjusted test frequency must satisfy: $f_o \leq 2N_Q/3H$.

(k) Compute required integer number of cycles, C.

To avoid inaccuracies in the FFT due to windowing errors, the time series should be sampled over an integer number of cycles. The integer C must satisfy: $(Tf_o - 1) < C \leq Tf_o$. C is the highest integer less than Tf_o.

(l) Adjust test frequency to collect C cycles.

Hence, the "matched" test frequency is $f_m = C/T$. If the matched frequency is significantly different from the desired frequency then a larger number of points should be chosen. In this research, 256 point time series were usually collected and the matched frequencies differed only slightly from the desired frequencies when eight or less principal harmonics are desired.

<u>(2) The MTSBASIC FFT Statement</u>

The MTSBASIC language incorporates the FFT statement which quickly returns the FFT of a time series using a machine code subroutine. This statement returns a close approximation to $X_d(nf_o)$ for a time series, $x(2^m\Delta t)$, containing 2^m equally spaced elements.

(3) Removing DC Offset

The mean value of time series collected for a standing wave is normally close to zero. The frequency matching subroutine implicitly ensures this. However, the mean value is rarely exactly zero. Poor accuracy of the FFT approximation to the DFT is obtained when the mean value of the time series is nonzero. This idiosyncracy is common to most commercial FFT subroutines.[622]

(4) Scaling of Time Series

The FFT algorithm requires an integer-valued time series. Since the PDP-11 is a 16-bit system, the maximum numerical resolution for an integer valued time series is simply $1/2^{16}$ or 1/65536. For maximum numerical precision, the integer-valued time series should be scaled to span the full integer range ±32767. Each element of the frequency spectrum, $X(nf_o)$, must be multiplied by the reciprocal of the scaling factor in the unscaling operation which is carried out immediately after the FFT is performed.

d. Polar and Rectangular Forms

We have discussed the frequency spectrum in its rectangular form. The FFT statement returns a set of N/2 ordered pairs from an N element time series. Each ordered pair consists of the real and imaginary parts of each element of $X(nf_o)$, which is obviously a series of complex numbers. This form for frequency spectra is the established convention for discrete Fourier transform results amongst mathematicians and physicists.

An equivalent convention for spectra is the polar form. Instead of real and imaginary parts, the polar convention uses amplitudes and phase angles * This method is more popular with rheologists since material properties are traditionally reported as combinations of amplitude ratios and phase angle differences.

Interconverting between rectangular and polar forms is trivial. The complex pair is easily deduced from the polar form using:

$$\mathrm{Re}[X(nf_o)] = A(nf_o) \cos \delta(nf_o) \quad \text{and} \tag{209}$$

$$\mathrm{Im}[X(nf_o)] = A(nf_o) \sin \delta(nf_o). \tag{210}$$

The polar pair is:

$$\delta(nf_o) = \arctan \{ \mathrm{Im}[X(nf_o)] / \mathrm{Re}[X(nf_o)] \}, \tag{211}$$

and

---

*Also called phase contents.

$$A(nf_o) = \left[\{Re[X(nf_o)]\}^2 + \{Im[X(nf_o)]\}^2 \right]^{\frac{1}{2}}. \tag{212}$$

The special problem with (211) is that regardless of the amplitude given by (212), so long as it is nonzero, it will return a phase content. Phase contents exist, even when amplitudes are negligible. This is why the polar form is not a popular convention amongst mathematicians and physicists.

For consistency with established literature in rheology, the polar form will be used almost exclusively in the present document. Both forms are important ways of looking at material property data.

e. Time Base

Complete specification of a time series, $x(nf_o)$, requires that a time zero be assigned to one element. This assignment for the time series is called its time base. Although this can be assigned arbitrarily to any element, it is usually assigned to the first element. Hence, complete specification of the frequency spectrum also involves a time base. All the spectra presented hereunder assign zero time to the first element of the time series.

The time base affects the phase spectrum but not the amplitude spectrum. This is why the polar form is popular with vibration analysts, since they concern themselves almost exclusively with amplitude spectra. The effect of shifting the time base by t_o on the phase spectrum, called frequency modulation, is discussed below.

f. Enhancing Resolution

Regardless of how well a rheometer drive system works, there will always be some discrepancy between actual and prescribed motion. For oscillatory shear, imperfections in the actual motion from the desired standing wave show up as line broadening on the strain frequency spectrum. The stress response will also exhibit line broadening. Hence, line breadth is a measure of cycle-to-cycle variability which can be derived from the DFT for the time series of an experimental waveform.

It is sometimes necessary to artificially narrow the line breadths.[623] This is particularly important when desired and undesired spectral components occur at nearby frequencies. For example, undesired components can be caused by mechanical or electrical resonant frequencies in the rheometer and related circuitry. Also, ground loops in capacitance proximeters can cause low level error at 60 Hz when imperfectly grounded. When desired and undesired components occur at nearby frequencies, such that their line breadths overlap, it can be difficult to resolve one peak from another. Here a mathematical filter called the Hanning window can be used to decrease individual line breadths and hence, enhance the resolution of an amplitude spectrum.[624] The Hanning window requires a preliminary operation on the time series before the FFT. The Hanning window capability has been built in to the spectral analysis software.

g. Broadband Noise Reduction

In the discussion of random shear we saw that broadband mechanical noise in the shear strain can cause deviations from simple shear in fluids with temperature dependent properties. Furthermore, we saw how to minimize such deviations by keeping the total test time below a specified value.[625]. Moreover, we considered broadband noise in the shear stress that can result from random shear. The discrete Fourier transform makes it easy to filter out broadband noise for periodic waveforms.

For nonperiodic waveforms, broadband noise can be minimized by taking an average of several time series before transforming. This is possible since the spectral components for broadband noise tend uniformly to zero with the number of signals averaged. Using signal averaging, accurate spectra can be obtained for low signal-to-noise ratio (S/N) waveforms using signal averaging. Sometimes the number of measurements required to obtain peaks which are well resolved from the background is impracticably high.

For periodic waveforms, the level of broadband noise can also be minimized by simply increasing the total number of points in the time series. This is normally sufficient for studying standing shear stress waves in molten plastics with a shear stress transducer.

Furthermore, since the DFT of a periodic waveform is a line spectrum, the desired spectral components are easily resolved from the background noise, because their frequencies are known a priori. Hence, if the noise levels at undesired frequencies are uniform, then the amplitude of this background noise can be easily subtracted from the entire spectrum. This provides a means of removing the effect of background noise on the desired spectral components.

h. Correcting Errors Due to Resonance

Errors due to resonance can easily be eliminated when corresponding spectral components are not near desired spectral components. This is as simple as setting the amplitudes of these spectral components to zero at the relevant frequencies. However, spurious higher harmonic components can be generated when the test frequency is an integer subharmonic of a system resonant frequency, that is, when $\omega = \omega_r/(2n+1)$.[626]

i. Subtracting Time Shifted Baseline

There is one final method of digital filtering also worth mentioning. When an error component shows up in a spectrum, and the frequency of this component is near a desired one, then the error component is difficult to resolve from the desired one. Increasing the frequency resolution by increasing the total number of points or the sampling rate helps here. However, when the frequency of the error component is exactly that of the desired frequency, increasing total points and adjusting sampling rate will not help.

For example, suppose that a baseline spectrum for the shear stress transducer output is computed from a time series with its time base taken as zero at exactly 12.00 noon. The spectrum shows broadband noise with a peak having an amplitude of .02 MPa at 60 Hz with phase angle $\pi/8$ radians. Suppose that an oscillatory shear test is done shortly thereafter at 60 Hz and a time series for the shear stress response is collected starting exactly 10 seconds after 12.00 noon. The shear stress spectrum computed from this time series, taking 12.00.10 as time zero shows a peak of amplitude 1.11 MPa at 60 Hz with phase content of $\pi/7$. But to give the baseline spectrum the same time base, the phase content of each of its spectral components must be multiplied by ωT.

The baseline spectrum may be obtained either before or after the measurement time series is collected Obviously, mechanical noise generated during the measurement and not present in the baseline series and hence, cannot be removed in this way.

i. Spectral Analysis in the Time Domain

To obtain an analytical expression for $X(nf_o)$, one must first obtain an analytical expression for $x(t)$. If no such expression is known, one can test the validity of an assumed expression or model. One can compute best fits for the parameters of the assumed model by statistical regression. This process of fitting $x(t)$ to the data set $x(n\Delta t)$ is called time series analysis.

$X(nf_o)$ is commonly approximated by fitting the time series to a truncated Fourier series. This approach has been used for determining $G'(\omega)$ and $G''(\omega)$ in small amplitude oscillatory shear[627] and for $G'(\omega,\gamma_o)$ and $G''(\omega,\gamma_o)$ in large amplitude oscillatory shear.[628] This approach has also been successfully used for determining amplitudes and phase angles of higher harmonics of shear stress in steady shear superposed on oscillatory shear.[629,630] This method works well when the truncated Fourier series is essentially correct. However, time series analyses are not suitable for low signal-to-noise measurements, because the existence of error components must be presupposed Furthermore, time series harmonic analysis requires more computations than harmonic analysis with the discrete Fourier transform

A related method called digital time-domain cross-correlation has also been used to determine linear[631] and slightly nonlinear viscoelastic properties for solid polymers in oscillatory shear.[632,633] However, this method can only be applied when the dependent variable is linearly related to the independent variable.[634] For example, the Rheometrics Mechanical Spectrometer incorporates digital hardware which determines the phase angle between the stress and the strain using time-domain cross-correlation. Furthermore, this hardware incorporates an analog third-order filter to improve resolution of stress and strain measurements. This approach has the effect of rejecting all frequency components other than the fundamental.[635] Hence, this approach makes it difficult to distinguish linear behavior from nonlinear behavior. Furthermore, it automatically removes any DC offset which is a measure of drift in the strain measurement or baseline drift in the torque and strain transducer calibrations.

k. Spectral Analysis Using Analog Circuitry

Phillipoff used an analog computer to assess the amplitudes and phase contents to the principal harmonics of stress for viscoelastic liquids in large amplitude oscillatory shear.[636] Analog circuits have also been used for real-time frequency analysis of nonlinear shear stress waves of viscoelastic fluids in oscillatory shear.[637,638]

4. Using Spectral Analysis to Get Viscoelastic Properties

Property measurement using the frequency domain requires that two spectra, those of the dependent and independent variables, be compared. For viscoelastic property measurements, for example, spectra of both the shear stress and the shear strain are required.

It is important to correct the phase spectra associated with each viscoelastic property measurement.[639] Failure to make such corrections can cause physically unrealistic observations.[640] For example, Phillipoff (1964) showed loops of shear stress against shear strain for viscoelastic liquids with negative areas.[641] This implies negative lost work and hence implies a violation of the second law of thermodynamics. Similarly, loops of shear stress against shear strain for a Newtonian[642,643] liquid in oscillatory shear were reported with phase lags greater than $\pi/2$. By definition, Newtonian liquids have phase lags of exactly $\pi/2$ in oscillatory shear.

a. Shear Strain Spectra

To the uninitiated, a spectrum of the shear strain might seem unnecessary since the shear strain is prescribed in an oscillatory shear test. Indeed the command strain wave for an oscillatory shear test will give a perfect displaced sinusoid as prescribed by the MTS harmonic function discussed above. However, the time base of the actual shear strain will be slightly different from the prescribed one depending on the frequency response of the servo-hydraulic system. Furthermore, at high frequencies small higher harmonics can sometimes be detected especially when the gain setting of the closed loop control system has not been optimized. Hence, the phase contents of the shear strain are unknown, a priori, and material properties such as the stress-strain phase difference, $\delta(\omega)$, can only be computed using the shear stress and strain spectra.

(1) Phase Correction for Shear Strain

The shear strain is measured using the MTS linear variable displacement transducer (LVDT) whose frequency response is simply that of the signal conditioner * This circuit has first order frequency response specified as -3dB attenuation at 1 kHz, and the time constant for the LVDT measurement

*Product Bulletin 440.22-4, Model 440.22 AC Transducer Conditioner, MTS Systems Corp., Eden Prairie, Minnesota (1979).

is .001 seconds. Hence, a phase angle, $\delta_e = \arctan(-.001\ \omega)$ should be subtracted from the phase contents of spectral components of strain.* For a proper oscillatory shear test, the fundamental should be the only significant peak in the shear strain amplitude spectrum.

Recall that in addition to the phase error, one must also compensate for corresponding attenuation, $A(\omega)$. For the shear strain, this is accomplished by multiplying the amplitude of each spectral component by $\sqrt{(.001^2\ \omega^2 + 1)}$. This correction is less than 1% at 22 Hz.

b. Local Shear Stress Spectra

The other important spectra, for viscoelastic property measurements, are those of the dependent variable, the locally measured shear stress.

(1) Phase Correction for Shear Stress

These too must be phase corrected for the frequency responses of the MTS signal conditioner and the capacitance amplifier. Since the responses of these conditioners are both first order, and since they are connected in series, the phase angle that must be subtracted from the phase contents of the shear stress spectra is the sum of the capacitance amplifier and DC conditioner component phase errors.

---

*See Chapter 5 in section on dynamic response of transducers for detailed explanation.

The shear stress signal conditioner circuit has a first order frequency response specified as -3dB attenuation at 1.6 kHz, and the time constant for the DC conditioner is .000625 seconds.* Furthermore, the capacitance probe amplifier circuit** has a first order frequency response specified as -3dB attenuation at 5 kHz, and the time constant for the proximeter is .0002 seconds.*** Another cause of phase error in the shear stress transducer is the squeezing flow of the fluid between the transducer cantilever and housing. The phase error due to squeezing flow, δ_s, must be determined empirically by dynamic calibration. Hence, the phase correction to shear stress measurements is $-\delta_e - \arctan(.0002\ \omega) + \arctan(.000625\ \omega) - \delta_s(\omega,\sigma_o)$, where δ_s can depend on both the frequency and the stress amplitude.

Compensation for the attenuation is composed of the product of three attenuation factors. $\sqrt{(.0002^2\ \omega^2 + 1)}\ \sqrt{(.00625^2\ \omega^2 + 1)}\ [1/A_s(\omega,\sigma_o)]$. Here, $A_s(\omega,\sigma_o)$ is the attenuation caused by the squeezing flow which is deducible from the dynamic calibration.

c. Total Force Spectra

---

*Product Specification 440.21-6, Model 440.21 DC Transducer Conditioner, MTS Systems Corp., Eden Prairie, Minnesota (1979).

**MTI probe amplifier model AS 1023-PA.

***Bulletin INS101, "Accumeasure System 1000: Accuracy Without Contact", MTI Instruments, 968 Albany-Shaker Road, Latham, New York.

Recall that the classical way of determining viscoelastic properties in sliding plate rheometers is to infer the shear stress from the measured total force. Total force spectra permit a good comparison between the classical results and the local shear stress measurement.

(1) Phase Correction for Total Force

The frequency response of the MTS load cell* is governed by the frequency response of its signal conditioning circuit.** This DC signal conditioner has first order frequency response specified as -3dB attenuation at 1.6 kHz, so the time constant for the DC conditioner is .000625 seconds.*** Hence, the phase error for each spectral component is. δ_e = arctan (-.000625 ω). The corresponding attenuation correction factor is $\sqrt{(.000625^2\omega^2)}$.

d. Determining Viscoelastic Properties

Results from the corrected amplitude spectra can be used to plot the amplitudes of each harmonic of the shear stress against the shear strain amplitude. The other relevant properties are the phase angles between the phase content of each spectral component of shear stress and the phase

*Model No. 661.19B-02.

**Product Bulletin 0285, 661.19A-1, MTS Systems Corp., Eden Prairie, Minnesota (1985).

***Product Specification 440.21-6, Model 440.21 DC Transducer Conditioner, MTS Systems Corp., Eden Prairie, Minnesota (1979).

content of the fundamental component of shear strain. We have seen, however, that the phase content of a spectral component depends on its time base. If the shear strain is $\gamma_0 \cos(\omega_0 t+\alpha)$, then the shear stress must be time shifted by $T = -\alpha/\omega$. In the frequency domain, this requires frequency modulation of the shear stress. Specifically, $-(\omega/\omega_0)\alpha$ must be added to the phase content of each spectral component of angular frequency ω.[644]

5. Differentiation and Integration Using Spectra

It is often useful to plot the shear stress against the shear rate to analyze viscoelastic response To obtain such a plot, we must obtain the derivative of shear strain. Furthermore, the lost work per cycle is the cyclic integral of shear stress with respect to shear strain. Since frequency spectra provide us with analytical expressions for the stress and strain, the computation from the DFT results of these derivatives and integrals is mathematically trivial. These techniques are called pseudodifferentiation and pseudointegration respectively. Pseudodifferentiation permits the intermediate refinement of digital filtering for noise reduction. This is particularly handy for high S/N waveforms since time domain methods may amplify this noise.[645,646]

It is also possible to use analog circuits to obtain the derivative of the shear rate.[647,648,649,650] However, care must be taken to phase correct for the phase error introduced by the analog circuit.

6. Confidence Intervals for Spectra

When the desired signal is easily distinguished from the noise, statistical confidence intervals for the DFT results can be determined. There are many ways to obtain such confidence intervals. If a value for S/N is chosen by inspecting the amplitude spectrum, then the rectangular forms for the spectral components can be used to obtain confidence intervals for the amplitudes. Letting the amplitude of the fundamental be A_o, the standard deviation of the complex parts of components having amplitudes not greater than $A_o/(S/N)$ is computed. Where this standard deviation, s_d, is computed from M points, the 95% confidence interval associated with amplitude $A(\omega)$ is $\pm 2s_d/\sqrt{M}$. Confidence intervals can then be drawn on the amplitude spectrum to determine, for example, whether spectral components are distinguishable from zero or not.

When the S/N ratio is overestimated, then the confidence interval estimates will be low. When the S/N ratio is underestimated, then the confidence interval estimates will be high. Hence, for conservative estimates of the confidence intervals, the selected S/N ratio should be just high enough to include the principal harmonics. Less conservative schemes for confidence interval assessment in spectral analyses have also been posited.[651]

7. Other Methods of Data Reduction

a. Linear Behavior

The properties of simple rubbers are commonly analyzed using the ratio of stress to strain, G, called the shear modulus. Although a powerful method for data reduction, the single number, G, does not tell us over what range of shear strains the material behavior is known to remain linear.

Similarly, linear viscoelastic material responses are often summarized as ratios of stress to strain. Recall that when the shear strain is cosinusoidal the shear stress is harmonic, so, $\sigma(t) = \sigma_o \cos(\omega t+\delta)$. Its amplitude, σ_o, is proportional to the shear strain amplitude. The ratio $G^*(\omega)$ decribes the material behavior. In polar form, its definition is.

$$G^*(\omega) = (\sigma_o/\gamma_o) \exp(i\delta) , \tag{213}$$

where $i = \sqrt{-1}$ $|G^*(\omega)| = (\sigma_o/\gamma_o)$ is called the magnitude of the complex modulus and $\delta(\omega)$ is called the mechanical loss angle. Linear viscoelastic properties are often analyzed using the polar forms for complex modulus but are more commonly expressed in rectangular form:

$$G^*(\omega) = G' + iG'' , \tag{214}$$

where $G' = (\sigma_o/\gamma_o) \cos \delta$, and $G''(\omega) = (\sigma_o/\gamma_o) \sin \delta$.

The use of the complex modulus is popular for both liquids and solids. Another ratio, the complex viscosity, is also commonly used for liquids. This is defined, in polar form, as:

$$\eta^*(\omega) = (\sigma_0'/\omega\gamma_0) \exp(i\delta) , \tag{215}$$

which has rectangular form:

$$\eta^*(\omega) = \eta'' - i\eta' , \tag{216}$$

where $\eta'' = (\sigma_0/\omega\gamma_0) \cos \delta$ and $\eta^* = (\sigma_0/\omega\gamma_0) \sin \delta$. These methods of analysis are feasible when the complex modulus is independent of strain amplitude.

Moduli do not tell us the range of strain within which the stress is linear. From the discussion of viscoelastic theory we know that two materials with the same $G^*(\omega)$ may have drastically different strain dependencies even at low values of strain. In fact, complex moduli are sometimes reported at single strain amplitudes without checking for linearity.

Furthermore, rectangular forms confound the phase shifts with the amplitude ratios. This makes interpretation of results difficult. For example, the strain amplitude dependence of phase shift made obvious with the plot of phase shift against strain amplitude on linear scales in Figure 11 is less visible in plots of G' and G" shown in Figure 142. Moreover, in the log-log plot of these data, the strain dependence is even less visible.* Interestingly, Figures 10 and 11 show the phase angle varies with strain amplitude, while the shear stress amplitude does not. Furthermore, phase error correction and expression of statistical confidence intervals becomes unnecessarily complicated when expressed as complex moduli or complex viscosities. Also, Booij has pointed out that the use of $\delta(\omega)$ is the best way of looking at linear results since it is not subject to calibration errors and is sensitive to differences between materials.[652]

For these reasons, the author prefers plots of stress amplitude and phase shift against strain amplitude on linear scales for analyzing oscillatory shear test results.

b. Analyzing Nonlinear Behavior

Since large amplitude oscillatory shear properties involve both strain and frequency dependencies, representing such properties concisely is more difficult than for the linear case In the technical literature, one finds a plethora of ways to analyze nonlinear material responses. Their levels of sophistication range from simple time series plots to the rigour of constitutive equations. Each approach has its merits, the pros and cons of which are discussed below using a single test recorded for a polystyrene melt on the new rheometer.

*The log-log representation of G' and G" against γ_0 is the most commonly used for strain sweep experiments which are usually performed in an effort to detect strain dependence. Paradoxically, one is least likely to notice strain dependence by looking at such log-log graphs.

(1) Time Traces

One simple way of analyzing oscillatory shear results is to plot both stress and strain against time.[653] This way is particularly useful for studying cycle-to-cycle variability. Slight differences between cycles caused by statistical variability are seen in time traces. Time traces are popular for displaying properties involving transitions to and from equilibrium such as stress growth and relaxation experiments, but are less popular for oscillatory shear test results

It is difficult to notice the presence of higher harmonics on a time domain plot. For example, the twofold asymmetry of a waveform may go unnoticed on a time trace Of course, one can always do the harmonic analysis of a time trace by reducing it to a series of numbers. However tedious, this procedure has been used successfully for harmonically analyzing the shear stress waves for viscoelastic liquids in oscillatory shear.[654] Doebelin has outlined a graphical procedure to simplify this process.[655]

Another interesting display is a time trace of the instantaneous lead angle of stress with respect to strain against time, $\delta(t)$. This method has been used to analyze the total torque for clays in large amplitude oscillatory parallel disk flow.[656]

(2) Loops

Another way of observing oscillatory shear results is to plot the shear stress against the shear strain.[657] When the stress response is harmonic, this gives an ellipse whose area depends on the axis scaling and the phase shift. When each axis is normalized and scaled identically, the area of the ellipse is proportional to the sine of the phase shift. Moreover, the phase angle is deducible from the ratio, R, of the lengths of the ellipse's minor to major axes:[658,659]

$$\delta = 2 \arctan R. \tag{217}$$

Hence, phase shift between harmonic waveforms of the same frequency can be obtained directly from the normalized equi-scaled loop. This method is especially handy when a quick measurement of phase lag is required from an oscillograph. Of course, for low S/N waveforms and for very low phase angles, precise measurement of the axis lengths is not possible. For such cases, DFT techniques are called for.

When the stress response is anharmonic, we have seen that the area of the loop depends on the amplitude and phase shift of the fundamental. When measuring nonlinear properties using oscillatory shear, the loop is an indispensable diagnotic tool. Loops of stress versus strain can be obtained quickly, and where an oscilloscope is used they are obtained in real time. They can tell the experimenter (1) when the stress becomes a standing wave, (2) whether the response is anharmonic or not, and (3) what the lost work is. For instance, melt fracture usually causes a non-standing stress wave, that is an unclosed loop with twofold asymmetry.

For liquids, it has been found that a plot of shear stress versus shear rate can accentuate the appearance of higher harmonics. Shear stress versus shear rate loops have been used to describe the nonlinear viscoelastic behavior of polymer melts in oscillatory shear. The shear rate for such loops can be obtained using either on-line analog circuitry,[660,661,662] time domain differentiation, or pseudodifferentiation of the strain.

In electrical engineering, loops are used extensively to study the behavior of circuitry in alternating currents. In this context, they are often called Lissajous figures.[663,664,665,666]

(3) Gross Features

Instead of measuring all the frequency components for the stress response, only certain gross features of the loop are sometimes reported. When determining the viscous dissipation in rubbers under vibratory loads, for example, one might be interested in the lost work per cycle, the higher harmonics being of no consequence to the lost work.[667,668] For molten plastics, however, the higher harmonics represent an interesting feature of the nonlinear viscoelasticity. However, to simplify the analysis of oscillatory shear test results, several approximate formats for data analysis are used.

Firstly, some report only the stress amplitude, σ_o, and the lost work per cycle, W_1, or simple functions of these.[669,670] Others report an equivalent phase angle for a hypothetical ellipse having the same lost work[671,672,*] The lost work per cycle is easily deduced from the area of the stress versus strain loop which can be obtained manually using a planimeter on loops of unfiltered waveforms[673] or by pseudointegration of shear stress with respect to the shear strain. Although the stress, $\sigma(t)$, can be written explicitly as a function of the amplitudes and phase contents of its spectral components, the overall stress amplitude cannot. Hence, σ_o can only be deduced numerically from the values of the spectral components of shear stress. Background noise makes σ_o difficult to obtain precisely from loops of unfiltered waveforms. The digitally filtered DFT results permit precise determination of σ_o under such circumstances. When only σ_o and lost work per cycle results are presented, no information is given about the shape of the stress response. In this sense, such methods address only the gross features of the loop.

Using simple functions of σ_o and W_1, Thurston (1981) pioneered the use of three-dimensional drawings to analyze the nonlinear viscoelastic behavior of biofluids with frequency and strain amplitude in a single summary diagram.[674,675] Stereoscopic pictures were used to provide the

*Not to be confused with the phase angle of the fundamental.

depth-perception required to separate the effects of shear strain and shear rate amplitudes.

Another useful approach to presenting nonlinear viscoelastic properties in oscillatory shear testing draws from an analogy with methods commonly used in electrical engineering. Here the root mean square value of a waveform is defined, A_{rms}, which can be obtained using appropriate analog circuitry.[676] It is also easily obtained from the amplitudes of its spectral components, A_i.[677]

$$A_{rms} = \left[\sum_{i=1}^{n} A_i^2 \right]^{1/2} \tag{218}$$

Although the higher harmonics do contribute to the root mean square amplitude of a waveform, the shape of the waveform is not accounted for in A_{rms}. This approach gives only the gross features of the waveform.

(4) Use of Constitutive Equations

Detailed reviews of the use of constitutive equations for analyzing nonlinear viscoelastic properties of liquids in oscillatory shear have been provided by Soong (1983), Tsang (1980) and Tee (1974).[678,679,680] A good summary judgment on these reviews would be that the theory of nonlinear viscoelasticity is not well enough advanced to be useful for routine reduction of large amplitude oscillatory shear test results. Even theories designed for shear strains less than unity have been only moderately successful, although they require mainframe computers to properly evaluate them.[681,682,683,684,685,686,687,688,689] Although considerable progress is being made on models for large amplitude oscillatory shear, such models remain developmental.[690,691,692] One use for theory in analyzing oscillatory shear data is a semitheoretical approach due to Vinogradov. Using the concept of equivalent phase angles mentioned above, strain amplitude dependent or "truncated" relaxation spectra are calculated.[693,694]

The objective of conveniently summing up the large amplitude oscillatory shear behavior of a polymeric liquid with a reasonable number of material constants seems remote. For the time being, the polymer engineer must be content to chose from the empirical methods reviewed above for summarizing this behavior.

VI. RESULTS

A. Calibration of the Shear Stress Transducer

1. Static Calibration Results

The computer program used for static calibration is listed in Appendix 4 Written in MTS-BASIC, this program features simultaneous calibration of both the load cell and the shear stress transducer. This is possible because the weights supported by the shear stress transducer are also suspended from the load cell. Typical curves obtained for the shear stress transducer and load cell calibration are shown in Figures 44a-44b. More or fewer data points can be collected depending on the level of noise present and the desired precision Linear regression gives the transducer sensitivities in terms of volts per unit equivalent shear stress. Since the offset is measured at the outset for each test with the test programs, only the slopes in V/Kg are used as inputs to the oscillatory shear test program given in Appendix 1. Hence, the relevant result is the slope of the curves, obtained from linear regressions of the voltage-weight data.

Appreciable noise is observed in the load cell output at elevated temperatures. However, using 80 data points for the linear regression gives a voltage/weight slope determination with 2% precision and 95% confidence.

Calibration drift is commonly a problem for experimental rheologists. In chapter 5 we described digital electronic circuitry designed to remove all the harmonics of the shear stress, including the one at zero frequency that measures baseline drift during a test. In general, drift in the transducer sensitivities poses a more serious problem than baseline drift. In extreme cases, recalibration between tests is required as was the case for the Fotonic sensor used by Soong.[695] Figure 45 shows a collection of static calibrations performed over a period of roughly two months on the new rheometer using beam #2 in the shear stress transducer. Over this period the shear stress sensitivity varied by less than ± 10% of its mean value and that some of this variability is due to temperature variations in the range from 20 to 200°C. Similar observations were made for static calibrations with beam #1.

2. Dynamic Calibration Results

A program for dynamic calibration was obtained by modifying the oscillatory shear test program. This required that the statements relating to strain be changed to those appropriate to the driving force. This was done because, in the dynamic calibration mode, a spring transmits the desired force to the transducer cantilever.

The spring stiffness* is determined by a linear regression of force-extension results for static tests on an INSTRON electromechanical tensile

*Also called spring rate or spring constant. This is the slope of the load-extension curve.

tester. The spring rate was determined by linear regression, shown in Figure 46, with a standard error of 0.26% from four observations.

A typical output for a dynamic calibration test routine is shown in Figure 47. The loss angle between driving force and measured equivalent shear stress is so small that it cannot be separated from background noise without the use of a frequency spectrum.

The effect of the squeezing flow of molten plastics on the dynamic response of the shear stress transducer is easily assessed by comparing the dynamic calibration results with and without polymer in the beam-housing annulus However, the phase angle of the dynamic calibration assembly can first be determined by performing a dynamic calibration on the shear stress transducer with no polymer present.

a. Response of the Calibration Assembly

The phase angle measured in a dynamic calibration on the clean transducer has two components. Firstly, there is the phase lead resulting from the mechanical losses and inertia associated with cantilever deflection. Secondly, there is the phase lag due to mechanical losses in the calibration assembly. The first contribution can be inferred from the damping factor and mode-one resonant frequency deduced from step response measurements and described in chapter 5.

Recall that since the clean beam is a second order system, the phase lead due to beam inertia is:

$$\delta_e = \arctan \{2\eta/(\omega/\omega_n - \omega_n/\omega)\}. \tag{219}$$

Also, from the damped free oscillation test results given in Table 3, $\eta = .00172$ and $\omega_r = 730$ Hz for beam #2.

Figure 50 compares two typical amplitude spectra for the shear stress transducer input* and output signals. The background noise in the output is ten times higher than the noise in spring extension.

Statistical analysis of these spectra, shown on linear scales in Figure 51, shows that only one peak is significantly different from zero. Recall that peaks at frequencies greater than 2/3 of the Nyquist frequency are subject to numerical inaccuracy[696] which explains the marginally significant peaks that occasionally occur near the Nyquist frequency in the output spectra.

Figure 52 shows typical phase spectra for the spring extension (upper plot) and the shear stress transducer output (lower plot) for a dry beam test. The phase content of the input is only slightly higher than that of the transducer output, hence, a slight phase lead has been measured. Only

* Using the spring rate, this is inferred from the spring extension which is given by the LVDT output.

the phase contents of components with amplitudes greater than the indicated background noise levels are included in these phase spectra.

Table 4: Dynamic Response of Calibration Assembly

f,Hz	δ_{in}	δ_{Cin}	δ_{out}	δ_{Cout}	δ_{cal}
1.00015	3.16236	3.168644	3.15474	3.171239	0.002595
0.100002	3.3355	3.336128	3.32798	3.329629	-0.00649
0.500009	3.19206	3.195201	3.18112	3.189369	-0.00583
2.0008	3.09782	3.110390	3.09084	3.123843	0 013453
5 002	2.05401	2.085428	2.04749	2.129928	0.044500

Table 4 shows the results of dynamic calibration tests done with the gap void at 200°C. The raw phase contents δ_{in} and δ_{out} are the uncorrected phase contents of the transducer input and output respectively. The corresponding corrected phase contents are:

$$\delta_{Cin} = \delta_{in} - \arctan(-.001\ \omega), \tag{220}$$

which accounts for the frequency response of the LVDT and related circuitry, and by:

$$\delta_{Cout} = \delta_{out} - \arctan(-.002\,\omega) - \arctan(-.000625\,\omega)$$

$$- \arctan\left[\frac{2\,(.00172)}{f/730 - 730/f}\right], \tag{221}$$

which accounts for the frequency responses of the MTS signal conditioner, the capacitance probe amplifier and the mechanical inertia of the beam respectively. A plot of the resulting phase lag computed for the calibration assembly, $\delta_{cal} = \delta_{Cout} - \delta_{Cin}$, is given in Figure 53. Hence, the calibration assembly behaves as a linear element. The time constant for this element, determined by linear regression of the data in Figure 53, gives a time constant for the calibration assembly of .0017 sec. Hence, the phase lag intrinsic to the calibration assembly is:

$$\delta_{cal} = \arctan(.0017\,\omega). \tag{222}$$

The small offset of -.009 radians or -½° observed in Figure 53 is due to inaccuracies in the phase corrections described above. Finally, signals were attenuated by less than 1% for all the calibration assembly tests, which is expected for a linear element.

b. Effect of Molten Polymer in the Annulus

The frequency response of the shear stress transducer with molten polystyrene in the annulus between the beam and the housing can now be determined. Since, this is the in-service condition of the shear stress transducer, the frequency response of the transducer can be used to error correct the phase contents of the spectral components of shear stress measured for molten polystyrene in oscillatory shear.

Figure 54 shows a typical plot of raw data which the operator obtains immediately after a dynamic calibration test. The time trace of the command equivalent shear stress (ESS) versus the actual ESS shows that the actual spring extension closely follows the desired harmonic function. The loop of load versus actual ESS consists mainly of bearing friction since the force amplitudes required for dynamic calibration of the shear stress transducer are much lower than amplitudes due to bearing friction.* The loop of shear stress transducer output versus ESS input shows the slight phase lead which is our measure of the dynamic response of the transducer. The phase lead is largely obscured by the background noise so that spectral analysis is called for. This background noise is also apparent in the time-trace of the shear stress transducer output during dynamic calibration, which is shown in Figure 55.

Figure 56 shows typical amplitude spectra for the shear stress transducer input and output for a dynamic calibration done with molten polystyrene in the transducer gap. Statistical analysis of these spectra, shown on linear scales in Figure 57, shows that only one peak is

---

*See Figure 43 for amplitude spectrum of bearing friction alone.

significantly different from zero, and this shows that both the input and output signals are harmonic, as is desired for dynamic calibration.

Figure 58 shows typical phase spectra for the shear stress transducer input and output for a dynamic calibration done with molten polystyrene in the transducer gap. The output phase content is slightly lower than that of the input which is a measure of the phase lead caused by the shear stress transducer.

As for the case of the clean beam calibration, the phase content of the shear stress transducer input was phase corrected using.

$$\delta_{Cin} = \delta_{in} - \arctan(-.001\ \omega), \tag{223}$$

which accounts for the frequency response of the LVDT and related circuitry, and the shear stress transducer output was phase corrected using:

$$\delta_{Cout} = \delta_{out} - \arctan(-.002\ \omega) - \arctan(-.000625\ \omega) - \arctan(.0017\ \omega), \tag{224}$$

which accounts for the frequency responses of the MTS signal conditioner, the capacitance probe amplifier and the frequency response of the dynamic calibration assembly. The phase response of the shear stress transducer is obtained using $\delta_{sst} = \delta_{Cout} - \delta_{Cin}$.

Table 5: Dynamic Response of SST with PS-filled Annulus

f, Hz	δ_{in}	δ_{Cin}	δ_{out}	δ_{Cout}	δ_{sst}
1.00015	3.16733	3.173614	3.11097	3.116782	-0.05683
0.100002	3.33635	3.336978	3.30022	3.300801	-0.03617
0.500009	3.19497	3.198111	3.13315	3.136055	-0.06205
2.0008	3.11089	3.123460	3.03293	3.044556	-0.07890
5.002	2.16227	2.193688	2 07414	2.103176	-0.09051

The phase response of the shear stress transducer in the in-service condition at several frequencies, recorded in Table 5, is shown in Figure 59. The phase error is small, negative and decreases logarithmically with frequency. Linear regression of these data gives:

$$\tan \delta_{sst} = -.0136 \ln f , \tag{225}$$

with a slight zero frequency offset of -.0669 which corresponds to -1.9°. This small offset is due to cumulative inaccuracies in the phase corrections described above.

(1) Effect of Shear Stress Amplitude

Figure 61 shows the effect of stress amplitude on the frequency response of the shear stress transducer. Over the range of stress amplitudes tested, the phase response was insensitive to shear stress amplitude.

(2) Effect of Temperature

Dynamic calibrations were performed at several temperatures with polystyrene melt in the gap. Surprisingly, the transducer frequency response was not sensitive to temperature and phase leads were small for temperatures spanning 130 to 200°C.

B. Transducer Background Noise

With the test programs given in Appendices 1 and 2, a subroutine is included that measures the mean offset levels of all baseline signals before the test is performed. Included in this routine is the calculation of the standard deviation in the baseline signal. This provides a quick assessment and record of the background noise levels present at the time of the test. These are recorded as 99% confidence intervals* for each signal. Such assessments permit the operator to eliminate unusually high background noise when it occurs. The time trace of the strain, and the force-strain and stress-strain loops are also recorded for each measurement. Such records are also invaluable when archival measurement records are to be used. Be this as it may, a more informative analysis of the background noise levels is obtained using spectral analysis.

1. Shear Stress Transducer Signal

---

*The 99% confidence interval is simply four times the standard deviation. It gives a good, quick estimate of the peak-to-peak noise levels for the baseline and hence, the real time measurement resolution. These values are denoted by (4s p-p).

The background noise levels in signal output are one good measure of the performance of a shear stress transducer. The availability of the DFT technique permits us to study the amplitude spectra of the background noise in shear stress transducer output under various conditions.

Figure 62 shows a typical time trace for the shear stress transducer output. Figures 63 through 66 are amplitude spectra obtained for the shear stress transducer output at various Nyquist frequencies. These were computed using 512 point DFT's taken at different sampling rates to give Nyquist frequencies spanning the range from 2.56 to 256 Hz. Since the lower frequency amplitude spectra, Figures 63 through 65, are essentially flat, we see that the background signal consists of broadband noise which is below 0.5 Pa in amplitude from zero to 25.6 Hz using beam #2. The level of this random noise will decrease with the total number of points sampled. In fact, in principle this noise level can be made to tend to zero if enough points are sampled.[697] In contrast, in the higher frequency amplitude spectrum we detect two distinct error components. The 60 Hz component is caused by ground loops that are common in capacitance proximeters employing guard-field technology.[698,699,700,701] An equally significant error component is also observed at 180 Hz. This is obviously the third harmonic of the 60 Hz peak and probably results from a ground loop as well. These peaks have amplitudes of roughly 4 Pa. A less significant error component having 1 Pa amplitude is also resolved at 30 Hz which is the second subharmonic of 60 Hz. Hence, it is best to avoid using test results with spectral components of shear stress at frequencies that are harmonically related to both 60 Hz and the shear strain.* These noise levels meet the manufacturer's specifications for the capacitance proximeter system incorporating the model ASP-5HT probe used with the 5-kHz (-3dB) frequency response probe amplifier model AS1023-PA.[702]

These baseline spectra were obtained with the hydraulic pump on to represent the true background conditions existing prior to and between actual measurements. In principle, floor vibration due to pump rotation could cause vibrations in the rheometer. In practice, however, activating the large, loud hydraulic pump does not significantly alter these background spectra. For example, Figure 67 shows a comparison of high frequency amplitude spectra with MTS hydraulic pump on and off.

2. Load Cell Signal

A spectral analysis of low-level background noise in the total force caused by bearing friction during large amplitude oscillatory shear testing was discussed under rheometer design.** There is a significant spurious peak of unknown origin at 50 Hz with amplitude .02 N. A baseline spectrum for the load cell output is given in Figure 68 showing significant error components at 60 Hz and at 180 Hz with amplitudes of roughly .008 and .004 N respectively.

*Remember that the method of time-shifting baseline described in Chapter 5 can be used to correct spectral components at frequencies harmonically related to the error components of noise when spectral components at such frequencies must be used.

**See Figure 43.

3. Displacement Transducer Signal

Background noise levels for the LVDT output are typically below the digital resolution of the data acquisition devices. Using a 1 mm shim thickness and the maximum resolution signal-conditioning amplifier setting, the digital resolution corresponds to about .5% shear strain.

C. Oscillatory Shear

The test program given in Appendix 1 was used for all oscillatory shear experiments.

1. Materials Studied

a. Molten Plastics

The new rheometer was evaluated using molten polystyrene in oscillatory shear and polypropylene in reciprocating exponential shear. The polystyrene, previously studied by Tee and Dealy,[703,704] was sold by Dow Chemical Canada Ltd under the name Styron 683. Its salient properties are. M_w = 3.3 x 10^5, solid-state density = 1.04 g/cc and melt index = 4.8. The molten polypropylene was previously studied by Mutel and Kamal.[276]

b. Polyisobutylene

Preliminary investigations, done on the modified prototype at room temperature, made use of Vistanex LM-MS. This commercial polyisobutylene homopolymer was supplied by the EXXON CHEMICAL COMPANY. It is ideal for rheometer evaluation and is commonly used for this purpose since it is molten at room temperature.[705,706,707,708,709,710] It also resists melt fracture well so that nonlinear viscoelastic properties are easily obtained before sample fracture. Commercially, this resin is principally used as a base for chewing gum and for hot-melt adhesives such as window caulking. It has a limiting low-shear viscosity of 1.04×10^5 Pa·s, a viscosity average molecular weight of 45,000 and its density has been measured as a function of temperature.[711,712]

The sample loading procedure for polyisobutylene is different from that of a molten plastic since it is in the molten state during loading. Using wet hands to prevent adhesion, a rectangular sample can be shaped and held until dry on one side. The sample can then easily be pressed onto the stationary plate around the active face of the transducer, taking care not to allow bubbles to be trapped between the polymer and the stationary plate. The rheometer is then closed and one proceeds as for the case of a molten plastic. This approach is simpler than the more commonly used method of heating the polymer overnight under vacuum and pouring the hot melt onto the stationary plate.

2. New Rheometer Using MTS-BASIC Programs

a. Small Amplitude Tests

(1) Low S/N

A common problem with performing small shear strain amplitude experiments at low frequency on a rheometer designed for nonlinear viscoelastic property measurements is that the background noise levels can begin to interfere with the low-level shear stress measurements. Small shear strain amplitude tests were done with molten polystyrene, Styron 683, at 190°C Figure 82 is a representative test record for a small amplitude oscillatory shear test This test was done with a shear strain double amplitude of .4 at .1 Hz and the signal to noise ratio is low. This is clear from the raw data loop of shear stress versus shear strain.

Figure 83 is the amplitude spectrum of the shear strain, which demonstrates the quality of the motion of the sliding plate The statistical analysis of this spectrum, plotted on expanded linear scales in Figure 84, shows that only the fundamental is significantly different from zero within a two-sigma confidence range. Furthermore, from the breadth of this peak we conclude that the precision on the frequency is better than the frequency resolution (DF), which is 1% of the driving frequency, and this is one good measure of rheometer performance. The corresponding phase spectrum, not shown, shows the phase content of the strain to be slightly higher than $\pi/2$ which is what it should be since the HTS harmonic function is a cosinusoid with $\pi/2$ phase content.

Figure 85 is the corresponding time trace for the shear stress response. Note the differences from cycle to cycle due to background noise. The corresponding shear stress spectrum in rectangular form, Figure 86, and the shear stress amplitude spectrum, Figure 87, show that only the fundamental contributes significantly to the material response. Furthermore, the log-amplitude of the shear stress, Figure 88, shows that the spectrum of the background noise is uniform. This type of noise is called white noise.

On occasion, a different type of experimental noise is observed such that the level of background noise decreases gradually with frequency. This is an error and is due to the rectangular window used and can be minimized by pretreating the time series in several ways before proceeding with the DFT. For example, in Figure 97 this sort of windowing error is noticeable. In practice, this type of error was occasionally observed. However, when windowing error does occur it is best to supplement the DFT of the rectangularly windowed time series with a specially filtered one. The analysis program given in Appendix 3 incorporates such an option. Consider Figure 98 which shows a Hanning windowed version of the spectrum given in Figure 97. The background noise is flatter at the low frequency end. Also, the peaks have been broadened and uniformly attenuated by a factor of .5, disadvantages characteristic of this type of digital filtering.

Those not familiar with such alternate windowing techniques, specifically the use of the Hanning window, are encouraged to consult Ramirez (1985) for further explanation.[713]

As discussed in chapter 5, meaningful phase spectra are generated by setting the phase contents of all noise components to zero, so that only the important phase contents are shown. This process is called digital filtering or noise-reduction. Figure 90 shows such a phase spectrum for the shear stress signal and Figure 89 shows the corresponding noise-reduced or digitally filtered amplitude spectrum. The phase lag of the fundamental of the shear stress is greater than zero and less than $\pi/2$. Otherwise stated, the shear stress response is thermodynamically plausible Also, here only the fundamental of the shear stress remains in the amplitude spectrum However, the statistical analysis shown in Figure 91 reveals the existence of very small higher harmonics that are barely significant at the 95% confidence level for the second, third and fourth harmonics Small even harmonics can be attributed to the effect of normal thrust on lateral cantilever deflection, which was discussed under transducer design.

Spectral analysis of the total force contrasts sharply with that of the shear stress. In both the rectangular spectra, Figure 92, and on the log-amplitude spectrum, Figure 93, higher harmonics are clearly evident. Higher harmonics of total force are also clearly in evidence in these spectra The noise-reduced amplitude spectrum and its corresponding phase contents are shown in Figures 94 and 95 respectively. Hence, the total force measurements are not qualitatively consistent with the shear stress measurements. The longstanding hypothesis that free-boundary errors are important is well supported. The statistical analysis of these data,

Figure 96, shows that higher harmonics up to and including the seventh one are significantly different from zero with better than a 2-sigma confidence level.

(2) High S/N

Figure 106 shows the frequency spectrum of shear stress for a small amplitude oscillatory shear test at a higher frequency. The spectrum is rich with odd higher harmonics that are not noticed on loops of stress versus strain or strain rate. The statistical analysis, shown in Figure 107, shows higher odd harmonics, including the 3rd, 5th and 7th, to be significant The even harmonics in such spectra are attributed to the effect of normal thrust A more precise determination of the amplitudes of these harmonics would best be achieved by collecting a larger time series, but increased RAM would be required so that larger, better resolved FFT's could be performed.

b. Effect of Thermal Degradation

It has been hypothesized that an advantage of sensing the shear stress locally, away from the free boundaries of the sample, is that experimental error due to oxidative degradation can be avoided for a considerable period of time without having to use expensive nitrogen blanketing. Figure 99 shows the comparison of the corrected phase angles for the total force and for the shear stress, both versus sample age. For the total force, considerable variation in phase angle is noticed in the total force after roughly 10 to 15 minutes. Corresponding curves showing the effect of sample age on shear stress and total force amplitudes are shown in Figures 100 and 101 respectively. A large variation in total force amplitude is observed for the total force while the shear stress response appears unaffected for a period of three hours. The solid state dimensions of the polystyrene plaque used for this test were 5.5 x 3.13 x .035 in. After insertion, using a shim thickness of .030 in, the contact area was inferred to have been 20 sq.in., which was confirmed by inspection after the test.

c. Large Amplitude Tests

Figures 69-81 pertain to a typical large amplitude oscillatory shear test performed on molten polystyrene (Styron 683) at 190°C with a shear strain double amplitude of 14 and a frequency of .2 Hz.

Figure 69 is a typical large amplitude oscillatory shear test record, obtained immediately after each test. The time trace of shear strain compares the command strain (continuous curve) with the actual strain inferred from the LVDT output signal (triangles). This curve gives the operator a quick impression of how closely the actual plate motion approached the desired motion. The total force versus shear strain loop and the shear stress versus shear strain loop quickly tell the operator whether the recorded waves are stationary during the interval of data collection. If standing waves are obtained, the operator can judge whether or not the loops are twofold symmetric. Here, the total force and the shear stress are also recorded during the first cycle.

Recall that a persistent lack of twofold symmetry suggests the presence of a fractured sample, which must usually be replaced. With the polystyrene melt, however, instances of the melt "healing" and returning to its original twofold symmetric state after about 5 minutes are commonly observed. Furthermore, twofold asymmetric standing waves are often observed at high shear rates which can repeatedly be reproduced even after performing several lower shear rate tests and then returning to the higher shear rate conditions.

Figure 70 shows a typical loop of the actual shear strain plotted against the command shear strain. Remember that since the frequency spectrum of the LVDT output is used for the final property determination, plots such as Figure 70 are used to check the harmonicity of the plate motion In this case the command motion closely approximates the desired harmonic function with only a slight phase lag between them. Some phase lag is inevitable in any servo-controlled actuator system.

Figures 71 and 72 show expanded plots of the shear stress transducer output and the load cell outputs respectively versus shear strain. These plots show raw data that have not undergone the small phase corrections and noise-reductions that can be performed using discrete Fourier transforms to improve accuracy and precision respectively.

Figure 73 is a typical counterclockwise loop of shear stress transducer output versus total force showing additional lost work due to free boundary errors arising in the total force measurement. The area of this loop is a measure of the amount of free boundary error incurred in the total force measurement.

Figures 74 and 75 are representative time traces of shear stress and load transducer output signals respectively. They show barely detectable anharmonicities and slight differences from cycle to cycle, which can be attributed to background noise.

(1) Time Domain Differentiation

As mentioned in Chapter 5, when the elements of a time series are equally spaced in time, the time series can be differentiated numerically by the method of Whitaker and Pigford.[714] The formula used for the derivative for each element, y_n, of the time series, $y(n\Delta t)$, is:

$$dy_n/dt = \sum_{X=-2}^{2} X\, y_{n+X} \,/\, (10\, \Delta t) \tag{226}$$

and the second derivative is:

$$d^2y_n/dt^2 = \sum_{X=-2}^{2} [X\, y_{n+X} \,/\, 7(\Delta t)^2] - 2 \sum_{X=-2}^{2} [y_{n+X} \,/\, 7(\Delta t)^2]. \tag{227}$$

Figure 76 is a typical counterclockwise loop of shear stress against shear strain rate in which anharmonicities in the shear stress are evidenced by the non-elliptical shape or pointiness of the loop.

There are an infinite number of derivatives that one might use to plot such loops. However, for liquids it would appear that the shear stress-shear rate loop best brings out the anharmonicities observed during nonlinear viscoelastic deformations. The method of Whitaker and Pigford is well suited to these experimental data, as this method does not amplify signal noise to an unacceptable degree even for the second derivatives. For example, Figures 77 and 78 show typical loops of the time derivative of shear stress, $d\sigma/dt$ or SSTR, versus shear strain and strain rate respectively The shear stress is plotted against the second derivative of shear strain, $d^2\gamma/dt^2$ or RATE OF CHANGE OF SR shown in Figure 79. Finally, the second time derivative of shear stress, $d^2\sigma/dt^2$ or DERIV SSTR, is plotted against the shear strain of Figure 80.

The test program given in Appendix 1 permits each of the aforementioned plots to be obtained immediately following the test. This gives the operator a complete time domain study of the raw data. Finally, a report on individual measurements is also obtained to complete the archival record. The report corresponding to Figures 69-80 is shown in Figure 81. This report contains sequentially:

(a) the data filename (OS208.DAT),
(b) material identification,
(c) test temperature,
(d) shear stress transducer beam number,
(e) test program name and version number (PGM),

(f) sample thickness (SHIM),

(g) operator identification,

(h) test frequency,

(i) shear strain double amplitude (SA),

(j) identification of collected cycle numbers,

(k) total number of data points (PPC),

(l) amplifier range settings (RS) for load, shear stress, shear strain channels,

(m) the baseline noise levels expressed as four times the standard deviation in the baseline signals before the test [NOISE (4S P-P)] for the load, shear stress and shear strain channels,

(n) the test date and time,

(o) the static calibration values for LVDT, load cell and shear stress transducer,

(p) the beam stiffness used in the static calibration,

(q) the capacitance probe model number,

(r) the identification of the electronic circuit used to compatibilize the capacitance amplifier with the MTS DC signal conditioner and,

(s) miscellaneous comments.

(2) Frequency Domain Analyses

In the previous section we noted several points of view that could be used to analyze the nonlinear viscoelastic response of a molten plastic to large amplitude oscillatory shear. These approaches share the disadvantage of not permitting digital filtering. As we saw for the small amplitude oscillatory shear test, frequency domain analyses permit one to resolve features of the material response that might otherwise go unnoticed. The following example underscores such advantages for the case of an anharmonic nonlinear viscoelastic response.

(3) Effect of Frequency

Table 6 summarizes a set of shear-stress response measurements on the polystyrene melt at 190°C in large amplitude oscillatory shear. All phase angles include appropriate phase corrections. The strain amplitude is nominally 5 Some slight differences between tests are a demonstration of the dynamic performance of the servo-controlled drive system. Figure 102 is a plot of these results showing the effect of frequency on the amplitudes of the principal harmonics of shear stress in large amplitude oscillatory shear Expanding the ordinate gives a better picture of the effect of frequency on the third and fifth harmonics shown respectively in Figures 103 and 104 The effect of frequency on the phase angles for the principal harmonics is shown in Figure 105. The loops corresponding to these are presented in Figures 108 and 109. The stress-rate loop accentuates the nonlinearities of the fluid, whereas the stress-strain loop does not.

Table 6: Effect of Frequency in LAOS

f,Hz	γ_o	σ_1	σ_3	σ_5	δ_1	δ_3	δ_5
0.500009	4.97816	.023937	.001378	.000128	4.61734	0.152020	5.309077
1.00015	4.98178	.027398	.001815	.000191	4.25997	5.631608	4.307595
0.200009	4.97698	.014484	.000855	.000129	4.53123	6.144380	4.660421

(4) Effect of Strain Amplitude

Table 7 summarizes the results of frequency domain analyses for a series of tests done at the same frequency, 0.2 Hz, over a wide range of shear strain amplitudes. Appropriate phase corrections were applied to all phase angle entries in Table 7.

Table 7: Effect of Strain Amplitude in LAOS

f,Hz	γ_o	σ_1	[illegible]	σ_5	δ_1	δ_3	δ_5
.200009	4.97698	.014484	.000855	.000129	1.251930	6.131927	4.647972
.200009	5.97686	.016175	.001088	0	1.255510	6.011647	0
.200009	2.49086	.009240	.000222	0	1.071560	5.222697	0
.200009	0.993945	.004506	.000045	0	.952220	4.379787	0
.200009	3.98398	.012634	.000561	0	1.157940	5.714087	0
.200009	0.496974	.002251	0	0	.929910	3.001137	0
.200009	6.97203	.017824	.001380	.000237	1.200560	0.193241	4.744892

These data are summarized in Figures 110-112. Corresponding loops of shear stress versus shear strain are shown in Figures 113-115 and loops of shear stress versus shear rate are shown in Figures 116-118. At 0.2 Hz the behavior of the polystyrene appears to be linear for strain amplitudes of .5 and 1. This is evidenced by the facts that (1) the stress versus shear rate loops are virtually elliptical, (2) the shear stress versus shear strain loops are virtually elliptical and (3) the phase angle of the fundamental is virtually independent of strain amplitude for $\gamma_o \leq 1$. Strictly speaking, linear behavior has not been observed since the harmonic analyses show a significant third harmonic content at $\gamma_o = 1$.

d. Melt Fracture

Oscillatory shear properties can be measured for the molten polystyrene for strain amplitudes from 5% up to levels that cause melt fracture. Hence, the full spectrum of oscillatory shear properties can be measured with the new rheometer. Melt fracture is judged to have occurred when the test report plots show a stress-strain loop that is (1) twofold asymmetric or (2) not closed. A typical example of a test report for a sample undergoing melt fracture is shown in Figure 119. Here, twofold asymmetry is prevalent in the shear stress versus shear strain loop but is not evident in the total force versus shear strain loop. This is because the total force measurement is dominated by flow occurring at the free boundaries. Hence, the flow in the middle of the sample seems not to govern the total force measurement.

e. Shear Stress Near the Free Boundary

Recall that the strain history used in the oscillatory shear test program is generated by an MTS harmonic function that is neither sinusoidal nor cosinusoidal. The actual strain history is:

$$\gamma = \gamma_o (1 + \cos \omega t) . \tag{228}$$

By locating the shear stress transducer near a boundary, one can probe end effects by studying the effect of a sign change in γ_o on the shear stress. With the shear stress transducer 50 mm away (d_{min} = 50 mm) from the nearest end of a rectangular sample, 16 cm long and 10 cm wide, one can probe end effects by performing pairs of otherwise identical oscillatory shear tests in opposite directions. Any difference due to the γ_o sign change can be attributed to end effects Now for a shim thickness of .755 mm, significant effects of sign change were observed at a plate displacement of 10.6 mm (D_{max} = 10.6 mm). This corresponds to a double amplitude of 14 shear strain units. When the test is performed such that the transducer moves toward the center of the sample, a twofold symmetric response is obtained. When the test is performed so that the transducer moves toward the free boundary, twofold asymmetry and overall attenuation is observed in the stress response. This sign change dependence is clearly illustrated in Figure 132.

Recall that the criterion for end effects given in the rheometer design section was $D_{max}/d_{min} < \Phi_c$. For the sample shown in Figure 132, $\Phi_c = 0.21$. Hence,

$$D_{max}/(L-D_T) < 1/5 \ , \tag{229}$$

would appear to be a good design criterion for oscillatory shear experiments on sliding plate rheometers.

3. Preliminary Results

a. Using Modified Prototype

A polyisobutylene resin was studied in large amplitude oscillatory shear at room temperature using the prototype rheometer incorporating an MTI Fotonic sensor.[715] Static calibration was perfomed by suspending weights from the transducer's new calibration hook. All data were collected as oscillographs of stress versus strain (left) and stress versus strain rate (right) loops. One such measurement is shown in Figure 120. These data are collected using the "chop" mode on a Tektronix analog storage oscilloscope. An analog circuit was used to obtain the shear rate from the LVDT signal in real time. The static calibration gave the following conversion from oscillograph grid to shear stress. 0.040 MPa per large division.

(1) Effect of Frequency in LAOS

Figure 121 shows four test results done at a constant strain amplitude of 16.98 at several frequencies. The stress versus strain rate loop becomes less elliptical as the frequency is increased. It has recently been shown that certain kinetic network theories[716,717] predict this behavior for large amplitude oscillatory shear.[718]

Figure 123 shows the results of a comparison between the stress amplitudes obtained in this work and those obtained by Soong.[719] Good agreement was found despite problems with drift in Fotonic sensor sensitivity. Only the shear stress amplitude, σ_o, has been plotted.*

(2) Polystyrene Using IBM PC

Some preliminary results for molten polystyrene were obtained at 130°C using beam #1 with the Tektronix oscilloscope and IBM personal computer-based data acquisition system. These results are presented in a recent paper.[720]

D. Other Strain Patterns

Software has been written to accommodate several other strain histories. These include (1) start-up and cessation of steady shear, (2) reciprocating start-up flow, (3) step strain, (4) reciprocating step strain, (5) cessation of exponential shearing and (6) reciprocating exponential shear.

---

*Not to be confused with the amplitude of the first harmonic, σ_1

In fact, since the actuator motion is programmable, the strain pattern can be specified arbitrarily so that, within the constraints of the actuator dynamic performance, any nonlinear viscoelastic shear property can be measured with the new rheometer.

1. Exponential Shear Tests

The test program for reciprocating exponential shear and for stress relaxation following exponential shearing is given in Appendix 2. Students of MTSBASIC should notice the strong similarity between this program and that used for oscillatory shear given in Appendix 1. The strain history for exponential shear is:

$$\gamma = \exp(\dot{\epsilon}_o t) - 1 \tag{230}$$

and the corresponding strain rate history is:

$$\dot{\gamma} = \dot{\epsilon}_o \exp(\dot{\epsilon}_o t) \tag{231}$$

where $\dot{\epsilon}_o$ is the initial shear rate. For reciprocating exponential shear, the returning part of the cycle is:

$$\gamma = \gamma_o - [\exp(\dot{\epsilon}_o t) - 1] \tag{232}$$

Hence the shear strain for the reciprocating exponential shear property is specified by two variables, the strain amplitude γ_0 and the strain exponent ϵ_0

A representative test record for a reciprocating exponential shear test on molten polypropylene is shown in Figure 124. Expanded versions of these plots are given in Figures 125-127 showing successively, the time trace of the shear strain, the loop of total force versus shear strain and the shear stress versus shear strain The loops include plots of the first cycle response in addition to the stationary loops As for the case of oscillatory shear, the loops of the raw data for the shear stress versus shear strain are different. The signed areas of these loops represent the lost work The apparent lost work is greater when the shear stress is inferred from the total force than when the shear stress transducer signal is used. This discrepancy between total force and local shear stress is underscored by the loop of shear stress versus force shown in Figure 128.

The loop of actual strain versus command strain, Figure 129, shows how closely the actual plate motion approaches the desired reciprocating exponential deformation. Actuator performance is excellent in the exponential shearing mode

A typical time trace of the shear stress response to reciprocating exponential shear is shown in Figure 130. The shear stress inflects. For positive stress this inflection is from concave-up to concave-down. Using the method of Whitaker and Pigford, described earlier in this chapter, the second time derivative of the shear stress, $d^2\sigma/dt^2$, can be computed. Figure 131 shows that when this is plotted against shear strain, the values of the strain at which the inflection takes place are easily identified. Here they are 2.33 and 7.27. When the loop is centered about the ordinate, these values imply an inflection strain of ±2.5.

a. Frequency Domain Analysis

Frequency domain analysis is a useful way of looking at the data from a reciprocating exponential shear test. Figure 133 shows the amplitude spectrum of the shear strain. From the frequency domain, we see that the reciprocating exponential shear test stimulates the fluid at several harmonically related odd frequencies. Over eight peaks, all with amplitudes significant relative to the fundamental, are observed with this DFT Hence, the amplitude spectrum of the shear stress response, Figure 134, also has peaks at the same frequencies. Corresponding phase contents for these spectra were not measured.

VII. CONCLUSION

A. Conclusions

1. On the Shear Stress Transducer

a. Static calibration revealed minimal drift in transducer sensitivity.

b. Dynamic calibration of the new rheometer showed the shear stress transducer to have frequency response good enough to permit accurate measurement of the nonlinear viscoelastic properties it was designed to measure.

2. On the Rheometer

a. The combination of (1) a sliding plate rheometer incorporating the new shear stress transducer for molten plastics, (2) a computer controlled, programmable, servohydraulic linear actuator and (3) a digital data acquistion system, constitutes a system having great flexibility in flow history selection, which required to measure nonlinear viscoelastic properties of molten plastics.

b. The incorporation of a shear stress transducer in a sliding plate rheometer is an effective means of measuring the nonlinear viscoelastic properties of molten plastics, particularly when the transducer incorporates a capacitance proximeter and when a servo-hydraulic linear actuator is used to drive the rheometer.

c. The incorporation of a hook in the side of the shear stress transducer cantilever permits effective calibration, both static and dynamic, of the new rheometer.

d. The shear stress spectrum for a molten plastic in oscillatory shear measured on the new rheometer consists of principal harmonics plus white noise.

3. Relating to Rheological Measurement

a For a molten plastic in oscillatory shear, the actual shear stress response and the stress response inferred from total force are different.

(1) The presence of higher harmonics is more pronounced in total force spectra than in shear stress spectra.

(2) The phase angle between the shear strain and the fundamental of the total force is always higher than the angle between the strain and the shear stress.

(3) Melt fracture is clearly evident in the shear stress signal, but may go undetected in the total force signal.

These phenomena are attributed to measurement errors caused by uncontrollable flows occurring near the sample free boundary.

4. Applying to Analysis

a. The use of spectral analysis permits slight higher harmonics to be detected for molten plastics in oscillatory shear, even at strain amplitudes as low as 0.2.

B. Contributions to Knowledge

The single most important contribution to knowledge of this research has been the design and evaluation of a sliding plate rheometer incorporating a shear stress transducer which permits the measurement of the nonlinear viscoelastic properties of molten plastics. The measurement of the errors due to the uncontrolled flow which arises when properties are inferred from total force is also an important contribution.

Another contribution to knowledge was made with the development of convenient methods for rheometer calibration. The method of static calibration is carried out at elevated temperature and does not require sample removal. The technique for dynamic calibration can also be performed at elevated temperature.

The investigation of the viscoelastic properties of molten plastics in transient simple shear tests incorporating shear rates that cause material responses spanning from linear viscoelasticity to sample fracture is a contribution to knowledge. Using the discrete Fourier transform, the methods of analysis for the viscoelastic properties of molten plastics have been advanced. This advancement provides improved accuracy in the viscoelastic property measurements by permitting phase-corrections, signal-averaging and noise-reduction on shear stress, total force and shear strain signals.

C. Recommendations

1. Pertaining to the Shear Stress Transducer

a Since squeezing flow in the annulus between the cantilever and the housing governs the frequency response of the transducer, there is an incentive to be able to use shear stress transducers having stiff cantilevers. Improvements in the frequency response of the shear stress transducer might be achieved with the use of a piezoelectric sensor whose intrinsically high rigidity would permit such very stiff cantilevers without sacrificing resolution in the shear stress. It is recommended that the feasibility of this method be evaluated at high temperatures.

b In its original conception, it was suggested that the shear stress transducer for molten plastics incorporate a linear servo-motor and be set up as a null-balance.[721,722] This more complicated approach could permit a high effective cantilever stiffness if the servo-motor has good frequency response. The use of the null-balance concept has recently been used for a new torque and normal thrust cell incorporated in a rotational rheometer.[723] It is recommended that the feasibility of this approach to shear stress transduction be investigated.

2. On the Rheometer

a. Since the displacement resolution provided by the MTS servohydraulic drive system is 9 microinches,* sample thicknesses as low as .9 mil could be accommodated for rheological testing. However, since shim thickness accuracy is only .001 inches, it is desirable to achieve tighter control of sample thickness. Cain[724] has suggested that shorter sides be used on the rheometer, so that thick shims could be ground with .05 mil accuracy to capitalize on the displacement resolution of the servohydraulic drive system. Another approach might be to design the rheometer to incorporate a continuously adjustable gap similar to Locati's sliding plate rheometer[725] or analogous to Tee's concentric cylinder rheometer, both of which have continuously adjustable sample thickness.[726,727] It is recommended that one such improvement in sample thickness accuracy be incorporated into future sliding plate rheometers.

b. The servo-control loop for the MTS hydraulic drive system is currently equipped with a load-control mode ordinarily used for force-controlled experiments on solids such as fatigue type tests. It is clearly possible to use the shear stress transducer output in this control loop to do shear stress controlled experiments on molten plastics. Here the molten plastic

*Simply the digital resolution of the LVDT acquisition system times the minimum travel range: $(1/2^{16})$ 0.6 inch.

itself becomes part of the control-loop in shear stress controlled tests which implies that the gain of the servo-controller circuitry should be tuned for each sample at each test rate. It is recommended that the feasibility of shear stress controlled experiments be evaluated in future work.

c. Recently, Meissner has studied the directional dependence of viscoelastic properties of polymer melts at low shear rates using a biaxial shear rheometer.[728,729] It has been suggested that the incorporation of a shear stress transducer into such a biaxial shear rheometer would permit the directional dependence of nonlinear viscoelastic properties to be measured.[730] A study of the feasibility of this way of measuring directional dependence of viscoelasticity of molten plastics is highly recommended.

3. <u>Relating to Rheological Measurement</u>

a. The advantages of using discrete Fourier transforms for data analysis in rheometry apply for most situations where rheometers are used for dynamic testing. Noise-reduction and signal-averaging, monitoring for slight deviations from linearity, time-shifting the baseline and non-linear viscoelastic property measurements are all made possible using DFT techniques. For these reasons, those using rheometers equipped with microcomputer controlled data acquisition are strongly encouraged to use frequency domain techniques for dynamic work.

4. Applying to Analysis

a It has been mentioned that frequency domain methods are equally useful for analyzing nonstationary waveforms such as stress relaxation data.[731] The advantages realized for oscillatory shear and demonstrated herein can also, in principle, be realized for other transient property measurements. The use of the "zoom" FFT, for analyzing transient test results is an especially exciting prospect for frequency domain analysis.[732,733,734] An assessment of the feasibility of using the DFT for analyzing transient properties other than oscillatory shear is highly recommended for future work.

b. Few theorists have used frequency domain analyses for studying the property predictions of mathematical models of the nonlinear viscoelasticity of polymeric liquids.[735] Engineers evaluating viscoelastic theory are encouraged to consider looking at mathematical predictions from the frequency domain point of view.

FIGURES

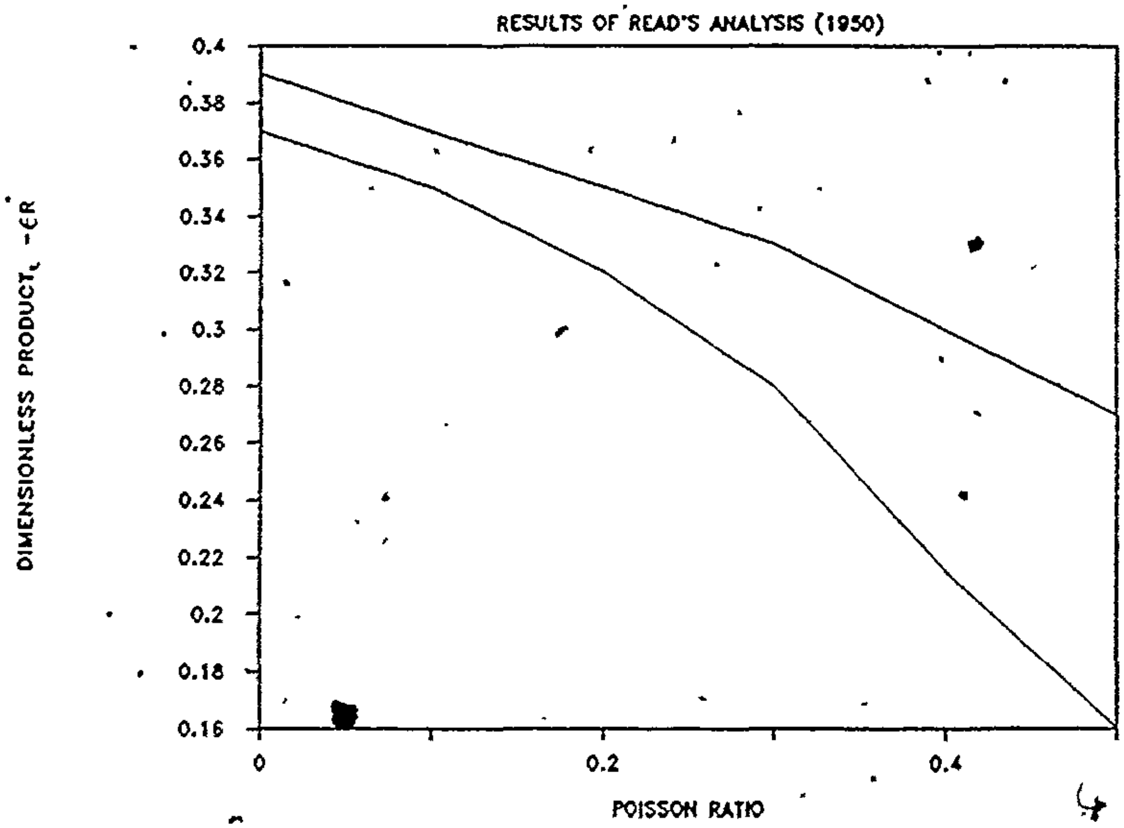

Figure 1 Upper and lower bounds to the free boundary error predicted for small shear strain using the thermodynamic analysis of Read (1950).

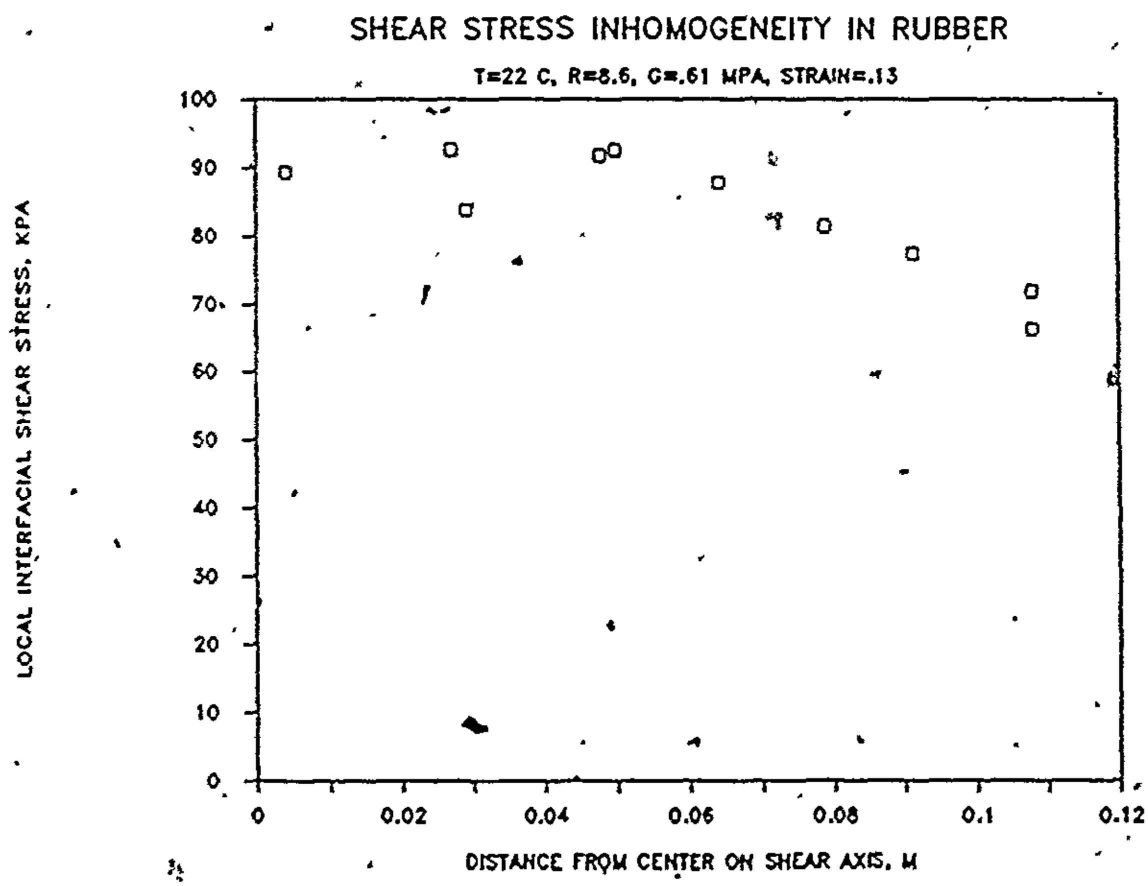

Figure 2. Shear stress inhomogeneity for rubber in simple shear measured with local shear stress transducer, T=22 C, R=8.6, G=.61 MPa, γ=0.13.

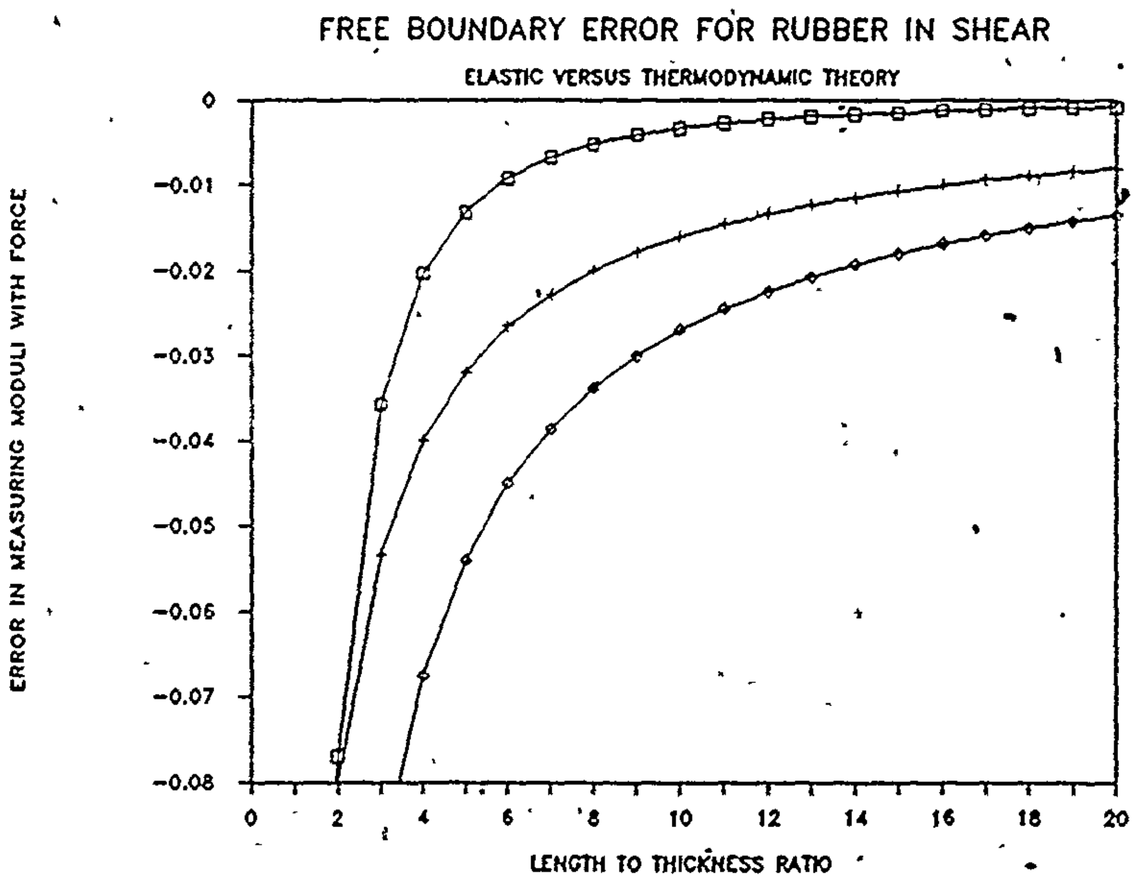

Figure 3. Free boundary error for rubber in simple shear using elastic (squares) and thermodynamic upper (diamonds) and lower (crosses) bounds.

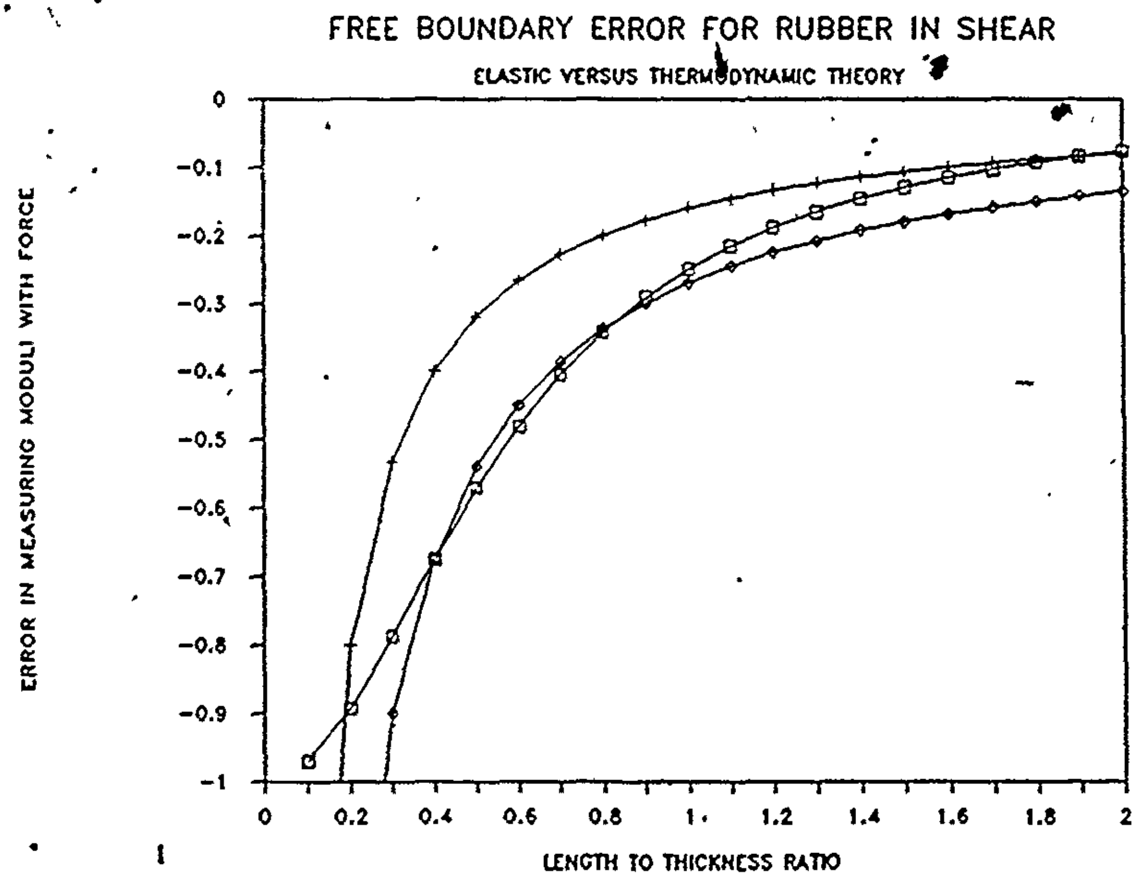

Figure 4: Free boundary error for rubber in simple shear using elastic (squares) and thermodynamic upper (diamonds) and lower (crosses) bounds.

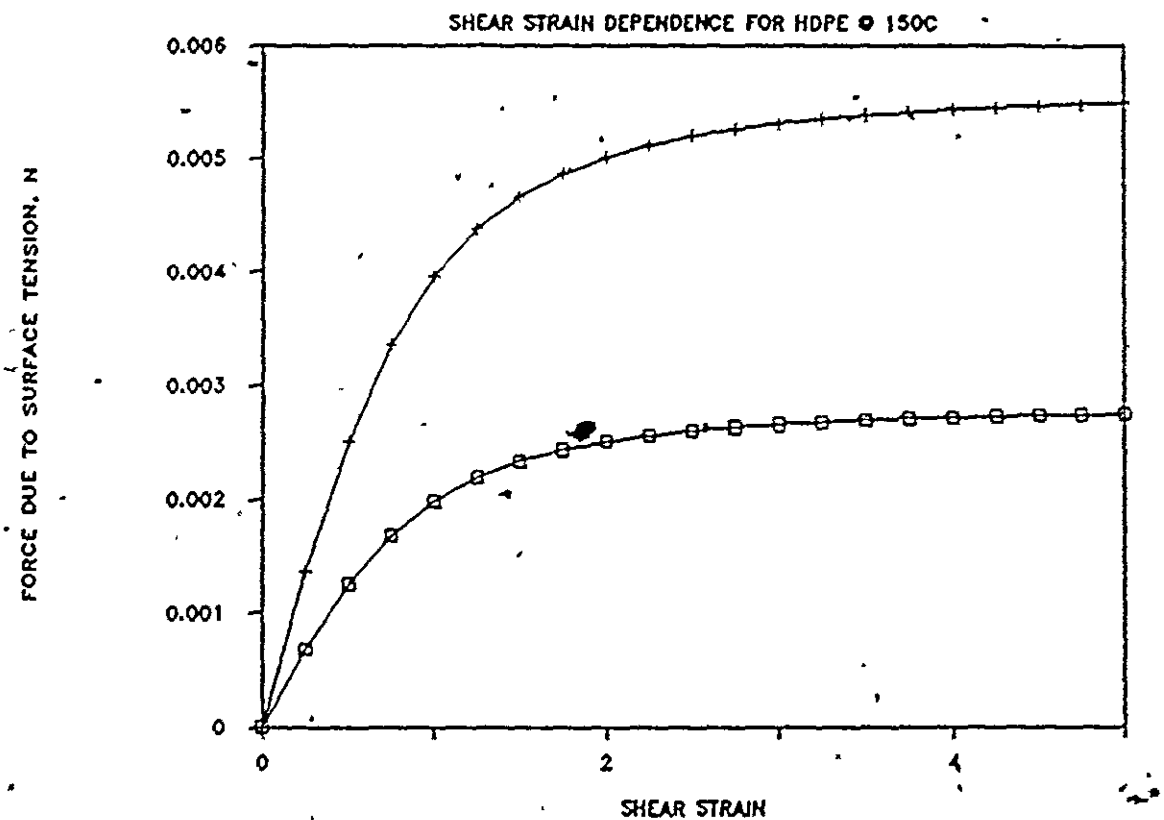

Figure 5: Shear strain dependence of force due to surface tension of free boundary computed for high density polyethylene at 150°C. Sample width of 5 cm (squares) and 10 cm (crosses).

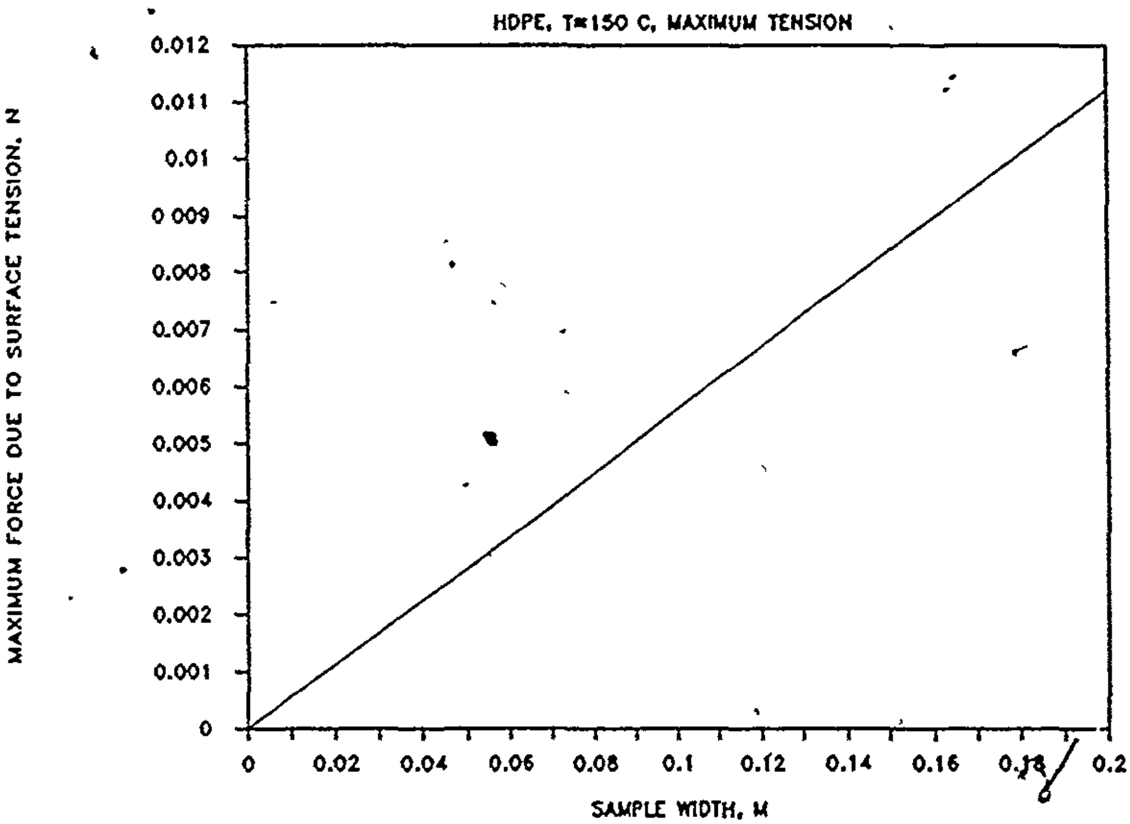

Figure 6. Width dependence of maximum force due to surface tension of free boundary for high density polyethylene at 150°C.

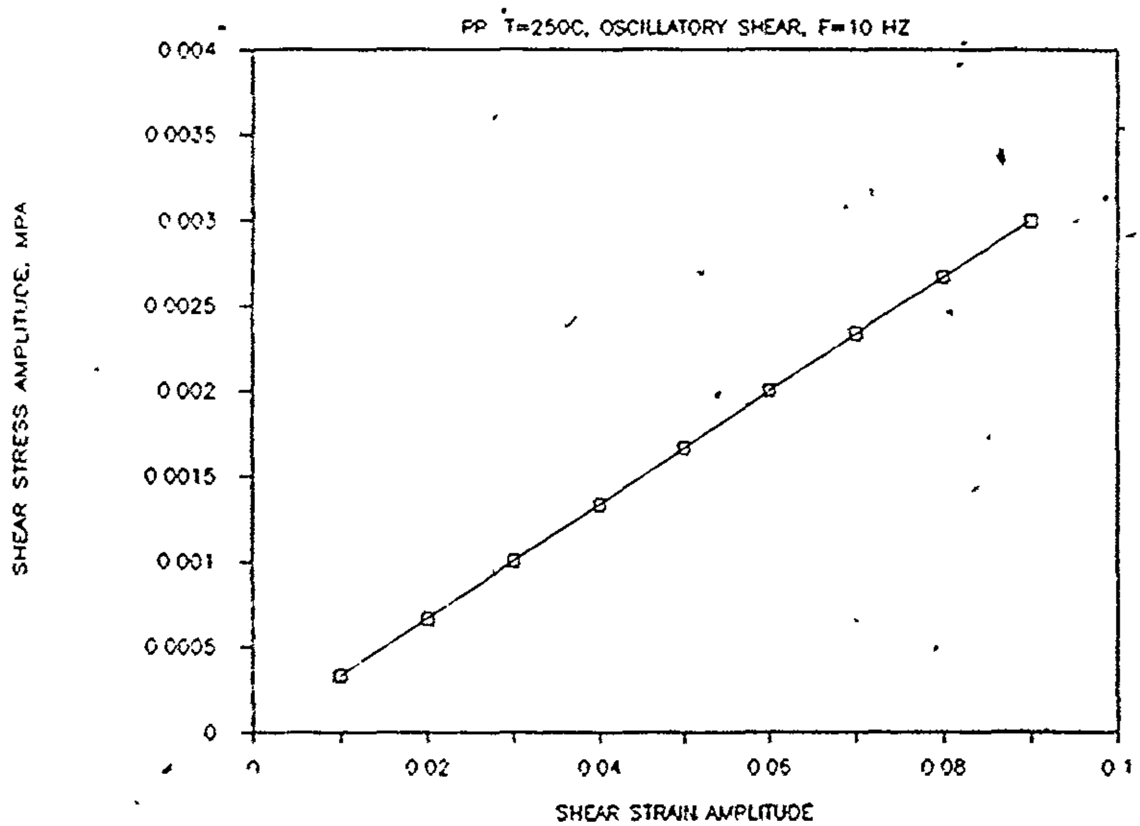

Figure 7a. Linear behavior of stress amplitude for polypropylene melt in oscillatory shear measured with rotational rheometer using cone-plate fixture, T = 250°C, f = 10 Hz.

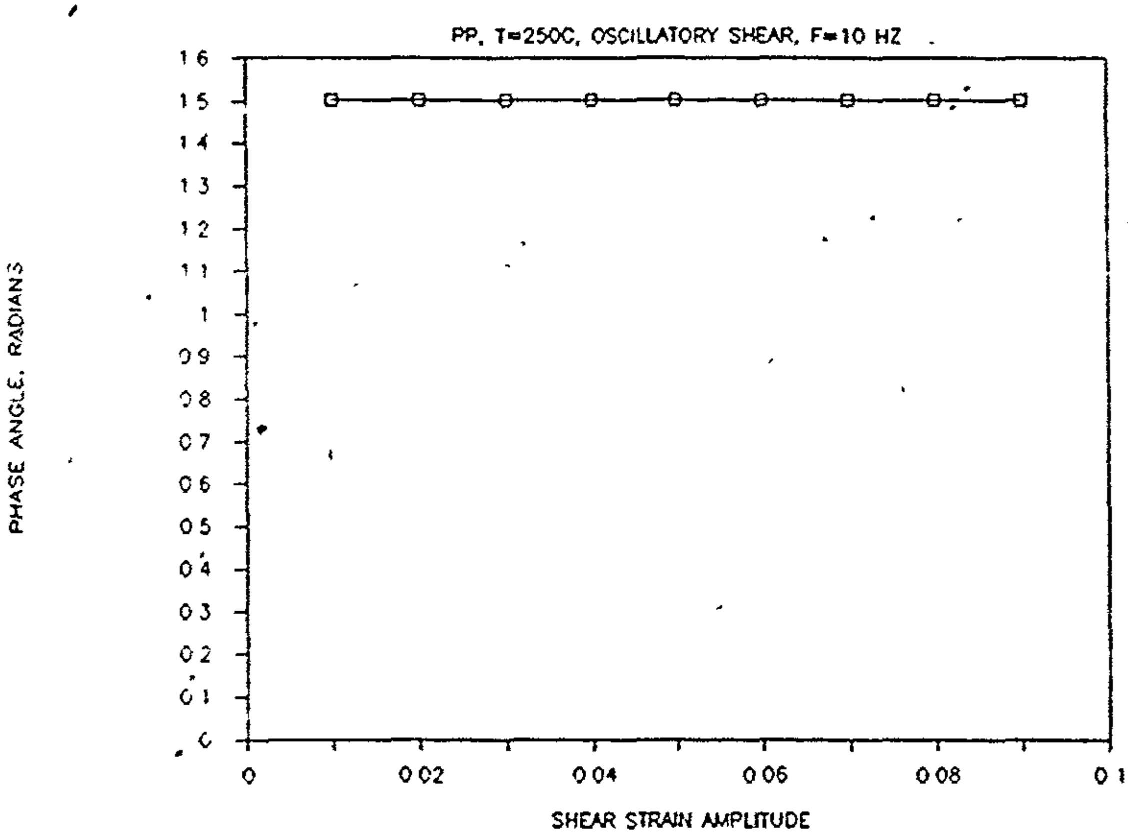

Figure 7b. Linear behavior of phase angle for polypropylene melt in oscillatory shear measured with rotational rheometer using cone-plate fixture, T = 250°C, f = 10 Hz.

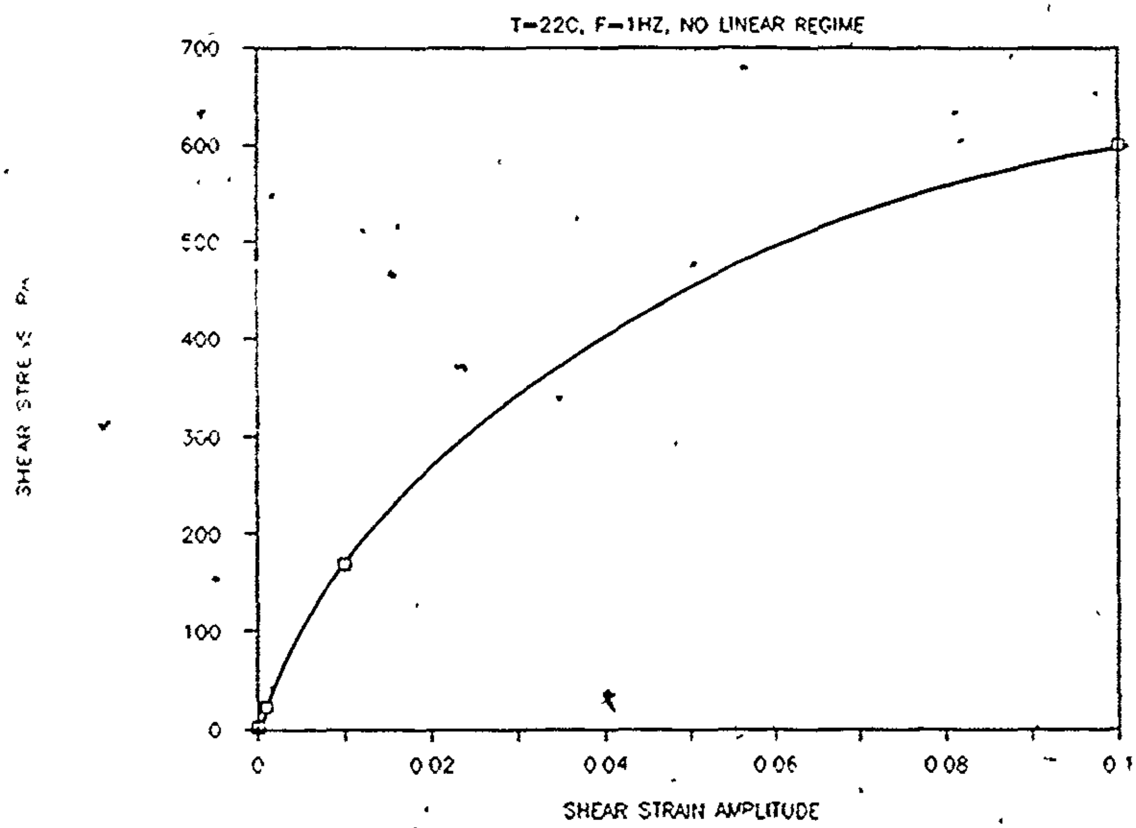

Figure 8a. Nonlinear behavior of stress amplitude for bread dough in oscillatory shear measured with sliding cylinder rheometer, T = 22°C, f = 1 Hz.

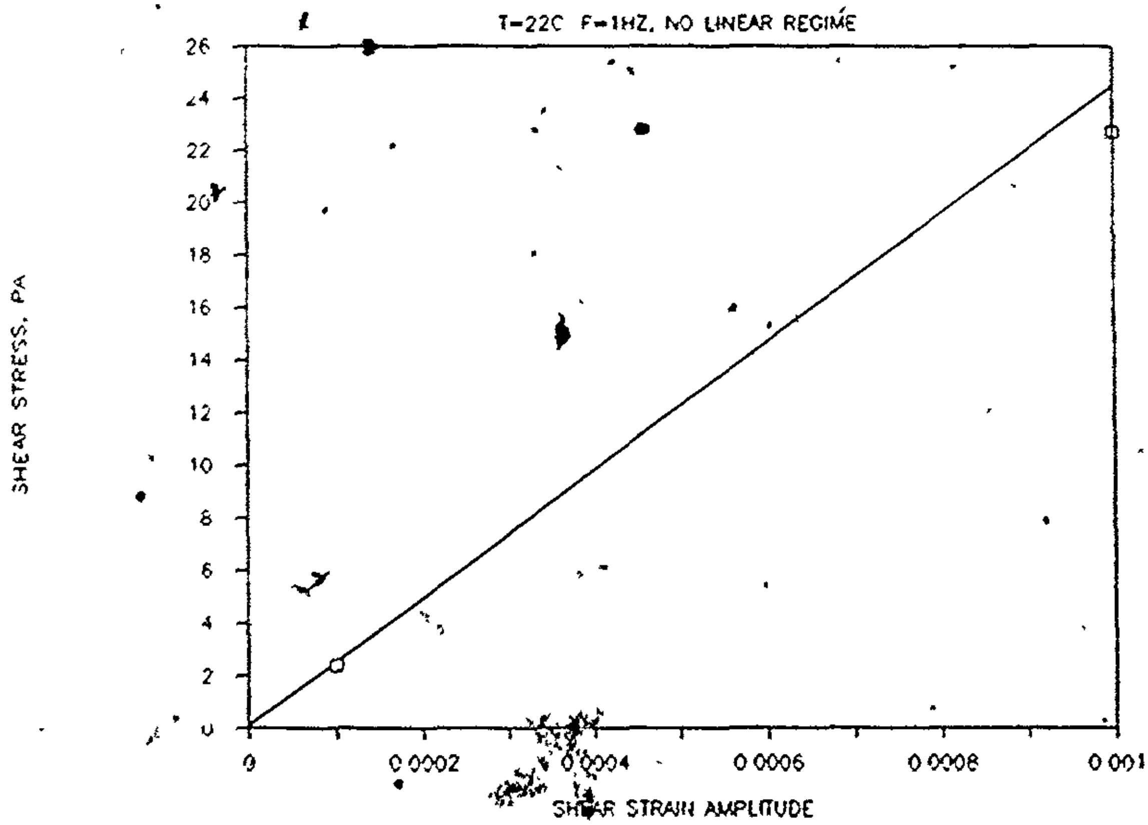

Figure 8b: Nonlinear behavior of stress amplitude for bread dough in oscillatory shear at low shear strain amplitudes measured with sliding cylinder rheometer, T = 22°C, f = 1 Hz.

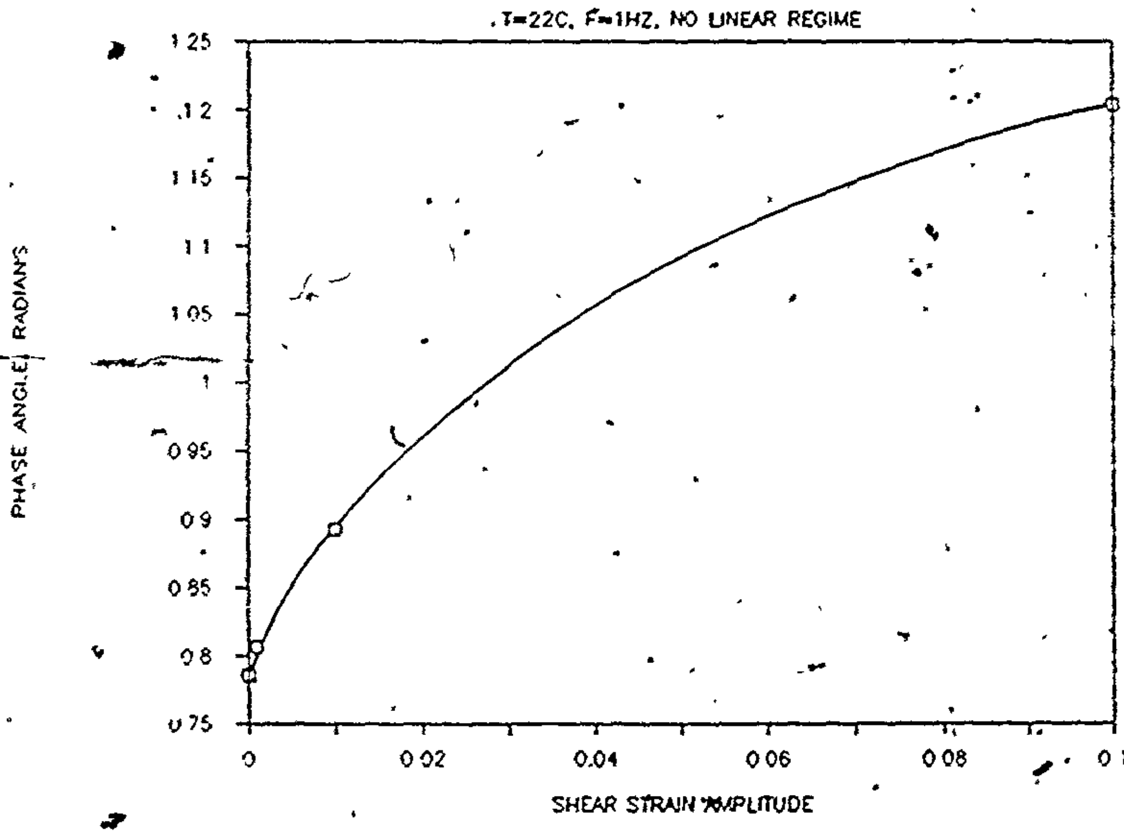

Figure 8c. Nonlinear behavior of phase angle for bread dough in oscillatory shear measured with sliding cylinder rheometer, T = 22°C, f = 1 Hz.

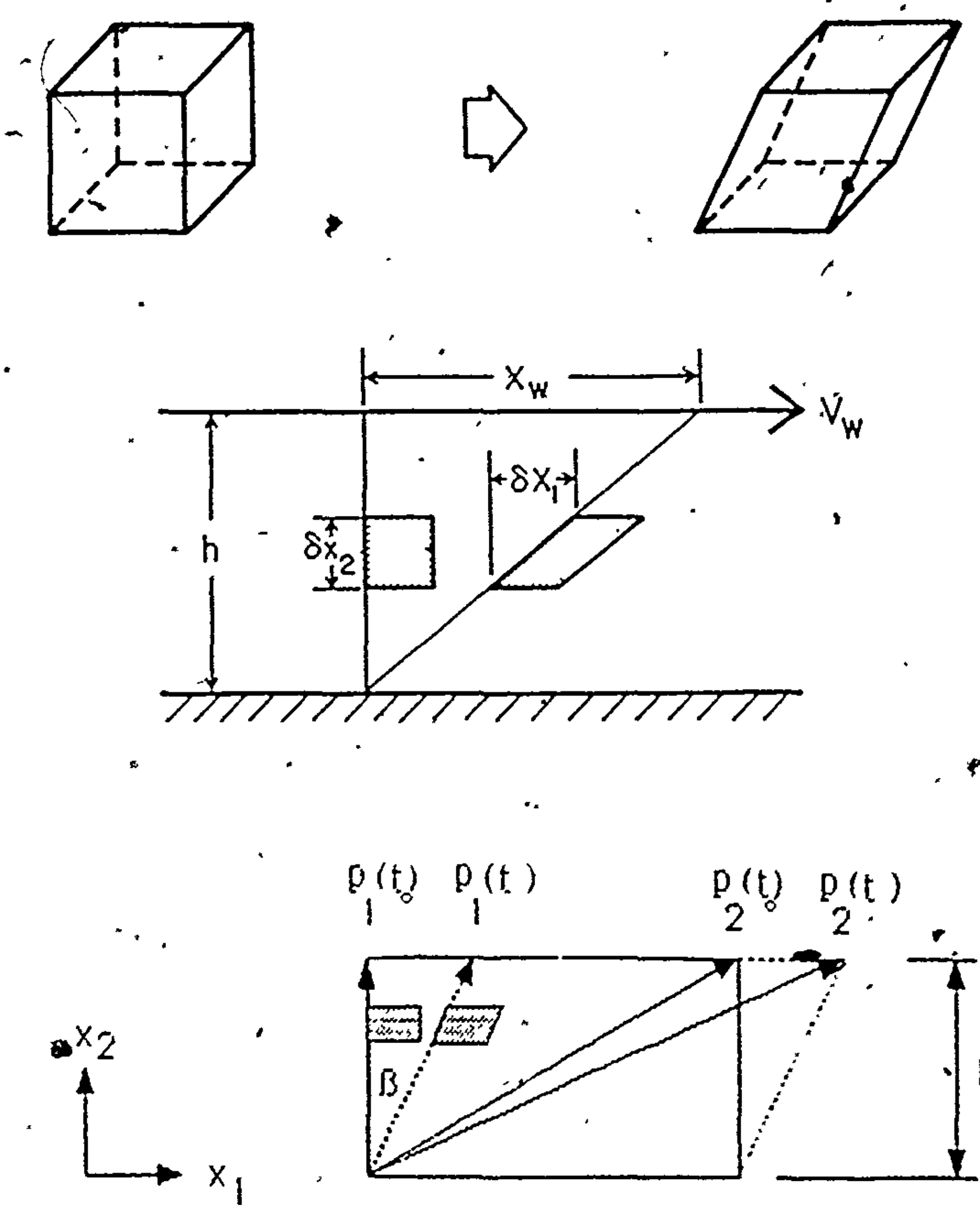

Figure 9 Illustration of simple shear deformation generated between sliding plates. The shear strain, the plate displacement per unit sample thickness, $\gamma = \delta X_1/\delta x_2$, is identically the tangent of the angle of shear, β.

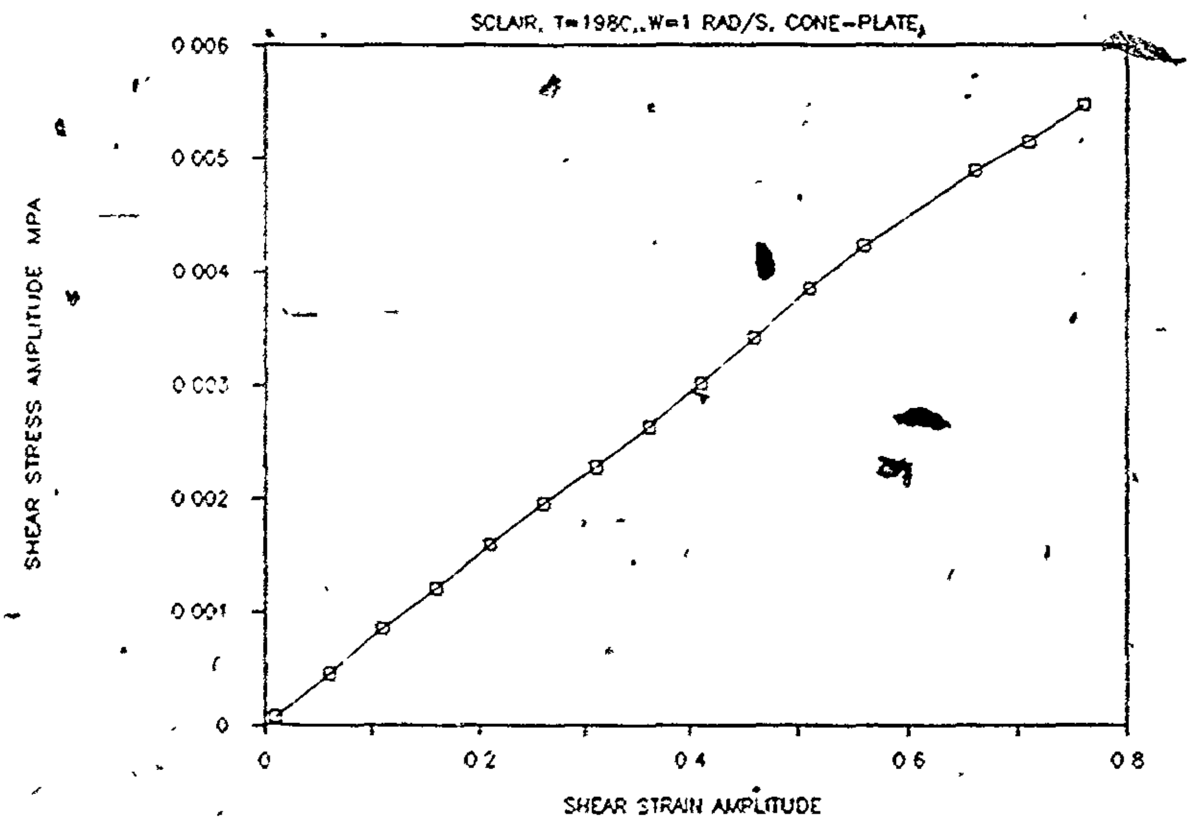

Figure 10. Linear behavior of shear stress amplitude for molten Sclair LDPE in oscillatory shear measured with rotational rheometer using cone-plate fixture, T = 198°C, ω = 1 rad/sec.

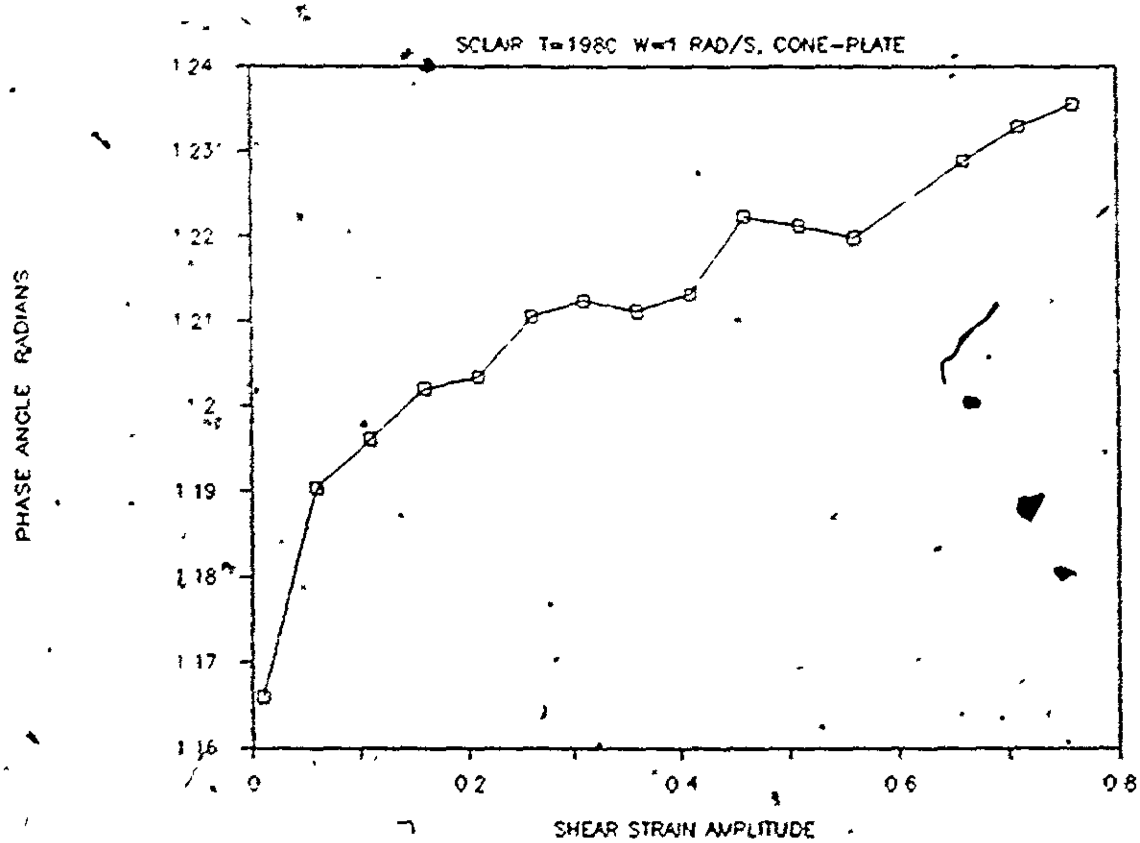

Figure 11. Nonlinear behavior of phase angle for molten Sclair LDPE measured with rotational rheometer using cone-plate fixture, T = 198°C, ω = 1 rad/sec.

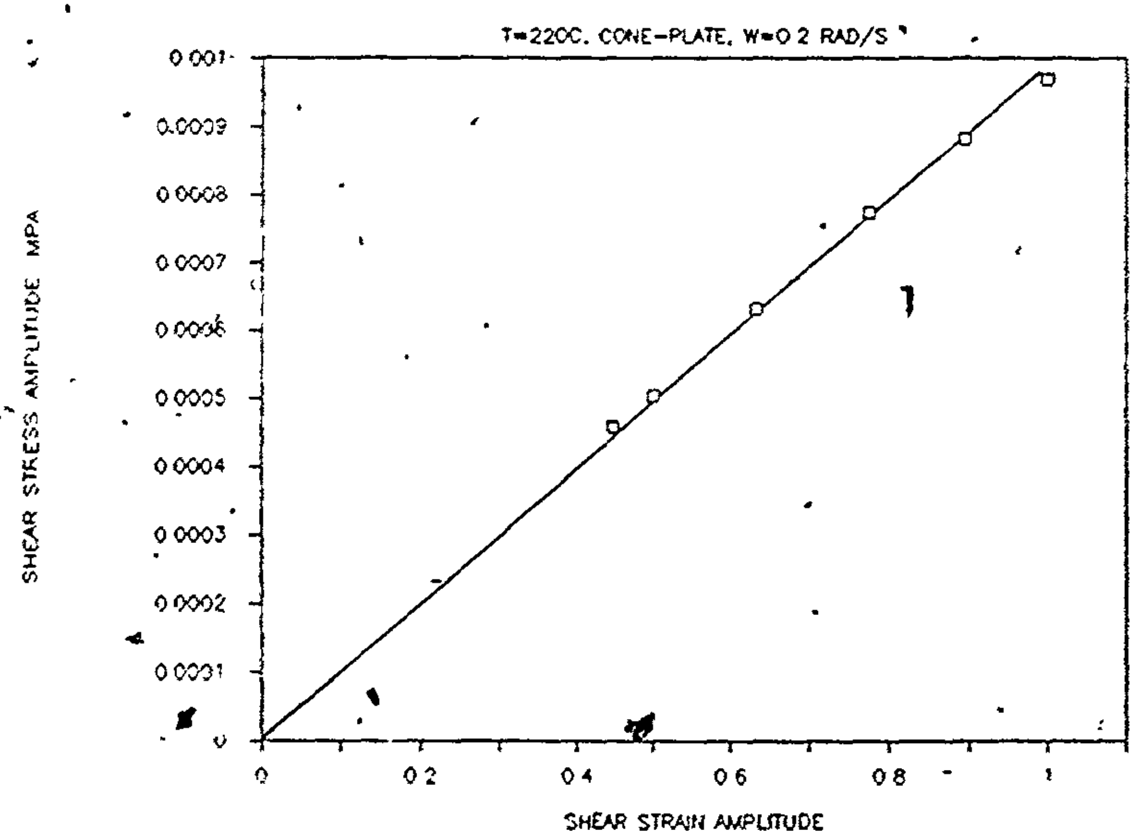

Figure 12a· Linear behavior of stress amplitude for polypropylene melt in oscillatory shear measured with rotational rheometer using cone-plate fixture, T = 220°C, ω = 0.2 rad/sec.

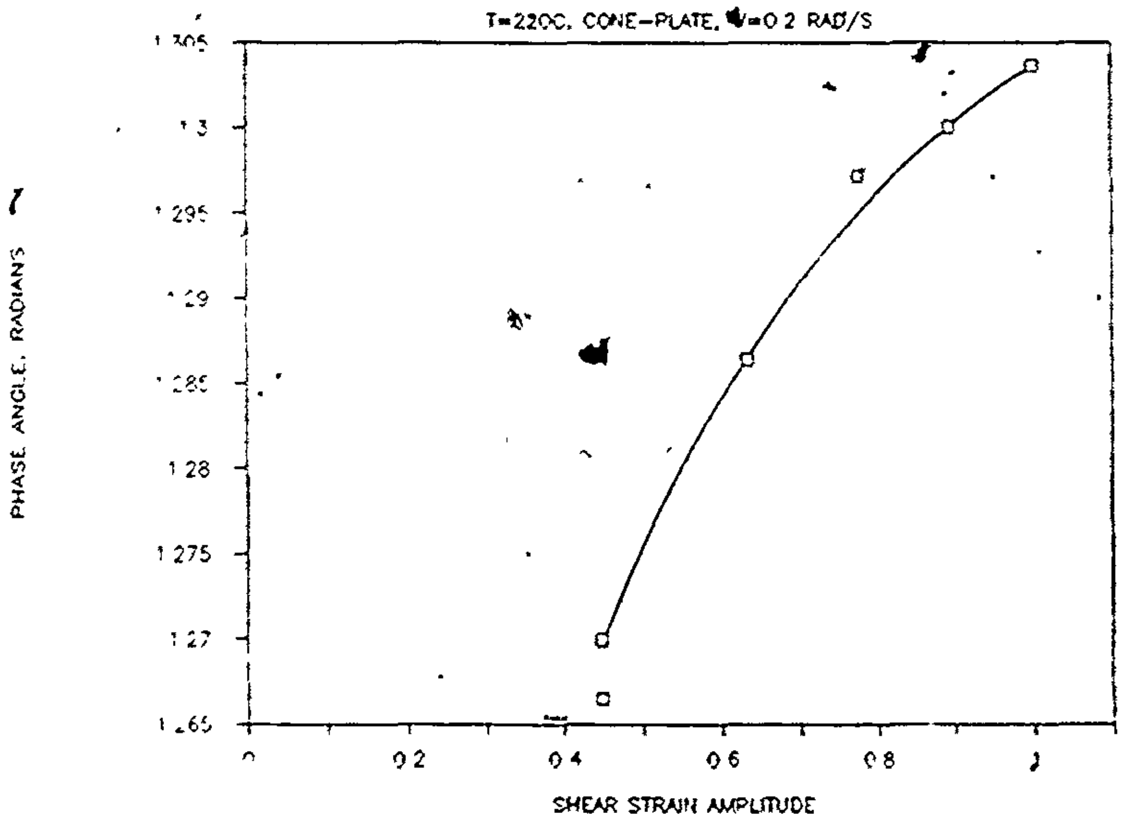

Figure 12b: Nonlinear behavior of phase angle for polypropylene melt in oscillatory shear measured with rotational rheometer using cone-plate fixture, T = 220°C, ω = 0.2 rad/sec.

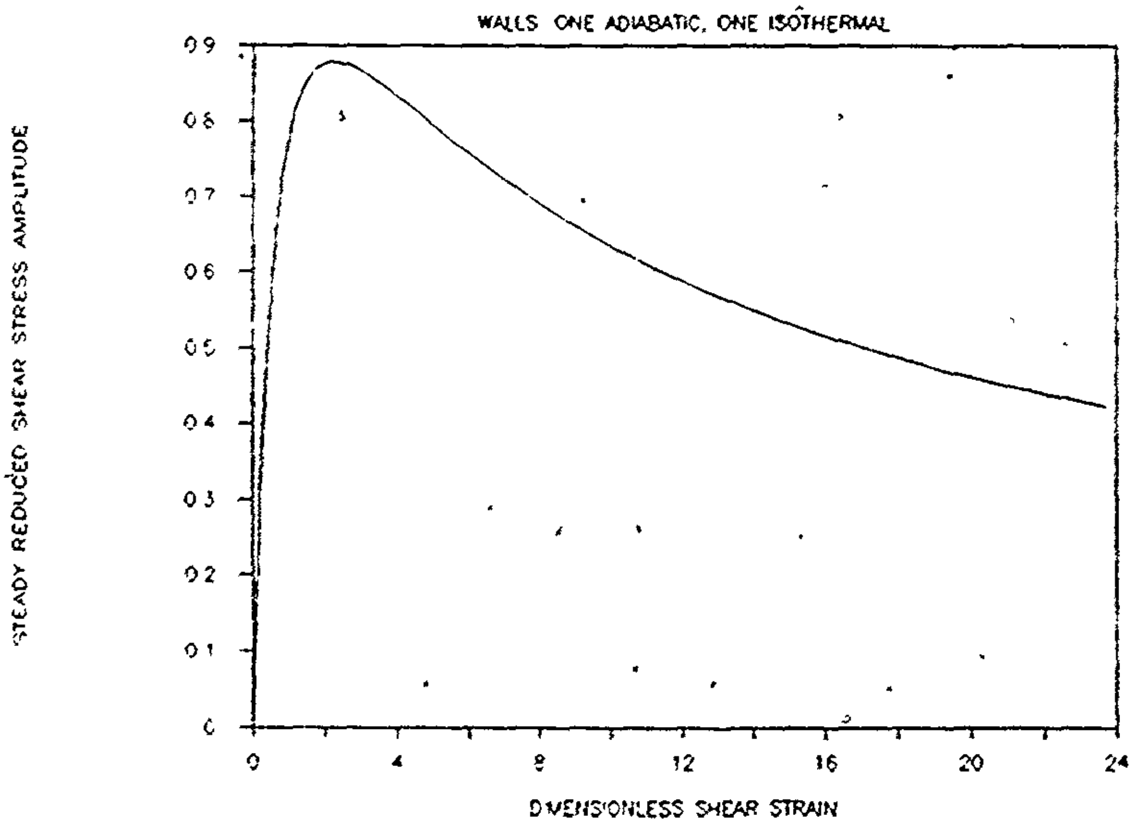

Figure 13: Effect of viscous heating on apparent oscillatory shear properties. The shear strain is double-valued with shear stress.

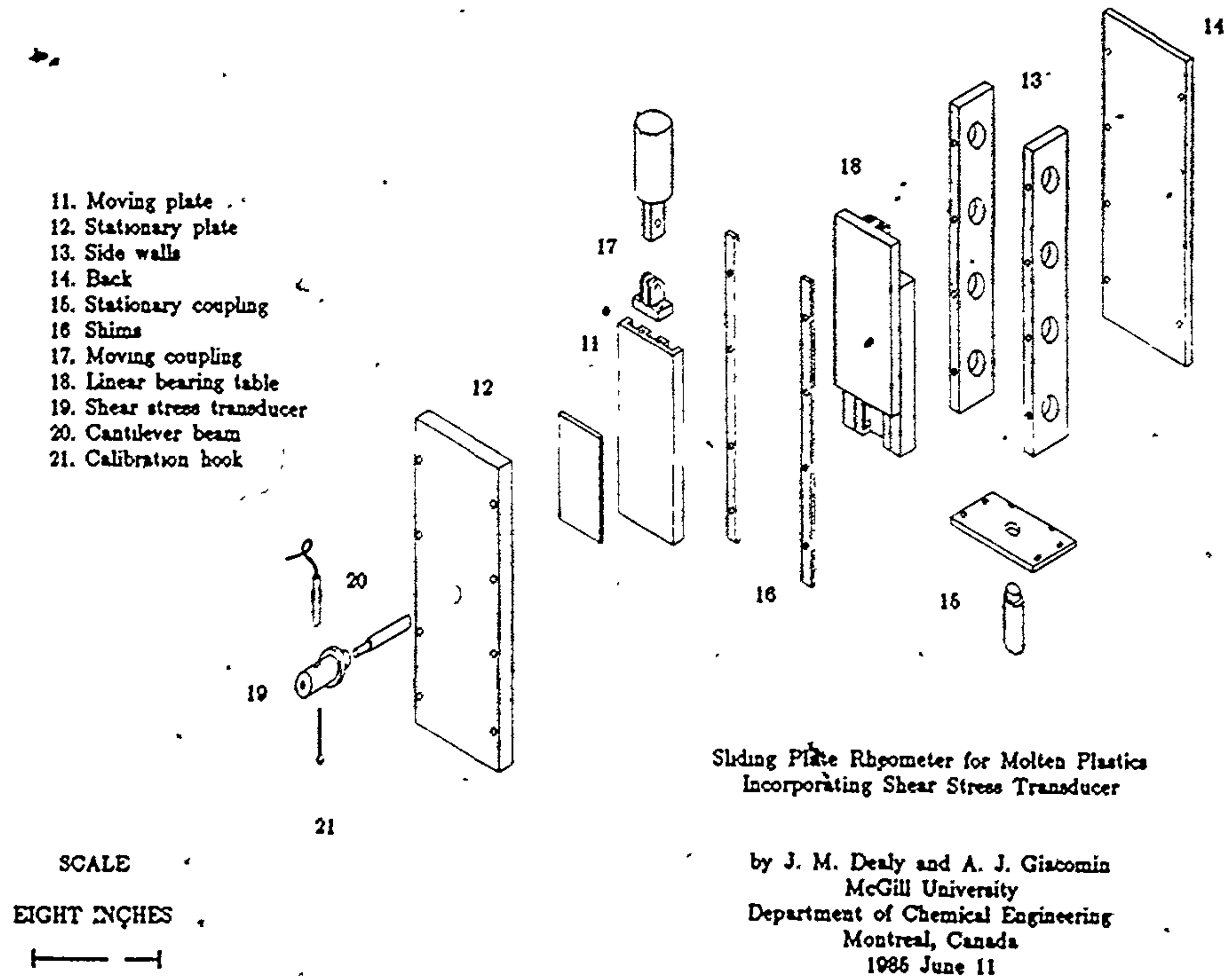

Figure 14. Isometric drawing with exploded view of sliding plate rheometer for molten plastics incorporating shear stress transducer.

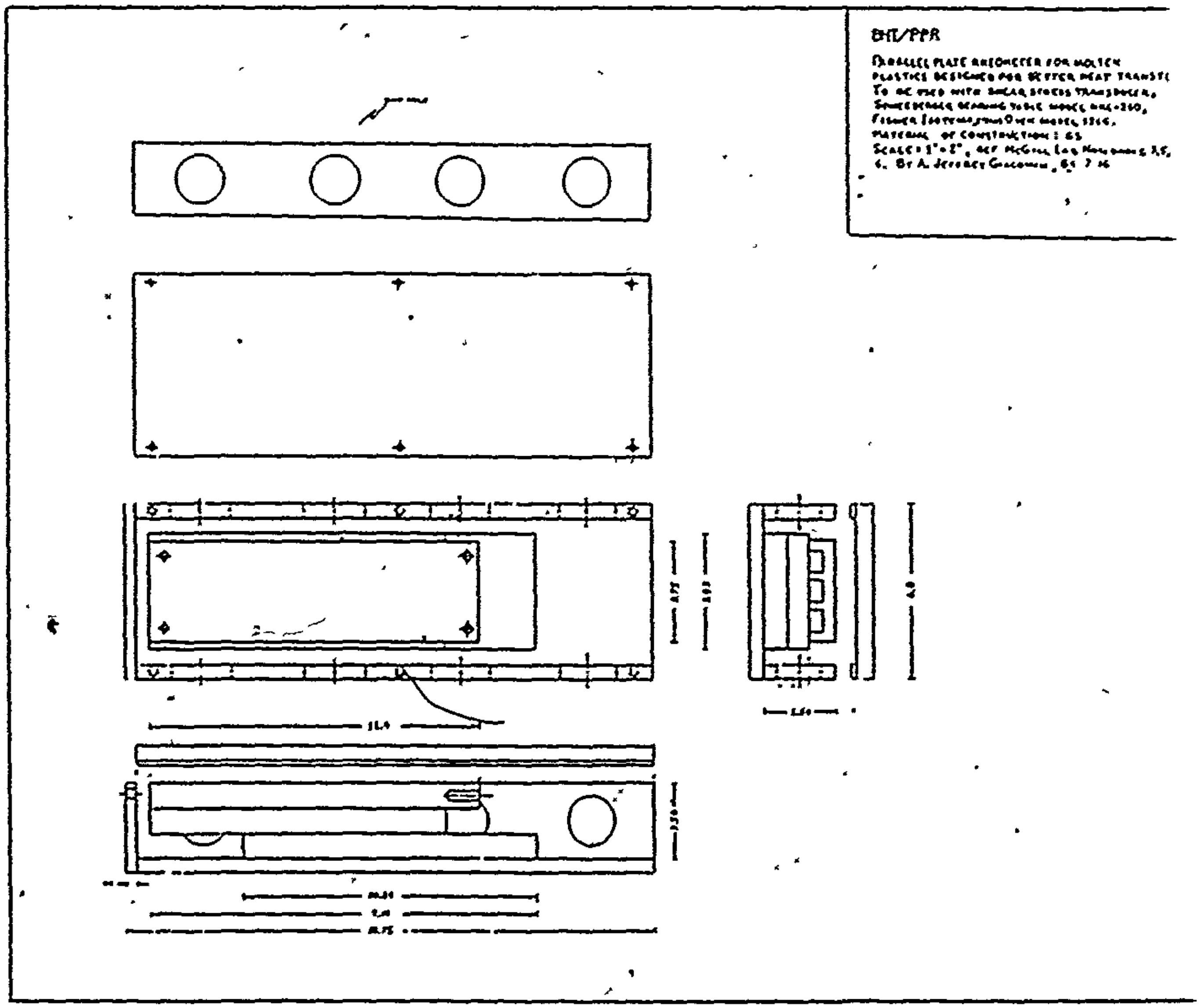

Figure 15. Engineering drawing for parallel plate rheometer for molten plastics designed for better heat transfer to be used with shear stress transducer, Schneeberger bearing table model NK6-260 and Fisher Isotemp oven model 126G.

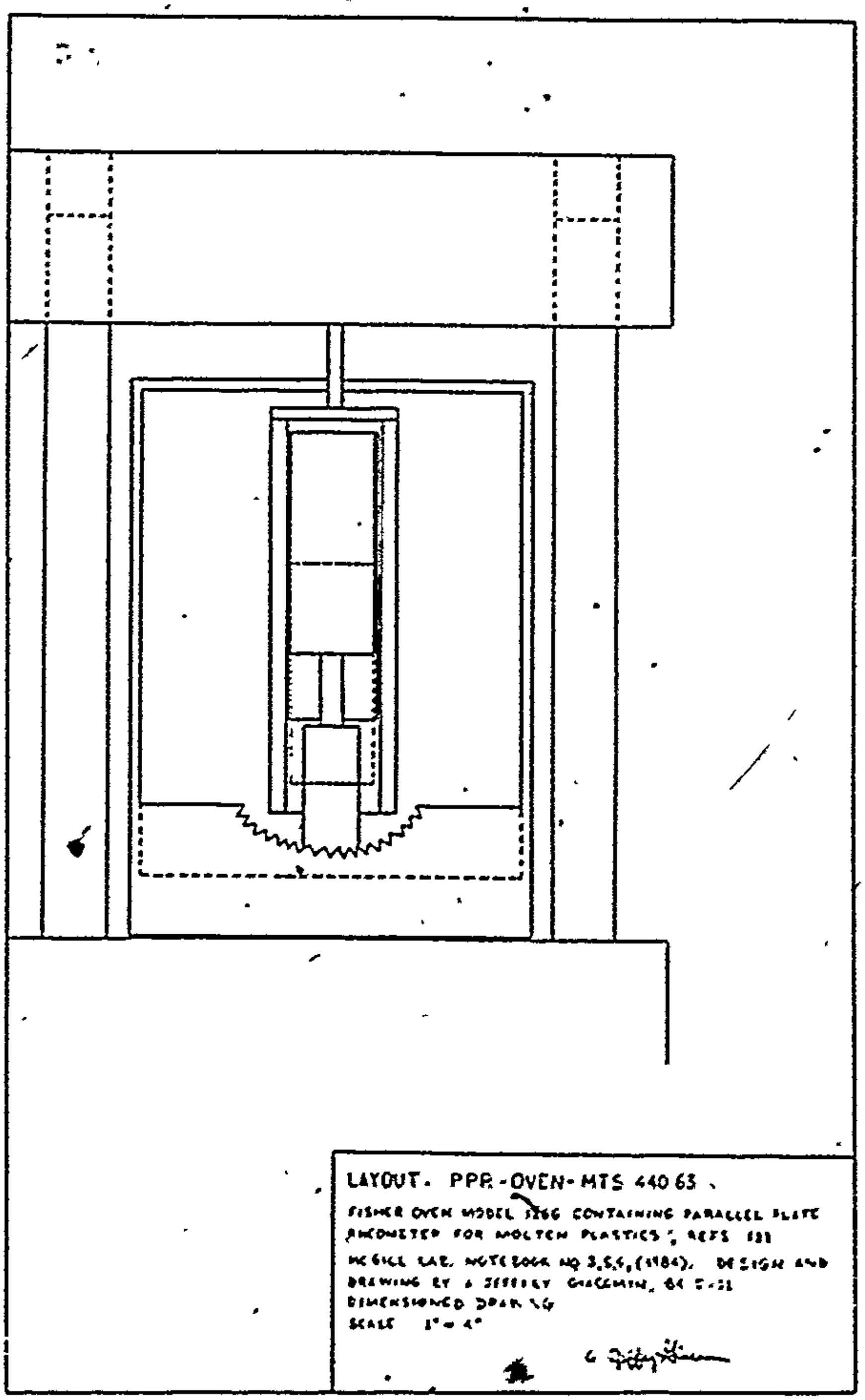

Figure 16 Layout of parallel plate rheometer, Fisher oven model 126G and materials testing system model MTS 440.63.

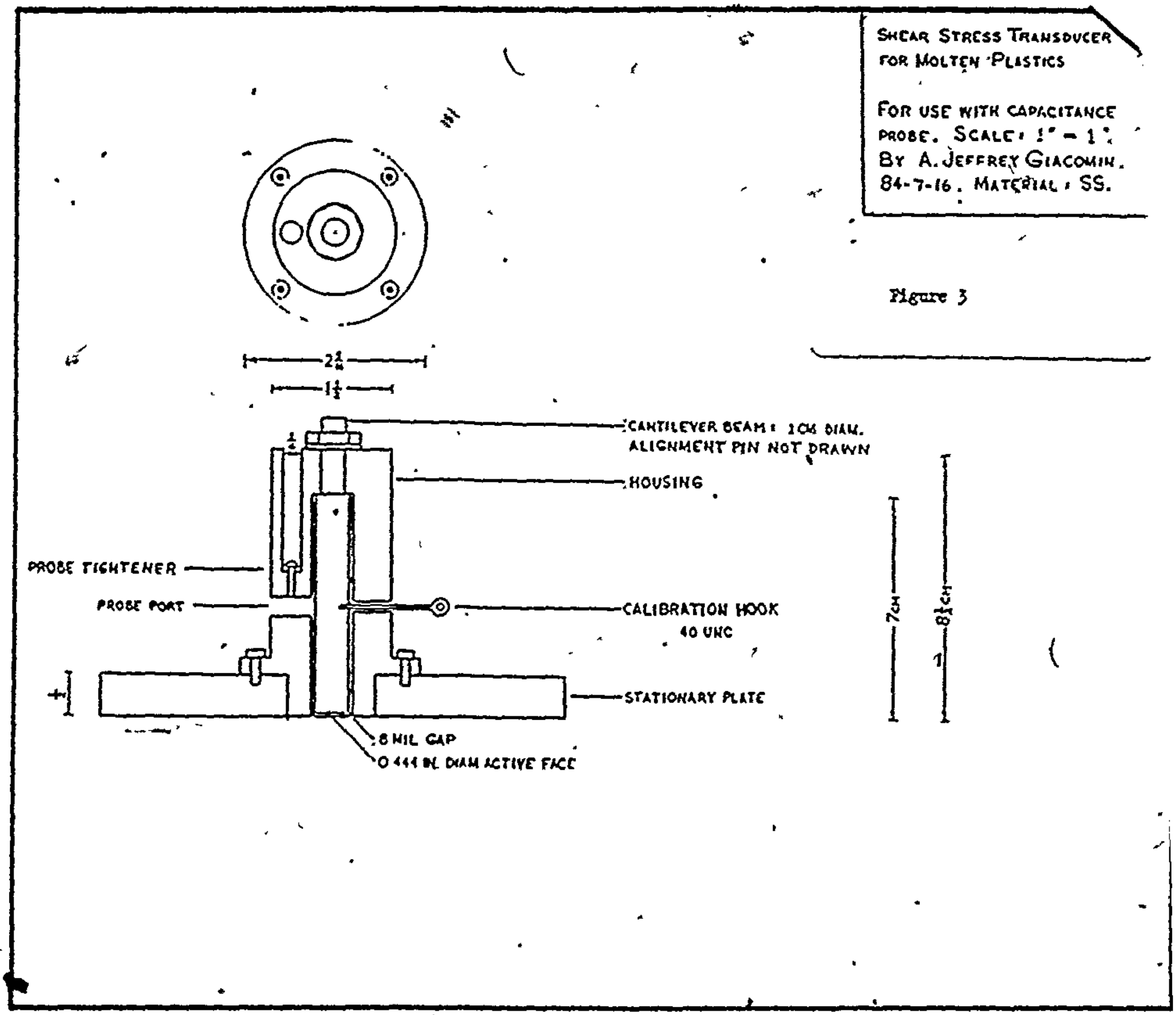

Figure 17: Engineering drawing for shear stress transducer for molten plastics for use with capacitance probe.

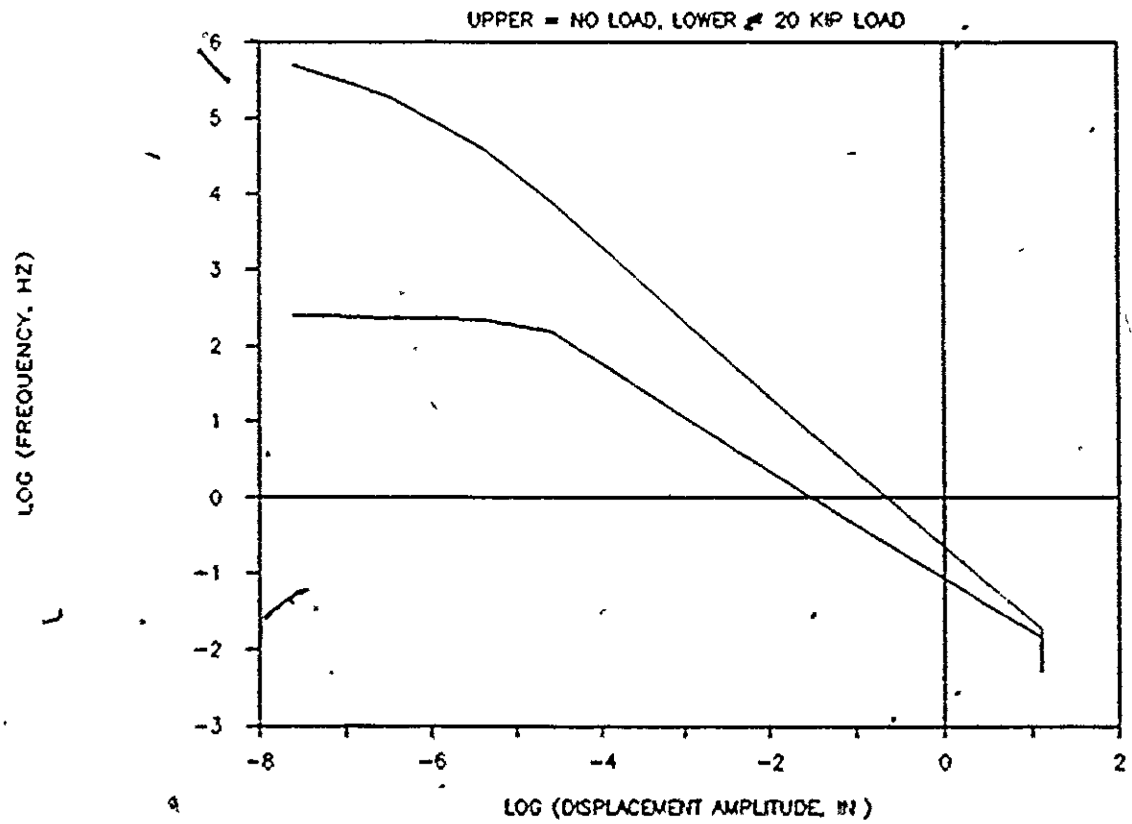

Figure 18. Actuator performance for oscillatory displacement (upper curve = no load, lower curve = 20 KIP load).

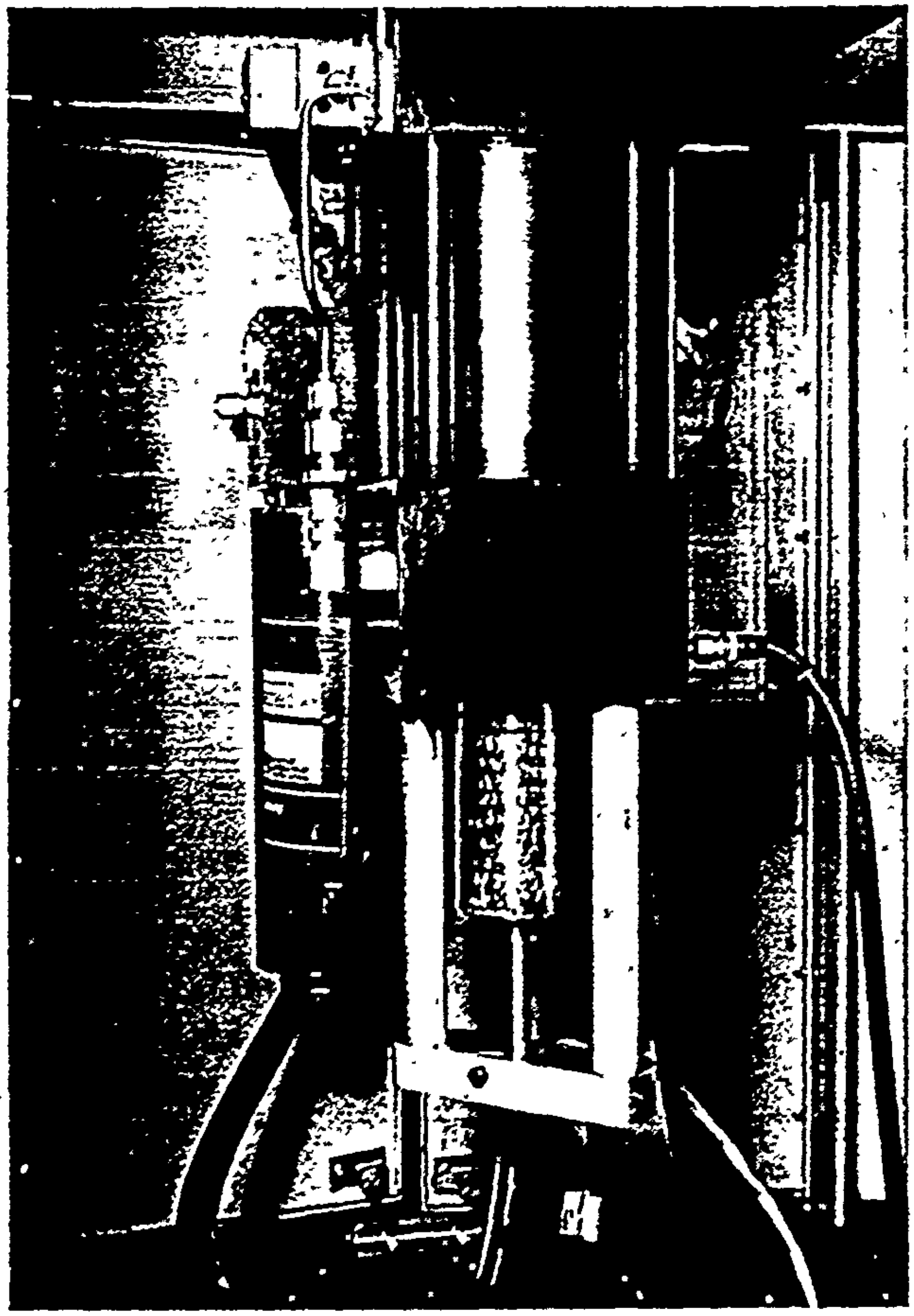

Figure 19: Front view of the MTS actuator showing exposed sections of piston and LVDT core. Bottles mounted near servo-valve (not shown) provide reservoir of high pressure fluid required for fast transient motions.

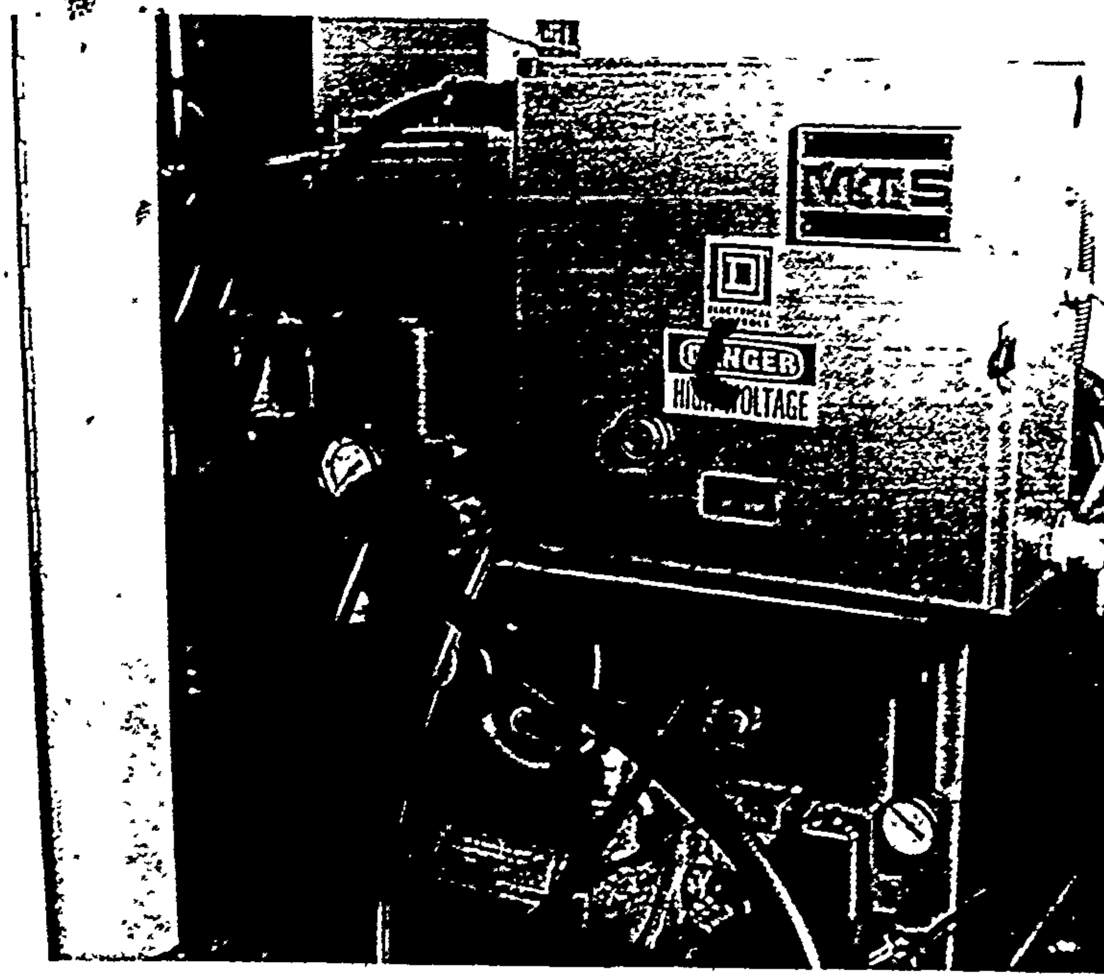

Figure 20. Hydraulic pump shown with heat exchanger (lower left), Bourdon oil pressure gauge (center, left), sight glass and thermometer for oil (lower right) and voltage transformer (upper left).

Figure 21: Author holds stationary plate open exposing baked-on residual polymer on moving plate.

Figure 22. Author shown applying sodium hydroxide aerosol to prepare sliding plate for cleaning at room temperature. Note stationary plate, suspended from oven roof, conveniently positioned for cleaning. Hydraulic pump is off, safety glasses and lab coat should be worn for this work.

Figure 23. Author shown cleaning sliding plate with wet cloth.

Figure 24. Author scrapes residual molten plastic from active face of shear stress transducer using brass scraper fashioned from brass sheet metal.

Figure 25· Author secures brass shim with set screw preparing for sample insertion.

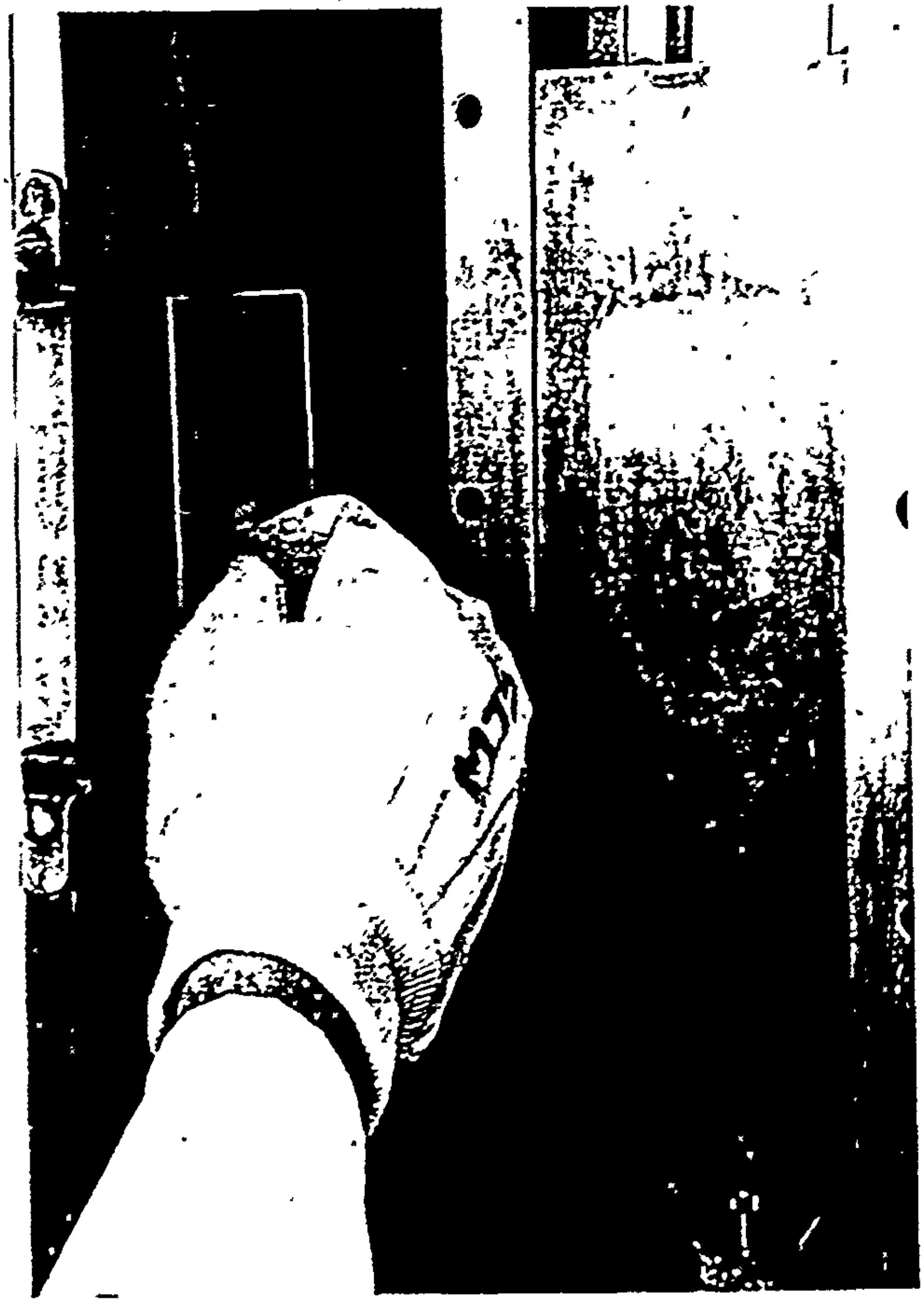

Figure 26 Rectangular plaque of solid plastic sticks to hot stationary plate over the active face of the shear stress transducer. Author carefully presses out air bubbles when the sample is still in solid state on outermost surface.

Figure 27 Stationary plate of rheometer is closed, squeezing fresh sample onto sliding plate. After removing delicate calibration hook from transducer, author uses left hand (not shown) on housing of shear stress transducer to guide stationary plate into position.

Figure 28. Using allen wrench, author tightens stationary plate onto sliding plate. This sets sample thickness to that of selected shim.

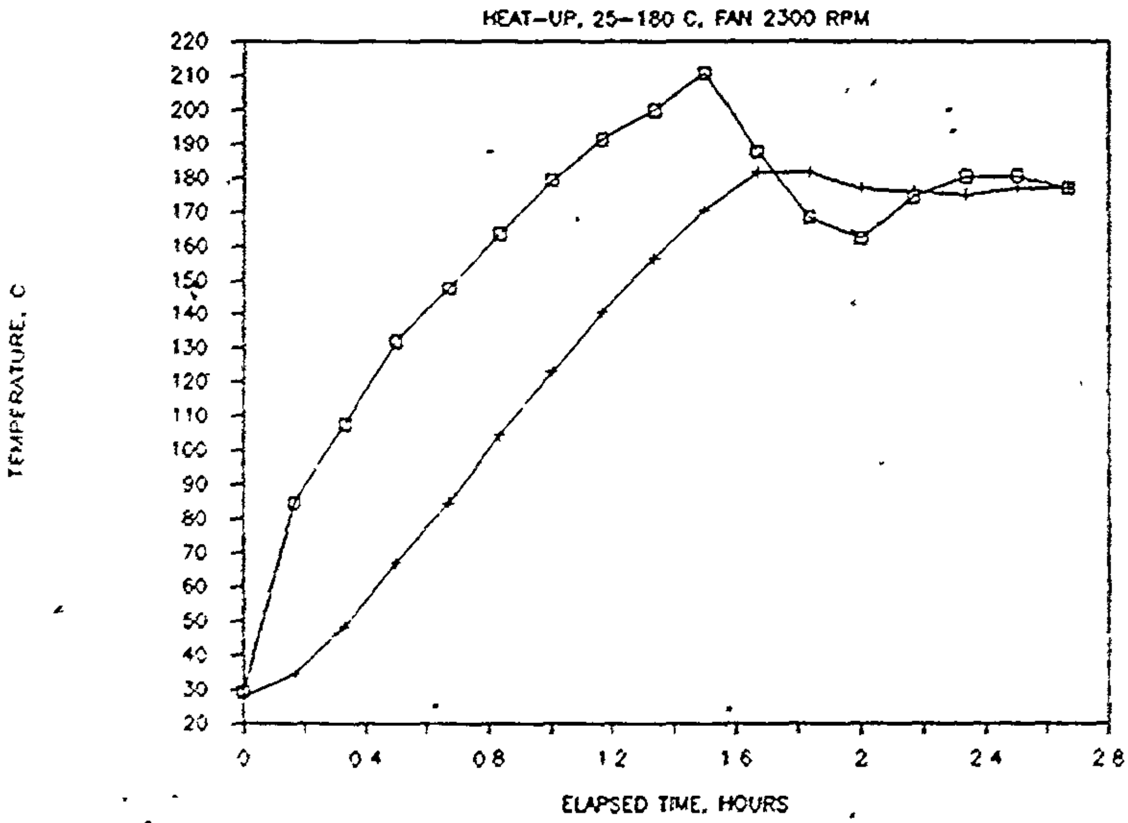

Figure 29: Oven heat-up performance. Note overshoot of oven air temperature (squares) and slight overshoot of rheometer temperature measured with thermocouple embedded in moving plate (crosses).

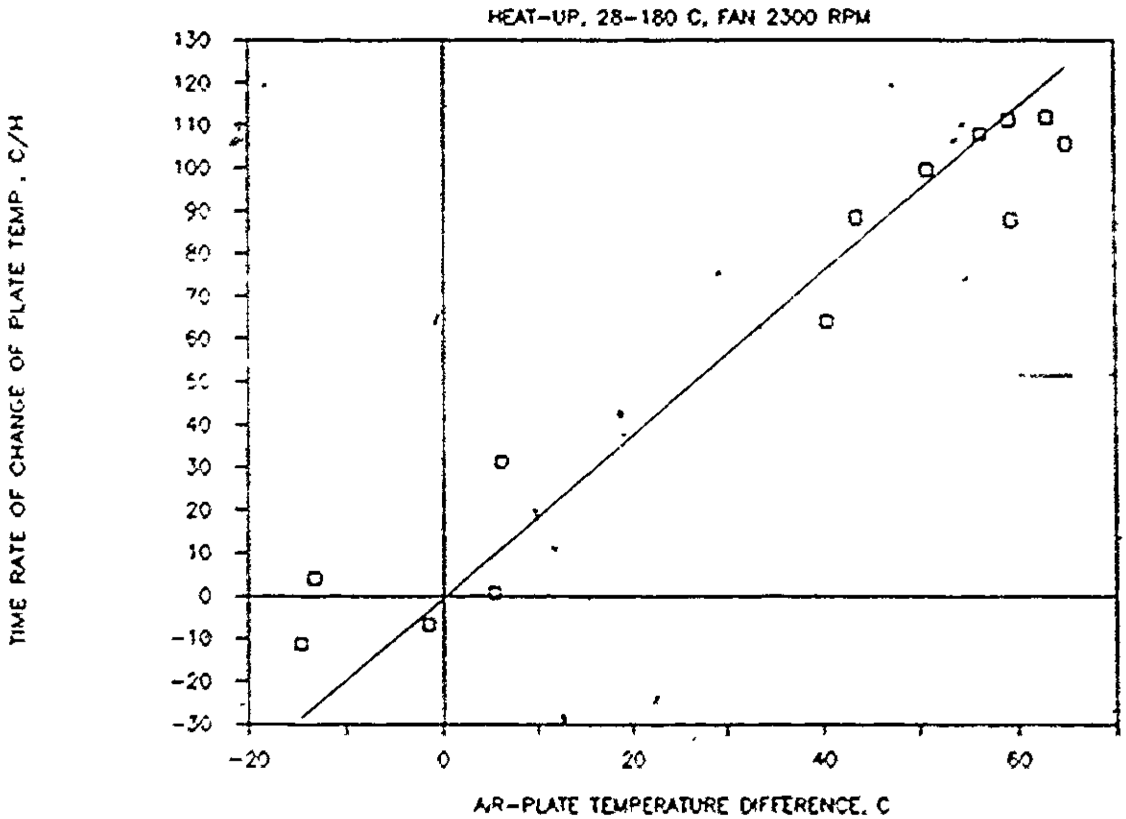

Figure 30. Newton's law approximation for oven heat-up from 28°C to 180°C with oven fan speed set at 2300 rpm.

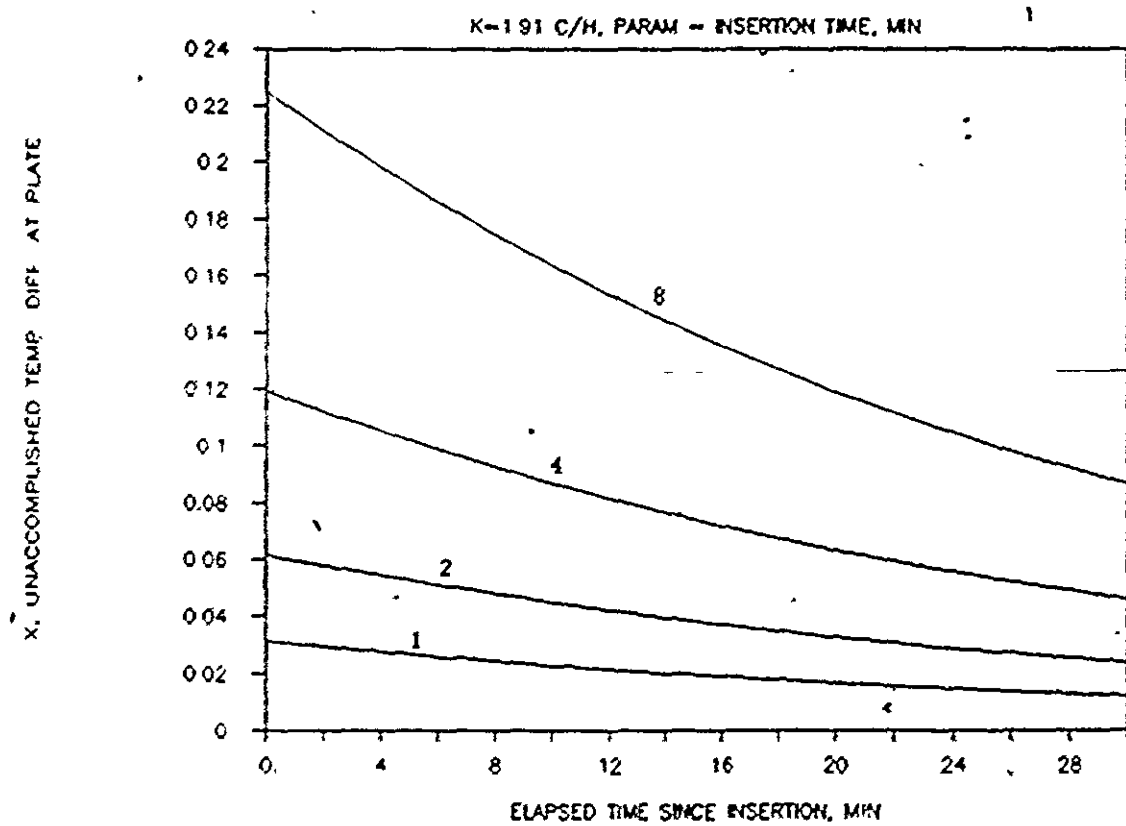

Figure 31: Post-insertion thermal response of rheometer plates.

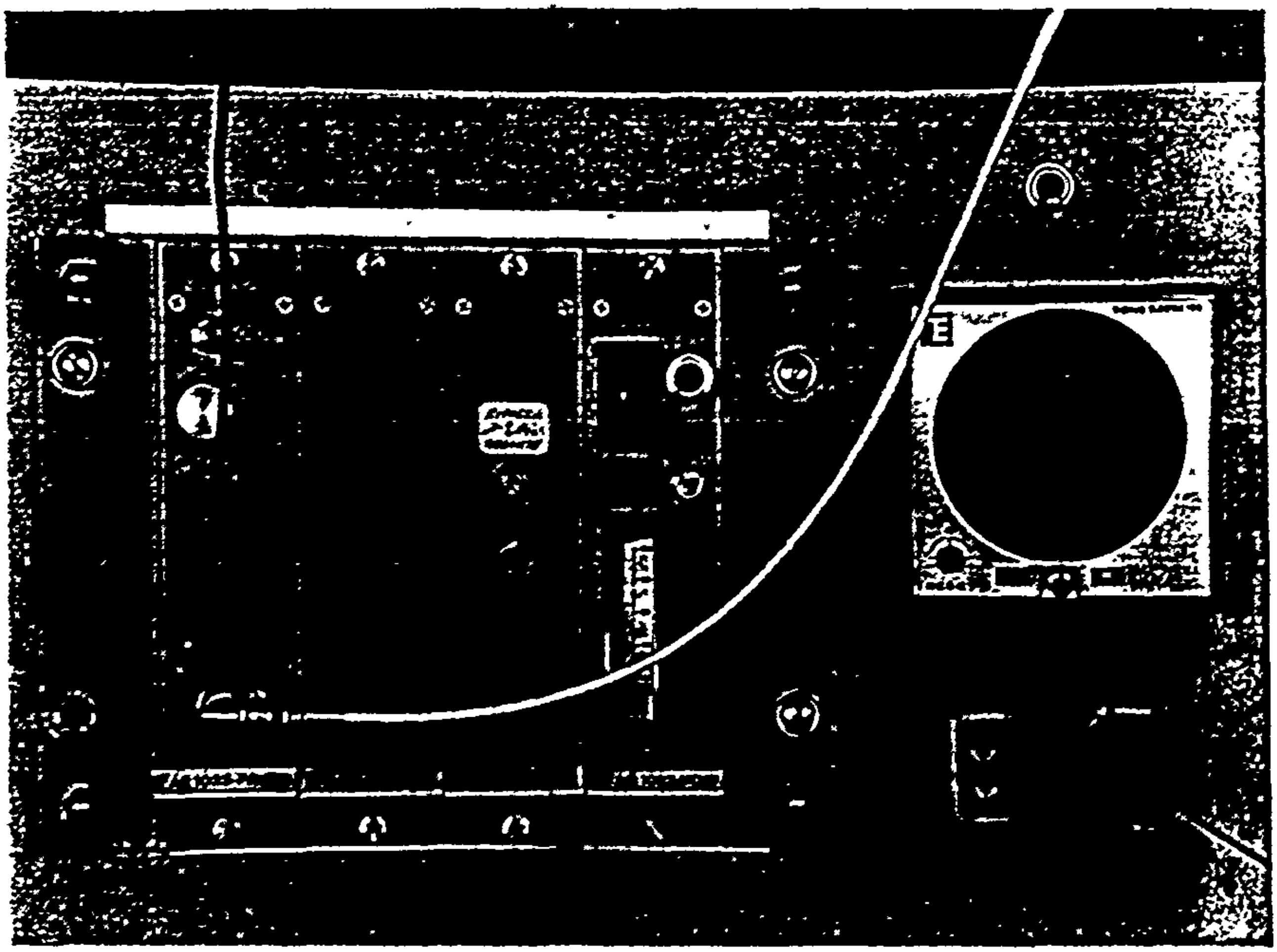

Figure 32 View of from panel showing Accumeasure System 1000 capacitance probe amplifier (left) and bandwidth proportional temperature controller for oven (right).

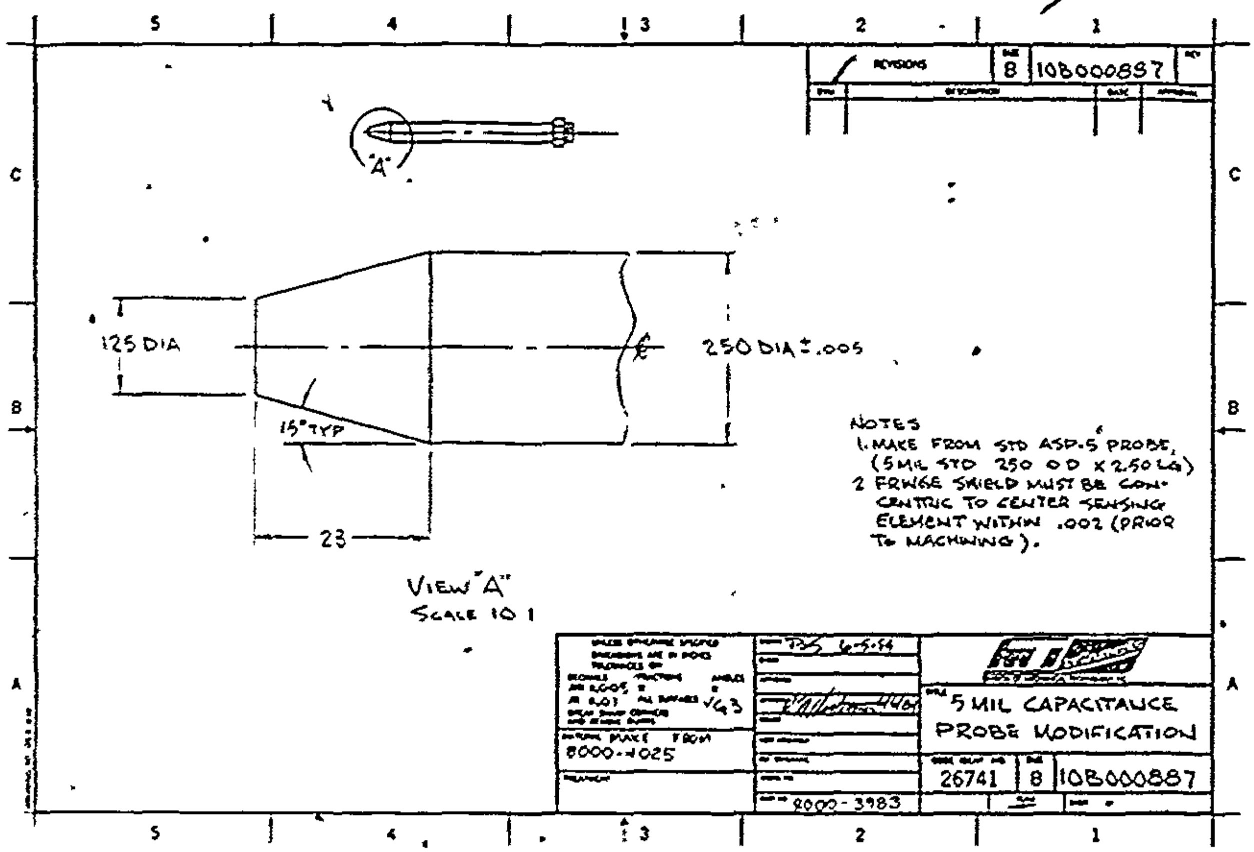

Figure 33· Engineering drawing of tapered capacitance probe. Untapered capacitance probes are difficult to position in the shear stress transducer.

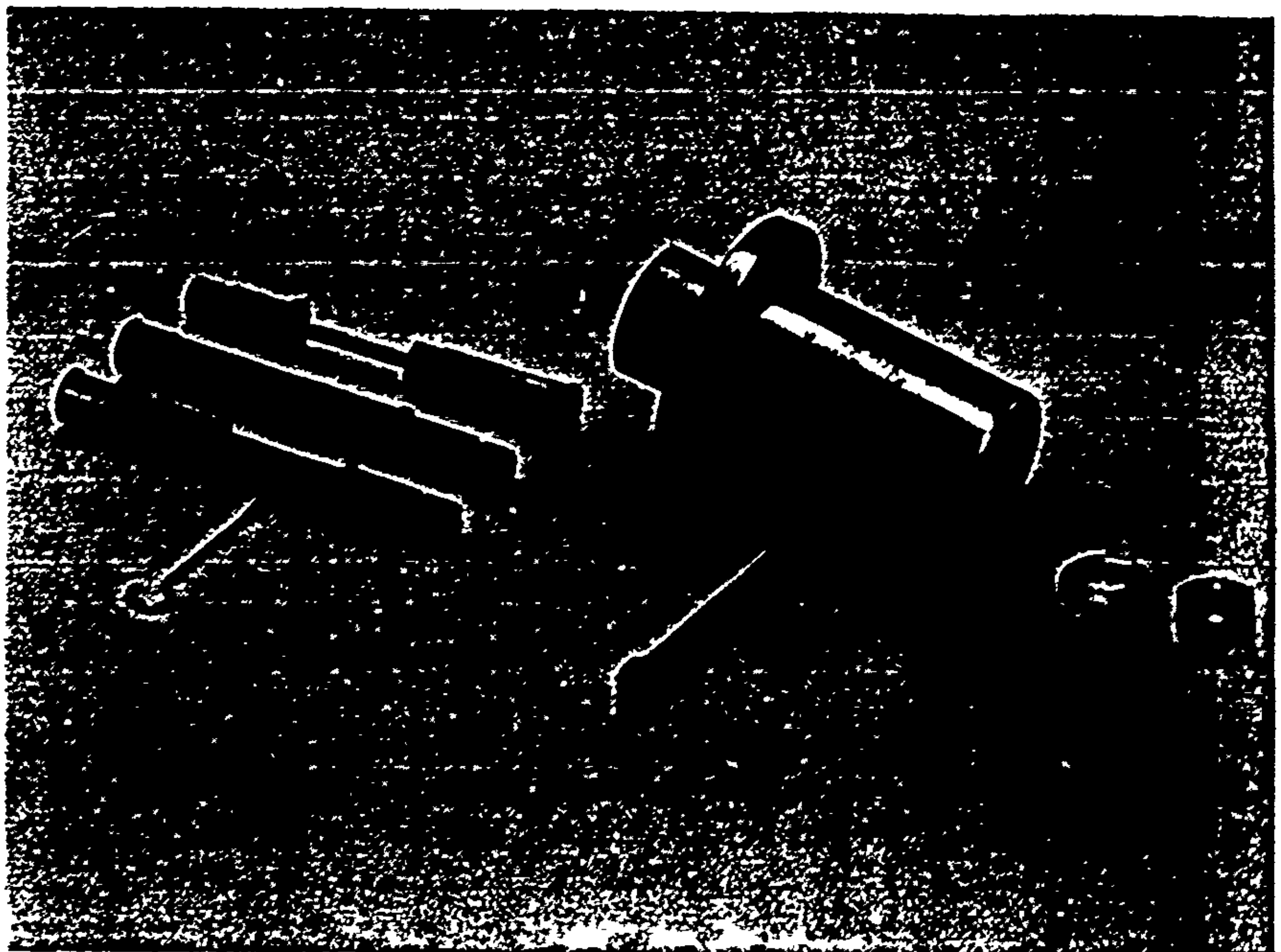

Figure 34. Disassembled shear stress transducer with three beams of different stiffnesses (upper left), calibration hook (lower left), capacitance probe (lower center) and cantilever housing (upper center). After the securing nut (extreme right) is removed, the transducer is disassembled by hand to prevent overstraining.

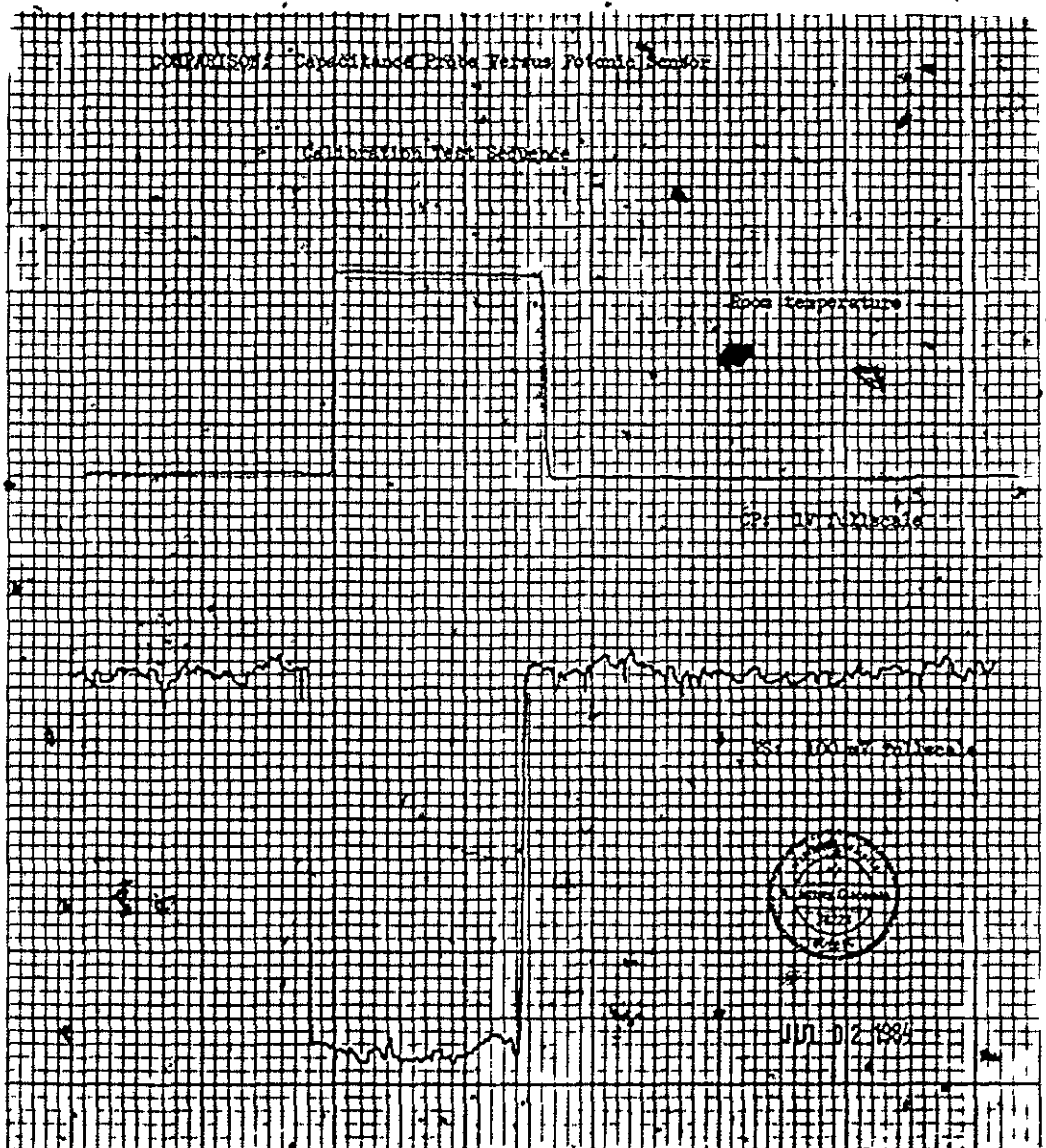

Figure 35 Comparison of capacitance proximeter output (upper curve) with Fotonic sensor output (lower curve) during static calibration at room temperature Note significant improvement in noise level of capacitance method over optical one.

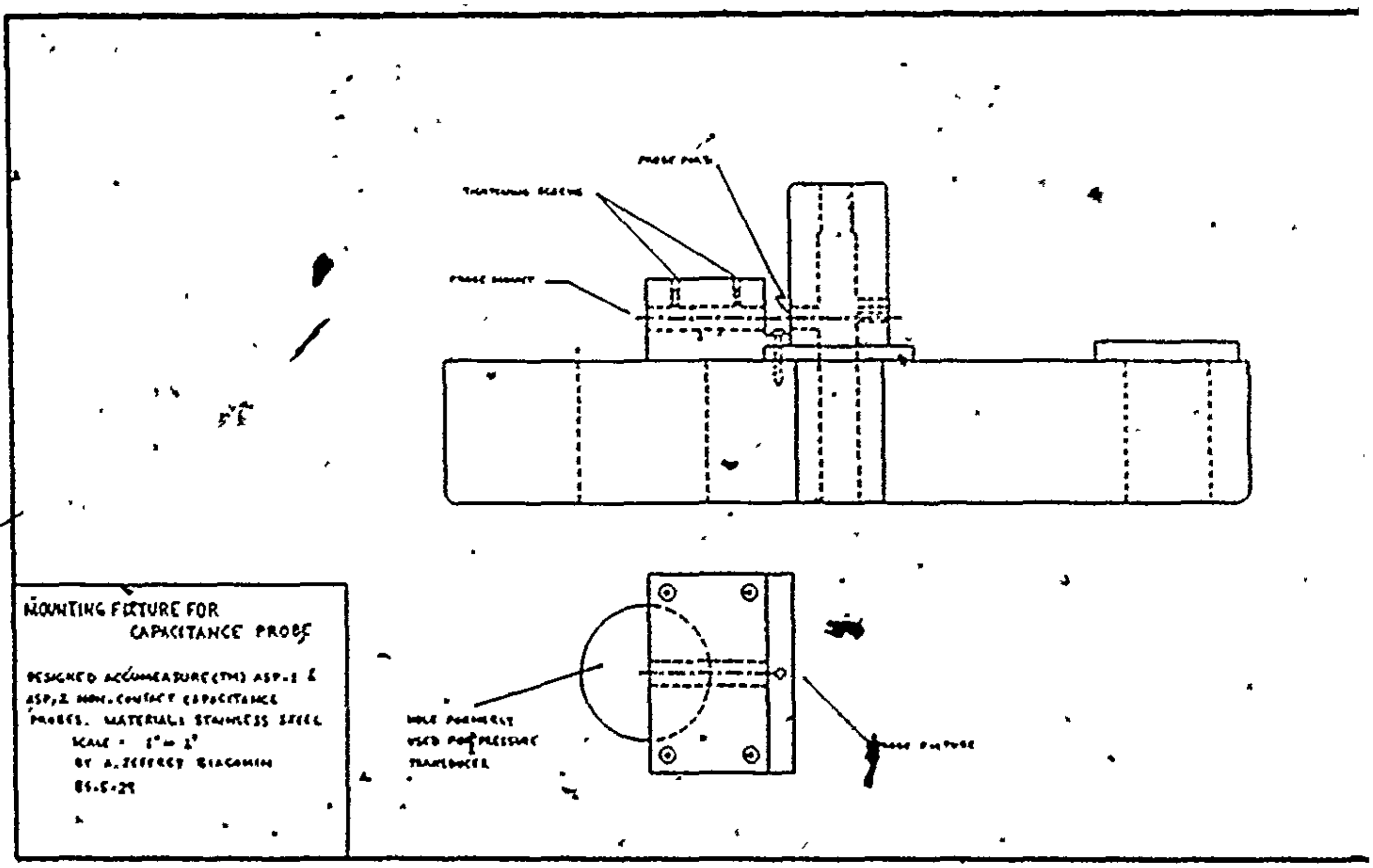

Figure 36. Mounting fixture for capacitance probe built for room temperature prototype rheometer for preliminary testing of capacitance proximeter.

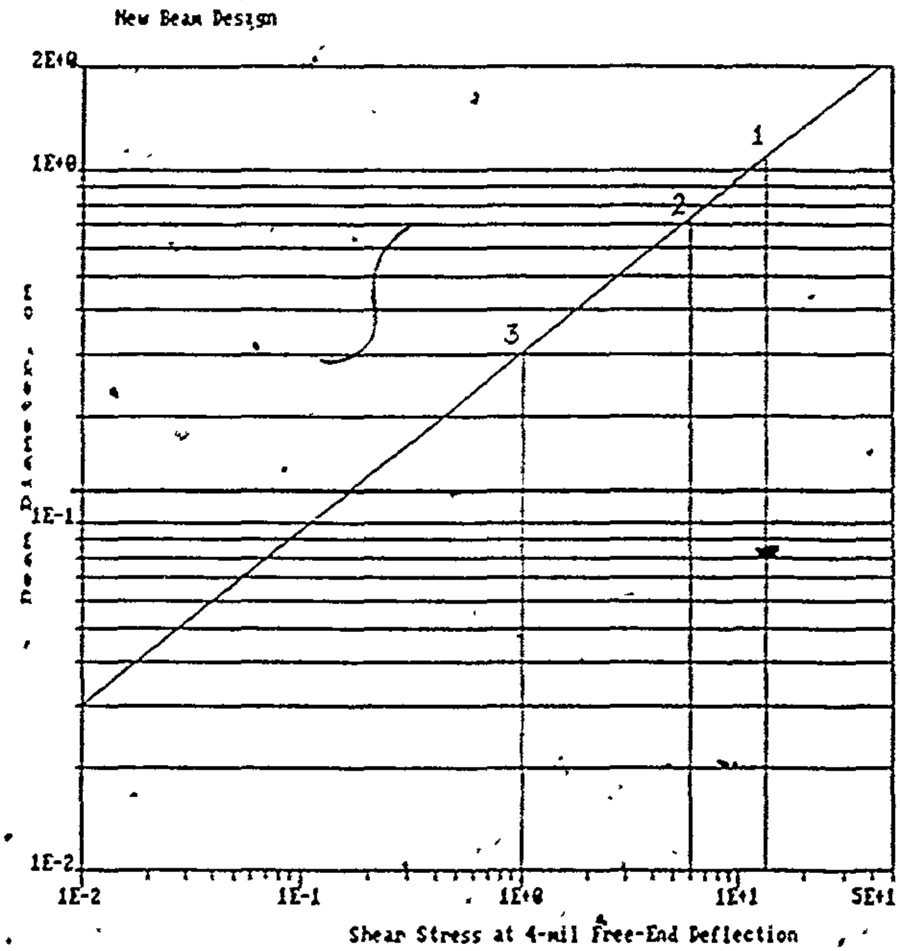

Figure 37 Design plot used for selecting beam diameters for the new shear stress transducer for molten plastics. Shear stress in Mdyn/sq.cm.

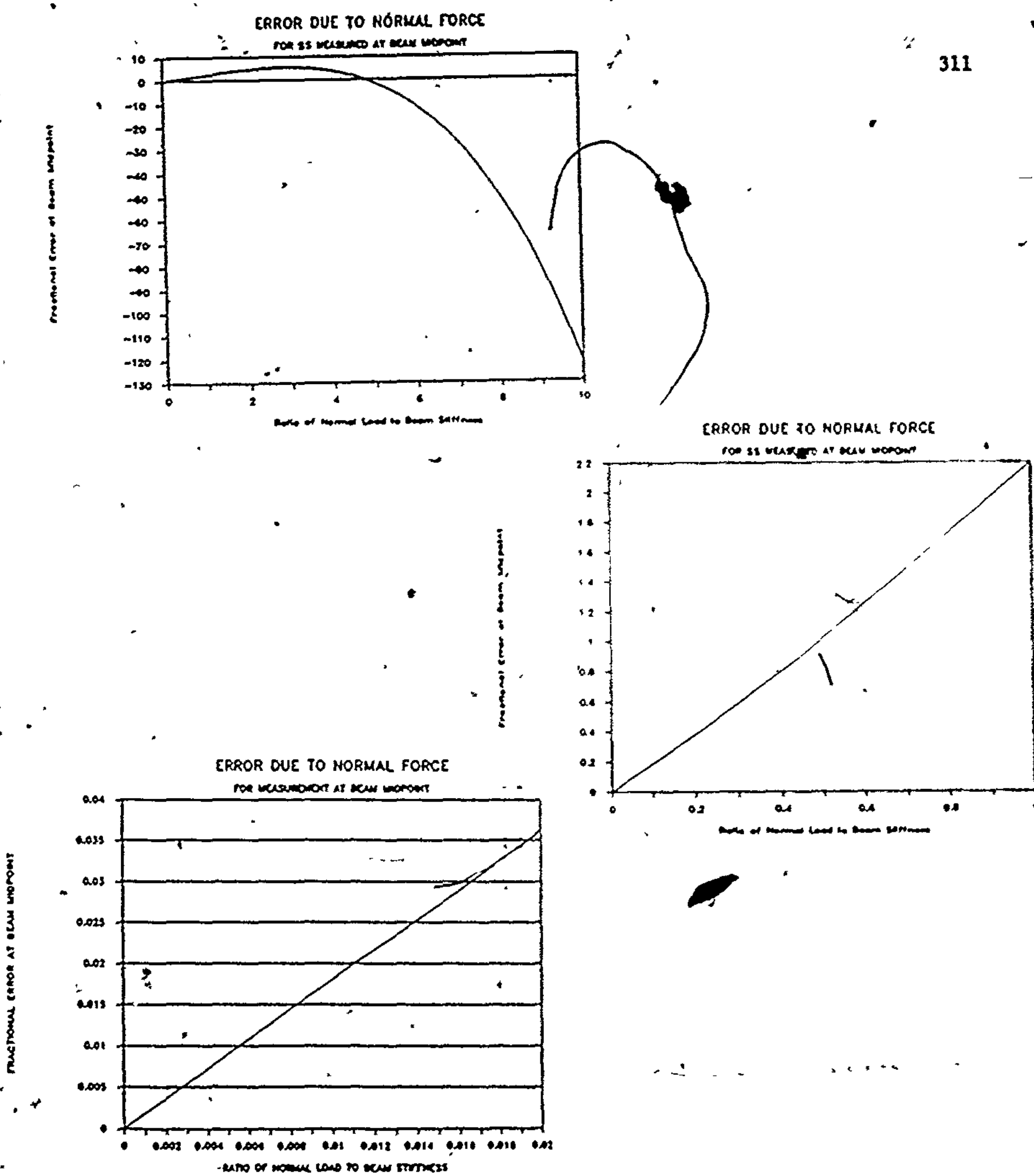

Figure 38. Potential error due to normal force as a function of normal load to stiffness ratio.

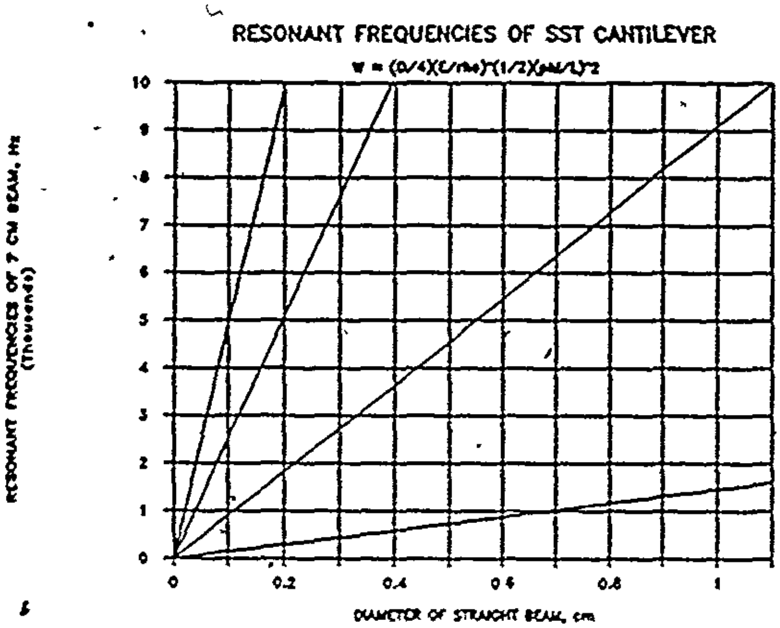

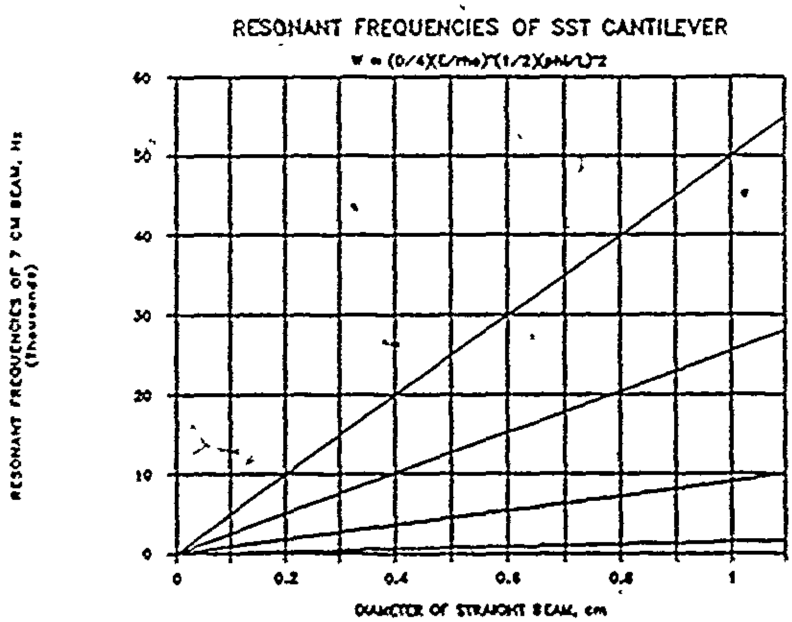

Figure 39: Diameter dependence of resonant frequencies for shear stress transducer straight cantilever.

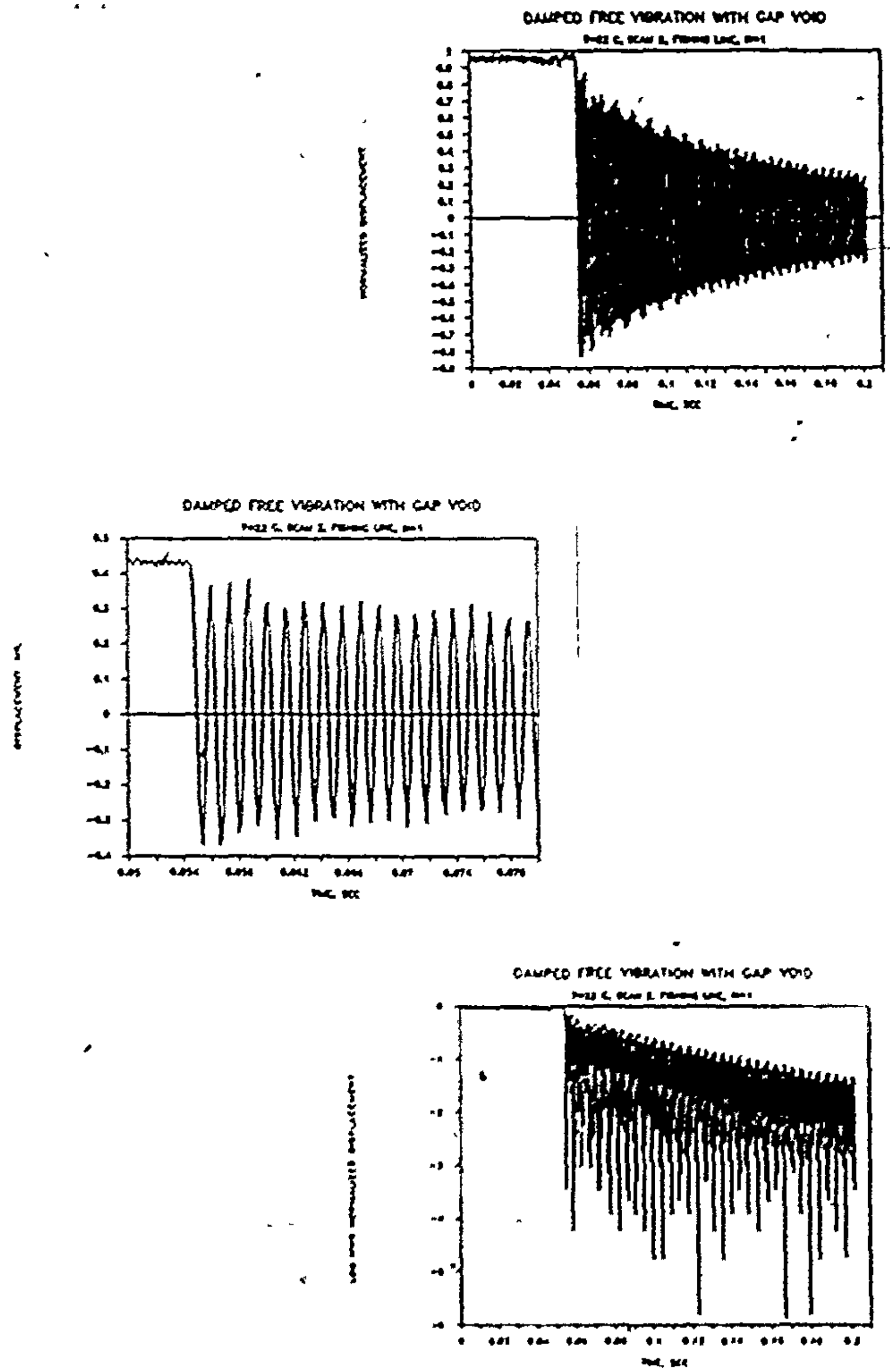

Figure 40   Damped free vibration of dry shear stress transducer beam #2 Similar results were obtained for beams #1 and #3.

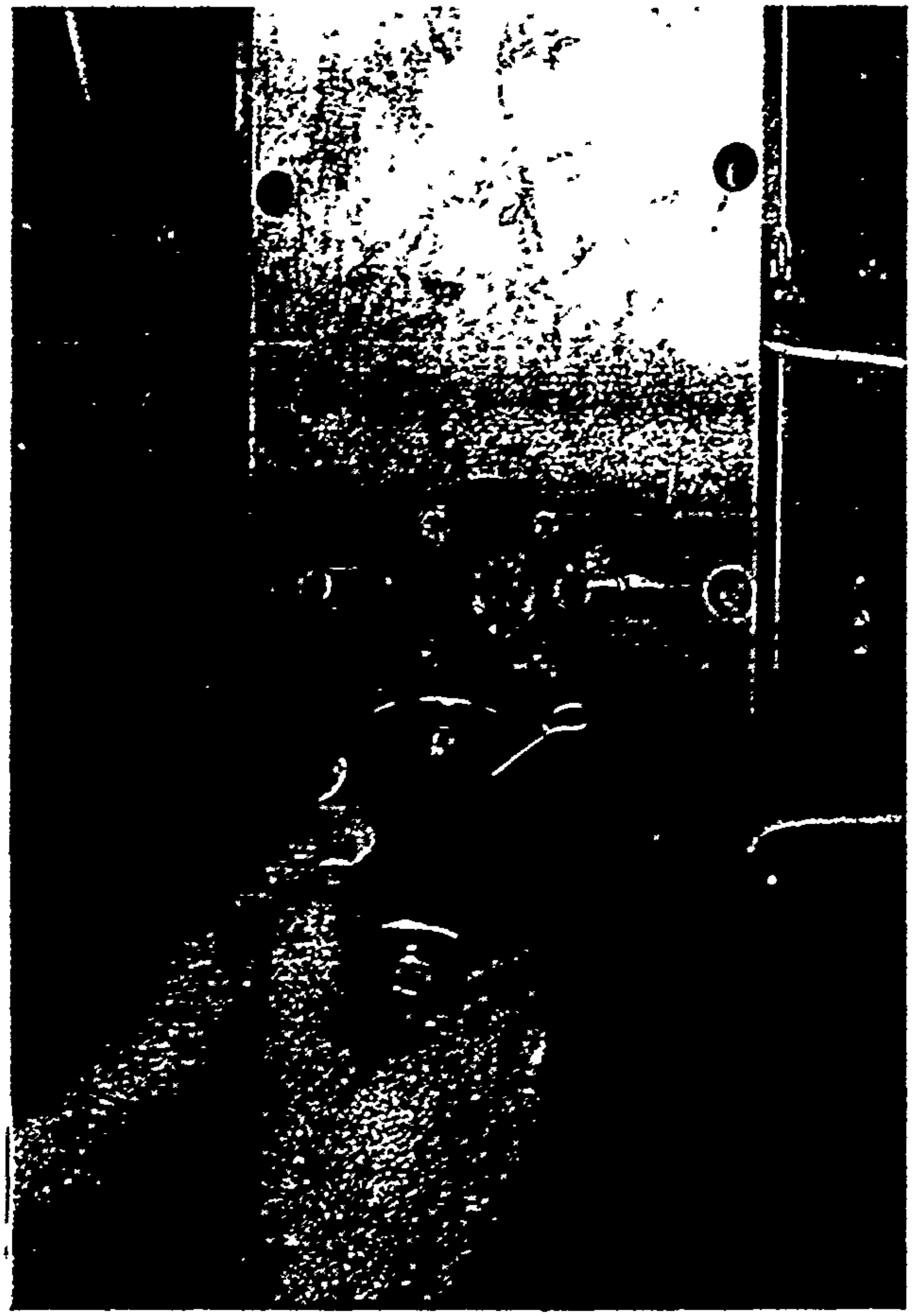

Figure 41: Author flush-mounting shear stress transducer in stationary plate showing deep-well thermocouple mounts on either side of transducer. Also, convenient handle on stationary plate shown at right.

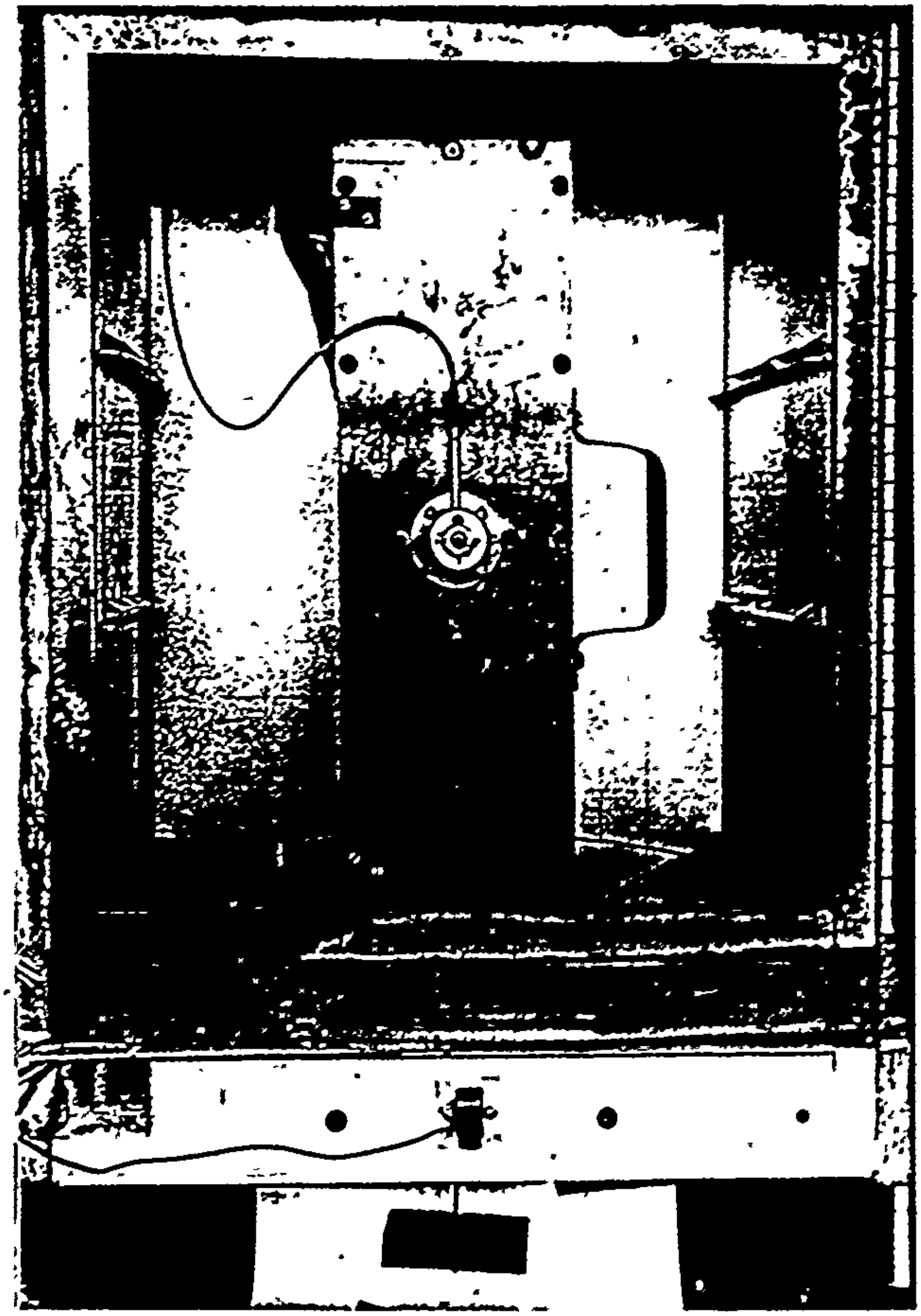

Figure 42. Static calibration assembly in use. Rectangular lead weight on dead-pan suspended under oven with chain from calibration hook. Capacitance probe, in measurement position, with cable passing through oven wall at rear (upper left). Wire for thermocouple, embedded in moving plate, also passes through oven wall at front (bottom center).

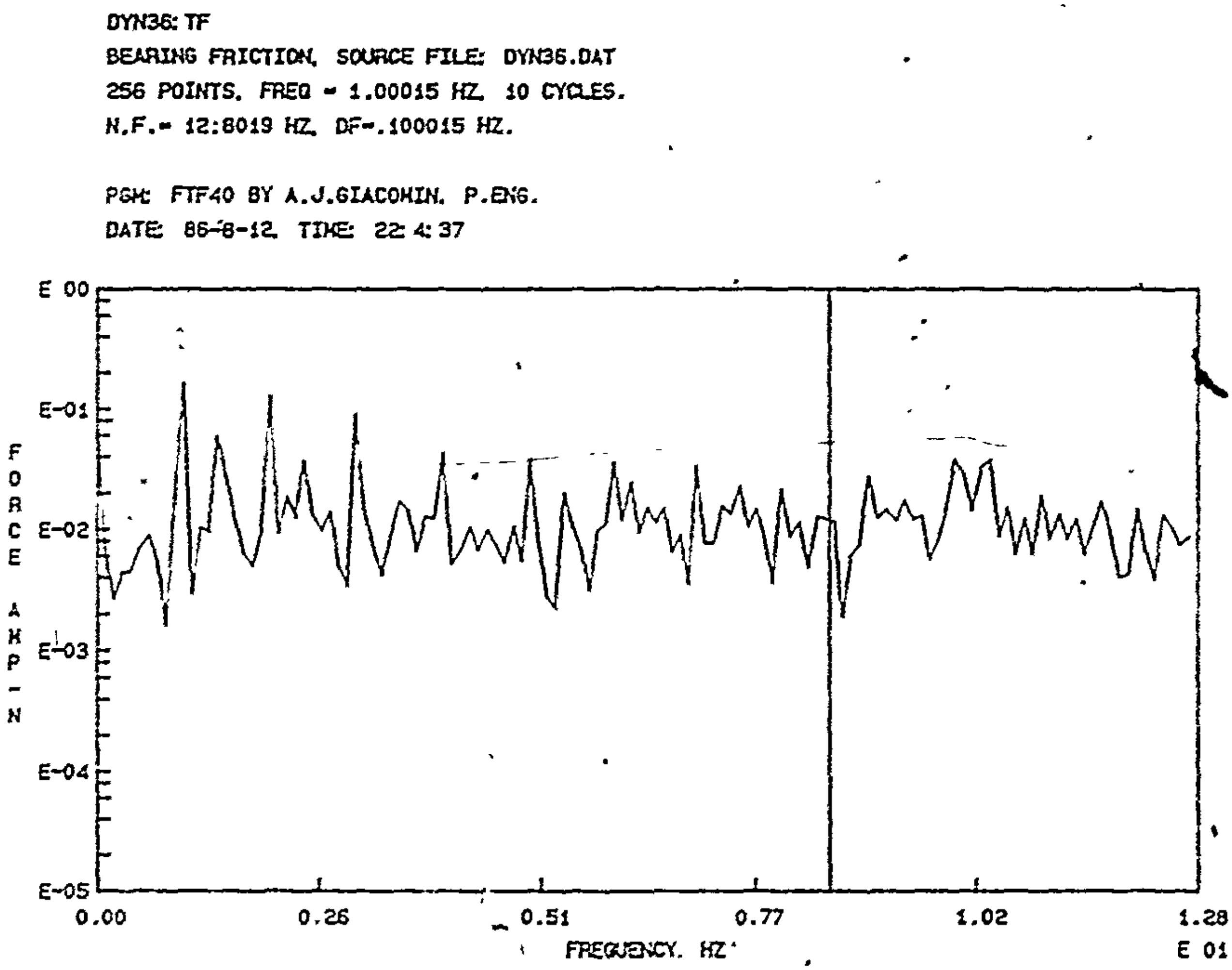

Figure 43 Amplitude spectrum of total force measured with HTS load cell during a 1 Hz oscillatory displacement of amplitude .6 inches. Since there is no sample in the rheometer for this test, this spectrum shows the contribution of bearing friction to the total force measurement in a typical oscillatory shear test.

DATE: 86-8-12. TIME: 17:56:54. BY: AJG

BEAM NO. 2. PROBE NO. ASP-5HT. T= 200 C.

PROGRAM: CAL17. 5 TESTS. 15 PTS/TEST.

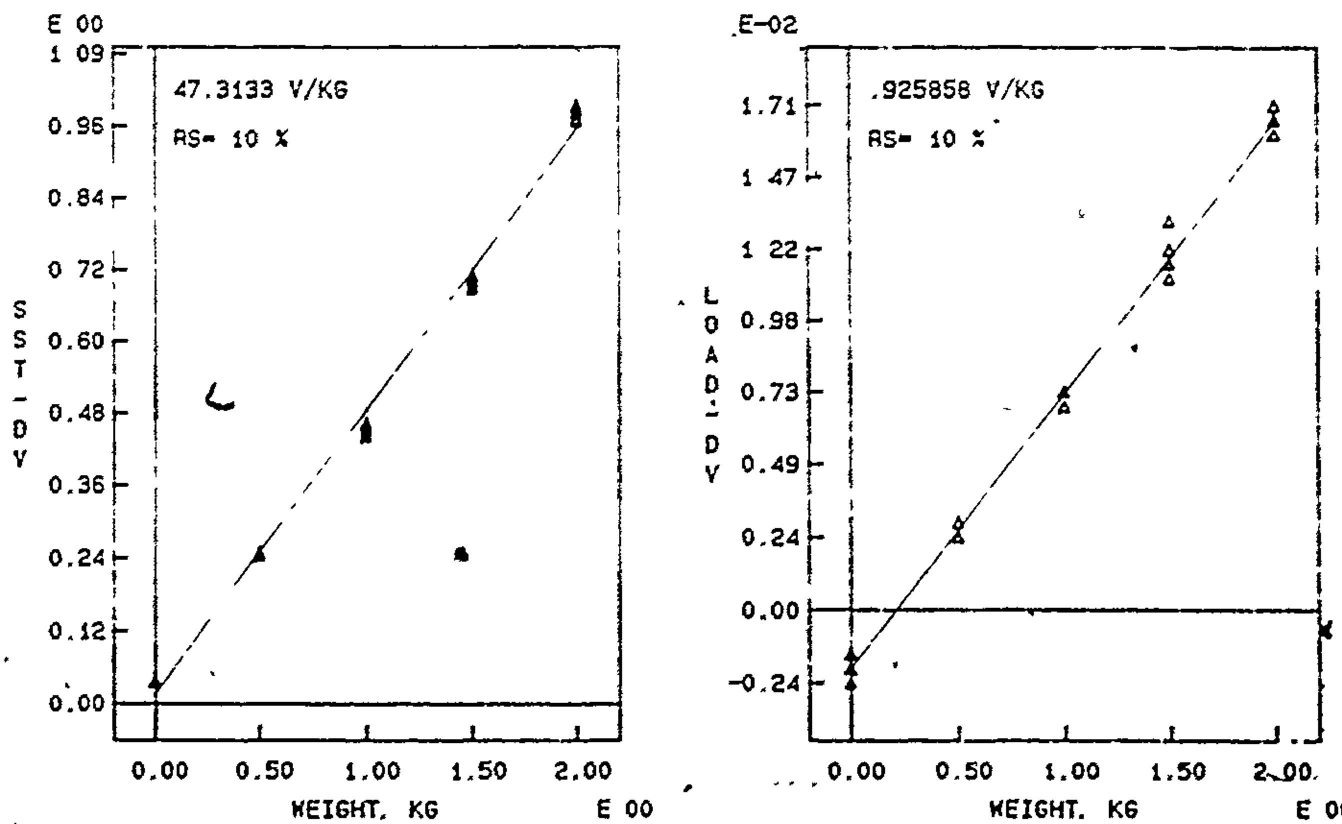

Figure 44a. Calibration data and regression lines drawn for static calibration of shear stress transducer (left) and load cell (right) using beam #2 at 200°C [1 DV = 10 V].

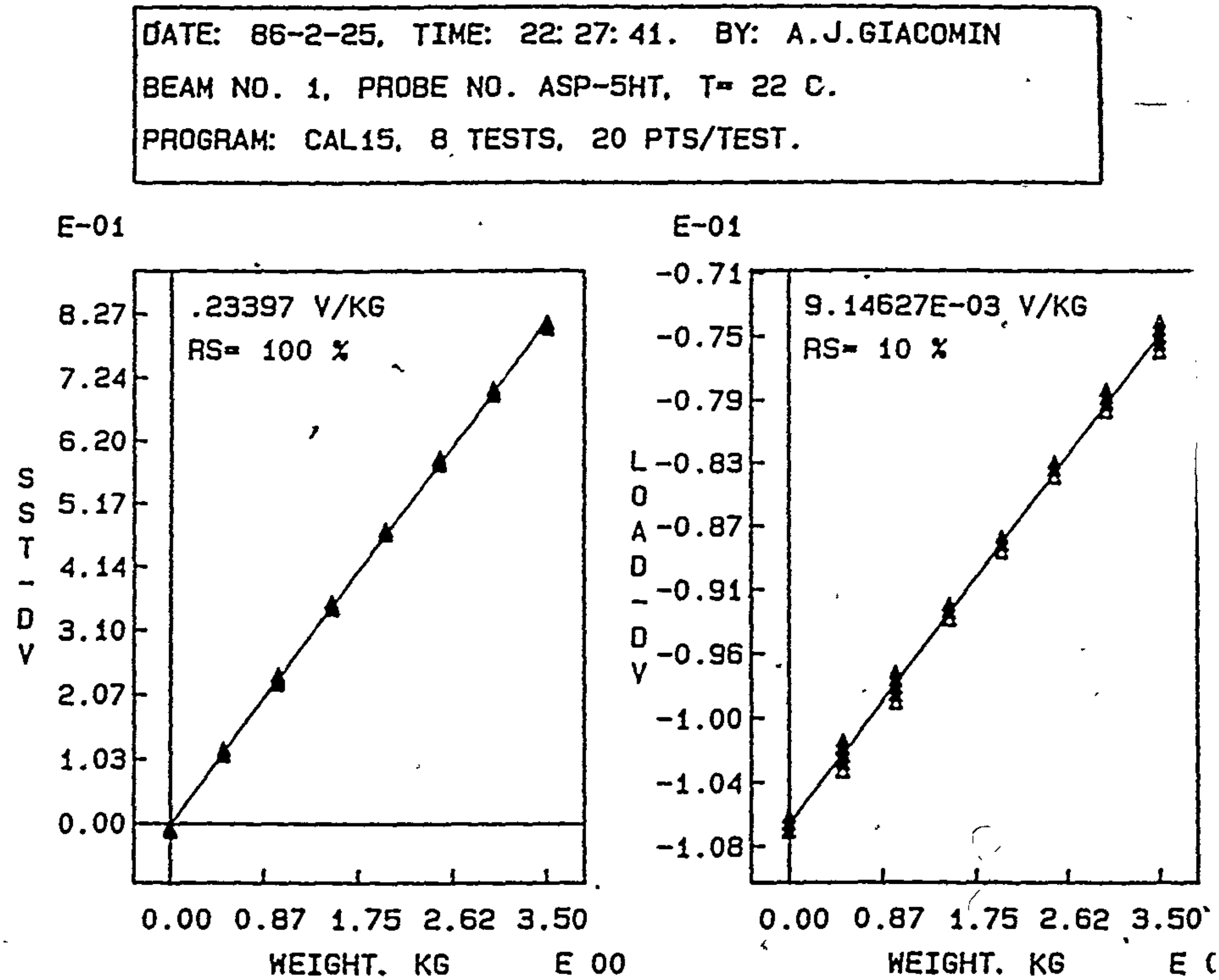

Figure 44b: Calibration data and regression lines drawn for static calibration of shear stress transducer (left) and load cell (right) using beam #1 at room temperature [1 DV = 10 V].

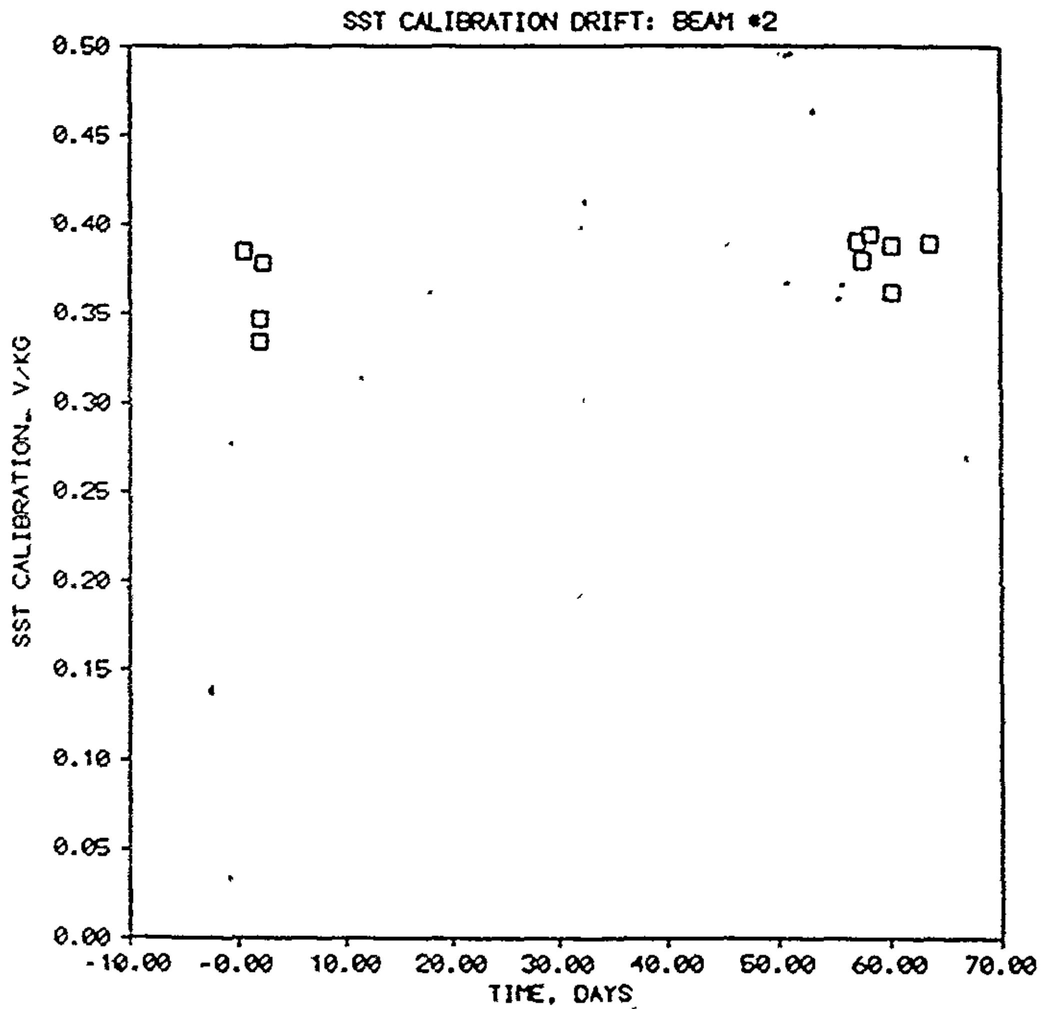

Figure 45 Shear stress transducer sensitivity measured using static calibration with beam #2 over period of roughly two months showing ± 10% drift.

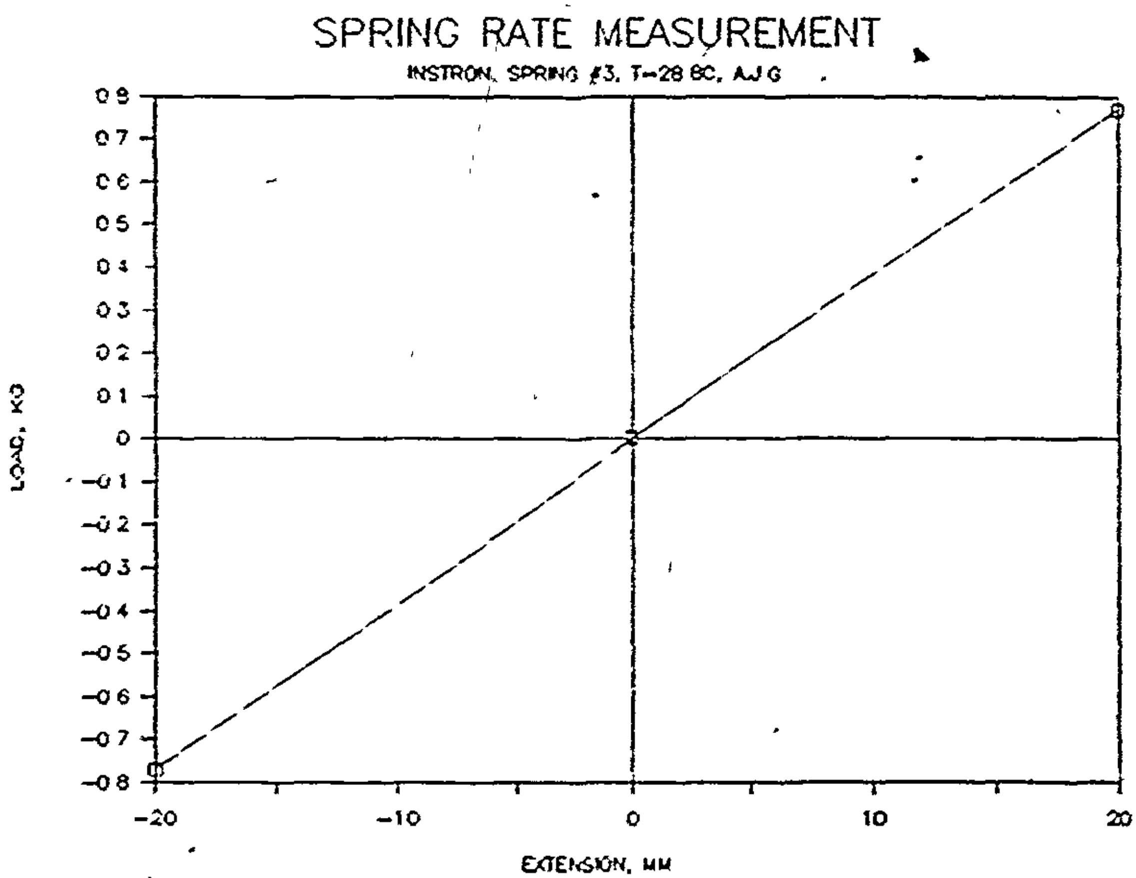

Figure 46: Spring rate determination by linear regression of load/extension data for static tests using INSTRON tensile tester. Standard error on spring rate was 0.26%.

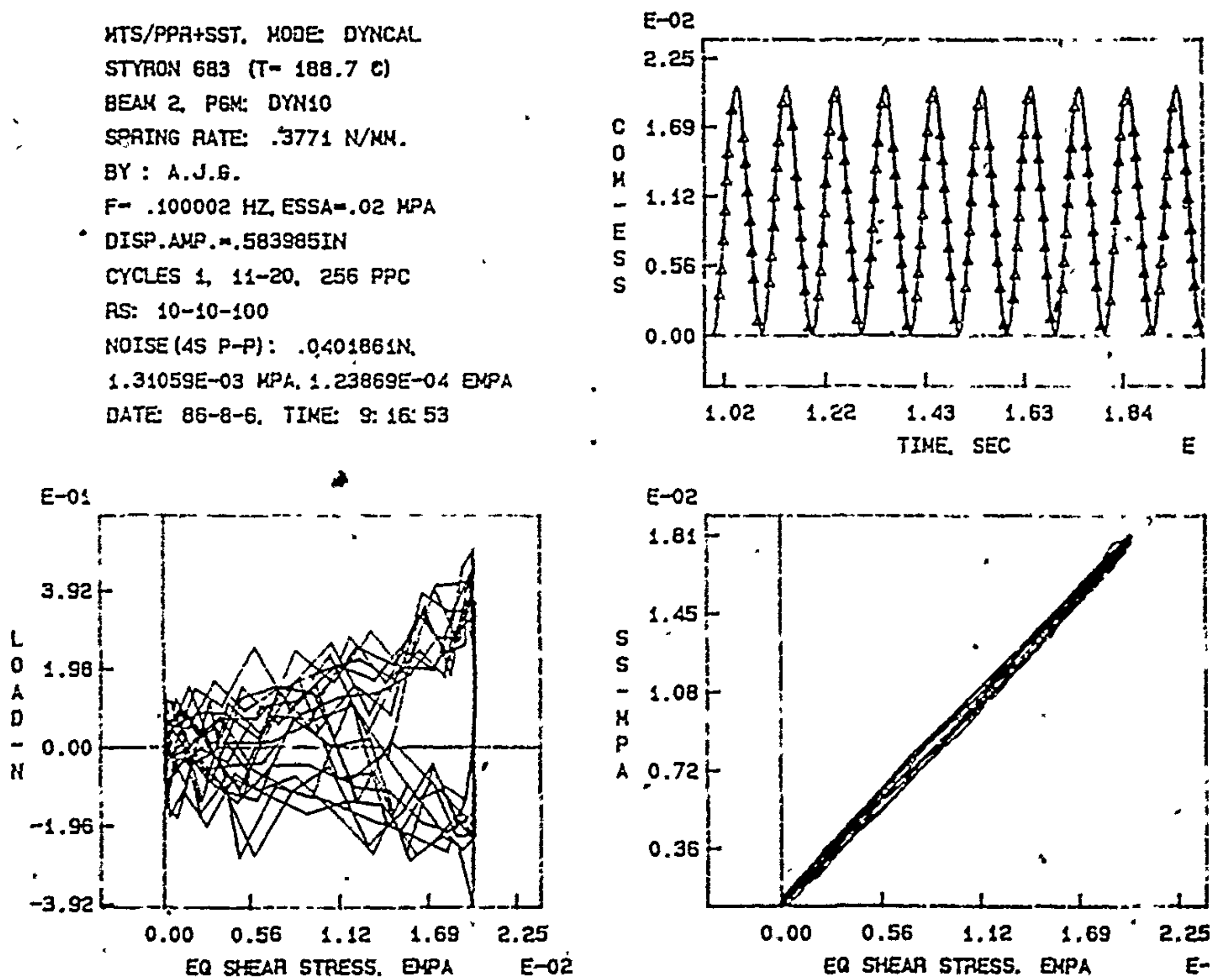

Figure 47. Typical result for dynamic calibration using Styron 683 in beam-housing gap after removing sample from rheometer. Figure on upper right shows the trace of the desired spring extension (solid curve) versus measured spring extension (triangles). Figure on lower right shows loop for measured shear stress versus applied equivalent shear stress.

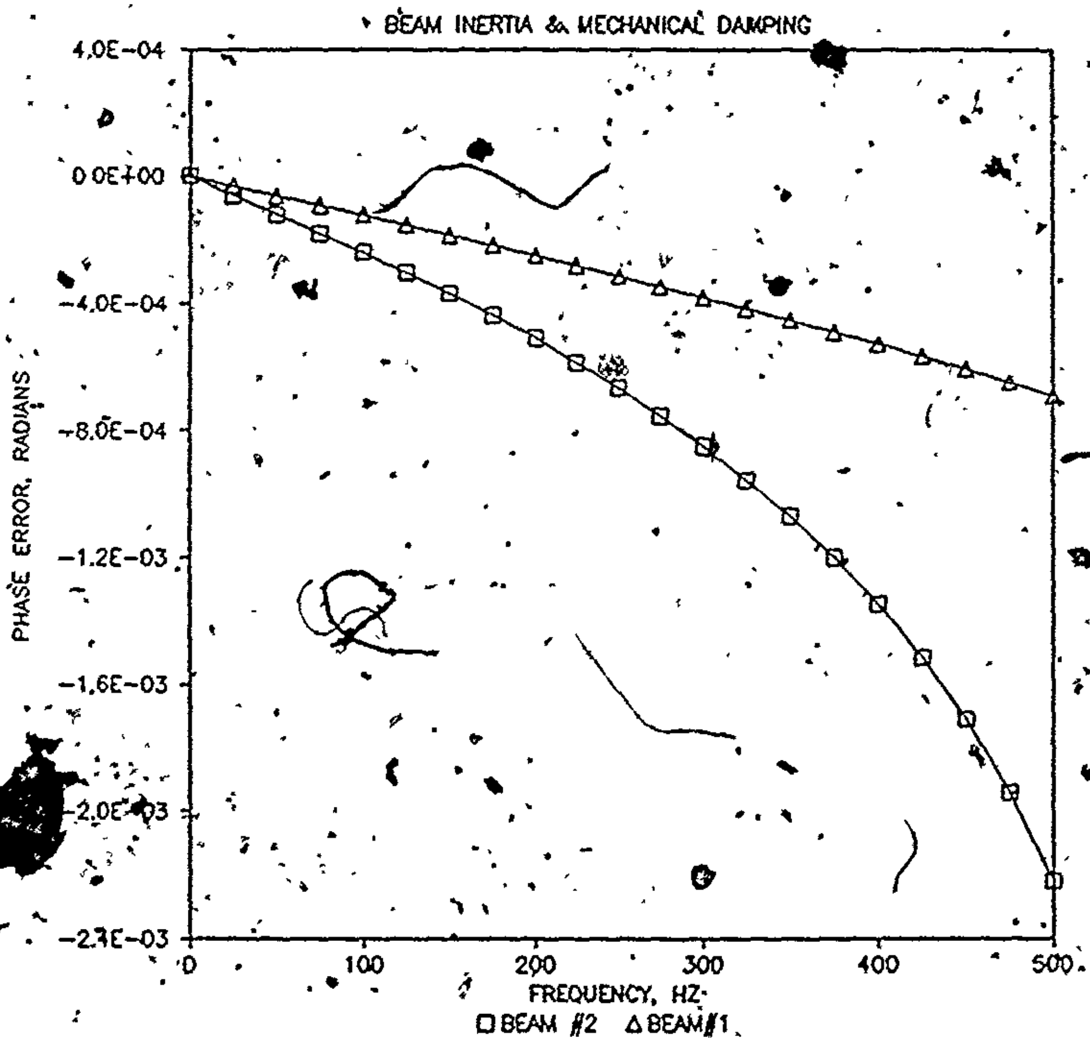

Figure 48: Second order frequency response curves for beam #1 (η=.00172, ω_r= 1440 Hz) and beam #2 (η=.00175, ω_r=730 Hz) with annulus void.

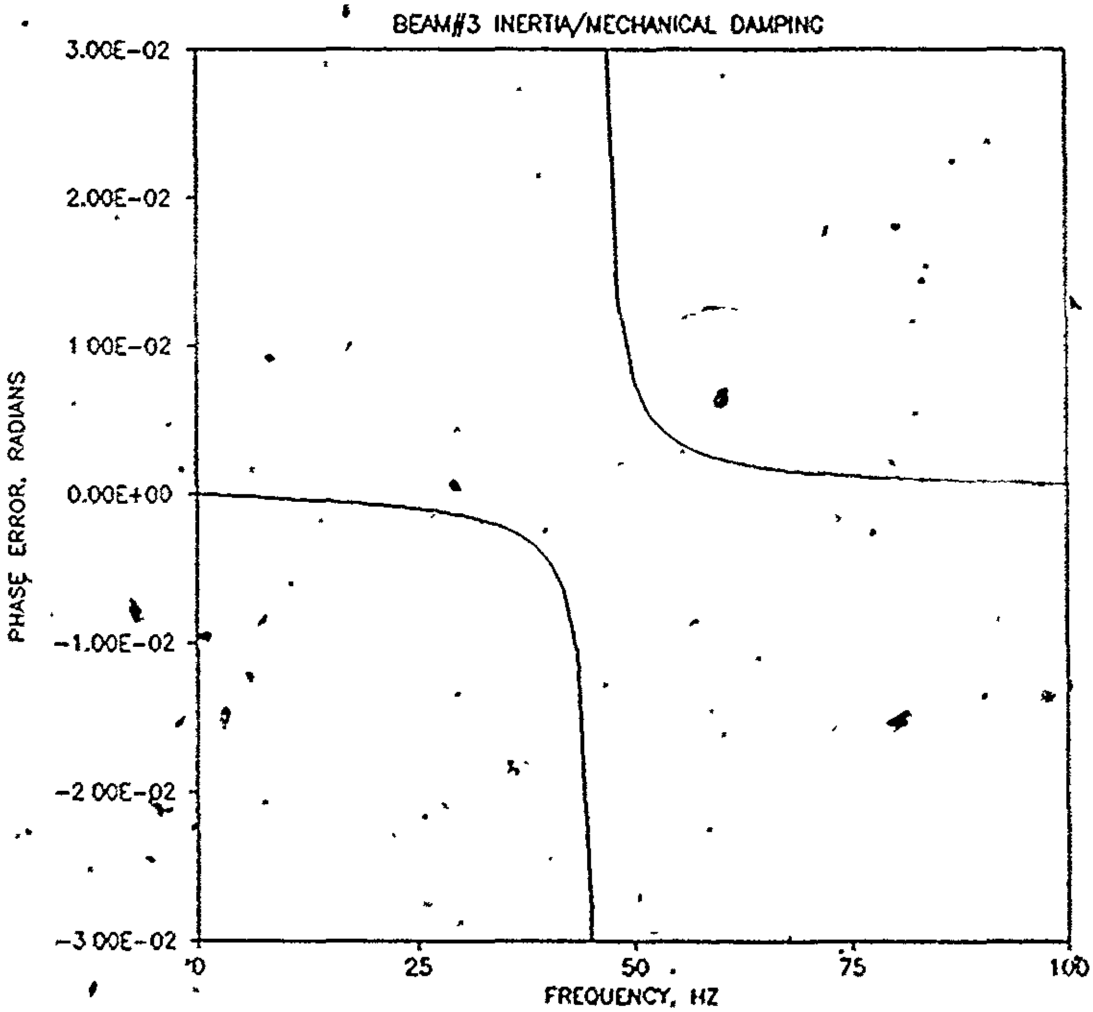

Figure 49. Second order frequency response curve for beam #3 (η=.00127, ω_n=46 Hz) with annulus void. Resonant frequency falls within expected measurement range.

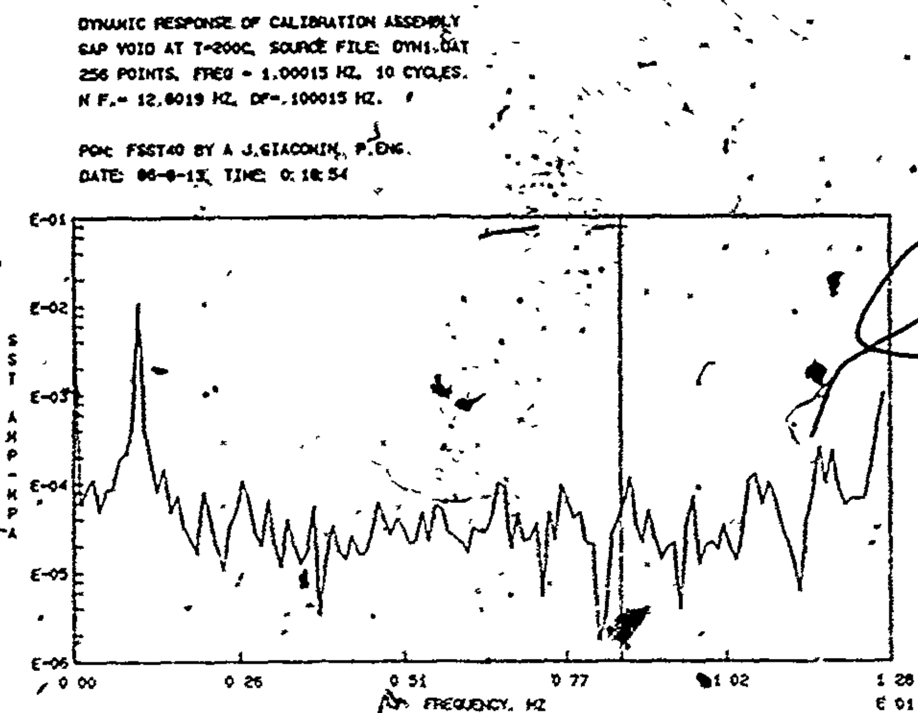

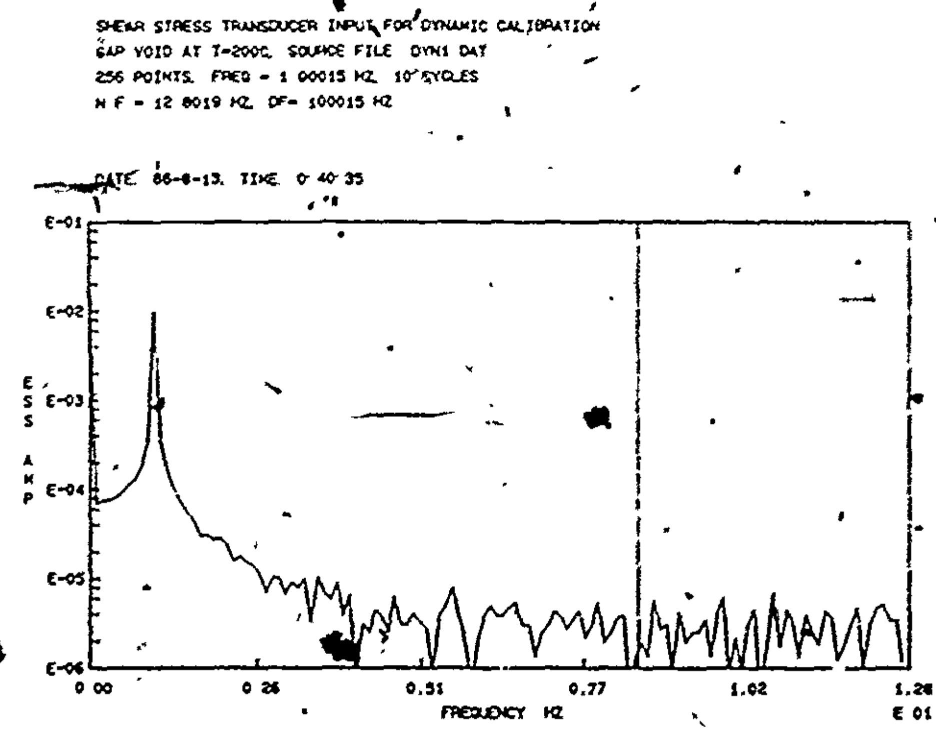

Figure 50: Typical amplitude spectra for the spring extension (lower plot) and the shear stress transducer output (upper plot) for a dry beam test.

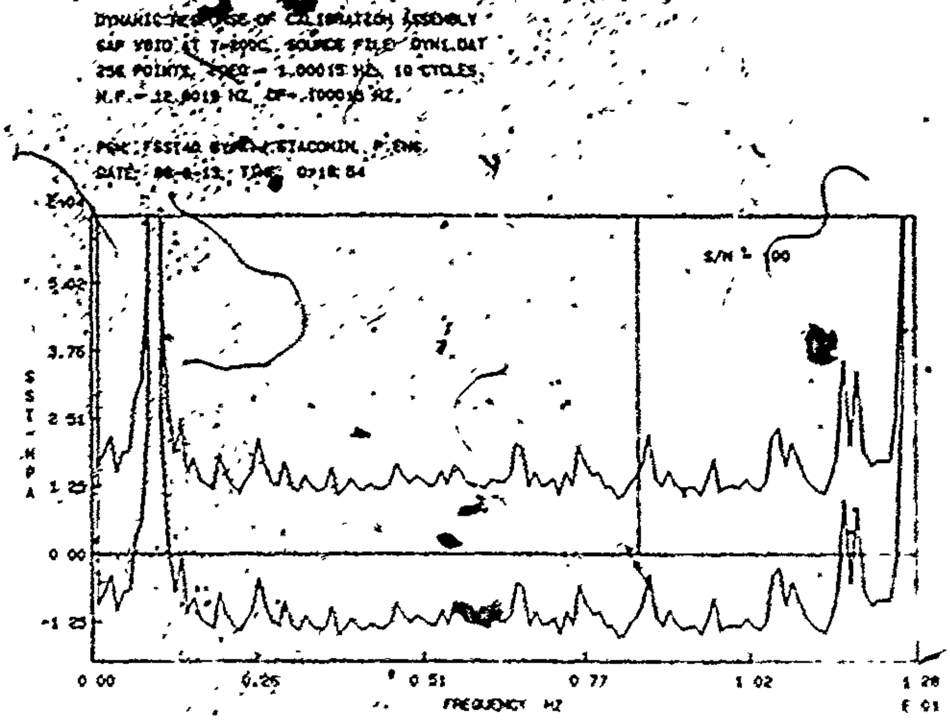

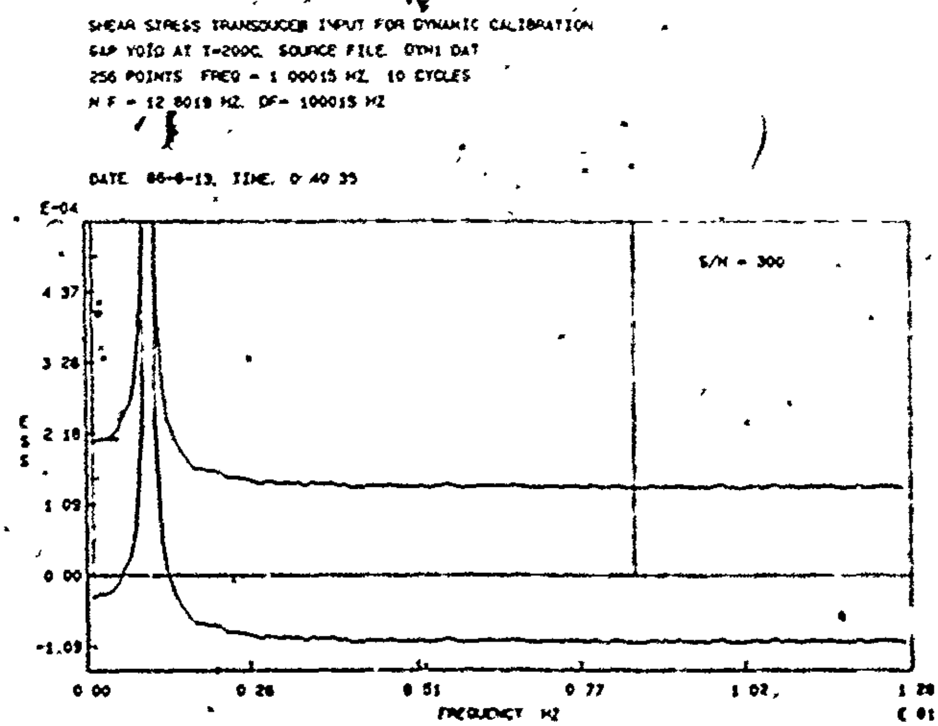

Figure 51: Statistical analysis of amplitude spectra for the spring extension (upper plot) and the shear stress transducer output (lower plot) for a dry beam test. Transducer input and dry response are harmonic as desired.

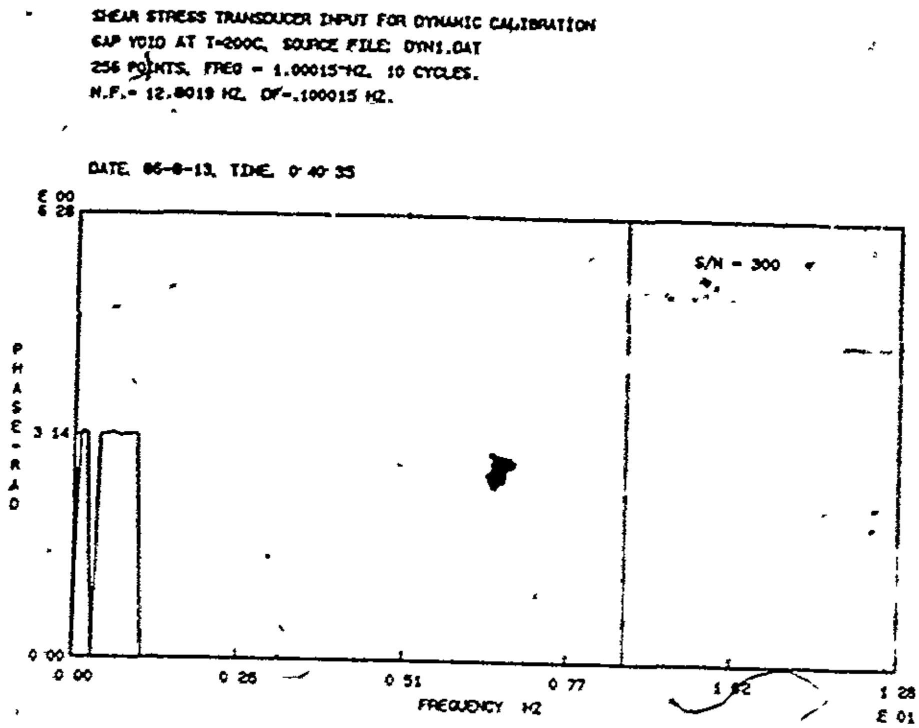

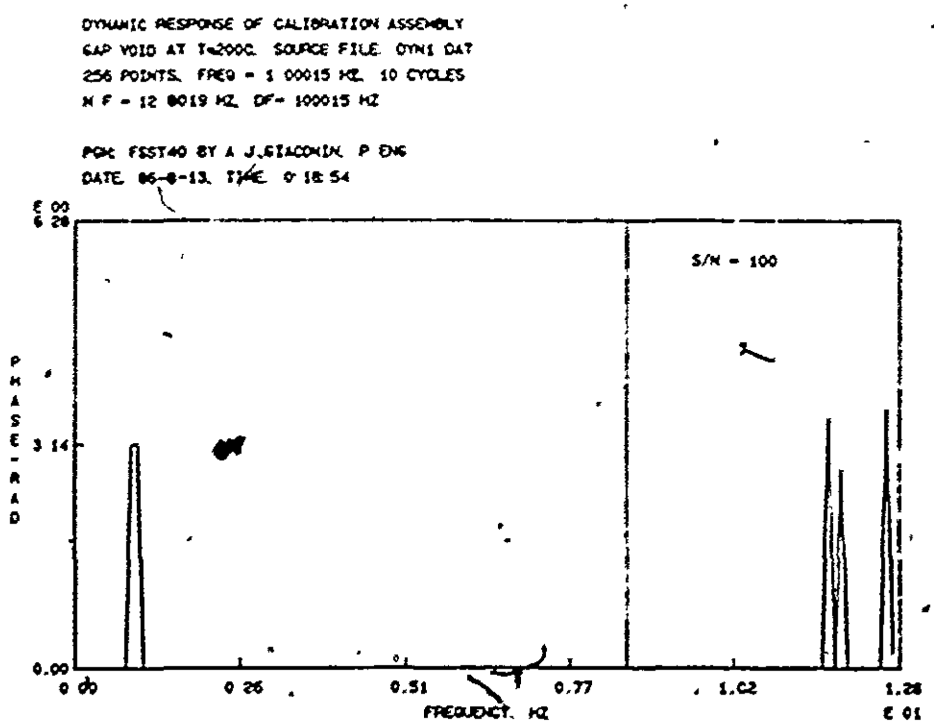

Figure 52· Typical phase spectra for the spring extension (upper plot) and the shear stress transducer output (lower plot) for a dry beam test.

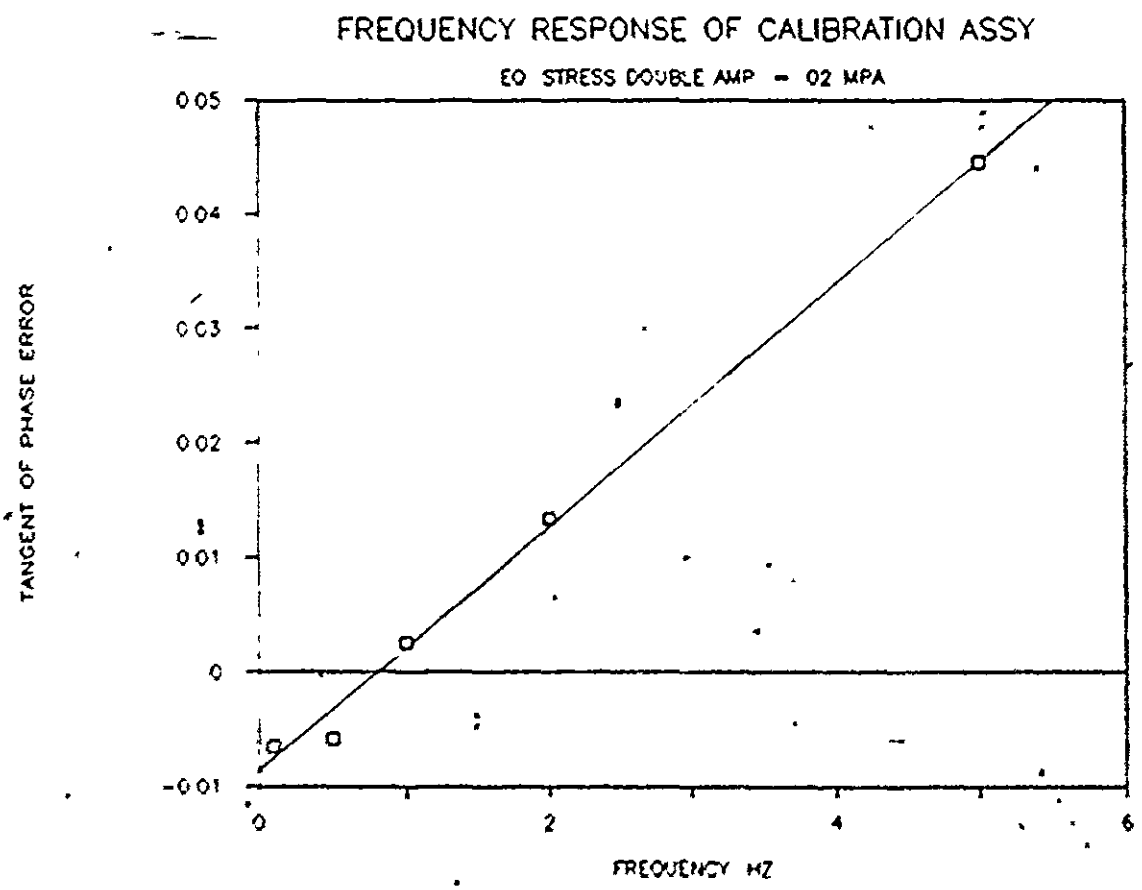

Figure 53. Linear frequency response of the calibration assembly.

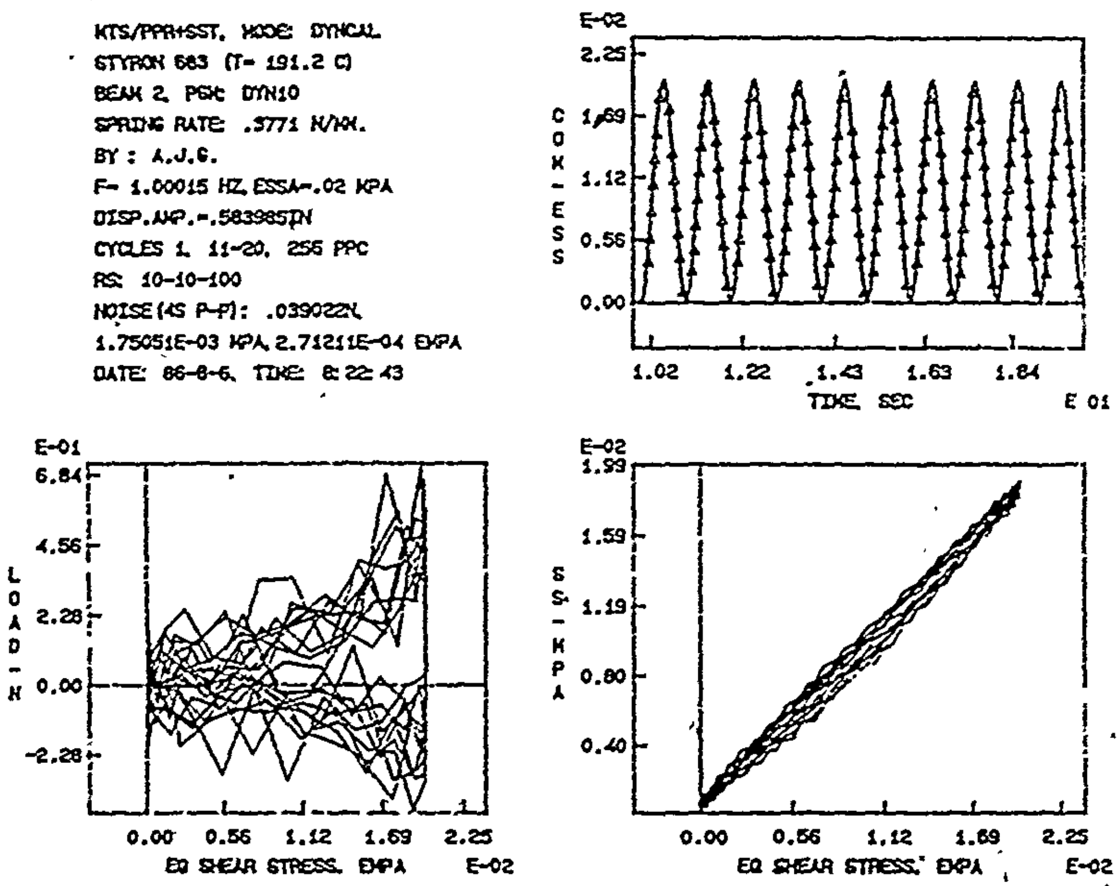

Figure 54: Typical loop plot obtained after a dynamic calibration test. Time trace (upper right) of equivalent shear stress (ESS) shows command ESS (continuous curve) versus actual ESS (triangles) which is inferred from LVDT output. Loop of shear stress output versus ESS input (lower right) and loop of force versus actual ESS (lower left).

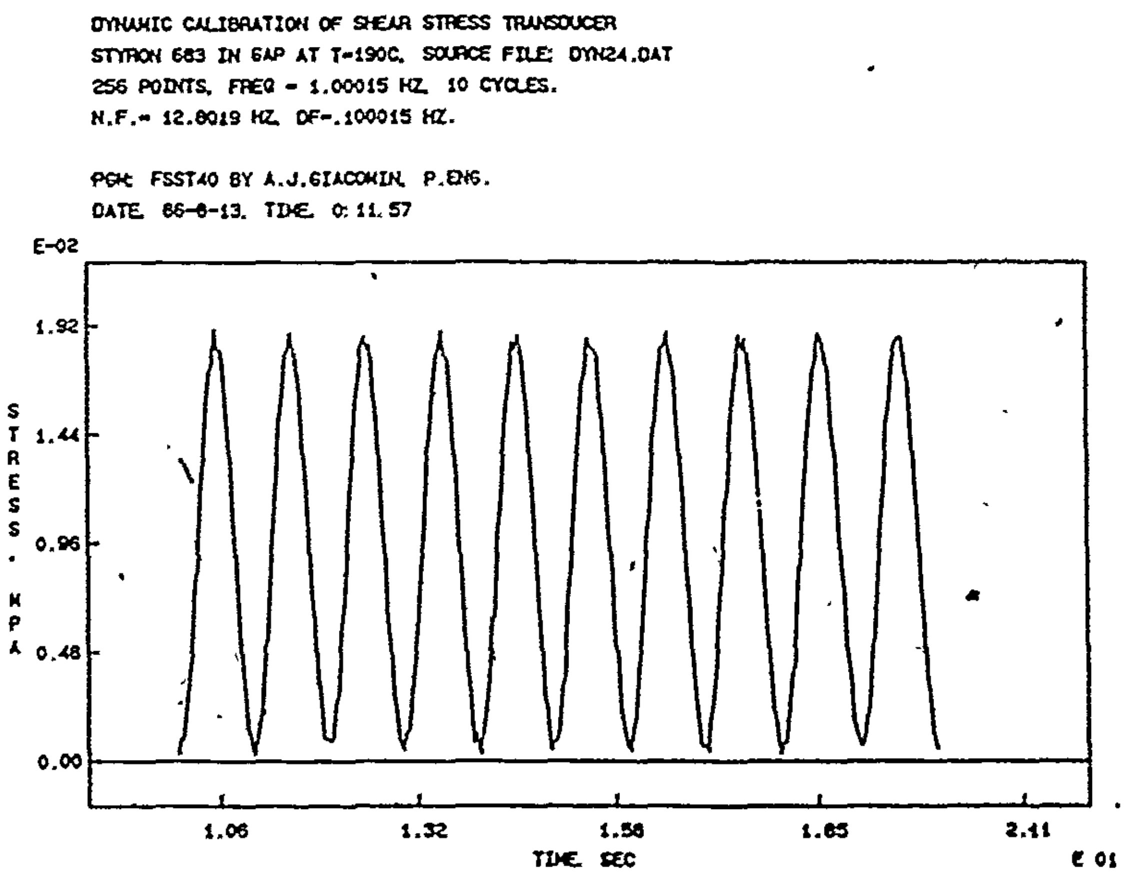

Figure 55: Time trace of the shear stress transducer output during a dynamic calibration test showing effect of background noise.

SHEAR STRESS TRANSDUCER INPUT FOR DYNAMIC CALIBRATION
STYRON 683 IN GAP AT T=190C. SOURCE FILE: DYN24.DAT
256 POINTS. FREQ = 1.00015 HZ. 10 CYCLES.
N.F.= 12.8019 HZ. DF=.100015 HZ.

DATE: 86-8-12. TIME: 23:22:21

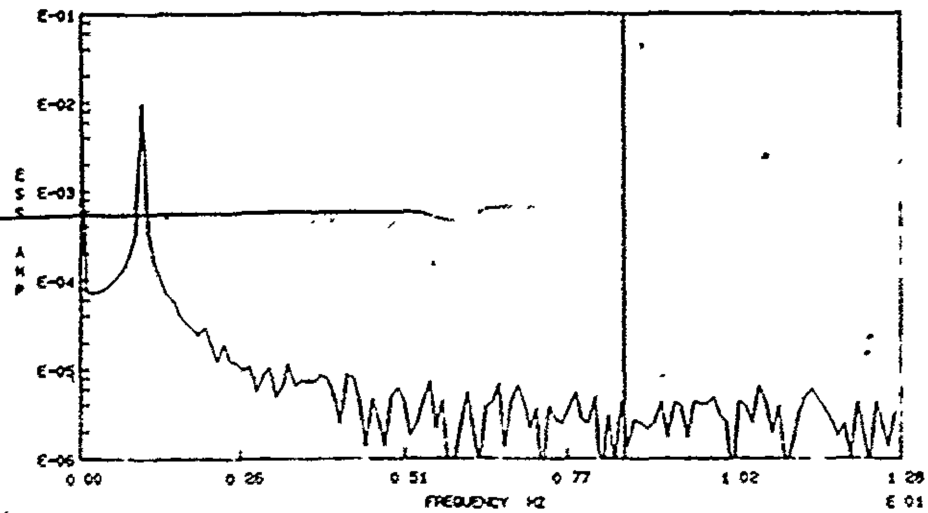

DYNAMIC-CALIBRATION OF SHEAR STRESS TRANSDUCER
STYRON 683 IN GAP AT T=190 C SOURCE FILE DYN24 DAT
256 POINTS. FREQ = 1 00015 HZ. 10 CYCLES
N F = 12 8019 HZ. DF= 100015 HZ

PGM: FSST40 BY A J GIACOMIN. P ENG
DATE. 86-8-12. TIME. 22:48:11

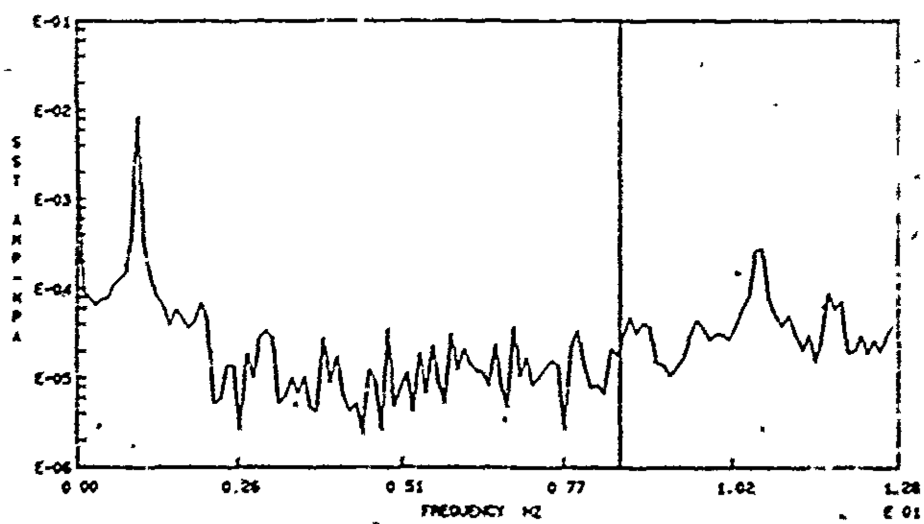

Figure 56· Typical amplitude spectra for the shear stress transducer input (upper plot) and the shear stress transducer output (lower plot) for a dynamic calibration done with molten polystyrene in transducer gap.

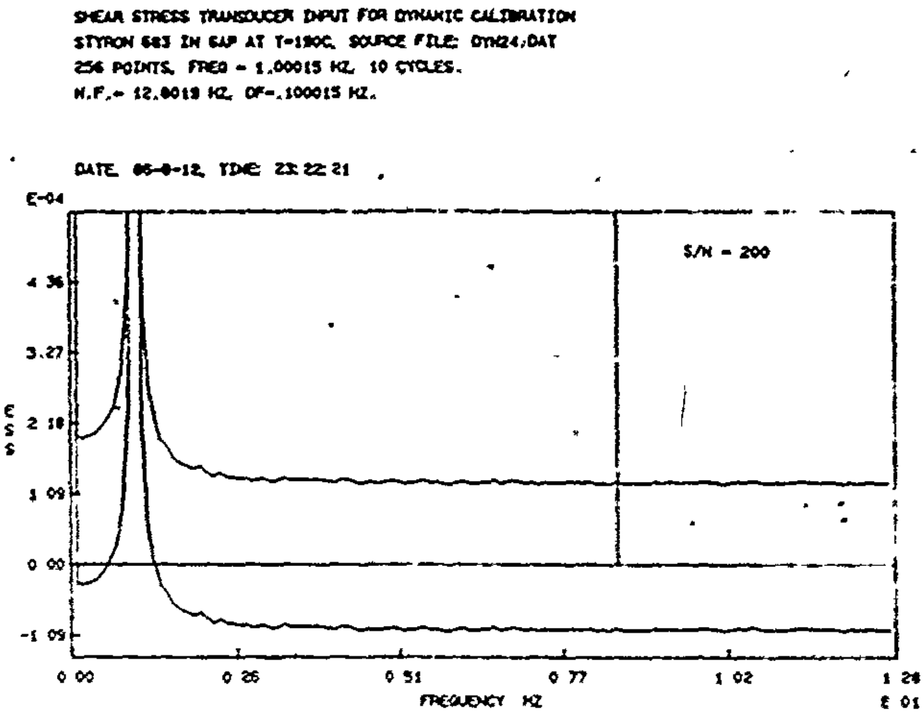

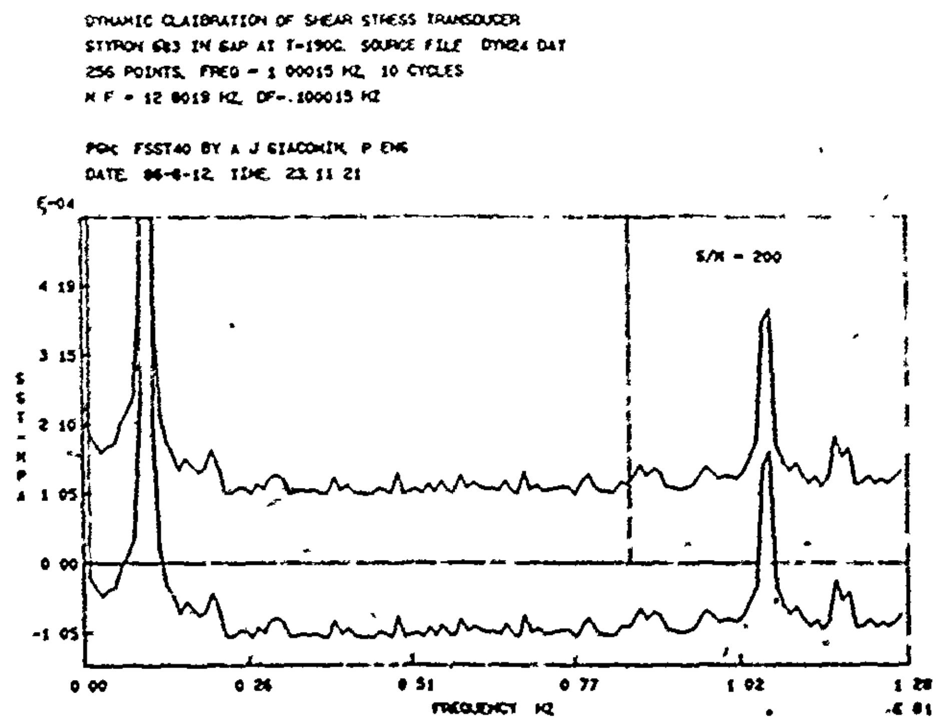

Figure 57. Statistical analysis of amplitude spectra for the shear stress transducer input (upper plot) and the shear stress transducer output (lower plot) for a dynamic calibration done with molten polystyrene in transducer gap. Transducer input and output are harmonic as desired.

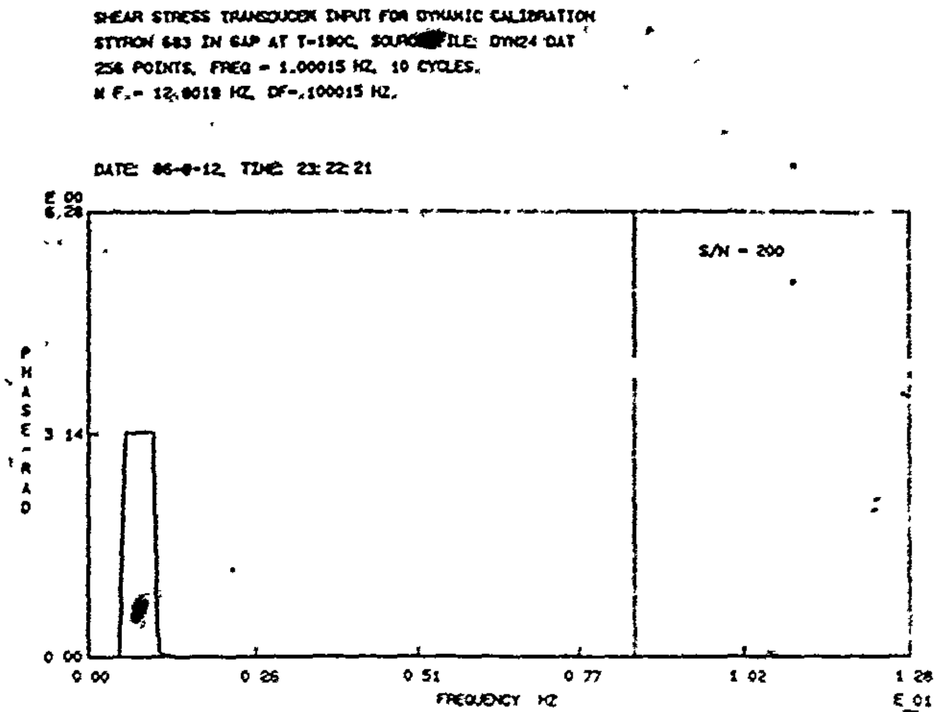

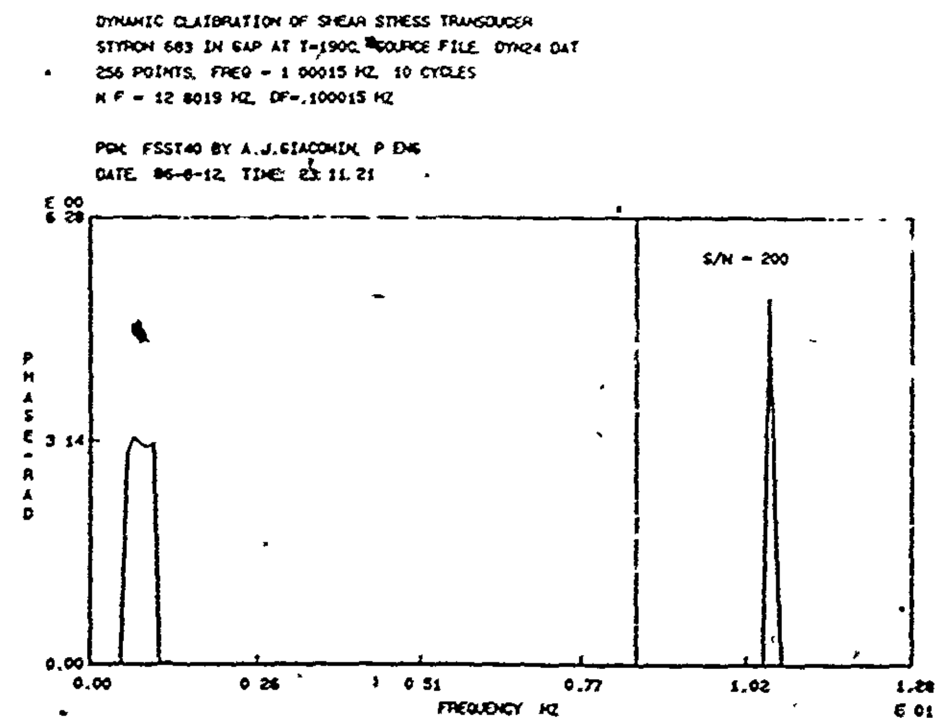

Figure 58: Typical phase spectra for the shear stress transducer input (upper plot) and the shear stress transducer output (lower plot) for a dynamic calibration done with molten polystyrene in transducer gap.

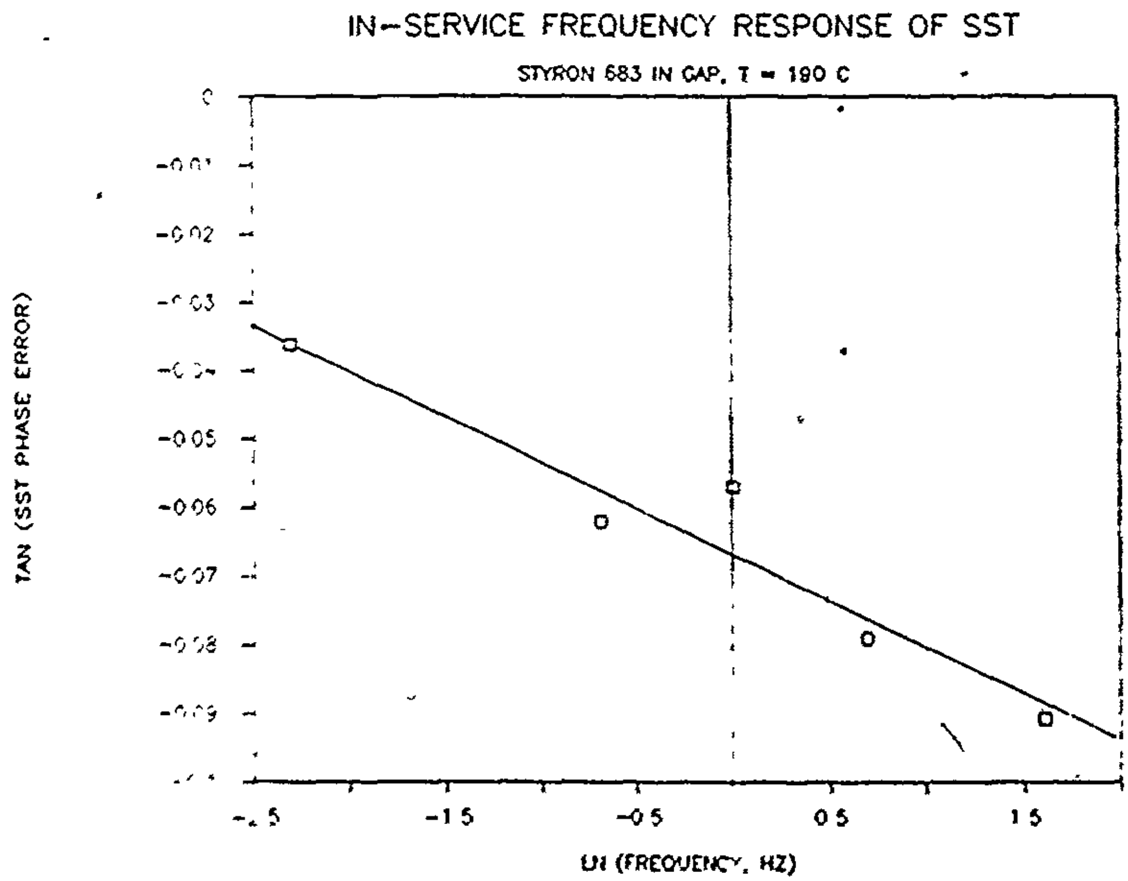

Figure 59   Frequency response results for the shear stress transducer at 190°C with molten polystyrene in the annulus between the housing and the cantilever.

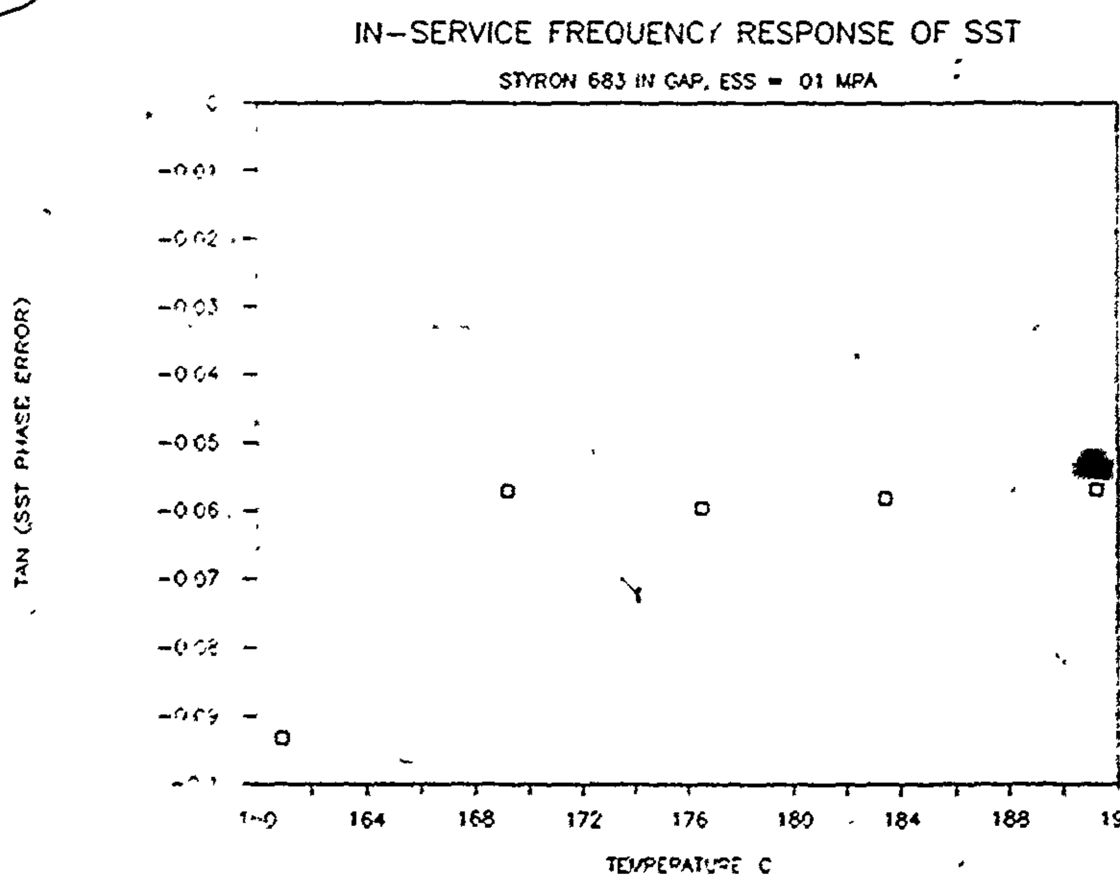

Figure 60: Slight temperature dependence of frequency response of the shear stress transducer with molten polystyrene in the transducer gap.

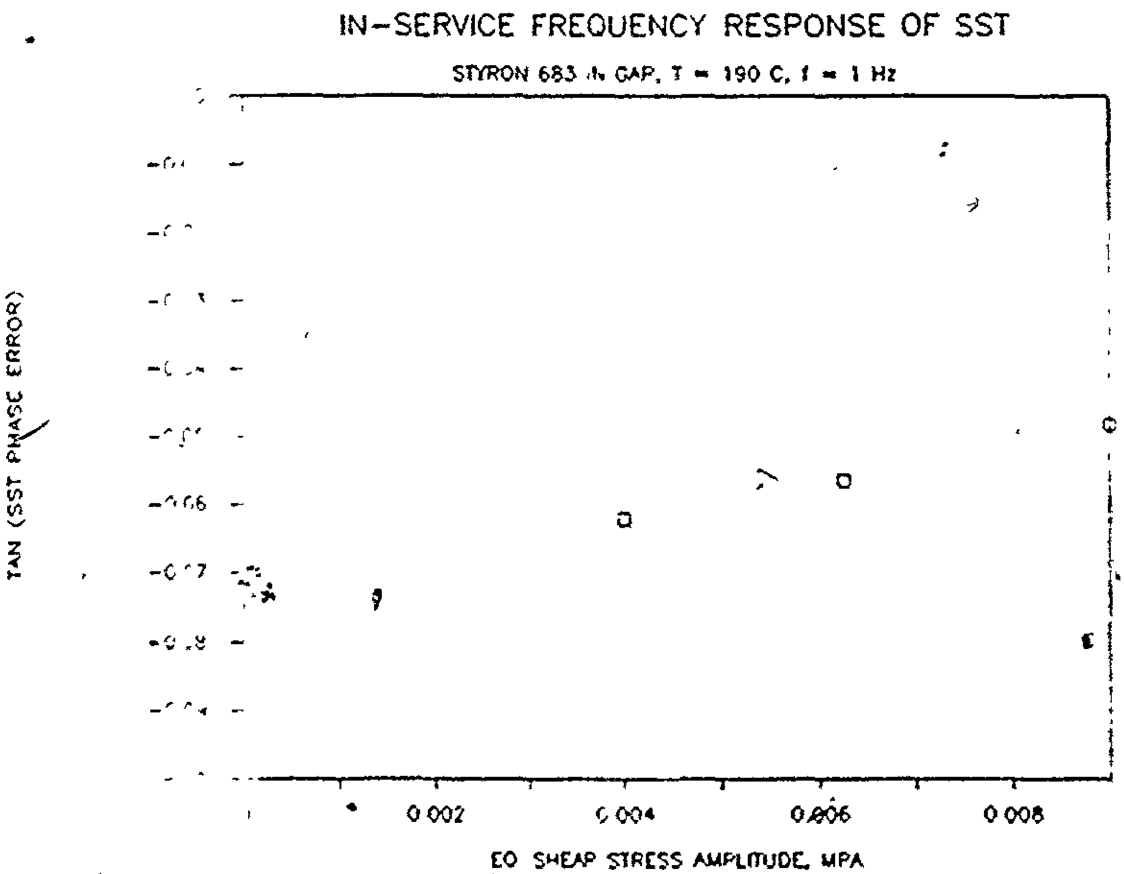

Figure 61. Test for the effect of shear stress amplitude on the frequency response of the shear stress transducer with polystyrene melt in the annulus between the cantilever and the housing.

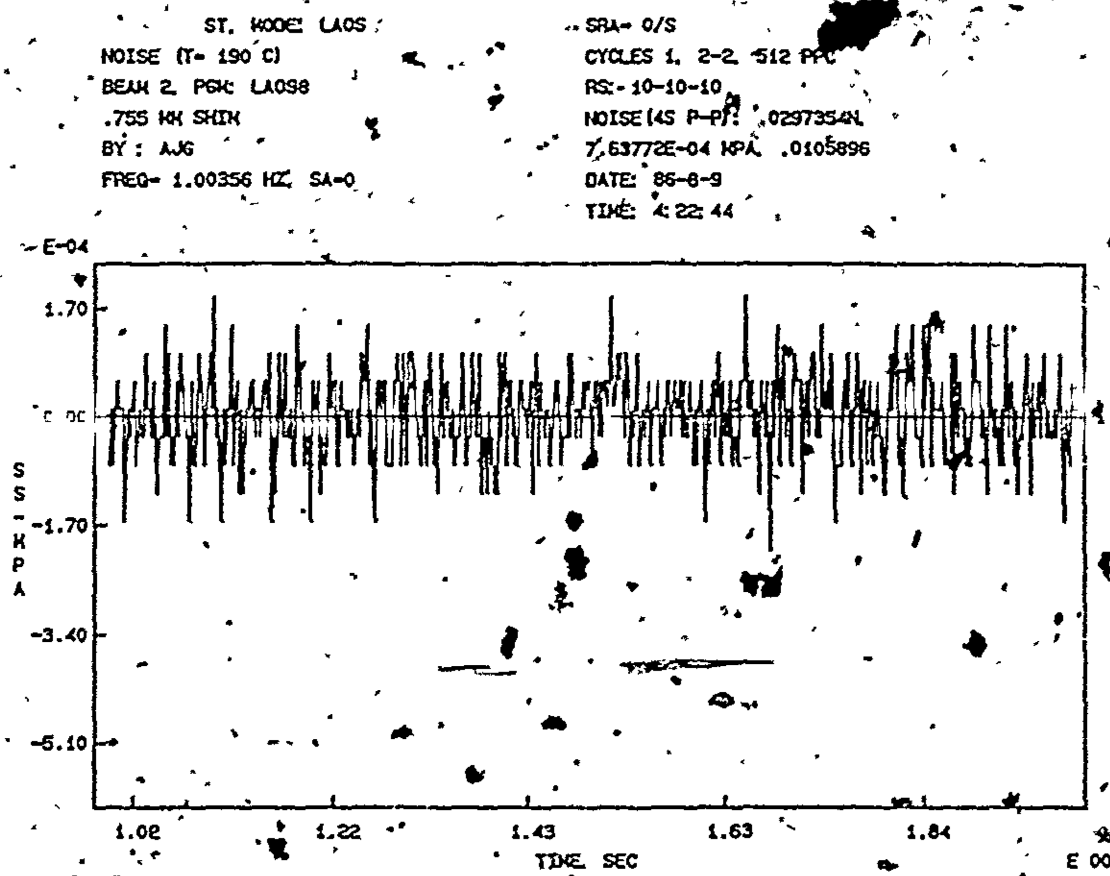

Figure 62: Typical time trace for the shear stress transducer output using beam #2.

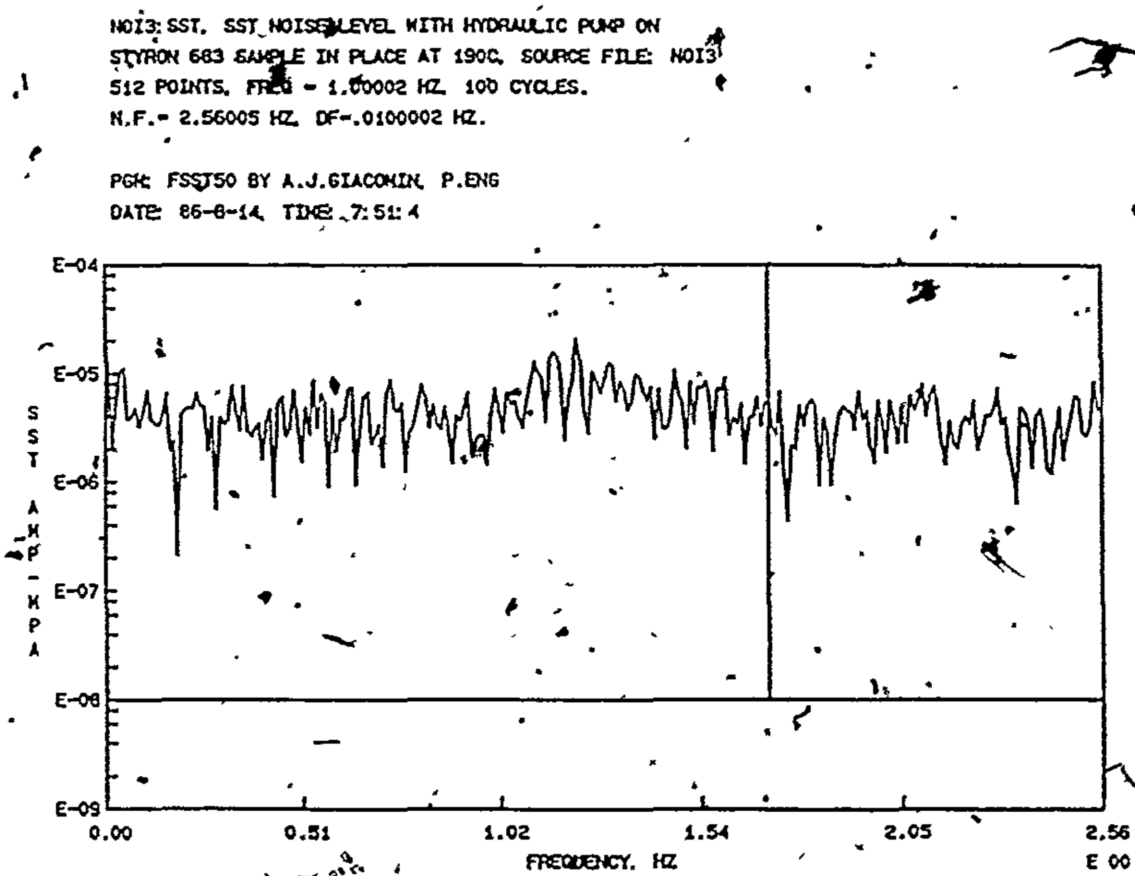

Figure 63. Low frequency amplitude spectrum of shear stress transducer output computed with 256 point DFT with 2.56 Hz Nyquist frequency.

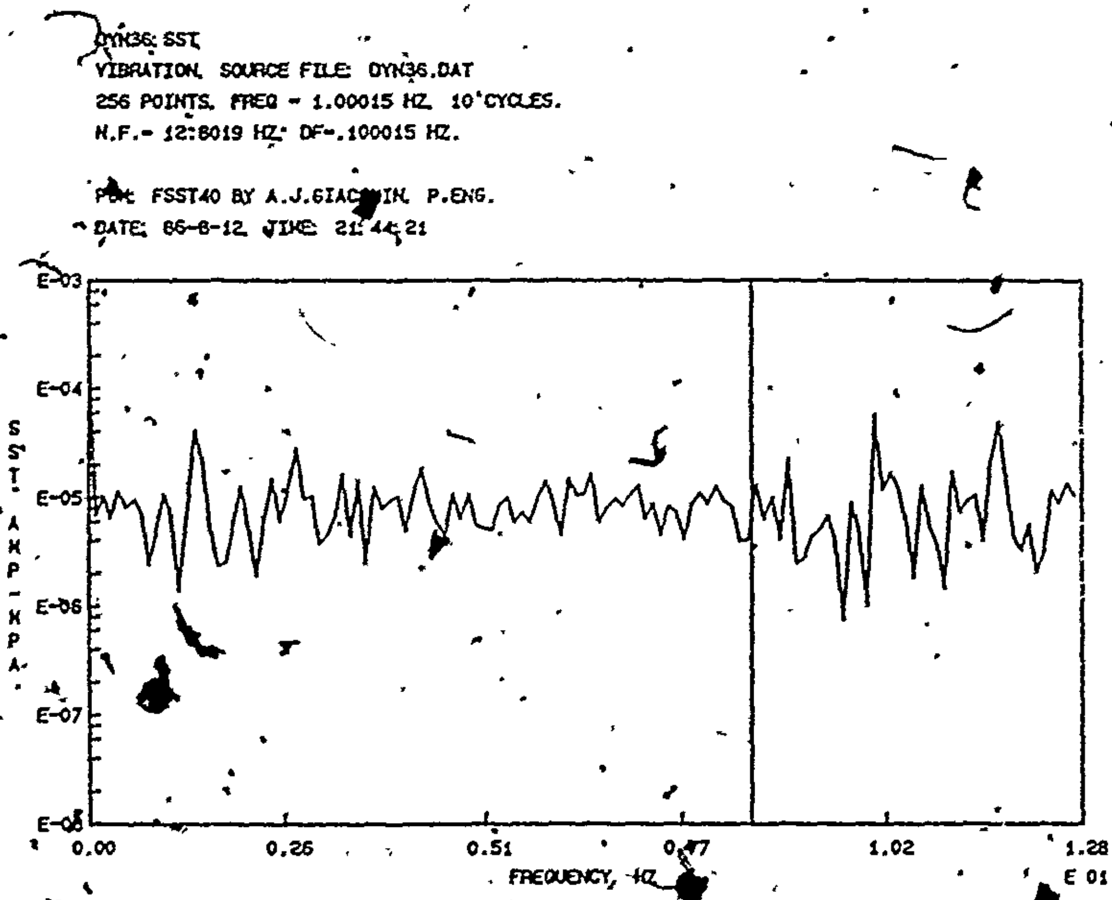

Figure 64: Low frequency amplitude spectrum of shear stress transducer output computed with 256 point DFT with 12.8 Hz Nyquist frequency.

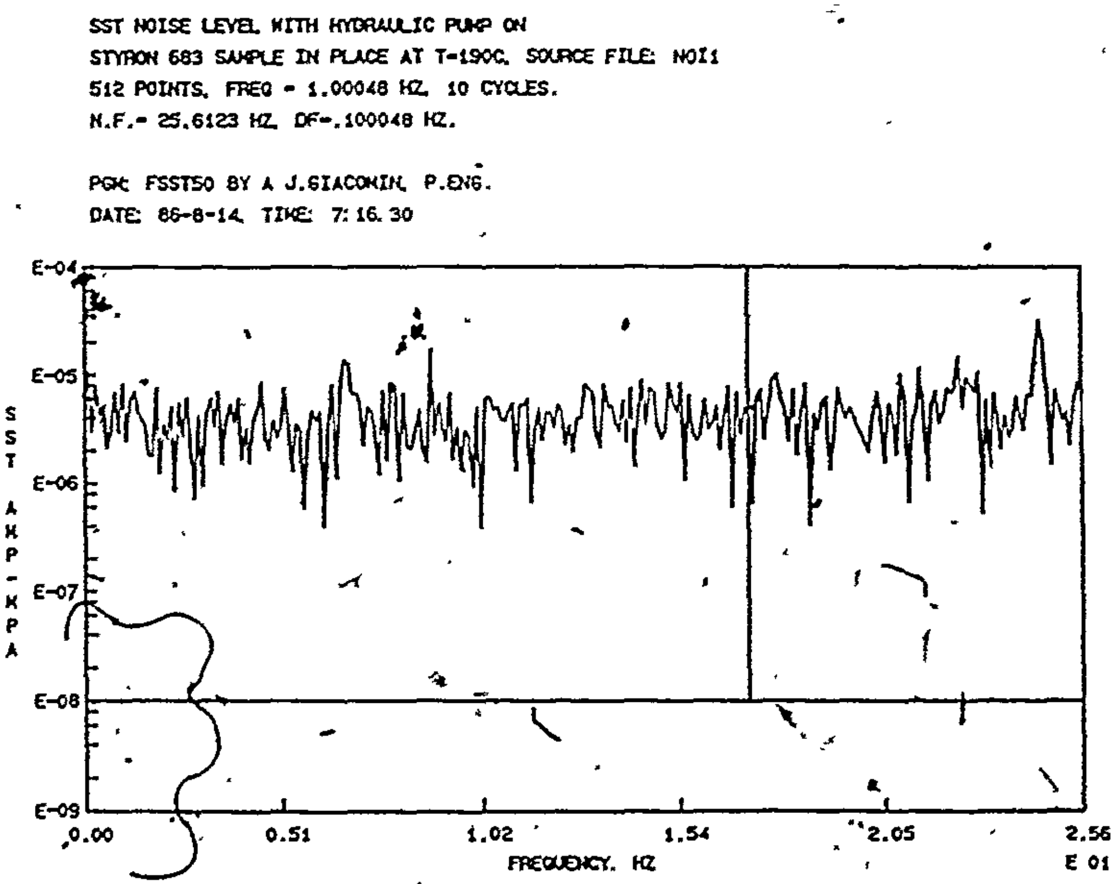

Figure 65: Intermediate frequency amplitude spectrum of shear stress transducer output computed with 256 point DFT with 25.6 Hz Nyquist frequency.

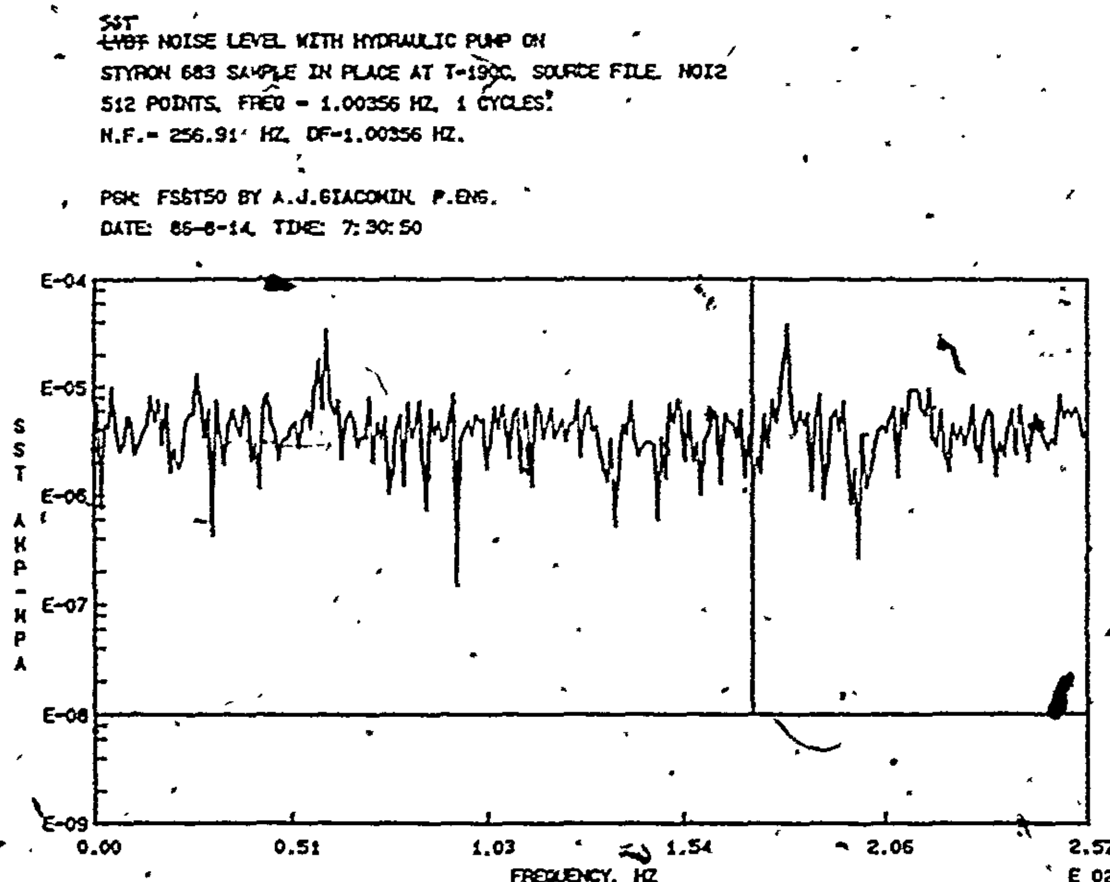

Figure 66: High frequency amplitude spectrum of shear stress transducer output computed with 256 point DFT with 256 Hz Nyquist frequency.

SST
NOISE LEVEL WITH HYDRAULIC PUMP ON
STYRON 683 SAMPLE IN PLACE AT T=190C, SOURCE FILE: NOI24
512 POINTS, FREQ = 1.00356 HZ, 1 CYCLES.
N.F.= 256.911 HZ, DF=1.00356 HZ.

PGM: FSST50 BY A.J.GIACOMIN, P.ENG.
DATE: 86-8-14, TIME: 7:30:50

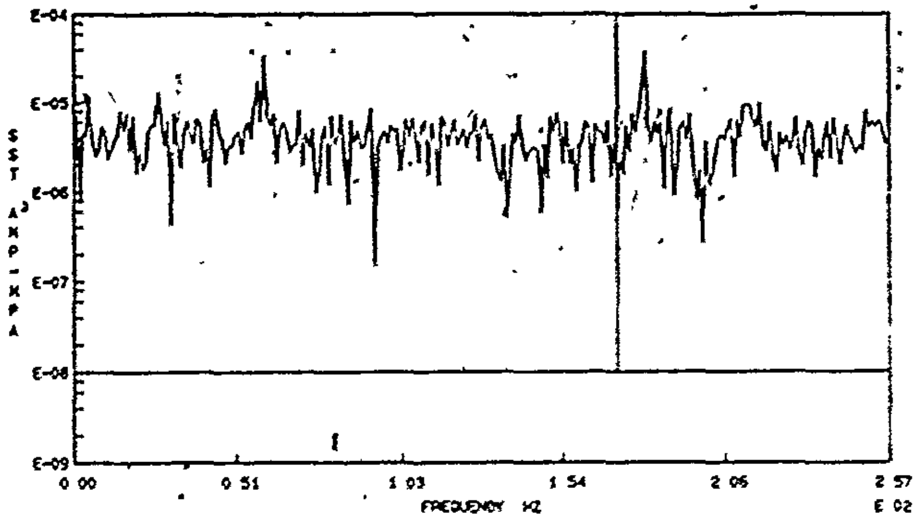

NOI4 SST, SST NOISE WITH HYDRAULIC PUMP OFF
STYRON 683 SAMPLE IN PLACE AT 190C, SOURCE FILE: NOI4
512 POINTS, FREQ = 1.00356 HZ, 1 CYCLES
N.F.= 256.911 HZ, DF=1.00356 HZ.

PGM: FSST50 BY A.J.GIACOMIN, P.ENG
DATE: 86-8-14, TIME: 7:58:2

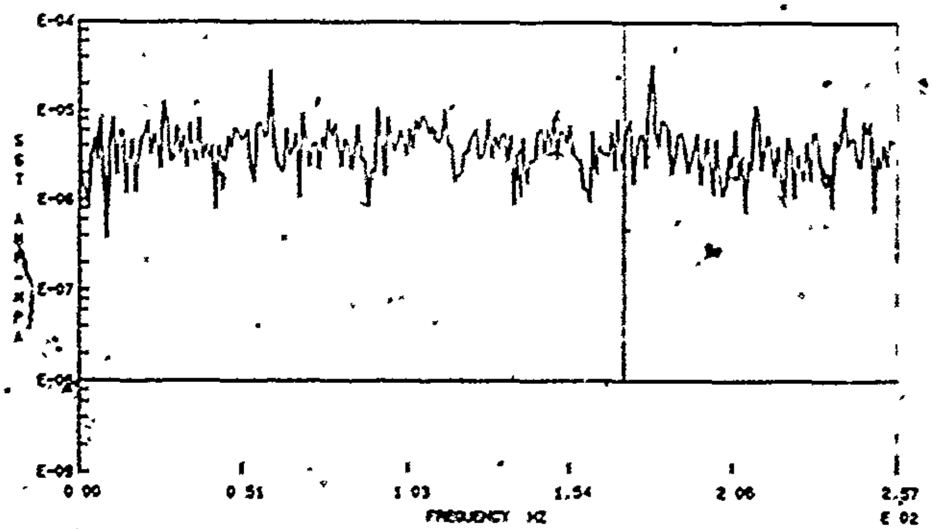

Figure 67. Comparison of high frequency amplitude spectra with MTS hydraulic pump on (upper plot) and off (lower plot).

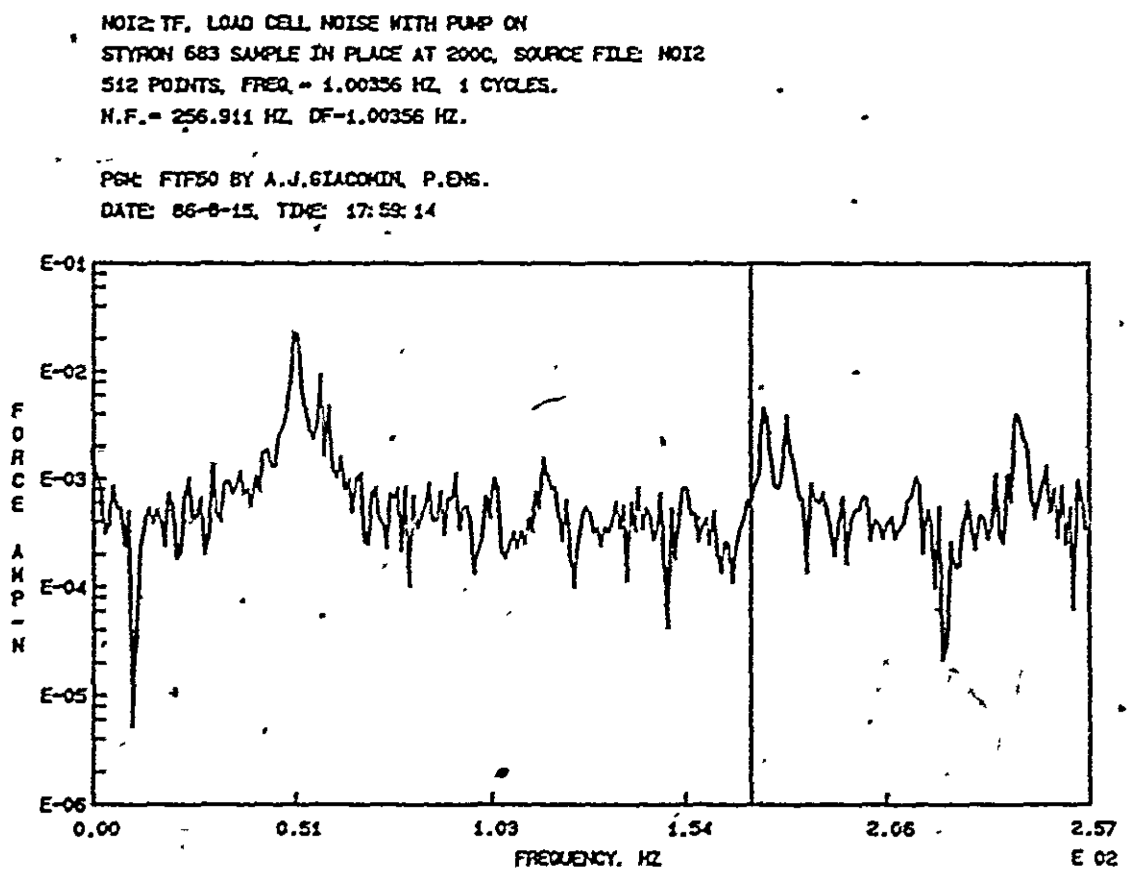

Figure 68. High frequency amplitude spectrum of load cell output computed with 256 point DFT with 256 Hz Nyquist frequency.

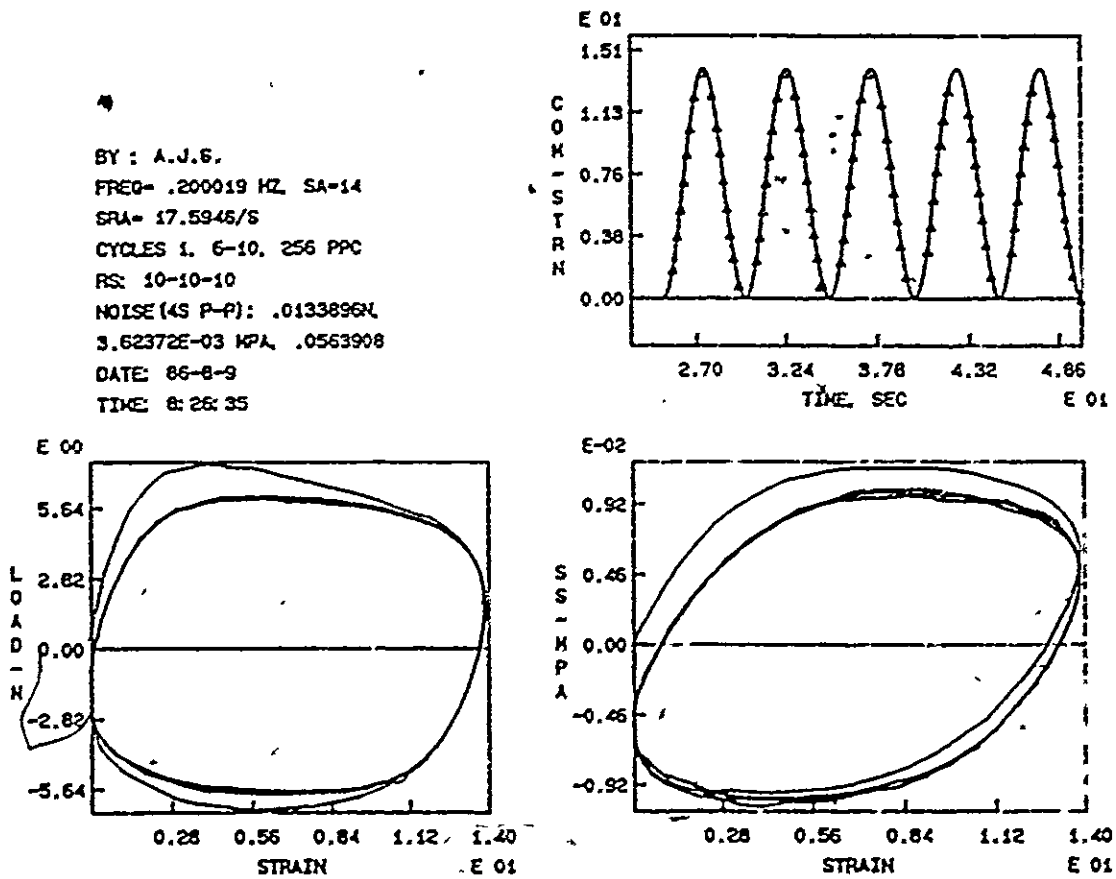

Figure 69: Typical large amplitude oscillatory shear test record obtained immediately after each test. Time trace of shear strain (upper right), total force versus shear strain loop (lower left) and shear stress versus shear strain loop (lower right).

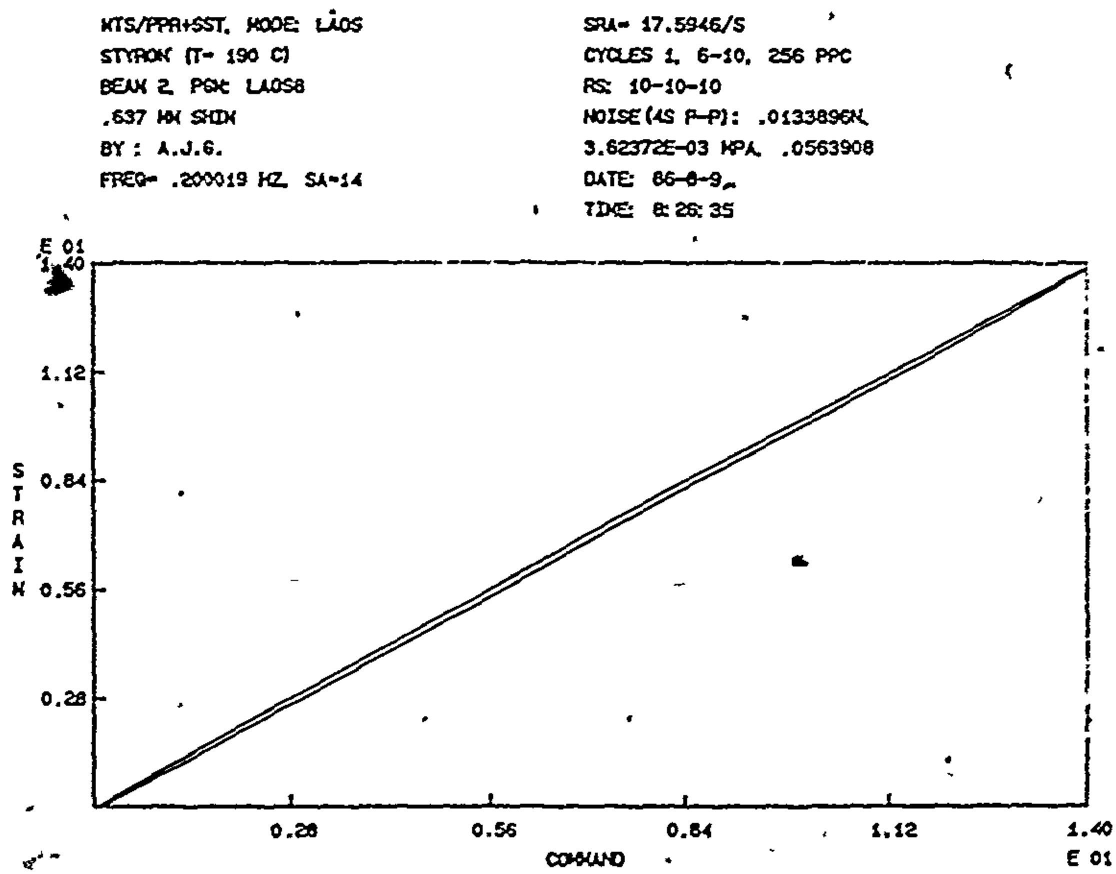

Figure 70: Typical clockwise loop of actual shear strain versus command shear strain showing slight phase lag for large amplitude oscillatory shear test done on molten polystyrene at T = 190°C. Since the loop is essentially elliptical, the actual shear strain is harmonic as desired.

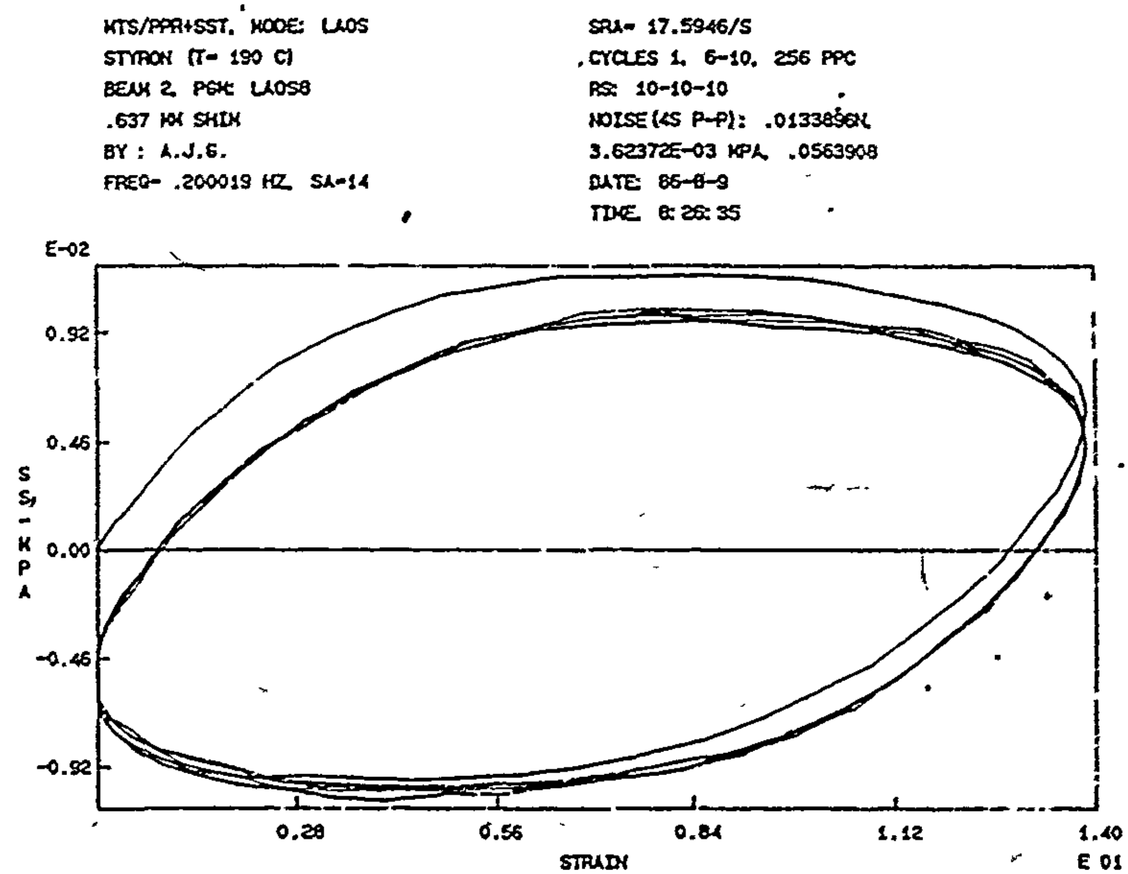

Figure 71: Typical clockwise loop of shear stress against actual shear strain showing large amount of lost work which is proportional to loop area. Large amplitude oscillatory shear test done on molten polystyrene at T = 190°C.

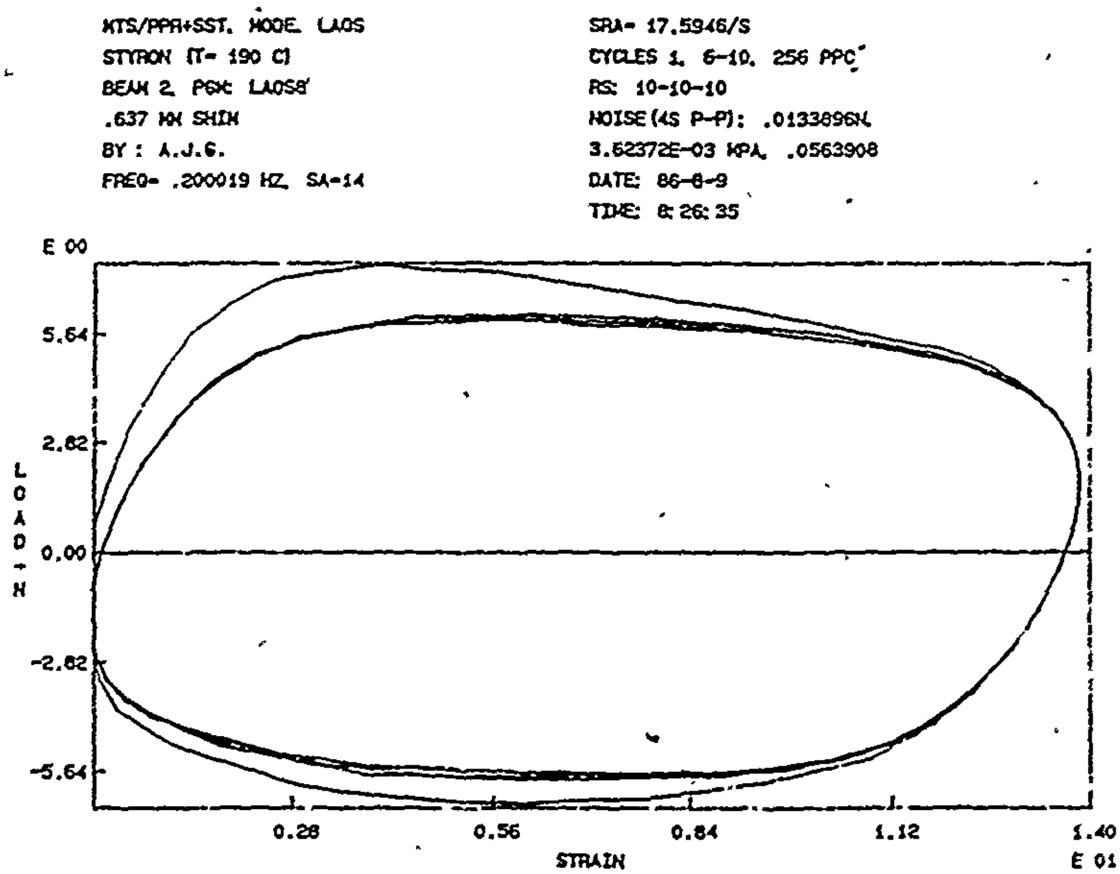

Figure 72: Typical clockwise loop of total force against actual shear strain showing large amount of apparent lost work which is proportional to loop area. Large amplitude oscillatory shear test done on molten polystyrene at T = 190°C.

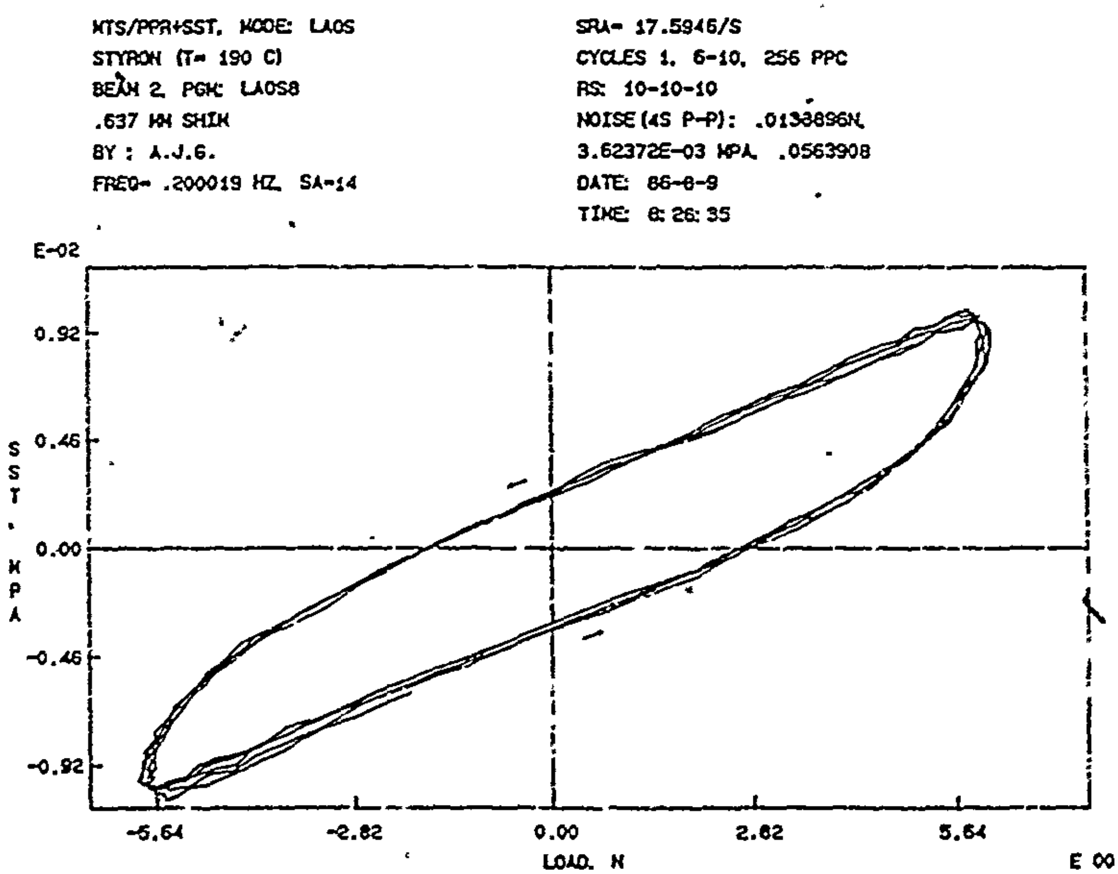

Figure 73: Typical counterclockwise loop of shear stress transducer output versus total force showing additional lost work due to free boundary effects Large amplitude oscillatory shear test done on molten polystyrene at T = 190°C.

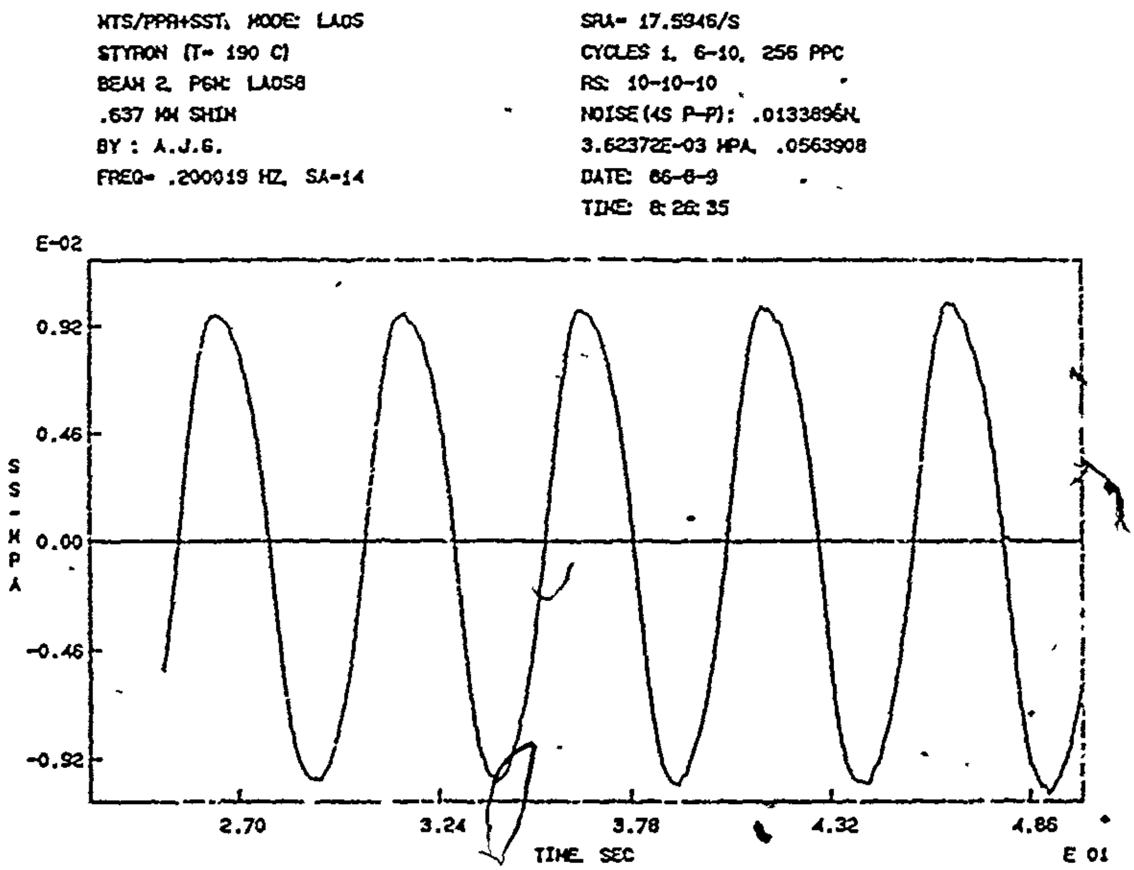

Figure 74· Time trace of shear stress transducer output with anharmonicity barely detectable and showing slight difference from cycle to cycle due to background noise. Large amplitude oscillatory shear test done on molten polystyrene at T = 190°C.

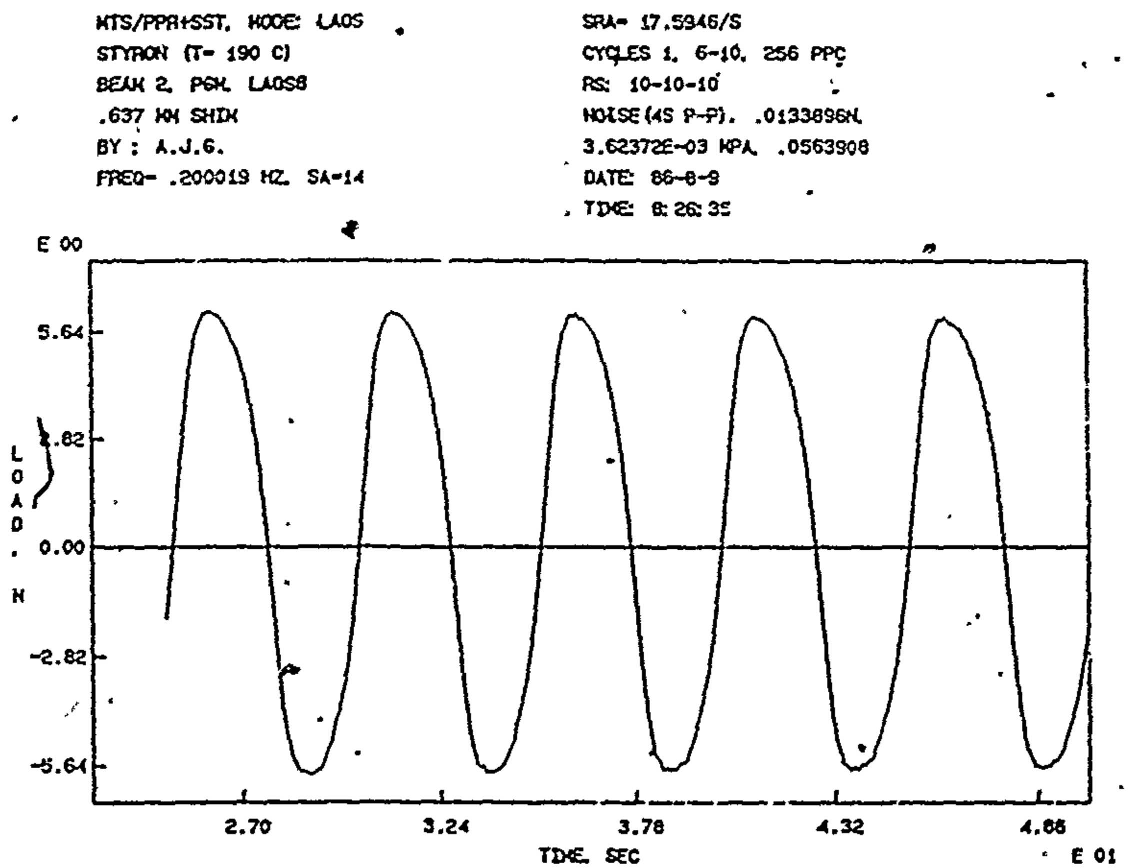

Figure 75: Time trace of load cell transducer output with anharmonicity barely detectable and showing slight difference from cycle to cycle due to background noise. Large amplitude oscillatory shear test done on molten polystyrene at T = 190°C.

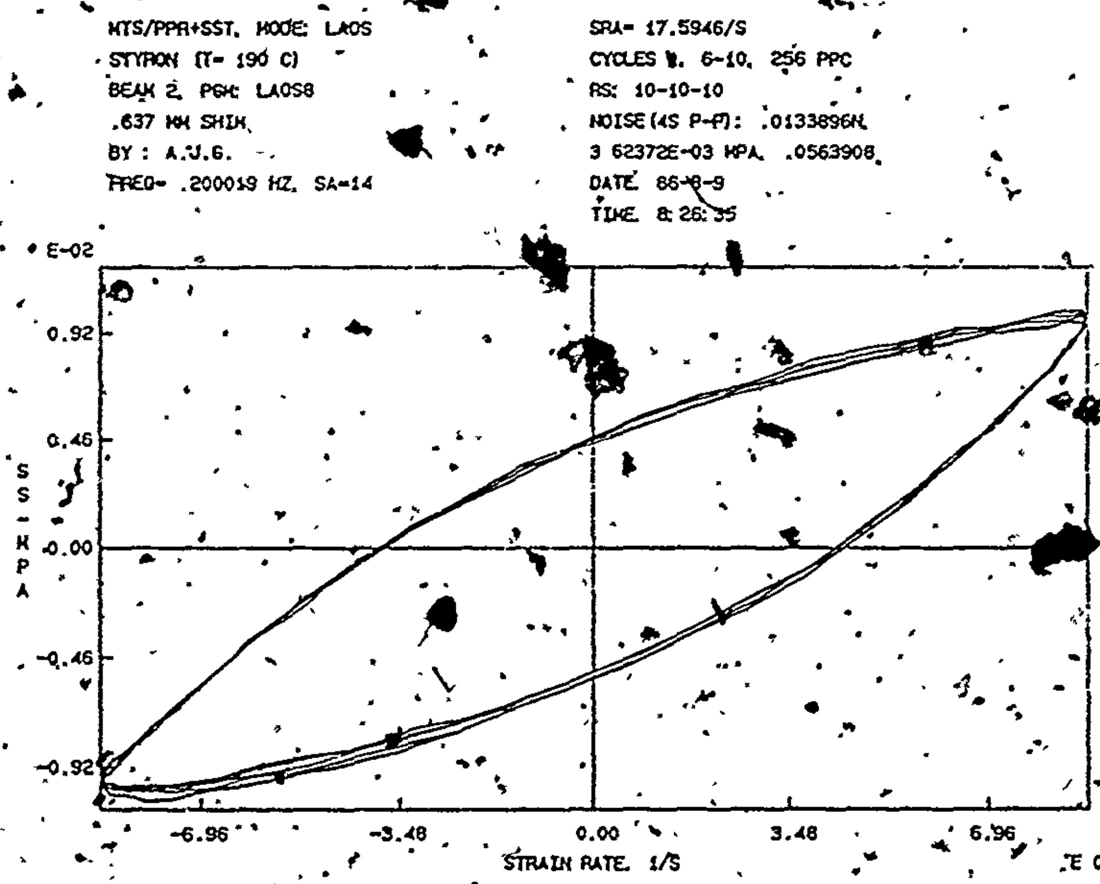

Figure 76. Typical counterclockwise loop of shear stress against actual shear strain rate, dγ/dt, clearly showing anharmonicities in the shear stress by the non-elliptical shape or [illegible]iness of the loop. Large amplitude oscillatory shear test done on molten polystyrene at T = 190°C.

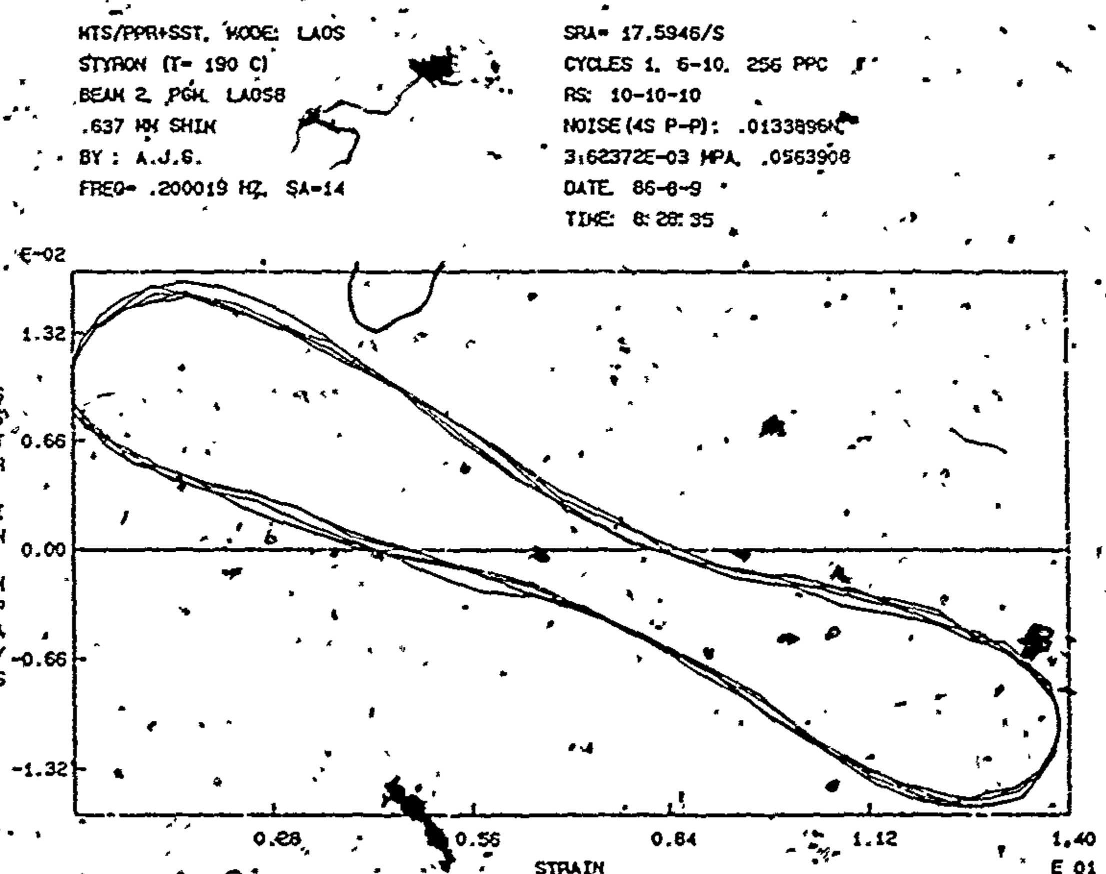

Figure 77: Typical loop of the rate of change of shear stress, $d\sigma/dt$, against actual shear strain clearly showing anharmonicities in the shear stress by the non-elliptical shape of the loop. Large amplitude oscillatory shear test done on molten polystyrene at T = 190°C.

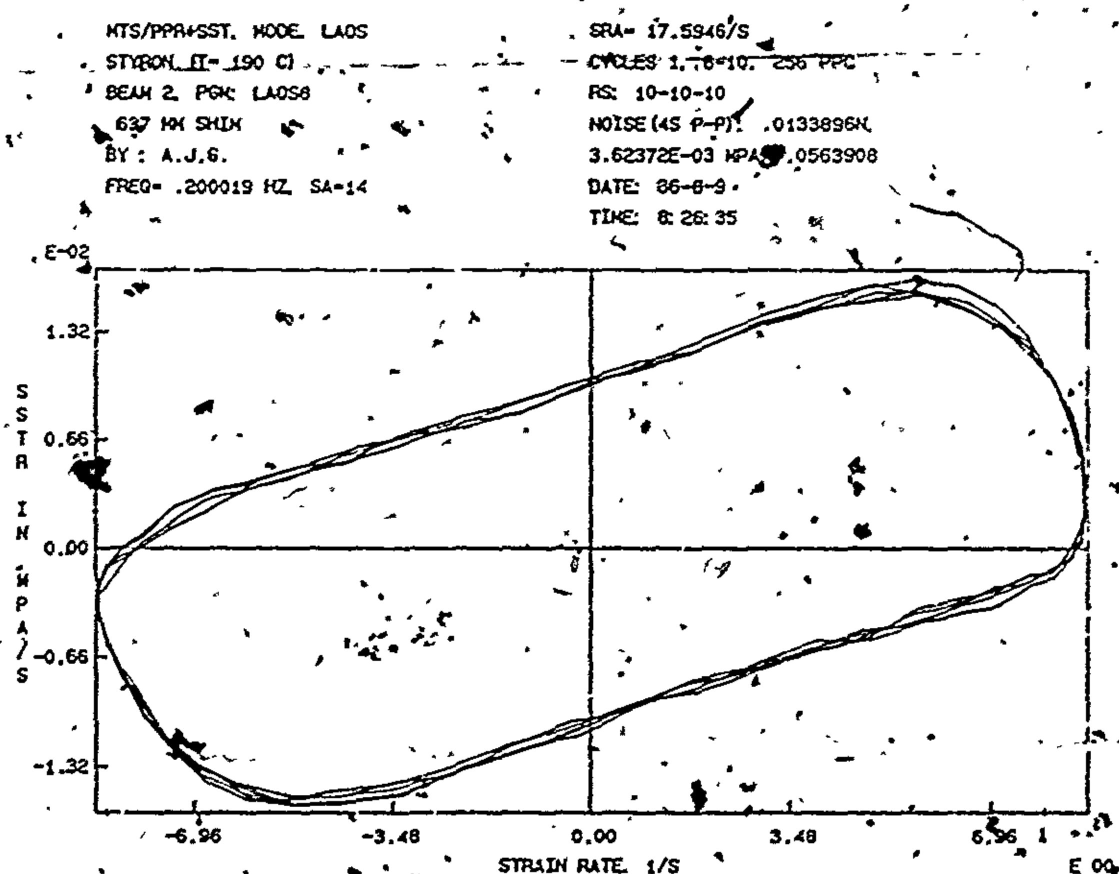

Figure 78: Typical loop of the rate of change of shear stress, $d\sigma/dt$, against actual shear strain rate, $d\gamma/dt$, clearly showing anharmonicities in the shear stress by the non-elliptical shape of the loop. Large amplitude oscillatory shear test done on molten polystyrene at T = 190°C.

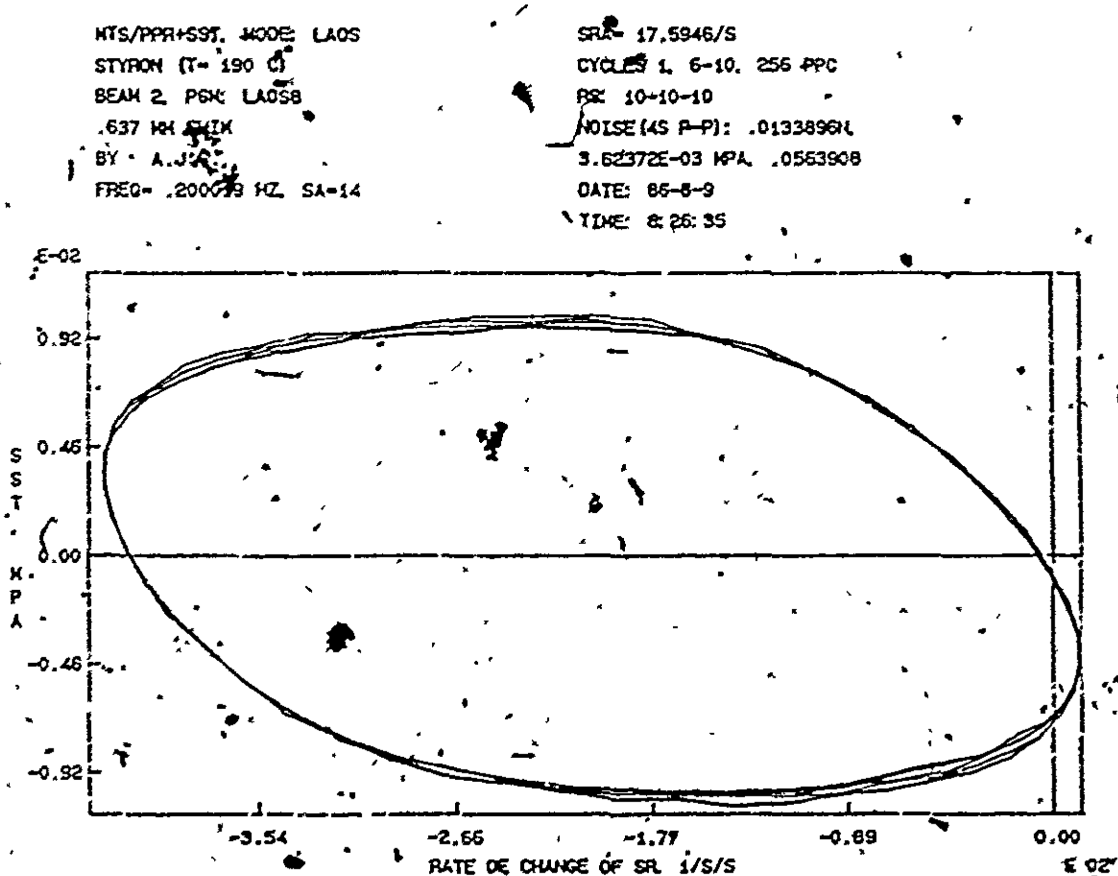

Figure 79· Typical counterclockwise loop of the shear stress, against the second time derivative of actual shear strain, $d^2\gamma/dt^2$, clearly showing anharmonicity in the shear stress by the non-elliptical shape of the loop. Large-amplitude oscillatory shear on molten polystyrene at T = 190°C.

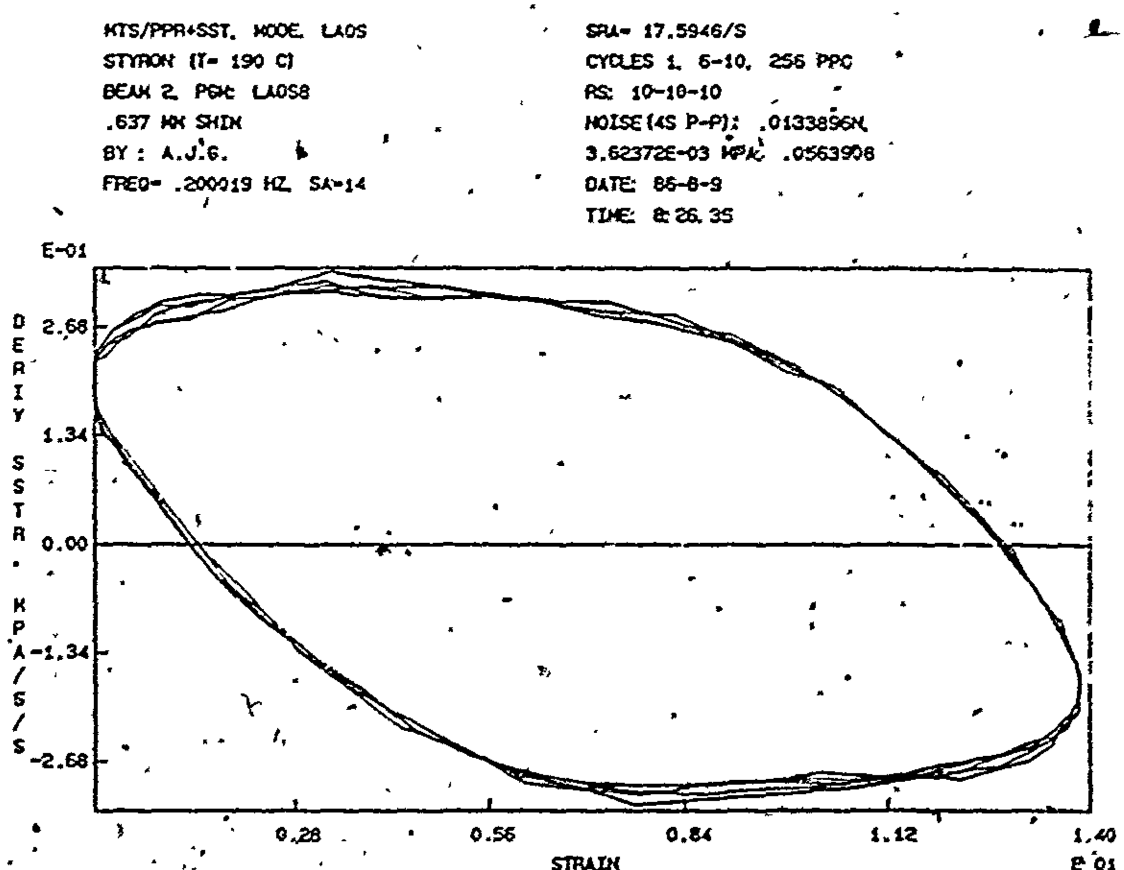

Figure 80· Typical loop of the second time derivative of shear stress, $d^2\sigma/dt^2$, against actual shear strain clearly showing anharmonicity in the shear stress by the non-elliptical shape of the loop. Large amplitude oscillatory shear test done on molten polystyrene at T = 190°C.

```
REPORT ON DU1:OS208.DAT &

STYRON (T= 190 C)              BEAM 2, PGM: LAOS8
.637 MM SHIM   BY : A.J.G.
FREQ= .200019 HZ, SA=14        SRA= 17.5946/S
CYCLES 1, 6-10, 256 PPC        RS: 10-10-10
NOISE(4S P-P): .0133896N,      3.62372E-03 MPA, .0563908
DATE: 86-8-9  TIME: 8:26:35
LVDT CAL=  4.81768  IN @ 10 V.
LOAD CAL=  .795328  V/KG HUNG MASS @ RS 100%
SST CAL=  .387894  V/KG HUNG MASS @ RS=100%
BEAM DEFLECTION CONST= .03504  MPA/KG
CAPACITANCE PROBE? ASP-5HT
ATTENUATION METHOD? BUILT-IN CIRCUIT.
COMMENTS? NONLINEAR VISCOELASTIC RESPONSE.
```

Figure 81: Archival record for an oscillatory shear test.

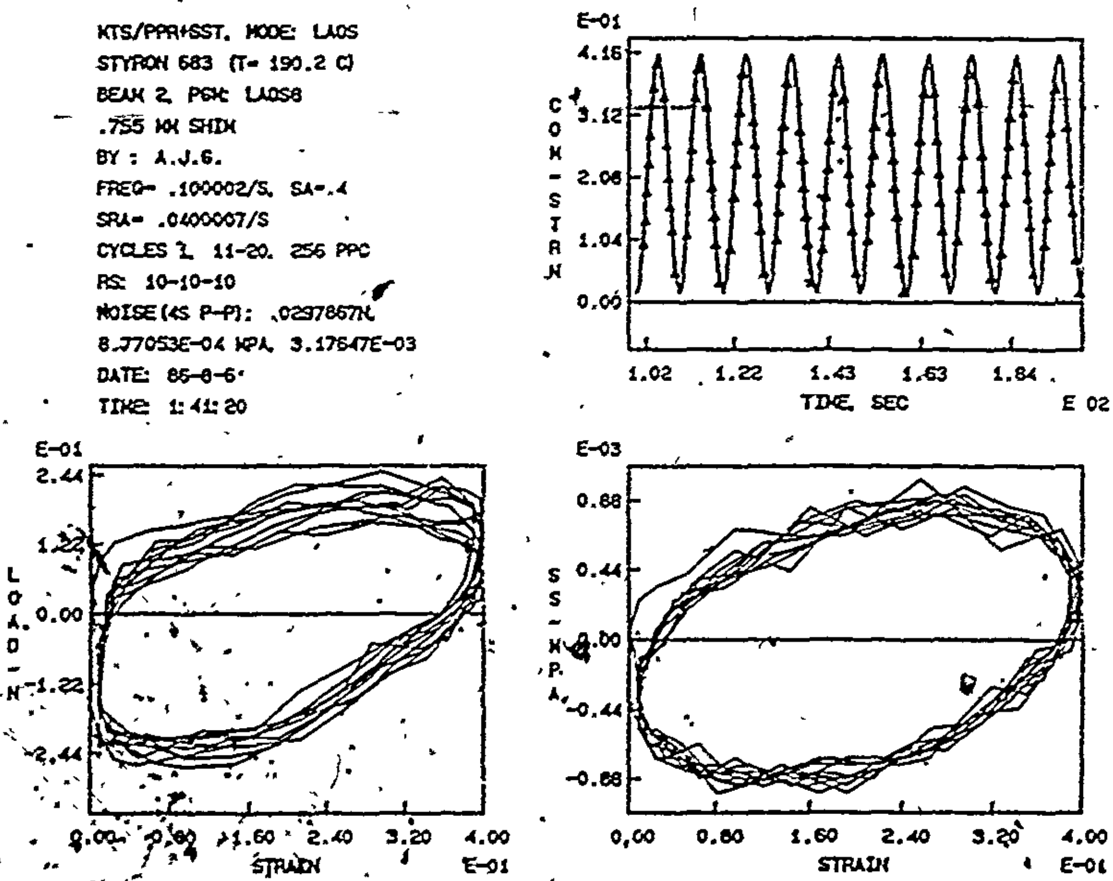

Figure 82: Small amplitude oscillatory shear test record. Low S/N observed for shear strain double amplitude of .4 at .1 Hz on molten polystyrene at T = 190°C.

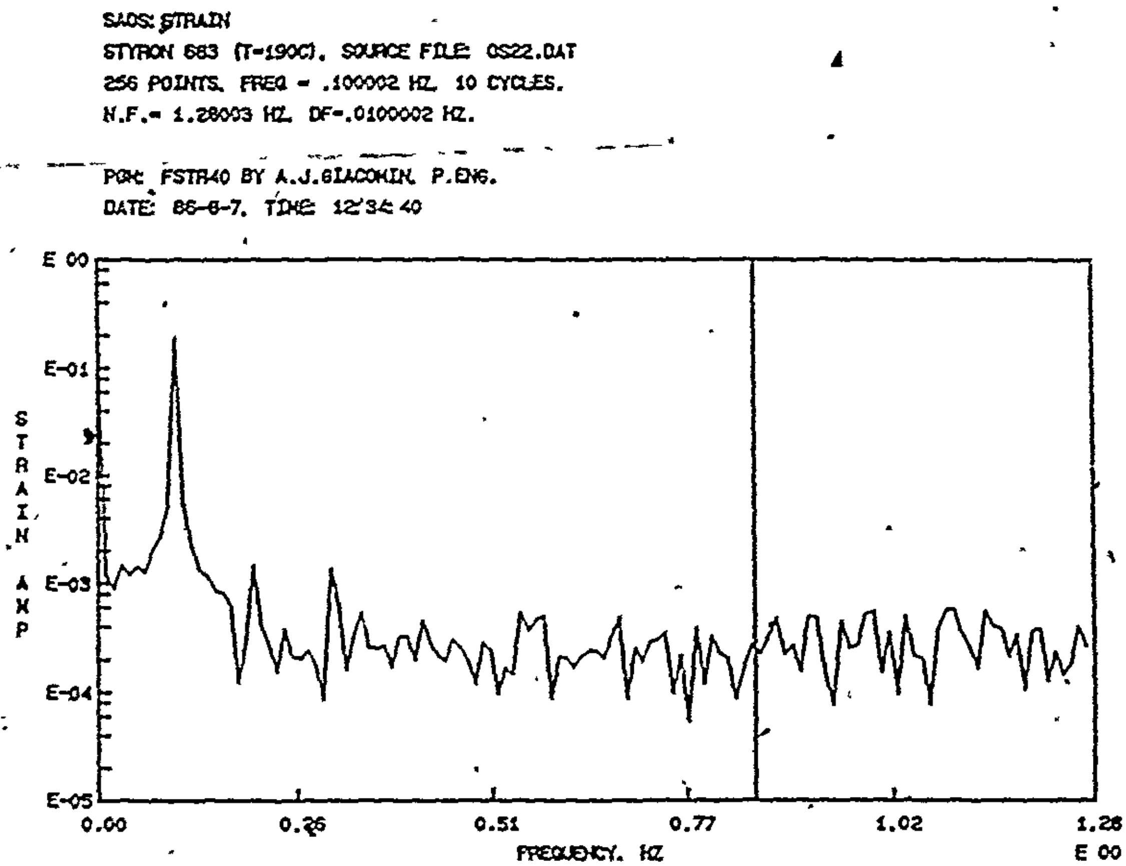

Figure 83: Spectral analysis of the actual shear strain for a small amplitude oscillatory shear test done on molten polystyrene at T = 190°C.

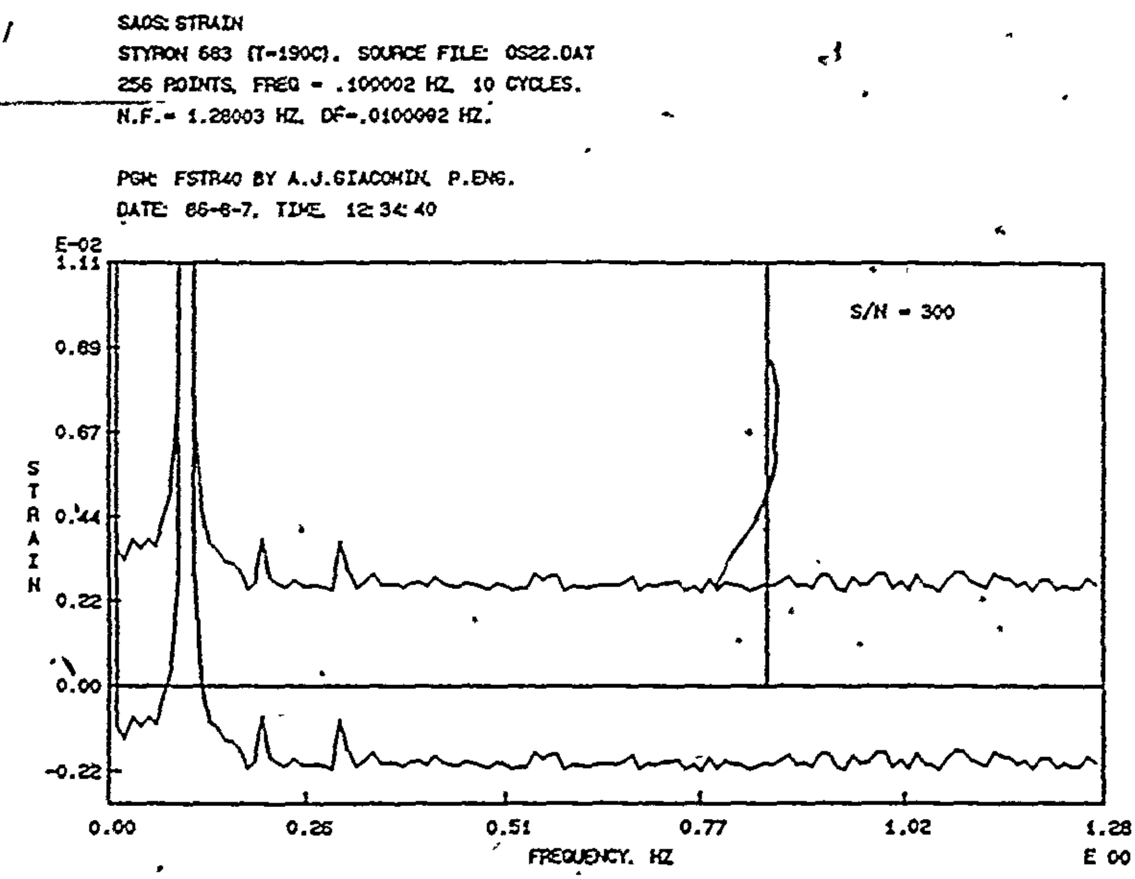

Figure 84. Upper and lower 95% confidence intervals for spectral analysis of the shear strain shown for a small amplitude oscillatory shear test done on molten polystyrene at T = 190°C. Computed with 256 point FFT and Nyquist frequency of 12.8 Hz.

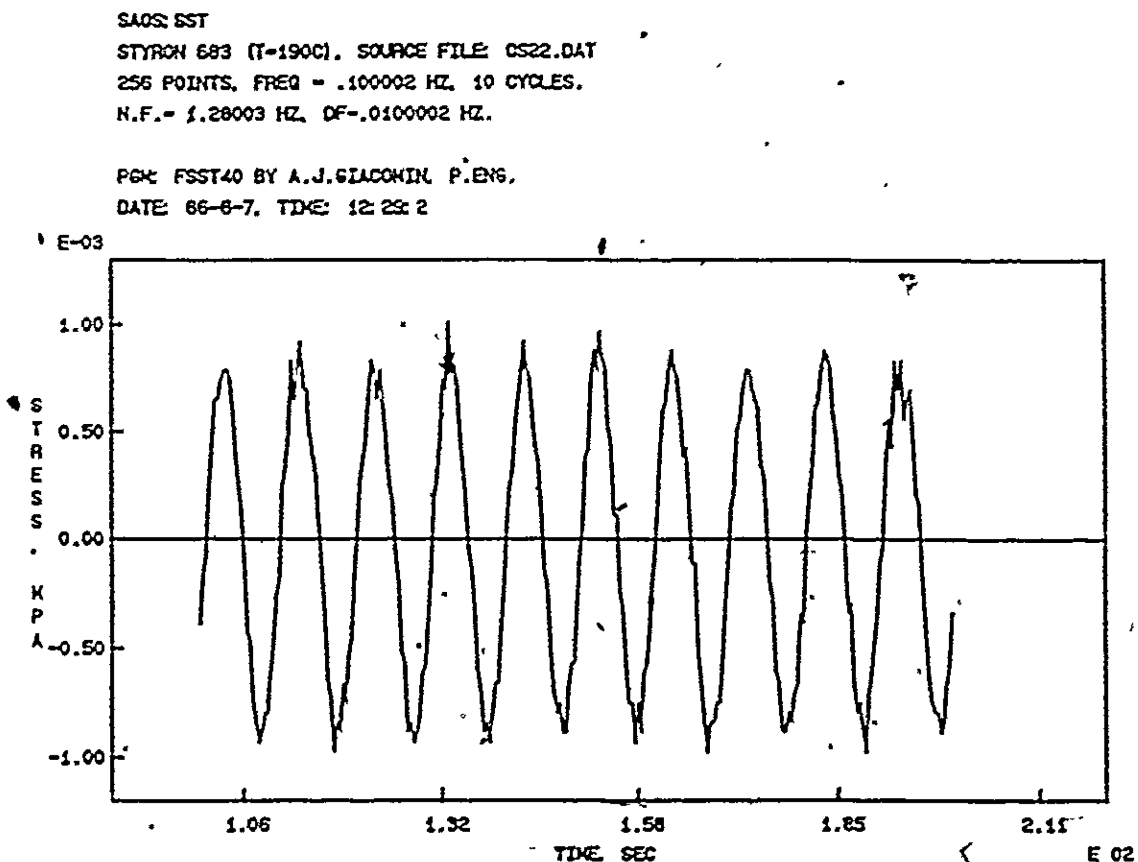

Figure 85: Time trace of the shear stress response to small amplitude, γ_o = .2, oscillatory shear test done at low frequency, f = .1 Hz, on molten polystyrene at T = 190°C. Cycle-to-cycle differences are due to background noise.

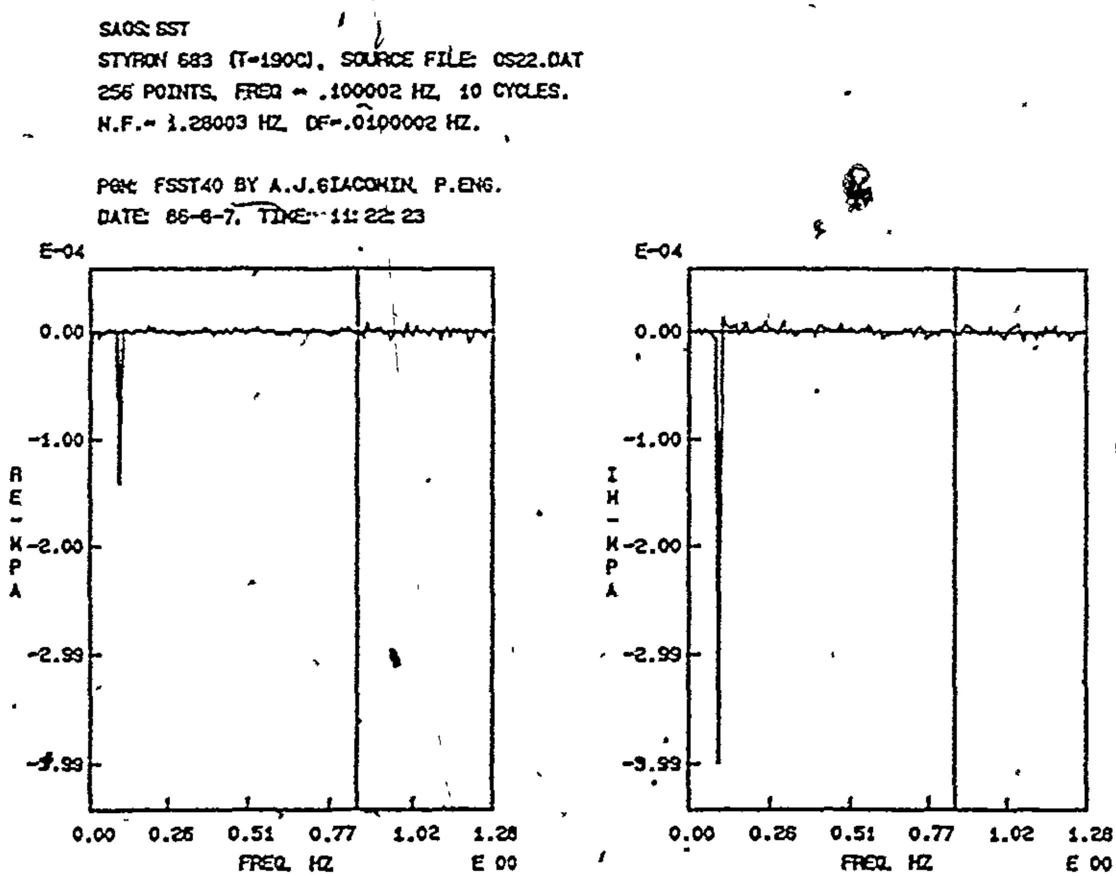

Figure 86 Spectral analysis in rectangular form of shear stress response in small amplitude, γ_0 = .2, oscillatory shear test done at low frequency, f = .1 Hz, on molten polystyrene at T = 190°C. The background noise observed on either side of the fundamental.

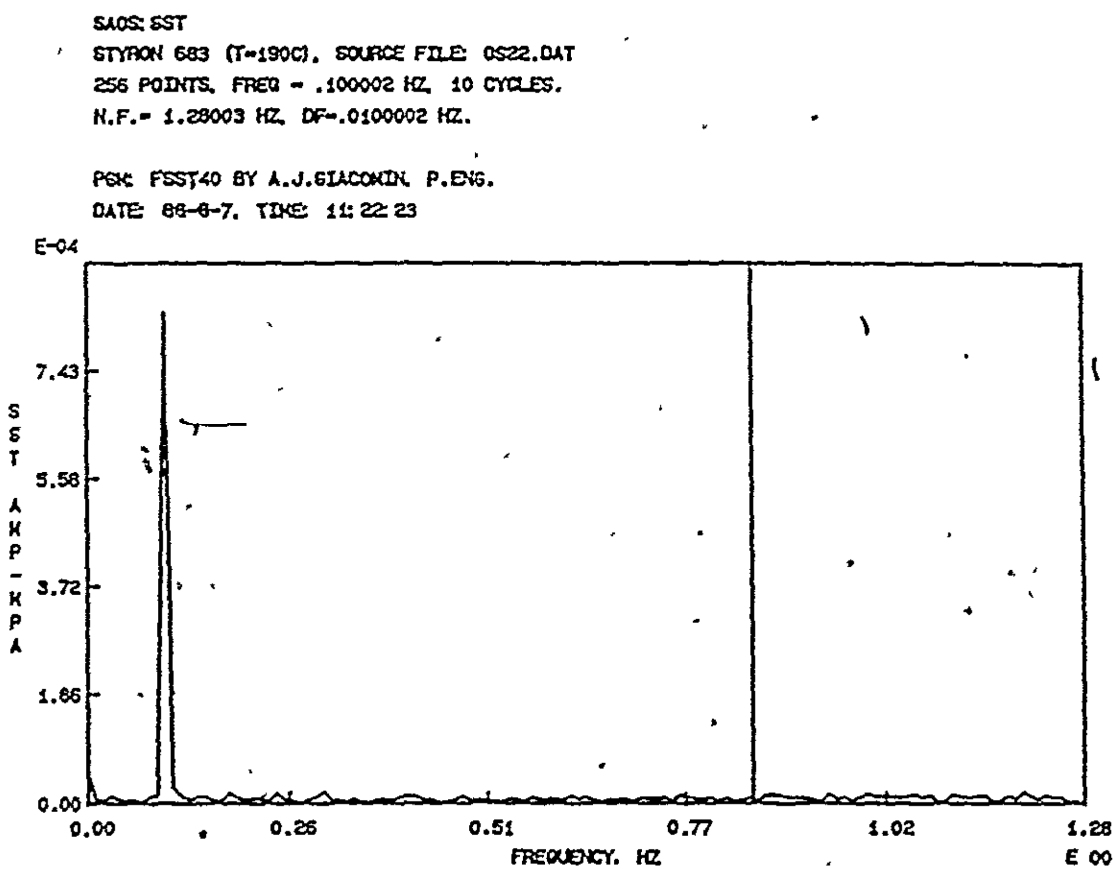

Figure 87. Amplitude spectrum of shear stress response in small amplitude, γ_o = .2, oscillatory shear test done at low frequency, f = .1 Hz, on molten polystyrene at T = 190°C. The background noise observed on either side of the fundamental.

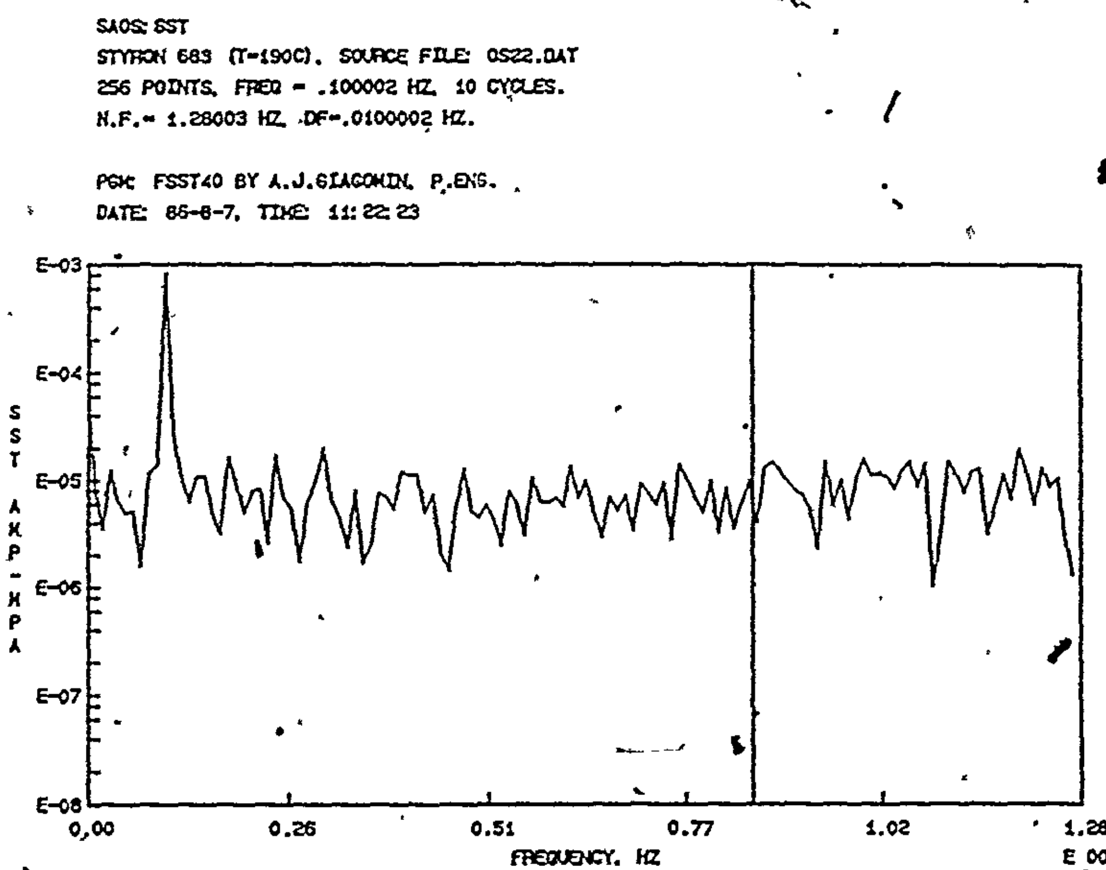

Figure 88: Log amplitude spectrum of shear stress response in small amplitude, $\gamma_0 = .2$, oscillatory shear test done at low frequency, $f = .1$ Hz, on molten polystyrene at $T = 190°C$. The spectrum of the background noise is flat.

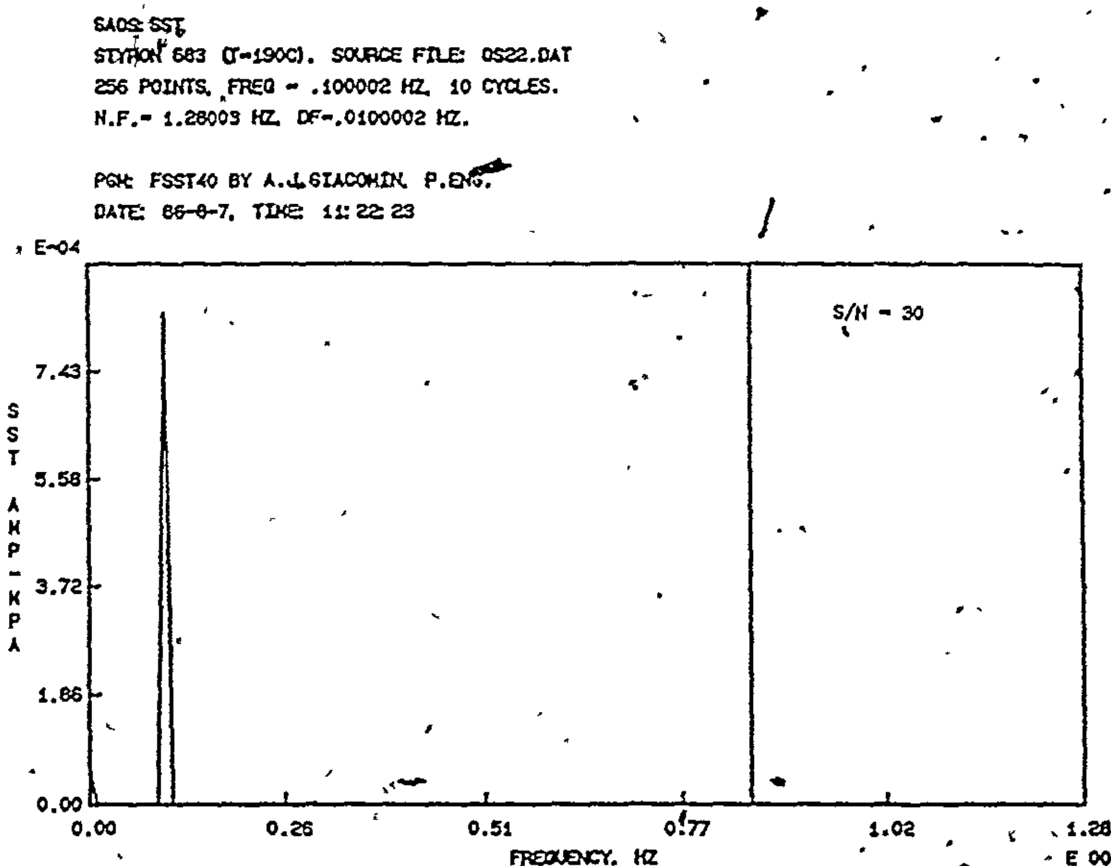

Figure 89: Noise-reduced amplitude spectrum of shear stress response in small amplitude, γ_0 = .2, oscillatory shear test done at low frequency, f = .1 Hz, on molten polystyrene at T = 190°C.

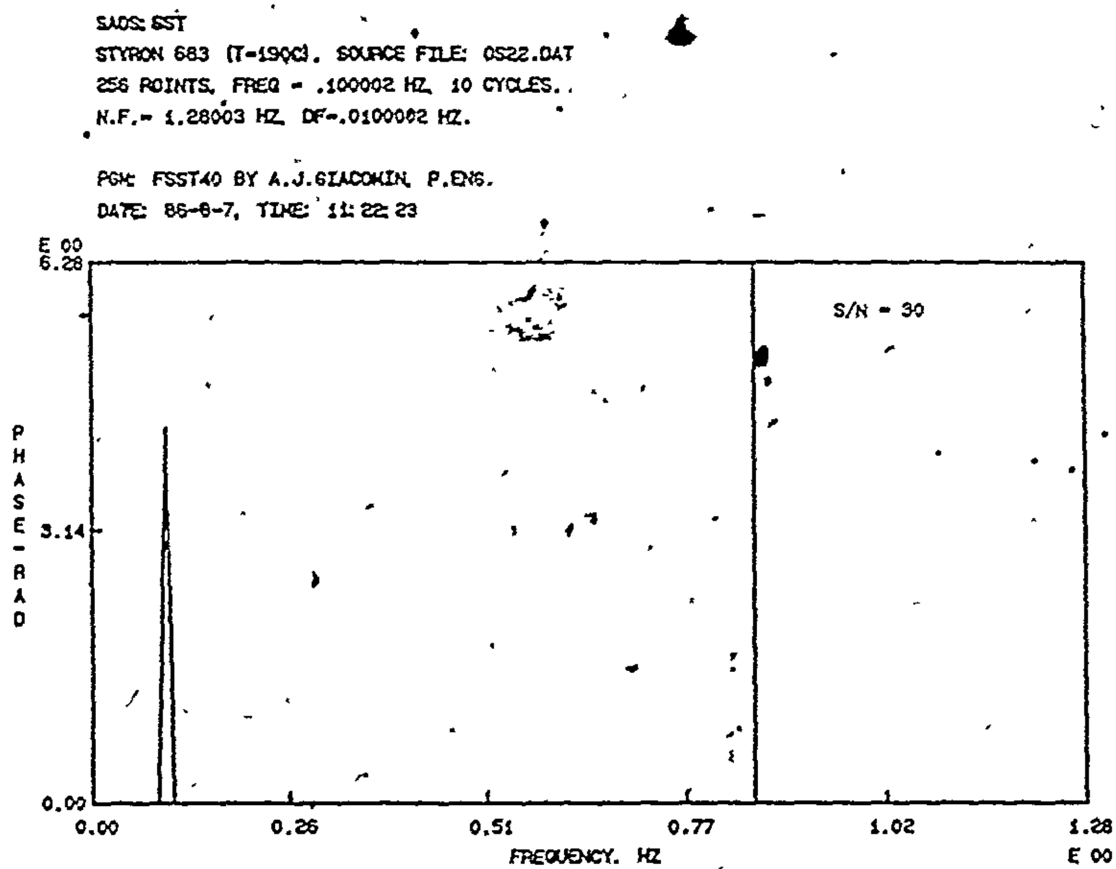

Figure 90. Uncorrected phase contents for noise-reduced amplitude spectrum of shear stress response in small amplitude, $\gamma_0 = .2$, oscillatory shear test done at low frequency, f = .1 Hz, on molten polystyrene at T = 190°C.

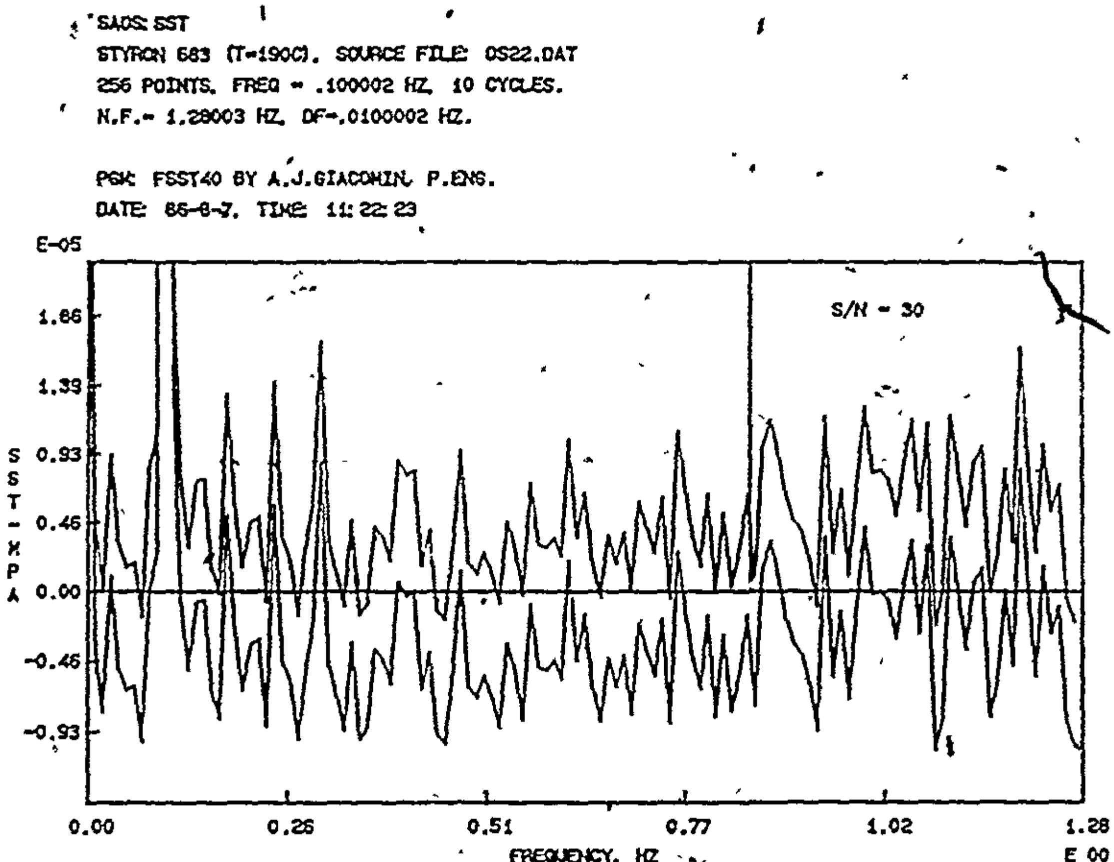

Figure 91: Upper and lower 95% confidence limits for the amplitude spectrum of shear stress response in small amplitude, γ_0 = .2, oscillatory shear test done at low frequency, f = .1 Hz, on molten polystyrene at T = 190°C Small higher harmonics can be resolved from the background noise observed on either side of the fundamental.

SAOS: FORCE
STYRON 683 (T=190C). SOURCE FILE: OS22.DAT
256 POINTS. FREQ = .100002 HZ. 10 CYCLES.
N.F.= 1.28003 HZ. DF=.0100002 HZ.

PGM: FTF40 BY A.J.GIACOMIN, P.ENG.
DATE: 86-8-7. TIME: 12:58:49

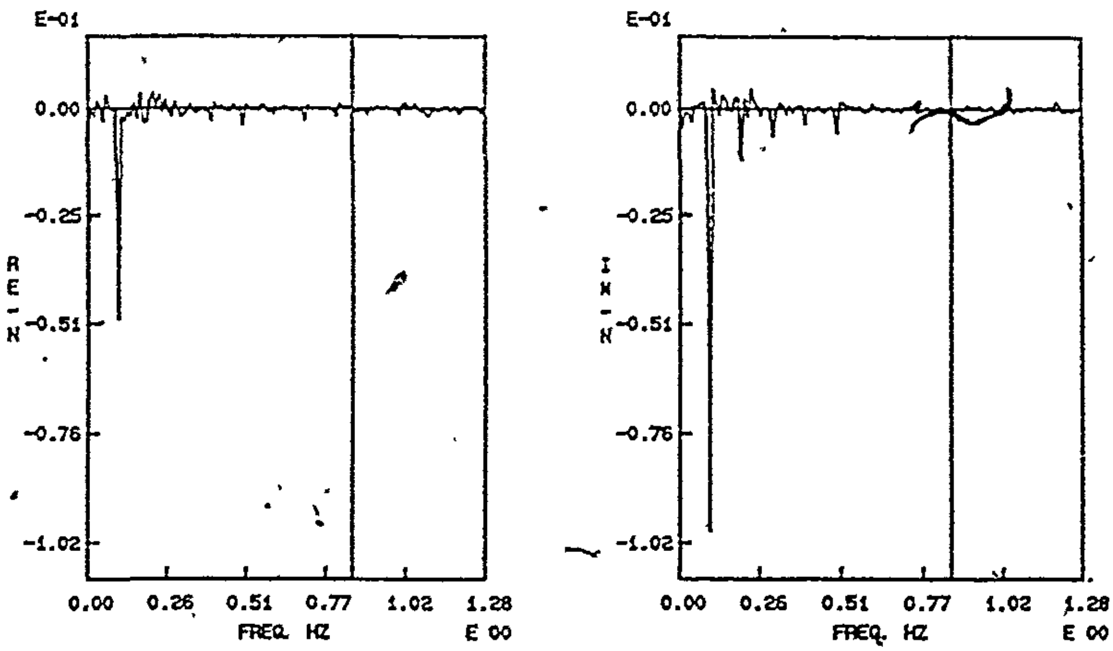

Figure 92: Spectral analysis in rectangular form of total force response to small amplitude, γ_0 = .2, oscillatory shear test done at low frequency, f = .1 Hz, on molten polystyrene at T = 190°C.

SAOS: FORCE
STYRON 683 (T=190C). SOURCE FILE: OS22.DAT
256 POINTS. FREQ = .100002 HZ. 10 CYCLES.
N.F.= 1.28003 HZ. DF=.0100002 HZ.

PGM: FTF40 BY A.J.GIACOMIN, P.ENG.
DATE: 86-6-7. TIME: 12:58:49

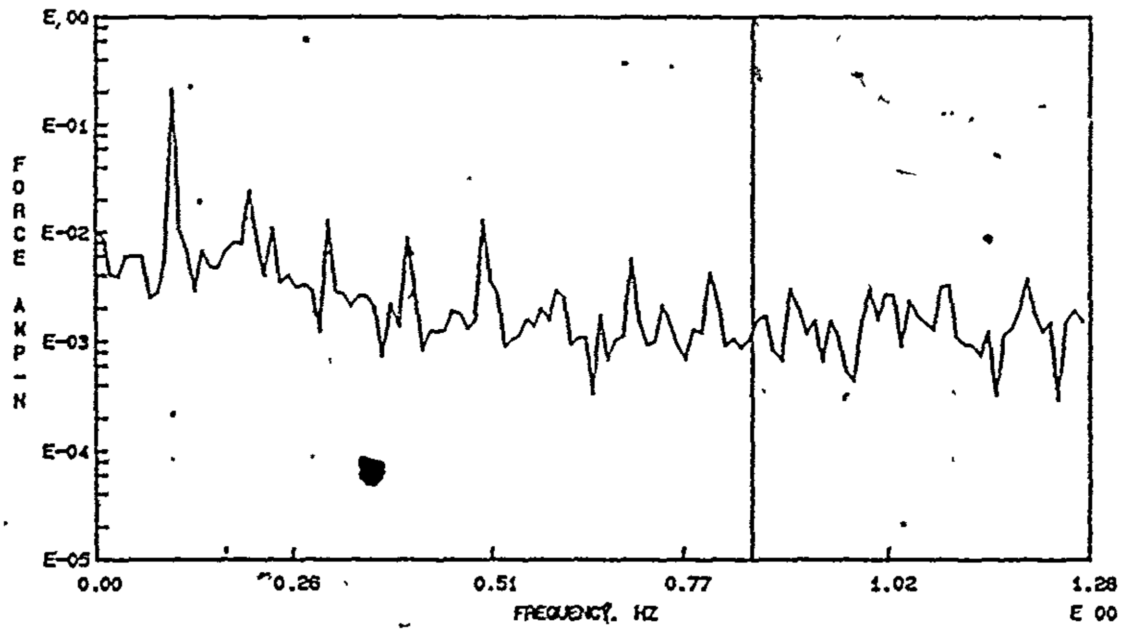

Figure 93: Log amplitude spectrum of total force response in small amplitude, $\gamma_0 = .2$, oscillatory shear test done at low frequency, f = .1 Hz, on molten polystyrene at T = 190°C. The spectrum of the background noise is flat.

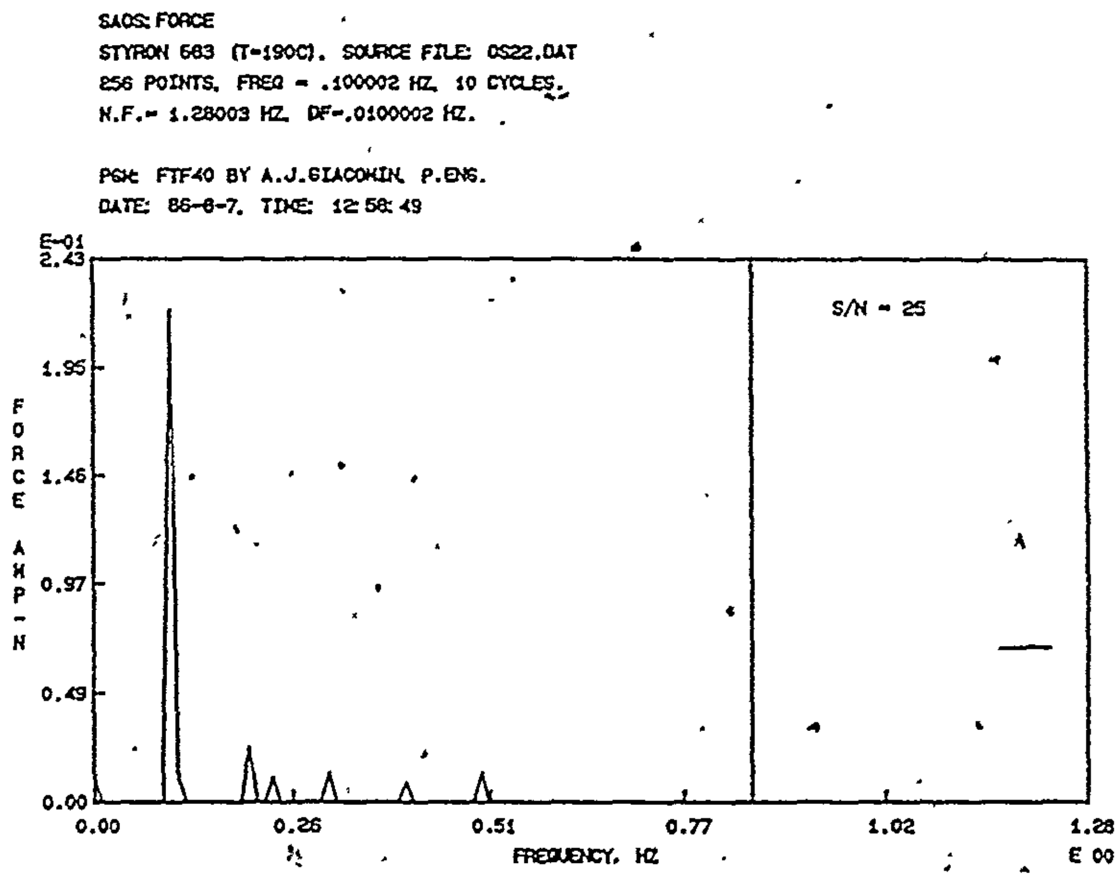

Figure 94: Noise-reduced amplitude spectrum of total force response in small amplitude, γ_0 = .2, oscillatory shear test done at low frequency, f = .1 Hz, on molten polystyrene at T = 190°C.

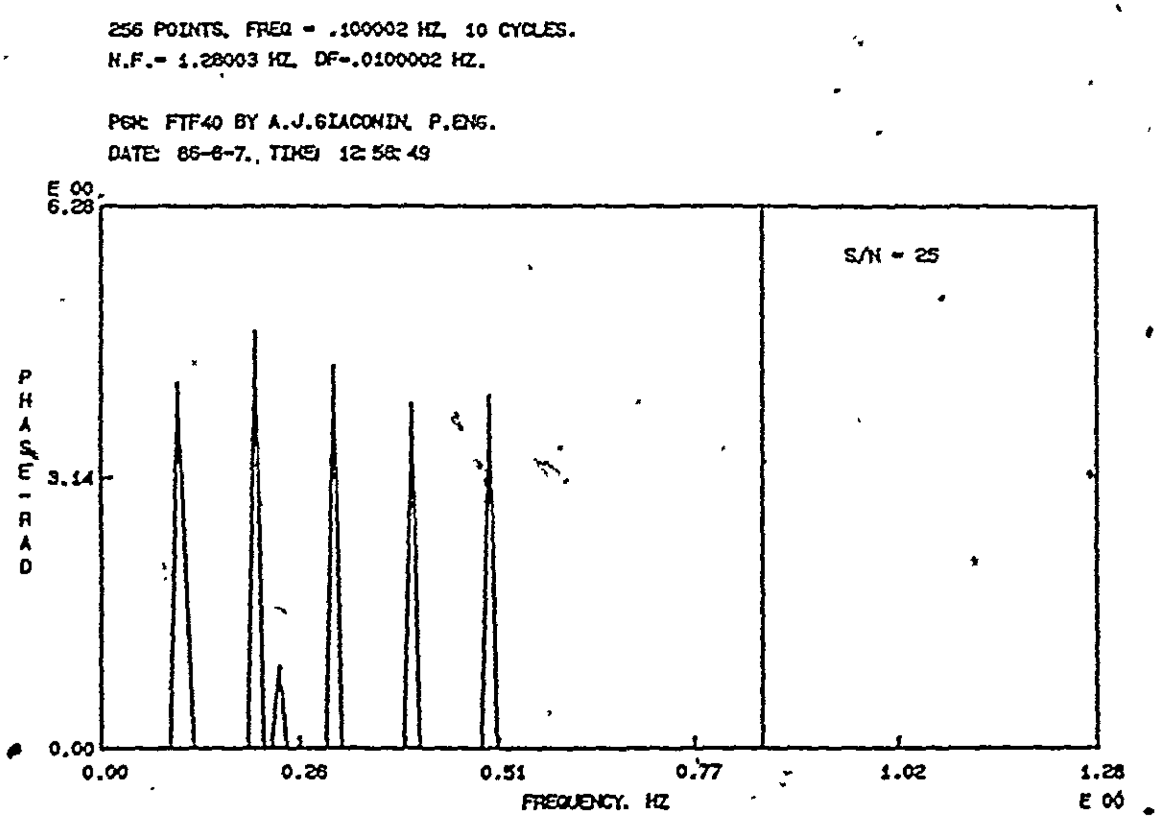

Figure 95: Uncorrected phase contents for noise-reduced amplitude spectrum of total force response in small amplitude, $\gamma_0 = .2$, oscillatory shear test done at low frequency, f = .1 Hz, on molten polystyrene at T = 190°C.

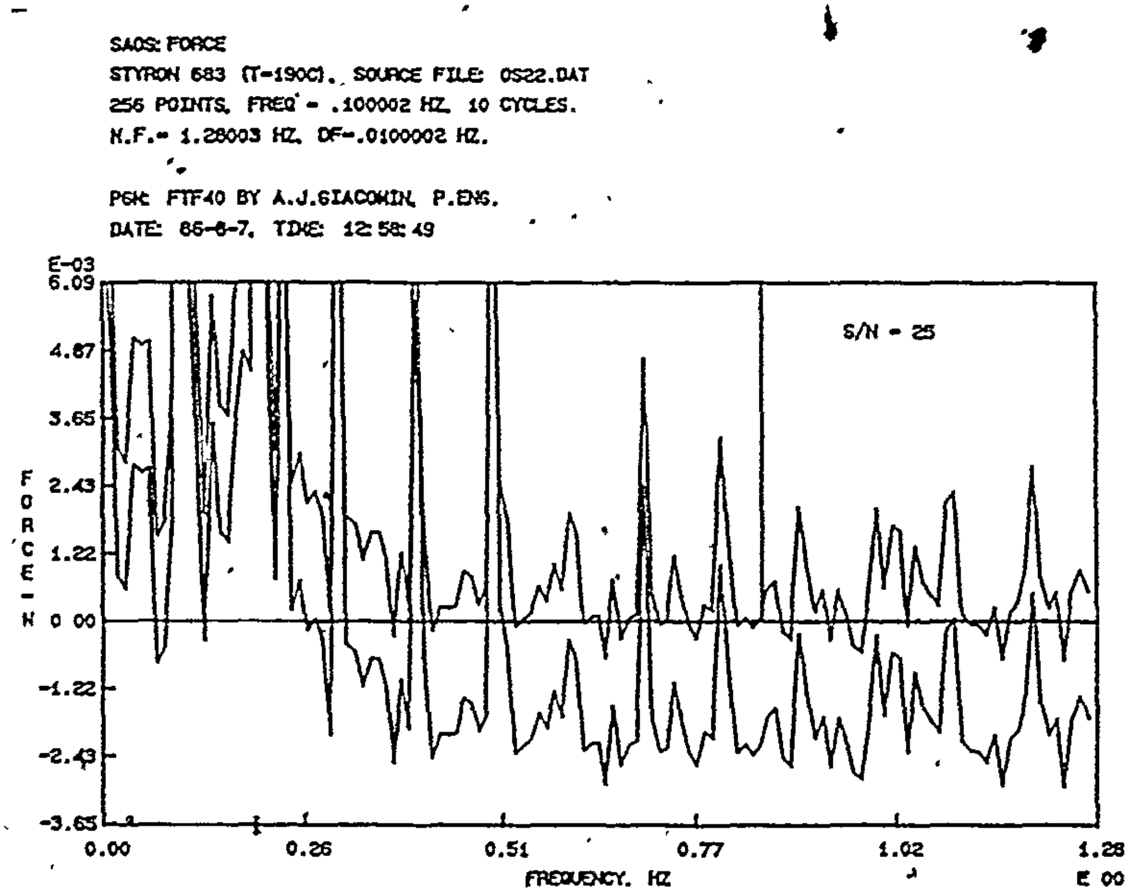

Figure 96: Upper and lower 95% confidence limits for the amplitude spectrum of shear stress response in small amplitude, $\gamma_0 = .2$, oscillatory shear test done at low frequency, $f = .1$ Hz, on molten polystyrene at $T = 190^0C$. Several well resolved higher harmonics are observed.

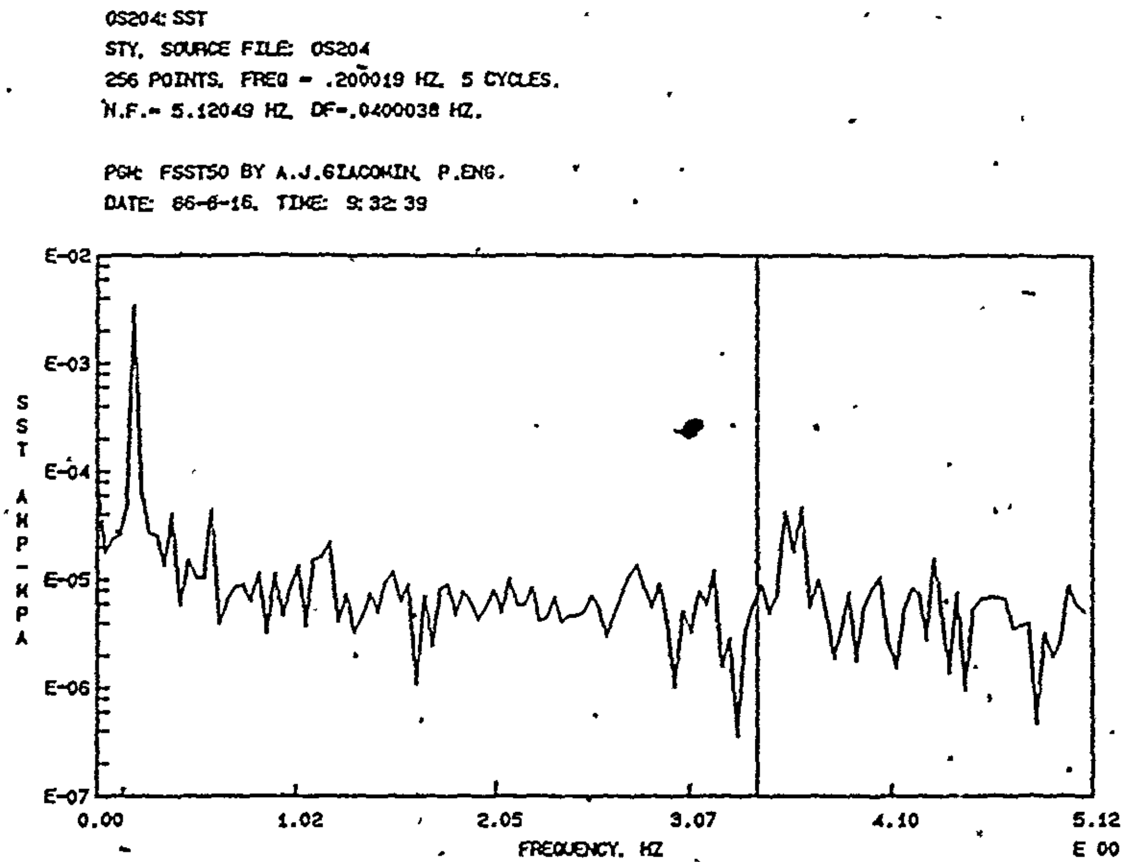

Figure 97: Spectral analysis of shear stress response to oscillatory shear computed with a 256-point FFT with Nyquist frequency 5.12 Hz using a rectangularly windowed time series.

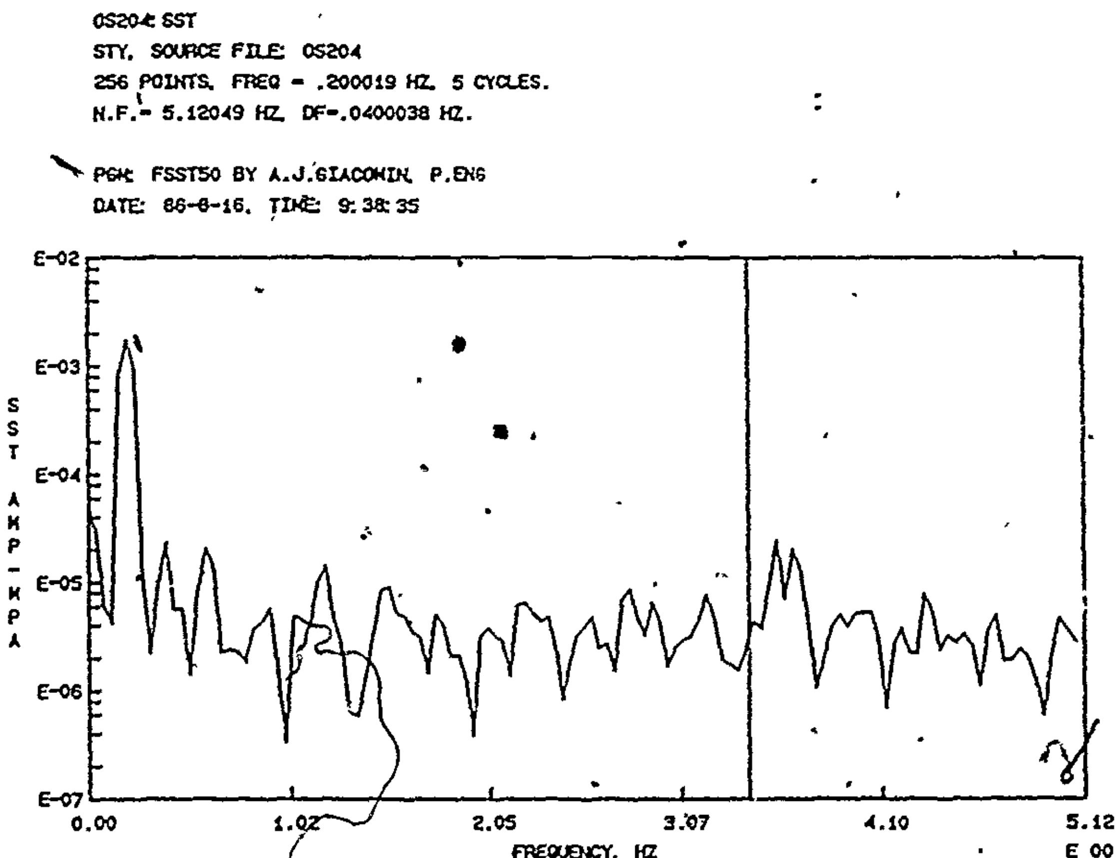

Figure 98. Spectral analysis of shear stress response to oscillatory shear computed with a 256-point FFT with Nyquist frequency 5.12 Hz using a Hanning windowed time series. Compare with Figure 97 to see the line-broadening and uniform peak attenuation effects of this digital filter.

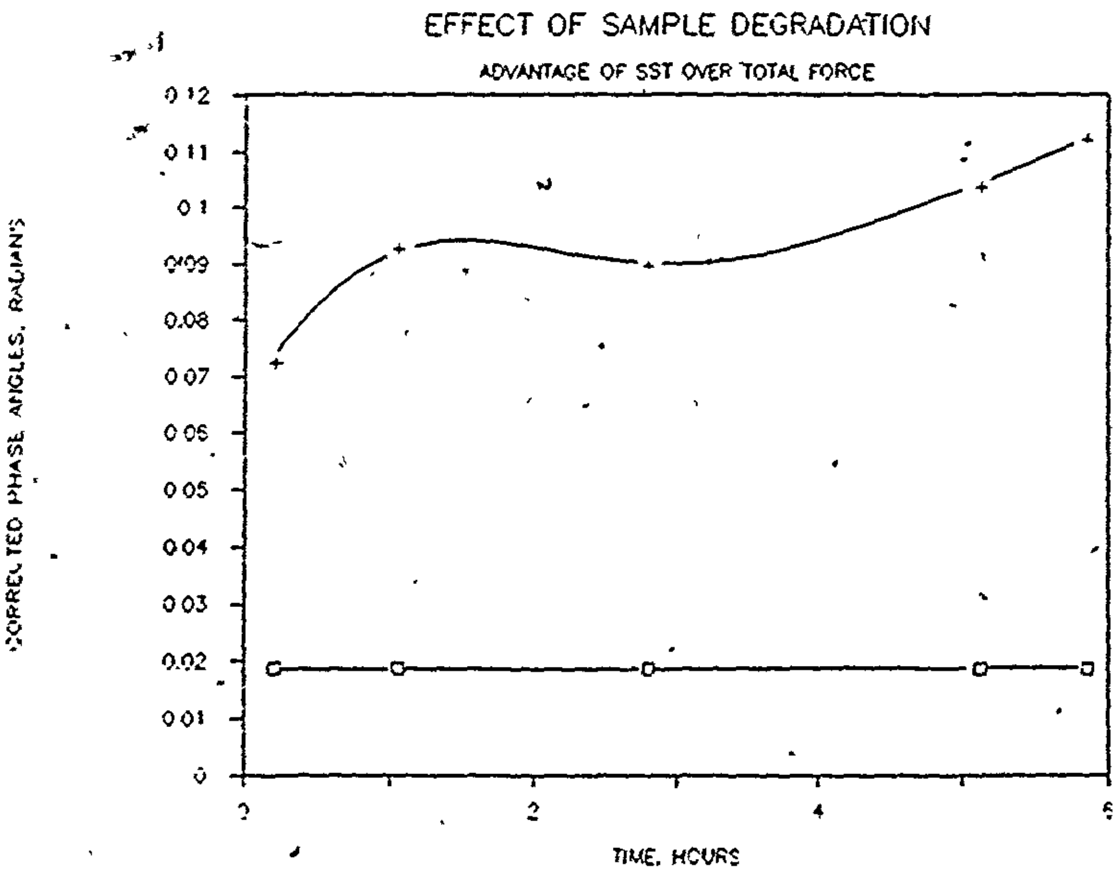

Figure 99: Comparison of the effects of sample age on corrected phase angles for shear stress (squares) and for total force (crosses) in small amplitude, $\gamma_o = .2$, oscillatory shear test done at low frequency, f = .1 Hz, on molten polystyrene at T = 190°C.

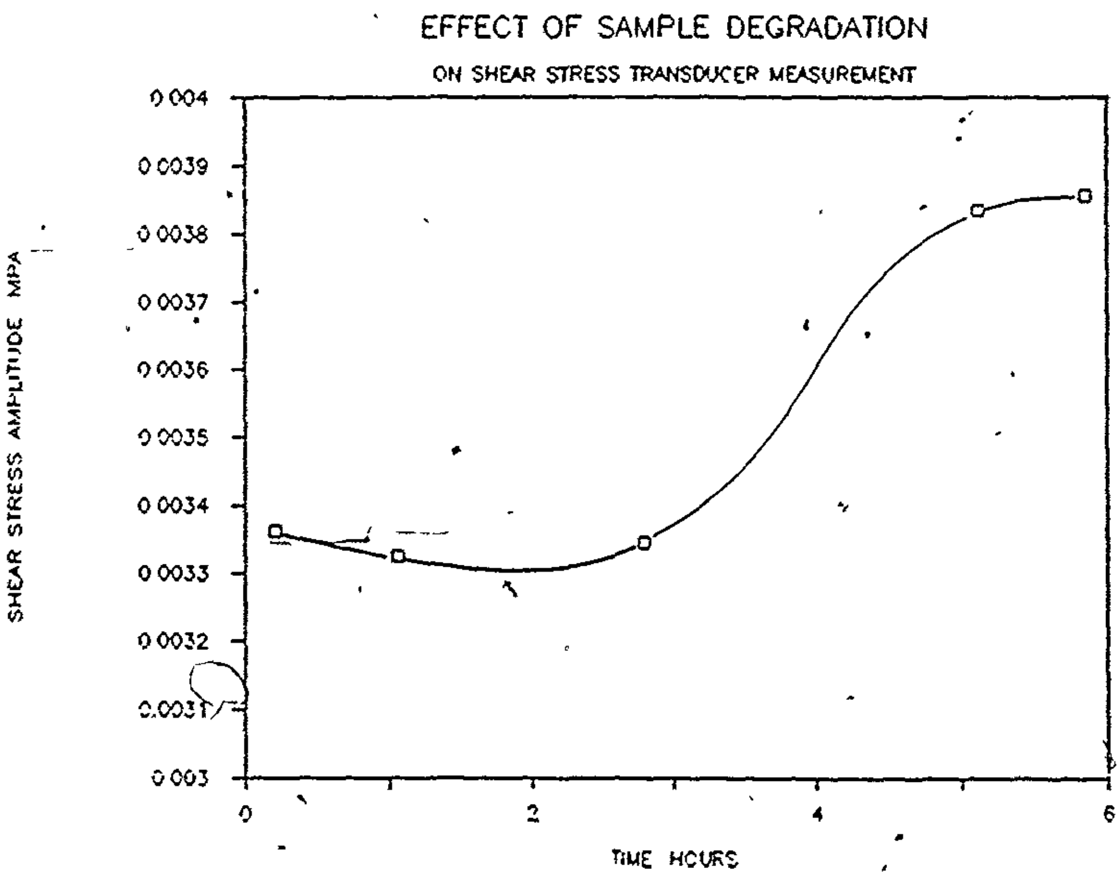

Figure 100: Effect of sample age on shear stress amplitude in small amplitude, γ_0 = .2, oscillatory shear test done at low frequency, f = .1 Hz, on molten polystyrene at T = 190°C.

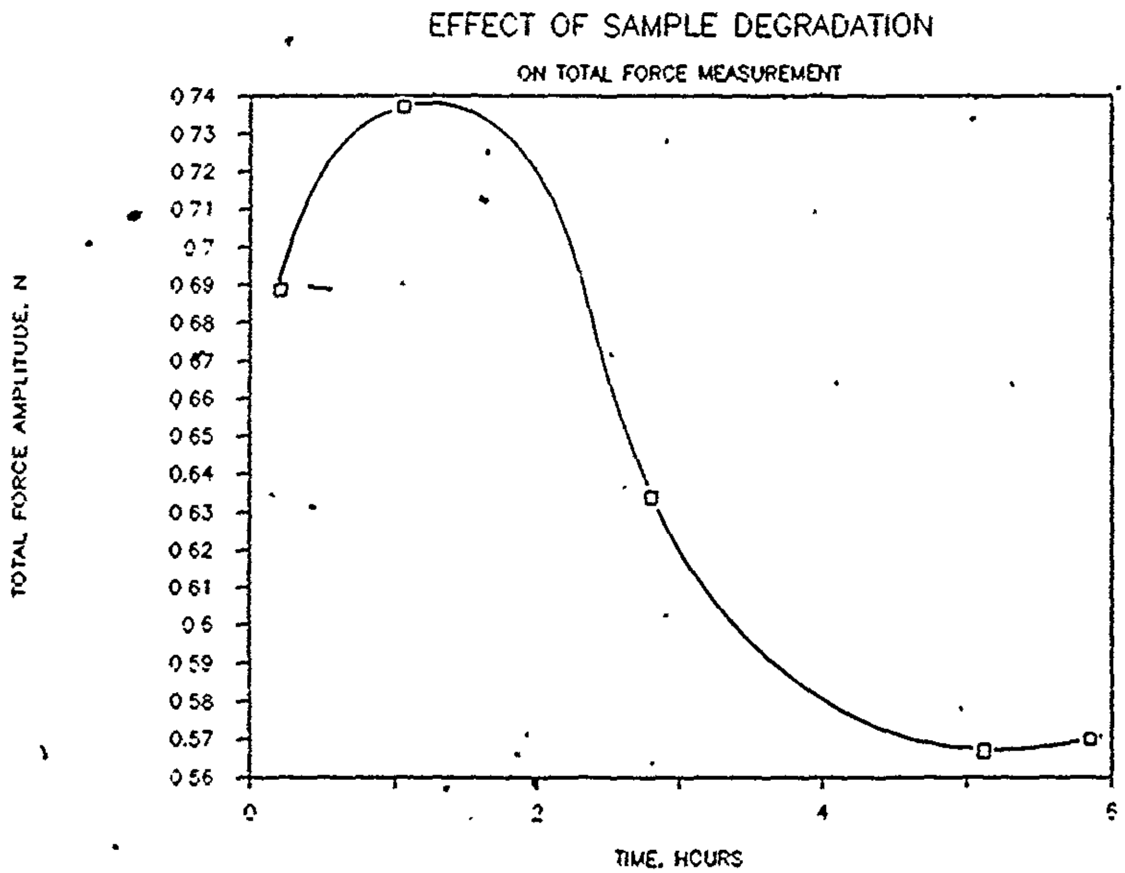

Figure 101: Effect of sample age on total force amplitude in small amplitude, γ_o = .2, oscillatory shear test done at low frequency, f = .1 Hz, on molten polystyrene at T = 190°C.

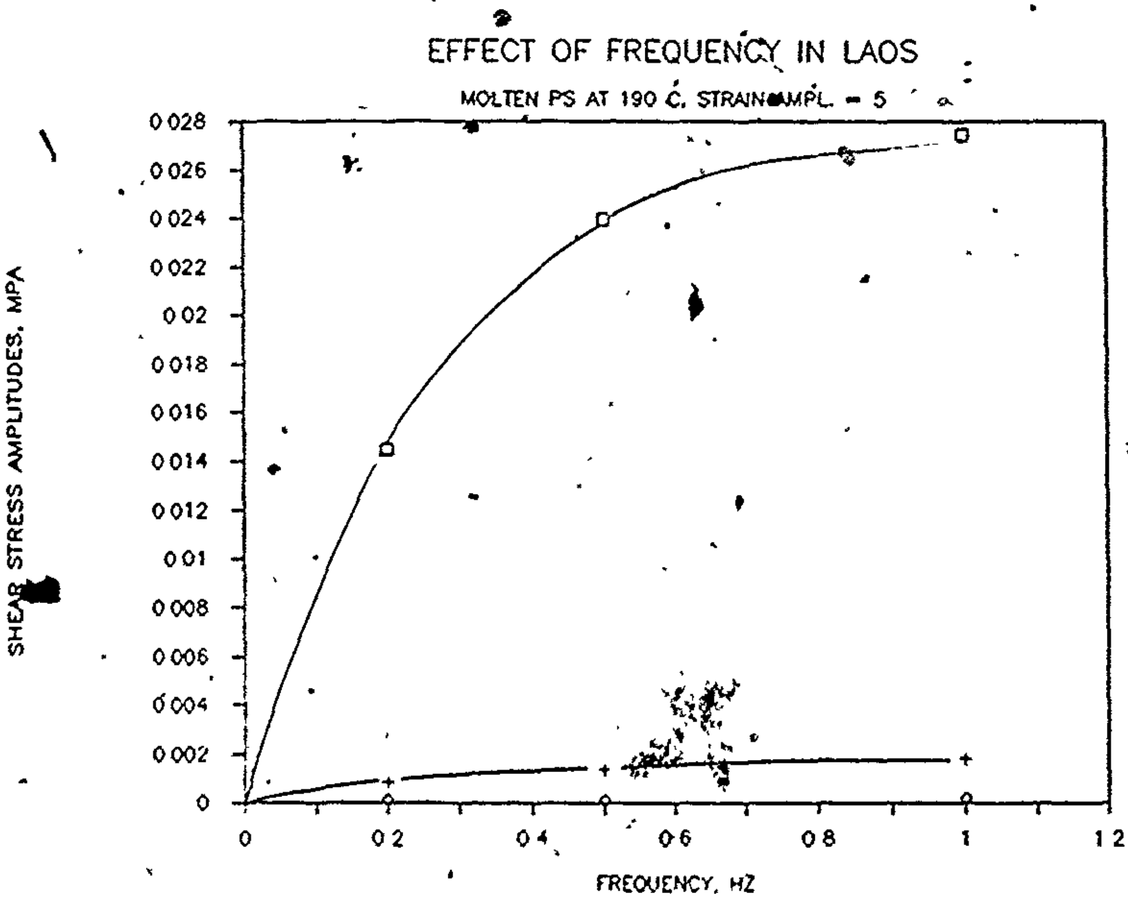

Figure 102. Effect of frequency on the principal harmonics of shear stress in large amplitude oscillatory shear, $\gamma_0 = 5$. Here the frequency dependence of the fundamental (squares) is made clear. Third (crosses) and fifth (diamonds) harmonics also displayed.

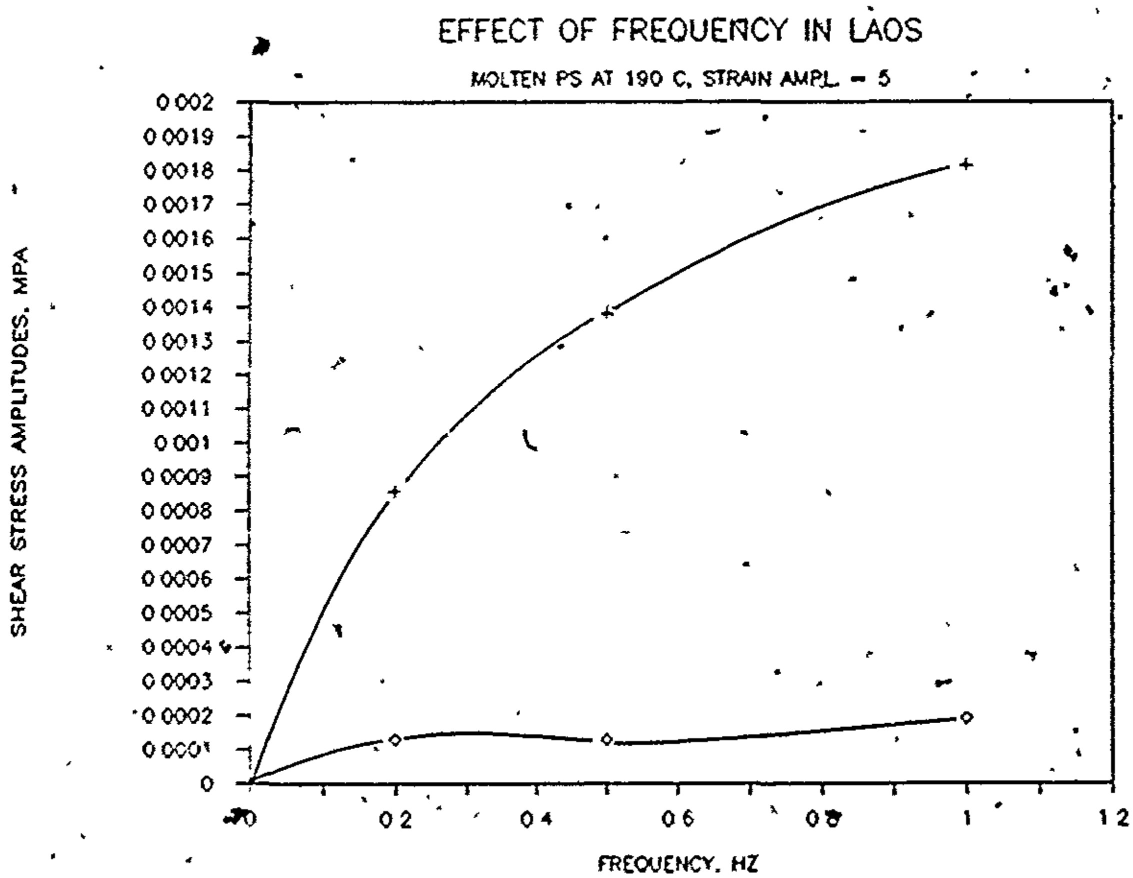

Figure 103: Effect of frequency on the principal harmonics of shear stress in large amplitude oscillatory shear, $\gamma_0 = 5$. Here the frequency dependence of the third harmonic (crosses) is made clear. Fifth harmonic (diamonds) is also displayed.

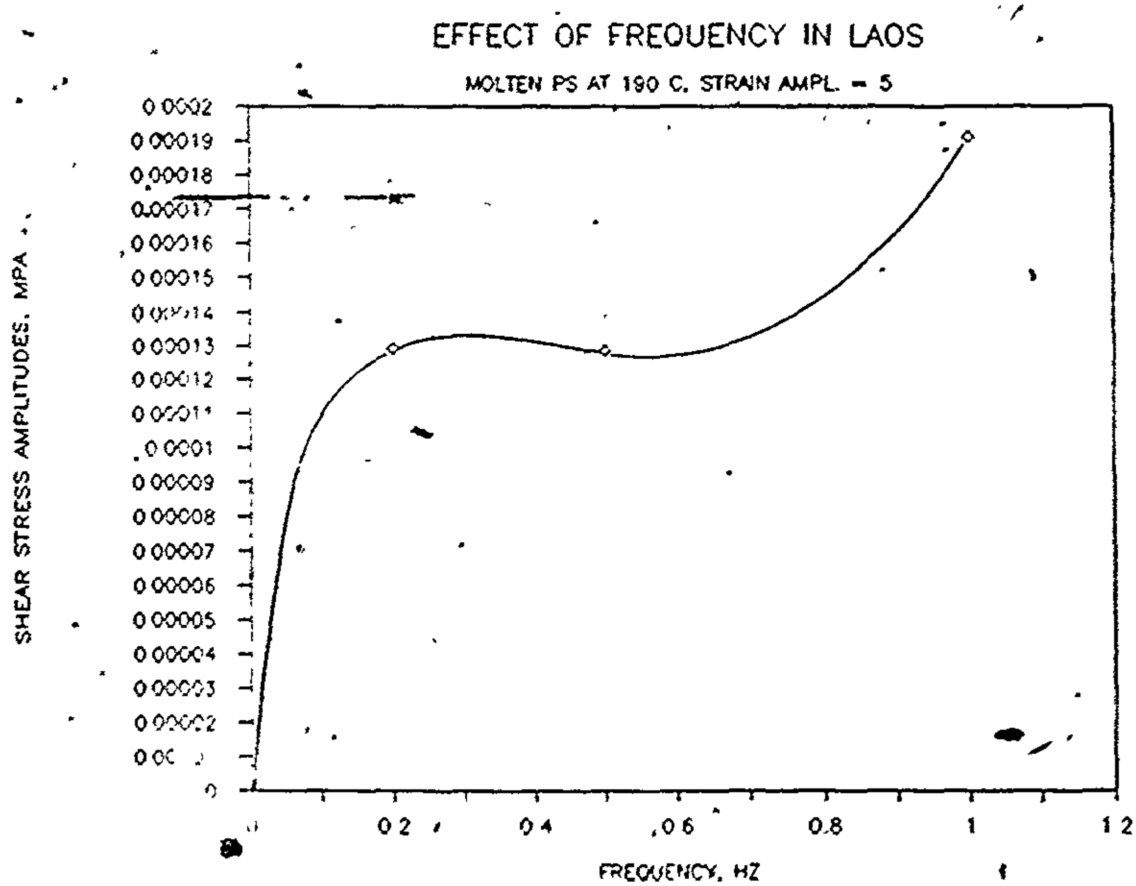

Figure 104. Effect of frequency on the principal harmonics of shear stress in large amplitude oscillatory shear, $\gamma_0 = 5$. Here the frequency dependence of the fifth harmonic (diamonds) is made clear.

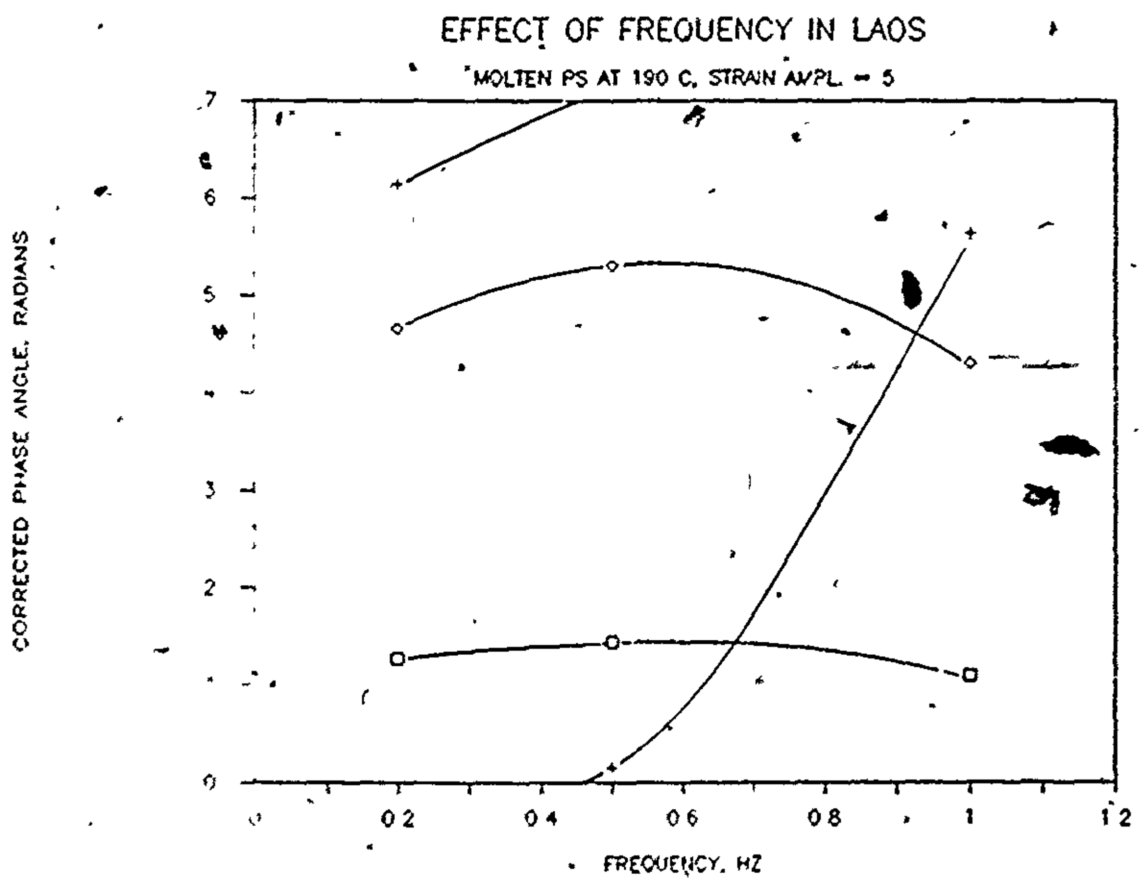

Figure 105: Effect of frequency on the error corrected phase angles of the fundamental (squares), third harmonics (crosses) and fifth harmonics (diamonds) of shear stress in large amplitude oscillatory shear, $\gamma_o = 5$.

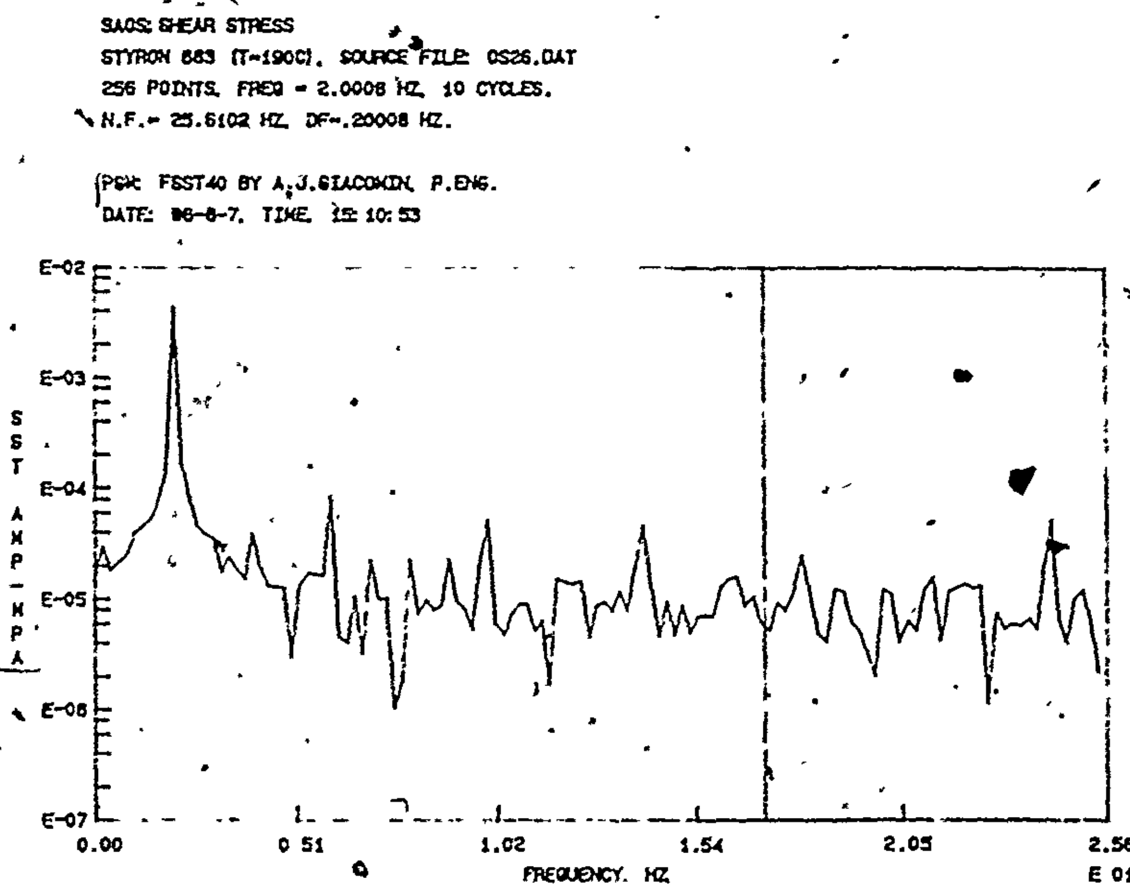

Figure 106. Amplitude spectrum rich with higher harmonics for shear stress response to small amplitude oscillatory shear for the molten polystyrene at 190°C and at 2 Hz with $\gamma_o = 0.2$.

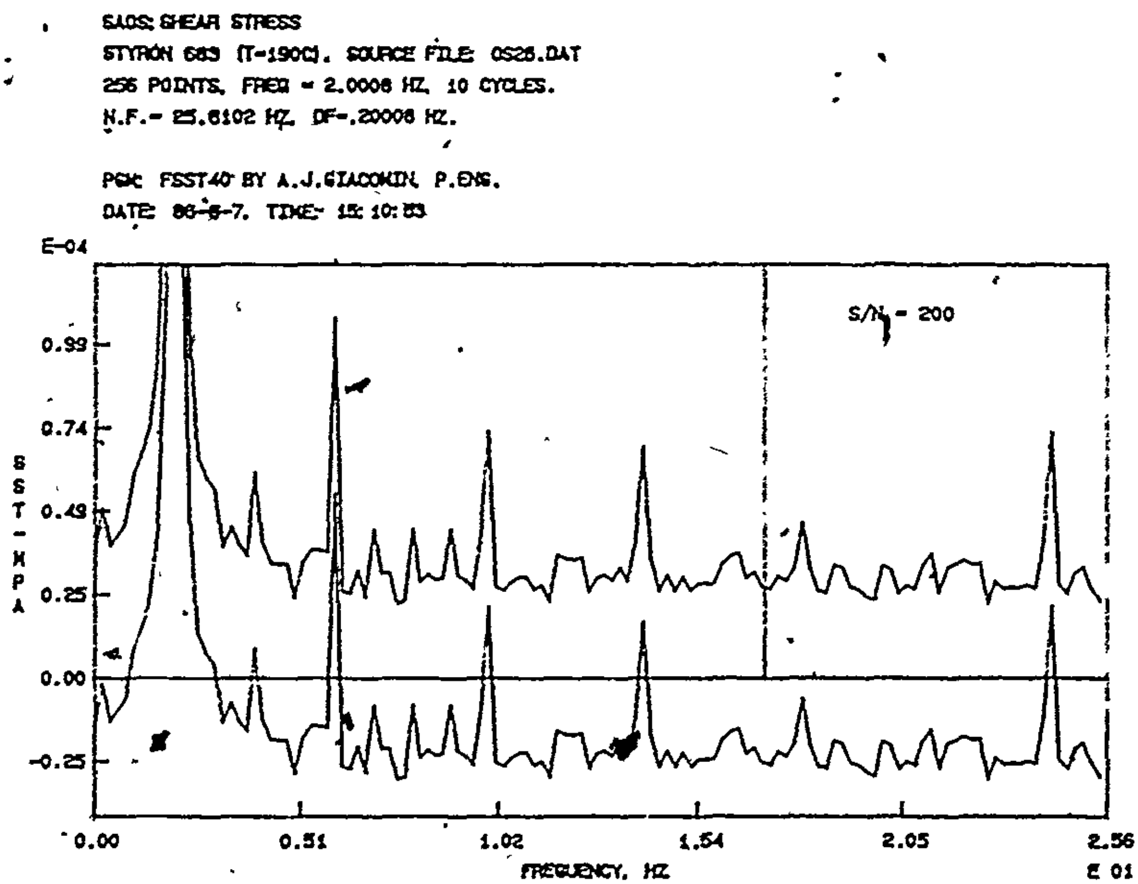

Figure 107: Statistical analysis of amplitude spectrum for the shear stress response to small amplitude oscillatory shear test done with molten polystyrene at 190°C.

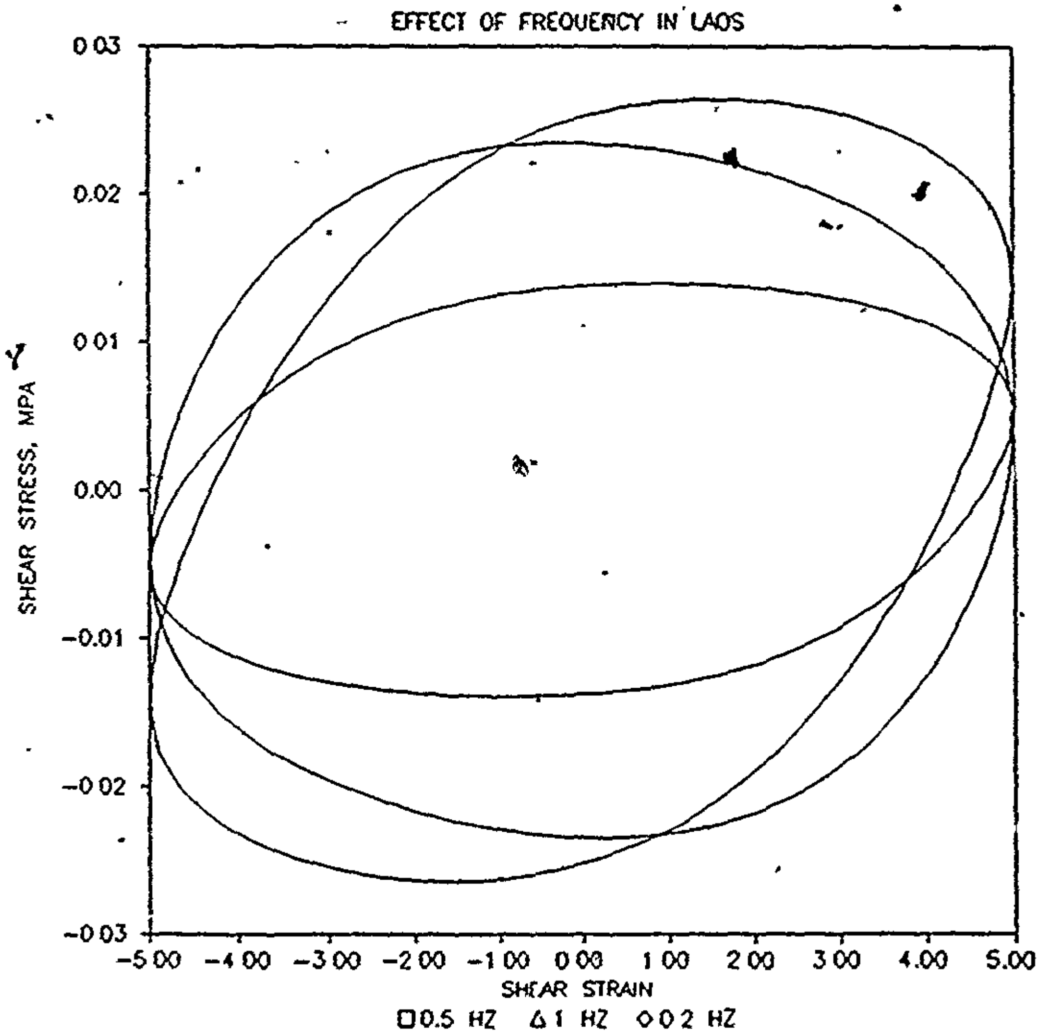

Figure 108. Shear stress versus shear strain loops for molten polystyrene in oscillatory shear at 190°C. Frequencies (from loop with lowest to highest stress amplitude) .2, .5 and 1 Hz.

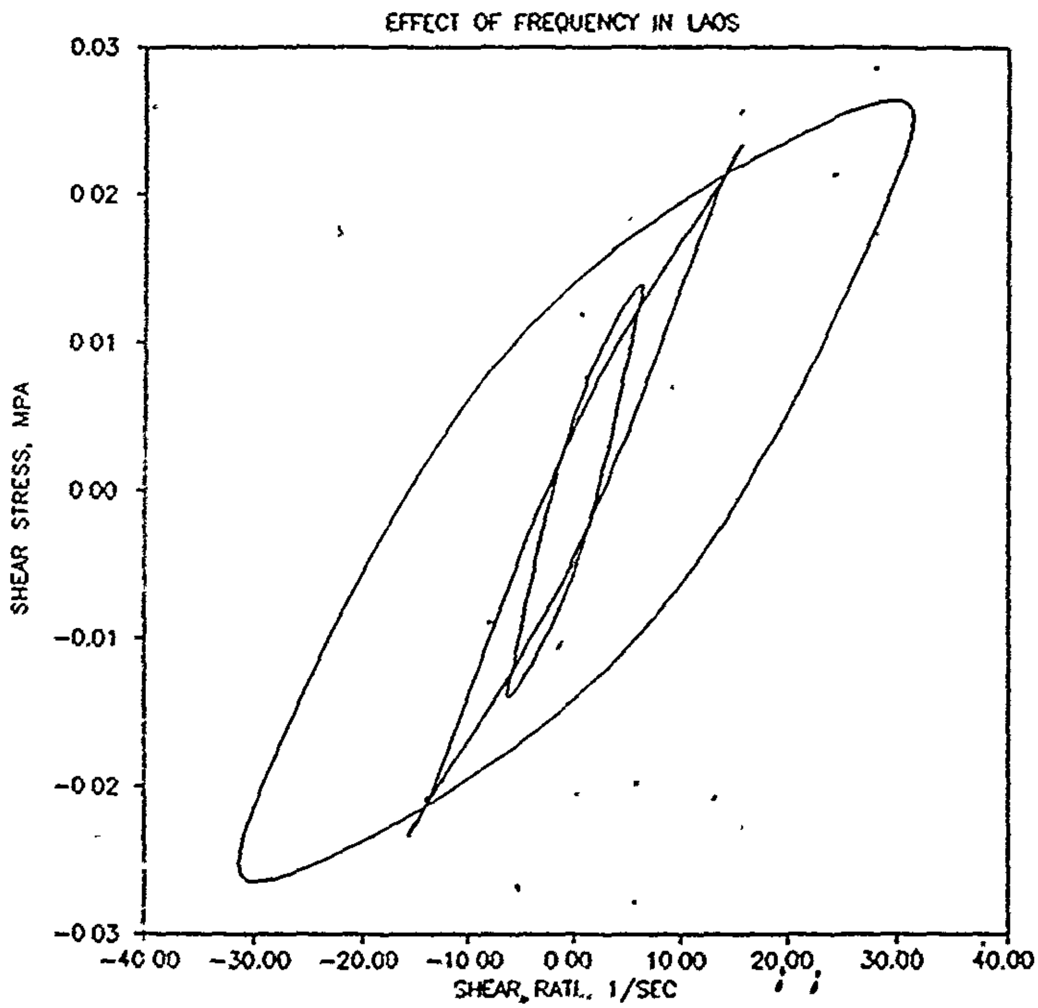

Figure 109: Shear stress versus shear strain rate loops for molten polystyrene in oscillatory shear at 190°C. Frequencies (from loop with lowest to highest stress amplitude) .2, .5 and 1 Hz. Constant strain amplitude, $\gamma_0 = 5$.

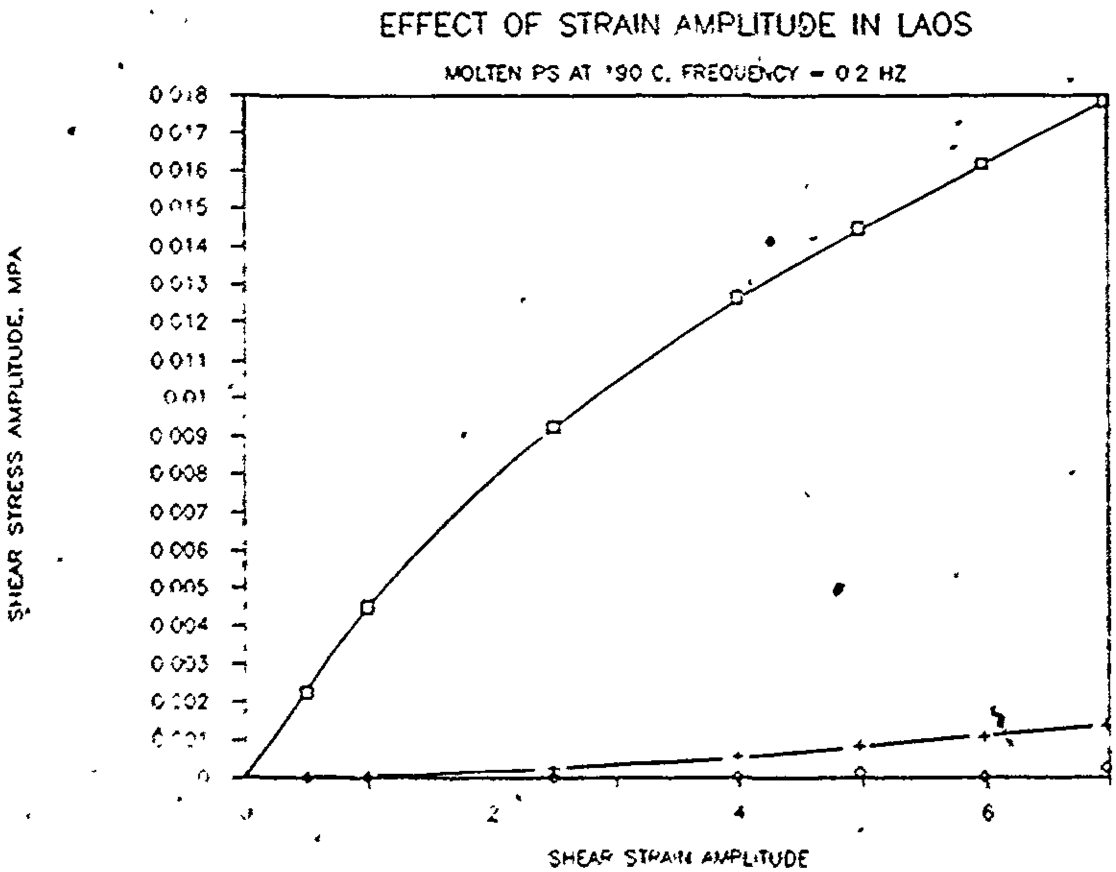

Figure 110: Effect of strain amplitude on the fundamental (squares), third harmonics (crosses) and fifth harmonics (diamonds) of shear stress in large amplitude oscillatory shear, f = .2 Hz. Here the strain amplitude dependence of the fundamental is made clear.

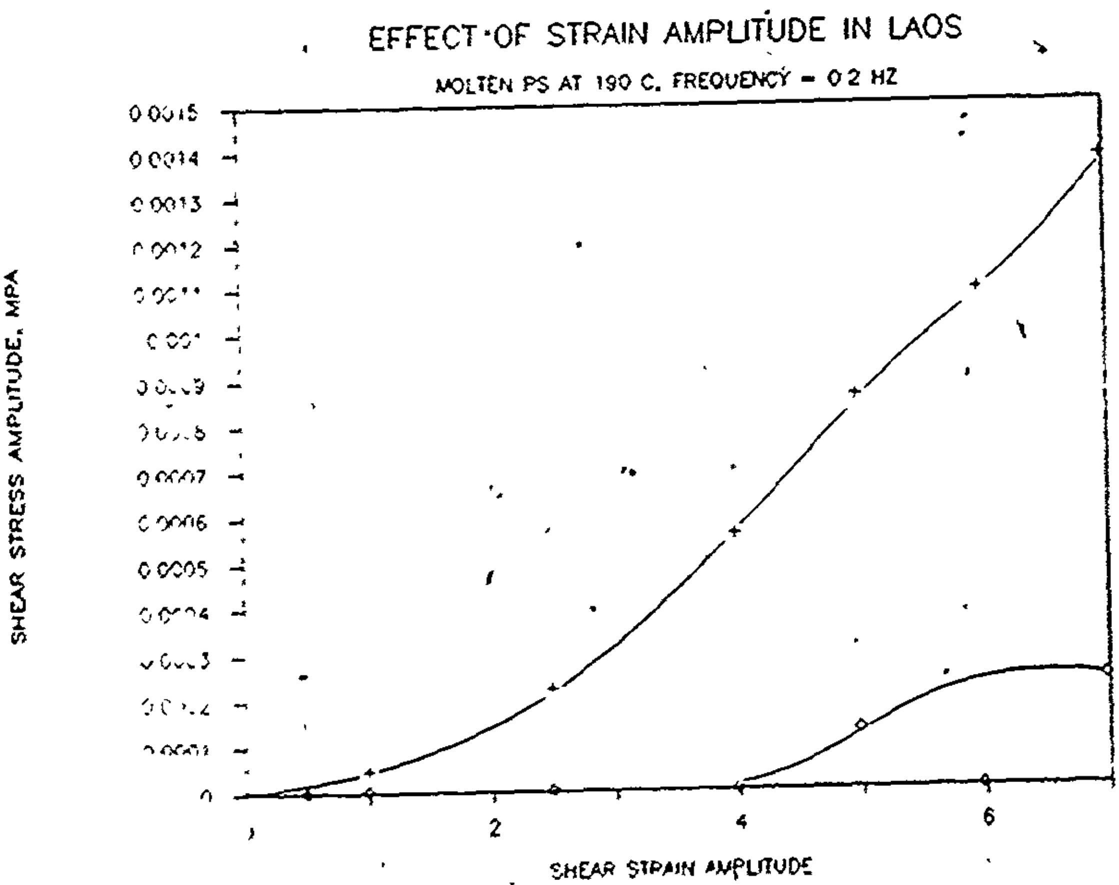

Figure 111: Effect of strain amplitude on the fundamental (squares), third harmonics (crosses) and fifth harmonics (diamonds) of shear stress in large amplitude oscillatory shear, f = .2 Hz. Here the strain amplitude dependence of the third and fifth harmonics is made clear.

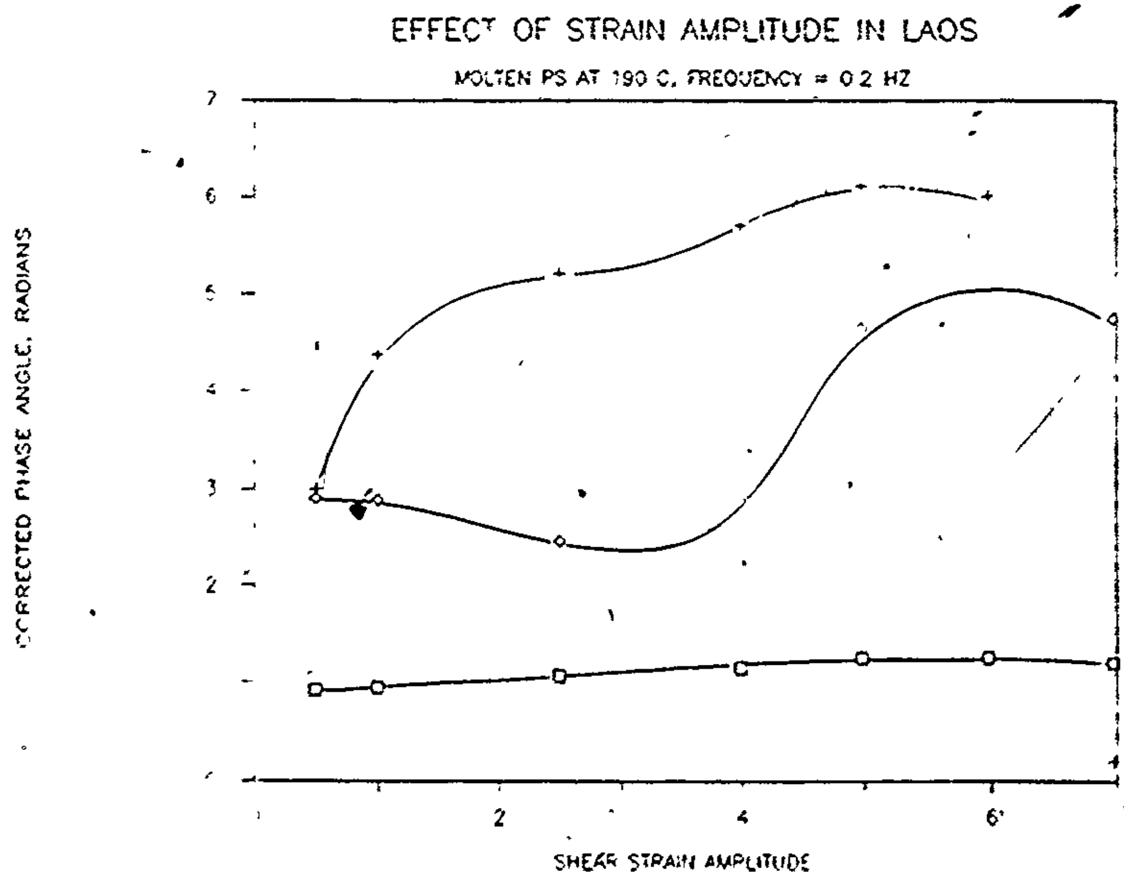

Figure 112: Effect of strain amplitude on the error corrected phase angles of the principal harmonics of shear stress in large amplitude oscillatory shear, f = 0.2 Hz. Fundamental (squares), 3rd harmonic (crosses) and 5th harmonic (diamonds).

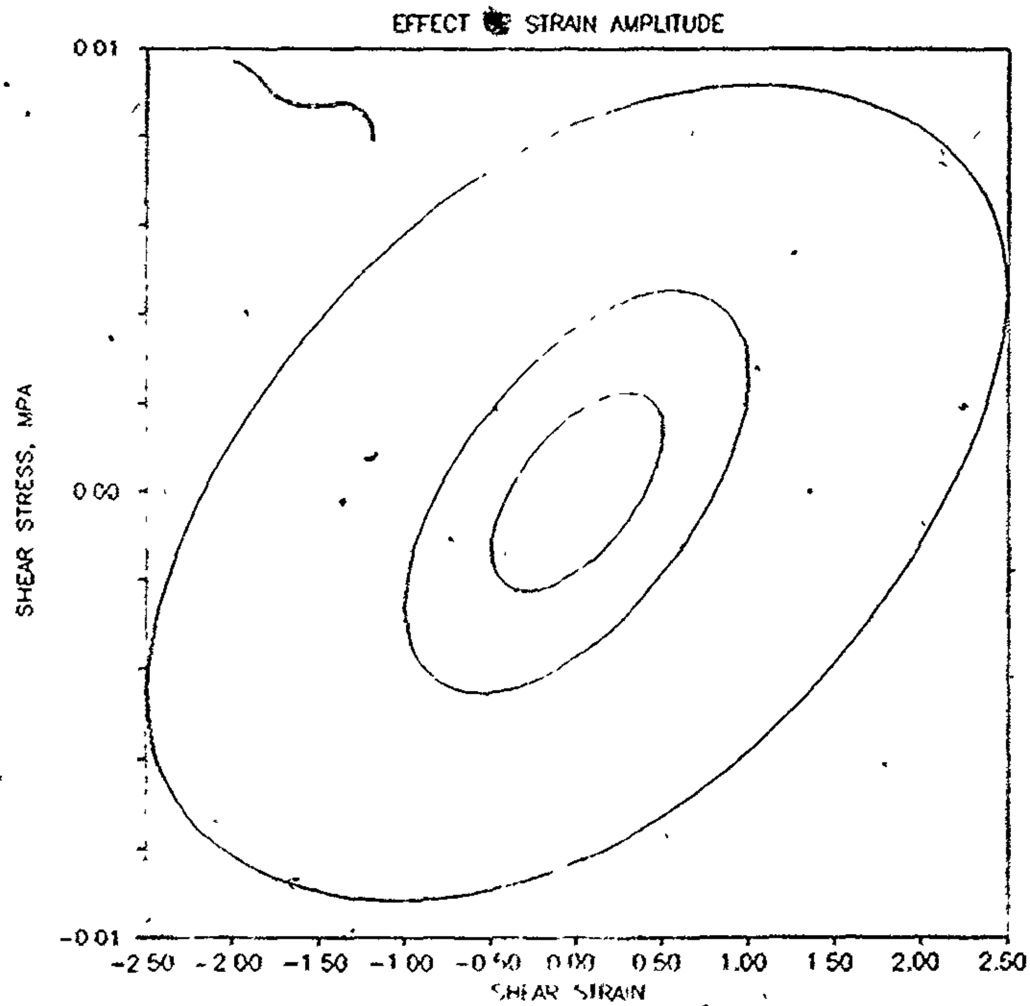

Figure 113. Shear stress versus shear strain loops for molten polystyrene in oscillatory shear at 190°C. Strain amplitudes (from innermost to outermost loops) are .5, 1 and 2.5. Constant frequency of 0.2 Hz.

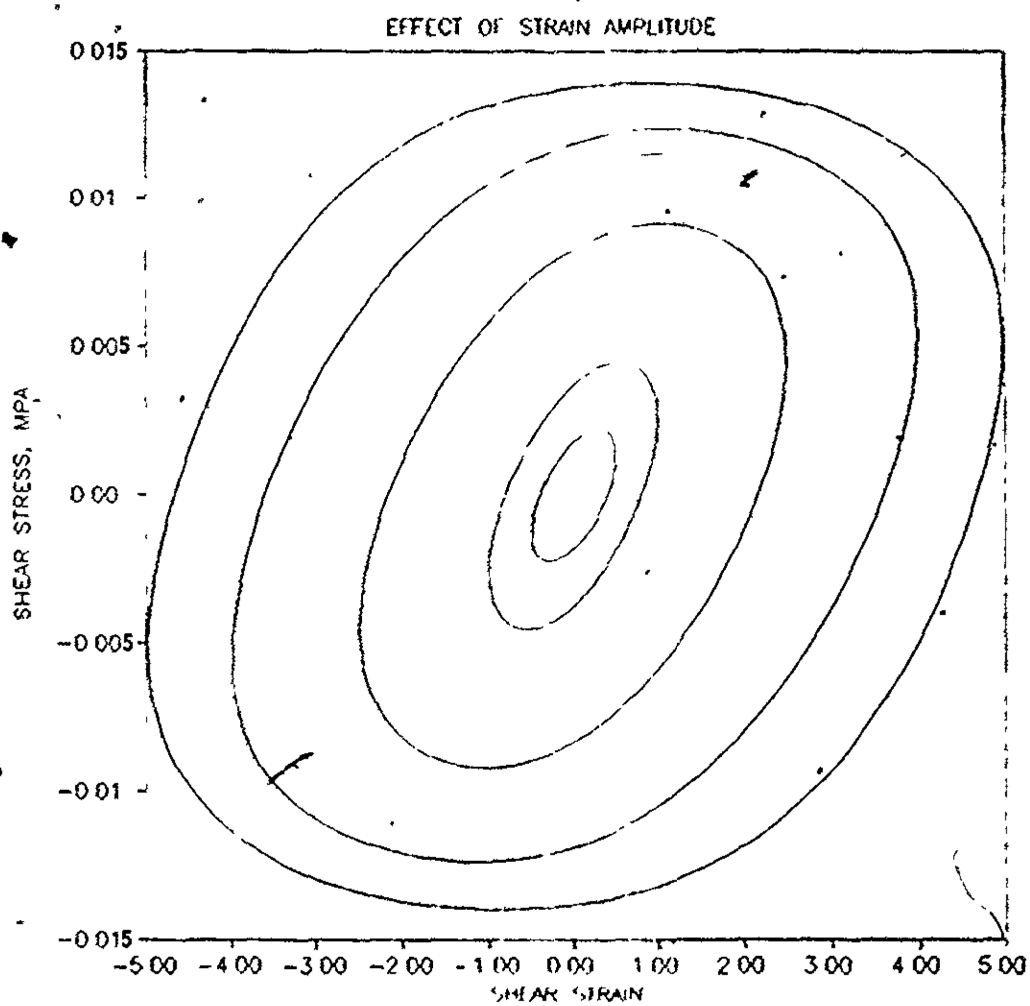

Figure 114. Shear stress versus shear strain loops for molten polystyrene in oscillatory shear at 190°C. Strain amplitudes (from innermost to outermost loops) are .5, 1, 2.5, 4, and 5. Constant frequency of 0.2 Hz.

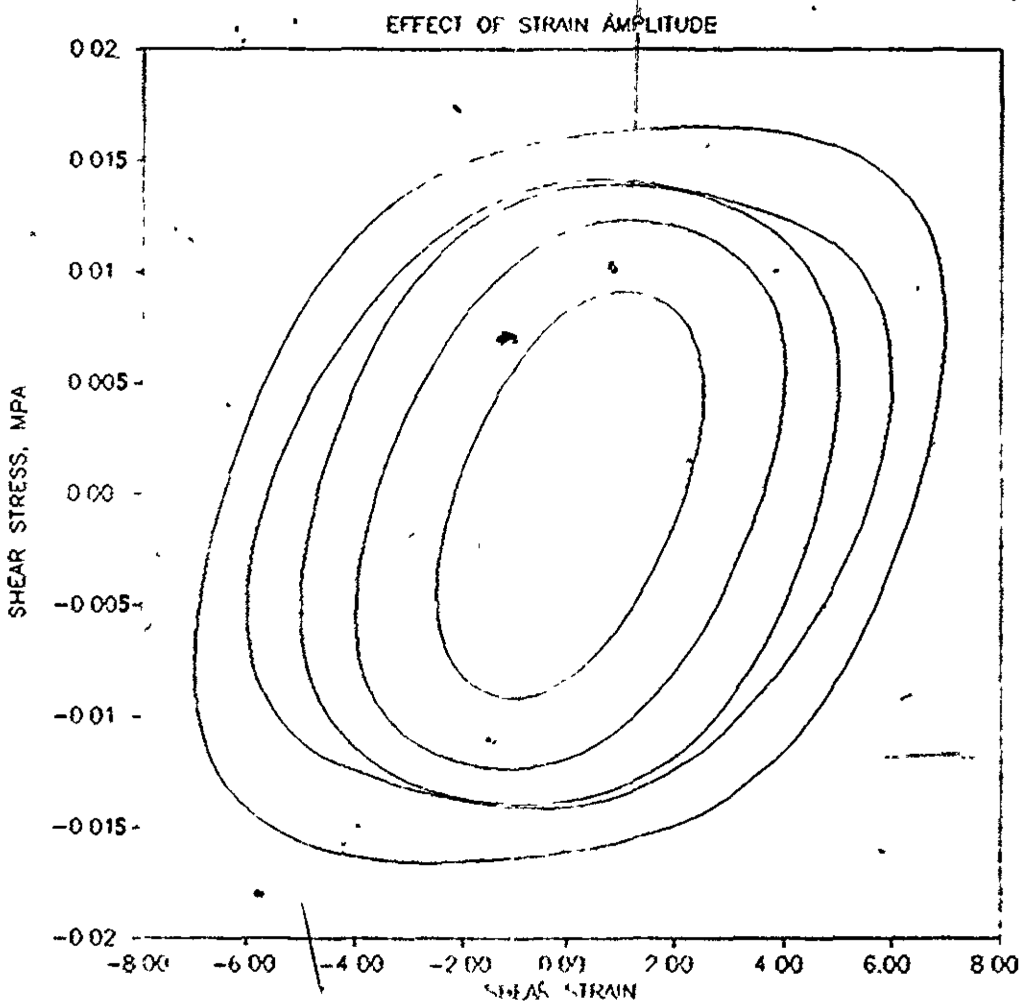

Figura 115: Shear stress versus shear strain loops for molten polystyrene in oscillatory shear at 190°C. Strain amplitudes (from innermost to outermost loops) are 2.5, 4, 5, 6 and 7. Constant frequency of 0.2 Hz.

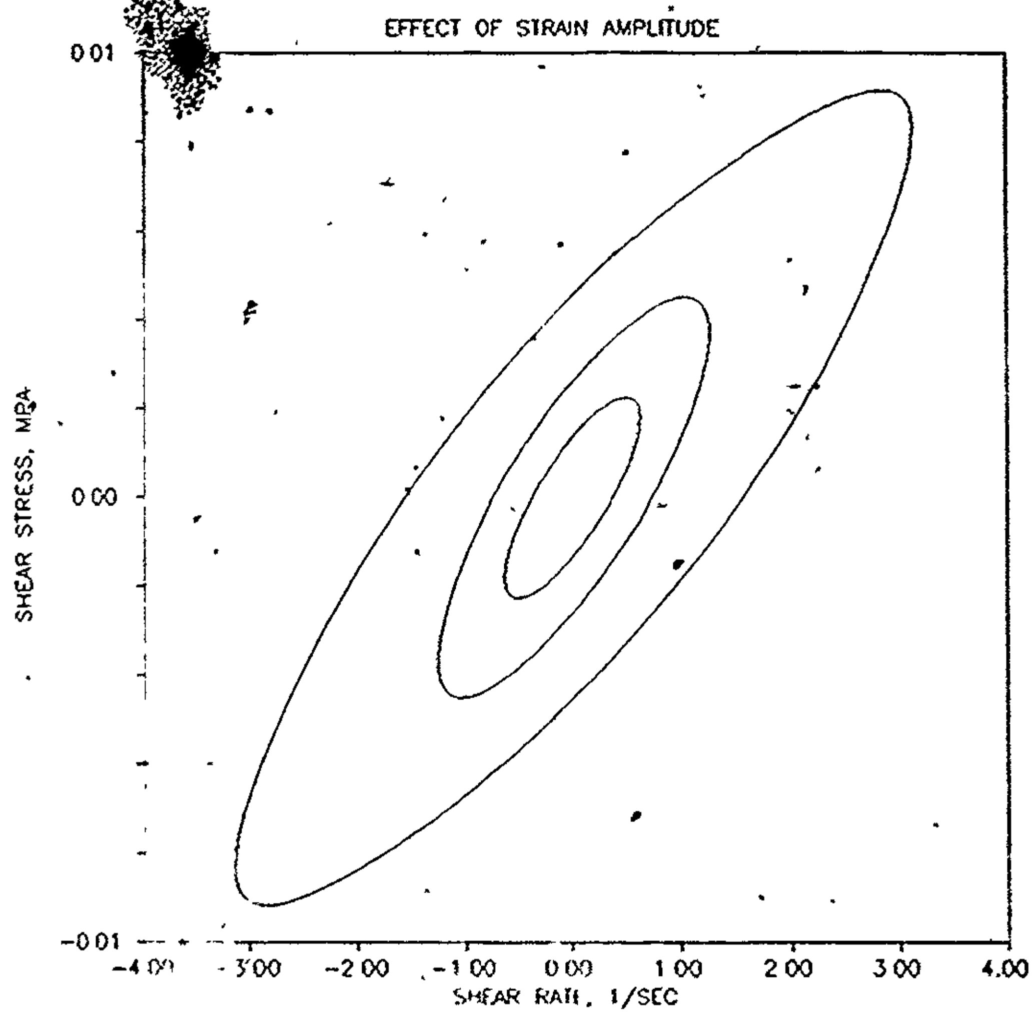

Figure 116. Shear stress versus shear strain rate loops for molten polystyrene in oscillatory shear at 190°C. Strain amplitudes (from innermost to outermost loops) are .5, 1 and 2.5. Constant frequency of 0.2 Hz.

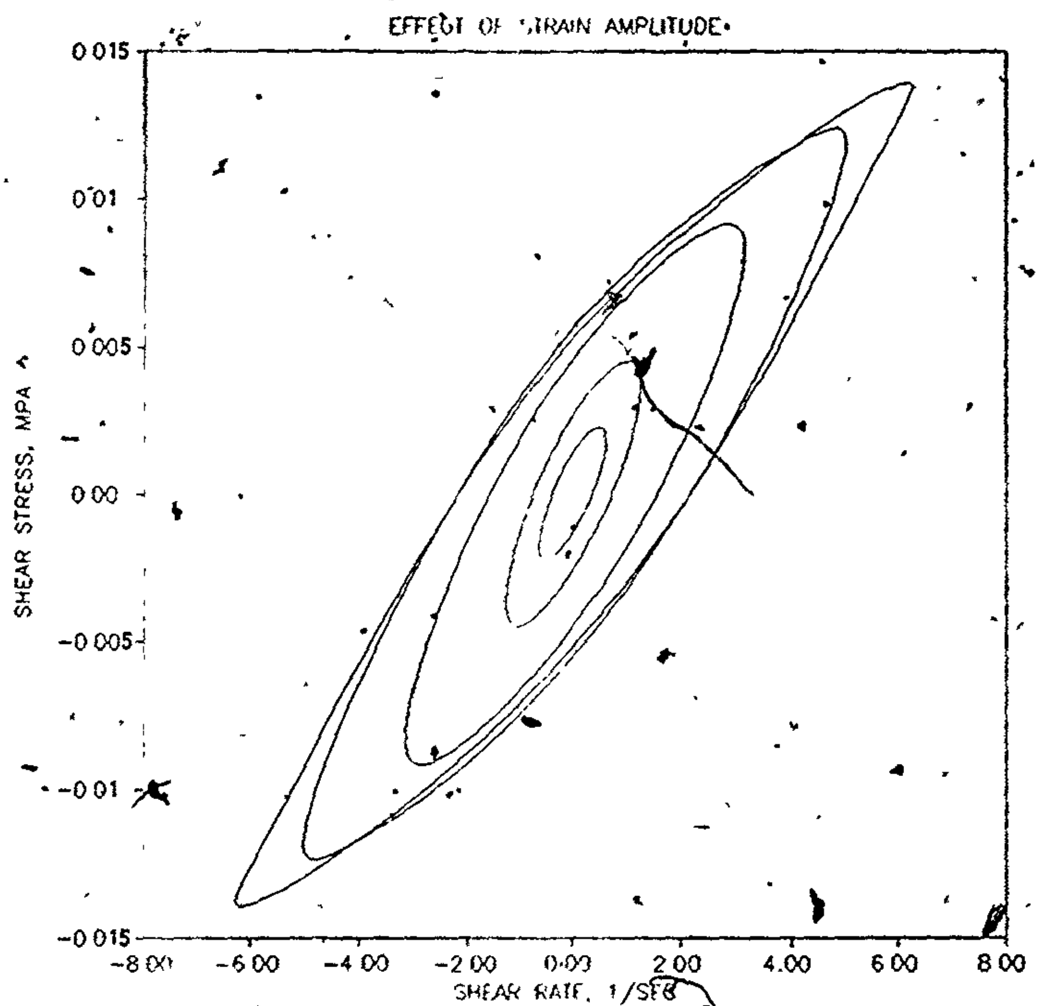

Figure 117: Shear stress versus shear strain rate loops for molten polystyrene in oscillatory shear at 190°C. Strain amplitudes (from innermost to outermost loops) are .5, 1, 2.5, 4, and 5. Constant frequency of 0.2 Hz.

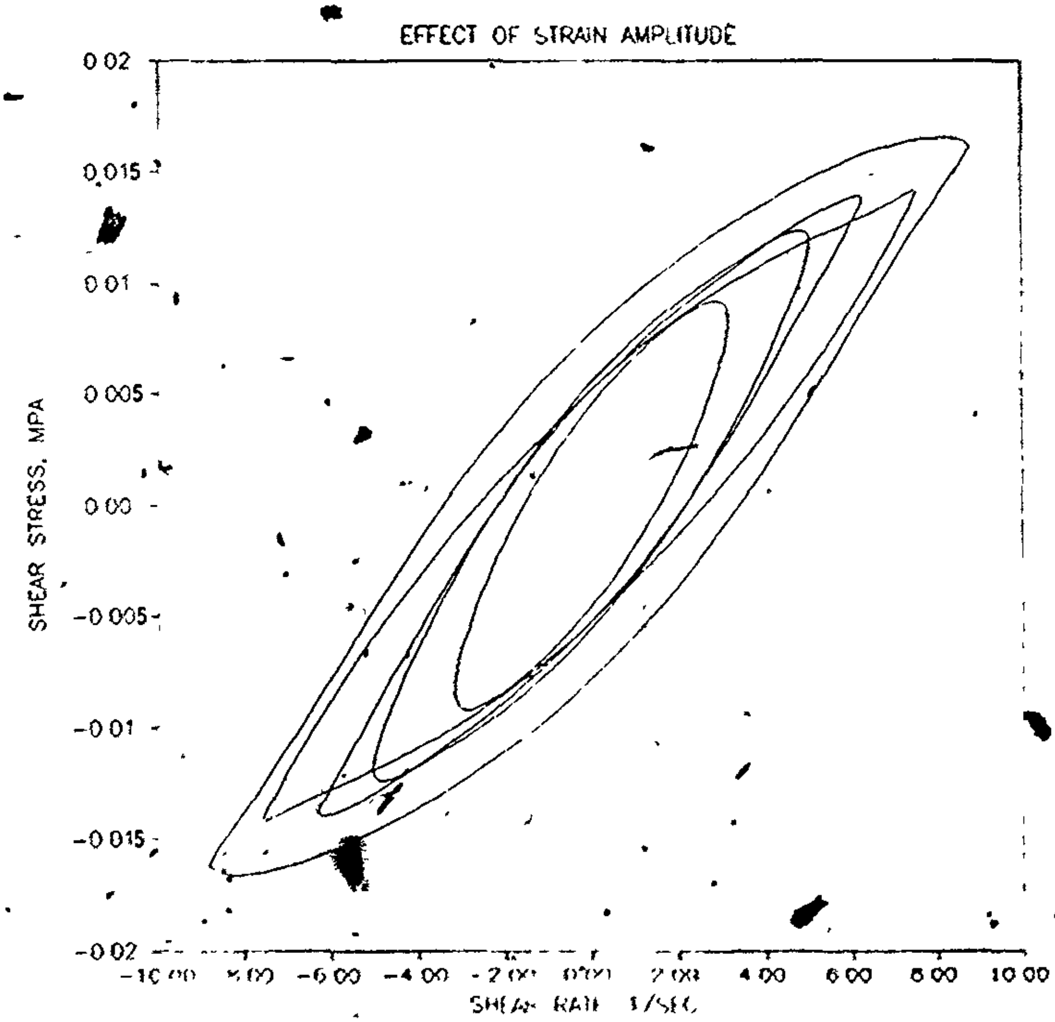

Figure 118. Shear stress versus shear strain rate loops for molten polystyrene in oscillatory shear at 190°C. Strain amplitudes (from innermost to outermost loops) are 2.5, 4, 5, 6 and 7. Constant frequency of 0.2 Hz.

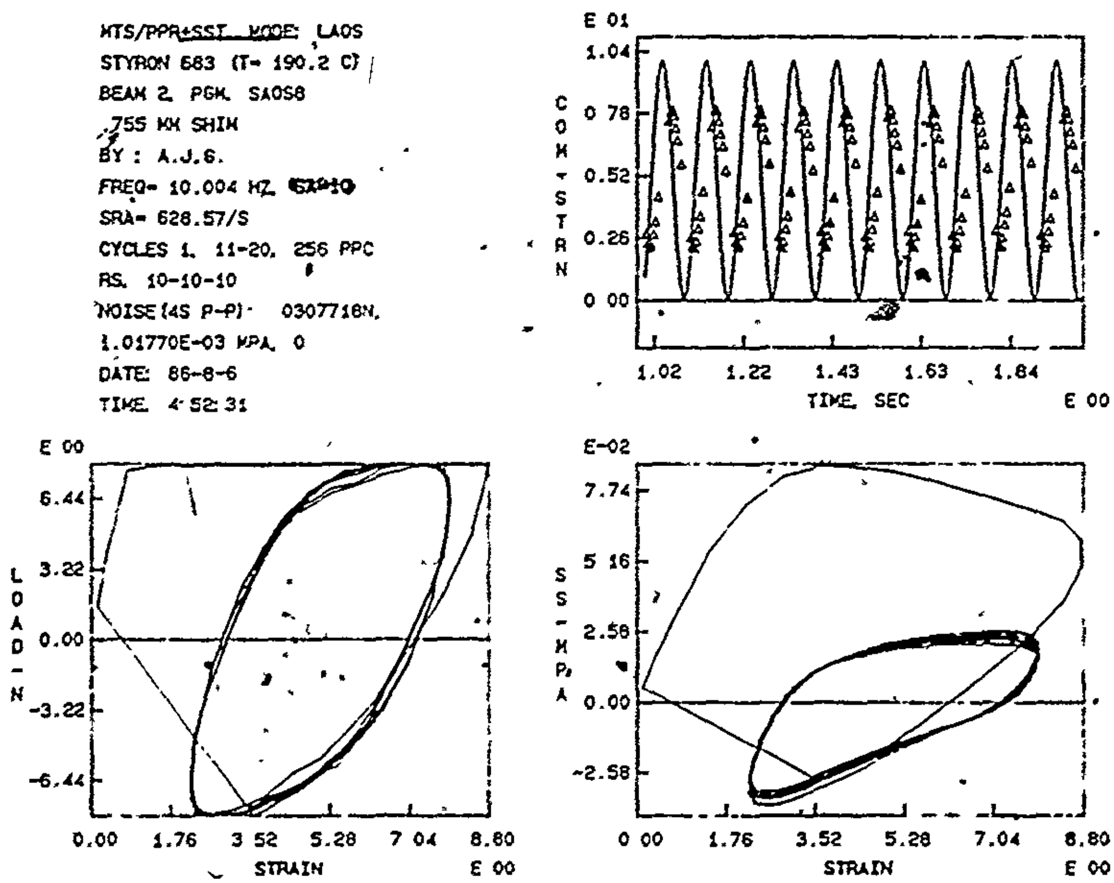

Figure 119: Shear stress versus shear strain rate loops for molten polystyrene in oscillatory shear after melt fracture at 190°C. Twofold asymmetry in stress-strain loop is not picked up in load-strain loop.

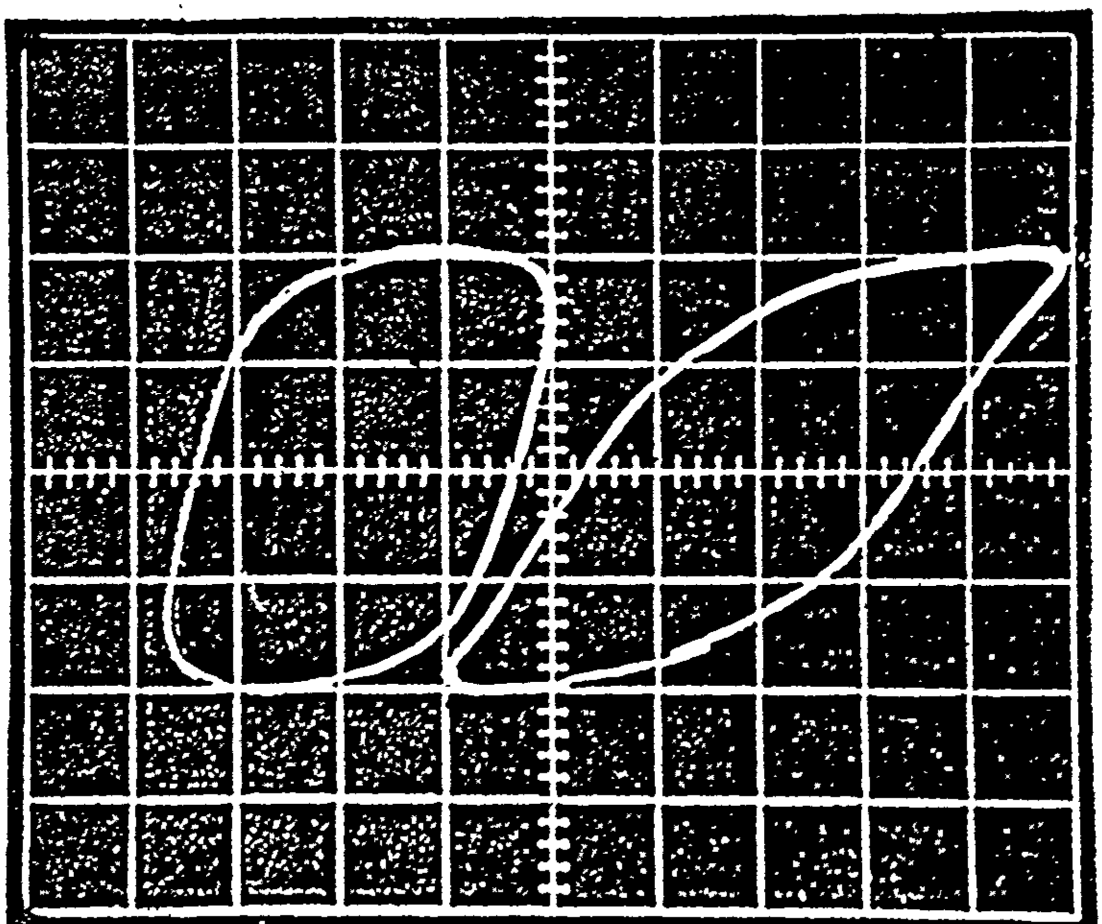

Figure 120 Nonlinear viscoelastic response of Vistanex LM-MS PIB in large amplitude oscillatory shear at room temperature. Left loop is shear stress versus shear strain, right loop is shear stress versus shear rate. Test conditions f = 0 20 Hz, σ_o = .0793 MPa, γ_o = 16 38.

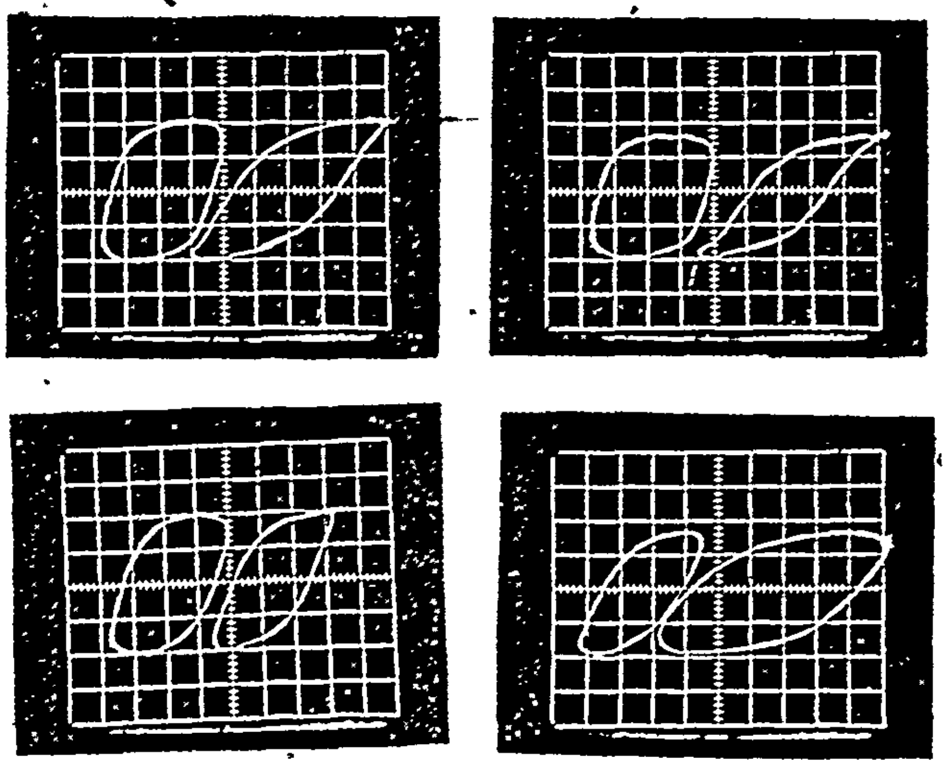

Figure 121: Effect of frequency on Vistanex LM-MS PIB in large amplitude oscillatory shear, γ_o = 16.38. Test conditions: f = 0.14 Hz, σ_o = .0714 MPa (upper right), f = 0.20 Hz, σ_o = .0793 MPa (upper left), f = .30 Hz, σ_o = .0793 MPa (lower left) and f=.45 Hz, σ_o = .0694 MPa (lower right).

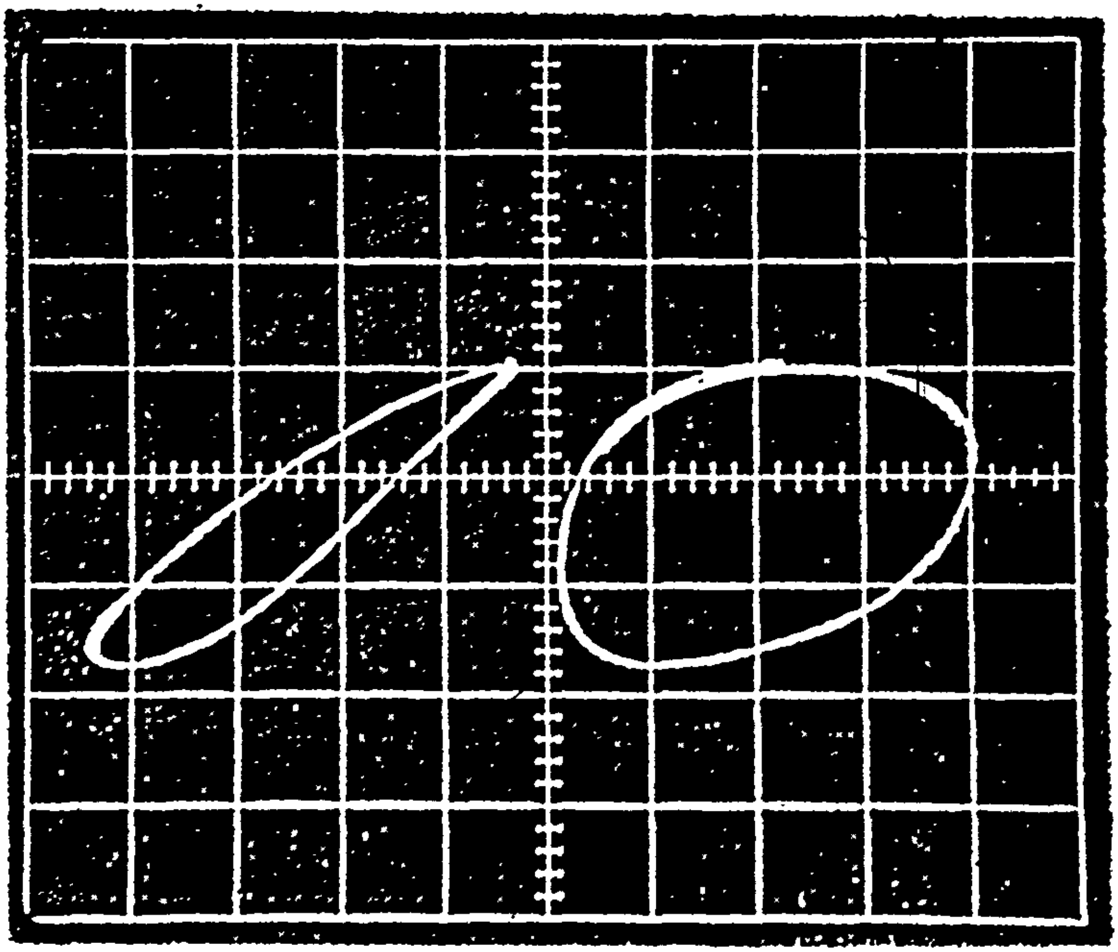

Figure 122 Melt fracture of Vistanex LM-MS PIB in large amplitude oscillatory shear at room temperature. Left loop is shear stress versus shear strain, right loop is shear stress versus shear rate. Test conditions: f = 0.88 Hz, σ_o = .0535 MPa, γ_o = 9.66.

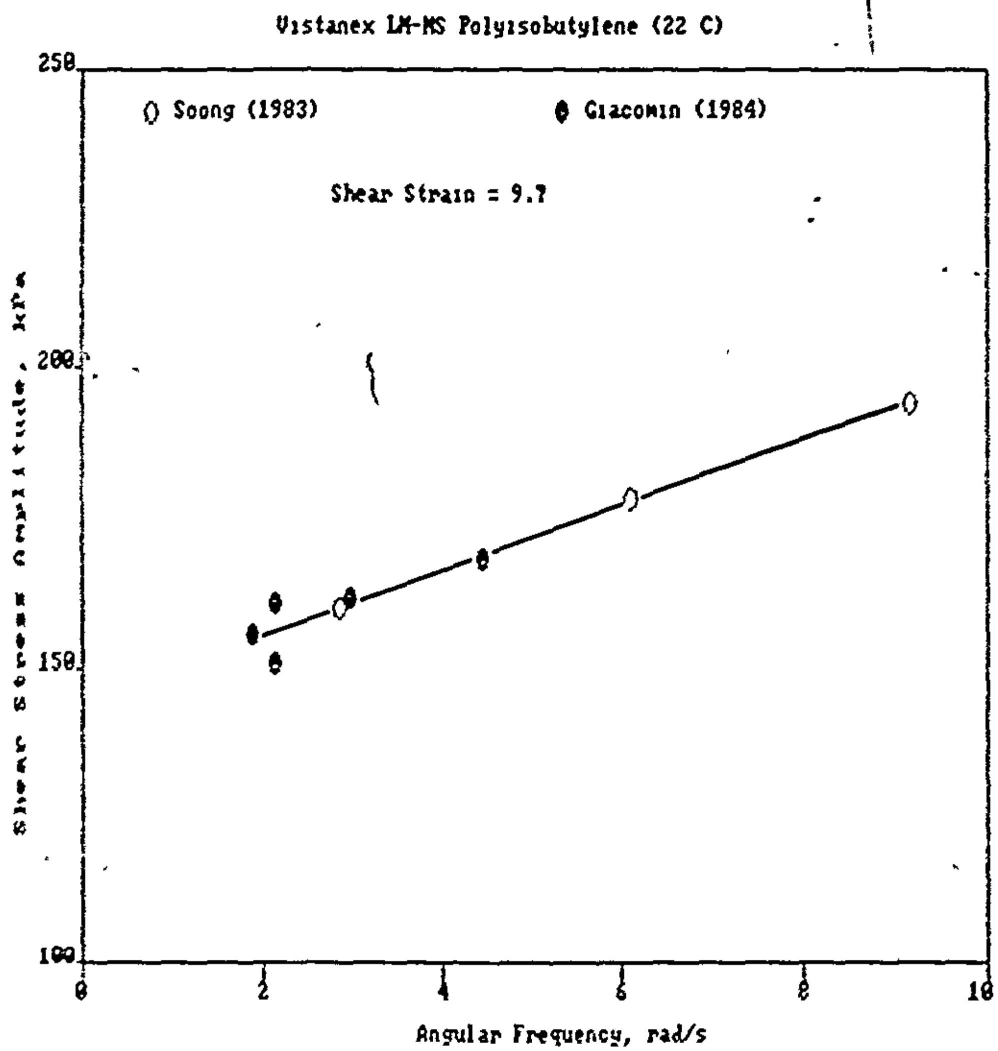

Figure 123: Comparison of large amplitude oscillatory shear results obtained by Giacomin (1984) on the room temperature prototype rheometer with those obtained by Soong (1983).

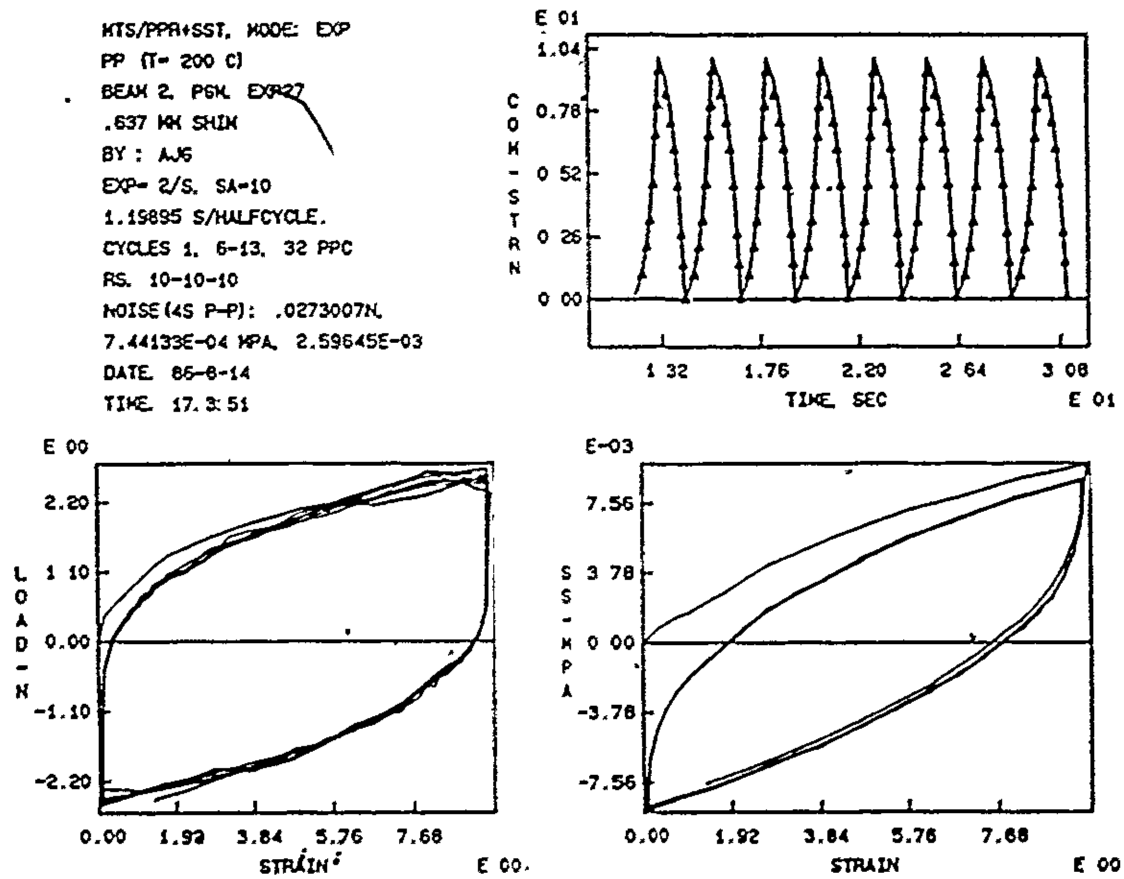

Figure 124. Representative reciprocating exponential shear test record. Test conditions. $\dot{\epsilon}_o$ = 2/sec, γ_o = 10, molten polypropylene, T = 200°C.

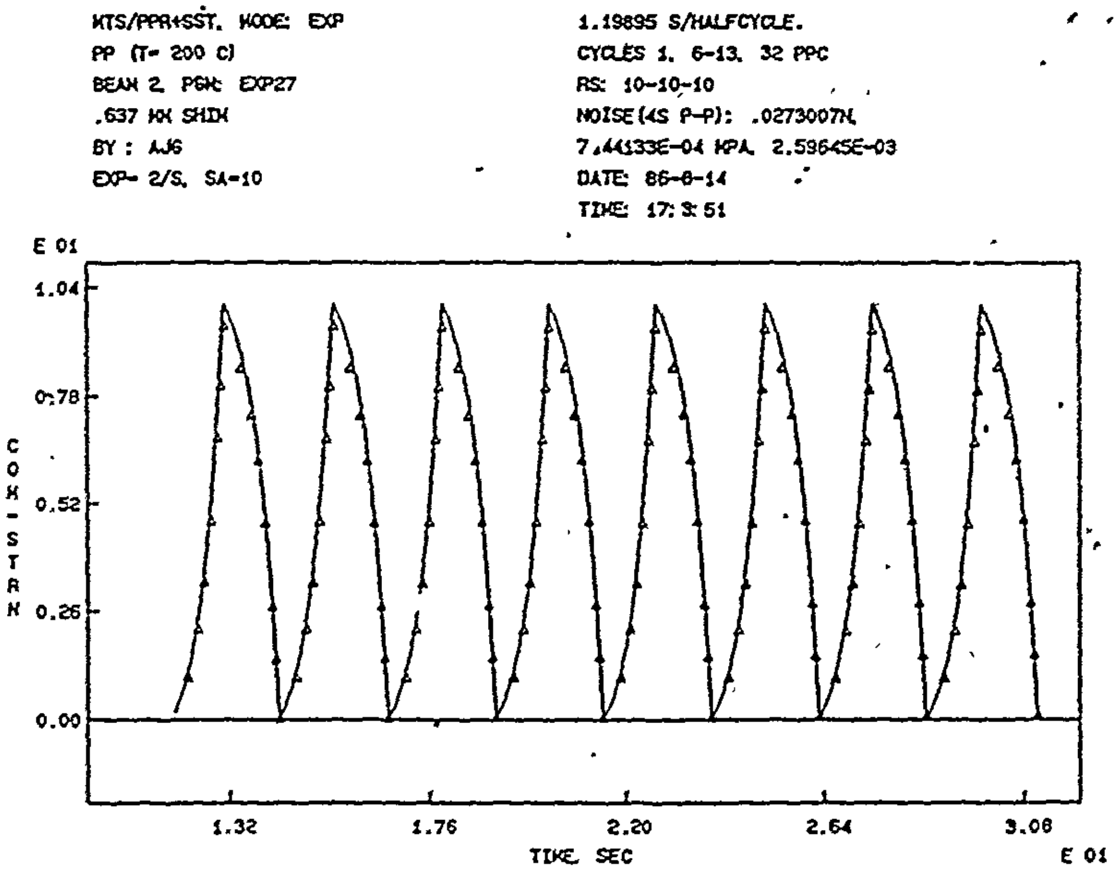

Figure 125: Time trace of shear strain for reciprocating exponential shear test Actual strain (triangles) closely follows command strain (curve). Test conditions: $\dot{\epsilon}_o = 2$/sec, $\gamma_o = 10$, molten polypropylene, T = 200°C.

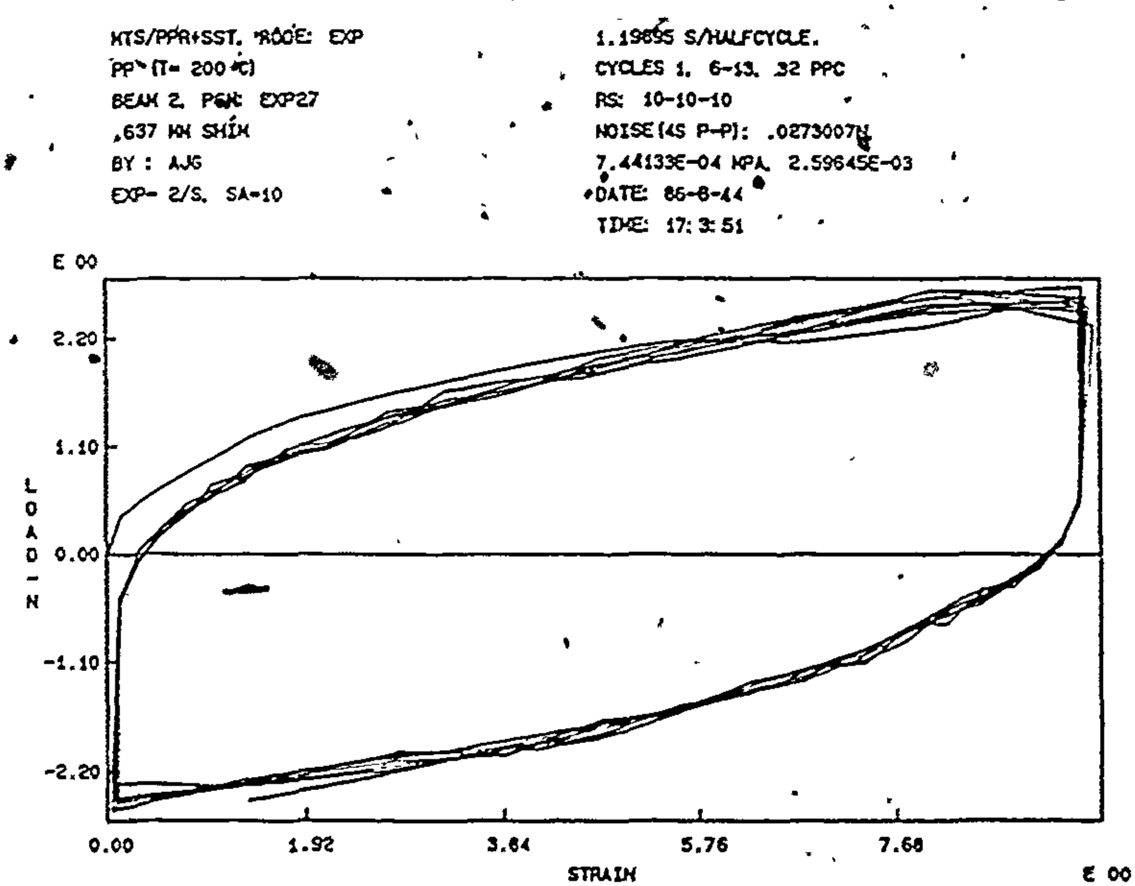

Figure 126. Loop of total force versus shear strain for reciprocation exponential shear test. Test conditions. $\dot{\epsilon}_0 = 2/\text{sec}$, $\gamma_0 = 10$, molten polypropylene, T = 200°C.

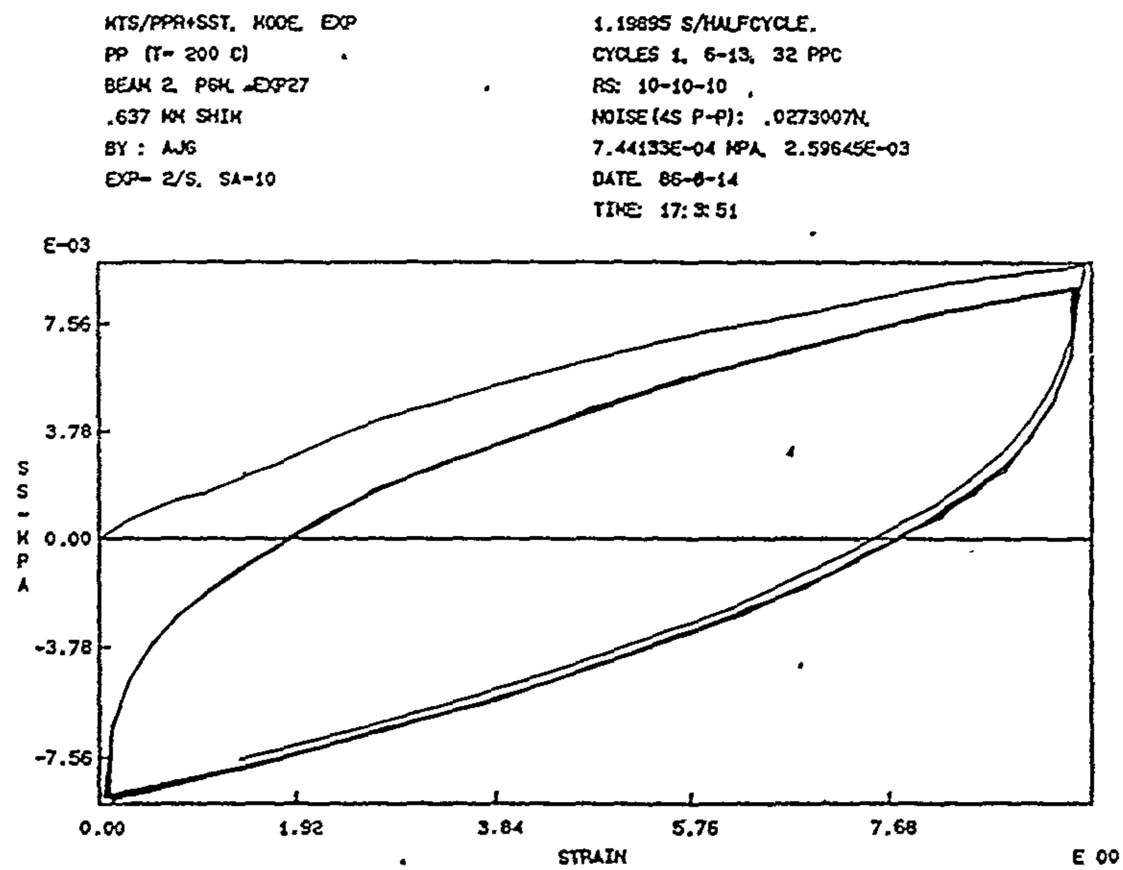

Figure 127. Loop of shear stress versus shear strain for reciprocation exponential shear test. Test conditions: $\epsilon_0 = 2/\mathrm{sec}$, $\gamma_0 = 10$, molten polypropylene, T = 200°C.

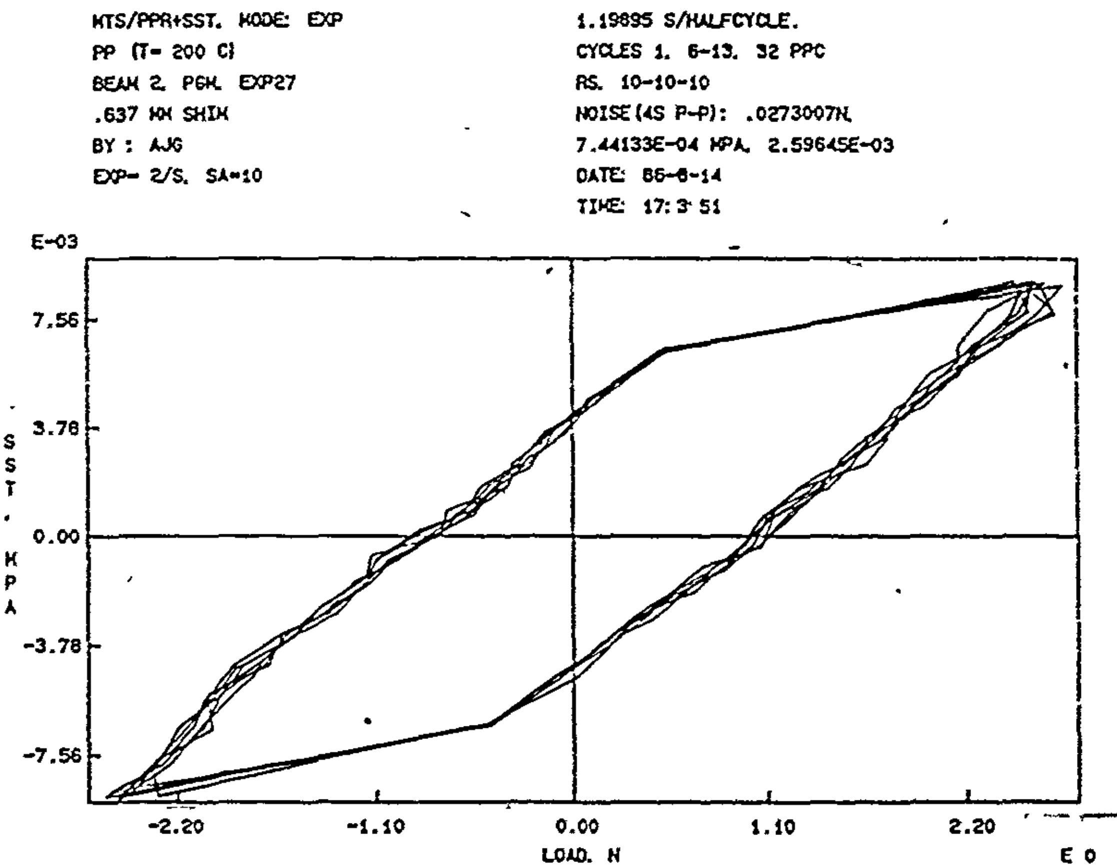

Figure 128. Loop of shear stress versus total force showing large discrepancy for reciprocating exponential shear test. Test conditions. $\epsilon_0 = 2/\text{sec}$, $\gamma_0 = 10$, molten polypropylene, T = 200°C.

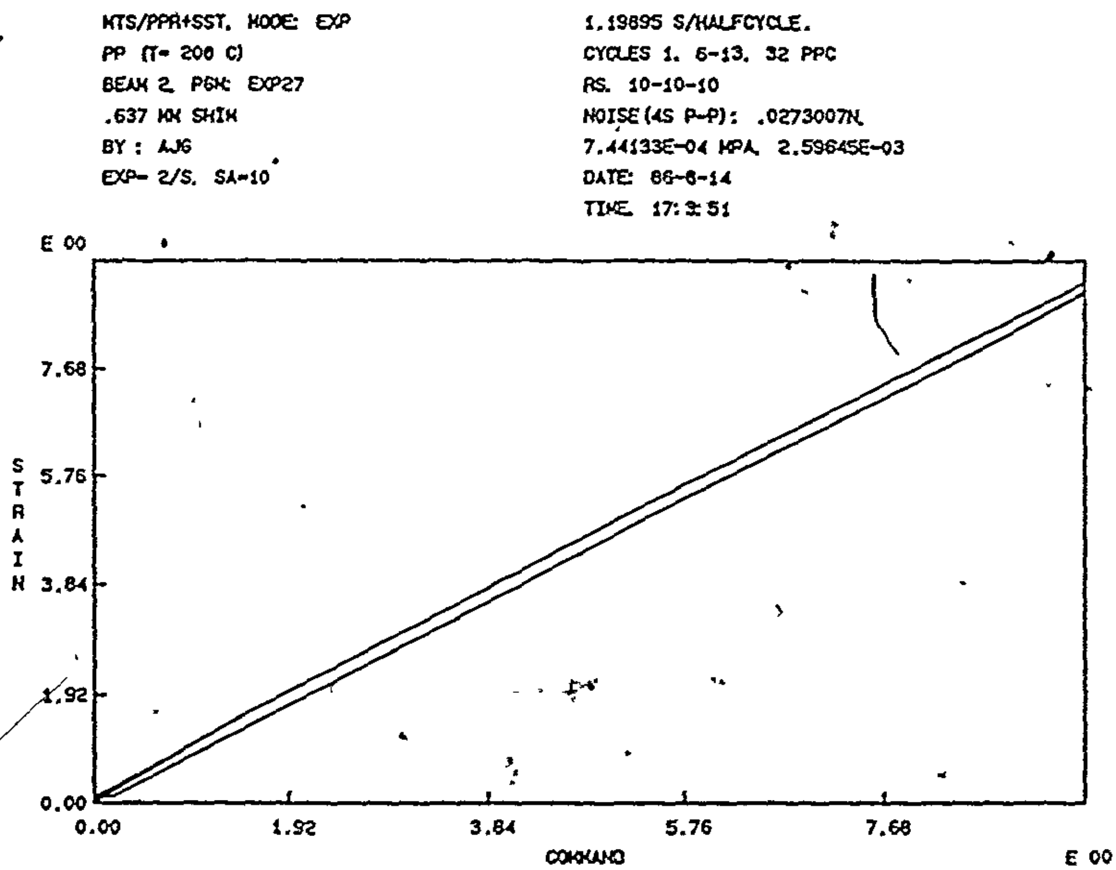

Figure 129 Loop of actual strain against command strain showing good execution of desired reciprocating exponential strain history. Test conditions: $\dot{\epsilon}_o$ = 2/sec, γ_o = 10, molten polypropylene, T = 200°C.

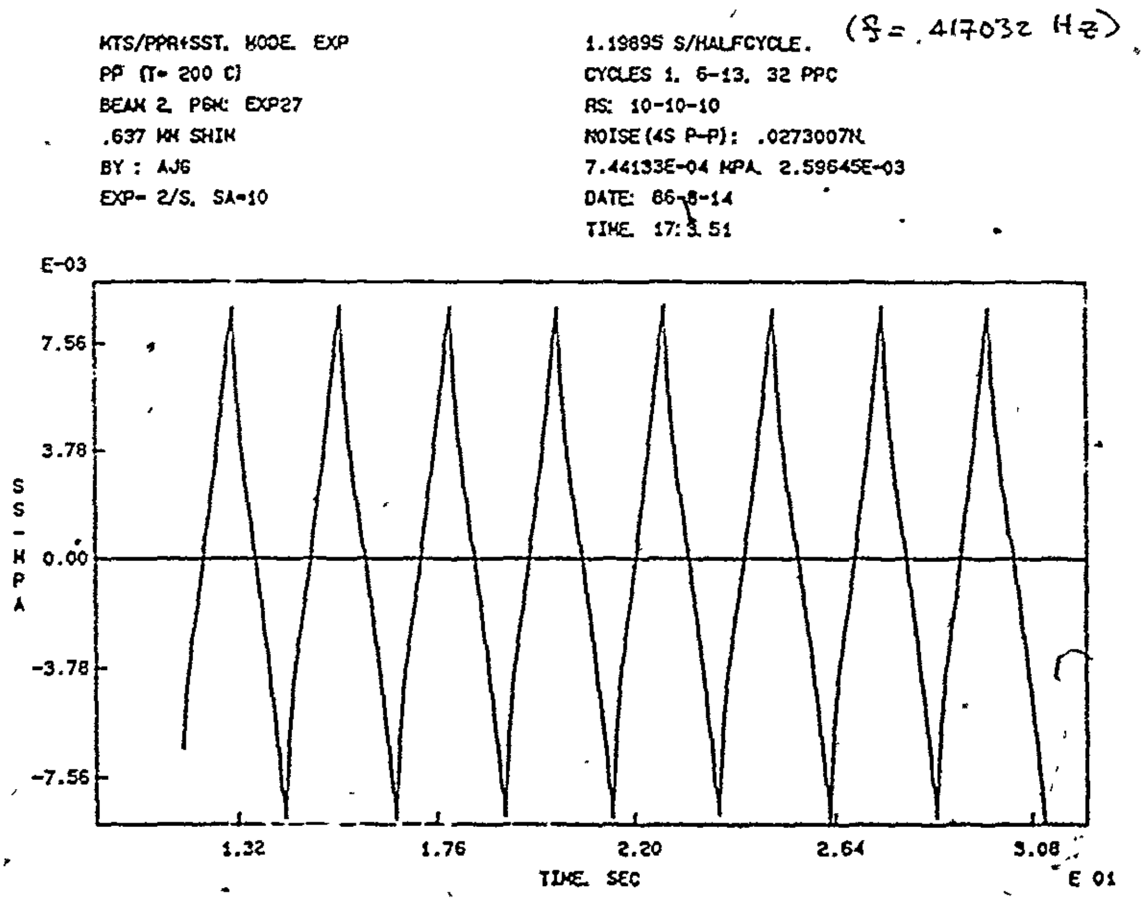

Figure 130. Time trace of shear stress for reciprocating exponential shear test showing inflections in shear stress. Test conditions. $\epsilon_0 = 2$/sec, $\gamma_0 = 10$, molten polypropylene, T = 200°C.

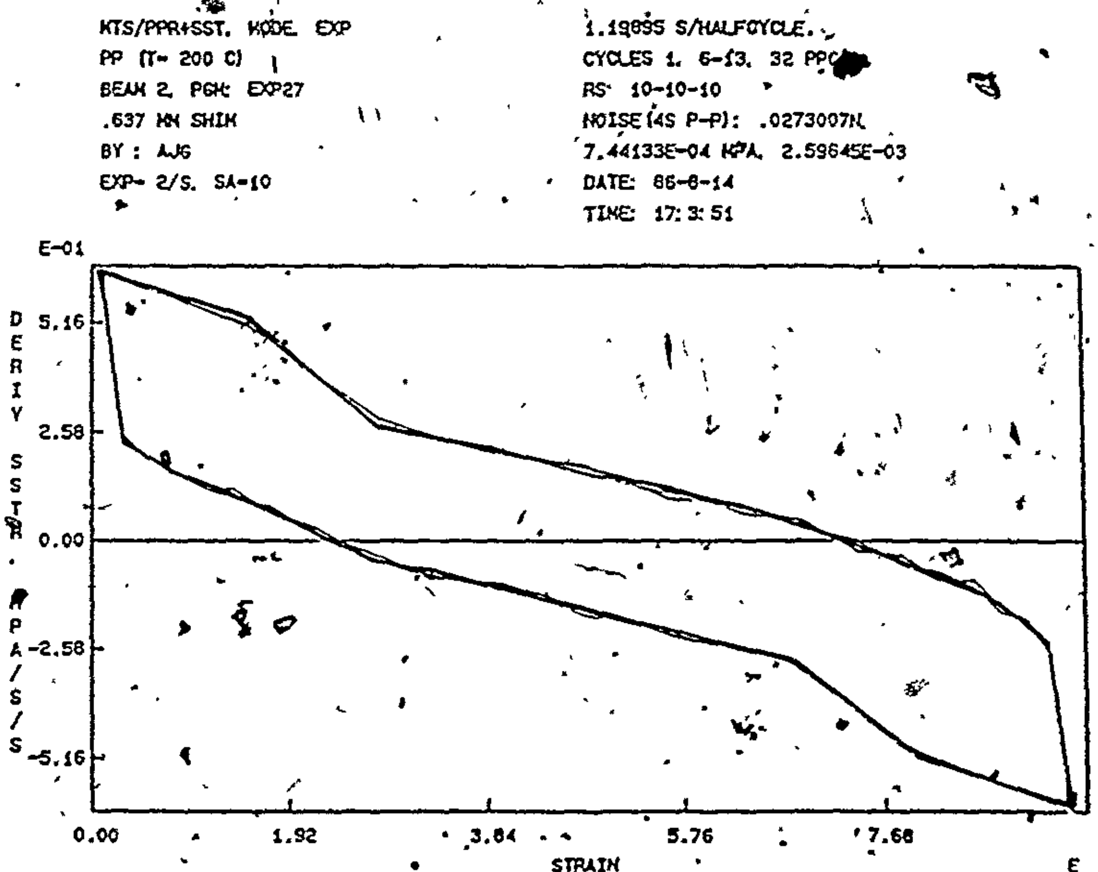

Figure 131: Loop of second time derivative of shear stress, $d^2\sigma/dt^2$, versus shear strain showing stress inflections at strains of 2.33 and 7.27. Test conditions: $\epsilon_0 = 2/\mathrm{sec}$, $\gamma_0 = 10$, molten polypropylene, $T = 200°C$.

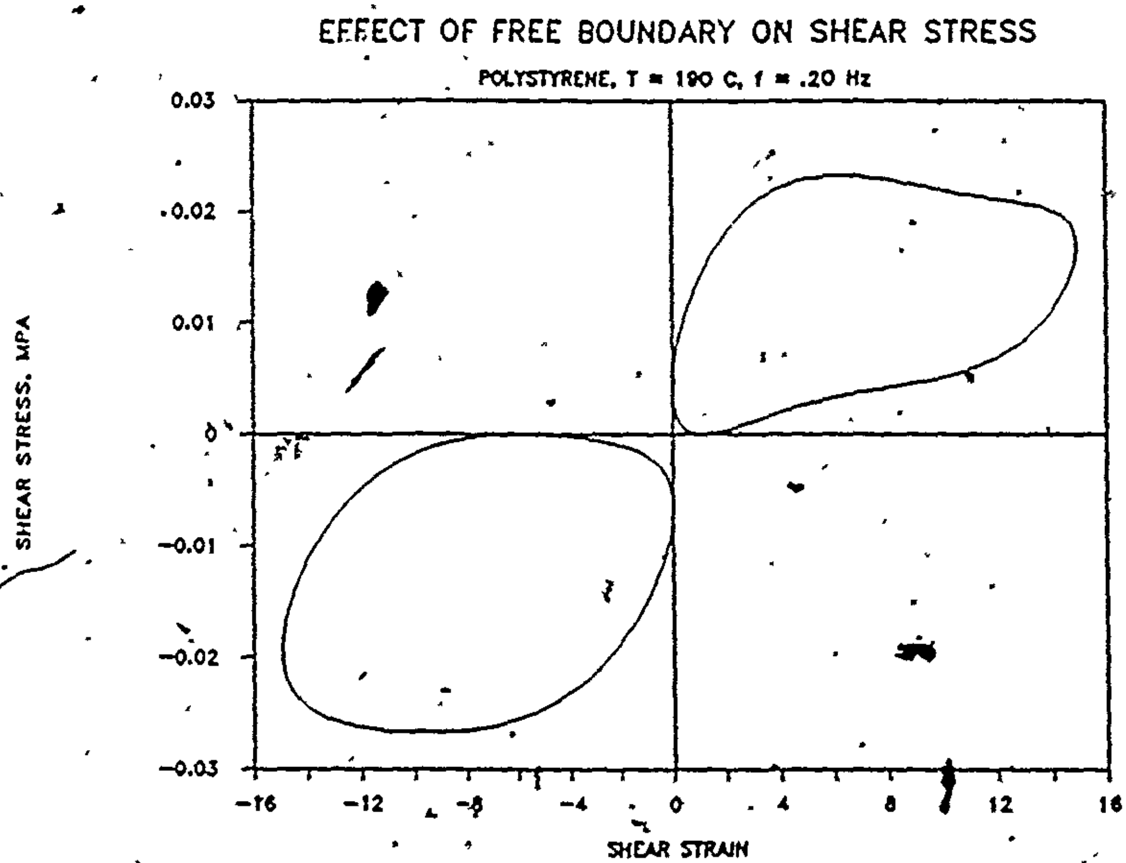

Figure 132. Results of special oscillatory shear test for end effects by mounting sample end near shear stress transducer. When transducer moves towards center of sample (left loop) twofold symmetric response is obtained. When transducer moves towards boundary (right loop), twofold asymmetry appears in the stress response.

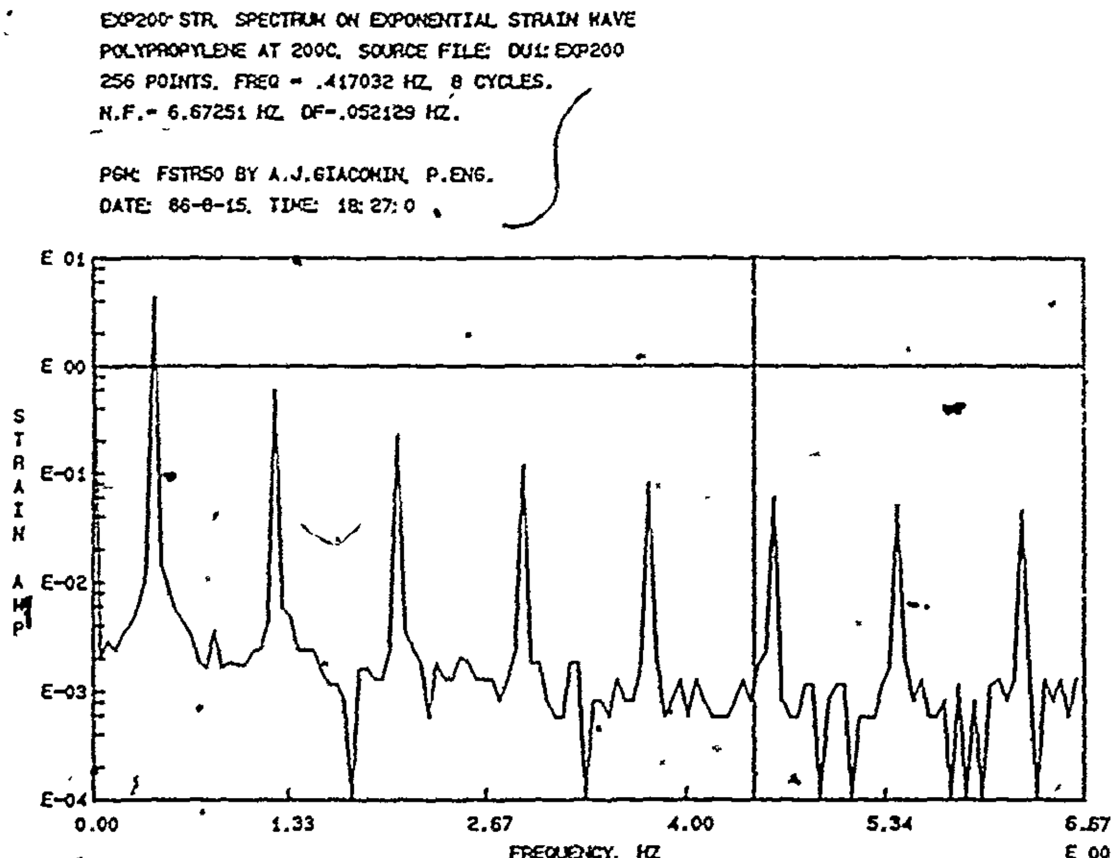

Figure 133: Amplitude spectrum for shear strain for reciprocating exponential shear test. Test conditions: $\epsilon_o = 2$/sec, $\gamma_o = 10$, molten polypropylene, T = 200°C.

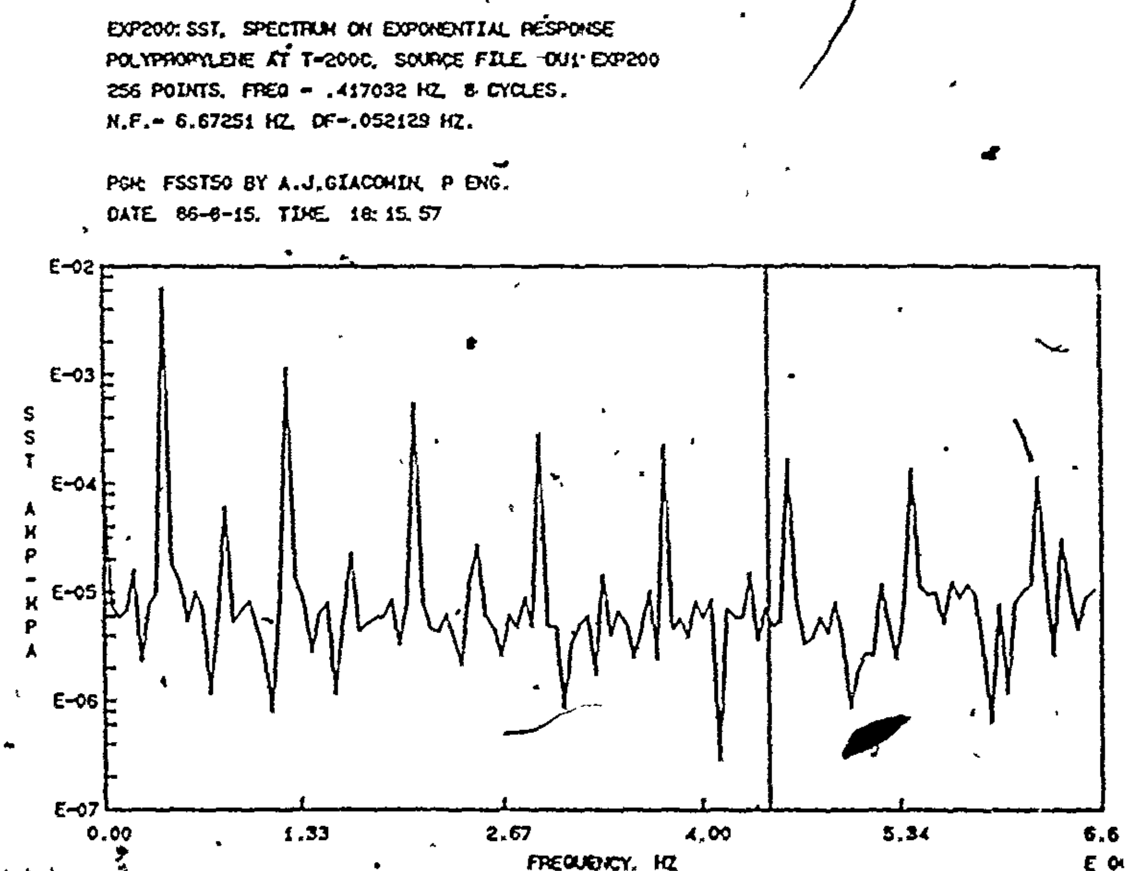

Figure 134. Amplitude spectrum for shear stress for reciprocating exponential shear test. Test conditions: $\epsilon_0 = 2/\mathrm{sec}$, $\gamma_0 = 10$, molten polypropylene, $T = 200°C$.

Figure 135: Handy accessories for high temperature rheometry: household oven cleaner (left), anti-seizing compound (center) and silicone oil (right).

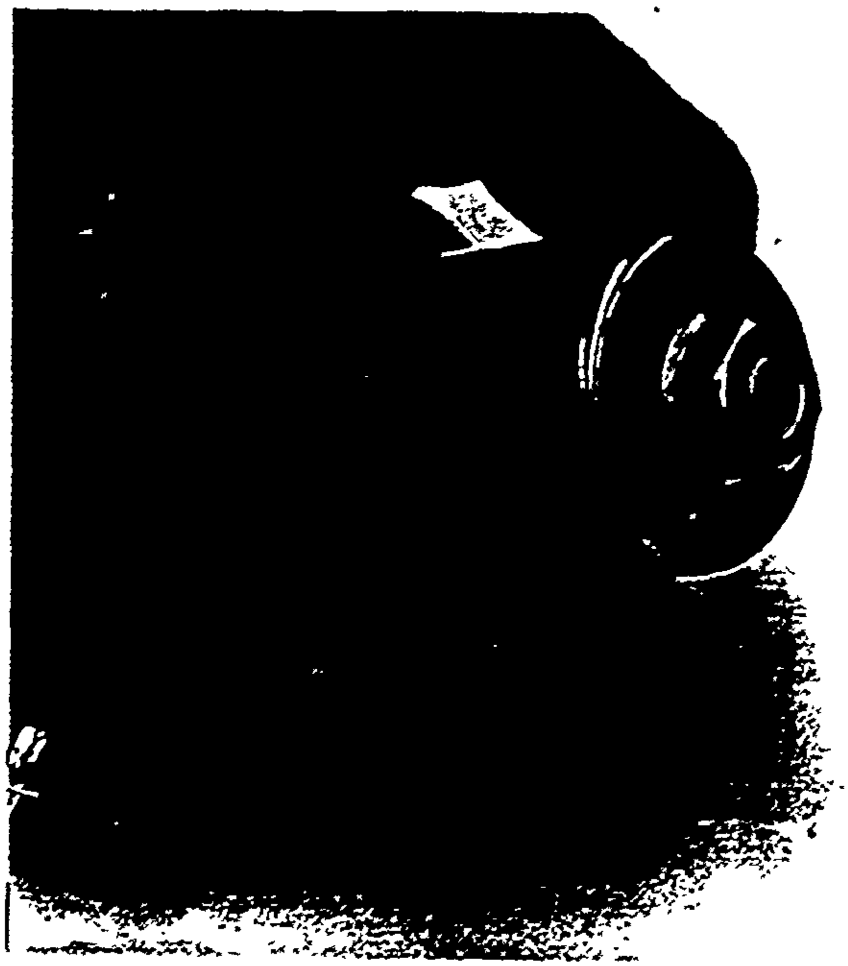

Figure 136: Fixed end of cantilever shown fully assembled. Port for set screw, used for securing capacitance probe, shown at left of nut.

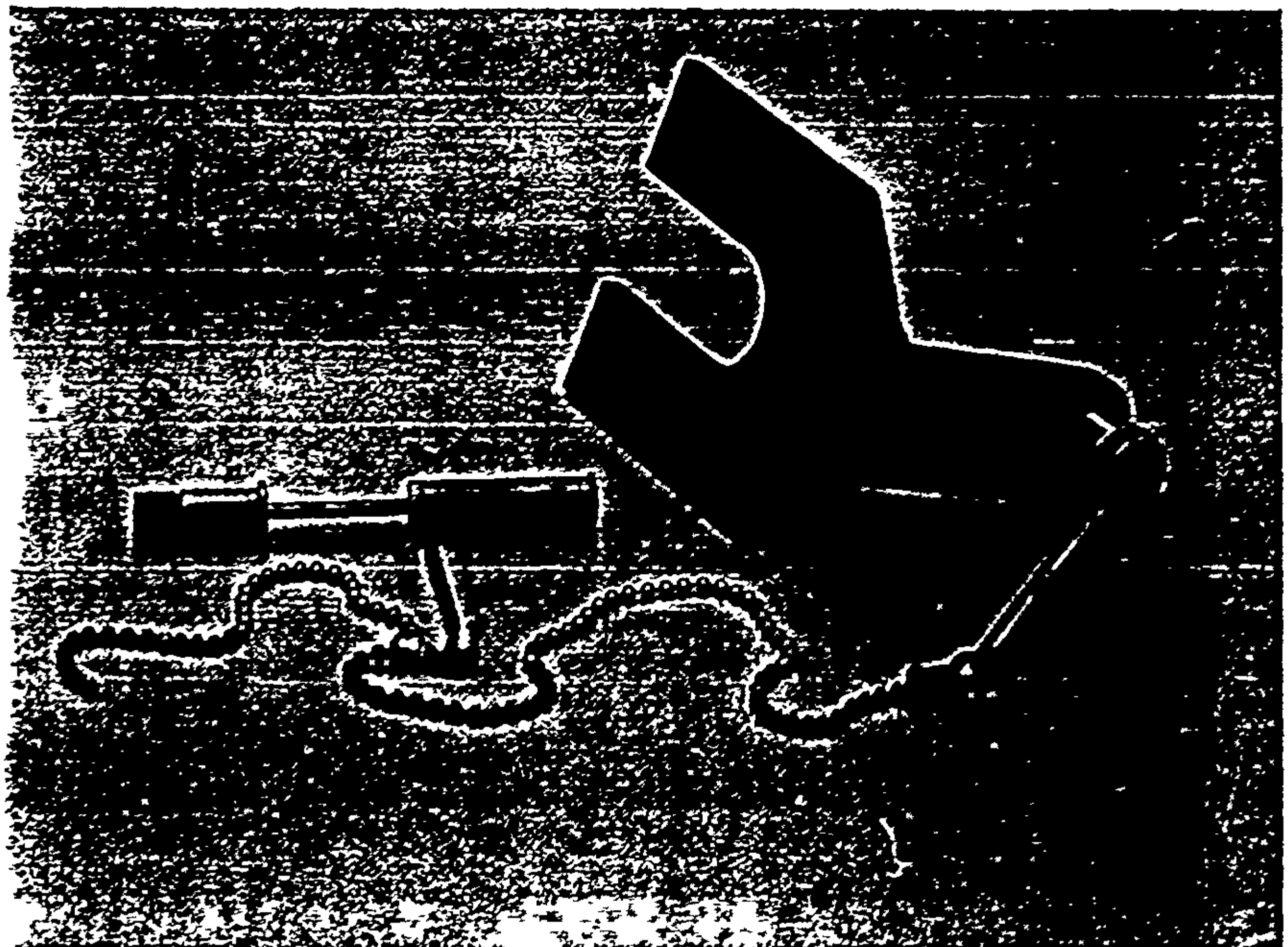

Figure 137· Dynamic calibration assembly showing cantilever with calibration hook (left), connecting chain, calibration spring (lower right), and the coupling to connect the spring to the moving actuator.

Figure 138 Active face of fully assembled shear stress transducer showing cantilever flush with housing. This housing will in turn be flush-mounted on the stationary plate.

Figure 139: Author shown adjusting the stand-off distance of the capacitance probe (in right hand) using allen key on set screw to secure probe.

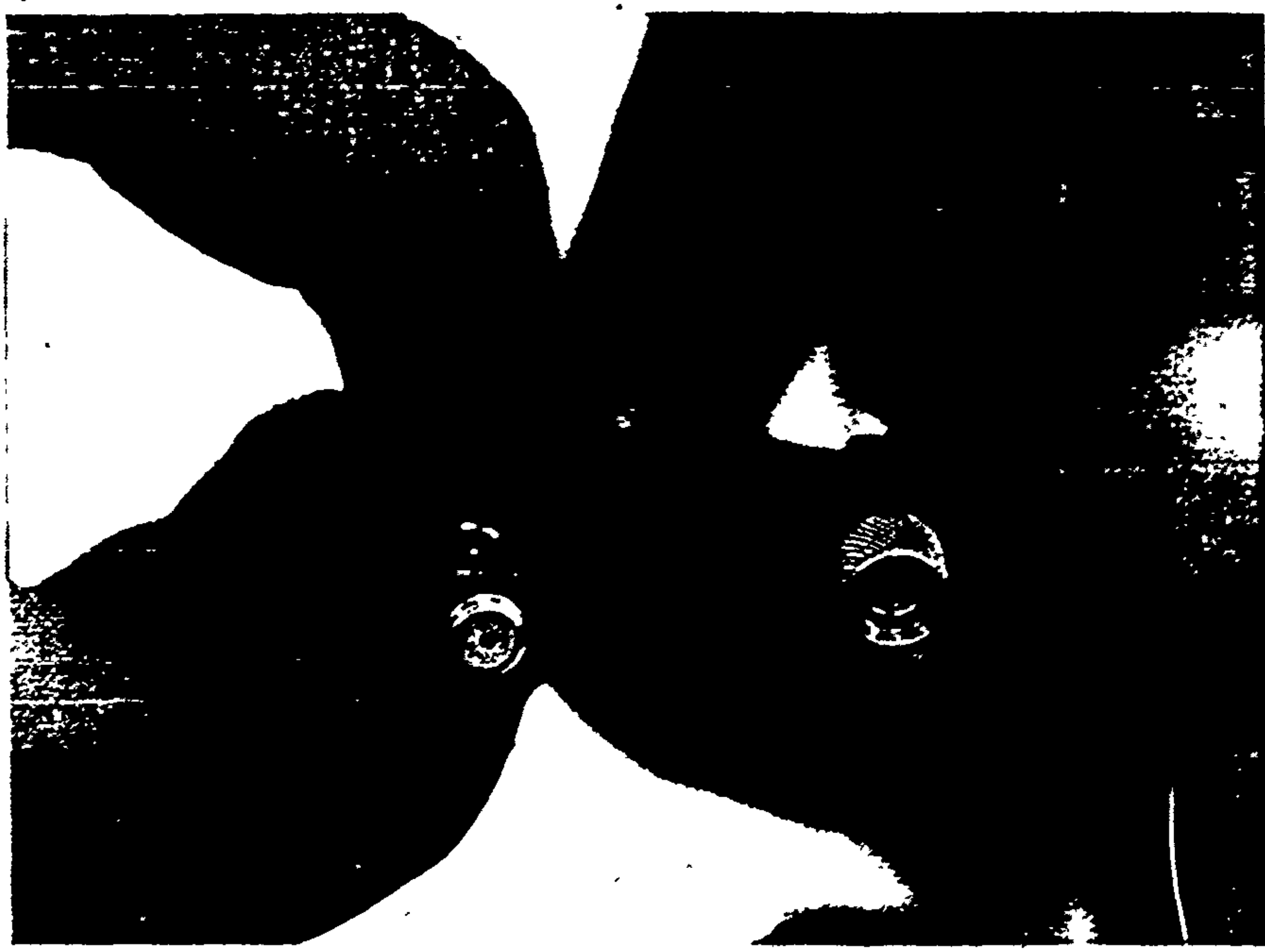

Figure 140. View of connecting end of capacitance probe (left) with special cable for high-temperature service.

Figure 141: Author conducts material test from terminal showing oven (upper right) which contains sliding plate rheometer (not shown) positioned below the MTS crosshead, load cell atop crosshead (barely visible), front panel of servo-hydraulic test system (center) and digital storage oscilloscope (lower right).

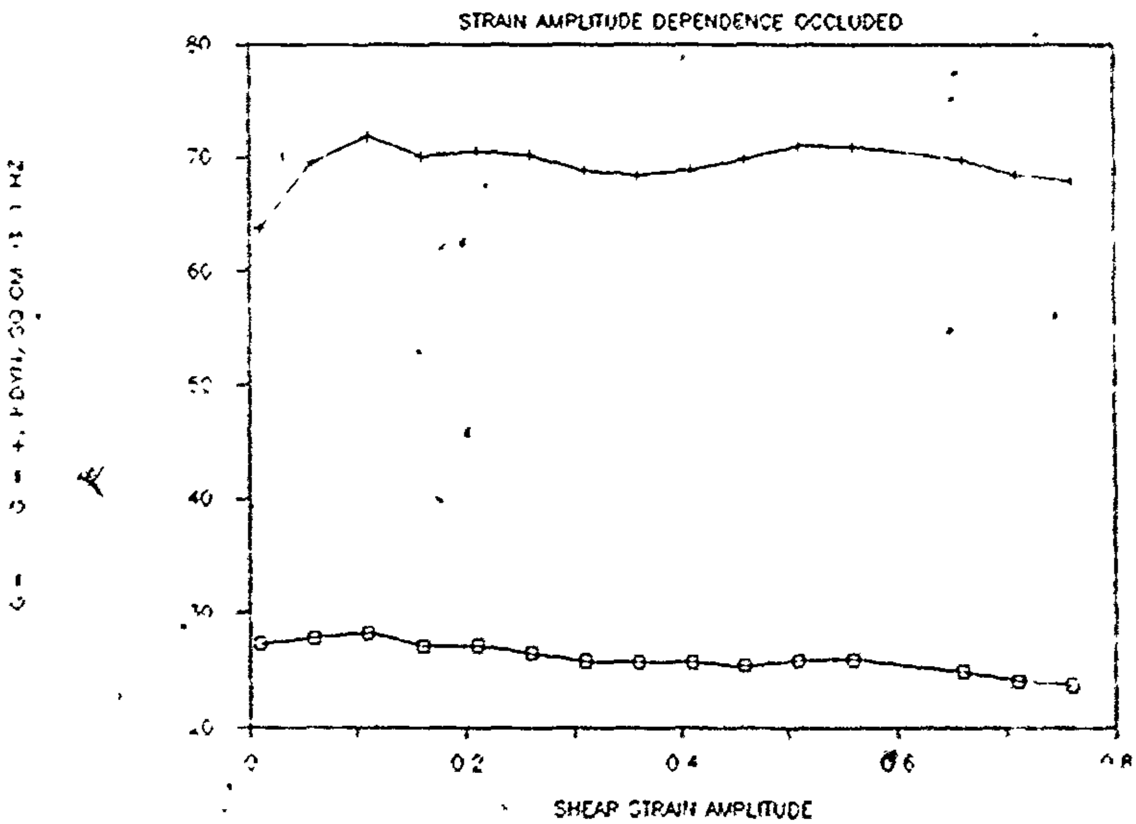

Figure 142. Behavior of molten Sclair LDPE in oscillatory shear measured with rotational rheometer using cone-plate fixture, T = 198°C, ω = 1 rad/sec.

APPENDIX 1: LAOS Test Program

```
LIST

LA0S8   5-Aug-86  MTS 773 MU BASIC V02.08

10 REM                  LARGE AMPLITUDE OSCILLATORY SHEAR
11 REM
12 REM                              BY
13 REM
14 REM                      A. JEFFREY GIACOMIN
15 REM
16 REM ACKNOWLEDGEMENTS: DR. P. CAIN, S. DOSHI, T. SAMURKAS.
17 REM
20 REM
30 REM ***** STARTING STATEMENTS *****
40 REM
50 GRATTACH(2,2,Y9)
52 GOSUB 700 \ REM STARTING SCREEN.
55 GOSUB 1200 \ REM GET TEST INFO.
58 GOSUB 800 \ REM REVISE CAL CONSTANTS.
61 GOSUB 600 \ REM TOTAL POINTS.
64 SETDIM VA1(N1,5),VA2(P8,5),X(1024)
67 GOSUB 1400 \ REM RETURN TO SETPT.
90 GOSUB 30010 \ REM MATCH TEST & DAP FREQUENCIES.
100 GOSUB 1100 \ REM GET TEST PARAMETERS
101 GOSUB 1300 \ REM GET SPECIFIC TEST INFO.
102 GOSUB 3900 \ REM BASELINES & STD DEVS
103 GOSUB 900 \ REM COLLECTS EXTREMA.
104 REM
105 REM
120 CKTIME(1,Z1,Z1) \ REM REDUNDANT.
130 FGREPT(1,"SIN", FREQ F1,2*P1,A1,0)
140 ADTIMED(2,VA1,,4,1,1,3) \ ADTIMED(1,VA2,,4,1,1,3) \ REM DACQ.
142 PRINT  \ Y8$="" \ PRINT "'RUN'"; \ INPUT Y8$ \ IF Y8$<>"RUN" THEN 142
144 FGGO \ ADINIT \ ADGO(1) \ REM COLLECTS 1ST.
150 ETIME \ SLEEP(S1) \ ADINIT \ ADGO(2) \ REM DELAYS DACQ UNTIL S1.
160 IF VA1<N1 THEN 160 \ REM ELEGANT STOP.
180 GOSUB 1400 \ REM RETURNS TO SETPT.
182 REM
183 REM ***** POST TEST PROCESSING *****
184 REM
188 GOSUB 1800 \ REM CONV UNITS & COMP TIME.
190 GOSUB 2000 \ REM FIX EXTREMA & CONV UNITS.
192 GOSUB 4400 \ REM PRINT NOISE LEVELS      \ GOSUB 3800 \ REM WAIT THEN CLS.
193 GOSUB 540 \ REM COMMENT PREP.
194 GOSUB 1600 \ REM DRAWS BUSY PLOT      \ GOSUB 3800 \ REM WAIT THEN CLS.
200 GOSUB 2300 \ REM DRAWS EXPANDED PLOT      \ GOSUB 3800 \ REM WAIT THEN CLS
210 GOSUB 4500 \ REM DIFFERENTIATES      \ GOSUB 3800 \ REM WAIT THEN CLS.
220 GOSUB 4800 \ REM DRAWS RATE PLOTS      \ GOSUB 3800 \ REM WAIT THEN CLS.
230 GOSUB 8500 \ REM SAVE TO FLOPPY
240 GOSUB 9500 \ REM PRINT REPORT      \ GOSUB 3800 \ REM WAIT THEN CLS.
340 END
350 REM
360 REM ***** START A GRAPH *****
370 REM
380 TEKMODE \ VTMODE \ PRINT "VT-240 (1) OR PLOTTER (2)"; \ INPUT A2
390 F9=1 \ IF A2=2 THEN PRINT "FRACTION OF FULLSIZE (.75)"; \ INPUT F9
400 Y8$="" \ IF A2=1 THEN 430
410 IF A2=2 THEN PRINT "PAPER INSERTED AND PEN READY"; \ INPUT Y8$
420 IF Y8$<>"Y" THEN 410 \ REM GOES TO PREV LINE.
430 IF A2=1 THEN TEKMODE(1,1)
440 IF A2=2 THEN GRON(2) \ IF A2=2 THEN SIZE(A2,108*F9,216*F9)
```

```
450 INPUT \ RETURN
470 REM
480 REM ***** AXES *****
490 REM
500 AXES(A2,0,0) \ AXES(A2,1.00000E+08,1.00000E+08)
510 AXES(A2,-1.00000E+08,-1.00000E+08)
520 RETURN
530 REM
540 REM ***** COMMENT PREP *****
550 REM
560 WHOAMI(A$) \ X1$="MTS/PPR+SST, MODE: LAOS".
561 X2$=M2$+" (T= "+M3$+" C)" \ REM MATERIAL NAME & TEMP.
562 X3$="BEAM "+M5$+", PGM: "+A$ \ REM BEAM & PROGRAM NUMBERS.
563 X4$=STR$(T1)+" MM SHIM"
564 REM SHIM THICKNESS & LOAD-SST-STRAIN RANGE SETTINGS.
565 X5$="BY : "+M4$ \ REM OPERATOR.
566 X6$="FREQ= "+STR$(F1)+"/S, SA="+STR$(G1)
567 X7$="SRA= "+STR$(G1*F1)+"/S"
568 X8$="CYCLES 1, "+STR$(P2+1)+"-"+STR$(P2+P3)+", "+STR$(P9)+" PPC"
569 X9$="RS: "+STR$(R3)+"-"+STR$(R4)+"-"+STR$(R2)
570 Y5$="NOISE(4S P-P): "+STR$(4*SQR(V2(1,1)))+"N," \ REM LOAD NOISE.
572 Y4$=STR$(4*SQR(V3(1,1)))+" MPA, "+STR$(4*SQR(V4(1,1))) \ REM SST,STR NOISE.
575 GDATE(Y9,M9,D9) \ Y7$="DATE: "+STR$(Y9)+"-"+STR$(M9)+"-"+STR$(D9)
576 GTIME(S9,M9,H9) \ Y6$="TIME: "+STR$(H9)+":"+STR$(M9)+":"+STR$(S9)
590 RETURN
600 REM
610 REM ***** NUMBER OF DATA POINTS *****
620 REM
630 PRINT \ PRINT "FOR FFT CHOOSE 2,4,8,16,32,64,128,256,512,1024 ..."
640 PRINT "TOTAL POINTS"; \ INPUT P9 \ N1=P9-1
650 PRINT "COLLECT AFTER CYCLE NUMBER"; \ INPUT P2
660 PRINT "HOW MANY CYCLES"; \ INPUT P3
662 PRINT "PERIODS OF RELAXATION"; \ INPUT P4
670 P8=P9/(P2+P4) \ REM POINTS IN 1ST CYCLE
675 P1=P2+P3 \ REM TOTAL CYCLES.
680 RETURN
700 REM
701 REM ***** STARTING SCREEN *****
702 REM
709 TEKMODE \ VTMODE \ WHOAMI(A$) \ PRINT "PROGRAM: ";A$ \ PRINT
710 GDATE(Y9,M9,D9) \ PRINT "DATE: ";Y9;"-";M9;"-";D9
720 GTIME(S9,M9,H9) [illegible] "TIME: ";H9;":";M9;":";S9 \ PRINT
730 PRINT "ZERO LO[illegible]OKE AND SST"
740 PRINT "SET SPA[illegible]2 AT 0 & 1." \ PRINT
750 RETURN
800 REM
810 REM ***** CALIBRATION CONSTANTS *****
820 REM
830 K1=4.916*.98 \ REM LVDT CAL, IN @ 10 V, REF. 12, 112.
840 K2=1.22375 \ REM LOAD CAL, V/KG HUNG MASS @ RS=100%, REF. 16,144.
845 K3=.378269 \ REM SST CAL, V/KG HUNG MASS @ RS=100%, REF.16,144.
850 K5=.03504 \ REM BEAM DEFLECTION CONSTANT IN MPA/KG.
860 PRINT \ PRINT "LVDT: ";K1;" IN @ 10V"
865 PRINT "LOAD: ";K2;" V/KG @ RS=100%"
870 PRINT "SST: ";K3;" V/KG @ RS=100%"
880 PRINT "BEAM DEFL: ";K5;" MPA/KG."
890 PRINT \ Y8$="" \ PRINT "UP-TO-DATE"; \ INPUT Y8$ \ IF Y8$<>"Y" THEN 890
895 RETURN
900 REM
910 REM ***** STORE LOAD, SST & STROKE EXTREMA *****
920 REM
930 DIM B1(1,1),C1(1,1),D1(1,1) \ REM LOAD,SST,STROKE.
940 ADRMAX(1,B1,1) \ ADRMAX(1,C1,2) \ ADRMAX(1,D1,3)
950 DIM B2(1,1),C2(1,1),D2(1,1) \ REM LOAD,SST,STROKE.
960 ADRMIN(1,B2,1) \ ADRMIN(1,C2,2) \ ADRMIN(1,D2,3)
970 REM
```

```
980 DIM B3(1,1),C3(1,1),D3(1,1) \ REM LOAD,SST,STROKE: 1ST.
990 ADRMAX(2,B3,1) \ ADRMAX(2,C3,2) \ ADRMAX(2,D3,3)
1000 DIM B4(1,1),C4(1,1),D4(1,1) \ REM LOAD,SST,STROKE: 1ST.
1010 ADRMIN(2,B4,1) \ ADRMIN(2,C4,2) \ ADRMIN(2,D4,3)
1020 RETURN
1100 REM
1110 REM ***** TEST PARAMETERS *****
1120 REM
1130 PRINT  \ PRINT "TEST PARAMETERS:" \ PRINT
1140 PRINT "STRAIN AMPLITUDE"; \ INPUT G1
1175 SI=P2/F1 \ REM SLEEP TIME.
1180 RETURN
1200 REM
1210 REM ***** GENERAL TEST INFO *****
1220 REM
1230 PRINT "NAME OR INITIALS"; \ INPUT M4$
1240 PRINT "MATERIAL"; \ INPUT M2$ \ PRINT "TEMPERATURE, C"; \ INPUT M3$
1250 PRINT "BEAM NUMBER", \ INPUT M5$ \ PRINT "SHIM THICKNESS, MM"; \ INPUT T1
1260 RETURN
1300 REM
1310 REM ***** SPECIFIC TEST INFO *****
1320 REM
1330 PRINT "LOAD RANGE SETTING/100"; \ INPUT R3
1340 PRINT "SST RANGE SETTING/100"; \ INPUT R4
1350 PRINT "STROKE RANGE SETTING/100"; \ INPUT R2
1360 A1=G1*100*T1/(R2*K1*25.4) \ REM ENDLEVEL CALCN.
1370 RETURN
1400 FGSTOP \ ADSTOP \ FGIMMED(1,"RAMP", TIME 2,0) \ REM RETURNS TO SETPT.
1405 CKSTOP
1410 RETURN
1500 REM
1502 REM ***** INTEGERS FOR SCALES *****
1504 REM
1506 REM ***** ABSCISSA MIN *****
1508 REM
1510 IF X1=0 THEN 1518 \ IF X1>0 THEN 1516
1512 X3=10^INT(LOG10(ABS(X1))-1)*INT((ABS(X1)/(10^INT(LOG10(ABS(X1))-1)))+1)
1514 X3=-X3 \ GO TO 1521
1516 X3=10^INT(LOG10(ABS(X1))-1)*INT((ABS(X1)/(10^INT(LOG10(ABS(X1))-1)))-1)
1518 IF X1=0 THEN X3=0
1520 REM
1521 REM ***** ABSCISSA MAX *****
1522 REM
1524 IF X2=0 THEN 1532 \ IF X2>0 THEN 1530
1526 X4=10^INT(LOG10(ABS(X2))-1)*INT((ABS(X2)/(10^INT(LOG10(ABS(X2))-1)))-1)
1528 X4=-X4 \ GO TO 1534
1530 X4=10^INT(LOG10(ABS(X2))-1)*INT((ABS(X2)/(10^INT(LOG10(ABS(X2))-1)))+1)
1532 IF X2=0 THEN X4=0
1534 REM
1535 REM ***** ORDINATE MIN *****
1536 REM
1538 IF Y1=0 THEN 1546 \ IF Y1>0 THEN 1544
1540 Y3=10^INT(LOG10(ABS(Y1))-1)*INT((ABS(Y1)/(10^INT(LOG10(ABS(Y1))-1)))+1)
1542 Y3=-Y3 \ GO TO 1546
1544 Y3=10^INT(LOG10(ABS(Y1))-1)*INT((ABS(Y1)/(10^INT(LOG10(ABS(Y1))-1)))-1)
1546 IF Y1=0 THEN Y3=0
1547 REM
1550 REM ***** ORDINATE MAX *****
1551 REM
1552 IF Y2=0 THEN 1560 \ IF Y2>0 THEN 1558
1554 Y4=10^INT(LOG10(ABS(Y2))-1)*INT((ABS(Y2)/(10^INT(LOG10(ABS(Y2))-1)))-1)
1556 Y4=-Y4 \ GO TO 1560
1558 Y4=10^INT(LOG10(ABS(Y2))-1)*INT((ABS(Y2)/(10^INT(LOG10(ABS(Y2))-1)))+1)
1560 IF Y2=0 THEN Y4=0
1562 REM
1566 SCALE(A2,0,X3,X4,Y3,Y4) \ X5=(X4-X3)/5 \ Y5=(Y4-Y3)/5
```

```
1570 RETURN
1600 REM ***** EXP GRAPHICS (BUSY PLOT) *****
1610 REM
1615 Y8$="" \ PRINT "SKIP BUSY PLOT"; \ INPUT Y8$ \ IF Y8$="Y" THEN RETURN
1620 GOSUB 360 \ REM START A GRAPH.
1630 GOSUB 6000 \ REM COMMENT.
1640 INVEC \ PHYL(A2,55*F9,100*F9,60*F9,100*F9)
1650 GOSUB 3320 \ REM PLOT COM-STRN VS. TIME *****
1721 INVEC \ PHYL(A2,0,40*F9,0,45*F9)
1722 GOSUB 2700 \ REM PLOT LOAD VS STRAIN.
1729 INVEC \ PHYL(A2,55*F9,100*F9,0,45*F9)
1730 GOSUB 2800 \ REM PLOT SST VS. STRAIN.
1740 INVEC \ GO TO 1615 \ REM 'SKIP' QUESTION      \ RETURN
1800 REM
1810 REM SUBTRACT BASELINES, CONVERT UNITS & COMPUTE TIME *****
1811 REM
1812 DIM Z2(1,1),Z3(1,1),Z4(1,1) \ REM BASELINES.
1813 DIM V2(1,1),V3(1,1),V4(1,1) \ REM STD DEV.
1814 Z2(1,1)=S2(1,1)*10*9.8*R3/100/K2 \ REM LOAD.
1815 V2(1,1)=V5(1,1)*10*9.8*R3/100/K2 \ REM LOAD.
1816 Z3(1,1)=S3(1,1)*10*K5*R4/100/K3 \ REM SST.
1817 V3(1,1)=V6(1,1)*10*K5*R4/100/K3 \ REM SST.
1818 Z4(1,1)=S4(1,1)*10*K1*25.4*R2/(10*100*T1) \ REM STRAIN.
1819 V4(1,1)=V7(1,1)*10*K1*25.4*R2/(10*100*T1) \ REM STRAIN.
1820 REM
1822 FOR I=0 TO N1
1830 VA1(I,1)=10*ELEVEL(VA1(I,1))*K1*25.4*R2/(10*100*T1) \ REM COMMAND.
1840 VA1(I,4)=10*ELEVEL(VA1(I,4))*K1*25.4*R2/(10*100*T1)-Z4(1,1) \ REM STRAIN.
1850 VA1(I,2)=10*ELEVEL(VA1(I,2))*9.8*R3/100/K2-Z2(1,1) \ REM LOAD TO NEWTONS.
1860 VA1(I,3)=10*ELEVEL(VA1(I,3))*K5*R4/100/K3-Z3(1,1) \ REM SST TO MPA.
1865 VA1(I,5)=S1+Z1*I \ REM S1 IS SLEEP TIME.
1870 NEXT I
1880 FOR I=0 TO P8
1890 VA2(I,1)=10*ELEVEL(VA2(I,1))*K1*25.4*R2/(10*100*T1) \ REM COMMAND.
1900 VA2(I,4)=10*ELEVEL(VA2(I,4))*K1*25.4*R2/(10*100*T1)-Z4(1,1) \ REM STRAIN.
1910 VA2(I,2)=10*ELEVEL(VA2(I,2))*9.8*R3/100/K2-Z2(1,1) \ REM LOAD TO NEWTONS.
1920 VA2(I,3)=10*ELEVEL(VA2(I,3))*K5*R4/100/K3-Z3(1,1) \ REM SST TO MPA.
1925 VA2(I,5)=Z1*I \ REM TIME FOR 1ST.
1930 NEXT I
1935 RETURN
2000 REM
2010 REM ***** FIX EXTREMA & CONVERT THEIR UNITS *****
2020 REM
2030 IF B3(1,1)>B1(1,1) THEN B1(1,1)=B3(1,1)
2040 IF C3(1,1)>C3(1,1) THEN C1(1,1)=C3(1,1)
2050 IF D3(1,1)>D1(1,1) THEN D1(1,1)=D3(1,1)
2060 REM
2070 IF B4(1,1)<B2(1,1) THEN B2(1,1)=B4(1,1)
2080 IF C4(1,1)<C2(1,1) THEN C2(1,1)=C4(1,1)
2090 IF D4(1,1)<D2(1,1) THEN D2(1,1)=D4(1,1)
2100 REM
2110 D1=(D1(1,1)/32767)*10*K1*25.4*R2/(10*100*T1)-Z4(1,1) \ REM CONV. TO STRN.
2120 D2=(D2(1,1)/32767)*10*K1*25.4*R2/(10*100*T1)-Z4(1,1) \ REM DITTO.
2130 C1=(C1(1,1)/32767)*10*K5*R4/100/K3-Z3(1,1) \ REM CONV. TO MPA.
2140 C2=(C2(1,1)/32767)*10*K5*R4/100/K3-Z3(1,1) \ REM CONV. TO MPA.
2150 B1=(B1(1,1)/32767)*10*9.8*R3/100/K2-Z2(1,1) \ REM CONV. TO NEWTONS.
2160 B2=(B2(1,1)/32767)*10*9.8*R3/100/K2-Z2(1,1) \ REM CONV. TO NEWTONS.
2170 REM
2180 N9=D1-D2 \ REM STRAIN RANGE.
2190 N8=C1-C2 \ REM SST RANGE IN MPA.
2200 N7=B1-B2 \ REM LOAD RANGE IN NEWTONS.
2210 RETURN
2300 REM
2310 REM ***** CHOOSE ENLARGED PLOT *****
2320 REM
2325 S8$="" \ PRINT "SKIP ENLARGED GRAPHICS"; \ INPUT S8$
```

```
2328 IF S8$="" THEN RETURN
2330 S8$="" \ PRINT "WHICH PLOT: SST,STRAIN,LOAD,LD-SST,TBASE"; \ INPUT S8$
2332 IF S8$="TBASE" THEN GOSUB 3220 \ REM SELECT TBASE.
2336 GOSUB 360 \ REM START A GRAPH        \ GOSUB 8000 \ REM COMMENT.
2338 PHYL(A2,0,100*F9,0,70*F9)
2340 IF S8$="SST" THEN GOSUB 2800
2342 IF S8$="STRAIN" THEN GOSUB 2800
2344 IF S8$="LOAD" THEN GOSUB 2700
2350 IF S8$="LD-SST" THEN GOSUB 3000
2362 IF S8$="COM-STR" THEN GOSUB 3320
2363 IF S8$="TLOAD" THEN GOSUB 3600
2364 IF S8$="TSST" THEN GOSUB 3700
2365 GOSUB 3800 \ REM WAIT THEN CLS.
2370 GO TO 2325 \ REM SKIP QUESTION.
2400 REM
2700 REM
2710 REM ***** PLOT LOAD VS. STRAIN *****
2720 REM
2730 X1=D2 \ X2=D1 \ Y1=B2 \ Y2=B1 \ GOSUB 1500 \ REM INT.
2732 GOSUB 470 \ REM AXES        \ GOSUB 2000 \ REM FIX EXTREMA & SCALE
2734 LABEL(A2,"STRAIN","LOAD-N",X5,Y5,1)
2736 FOR I=0 TO N1 \ PLOT(A2,VA1(I,4),VA1(I,2)) \ REM (STRAIN,LOAD)       \ NEXT I
2738 INVEC \ FOR I=0 TO P8 \ PLOT(A2,VA2(I,4),VA2(I,2)) \ REM 1ST       \ NEXT I
2739 RETURN
2800 REM ***** PLOT SST VS STRAIN.
2810 REM
2820 X1=D2 \ X2=D1 \ Y1=C2 \ Y2=C1 \ GOSUB 1500 \ REM INT
2822 GOSUB 470 \ REM AXES        \ GOSUB 2000 \ REM FIX EXTREMA & SCALE
2824 LABEL(A2,"STRAIN","SS-MPA",X5,Y5,1)
2826 FOR I=0 TO N1 \ PLOT(A2,VA1(I,4),VA1(I,3)) \ REM (STRAIN,SST)       \ NEXT I
2828 INVEC \ FOR I=0 TO P8 \ PLOT(A2,VA2(I,4),VA2(I,3)) \ REM 1ST       \ NEXT I
2829 RETURN
2900 REM
2910 REM ***** PLOT STRAIN-COMMAND *****
2920 REM
2922 X1=D2 \ X2=D1 \ Y1=X1 \ Y2=X2 \ GOSUB 1500 \ REM INT
2924 GOSUB 470 \ REM AXES        \ GOSUB 2000 \ REM FIX EXTREMA & SCALE.
2926 LABEL(A2,"COMMAND","STRAIN",X5,Y5,1)
2928 FOR I=0 TO N1 \ PLOT(A2,VA1(I,1),VA1(I,4)) \ REM(COMM,STRN)       \ NEXT I
2929 RETURN
3000 REM
3010 REM ***** PLOT LOAD VS. SST *****
3020 REM
3022 X1=B2 \ X2=B1 \ Y1=C2 \ Y2=C1 \ GOSUB 1500 \ REM INT.
3024 GOSUB 470 \ REM AXES        \ GOSUB 2000 \ REM FIX EXTREMA & SCALE.
3026 LABEL(A2,"LOAD, N","SST, MPA",X5,Y5,1)
3028 FOR I=0 TO N1 \ PLOT(A2,VA1(I,2),VA1(I,3)) \ REM (SST,LD)       \ NEXT I
3030 RETURN
3200 REM
3220 REM ***** TBASE GRAPHICS *****
3240 REM
3280 S8$="" \ PRINT "WHICH TBASE PLOT: COM-STR,TLOAD OR TSST"; \ INPUT S8$
3300 RETURN
3320 REM
3340 REM ***** PLOT COM-STRN VS. TIME *****
3360 REM
3380 X1=VA1(0,5) \ X2=VA1(N1,5) \ Y1=-.2*G1 \ Y2=1.1*G1 \ GOSUB 1500 \ REM INT
3400 GOSUB 470 \ REM AXES        \ GOSUB 2000 \ REM FIX EXTREMA & SCALE
3420 LABEL(A2,"TIME, SEC","COM-STRN",X5,Y5,1)
3440 FOR I=0 TO N1
3460 PLOT(A2,VA1(I,5),VA1(I,1)) \ REM (T,COMM)
3480 N2=ABS(VA1(I,1)-V9) \ IF N2<ABS(.1*G1) THEN 3540 \ REM CRIT FOR MARK.
3500 V9=VA1(I,1) \ REM RESETS V9.
3520 MARK(A2,1,VA1(I,5),VA1(I,4)) \ REM (T,STRAIN)
3540 NEXT I \ INVEC \ RETURN
3600 REM
```

```
3610 REM ***** LOAD VS. TIME *****
3620 REM
3630 X1=VA1(0,5) \ X2=VA1(N1,5) \ Y1=B2 \ Y2=B1 \ GOSUB 1500 \ REM INT
3640 GOSUB 470 \ REM AXES        \ GOSUB 2000 \ REM FIX EXTREMA & SCALE.
3650 LABEL(A2,"TIME, SEC","LOAD, N",X5,Y5,1)
3660 FOR I=0 TO N1 \ PLOT(A2,VA1(I,5),VA1(I,2)) \ REM (T,LD)        \ NEXT I
3670 RETURN
3700 REM
3710 REM ***** PLOT SST VS. TIME *****
3720 REM
3730 X1=VA1(0,5) \ X2=VA1(N1,5) \ Y1=C2 \ Y2=C1 \ GOSUB 1500 \ REM INT
3740 GOSUB 470 \ REM AXES        \ GOSUB 2000 \ REM FIX EXTREMA & SCALE.
3750 LABEL(A2,"TIME, SEC","SS-MPA",X5,Y5,1)
3760 FOR I=0 TO N1 \ PLOT(A2,VA1(I,5),VA1(I,3)) \ REM (T,SST)       \ NEXT I
3770 RETURN
3800 REM
3810 REM ***** WAIT THEN CLS *****
3820 REM
3830 Y8$="" \ INPUT Y8$ \ Y8$="" \ TEKMODE \ VTMODE \ IF A2=2 THEN GROFF(2)
3840 RETURN
3900 REM
3910 REM ***** SUBTRACTOR CIRCUIT *****
3920 REM
3922 DIM S2(1,1),S3(1,1),S4(1,1),V5(1,1),V6(1,1),V7(1,1)
3924 PRINT
3925 Y8$="" \ PRINT "SKIP SUBTRACTOR"; \ INPUT Y8$ \ IF Y8$="Y" THEN RETURN
3930 Q1=200 \ SETDIM VA3(Q1,5) \ REM SETS TOTAL PTS.
3940 GOSUB 1400 \ REM RETURN TO SETPT.
3960 CKTIME(1,.02) \ ADTIMED(3,VA3,,4,1,1,3) \ REM DACQ
3970 PRINT "LOAD,SST & STROKE ZEROED ON DIALS"; \ INPUT Y8$
3990 ADINIT \ ADGO(3) \ IF VA3<Q1 THEN 3990 \ REM ELEGANT STOP.
3995 GOSUB 1400 \ REM RETURNS TO SETPT.
4000 IF Y8$<>"Y" THEN 3970
4010 REM
4020 REM CALCULATE MEANS.
4030 REM
4040 FOR I=0 TO Q1
4050 S2(1,1)=S2(1,1)+VA3(I,2)
4051 S3(1,1)=S3(1,1)+VA3(I,3)
4052 S4(1,1)=S4(1,1)+VA3(I,4)
4060 NEXT I
4070 S2(1,1)=S2(1,1)/(Q1+1)/32767
4071 S3(1,1)=S3(1,1)/(Q1+1)/32767
4072 S4(1,1)=S4(1,1)/(Q1+1)/32767
4080 REM
4090 REM CALCULATE S^2.
4100 REM
4200 FOR I=0 TO Q1 \ REM SUMS OF SQS OF RESIDS.
4210 V5(1,1)=V5(1,1)+(VA3(I,2)/32767-S2(1,1))^2
4220 V6(1,1)=V6(1,1)+(VA3(I,3)/32767-S3(1,1))^2
4230 V7(1,1)=V7(1,1)+(VA3(I,4)/32767-S4(1,1))^2
4240 NEXT I
4241 V5(1,1)=V5(1,1)/Q1
4242 V6(1,1)=V6(1,1)/Q1
4243 V7(1,1)=V7(1,1)/Q1 \ REM SUMS OF SQS OF RESIDS.
4244 PRINT S2(1,1),S3(1,1),S4(1,1)
4245 PRINT V5(1,1),V6(1,1),V7(1,1)
4270 RETURN
4400 REM
4410 REM ***** PRINT NOISE LEVELS *****
4412 REM
4420 PRINT "LOAD NOISE P-P ";4*SQR(V2(1,1));" N (2 SIGMA)."
4430 PRINT "SST NOISE P-P ";4*SQR(V3(1,1));" MPA (2 SIGMA)."
4440 PRINT "STRAIN NOISE P-P ";4*SQR(V4(1,1));" (2 SIGMA)."
4450 RETURN
4500 REM
```

```
4510 REM ***** THE DIFFERENTIATOR *****
4520 REM
4525 Y8$="" \ PRINT "DIFFERENTIATE"; \ INPUT Y8$ \ IF Y8$<>"Y" THEN RETURN
4526 REM
4530 REM 5-PT LS TECHNIQUE, REF. WHITAKER, S. AND  R.L. PIGFORD,
4540 REM IND.ENG.CHEM., 52(2),185-187 (1960).
4560 SETDIM VA5(N1,4) \ REM SR,D(SR)/DT,SSTR,D(SSTR)/DT
4562 SETDIM W4(2,4)
4563 PRINT "GOT THIS FAR!"
4565 REM
4570 FOR I=2 TO N1-2
4580 VA5(I,1)=(-2*VA1(I-2,4)-VA1(I-1,4)+VA1(I+1,4)+2*VA1(I+2,4))/(10*Z1)
4590 VA5(I,3)=(-2*VA1(I-2,3)-VA1(I-1,3)+VA1(I+1,3)+2*VA1(I+2,3))/(10*Z1)
4600 VA5(I,2)=(4*VA1(I-2,4)-VA1(I-1,4)+VA1(I+1,4)+4*VA1(I+2,4))
4610 VA5(I,2)=VA5(I,2)-2*(VA1(I-2,4)+VA1(I-1,4)+VA1(I,4)+VA1(I+1,4)+VA1(I+2,4))
4620 VA5(I,2)=VA5(I,2)/(7*Z1^2)
4630 VA5(I,4)=(4*VA1(I-2,3)-VA1(I-1,3)+VA1(I+1,3)+4*VA1(I+2,3))
4640 VA5(I,4)=VA5(I,4)-2*(VA1(I-2,3)+VA1(I-1,3)+VA1(I,3)+VA1(I+1,3)+VA1(I+2,3))
4650 VA5(I,4)=VA5(I,4)/(7*Z1^2)
4660 REM
4665 REM ***** FIND RATE EXTREMA *****
4666 REM
4690 FOR J=1 TO 4
4695 REM VA5(I,J) CONTAINS SR,D(SR)/DT,SSTR,D(SSTR)/DT FOR J=1-4.
4700 IF VA5(I,J)>W4(1,J) THEN W4(1,J)=VA5(I,J) \ REM MAXIMA.
4710 IF VA5(I,J)<W4(2,J) THEN W4(2,J)=VA5(I,J) \ REM MINIMA.
4720 NEXT J
4730 NEXT I
4740 RETURN
4800 REM
4810 REM ***** CHOOSE RATE PLOT *****
4815 REM
4820 S8$="" \ PRINT "SKIP RATE PLOTS"; \ INPUT S8$ \ IF S8$="Y" THEN RETURN
4830 S8$="" \ PRINT "PLOT: SST-SR,SSTR-STR,SSTR-SR,SST-DSR/DT,DSSTR/DT-STR";
4831 PRINT "OR TBASE"; \ INPUT S8$
4832 GOSUB 360 \ REM START A GRAPH       \ GOSUB 8000 \ REM COMMENT.
4834 PHYL(A2,0,100*F9,0,70*F9)
4840 IF S8$="SST-SR" THEN GOSUB 5010
4850 IF S8$="SSTR-STR" THEN GOSUB 5100
4851 IF S8$="SSTR-SR" THEN GOSUB 5200
4852 IF S8$="SST-DSR/DT" THEN GOSUB 5400
4853 IF S8$="DSSTR/DT-STR" THEN GOSUB 5500
4854 IF S8$="TBASE" THEN GOSUB 10000 \ REM CHOOSE TBASE
4855 IF S8$="SR" THEN GOSUB 10100
4856 IF S8$="DSR/DT" THEN GOSUB 10200
4857 IF S8$="SSTR" THEN GOSUB 10300
4858 IF S8$="DSSTR/DT" THEN GOSUB 10400
4890 GOSUB 3800 \ REM WAIT THEN CLS.
4895 GO TO 4820 \ REM SKIP QUESTION.
5000 REM
5010 REM ***** PLOT SST VS. SR *****
5020 REM
5030 X1=W4(2,1) \ X2=W4(1,1) \ Y1=C2 \ Y2=C1 \ GOSUB 1500 \ REM INT
5040 GOSUB 470 \ REM AXES       \ GOSUB 2000 \ REM FIX EXTREMA & SCALE.
5050 LABEL(A2,"STRAIN RATE, 1/S","SS-MPA",X5,Y5,1)
5060 FOR I=3 TO N1-2 \ PLOT(A2,VA5(I,1),VA1(I,3)) \ REM(SR,SST)       \ NEXT I
5070 RETURN
5100 REM
5110 REM ***** PLOT SSTR VS. STRAIN *****
5120 REM
5130 X1=D2 \ X2=D1 \ Y1=W4(2,3) \ Y2=W4(1,3) \ GOSUB 1500 \ REM INT
5140 GOSUB 470 \ REM AXES       \ GOSUB 2000 \ REM FIX EXTREMA & SCALE.
5150 LABEL(A2,"STRAIN","SSTR IN MPA/S",X5,Y5,1)
5160 FOR I=3 TO N1-2 \ PLOT(A2,VA1(I,4),VA5(I,3)) \ REM (SSTR,STRAIN)       \ NI
5170 RETURN
5200 REM
```

```
5210 REM ***** PLOT SSTR VS. SR *****
5220 REM
5230 X1=W4(2,1) \ X2=W4(1,1) \ Y1=W4(2,3) \ Y2=W4(1,3) \ GOSUB 1500 \ REM INT.
5240 GOSUB 470 \ REM AXES       \ GOSUB 2000 \ REM FIX EXTREMA & SCALE.
5250 LABEL(A2,"STRAIN RATE, 1/S","SSTR IN MPA/S",X5,Y5,1)
5260 FOR I=3 TO N1-2 \ PLOT(A2,VA5(I,1),VA5(I,3)) \ REM (SR,SSTR)      \ NEXT I
5270 RETURN
5400 REM
5410 REM ***** PLOT SST VS. DSR/DT *****
5420 REM
5430 X1=W4(2,2) \ X2=W4(1,2) \ Y1=C2 \ Y2=C1 \ GOSUB 1500 \ REM INT.
5440 GOSUB 470 \ REM AXES       \ GOSUB 2000 \ REM FIX EXTREMA & SCALE.
5450 LABEL(A2,"RATE OF CHANGE OF SR, 1/S/S","SST, MPA",X5,Y5,1)
5460 FOR I=3 TO N1-2 \ PLOT(A2,VA5(I,2),VA1(I,3)) \ REM (DSR/DT,SST)
5470 NEXT I \ RETURN
5500 REM
5510 REM ***** PLOT D(SSTR)/DT VS. STR *****
5520 REM
5530 X1=D2 \ X2=D1 \ Y1=W4(2,4) \ Y2=W4(1,4) \ GOSUB 1500 \ REM INT.
5540 GOSUB 470 \ REM AXES       \ GOSUB 2000 \ REM FIX EXTREMA & SCALE.
5550 LABEL(A2,"STRAIN","DERIV SSTR, MPA/S/S",X5,Y5,1)
5560 FOR I=3 TO N1-2 \ PLOT(A2,VA1(I,4),VA5(I,4)) \ REM (STR,DSSTR/DT)
5570 NEXT I \ RETURN
6000 REM
6010 REM ***** BUSY PLOT COMMENTS *****
6020 REM
6025 INVEC \ PHYL(A2,0,100*F9,0,100*F9) \ SCALE(A2,0,0,100,0,100)
6030 COMM(A2,X1$,1,100) \ REM METHOD & MODE.
6035 COMM(A2,X2$,1,96) \ REM MATERIAL NAME & TEMP.
6040 COMM(A2,X3$,1,92) \ REM BEAM & PROGRAM NUMBERS.
6045 COMM(A2,X4$,1,88) \ REM SHIM THICKNESS
6050 COMM(A2,X5$,1,84) \ REM OPERATOR.
6060 COMM(A2,X6$,1,80) \ REM EXPONENT & STRAIN AMP.
6070 COMM(A2,X7$,1,76) \ REM HALFCYCLE TIME.
6080 COMM(A2,X8$,1,72) \ REM WHICH CYCLES & PTS/CYCLE.
6085 COMM(A2,X9$,1,68) \ REM LOAD-SST-STRAIN RS.
6090 COMM(A2,Y5$,1,64) \ REM LOAD NOISE.
6095 COMM(A2,Y4$,1,60) \ REM SST,STR NOISE.
7010 COMM(A2,Y7$,1,56) \ REM DATE.
7015 COMM(A2,Y6$,1,52) \ REM TIME.
7020 RETURN
8000 REM
8010 REM ***** ENLARGED PLOT COMMENTS *****
8020 REM
8030 INVEC \ PHYL(A2,0,100*F9,0,100*F9) \ SCALE(A2,0,0,100,0,100)
8040 COMM(A2,X1$,1,100) \ REM METHOD & MODE
8050 COMM(A2,X2$,1,96) \ REM MATERIAL NAME & TEMP.
8051 COMM(A2,X3$,1,92) \ REM BEAM & PROGRAM NUMBERS.
8052 COMM(A2,X4$,1,88) \ REM SHIM THICKNESS.
8053 COMM(A2,X5$,1,84) \ REM OPERATOR.
8060 COMM(A2,X6$,1,80) \ REM EXPONENT & STRAIN AMP.
8070 COMM(A2,X7$,50,100) \ REM HALFCYCLE TIME.
8080 COMM(A2,X8$,50,96) \ REM WHICH CYCLES & PTS/CYCLE.
8085 COMM(A2,X9$,50,92) \ REM LOAD-SST-STRAIN RS.
8090 COMM(A2,Y5$,50,88) \ REM LOAD NOISE.
8095 COMM(A2,Y4$,50,84) \ REM SST,STR NOISE.
8100 COMM(A2,Y7$,50,80) \ REM DATE.
8110 COMM(A2,Y6$,50,76) \ REM TIME.
8120 RETURN
8500 REM
8510 REM ***** SAVE TO FLOPPY *****
8520 REM
8530 TEKMODE \ VTMODE
8540 Y8$="" \ PRINT N1+1;"DATA PTS. SAVE"; \ INPUT Y8$
8550 IF Y8$="N" THEN 8650
8560 PRINT "TEST FILENAME"; \ INPUT F1$
```

```
8570 F2$="DU1:"+F1$
8580 A$=F2$ \ GOSUB 9000 \ REM CHECKS FOR PRIORS.
8650 Y8$="" \ PRINT "SAVE 1ST CYCLE"; \ INPUT Y8$
8660 IF Y8$="N" THEN RETURN
8670 PRINT "1ST CYCLE FILENAME"; \ INPUT F3$
8680 F4$="DU1:"+F3$
8690 A$=F4$ \ GOSUB 9000 \ REM CHECKS FOR PRIORS.
8700 RETURN
9000 REM
9010 REM ***** CHECKS FOR PRIORS *****
9020 REM
9030 FINDFILE(A$,S9) \ REM CHECKS FOR EXISTENCE.
9040 Y8$="" \ IF S9<>-8 THEN PRINT A$;" MAY EXIST, OVERWRITE"; \ INPUT Y8$
9050 IF Y8$="N" THEN RETURN
9052 IF A$=F2$ THEN GOSUB 9200
9053 IF A$=F4$ THEN GOSUB 9300
9060 RETURN \ REM DEFAULTS WITH RETURN.
9070 REM
9200 REM
9210 REM ***** SAVE A FILE TO FLOPPY *****
9220 REM
9230 OPEN A$ FOR OUTPUT AS FILE #1 DOUBLE BUF
9240 FOR I=0 TO N1
9245 PRINT #1,VA1(I,1);",";VA1(I,2);",";VA1(I,3);",";VA1(I,4);",";VA1(I,5)
9250 NEXT I
9260 CLOSE
9270 GO TO 9060
9300 REM
9301 REM ***** SAVES FIRST CYCLE TO FLOPPY *****
9302 REM
9303 OPEN A$ FOR OUTPUT AS FILE #2 DOUBLE BUF
9304 FOR I=0 TO P8
9310 PRINT #2;VA2(I,1);",";VA2(I,2);",";VA2(I,3);",";VA2(I,4);",";VA2(I,5)
9320 NEXT I
9330 CLOSE
9340 RETURN
9500 REM
9510 REM ***** PRINT REPORT FOR FILE ON FLOPPY *****
9520 REM
9530 PRINT  \ PRINT  \ PRINT  \ PRINT  \ PRINT "REPORT ON ";F2$;" & ";F4$
9540 PRINT
9550 PRINT X2$,X3$
9560 PRINT X4$,X5$
9570 PRINT X6$,X7$
9580 PRINT X8$,X9$
9590 PRINT Y5$,Y4$
9600 PRINT Y7$,Y6$
9610 PRINT "LVDT CAL= ";K1;" IN @ 10 V."
9620 PRINT "LOAD CAL= ";K2;" V/KG HUNG MASS @ RS 100%"
9630 PRINT "SST CAL= ";K3;" V/KG HUNG MASS @ RS=100%"
9640 PRINT "BEAM DEFLECTION CONST=";K5;" MPA/KG"
9650 PRINT "CAPACITANCE PROBE"; \ INPUT Y8$
9660 PRINT "ATTENUATION METHOD"; \ INPUT Y8$
9665 PRINT "COMMENTS"; \ INPUT Y8$
9670 PRINT  \ PRINT  \ PRINT  \ PRINT  \ PRINT  \ PRINT  \ PRINT  \ PRINT
9680 CLOSE  \ RETURN
10000 REM
10010 REM ***** CHOOSE TBASE DERIV GRAPHICS *****
10020 REM
10030 S8$="" \ PRINT "TBASE PLOT: SR,DSR/DT,SSTR OR DSSTR/DT"; \ INPUT S8$
10040 RETURN
10100 REM
10110 REM ***** PLOT SR VS. TIME *****
10120 REM
10130 X1=VA1(0,5) \ X2=VA1(N1,5) \ Y1=H4(2,1) \ Y2=H4(1,1)
10140 GOSUB 470   REM AXES     \ GOSUB 2000 \ REM FIX EXTREMA & SCALE.
```

```
10150 LABEL(A2,"TIME, SEC","STRAIN RATE, 1/S",X5,Y5,1)
10160 FOR I=3 TO N1-2 \ PLOT(A2,VA1(I,5),VA5(I,1)) \ REM (T,SR)    \ NEXT I
10170 RETURN
10200 REM
10210 REM ***** PLOT D(SR)/DT VS. TIME *****
10220 REM
10230 X1=VA1(0,5) \ X2=VA1(N1,5) \ Y1=W4(2,2) \ Y2=W4(1,2)
10240 GOSUB 470 \ REM AXES     \ GOSUB 2000 \ REM FIX EXTREMA & SCALE.
10250 LABEL(A2,"TIME, SEC","STRAIN RATE, 1/S",X5,Y5,1)
10260 FOR I=3 TO N1-2 \ PLOT(A2,VA1(I,5),VA5(I,2)) \ REM (T,DSR/DT)     \ NEXT I
10270 RETURN
10300 REM
10310 REM ***** PLOT SSTR VS. TIME *****
10320 REM
10330 X1=VA1(0,5) \ X2=VA1(N1,5) \ Y1=W4(2,3) \ Y2=W4(1,3)
10340 GOSUB 470 \ REM AXES     \ GOSUB 2000 \ REM FIX EXTREMA & SCALE.
10350 LABEL(A2,"TIME, SEC","SSTR, MPA/S",X5,Y5,1)
10360 FOR I=3 TO N1-2 \ PLOT(A2,VA1(I,5),VA5(I,3)) \ REM (T,SSTR)     \ NEXT I
10370 RETURN
10400 REM
10410 REM ***** D(SSTR)/DT VS. TIME *****
10420 REM
10430 X1=VA1(0,5) \ X2=VA1(N1,5) \ Y1=W4(2,4) \ Y2=W4(1,4)
10440 LABEL(A2,"TIME, SEC","DERIV SSTR, MPS/S/S",X5,Y5,1)
10450 FOR I=3 TO N1-2 \ PLOT(A2,VA1(I,5),VA5(I,4)) \ REM (T,DSSTR/DT)     \ NEXI
10460 RETURN
30000 REM
30010 REM ***** MATCH TEST & DAP FREQUENCIES *****
30020 REM
30030 TEKMODE \ VTMODE
30040 PRINT "DESIRED FREQUENCY"; \ INPUT F0
30050 Z1=P3/(F0*N1)
30060 IF Z1>1.00000E-03 THEN 30070 \ P3=P3+1 \ GO TO 30050 \ REM TESTS Z1.
30070 CKTIME(1,Z1,Z1)
30080 Z=INT(F0*N1*Z1+1) \ REM ESTIMATES Z.
30090 F1=Z/(N1*Z1) \ REM NEW FREQ.
30100 PRINT "MATCHED FREQUENCY IS ";F1;" HZ."
30110 PRINT P3;" CYCLES REQUIRED."
30120 PRINT "NYQUIST FREQ. OF ";1/2/Z1;" HZ."
30130 PRINT "FREQ RESOLN. OF ";1/(N1+1)/Z1;" HZ."
30140 PRINT "TOTAL POINTS = ";N1+1
30150 Y8$="" \ PRINT "SATISFACTORY"; \ INPUT Y8$
30160 IF Y8$="N" THEN 61
30170 RETURN
30180 REM

Ready
```

APPENDIX 2: Exponential Shear Test Program

```
.TYPE EXP27.BAS
10 REM                         STRONG FLOWS
11 REM
12 REM                              BY
13 REM
14 REM                     A. JEFFREY GIACOMIN
15 REM
16 REM ACKNOWLEDGEMENTS: DR. P. CAIN, S. DOSHI, T. SAMURKAS.
17 REM
20 REM
30 REM ***** STARTING STATEMENTS *****
40 REM
50 GRATTACH(2,2,Y9)
52 GOSUB 700 \ REM STARTING SCREEN.
55 GOSUB 1200 \ REM GET TEST INFO.
58 GOSUB 800 \ REM REVISE CAL CONSTANTS.
61 GOSUB 600 \ REM TOTAL POINTS.
64 SETDIM VA1(N1,5),VA2(P8,5),X(1024)
67 GOSUB 1400 \ REM RETURN TO SETPT.
100 GOSUB 1100 \ REM GET TEST PARAMETERS
101 GOSUB 1300 \ REM GET SPECIFIC TEST INFO.
102 GOSUB 3900 \ REM BASELINES & STD DEVS
103 GOSUB 900 \ REM COLLECTS EXTREMA.
104 REM
105 REM
107 REM ***** PREPARES X(I) FOR FGSHAPE *****
109 REM
110 A1=(100*T1/(R2*K1*25.4))*(EXP(E9*1024*T2/1024)-1) \ REM ENDLEVEL.
111 FOR I=0 TO 1024
112 X(I)=(EXP(E9*I*T2/1024)-1)/(EXP(E9*1024*T2/1024)-1) \ REM X(I) NORMALIZED.
114 NEXT I
115 REM
125 CKTIME(1,2*T2/P9,Z1) \ REM CYCLE TIME/PTS PER CYCLE.
130 FGSHAPE(1,X) \ FGREPT(1,"AUX", TIME T2,2*P1,A1,0)
140 ADTIMED(2,VA1,,4,1,1,3) \ ADTIMED(1,VA2,,4,1,1,3) \ REM DACQ.
142 PRINT \ Y8$="" \ PRINT "'RUN'"; \ INPUT Y8$ \ IF Y8$<>"RUN" THEN 142
144 FGGO \ ADINIT \ ADGO(1) \ REM COLLECTS 1ST.
150 ETIME \ SLEEP(S1) \ ADINIT \ ADGO(2) \ REM DELAYS DACQ UNTIL S1.
160 IF VA1<N1 THEN 160 \ REM ELEGANT STOP.
180 GOSUB 1400 \ REM RETURNS TO SETPT.
182 REM
183 REM ***** POST TEST PROCESSING *****
184 REM
188 GOSUB 1800 \ REM CONV UNITS & COMP TIME.
190 GOSUB 2000 \ REM FIX EXTREMA & CONV UNITS.
192 GOSUB 4400 \ REM PRINT NOISE LEVELS        \ GOSUB 3800 \ REM WAIT THEN CL.
193 GOSUB 540 \ REM COMMENT PREP.
194 GOSUB 1600 \ REM DRAWS BUSY PLOT         \ GOSUB 3800 \ REM WAIT THEN CLS.
200 GOSUB 2300 \ REM DRAWS EXPANDED PLOT        \ GOSUB 3800 \ REM WAIT THEN CLS
210 GOSUB 4500 \ REM DIFFERENTIATES          \ GOSUB 3800 \ REM WAIT THEN CLS.
220 GOSUB 4800 \ REM DRAWS RATE PLOTS         \ GOSUB 3800 \ REM WAIT THEN CLS.
230 GOSUB 8500 \ REM SAVE TO FLOPPY
240 GOSUB 9500 \ REM PRINT REPORT.          \ GOSUB 3800 \ REM WAIT THEN CLS.
340 END
350 REM
360 REM ***** START A GRAPH *****
370 REM
380 TEKMODE \ VTMODE \ PRINT "VT-240 (1) OR PLOTTER (2)"; \ INPUT A2
390 F9=1 \ IF A2=2 THEN PRINT "FRACTION OF FULLSIZE (.75)"; \ INPUT F9
400 Y8$="" \ IF A2=1 THEN 430
410 IF A2=2 THEN PRINT "PAPER INSERTED AND PEN READY"; \ INPUT Y8$
420 IF Y8$<>"Y" THEN 410 \ REM GOES TO PREV LINE.
```

```
430 IF A2=1 THEN TEKMODE(1,1)
440 IF A2=2 THEN GRON(2) \ IF A2=2 THEN SIZE(A2,108*F9,216*F9)
450 INVEC(A2) \ RETURN
470 REM
480 REM ***** AXES *****
490 REM
500 AXES(A2,0,0) \ AXES(A2,1.00000E+08,1.00000E+08)
510 AXES(A2,-1.00000E+08,-1.00000E+08)
520 RETURN
530 REM
540 REM ***** COMMENT PREP *****
550 REM
560 WHOAMI(A$) \ X1$="MTS/PPR+SST, MODE: EXP"
561 X2$=M2$+" (T= "+M3$+" C)" \ REM MATERIAL NAME & TEMP.
562 X3$="BEAM "+M5$+", PGM: "+A$ \ REM BEAM & PROGRAM NUMBERS.
563 X4$=STR$(T1)+" MM SHIM"
564 REM SHIM THICKNESS & LOAD-SST-STRAIN RANGE SETTINGS.
565 X5$="BY : "+M4$ \ REM OPERATOR.
566 X6$="EXP= "+STR$(E9)+"/S, SA="+STR$(G1)
567 X7$=STR$(T2)+" S/HALFCYCLE."
568 X8$="CYCLES 1, "+STR$(P2+1)+"-"+STR$(P2+P3)+", "+STR$(P9)+" PPC"
569 X9$="RS: "+STR$(R3)+"-"+STR$(R4)+"-"+STR$(R2)
570 Y5$="NOISE(4S P-P): "+STR$(4*SQR(V2(1,1)))+"N," \ REM LOAD NOISE.
572 Y4$=STR$(4*SQR(V3(1,1)))+" MPA, "+STR$(4*SQR(V4(1,1))) \ REM SST,STR NOISE.
575 GDATE(Y9,M9,D9) \ Y7$="DATE: "+STR$(Y9)+"-"+STR$(M9)+"-"+STR$(D9)
576 GTIME(S9,M9,H9) \ Y6$="TIME: "+STR$(H9)+":"+STR$(M9)+":"+STR$(S9)
590 RETURN
600 REM
610 REM ***** NUMBER OF DATA POINTS *****
620 REM
630 PRINT \ PRINT "FOR FFT CHOOSE 2,4,8,16,32,64,128,256,512,1014 ..."
640 PRINT "POINTS PER CYCLE"; \ INPUT P9
650 PRINT "COLLECT AFTER CYCLE NUMBER"; \ INPUT P2
660 PRINT "HOW MANY CYCLES"; \ INPUT P3
662 PRINT "PERIODS OF RELAXATION"; \ INPUT P4
670 N1=(P3+P4)*P9-1 \ REM TOTAL POINTS.        \ P8=P9-1 \ REM POINTS IN 1ST CY.
675 P1=P2+P3 \ REM TOTAL CYCLES.
680 RETURN
700 REM
701 REM ***** STARTING SCREEN *****
702 REM
709 TEKMODE \ VTMODE \ WHOAMI(A$) \ PRINT "PROGRAM: ";A$ \ PRINT
710 GDATE(Y9,M9,D9) \ PRINT "DATE: ";Y9;"-";M9;"-";D9
720 GTIME(S9,M9,H9) \ PRINT "TIME: ";H9;":";M9;":";S9 \ PRINT
730 PRINT "ZERO LOAD, STROKE AND SST"
740 PRINT "SET SPANS 1 & 2 AT 0 & 1." \ PRINT
750 RETURN
800 REM
810 REM ***** CALIBRATION CONSTANTS *****
820 REM
830 K1=4.916*.98 \ REM LVDT CAL, IN @ 10 V, REF. 12, 112.
840 K2=.956562 \ REM LOAD CAL, V/KG HUNG MASS @ RS=100%, REF. 14,45.
845 K3=.448503 \ REM SST CAL, V/KG HUNG MASS @ RS=100%, REF.14,45.
850 K5=.03504 \ REM BEAM DEFLECTION CONSTANT IN MPA/KG.
860 PRINT \ PRINT "LVDT: ";K1;" IN @ 10V"
865 PRINT "LOAD: ";K2;" V/KG @ RS=100%"
870 PRINT "SST: ";K3;" V/KG @ RS=100%"
880 PRINT "BEAM DEFL: ";K5;" MPA/KG."
890 PRINT \ Y8$="" \ PRINT "UP-TO-DATE"; \ INPUT Y8$ \ IF Y8$<>"Y" THEN 890
895 RETURN
900 REM
910 REM ***** STORE LOAD, SST & STROKE EXTREMA *****
920 REM
930 DIM B1(1,1),C1(1,1),D1(1,1) \ REM LOAD,SST,STROKE.
940 ADRMAX(1,B1,1) \ ADRMAX(1,C1,2) \ ADRMAX(1,D1,3)
950 DIM B2(1,1),C2(1,1),D2(1,1) \ REM LOAD,SST,STROKE.
```

```
960 ADRMIN(1,B2,1) \ ADRMIN(1,C2,2) \ ADRMIN(1,D2,3)
970 REM
980 DIM B3(1,1),C3(1,1),D3(1,1) \ REM LOAD,SST,STROKE: 1ST.
990 ADRMAX(2,B3,1) \ ADRMAX(2,C3,2) \ ADRMAX(2,D3,3)
1000 DIM B4(1,1),C4(1,1),D4(1,1) \ REM LOAD,SST,STROKE: 1ST.
1010 ADRMIN(2,B4,1) \ ADRMIN(2,C4,2) \ ADRMIN(2,D4,3)
1020 RETURN
1100 REM
1110 REM ***** TEST PARAMETERS *****
1120 REM
1130 PRINT ' \ PRINT "TEST PARAMETERS:" \ PRINT
1140 PRINT "STRAIN AMPLITUDE"; \ INPUT G1
1160 PRINT "EXPONENT, 1/S"; \ INPUT E9
1170 T2=(LOG(G1+1))/E9 \ REM HALFCYCLE TIME.
1175 S1=P2*2*T2 \ REM SLEEP TIME.
1180 RETURN
1200 REM
1210 REM ***** GENERAL TEST INFO *****
1220 REM
1230 PRINT "NAME OR INITIALS"; \ INPUT M4$
1240 PRINT "MATERIAL"; \ INPUT M2$ \ PRINT "TEMPERATURE, C"; \ INPUT M3$
1250 PRINT "BEAM NUMBER"; \ INPUT M5$ \ PRINT "SHIM THICKNESS, MM"; \ INPUT T1
1260 RETURN
1300 REM
1310 REM ***** SPECIFIC TEST INFO *****
1320 REM
1330 PRINT "LOAD RANGE SETTING/100"; \ INPUT R3
1340 PRINT "SST RANGE SETTING/100"; \ INPUT R4
1350 PRINT "STROKE RANGE SETTING/100"; \ INPUT R2
1370 RETURN
1400 FGSTOP \ ADSTOP \ FGIMMED(1,"RAMP", TIME 2,0) \ REM RETURNS TO SETPT.
1405 CKSTOP
1410 RETURN
1500 REM
1502 REM ***** INTEGERS FOR SCALES *****
1504 REM
1506 REM ***** ABSCISSA MIN *****
1508 REM
1510 IF X1=0 THEN 1518 \ IF X1>0 THEN 1516
1512 X3=10^INT(LOG10(ABS(X1))-1)*INT((ABS(X1)/(10^INT(LOG10(ABS(X1))-1)))+1)
1514 X3=-X3 \ GO TO 1521
1516 X3=10^INT(LOG10(ABS(X1))-1)*INT((ABS(X1)/(10^INT(LOG10(ABS(X1))-1)))-1)
1518 IF X1=0 THEN X3=0
1520 REM
1521 REM ***** ABSCISSA MAX *****
1522 REM
1524 IF X2=0 THEN 1532 \ IF X2>0 THEN 1530
1526 X4=10^INT(LOG10(ABS(X2))-1)*INT((ABS(X2)/(10^INT(LOG10(ABS(X2))-1)))-1)
1528 X4=-X4 \ GO TO 1534
1530 X4=10^INT(LOG10(ABS(X2))-1)*INT((ABS(X2)/(10^INT(LOG10(ABS(X2))-1)))+1)
1532 IF X2=0 THEN X4=0
1534 REM
1535 REM ***** ORDINATE MIN *****
1536 REM
1538 IF Y1=0 THEN 1546 \ IF Y1>0 THEN 1544
1540 Y3=10^INT(LOG10(ABS(Y1))-1)*INT((ABS(Y1)/(10^INT(LOG10(ABS(Y1))-1)))+1)
1542 Y3=-Y3 \ GO TO 1546
1544 Y3=10^INT(LOG10(ABS(Y1))-1)*INT((ABS(Y1)/(10^INT(LOG10(ABS(Y1))-1)))-1)
1546 IF Y1=0 THEN Y3=0
1547 REM
1550 REM ***** ORDINATE MAX *****
1551 REM
1552 IF Y2=0 THEN 1560 \ IF Y2>0 THEN 1558
1554 Y4=10^INT(LOG10(ABS(Y2))-1)*INT((ABS(Y2)/(10^INT(LOG10(ABS(Y2))-1)))-1)
1556 Y4=-Y4 \ GO TO 1560
1558 Y4=10^INT(LOG10(ABS(Y2))-1)*INT((ABS(Y2)/(10^INT(LOG10(ABS(Y2))-1)))+1)
```

```
1560 IF Y2=0 THEN Y4=0
1562 REM
1566 SCALE(A2,0,X3,X4,Y3,Y4) \ X5=(X4-X3)/5 \ Y5=(Y4-Y3)/5
1570 RETURN
1600 REM ***** EXP GRAPHICS (BUSY PLOT) *****
1610 REM
1615 Y8$="" \ PRINT "SKIP BUSY PLOT"; \ INPUT Y8$ \ IF Y8$="Y" THEN RETURN
1620 GOSUB 360 \ REM START A GRAPH.
1630 GOSUB 6000 \ REM COMMENT.
1640 INVEC(A2) \ PHYL(A2,50*F9,100*F9,60*F9,100*F9)
1650 GOSUB 3320 \ REM PLOT COM-STRN VS. TIME *****
1721 INVEC(A2) \ PHYL(A2,0,40*F9,0,45*F9)
1722 GOSUB 2700 \ REM PLOT LOAD VS STRAIN.
1729 INVEC(A2) \ PHYL(A2,55*F9,100*F9,0,45*F9)
1730 GOSUB 2800 \ REM PLOT SST VS. STRAIN.
1740 INVEC(A2) \ GO TO 1615 \ REM 'SKIP' QUESTION         \ RETURN
1800 REM
1810 REM SUBTRACT BASELINES, CONVERT UNITS & COMPUTE TIME *****
1811 REM
1812 DIM Z2(1,1),Z3(1,1),Z4(1,1) \ REM BASELINES.
1813 DIM V2(1,1),V3(1,1),V4(1,1) \ REM STD DEV.
1814 Z2(1,1)=S2(1,1)*10*9.8*R3/100/K2 \ REM LOAD.
1815 V2(1,1)=V5(1,1)*10*9.8*R3/100/K2 \ REM LOAD.
1816 Z3(1,1)=S3(1,1)*10*K5*R4/100/K3 \ REM SST.
1817 V3(1,1)=V6(1,1)*10*K5*R4/100/K3 \ REM SST.
1818 Z4(1,1)=S4(1,1)*10*K1*25.4*R2/(10*100*T1) \ REM STRAIN.
1819 V4(1,1)=V7(1,1)*10*K1*25.4*R2/(10*100*T1) \ REM STRAIN.
1820 REM
1822 FOR I=0 TO N1
1830 VA1(I,1)=10*ELEVEL(VA1(I,1))*K1*25.4*R2/(10*100*T1) \ REM COMMAND.
1840 VA1(I,4)=10*ELEVEL(VA1(I,4))*K1*25.4*R2/(10*100*T1)-Z4(1,1) \ REM STRAIN.
1850 VA1(I,2)=10*ELEVEL(VA1(I,2))*9.8*R3/100/K2-Z2(1,1) \ REM LOAD TO NEWTONS.
1860 VA1(I,3)=10*ELEVEL(VA1(I,3))*K5*R4/100/K3-Z3(1,1) \ REM SST TO MPA.
1865 VA1(I,5)=S1+Z1*I \ REM S1 IS SLEEP TIME.
1870 NEXT I
1880 FOR I=0 TO P8
1890 VA2(I,1)=10*ELEVEL(VA2(I,1))*K1*25.4*R2/(10*100*T1) \ REM COMMAND.
1900 VA2(I,4)=10*ELEVEL(VA2(I,4))*K1*25.4*R2/(10*100*T1)-Z4(1,1) \ REM STRAIN.
1910 VA2(I,2)=10*ELEVEL(VA2(I,2))*9.8*R3/100/K2-Z2(1,1) \ REM LOAD TO NEWTONS.
1920 VA2(I,3)=10*ELEVEL(VA2(I,3))*K5*R4/100/K3-Z3(1,1) \ REM SST TO MPA.
1925 VA2(I,5)=Z1*I \ REM TIME FOR 1ST.
1930 NEXT I
1935 RETURN
2000 REM
2010 REM ***** FIX EXTREMA & CONVERT THEIR UNITS *****
2020 REM
2030 IF B3(1,1)>B1(1,1) THEN B1(1,1)=B3(1,1)
2040 IF C3(1,1)>C3(1,1) THEN C1(1,1)=C3(1,1)
2050 IF D3(1,1)>D1(1,1) THEN D1(1,1)=D3(1,1)
2060 REM
2070 IF B4(1,1)<B2(1,1) THEN B2(1,1)=B4(1,1)
2080 IF C4(1,1)<C2(1,1) THEN C2(1,1)=C4(1,1)
2090 IF D4(1,1)<D2(1,1) THEN D2(1,1)=D4(1,1)
2100 REM
2110 D1=(D1(1,1)/32767)*10*K1*25.4*R2/(10*100*T1)-Z4(1,1) \ REM CONV. TO STRN.
2120 D2=(D2(1,1)/32767)*10*K1*25.4*R2/(10*100*T1)-Z4(1,1) \ REM DITTO.
2130 C1=(C1(1,1)/32767)*10*K5*R4/100/K3-Z3(1,1) \ REM CONV. TO MPA.
2140 C2=(C2(1,1)/32767)*10*K5*R4/100/K3-Z3(1,1) \ REM CONV. TO MPA.
2150 B1=(B1(1,1)/32767)*10*9.8*R3/100/K2-Z2(1,1) \ REM CONV. TO NEWTONS.
2160 B2=(B2(1,1)/32767)*10*9.8*R3/100/K2-Z2(1,1) \ REM CONV. TO NEWTONS.
2170 REM
2180 N9=D1-D2 \ REM STRAIN RANGE.
2190 N8=C1-C2 \ REM SST RANGE IN MPA.
2200 N7=B1-B2 \ REM LOAD RANGE IN NEWTONS.
2210 RETURN
2300 REM
```

```
2310 REM ***** CHOOSE ENLARGED PLOT *****
2320 REM
2325 S8$="" \ PRINT "SKIP ENLARGED GRAPHICS"; \ INPUT S8$
2328 IF S8$="Y" THEN RETURN
2330 S8$="" \ PRINT "WHICH PLOT; SST,STRAIN,LOAD,LD-SST,TBASE"; \ INPUT S8$
2332 IF S8$="TBASE" THEN GOSUB 3220 \ REM SELECT TBASE.
2336 GOSUB 360 \ REM START A GRAPH          \ GOSUB 8000 \ REM REPRINT.
2338 PHYL(A2,0,100*F9,0,70*F9)
2340 IF S8$="SST" THEN GOSUB 2800
2342 IF S8$="STRAIN" THEN GOSUB 2900
2344 IF S8$="LOAD" THEN GOSUB 2700.
2350 IF S8$="LD-SST" THEN GOSUB 3000
2362 IF S8$="COM-STR" THEN GOSUB 3320
2363 IF S8$="TLOAD" THEN GOSUB 3600
2364 IF S8$="TSST" THEN GOSUB 3700
2365 GOSUB 3800 \ REM WAIT THEN CLS
2370 GO TO 2325 \ REM SKIP QUESTION.
2400 REM
2700 REM
2710 REM ***** PLOT LOAD VS. STRAIN *****
2720 REM
2730 X1=D2 \ X2=D1 \ Y1=B2 \ Y2=B1 \ GOSUB 1500 \ REM INT
2732 GOSUB 470 \ REM AXES         \ GOSUB 2000 \ REM FIX EXTREMA & SCALE
2734 LABEL(A2,"STRAIN","LOAD-N",X5,Y5,1)
2736 FOR I=0 TO N1 \ PLOT(A2,VA1(I,4),VA1(I,2)) \ REM (STRAIN,LOAD)          \ NI
2738 INVEC(A2) \ FOR I=0 TO P8 \ PLOT(A2,VA2(I,4),VA2(I,2)) \ REM 1ST          \I
2739 RETURN
2800 REM ***** PLOT SST VS STRAIN.
2810 REM
2820 X1=D2 \ X2=D1 \ Y1=C2 \ Y2=C1 \ GOSUB 1500 \ REM INT.
2822 GOSUB 470 \ REM AXES         \ GOSUB 2000 \ REM FIX EXTREMA & SCALE
2824 LABEL(A2,"STRAIN","SS-MPA",X5,Y5,1)
2826 FOR I=0 TO N1 \ PLOT(A2,VA1(I,4),VA1(I,3)) \ REM (STRAIN,SST)          \ NEXI
2828 INVEC(A2) \ FOR I=0 TO P8 \ PLOT(A2,VA2(I,4),VA2(I,3)) \ REM 1ST          \I
2829 RETURN
2900 REM
2910 REM ***** PLOT STRAIN-COMMAND *****
2920 REM
2922 X1=D2 \ X2=D1 \ Y1=X1 \ Y2=X2 \ GOSUB 1500 \ REM INT
2924 GOSUB 470 \ REM AXES         \ GOSUB 2000 \ REM FIX EXTREMA & SCALE.
2926 LABEL(A2,"COMMAND","STRAIN",X5,Y5,1)
2928 FOR I=0 TO N1 \ PLOT(A2,VA1(I,1),VA1(I,4)) \ REM(COMM,STRN)          \ NEXTI
2929 RETURN
3000 REM
3010 REM ***** PLOT LOAD VS. SST *****
3020 REM
3022 X1=B2 \ X2=B1 \ Y1=C2 \ Y2=C1 \ GOSUB 1500 \ REM INT.
3024 GOSUB 470 \ REM AXES         \ GOSUB 2000 \ REM FIX EXTREMA & SCALE.
3026 LABEL(A2,"LOAD, N","SST, MPA",X5,Y5,1)
3028 FOR I=0 TO N1 \ PLOT(A2,VA1(I,2),VA1(I,3)) \ REM (SST,LD)          \ NEXT I
3030 RETURN
3200 REM
3220 REM ***** TBASE GRAPHICS *****
3240 REM
3280 S8$="" \ PRINT "WHICH TBASE PLOT: COM-STR,TLOAD OR TSST"; \ INPUT S8$
3300 RETURN
3320 REM
3340 REM ***** PLOT COM-STRN VS. TIME *****
3360 REM
3380 X1=VA1(0,5) \ X2=VA1(N1,5) \ Y1=-.2*G1 \ Y2=1.2*G1 \ GOSUB 1500 \ REM INT
3400 GOSUB 470 \ REM AXES         \ GOSUB 2000 \ REM FIX EXTREMA & SCALE
3420 LABEL(A2,"TIME, SEC","COM-STRN",X5,Y5,1)
3440 FOR I=0 TO N1
3460 PLOT(A2,VA1(I,5),VA1(I,1)) \ REM (T,COMM)
3480 N2=ABS(VA1(I,1)-V9) \ IF N2<ABS(.1*G1) THEN 3540 \ REM CRIT FOR MARK.
3500 V9=VA1(I.1) \ REM RESETS V9.
```

```
3520 MARK(A2,1,VA1(I,5),VA1(I,4)) \ REM (T,STRAIN)
3540 NEXT I \ INVEC(A2) \ RETURN
3600 REM
3610 REM ***** LOAD VS. TIME *****
3620 REM
3630 X1=VA1(0,5) \ X2=VA1(N1,5) \ Y1=B2 \ Y2=B1 \ GOSUB 1500 \ REM INT
3640 GOSUB 470 \ REM AXES           \ GOSUB 2000 \ REM FIX EXTREMA & SCALE.
3650 LABEL(A2,"TIME, SEC","LOAD, N",X5,Y5,1)
3660 FOR I=0 TO N1 \ PLOT(A2,VA1(I,5),VA1(I,2)) \ REM (T,LD)          \ NEXT I
3670 RETURN
3700 REM
3710 REM ***** PLOT SST VS. TIME *****
3720 REM
3730 X1=VA1(0,5) \ X2=VA1(N1,5) \ Y1=C2 \ Y2=C1 \ GOSUB 1500 \ REM INT
3740 GOSUB 470 \ REM AXES           \ GOSUB 2000 \ REM FIX EXTREMA & SCALE.
3750 LABEL(A2,"TIME, SEC","SS-MPA",X5,Y5,1)
3760 FOR I=0 TO N1 \ PLOT(A2,VA1(I,5),VA1(I,3)) \ REM (T,SST)         \ NEXT I
3770 RETURN
3800 REM
3810 REM ***** WAIT THEN CLS *****
3820 REM
3830 Y8$="" \ INPUT Y8$ \ Y8$="" \ TEKMODE \ VTMODE \ IF A2=2 THEN GROFF(2)
3840 RETURN
3900 REM
3910 REM ***** SUBTRACTOR CIRCUIT *****
3920 REM
3922 DIM S2(1,1),S3(1,1),S4(1,1),V5(1,1),V6(1,1),V7(1,1)
3924 PRINT
3925 Y8$="" \ PRINT "SKIP SUBTRACTOR"; \ INPUT Y8$ \ IF Y8$="Y" THEN RETURN
3930 Q1=200 \ SETDIM VA3(Q1,5) \ REM SETS TOTAL PTS.
3940 GOSUB 1400 \ REM RETURN TO SETPT.
3960 CKTIME(1,.02) \ ADTIMED(3,VA3,,4,1,1,3) \ REM DACQ
3970 PRINT "LOAD,SST & STROKE ZEROED ON DIALS"; \ INPUT Y8$
3990 ADINIT \ ADGO(3) \ IF VA3<Q1 THEN 3990 \ REM ELEGANT STOP.
3995 GOSUB 1400 \ REM RETURNS TO SETPT.
4000 IF Y8$<>"Y" THEN 3970
4010 REM
4020 REM CALCULATE MEANS.
4030 REM
4040 FOR I=0 TO Q1
4050 S2(1,1)=S2(1,1)+VA3(I,2)
4051 S3(1,1)=S3(1,1)+VA3(I,3)
4052 S4(1,1)=S4(1,1)+VA3(I,4)
4060 NEXT I
4070 S2(1,1)=S2(1,1)/(Q1+1)/32767
4071 S3(1,1)=S3(1,1)/(Q1+1)/32767
4072 S4(1,1)=S4(1,1)/(Q1+1)/32767
4080 REM
4090 REM CALCULATE S^2.
4100 REM
4200 FOR I=0 TO Q1 \ REM SUMS OF SQS OF RESIDS.
4210 V5(1,1)=V5(1,1)+(VA3(I,2)/32767-S2(1,1))^2
4220 V6(1,1)=V6(1,1)+(VA3(I,3)/32767-S3(1,1))^2
4230 V7(1,1)=V7(1,1)+(VA3(I,4)/32767-S4(1,1))^2
4240 NEXT I
4241 V5(1,1)=V5(1,1)/Q1
4242 V6(1,1)=V6(1,1)/Q1
4243 V7(1,1)=V7(1,1)/Q1 \ REM SUMS OF SQS OF RESIDS.
4244 PRINT S2(1,1),S3(1,1),S4(1,1)
4245 PRINT V5(1,1),V6(1,1),V7(1,1)
4270 RETURN
4400 REM
4410 REM ***** PRINT NOISE LEVELS *****
4412 REM
4420 PRINT "LOAD NOISE P-P ";4*SQR(V2(1,1));" N (2 SIGMA)."
4430 PRINT "SST NOISE P-P ";4*SQR(V3(1,1));" MPA (2 SIGMA)."
```

```
4440 PRINT "STRAIN NOISE P-P ";4*SQR(V4(1,1));" (2 SIGMA)."
4450 RETURN
4500 REM
4510 REM ***** THE DIFFERENTIATOR *****
4520 REM
4525 Y8$="" \ PRINT"DIFFERENTIATE"; \ INPUT Y8$ \ IF Y8$<>"Y" THEN RETURN
4526 REM
4530 REM 5-PT LS TECHNIQUE, REF. WHITAKER, S. AND  R.L. PIGFORD,
4540 REM IND.ENG.CHEM., 52(2),185-187 (1960).
4560 SETDIM VA5(N1,4) \ REM SR,D(SR)/DT,SSTR,D(SSTR)/DT
4562 SETDIM W4(2,4)
4563 PRINT "GOT THIS FAR!"
4565 REM
4570 FOR I=2 TO N1-2
4580 VA5(I,1)=(-2*VA1(I-2,4)-VA1(I-1,4)+VA1(I+1,4)+2*VA1(I+2,4))/(10*Z1)
4590 VA5(I,3)=(-2*VA1(I-2,3)-VA1(I-1,3)+VA1(I+1,3)+2*VA1(I+2,3))/(10*Z1)
4600 VA5(I,2)=(4*VA1(I-2,4)-VA1(I-1,4)+VA1(I+1,4)+4*VA1(I+2,4))
4610 VA5(I,2)=VA5(I,2)-2*(VA1(I-2,4)+VA1(I-1,4)+VA1(I,4)+VA1(I+1,4)+VA1(I+2,4))
4620 VA5(I,2)=VA5(I,2)/(7*Z1^2)
4630 VA5(I,4)=(4*VA1(I-2,3)-VA1(I-1,3)+VA1(I+1,3)+4*VA1(I+2,3))
4640 VA5(I,4)=VA5(I,4)-2*(VA1(I-2,3)+VA1(I-1,3)+VA1(I,3)+VA1(I+1,3)+VA1(I+2,3))
4650 VA5(I,4)=VA5(I,4)/(7*Z1^2)
4652 NEXT I
4660 REM
4665 REM ***** FIND RATE EXTREMA *****
4666 REM
4668 FOR I=0 TO N1
4690 FOR J=1 TO 4
4695 REM VA5(I,J) CONTAINS SR,D(SR)/DT,SSTR,D(SSTR)/DT FOR J=1-4.
4700 IF VA5(I,J)>W4(1,J) THEN W4(1,J)=VA5(I,J) \ REM MAXIMA.
4710 IF VA5(I,J)<W4(2,J) THEN W4(2,J)=VA5(I,J) \ REM MINIMA.
4720 NEXT J
4730 NEXT I
4740 RETURN
4800 REM
4810 REM ***** CHOOSE RATE PLOT *****
4815 REM
4820 S8$="" \ PRINT "SKIP RATE PLOTS"; \ INPUT S8$ \ IF S8$="Y" THEN RETURN
4830 S8$="" \ PRINT "PLOT: SST-SR,SSTR-STR,SSTR-SR,SST-DSR/DT,DSSTR/DT-STR";
4831 PRINT "OR TBASE"; \ INPUT S8$
4832 GOSUB 360 \ REM START A GRAPH          \ GOSUB 8000 \ REM COMMENT.
4834 PHYL(A2,0,100*F9,0,70*F9) \
4840 IF S8$="SST-SR" THEN GOSUB 5000
4850 IF S8$="SSTR-STR" THEN GOSUB 5100
4851 IF S8$="SSTR-SR" THEN GOSUB 5200
4852 IF S8$="SST-DSR/DT" THEN GOSUB 5400
4853 IF S8$="DSSTR/DT-STR" THEN GOSUB 5600
4854 IF S8$="TBASE" THEN GOSUB 10000 \ REM CHOOSE TBASE
4855 IF S8$="SR" THEN GOSUB 10100
4856 IF S8$="DSR/DT" THEN GOSUB 10200
4857 IF S8$="SSTR" THEN GOSUB 10300
4858 IF S8$="DSSTR/DT" THEN GOSUB 10400
4890 GOSUB 3800 \ REM WAIT THEN CLS.
4895 GO TO 4820 \ REM SKIP QUESTION.
5000 REM
5010 REM ***** PLOT SST VS. SR *****
5020 REM
5030 X1=W4(2,1) \ X2=W4(1,1) \ Y1=C2 \ Y2=C1 \ GOSUB 1500 \ REM INT
5040 GOSUB 470 \ REM AXES          \ GOSUB 2000 \ REM FIX EXTREMA & SCALE.
5050 LABEL(A2,"STRAIN RATE, 1/S","SS-MPA",X5,Y5,1)
5060 FOR I=3 TO N1-2 \ PLOT(A2,VA5(I,1),VA1(I,3)) \ REM(SR,SST)        \ NEXT I
5070 RETURN
5100 REM
5110 REM ***** PLOT SSTR VS. STRAIN *****
5120 REM
5130 X1=D2 \ X2=D1 \ Y1=W4(2.3) \ Y2=W4(1.3) \ GOSUB 1500 \ REM INT
```

```
5140 GOSUB 470 \ REM AXES          \ GOSUB 2000 \ REM FIX EXTREMA & SCALE.
5150 LABEL(A2,"STRAIN","SSTR IN MPA/S",X5,Y5,1)
5160 FOR I=3 TO N1-2 \ PLOT(A2,VA1(I,4),VA5(I,3)) \ REM (SSTR,STRAIN)          \I
5170 RETURN
5200 REM
5210 REM ***** PLOT SSTR VS. SR *****
5220 REM
5230 X1=W4(2,1) \ X2=W4(1,1) \ Y1=W4(2,3) \ Y2=W4(1,3) \ GOSUB 1500 \ REM INT.
5240 GOSUB 470 \ REM AXES          \ GOSUB 2000 \ REM FIX EXTREMA & SCALE.
5250 LABEL(A2,"STRAIN RATE, 1/S","SSTR IN MPA/S",X5,Y5,1)
5260 FOR I=3 TO N1-2 \ PLOT(A2,VA5(I,1),VA5(I,3)) \ REM (SR,SSTR)          \ NEXTI
5270 RETURN
5400 REM
5410 REM ***** PLOT SST VS. DSR/DT *****
5420 REM
5430 X1=W4(2,2) \ X2=W4(1,2) \ Y1=C2 \ Y2=C1 \ GOSUB 1500 \ REM INT.
5440 GOSUB 470 \ REM AXES          \ GOSUB 2000 \ REM FIX EXTREMA & SCALE.
5450 LABEL(A2,"RATE OF CHANGE OF SR, 1/S/S","SST, MPA",X5,Y5,1)
5460 FOR I=3 TO N1-2 \ PLOT(A2,VA5(I,2),VA1(I,3)) \ REM (DSR/DT,SST)
5470 NEXT I \ RETURN
5500 REM
5510 REM ***** PLOT D(SSTR)/DT VS. STR *****
5520 REM
5530 X1=D2 \ X2=D1 \ Y1=W4(2,4) \ Y2=W4(1,4) \ GOSUB 1500 \ REM INT.
5540 GOSUB 470 \ REM AXES          \ GOSUB 2000 \ REM FIX EXTREMA & SCALE.
5550 LABEL(A2,"STRAIN","DERIV SSTR, MPA/S/S",X5,Y5,1)
5560 FOR I=3 TO N1-2 \ PLOT(A2,VA1(I,4),VA5(I,4)) \ REM (STR,DSSTR/DT)
5570 NEXT I \ RETURN
6000 REM
6010 REM ***** BUSY PLOT COMMENTS *****
6020 REM
6025 INVEC(A2) \ PHYL(A2,0,100*F9,0,100*F9) \ SCALE(A2,0,0,100,0,100)
6030 COMM(A2,X1$,1,100) \ REM METHOD & MODE.
6035 COMM(A2,X2$,1,96) \ REM MATERIAL NAME & TEMP.
6040 COMM(A2,X3$,1,92) \ REM BEAM & PROGRAM NUMBERS.
6045 COMM(A2,X4$,1,88) \ REM SHIM THICKNESS
6050 COMM(A2,X5$,1,84) \ REM OPERATOR.
6060 COMM(A2,X6$,1,80) \ REM EXPONENT & STRAIN AMP.
6070 COMM(A2,X7$,1,76) \ REM HALFCYCLE TIME.
6080 COMM(A2,X8$,1,72) \ REM WHICH CYCLES & PTS/CYCLE.
6085 COMM(A2,X9$,1,68) \ REM LOAD-SST-STRAIN RS.
6090 COMM(A2,Y5$,1,64) \ REM LOAD NOISE.
6095 COMM(A2,Y4$,1,60) \ REM SST,STR NOISE.
7010 COMM(A2,Y7$,1,56) \ REM DATE.
7015 COMM(A2,Y6$,1,52) \ REM TIME.
7020 RETURN
8000 REM
8010 REM ***** ENLARGED PLOT COMMENTS *****
8020 REM
8030 INVEC(A2) \ PHYL(A2,0,100*F9,0,100*F9) \ SCALE(A2,0,0,100,0,100)
8040 COMM(A2,X1$,1,100) \ REM METHOD & MODE
8050 COMM(A2,X2$,1,96) \ REM MATERIAL NAME & TEMP.
8051 COMM(A2,X3$,1,92) \ REM BEAM & PROGRAM NUMBERS.
8052 COMM(A2,X4$,1,88) \ REM SHIM THICKNESS.
8053 COMM(A2,X5$,1,84) \ REM OPERATOR.
8060 COMM(A2,X6$,1,80) \ REM EXPONENT & STRAIN AMP.
8070 COMM(A2,X7$,50,100) \ REM HALFCYCLE TIME.
8080 COMM(A2,X8$,50,96) \ REM WHICH CYCLES & PTS/CYCLE.
8085 COMM(A2,X9$,50,92) \ REM LOAD-SST-STRAIN RS.
8090 COMM(A2,Y5$,50,88) \ REM LOAD NOISE.
8095 COMM(A2,Y4$,50,84) \ REM SST,STR NOISE.
8100 COMM(A2,Y7$,50,80) \ REM DATE.
8110 COMM(A2,Y6$,50,76) \ REM TIME.
8120 RETURN
8500 REM
8510 REM ***** SAVE TO FLOPPY *****
```

```
8520 REM
8530 TEKMODE \ VTMODE
8540 Y8$="" \ PRINT N1;"DATA PTS. SAVE"; \ INPUT Y8$
8550 IF Y8$="N" THEN 8650
8560 PRINT "TEST FILENAME"; \ INPUT F1$
8570 F2$="DU1:"+F1$
8580 A$=F2$ \ GOSUB 9000 \ REM CHECKS FOR PRIORS.
8650 Y8$="" \ PRINT "SAVE 1ST CYCLE"; \ INPUT Y8$
8660 IF Y8$="N" THEN RETURN
8670 PRINT "1ST CYCLE FILENAME"; \ INPUT F3$
8680 F4$="DU1:"+F3$
8690 A$=F4$ \ GOSUB 9000 \ REM CHECKS FOR PRIORS.
8700 RETURN
9000 REM
9010 REM ***** CHECKS FOR PRIORS *****
9020 REM
9030 FINDFILE(A$,S9) \ REM CHECKS FOR EXISTENCE.
9040 Y8$="" \ IF S9<>-8 THEN PRINT A$;" MAY EXIST, OVERWRITE"; \ INPUT Y8$
9050 IF Y8$<>"Y" THEN GOSUB 9200
9060 RETURN \ REM DEFAULTS WITH RETURN.
9070 REM
9200 REM
9210 REM ***** SAVE A FILE TO FLOPPY *****
9220 REM
9230 OPEN A$ FOR OUTPUT AS FILE #1 DOUBLE BUF
9240 FOR I=0 TO N1
9245 PRINT #1,VA1(I,1);",";VA1(I,2);",";VA1(I,3);",";VA1(I,4);",";VA1(I,5)
9250 NEXT I
9260 CLOSE
9270 RETURN
9500 REM
9510 REM ***** PRINT REPORT FOR FILE ON FLOPPY *****
9520 REM
9530 PRINT  \ PRINT  \ PRINT  \ PRINT  \ PRINT "REPORT ON ";F2$;" & ";F4$
9540 PRINT
9550 PRINT X2$,X3$
9560 PRINT X4$,X5$
9570 PRINT X6$,X7$
9580 PRINT X8$,X9$
9590 PRINT Y5$,Y4$
9600 PRINT Y7$,Y6$
9610 PRINT "LVDT CAL= ";K1;" IN @ 10 V."
9620 PRINT "LOAD CAL= ";K2;" V/KG HUNG MASS @ RS 100%"
9630 PRINT "SST CAL= ";K3;" V/KG HUNG MASS @ RS=100%"
9640 PRINT "BEAM DEFLECTION CONST=";K5;" MPA/KG"
9650 PRINT "CAPACITANCE PROBE"; \ INPUT Y8$
9660 PRINT "ATTENUATION METHOD"; \ INPUT Y8$
9670 PRINT  \ PRINT  \ PRINT  \ PRINT
9680 CLOSE  \ RETURN
10000 REM
10010 REM ***** CHOOSE TBASE DERIV GRAPHICS *****
10020 REM
10030 S8$="" \ PRINT "TBASE PLOT: SR,DSR/DT,SSTR OR DSSTR/DT"; \ INPUT S8$
10040 RETURN
10100 REM
10110 REM ***** PLOT SR VS. TIME *****
10120 REM
10130 X1=VA1(0,5) \ X2=VA1(N1,5) \ Y1=W4(2,1) \ Y2=W4(1,1)
10140 GOSUB 470 \ REM AXES        \ GOSUB 2000 \ REM FIX EXTREMA & SCALE.
10150 LABEL(A2,"TIME, SEC","STRAIN RATE, 1/S",X5,Y5,1)
10160 FOR I=3 TO N1-2 \ PLOT(A2,VA1(I,5),VA5(I,1)) \ REM (T,SR)       \ NEXT I
10170 RETURN
10200 REM
10210 REM ***** PLOT D(SR)/DT VS. TIME *****
10220 REM
10230 X1=VA1(0.5) \ X2=VA1(N1.5) \ Y1=W4(2.2) \ Y2=W4(1.2)
```

```
10240 GOSUB 470 \ REM AXES        \ GOSUB 2000 \ REM FIX EXTREMA & SCALE.
10250 LABEL(A2,"TIME, SEC","STRAIN RATE, 1/S",X5,Y5,1)
10260 FOR I=3 TO N1-2 \ PLOT(A2,VA1(I,5),VA5(I,2)) \ REM (T,DSR/DT)       \ NEXI
10270 RETURN
10300 REM
10310 REM ***** PLOT SSTR VS. TIME *****
10320 REM
10330 X1=VA1(0,5) \ X2=VA1(N1,5) \ Y1=H4(2,3) \ Y2=H4(1,3)
10340 GOSUB 470 \ REM AXES       \ GOSUB 2000 \ REM FIX EXTREMA & SCALE.
10350 LABEL(A2,"TIME, SEC","SSTR, MPA/S",X5,Y5,1)
10360 FOR I=3 TO N1-2 \ PLOT(A2,VA1(I,5),VA5(I,3)) \ REM (T,SSTR)        \ NEXTI
10370 RETURN
10400 REM
10410 REM ***** D(SSTR)/DT VS. TIME *****
10420 REM
10430 X1=VA1(0,5) \ X2=VA1(N1,5) \ Y1=H4(2,4) \ Y2=H4(1,4)
10440 LABEL(A2,"TIME, SEC","DERIV SSTR, MPS/S/S",X5,Y5,1)
10450 FOR I=3 TO N1-2 \ PLOT(A2,VA1(I,5),VA5(I,4)) \ REM (T,DSSTR/DT)       \ NI
10460 RETURN
10600 REM
10610 REM ***** INTEGRATOR: TRAP RULE *****
10620 REM
10621 Y8$="" \ PRINT "INTEGRATE"; \ INPUT Y8$ \ IF Y8$<>"Y" THEN RETURN
10625 SETDIM (H9(N1+1,2)) \ REM H9(I,1)=INT(SST)DG & H9(I,2)=INT(LOAD)DG
10630 FOR I=0 TO N1
10640 H9(I,1)=H9(I-1,1)+(VA1(I,4)-VA1(I-1,4))*(VA1(I,3)+VA1(I-1,3))/2
10650 H9(I,2)=H9(I-1,2)+(VA1(I,4)-VA1(I-1,4))*(VA1(I,2)+VA1(I-2,2))/2
10660 NEXT I
10670 H9(N1+1,1)=H9(N1,1)+(VA1(N1,4)-VA1(0,4))*(VA1(N1,3)+VA1(0,3))/2
10680 H9(N1+1,2)=H9(N1,2)+(VA1(N1,4)-VA1(0,4))*(VA1(N1,2)+VA1(0,2))/2
10690 REM
```

APPENDIX 3: Program for Spectral Analysis

```
.TYPE FSST40.TXT,FSTR40.TXT,FTF40.TXT
10 REM   SPECTRAL ANALYSIS OF SHEAR STRESS FOR OSCILLATORY SHEAR
20 REM
30 REM                              BY
40 REM
50 REM                       A. JEFFREY GIACOMIN
60 REM
70 REM ACKNOWLEDGEMENTS: DR. P. CAIN, S. DOSHI.
90 REM
95 GRATTACH(2,2,Y9)
100 TEKMODE \ VTMODE
102 PRINT  \ PRINT "TOTAL POINTS (<1024)": \ INPUT N1
105 SETDIM S(N1),X(N1+2)
106 DIM R(2),I(2)
108 SETDIM VA1(N1,5)
110 SETDIM VA2(N1+2,2)
120 GOSUB 21340 \ REM SELECT FREQUENCY.
125 GOSUB 21230 \ REM NUMBER OF CYCLES & T1.
128 GOSUB 30000 \ REM READ DATA FILE.
135 REM
140 REM ***** POST TEST PROCESSING *****
145 REM
146 GOSUB 25200 \ REM PREPARE COMMENTS.
155 GOSUB 24000 \ REM REMOVE DC OFFSET.
160 GOSUB 20430 \ REM USE HANNING WINDOW.
165 GOSUB 22500 \ REM FIND STRESS & STRAIN EXTREMA.
170 GOSUB 22000 \ REM PLOT WINDOWED DATA    \ GOSUB 3800 \ REM WAIT THEN CLS.
172 GOSUB 24600 \ REM NORMALIZE X(I)
174 GOSUB 22700 \ REM CONV TO BIN, INTEGERIZE.
180 GOSUB 20530 \ REM PERFORM FFT.
185 GOSUB 22900 \ REM SCALE, CONVERT BACK TO ENGG UNITS.
187 GOSUB 24700 \ REM PLOT SPECTRUM IN RECT COORDS.
190 GOSUB 20640 \ REM PLOT AMP SPECTRUM   \ GOSUB 3800 \ REM WAIT THEN CLS.
195 GOSUB 31000 \ REM PLOT LOG-AMP SPECTRUM
200 GOSUB 23000 \ REM PREPARE FOR PHASE SPECTRUM
210 GOSUB 23200 \ REM PLOT CUT-OFF PHASE SPECTRUM  \ GOSUB 3800
220 GOSUB 26000 \ REM PLOT CUT-OFF AMP SPECTRUM    \ GOSUB 3800
230 GOSUB 31500 \ REM PRINT FFT REPORT ON CUT-OFF SPECTRUM.
240 GOSUB 32000 \ REM STATISTICAL NOISE ANALYSIS.
250 GOSUB 32200 \ REM PLOT AMP SPECTRUM WITH CONF LIMS.
260 GOSUB 32500 \ REM PRINT REPORT ON NOISE SUBTRACTED SPECTRUM.
330 STOP
340 END
350 REM
360 REM ***** START A GRAPH *****
370 REM
380 TEKMODE \ VTMODE \ PRINT "VT-240 (1) OR PLOTTER (2)"; \ INPUT A2
390 F9=1 \ IF A2=2 THEN PRINT "FRACTION OF FULLSIZE (.75)"; \ INPUT F9
400 Y8$="" \ IF A2=1 THEN 430
410 IF A2=2 THEN PRINT "PAPER INSERTED AND PEN READY"; \ INPUT Y8$
420 IF Y8$<>"Y" THEN 410 \ REM GOES TO PREV LINE.
430 IF A2=1 THEN TEKMODE(1,1)
440 IF A2=2 THEN GRON(2) \ IF A2=2 THEN SIZE(A2,108*F9.216*F9)
450 INVEC(A2) \ RETURN
470 REM
480 REM ***** AXES *****
490 REM
500 AXES(A2,0,0) \ AXES(A2,1.00000E+08,1.00000E+08)
510 AXES(A2,-1.00000E+08,-1.00000E+08)
520 RETURN
530 REM
```

```
540 REM ***** LOG-AXES *****
550 REM
555 AXES(A2,0,1)
560 AXES(A2,1.00000E+08,1.00000E+08) \ AXES(A2,1.00000E-08,1.00000E-08)
570 RETURN
700 REM
701 REM ***** STARTING SCREEN *****
702 REM
709 TEKMODE \ VTMODE \ WHOAMI(A$) \ PRINT "PROGRAM: ";A$ \ PRINT
710 GDATE(Y9,M9,D9) \ PRINT "DATE: ";Y9;"-";M9;"-";D9
720 GTIME(S9,M9,H9) \ PRINT "TIME: ";H9;":";M9;":";S9 \ PRINT
730 PRINT "ZERO LOAD, STROKE AND SST"
740 PRINT "SET SPANS 1 & 2 AT 0 & 1." \ PRINT
750 RETURN
1500 REM
1502 REM ***** INTEGERS FOR SCALES *****
1504 REM
1506 REM ***** AUGMENT SCALING LIMITS ****
1508 REM
1510 IF X2=1/2/T1 THEN 1514 \ REM SKIP AUGMENT FOR FREQ AXIS.
1512 X1=X1-ABS(X1-X2)/10 \ X2=X2+ABS(X1-X2)/10
1514 Y1=Y1-ABS(Y1-Y2)/10 \ Y2=Y2+ABS(Y1-Y2)/10
1559 REM
1560 REM ***** ABSCISSA MIN *****
1561 REM
1562 IF X1=0 THEN 1566 \ IF X1>0 THEN 1565
1563 X3=10^INT(LOG10(ABS(X1))-1)*INT((ABS(X1)/(10^INT(LOG10(ABS(X1))-1)))+1)
1564 X3=-X3 \ GO TO 1568
1565 X3=10^INT(LOG10(ABS(X1))-1)*INT((ABS(X1)/(10^INT(LOG10(ABS(X1))-1)))-1)
1566 IF X1=0 THEN X3=0
1567 REM
1568 REM ***** ABSCISSA MAX *****
1569 REM
1570 IF X2=0 THEN 1574 \ IF X2>0 THEN 1573
1571 X4=10^INT(LOG10(ABS(X2))-1)*INT((ABS(X2)/(10^INT(LOG10(ABS(X2))-1)))-1)
1572 X4=-X4 \ GO TO 1575
1573 X4=10^INT(LOG10(ABS(X2))-1)*INT((ABS(X2)/(10^INT(LOG10(ABS(X2))-1)))+1)
1574 IF X2=0 THEN X4=0
1575 REM
1576 REM ***** ORDINATE MIN *****
1577 REM
1578 IF Y1=0 THEN 1582 \ IF Y1>0 THEN 1581
1579 Y3=10^INT(LOG10(ABS(Y1))-1)*INT((ABS(Y1)/(10^INT(LOG10(ABS(Y1))-1)))+1)
1580 Y3=-Y3 \ GO TO 1582
1581 Y3=10^INT(LOG10(ABS(Y1))-1)*INT((ABS(Y1)/(10^INT(LOG10(ABS(Y1))-1)))-1)
1582 IF Y1=0 THEN Y3=0
1583 REM
1584 REM ***** ORDINATE MAX *****
1585 REM
1586 IF Y2=0 THEN 1590 \ IF Y2>0 THEN 1589
1587 Y4=10^INT(LOG10(ABS(Y2))-1)*INT((ABS(Y2)/(10^INT(LOG10(ABS(Y2))-1)))-1)
1588 Y4=-Y4 \ GO TO 1590
1589 Y4=10^INT(LOG10(ABS(Y2))-1)*INT((ABS(Y2)/(10^INT(LOG10(ABS(Y2))-1)))+1)
1590 IF Y2=0 THEN Y4=0
1591 REM
1592 X5=ABS(X4-X3)/5 \ Y5=ABS(Y4-Y3)/5
1593 IF X2=1/2/T1 THEN RETURN \ REM DO NOT SCALE FOR FREQ DOMAIN.
1594 SCALE(A2,0,X3,X4,Y3,Y4) \ X5=(X4-X3)/5 \ Y5=(Y4-Y3)/5
1597 RETURN
3800 REM
3810 REM ***** WAIT THEN CLS *****
3820 REM
3830 Y8$="" \ INPUT Y8$ \ Y8$="" \ TEKMODE \ VTMODE \ IF A2=2 THEN GROFF(2)
3840 RETURN
4500 REM
6000 REM
```

```
6010 REM ***** BUSY PLOT COMMENTS *****
6020 REM
6025 INVEC(A2) \ PHYL(A2,0,100*F9,0,100*F9) \ SCALE(A2,0,0,100.0,100)
6030 COMM(A2,X1$,1,100) \ REM METHOD & MODE.
6035 COMM(A2,X2$,1,96) \ REM MATERIAL NAME & TEMP.
6040 COMM(A2,X3$,1,92) \ REM BEAM & PROGRAM NUMBERS.
6045 COMM(A2,X4$,1,88) \ REM SHIM THICKNESS
6050 COMM(A2,X5$,1,84) \ REM OPERATOR.
6060 COMM(A2,X6$,1,80) \ REM EXPONENT & STRAIN AMP.
6070 COMM(A2,X7$,1,76) \ REM HALFCYCLE TIME.
6080 COMM(A2,X8$,1,72) \ REM WHICH CYCLES & PTS/CYCLE.
6085 COMM(A2,X9$,1,68) \ REM LOAD-SST-STRAIN RS.
6090 COMM(A2,Y5$,1,64) \ REM LOAD NOISE.
6095 COMM(A2,Y4$,1,60) \ REM SST,STR NOISE.
7010 COMM(A2,Y7$,1,56) \ REM DATE.
7015 COMM(A2,Y6$,1,52) \ REM TIME.
7020 RETURN
8000 REM
8010 REM ***** ENLARGED PLOT COMMENTS *****
8020 REM
8030 INVEC(A2) \ PHYL(A2,0,100*F9,0,100*F9) \ SCALE(A2,0,0,100,0,100)
8040 COMM(A2,X1$,1,100) \ REM METHOD & MODE
8050 COMM(A2,X2$,1,96) \ REM MATERIAL NAME & TEMP.
8051 COMM(A2,X3$,1,92) \ REM BEAM & PROGRAM NUMBERS.
8052 COMM(A2,X4$,1,88) \ REM SHIM THICKNESS.
8060 COMM(A2,X6$,1,80) \ REM EXPONENT & STRAIN AMP.
8070 COMM(A2,X7$,1,76) \ REM HALFCYCLE TIME.
8120 RETURN
8500 REM
8510 REM ***** SAVE TO FLOPPY *****
8520 REM
8530 TEKMODE \ VTMODE
8540 Y8$="" \ PRINT N1;"DATA PTS. SAVE"; \ INPUT Y8$
8550 IF Y8$="N" THEN 8650
8560 PRINT "TEST FILENAME"; \ INPUT F1$
8570 F2$="DU1:"+F1$
8580 A$=F2$ \ GOSUB 9000 \ REM CHECKS FOR PRIORS.
8650 Y8$="" \ PRINT "SAVE 1ST CYCLE"; \ INPUT Y8$
8660 IF Y8$="N" THEN RETURN
8670 PRINT "1ST CYCLE FILENAME"; \ INPUT F3$
8680 F4$="DU1:"+F3$
8690 A$=F4$ \ GOSUB 9000 \ REM CHECKS FOR PRIORS.
8700 RETURN
9000 REM
9010 REM ***** CHECKS FOR PRIORS *****
9020 REM
9030 FINDFILE(A$,S9) \ REM CHECKS FOR EXISTENCE.
9040 Y8$="" \ IF S9<>-8 THEN PRINT A$;" MAY EXIST, OVERWRITE"; \ INPUT Y8$
9050 IF Y8$<>"Y" THEN GOSUB 9200
9060 RETURN \ REM DEFAULTS WITH RETURN.
9070 REM
9200 REM
9210 REM ***** SAVE A FILE TO FLOPPY *****
9220 REM
9230 OPEN A$ FOR OUTPUT AS FILE #1 DOUBLE BUF
9240 FOR I=0 TO N1-1 \ PRINT #1,VA1(I,1),VA1(I,2),VA1(I,3),VA1(I,4),VA1(I,5)
9250 NEXT I
9260 CLOSE
9270 RETURN
9500 REM
9510 REM ***** PRINT REPORT FOR FILE ON FLOPPY *****
9520 REM
9530 PRINT \ PRINT \ PRINT \ PRINT \ PRINT "REPORT ON ";F2$;" & ";F4$
9540 PRINT
9550 PRINT X2$,X3$
9560 PRINT X4$,X5$
```

```
9570 PRINT X6$,X7$
9580 PRINT X8$,X9$
9590 PRINT Y5$,Y4$
9600 PRINT Y7$,Y6$
9610 PRINT "LVDT CAL= ";K1;" IN @ 10 V."
9620 PRINT "LOAD CAL= ";K2;" V/KG HUNG MASS @ RS 100%"
9630 PRINT "SST CAL= ";K3;" V/KG HUNG MASS @ RS=100%"
9640 PRINT "BEAM DEFLECTION CONST=";K5;" MPA/KG"
9650 PRINT "CAPACITANCE PROBE"; \ INPUT Y8$
9660 PRINT "ATTENUATION METHOD"; \ INPUT Y8$
9670 PRINT  \ PRINT  \ PRINT  \ PRINT
9680 CLOSE  \ RETURN
20000 REM
20430 REM
20440 REM ***** HANNING WINDOW FOR STRESS (REF. 14,8) *****
20450 REM
20451 Y8$="" \ PRINT "WINDOW: HANNING (1) OR RECT (2)"; \ INPUT Y8$
20455 FOR I=0 TO N1-1
20490 IF Y8$="1" THEN X(I)=VA1(I,3)*.5*(1-COS(2*PI*I/(N1-1))) \ REM HANNING WIN.
20491 IF Y8$="2" THEN X(I)=VA1(I,3) \ REM RECT WINDOW.
20496 NEXT I
20500 RETURN
20530 REM
20540 REM ***** FORWARD FFT *****
20550 REM
20560 PRINT "FORWARD FFT IN PROGRESS"
20570 X=0
20575 SINS(S,N1) \ REM PRECALCULATES SINE-COSINE TABLE.
20580 PACK(X(0),N1)
20590 FFTI(0,X(0),X(0))
20600 UNPK(X(0),N1)
20620 R(2)=2*2^X*X(2*Z)/32767 \ I(2)=2*2^X*X(2*Z+1)/32767
20630 RETURN
20640 REM
20650 REM ***** PLOT AMPLITUDE SPECTRUM *****
20660 REM
20670 TEKMODE \ ERASE
20680 GOSUB 360 \ REM START A GRAPH  \ GOSUB 8000 \ REM COMMENT.
20684 PHYL(A2,0,100*F9,0,70*F9)
20685 GOSUB 31300 \ REM MAX AMP.
20686 REM H9=H9/40  \ REM BLOW UP CRESTS.
20688 SCALE(A2,0,0,1/(2*T1),0,1.1*H9)
20692 LABEL(A2,'FREQUENCY, HZ','SST AMP-MPA',1/10/T1,1.1*H9/5,1)
20696 GOSUB 470 \ REM AXES
20704 FOR I=0 TO N1-1 STEP 2
20708 A=2*SQR(X(I)^2+X(I+1)^2)
20712 PLOT(A2,I/N1/2/T1,A) \ REM (FREQ,AMP)
20713 NEXT I
20716 INVEC(A2) \ PLOT(A2,1/(3*T1),0) \ PLOT(A2,1/(3*T1),1.1*H9)
20720 RETURN
20820 REM
20830 REM ***** REAL/IMAG. GRAPHICS ****
20840 REM
20850 INVEC(A2)
20860 TEKMODE(1,1) \ ERASE
20870 PHYL(A2,0,100,0,90)
20880 SCALE(A2,1,-.2,.2,-.2,.2)
20890 LABEL(A2,"REAL","IMAGINARY",1/5,1/5,1)
20900 GOSUB 20380 \ REM AXES
20910 FOR I=1 TO 2
20920 PLOT(A2,0,0) \ PLOT(A2,R(I),I(I))
20930 MARK(1,I,R(I),I(I))
20940 NEXT I
20950 INPUT A9$
20960 VTMODE
20970 A1=ATN(I(1)/R(1)) \ A2=ATN(I(2)/R(2))
```

```
20980 S=SQR(R(1)^2+I(1)^2) \ T=SQR(R(2)^2+I(2)^2)
20990 PRINT 'STRAIN PHASE =';A1,'STRESS PHASE =';A2
21000 REM T0 IS SCALE FACTOR FOR STRESS
21010 T0=1
21020 REM S0 IS SCALE FACTOR FOR STRAIN
21030 S0=1
21040 PRINT "G'=";T*T0*COS(A2-A1)/S/S0,'G"=';T*T0*SIN(A2-A1)/S/S0
21050 PRINT ' <CR> TO CONTINUE'; \ INPUT A$
21060 TEKMODE \ ERASE
21070 PHYL(A2,0,100,0,45)
21080 SCALE(A2,1,0,40*F1,.01,10)
21090 LABEL(A2,'FREQUENCY','G*',1/10/T1,10,1)
21100 FOR J=1 TO N1/2
21110 G=T0*SQR(VA2(J*2,2)^2+VA2(J*2+1,2)^2)/S0/SQR(VA2(J*2,1)^2+VA2(J*2+1,2)^2)
21120 PLOT(A2,J/N1/T1,G)
21130 NEXT J
21140 PHYL(A2,0,100,55,90)
21150 SCALE(A2,1,0,40*F1,-2,2)
21160 LABEL(A2,'FREQUENCY','TAN DELTA',1/10/T1,10,1)
21170 FOR J=0 TO N1/2
21180 A=ATN(VA2(2*J+1,2)/VA2(2*J,2))-ATN(VA2(2*J+1,1)/VA2(2*J,1))
21190 PLOT(A2,J/T1/N1,A)
21200 NEXT J
21210 GO TO 4140
21220 FGSTOP \ END
21230 REM
21240 REM ***** MATCH TEST & DAP FREQUENCIES FOR FFT *****
21250 REM
21260 PRINT "NUMBER OF CYCLES"; \ INPUT C
21270 T1=(C/F1)/NI \ REM DT.
21330 RETURN
21340 REM
21350 REM ***** SELECT FREQUENCY *****
21360 REM
21370 VTMODE \ PRINT "FREQUENCY, HZ"; \ INPUT F1
21380 RETURN
21390 REM
21400 REM ***** SIMULATE DATA IN VA1 *****
21410 REM
21420 Y8$="" \ PRINT "SKIP SIMULATION"; \ INPUT Y8$ \ IF Y8$="Y" THEN RETURN
21440 FOR I=0 TO N1
21450 VA1(I,5)=I*C/F1/INT(N1*N2) \ REM TIME
21455 IF I>N1*N2 THEN 21500 \ REM ZERO AFTER C CYCLES.
21460 VA1(I,4)=G1*COS(2*PI*F1*VA1(I,5)) \ REM STRAIN.
21470 VA1(I,3)=L1(1)*COS(2*PI*F1*VA1(I,5)+D1(1)) \ REM STRESS FUNDAMENTAL.
21475 VA1(I,3)=VA1(I,3)+L1(2)*COS(2*2*PI*F1*VA1(I,5)+D1(2)) \ REM STRESS, 2ND.
21480 VA1(I,3)=VA1(I,3)+L1(3)*COS(3*2*PI*F1*VA1(I,5)+D1(3)) \ REM STRESS, 3RD.
21490 VA1(I,3)=VA1(I,3)+(B1/2)*(2*RND-1)
21495 VA1(I,3)=VA1(I,3)+L1(0) \ REM DC OFFSET STRESS.
21500 NEXT I
21510 RETURN
21520 REM
21530 REM ***** PARAMETERS FOR HARMONICALLY RELATED COSINUSOIDS *****
21540 REM
21550 DIM L1(10),D1(10)
21560 PRINT "STRAIN AMPLITUDE"; \ INPUT G1
21570 PRINT "STRESS AMPLITUDE FUNDAMENTAL, MPA"; \ INPUT L1(1)
21575 PRINT "STRESS AMPLITUDE, 2ND HARMONIC, MPA"; \ INPUT L1(2)
21580 PRINT "STRESS AMPLITUDE, 3RD HARMONIC, MPA"; \ INPUT L1(3)
21590 PRINT "PHASE LAG OF FUNDAMENTAL, RADS"; \ INPUT D1(1)
21595 PRINT "PHASE LAG OF 2ND HARMONIC, RADS"; \ INPUT D1(2)
21600 PRINT "PHASE LAG OF 3RD HARMONIC, RADS"; \ INPUT D1(3)
21605 PRINT "DC OFFSET STRESS, MPA"; \ INPUT L1(0)
21610 PRINT "BROADBAND NOISE (P-P) IN STRESS, MPA"; \ INPUT B1
21615 PRINT "FRACTION OF TOTAL POINTS IN";C;" CYCLES"; \ INPUT N2
21620 RETURN
```

```
22000 REM
22010 REM ***** SELECT WINDOW PLOT *****
22020 REM
22030 Y8$="" \ PRINT "SKIP WINDOW PLOTS"; \ INPUT Y8$ \ IF Y8$="Y" THEN RETURN
22040 Y8$="" \ PRINT "WINDOWED STRESS OR STRAIN"; \ INPUT Y8$
22045 GOSUB 360 \ REM START A GRAPH   \ GOSUB 8000 \ REM COMMENT.
22048 PHYL(A2,0,F9*100,0,F9*70)
22050 IF Y8$="STRESS" THEN GOSUB 22100
22090 REM
22100 REM ***** PLOT RECTANGULARLY WINDOWED STRESS WAVE *****
22110 REM
22120 X1=VA1(0,5) \ X2=VA1(N1-1,5) \ Y1=M8(1) \ Y2=M8(2) \ GOSUB 1500 \ REM INT
22130 GOSUB 470 \ REM AXES
22140 LABEL(A2,"TIME, SEC","STRESS, MPA",X5,Y5,1)
22150 FOR I=0 TO N1-1 \ PLOT(A2,VA1(I,5),VA1(I,3)) \ REM SIMUL(T,SST)   \ NEXT I
22155 REM
22160 REM ***** PLOT HANNING WINDOWED STRESS WAVE *****
22170 INVEC(A2)
22180 FOR I=0 TO N1-1 \ PLOT(A2,VA1(I,5),X(I)) \ REM SIMUL(T,HAM-SST)    \ NEXTI
22190 RETURN
22500 REM
22510 REM ***** FIND STRESS & STRAIN EXTREMA *****
22520 REM
22530 DIM M8(2),M9(2)
22540 FOR I=1 TO 2 \ REM MIN, MAX.
22550 M8(I)=VA1(0,3) \ M9(I)=VA1(0,4) \ REM STRESS & STRAIN.
22560 NEXT I
22570 FOR I=0 TO N1
22580 IF VA1(I,3)<M8(1) THEN M8(1)=VA1(I,3) \ REM STRESS MIN.
22590 IF VA1(I,3)>M8(2) THEN M8(2)=VA1(I,3) \ REM STRESS MAX.
22600 IF VA1(I,4)<M9(1) THEN M9(1)=VA1(I,4) \ REM STRAIN MIN.
22610 IF VA1(I,4)>M9(2) THEN M9(2)=VA1(I,4) \ REM STRAIN MAX.
22620 NEXT I
22630 RETURN
22700 REM
22710 REM ***** CONV TO BIN, INTEGERIZE *****
22720 REM
22770 FOR I=0 TO N1-1
22800 X(I)=INT(32767*X(I)) \ REM CONV TO BIN, INTEGERIZE.
22810 NEXT I
22820 RETURN
22900 REM
22910 REM ***** CONVERT BACK TO ENGG UNITS *****
22920 REM
22924 PRINT "SCALE=";X \ REM TROUBLESHOOTER.
22925 FOR I=0 TO N1-1 \ X(I)=2^X*X(I) \ NEXT I \ REM RESCALE AFTER FFT.
22926 FOR I=0 TO N1-1 \ X(I)=X(I)*V9 \ NEXT I \ REM UNNORMALIZE.
22930 FOR I=0 TO N1-1 \ X(I)=X(I)/32767 \ NEXT I \ REM BIN/ENGG CONV.
22950 Y8$="" \ PRINT "RESTORE OFFSET"; \ INPUT Y8$
22975 IF Y8$="Y" THEN X(0)=X(0)+M(0) \ REM RESTORES OFFSET
22980 RETURN
23000 REM
23010 REM ***** PREPARE FOR PHASE SPECTRUM *****
23020 REM
23030 PRINT "S/N ESTIMATE FROM AMP SPECTRUM"; \ INPUT N0
23160 RETURN
23200 REM
23210 REM ***** PLOT PHASE SPECTRUM *****
23220 REM
23230 TEKMODE \ ERASE
23240 GOSUB 360 \ REM START A GRAPH  \ GOSUB 8000 \ REM COMMENT.
23250 PHYL(A2,0,100*F9,0,70*F9)
23252 GOSUB 31300 \ REM MAX AMP.
23255 GOSUB 27000 \ REM S/N COMMENT.
23260 GOSUB 470 \ REM AXES
23262 SCALE(A2,0,0,1/(2*T1),0,2*PI)
```

```
23264 LABEL(A2,"FREQUENCY, HZ","PHASE-RAD",1/10/T1,PI,1)
23270 FOR I=0 TO N1-1 STEP 2
23275 GOSUB 26710 \ REM PHASE CALCULATIONS.
23320 PLOT(A2,I/N1/(2*T1),P) \ REM (FREQ,PHASE)
23325 NEXT I
23326 INVEC(A2) \ PLOT(A2,1/3/T1,0) \ PLOT(A2,1/3/T1,2*PI)
23330 RETURN
23500 REM
23510 REM ***** ARCTANGENT FOR CONTINUOUS PHASE *****
23520 REM
23525 P=0
23530 S=SGN(X(I))*SGN(X(I+1)) \ REM >0 FOR 1ST/3RD, <0 FOR 2ND/4TH.
23540 IF S<>0 THEN 23600
23550 IF X(I+1)>0 THEN P=PI/2 \ IF X(I+1)<0 THEN P=-PI/2 \ REM IM(X)=0
23555 IF X(I)=0 THEN P=0 \ REM RE(X)=0
23560 RETURN
23600 IF S>0 THEN 23700
23610 IF X(I)<0 THEN P=ATN(X(I+1)/X(I))+PI \ REM 2ND QUADRANT.
23620 IF X(I)>0 THEN P=ATN(X(I+1)/X(I))+2*PI \ REM 4TH QUADRANT.
23630 RETURN
23700 IF X(I+1)>0 THEN P=ATN(X(I+1)/X(I)) \ REM 1ST QUADRANT.
23710 IF X(I+1)<0 THEN P=ATN(X(I+1)/X(I))+PI \ REM 3RD QUADRANT.
23720 RETURN
24000 REM
24010 REM ***** REMOVE DC OFFSET *****
24020 REM
24500 DIM M(2)
24510 M(0)=0
24520 FOR I=0 TO N1-1 \ M(0)=M(0)+X(I) \ NEXT I \ M(0)=M(0)/N1
24530 FOR I=0 TO N1-1 \ X(I)=X(I)-M(0) \ NEXT I \ REM SUBTRACT OFFSET.
24535 PRINT M(0)
24540 RETURN
24600 REM
24610 REM ***** NORMALIZE X(I) *****
24620 REM
24625 V9=X(0)
24630 FOR I=0 TO N1-1 \ IF ABS(X(I))>ABS(V9) THEN V9=ABS(X(I))
24632 NEXT I
24635 FOR I=0 TO N1-1 \ X(I)=X(I)/V9 \ NEXT I \ REM NORMALIZES.
24640 RETURN
24700 REM
24710 REM ***** PLOT SPECTRUM IN RECT COORDS *****
24720 REM
24730 TEKMODE \ ERASE
24740 GOSUB 360 \ REM START A GRAPH   \ GOSUB 8000 \ REM COMMENT.
24744 GOSUB 25000 \ REM RECT EXTREMA.
24765 PHYL(A2,0,40*F9,0,70*F9)
24766 X1=0 \ X2=1/2/T1 \ Y1=H9(2) \ Y2=H9(1)
24768 GOSUB 1500 \ REM INT.
24770 SCALE(A2,0,0,1/2/T1,Y3,Y4) \ REM OVERRIDES PREVIOUS GOSUB.
24775 LABEL(A2,"FREQ, HZ","RE-MPA",1/2/T1/5,Y5,1)
24780 GOSUB 470 \ REM AXES.
24790 FOR I=0 TO N1-1 STEP 2 \ REM STEP 2 IMPORTANT.
24800 PLOT(A2,I/(N1-1)/2/T1,X(I)) \ REM (FREQ,REAL)
24810 NEXT I
24820 INVEC(A2) \ PLOT(A2,1/3/T1,Y3) \ PLOT(A2,1/3/T1,Y4) \ REM SAFELINE.
24830 PHYL(A2,60*F9,100*F9,0,70*F9)
24840 SCALE(A2,0,0,1/2/T1,Y3,Y4) \ REM OVERRIDES PREVIOUS GOSUB.
24850 LABEL(A2,"FREQ, HZ","IM-MPA",1/2/T1/5,Y5,1)
24860 GOSUB 470 \ REM AXES
24870 FOR I=0 TO N1-1 STEP 2 \ REM STEP 2 IMPORTANT.
24880 PLOT(A2,I/N1/2/T1,X(I+1)) \ REM (FREQ,IMAG)
24885 NEXT I
24886 INVEC(A2) \ PLOT(A2,1/3/T1,Y3) \ PLOT(A2,1/3/T1,Y4) \ REM SAFELINE.
24900 GOSUB 3800 \ REM WAIT THEN CLS  \ RETURN
25000 REM
```

```
25010 REM ***** FIND RECTANGULAR EXTREMA *****
25020 REM
25025 SETDIM H8(2),H9(2)
25026 FOR I=1 TO 2 \ H8(I)=X(1) \ H9(I)=X(0) \ NEXT I
25030 FOR I=0 TO N1-1 STEP 2
25040 IF X(I)>H9(1) THEN H9(1)=X(I) \ REM REAL MAX.
25050 IF X(I+1)>H8(1) THEN H8(1)=X(I+1) \ REM IMAG MAX.
25060 IF X(I)<H9(2) THEN H9(2)=X(I) \ REM REAL MIN.
25070 IF X(I+1)<H8(2) THEN H8(2)=X(I+1) \ REM IMAG MIN.
25080 NEXT I
25082 IF H8(1)>H9(1) THEN H9(1)=H8(1) \ REM COMMON MAX.
25084 IF H8(2)<H9(2) THEN H9(2)=H8(2) \ REM COMMON MIN.
25090 RETURN
25200 REM
25210 REM ***** COMMENTS *****
25220 REM
25230 PRINT "TITLE"; \ INPUT X1$
25235 PRINT "MATERIAL"; \ INPUT X2$
25240 X2$=X2$+", SOURCE FILE: "+C1$
25256 X3$=STR$(N1)+" POINTS, FREQ = "+STR$(F1)+" HZ, "+STR$(C)+" CYCLES."
25257 X4$="NF = "+STR$(1/2/T1)+" HZ, DF="+STR$(1/T1/N1)+" HZ."
25270 WHOAMI(A$) \ X6$="PGM; "+A$+" BY A.J.GIACOMIN, P.ENG."
25300 GDATE(Y9,M9,D9) \ X7$="DATE: "+STR$(Y9)+"-"+STR$(M9)+"-"+STR$(D9)
25310 GTIME(S9,M9,H9) \ X7$=X7$+", TIME. "+STR$(H9)+":"+STR$(M9)+":"+STR$(S9)
25380 RETURN
26000 REM
26010 REM ***** PLOT FILTERED AMP SPECTRUM *****
26020 REM
26030 TEKMODE \ ERASE
26040 GOSUB 360 \ REM START A GRAPH  \ GOSUB 8000 \ REM COMMENT.
26050 PHYL(A2,0,100*F9,0,70*F9)
26055 GOSUB 27000 \ REM S/N COMMENT.
26060 GOSUB 31300 \ REM MAX AMP.
26110 SCALE(A2,0,0,1/(2*T1),0,1.1*H9)
26120 LABEL(A2,'FREQUENCY, HZ','SST AMP-MPA',1/10/T1,1.1*H9/5,1)
26130 GOSUB 470 \ REM AXES
26145 FOR I=0 TO N1-1 STEP 2
26150 A=2*SQR(X(I)^2+X(I+1)^2)
26152 IF A<H9/N0 THEN A=0
26153 PLOT(A2,I/N1/2/T1,A) \ REM (FREQ,AMP)
26154 NEXT I
26180 JNVEC(A2) \ PLOT(A2,1/(3*T1),0) \ PLOT(A2,1/(3*T1),1.1*H9)
26190 RETURN
26700 REM
26710 REM ***** PHASE CALCULATION *****
26720 REM
26800 GOSUB 23500 \ REM  ARCTANGENT FOR CONTINUOUS PHASE.
26810 REM SETS PHASE TO ZERO WHEN AMPLITUDE INSIGNIFICANT.
26820 A=2*SQR(X(I)^2+X(I+1)^2)
26822 IF N5<>0 THEN 26840
26824 IF A<H9/N0 THEN P=0
26830 REM P=P+PI/2 \ REM CHANGES FROM COS BASED TO SIN BASED FFT.
26840 IF P>=2*PI THEN P=P-2*PI
26850 RETURN
27000 REM
27010 REM ***** S/N COMMENT *****
27020 REM
27030 X8$="S/N = "+STR$(N0)
27040 COMM(A2,X8$,75,90)
27050 RETURN
30000 REM
30010 REM ***** LOADS FILE *****
30020 REM
30030 PRINT "FILENAME"; \ INPUT C1$
30040 OPEN C1$ FOR INPUT AS FILE #1
30050 FOR I=0 TO N1
```

```
30060 INPUT #1,A1,A6,A3,A4,A5
30080 VA1(I,1)=A1 \ VA1(I,2)=A6 \ VA1(I,3)=A3 \ VA1(I,4)=A4 \ VA1(I,5)=A5
30085 IF END #1 THEN 30100
30090 NEXT I
30100 CLOSE #1
30110 RETURN
30120 REM
31000 REM
31010 REM ****** PLOT LOG-AMP SPECTRUM *****
31020 REM
31030 TEKMODE \ ERASE
31040 GOSUB 360 \ REM START A GRAPH  \ GOSUB 8000 \ REM COMMENT
31050 PHYL(A2,0,100*F9,0,70*F9)
31075 GOSUB 31300 \ REM MAX AMP.
31105 Y1=10^(INT(LOG10(H9))+1) \ Y2=Y1/100000
31110 SCALE(A2,1,0,1/2/T1,Y2,Y1)
31120 LABEL(A2,"FREQUENCY, HZ","SST AMP-MPA",1/10/T1,2,1)
31130 GOSUB 540 \ REM AXES
31140 FOR I=0 TO N1-1 STEP 2
31150 A=2*SQR(X(I)^2+X(I+1)^2) \ REM BY DEFN.
31160 IF Y2<=0 THEN A=Y2/1000 \ REM FOR ZEROES.
31170 PLOT(A2,I/N1/2/T1,A)
31180 NEXT I
31190 INVEC(A2) \ PLOT(A2,1/3/T1,1.00000E-08) \ PLOT(A2,1/3/T1,1.00000E+08)
31200 GOSUB 3800 \ REM WAIT  \ RETURN
31300 REM
31310 REM ***** FINDS MAX AMP *****
31320 REM
31322 H9=X(0) \ REM STARTING VALUE.
31325 FOR I=0 TO N1-1 STEP 2
31340 A=2*SQR(X(I)^2+X(I+1)^2)
31350 IF A>H9 THEN H9=A \ REM MAX AMP.
31360 NEXT I \ RETURN
31500 REM
31510 REM ***** PRINTED REPORT ON FFT *****
31520 REM
31530 PRINT "REPORT FORTHCOMING: CTRL PRT-SCR TO PRINT"
31540 GOSUB 3800 \ REM WAIT
31570 PRINT  \ PRINT \ PRINT
31580 PRINT "REPORT ON ";X1$
31590 PRINT
31600 PRINT X2$ \ PRINT X3$ \ PRINT X4$
31610 PRINT X6$ \ PRINT X7$
31620 PRINT "S/N= ";N0
31630 PRINT
31640 PRINT
31650 GOSUB 31300 \ REM MAX AMP.
31660 PRINT "FREQ,HZ","REAL,MPA","IMAG,MPA","AMP,MPA","PHASE,RAD"
31670 PRINT
31680 FOR I=0 TO N1-1 STEP 2
31690 A=2*SQR(X(I)^2+X(I+1)^2) \ REM AMPLITUDE.
31700 IF A<H9/N0 THEN 31730
31710 GOSUB 26710 \ REM PHASE CALCULATIONS.
31720 PRINT I/N1/2/T1,X(I),X(I+1),2*SQR(X(I)^2+X(I+1)^2),P
31730 NEXT I
31740 PRINT  \ PRINT \ PRINT
31750 GOSUB 3800 \ REM WAIT
31760 PRINT "TOGGLE CTRL-PRT OFF" \ GOSUB 3800 \ REM WAIT
31770 RETURN
32000 REM
32010 REM ***** STATS: MEAN & STD DEV OF NOISE *****
32020 REM
32030 N4=0 \ N8=0 \ N5=0 \ K4=0 \ REM INIT VALUES.
32050 FOR I=0 TO N1-1 STEP 2
32055 A=2*SQR(X(I)^2+X(I+1)^2)
32060 IF A>H9/N0 THEN 32078
```

```
32065 N8=N8+X(I)+X(I+1) \ REM FOR RECT MEAN.
32070 N4=N4+2*SQR(X(I)^2+X(I+1)^2) \ REM FOR POLAR MEAN.
32074 K4=K4+1 \ REM COUNTER.
32078 NEXT I
32080 N4=N4/K4 \ REM POLAR STAT MEAN.
32081 N8=N8/2/K4 \ REM RECT STAT MEAN.
32082 FOR I=0 TO N1-1 STEP 2
32086 N5=N5+(X(I)-N8)^2+(X(I+1)-N8)^2 \ REM SUM SQRS RECT. RESIDS.
32090 NEXT I
32098 N5=N5/2/K4 \ REM VARIANCE OF NOISE IN RECT.
32100 N5=SQR(N5/(K4-1)) \ REM STD. DEV. IN RECT. COORDS.
32120 PRINT "POLAR MEAN: ";N4;", RECT STD DEV: ";N5
32140 GOSUB 3800 \ REM WAIT.
32150 RETURN
32200 REM
32210 REM ***** PLOT NOISE SUBTRACTED AMP SPECTRUM *****
32211 REM              WITH CONFIDENCE INTERVALS
32220 REM
32230 TEKMODE \ ERASE
32240 GOSUB 360 \ REM START GRAPH \ GOSUB 8000 \ REM COMMENT
32250 PHYL(A2,0,100*F9,0,70*F9)
32260 GOSUB 27000 \ REM S/N COMMENT.
32275 GOSUB 31300 \ REM MAX AMP.
32276 H9=H9/40 \ REM MAGNIFY TRUNKS.
32280 SCALE(A2,0,0,1/2/T1,-N4-2*N5,1.1*H9)
32290 LABEL(A2,'FREQUENCY, HZ','SST-MPA',1/10/T1,1.1*H9/5,1)
32300 GOSUB 470 \ REM AXES.
32360 INVEC(A2) \ PLOT(A2,1/3/T1,0) \ PLOT(A2,1/3/T1,1.1*H9)
32365 REM UPPER CONF LIMIT.
32370 INVEC(A2) \ FOR I=0 TO N1-1 STEP 2
32380 A=2*SQR(X(I)^2+X(I+1)^2)-N4+SQR(2*2*N5^2) \ REM 95% CONF.
32390 PLOT(A2,I/N1/2/T1,A) \ REM (FREQ, UPPER LIM)
32400 NEXT I
32410 REM LOWER CONF LIMIT.
32420 INVEC(A2) \ FOR I=0 TO N1-1 STEP 2
32430 A=2*SQR(X(I)^2+X(I+1)^2)-N4-N5*SQR(2) \ REM 95% CONF.
32440 PLOT(A2,I/N1/2/T1,A) \ REM (FREQ, LOWER LIM)
32450 NEXT I
32480 GOSUB 3800 \ REM WAIT
32490 RETURN
32500 REM
32510 REM ***** PRINT REPORT ON NOISE SUBTRACTED SPECTRUM *****
32520 REM
32530 PRINT "STAT REPORT FORTHCOMING: CTRL PRT-SCR TO PRINT"
32540 GOSUB 3800 \ REM WAIT
32570 PRINT \ PRINT \ PRINT
32580 PRINT "REPORT ON ";X1$
32585 PRINT "COMPONENTS KNOWN WITH AT LEAST 95% CONFIDENCE"
32590 PRINT
32595 PRINT "POLAR MEAN: ";N4;", RECT STD DEV: ";N5
32600 PRINT X2$ \ PRINT X3$ \ PRINT X4$
32610 PRINT "S/N= ";N0
326[illegible] PRINT X6$ \ PRINT X7$
32630 PRINT \ PRINT
32650 GOSUB 31300 \ REM MAX AMP.
32660 PRINT "FREQ,HZ","REAL,MPA","IMAG,MPA","AMP,MPA","PHASE,RAD"
32680 FOR I=0 TO N1-1 STEP 2
32690 A=2*SQR(X(I)^2+X(I+1)^2)-N4 \ REM NOISE SUBTRACTED AMP.
32700 IF A<N5*SQR(2) THEN 32730
32710 GOSUB 26710 \ REM PHASE CALCULATIONS.
32720 PRINT I/N1/2/T1,X(I),X(I+1),A,P
32730 NEXT I
32740 PRINT \ PRINT \ PRINT
32750 GOSUB 3800 \ REM WAIT
32760 PRINT "TOGGLE CTRL-PRT OFF" \ GOSUB 3800 \ REM WAIT
32765 RETURN
```

```
10 REM    SPECTRAL ANALYSIS OF STRAIN FOR OSCILLATORY SHEAR
20 REM
30 REM                                 BY
40 REM
50 REM                       A. JEFFREY GIACOMIN
60 REM
70 REM ACKNOWLEDGEMENTS: DR. P. CA[illegible] S. DOSHI.
90 REM
95 GRATTACH(2,2,Y9)
100 TEKMODE \ VTMODE
102 PRINT  \ PRINT "TOTAL POINTS (<1024)"; \ INPUT N1
105 SETDIM S(N1),X(N1+2)
106 DIM R(2),I(2)
108 SETDIM VA1(N1,5)
110 SETDIM VA2(N1+2,2)
120 GOSUB 21340 \ REM SELECT FREQUENCY.
125 GOSUB 21230 \ REM NUMBER OF CYCLES & T1.
128 GOSUB 30000 \ REM READ DATA FILE.
135 REM
140 REM ***** POST TEST PROCESSING *****
145 REM
146 GOSUB 25200 \ REM PREPARE COMMENTS.
155 GOSUB 24000 \ REM REMOVE DC OFFSET.
160 GOSUB 20430 \ REM USE HANNING WINDOW.
165 GOSUB 22500 \ REM FIND STRESS & STRAIN EXTREMA.
170 GOSUB 22000 \ REM PLOT WINDOWED DATA    \ GOSUB 3800 \ REM WAIT THEN CLS.
172 GOSUB 24600 \ REM NORMALIZE X(I)
174 GOSUB 22700 \ REM CONV TO BIN, INTEGERIZE.
180 GOSUB 20530 \ REM PERFORM FFT.
185 GOSUB 22900 \ REM SCALE, CONVERT BACK TO ENGG UNITS.
187 GOSUB 24700 \ REM PLOT SPECTRUM IN RECT COORDS.
190 GOSUB 20640 \ REM PLOT AMP SPECTRUM  \ GOSUB 3800 \ REM WAIT THEN CLS.
195 GOSUB 31000 \ REM PLOT LOG-AMP SPECTRUM
200 GOSUB 23000 \ REM PREPARE FOR PHASE SPECTRUM
210 GOSUB 23200 \ REM PLOT CUT-OFF PHASE SPECTRUM  \ GOSUB 3800
220 GOSUB 26000 \ REM PLOT CUT-OFF AMP SPECTRUM    \ GOSUB 3800
230 GOSUB 31500 \ REM PRINT FFT REPORT ON CUT-OFF SPECTRUM.
240 GOSUB 32000 \ REM STATISTICAL NOISE ANALYSIS.
250 GOSUB 32200 \ REM PLOT AMP SPECTRUM WITH CONF LIMS.
260 GOSUB 32500 \ REM PRINT REPORT ON NOISE SUBTRACTED SPECTRUM.
330 STOP
340 END
350 REM
360 REM ***** START A GRAPH *****
370 REM
380 TEKMODE \ VTMODE \ PRINT "VT-240 (1) OR PLOTTER (2)"; \ INPUT A2
390 F9=1 \ IF A2=2 THEN PRINT "FRACTION OF FULLSIZE (.75)"; \ INPUT F9
400 Y8$="" \ IF A2=1 THEN 430
410 IF A2=2 THEN PRINT "PAPER INSERTED AND PEN READY"; \ INPUT Y8$
420 IF Y8$<>"Y" THEN 410 \ REM GOES TO PREV LINE.
430 IF A2=1 THEN TEKMODE(1,1)
440 IF A2=2 THEN GRON(2) \ IF A2=2 THEN SIZE(A2,108*F9,216*F9)
450 MVEC(A2) \ RETURN
470 REM
480 REM ***** AXES *****
490 REM
500 AXES(A2,0,0) \ AXES(A2,1.00000E+08,1.00000E+08)
510 AXES(A2,-1.00000E+08,-1.00000E+08)
520 RETURN
530 REM
540 REM ***** LOG-AXES *****
550 REM
555 AXES(A2,0,1)
560 AXES(A2,1.00000E+08,1.00000E+08) \ AXES(A2,1.00000E-08,1.00000E-08)
570 RETURN
```

```
700 REM
701 REM ***** STARTING SCREEN *****
702 REM
709 TEKMODE \ VTMODE \ WHOAMI(A$) \ PRINT "PROGRAM: ";A$ \ PRINT
710 GDATE(Y9,M9,D9) \ PRINT "DATE: ";Y9;"-";M9;"-";D9
720 GTIME(S9,M9,H9) \ PRINT "TIME: ";H9;":";M9;":";S9 \ PRINT
730 PRINT "ZERO LOAD, STROKE AND SST"
740 PRINT "SET SPANS 1 & 2 AT 0 & 1." \ PRINT
750 RETURN
1500 REM
1502 REM ***** INTEGERS FOR SCALES *****
1504 REM
1506 REM ***** AUGMENT SCALING LIMITS ****
1508 REM
1510 IF X2=1/2/T1 THEN 1514 \ REM SKIP AUGMENT FOR FREQ AXIS.
1512 X1=X1-ABS(X1-X2)/10 \ X2=X2+ABS(X1-X2)/10
1514 Y1=Y1-ABS(Y1-Y2)/10 \ Y2=Y2+ABS(Y1-Y2)/10
1559 REM
1560 REM ***** ABSCISSA MIN *****
1561 REM
1562 IF X1=0 THEN 1566 \ IF X1>0 THEN 1565
1563 X3=10^INT(LOG10(ABS(X1))-1)*INT((ABS(X1)/(10^INT(LOG10(ABS(X1))-1)))+1)
1564 X3=-X3 \ GO TO 1568
1565 X3=10^INT(LOG10(ABS(X1))-1)*INT((ABS(X1)/(10^INT(LOG10(ABS(X1))-1)))-1)
1566 IF X1=0 THEN X3=0
1567 REM
1568 REM ***** ABSCISSA MAX *****
1569 REM
1570 IF X2=0 THEN 1574 \ IF X2>0 THEN 1573
1571 X4=10^INT(LOG10(ABS(X2))-1)*INT((ABS(X2)/(10^INT(LOG10(ABS(X2))-1)))-1)
1572 X4=-X4 \ GO TO 1575
1573 X4=10^INT(LOG10(ABS(X2))-1)*INT((ABS(X2)/(10^INT(LOG10(ABS(X2))-1)))+1)
1574 IF X2=0 THEN X4=0
1575 REM
1576 REM ***** ORDINATE MIN *****
1577 REM
1578 IF Y1=0 THEN 1582 \ IF Y1>0 THEN 1581
1579 Y3=10^INT(LOG10(ABS(Y1))-1)*INT((ABS(Y1)/(10^INT(LOG10(ABS(Y1))-1)))+1)
1580 Y3=-Y3 \ GO TO 1582
1581 Y3=10^INT(LOG10(ABS(Y1))-1)*INT((ABS(Y1)/(10^INT(LOG10(ABS(Y1))-1)))-1)
1582 IF Y1=0 THEN Y3=0
1583 REM
1584 REM ***** ORDINATE MAX *****
1585 REM
1586 IF Y2=0 THEN 1590 \ IF Y2>0 THEN 1589
1587 Y4=10^INT(LOG10(ABS(Y2))-1)*INT((ABS(Y2)/(10^INT(LOG10(ABS(Y2))-1)))+1)
1588 Y4=-Y4 \ GO TO 1590
1589 Y4=10^INT(LOG10(ABS(Y2))-1)*INT((ABS(Y2)/(10^INT(LOG10(ABS(Y2))-1)))+1)
1590 IF Y2=0 THEN Y4=0
1591 REM
1592 X5=ABS(X4-X3)/5 \ Y5=ABS(Y4-Y3)/5
1593 IF X2=1/2/T1 THEN RETURN \ REM DO NOT SCALE FOR FREQ DOMAIN.
1594 SCALE(A2,0,X3,X4,Y3,Y4) \ X5=(X4-X3)/5 \ Y5=(Y4-Y3)/5
1597 RETURN
3800 REM
3810 REM ***** WAIT THEN CLS *****
3820 REM
3830 Y8$="" \ INPUT Y8$ \ Y8$="" \ TEKMODE \ VTMODE \ IF A2=2 THEN GROFF(A2)
3840 RETURN
4500 REM
6000 REM
6010 REM ***** BUSY PLOT COMMENTS *****
6020 REM
6025 INVEC(A2) \ PHYL(A2,0,100*F9,0,100*F9) \ SCALE(A2,0,0,100,0,100)
6030 COMM(A2,X1$,1,100) \ REM METHOD & MODE.
6035 COMM(A2,X2$,1,96) \ REM MATERIAL NAME & TEMP.
```

```
6040 COMM(A2,X3$,1,92) \ REM BEAM & PROGRAM NUMBERS.
6045 COMM(A2,X4$,1,88) \ REM SHIM THICKNESS'
6050 COMM(A2,X5$,1,84) \ REM OPERATOR.
6060 COMM(A2,X6$,1,80) \ REM EXPONENT & STRAIN AMP.
6070 COMM(A2,X7$,1,76) \ REM HALFCYCLE TIME.
6080 COMM(A2,X8$,1,72) \ REM WHICH CYCLES & PTS/CYCLE.
6085 COMM(A2,X9$,1,68) \ REM LOAD-SST-STRAIN RS.
6090 COMM(A2,Y5$,1,64) \ REM LOAD NOISE.
6095 COMM(A2,Y4$,1,60) \ REM SST,STR NOISE.
7010 COMM(A2,Y7$,1,56) \ REM DATE.
7015 COMM(A2,Y6$,1,52) \ REM TIME.
7020 RETURN
8000 REM
8010 REM ***** ENLARGED PLOT COMMENTS *****
8020 REM
8030 INVEC(A2) \ PHYL(A2,0,100*F9,0,100*F9) \ SCALE(A2,0,0,100,0,100)
8040 COMM(A2,X1$,1,100) \ REM METHOD & MODE
8050 COMM(A2,X2$,1,96) \ REM MATERIAL NAME & TEMP.
8051 COMM(A2,X3$,1,92) \ REM BEAM & PROGRAM NUMBERS.
8052 COMM(A2,X4$,1,88) \ REM SHIM THICKNESS.
8060 COMM(A2,X6$,1,80) \ REM EXPONENT & STRAIN AMP.
8070 COMM(A2,X7$,1,76) \ REM HALFCYCLE TIME.
8120 RETURN
8500 REM
8510 REM ***** SAVE TO FLOPPY *****
8520 REM
8530 TEKMODE \ VTMODE
8540 Y8$="" \ PRINT N1;"DATA PTS. SAVE"; \ INPUT Y8$
8550 IF Y8$="N" THEN 8650
8560 PRINT "TEST FILENAME"; \ INPUT F1$
8570 F2$="DU1:"+F1$
8580 A$=F2$ \ GOSUB 9000 \ REM CHECKS FOR PRIORS.
8650 Y8$="" \ PRINT "SAVE 1ST CYCLE"; \ INPUT Y8$
8660 IF Y8$="N" THEN RETURN
8670 PRINT "1ST CYCLE FILENAME"; \ INPUT F3$
8680 F4$="DU1:"+F3$
8690 A$=F4$ \ GOSUB 9000 \ REM CHECKS FOR PRIORS.
8700 RETURN
9000 REM
9010 REM ***** CHECKS FOR PRIORS *****
9020 REM
9030 FINDFILE(A$,S9) \ REM CHECKS FOR EXISTENCE.
9040 Y8$="" \ IF S9<>-8 THEN PRINT A$;" MAY EXIST, OVERWRITE"; \ INPUT Y8$
9050 IF Y8$<>"Y" THEN GOSUB 9200
9060 RETURN \ REM DEFAULTS WITH RETURN.
9070 REM
9200 REM
9210 REM ***** SAVE A FILE TO FLOPPY *****
9220 REM
9230 OPEN A$ FOR OUTPUT AS FILE #1 DOUBLE BUF
9240 FOR I=0 TO N1-1 \ PRINT #1,VA1(I,1),VA1(I,2),VA1(I,4),VA1(I,4),VA1(I,5)
9250 NEXT I
9260 CLOSE
9270 RETURN
9500 REM
9510 REM ***** PRINT REPORT FOR FILE ON FLOPPY *****
9520 REM
9530 PRINT \ PRINT \ PRINT \ PRINT \ PRINT "REPORT ON ",F2$;" & ";F4$
9540 PRINT
9550 PRINT X2$,X3$
9560 PRINT X4$,X5$
9570 PRINT X6$,X7$
9580 PRINT X8$,X9$
9590 PRINT Y5$,Y4$
9600 PRINT Y7$,Y6$
9610 PRINT "LVDT CAL= ";K1;" IN 4 10 V."
```

```
9620 PRINT "LOAD CAL= ";K2;" V/KG HUNG MASS @ RS 100%"
9630 PRINT "SST CAL= ";K3;" V/KG HUNG MASS @ RS=100%"
9640 PRINT "BEAM DEFLECTION CONST=";K5;" MPA/KG"
9650 PRINT "CAPACITANCE PROBE"; \ INPUT Y8$
9660 PRINT "ATTENUATION METHOD"; \ INPUT Y8$
9670 PRINT  \ PRINT  \ PRINT  \ PRINT
9680 CLOSE  \ RETURN
20000 REM
20430 REM
20440 REM ***** HANNING WINDOW FOR STRESS (REF. 1478) *****
20450 REM
20451 Y8$="" \ PRINT "WINDOW: HANNING (1) OR RECT (2)"; \ INPUT Y8$
20455 FOR I=0 TO N1-1
20490 IF Y8$="1" THEN X(I)=VA1(I,4)*.5*(1-COS(2*PI*I/(N1-1))) \ REM HANNING WIN.
20491 IF Y8$="2" THEN X(I)=VA1(I,4) \ REM RECT WINDOW.
20496 NEXT I
20500 RETURN
20530 REM
20540 REM ***** FORWARD FFT *****
20550 REM
20560 PRINT "FORWARD FFT IN PROGRESS"
20570 X=0
20575 SINS(S,N1) \ REM PRECALCULATES SINE-COSINE TABLE.
20580 PACK(X(0),N1)
20590 FFTI(0,X(0),X(0))
20600 UNPK(X(0),N1)
20620 R(2)=2*2^X*X(2*Z)/32767 \ I(2)=2*2^X*X(2*Z+1)/32767
20630 RETURN
20640 REM
20650 REM ***** PLOT AMPLITUDE SPECTRUM *****
20660 REM
20670 TEKMODE \ ERASE
20680 GOSUB 360 \ REM START A GRAPH  \ GOSUB 6000 \ REM COMMENT.
20684 PHYL(A2,0,100*F9,0,70*F9)
20685 GOSUB 31300 \ REM MAX AMP.
20686 REM H9=H9/40  \ REM BLOW UP CRESTS.
20688 SCALE(A2,0,0,1/(2*T1),0,1.1*H9)
20692 LABEL(A2,'FREQUENCY, HZ','STRAIN AMP',1/10/T1,1.1*H9/5,1)
20696 GOSUB 470 \ REM AXES
20704 FOR I=0 TO N1-1 STEP 2
20708 A=2*SQR(X(I)^2+X(I+1)^2)
20712 PLOT(A2,I/N1/2/T1,A) \ REM (FREQ,AMP)
20713 NEXT I
20716 INVEC(A2) \ PLOT(A2,1/(3*T1),0) \ PLOT(A2,1/(3*T1),1.1*H9)
20720 RETURN
20820 REM
20830 REM ***** REAL/IMAG. GRAPHICS ****
20840 REM
20850 INVEC(A2)
20860 TEKMODE(1,1) \ ERASE
20870 PHYL(A2,0,100,0,90)
20880 SCALE(A2,1,-.2,.2,-.2,.2)
20890 LABEL(A2,"REAL","IMAGINARY",1/5,1/5,1)
20900 GOSUB 20380 \ REM AXES
20910 FOR I=1 TO 2
20920 PLOT(A2,0,0) \ PLOT(A2,R(I),I(I))
20930 MARK(1,I,R(I),I(I))
20940 NEXT I
20950 INPUT A9$
20960 VTMODE
20970 A1=ATN(I(1)/R(1)) \ A2=ATN(I(2)/R(2))
20980 S=SQR(R(1)^2+I(1)^2) \ T=SQR(R(2)^2+I(2)^2)
20990 PRINT "STRAIN PHASE =";A1,"STRESS PHASE =";A2
21000 REM T0 IS SCALE FACTOR FOR STRESS
21010 T0=1
21020 REM S0 IS SCALE FACTOR FOR STRAIN
```

```
21030 S0=1
21040 PRINT "G'=";T*T0*COS(A2-A1)/S/S0,'G"=';T*T0*SIN(A2-A1)/S/S0
21050 PRINT ' (CR) TO CONTINUE'; \ INPUT A$
21060 TEKMODE \ ERASE
21070 PHYL(A2,0,100,0,45)
21080 SCALE(A2,1,0,40*F1,.01,10)
21090 LABEL(A2,'FREQUENCY','G*',1/10/T1,10,1)
21100 FOR J=1 TO N1/2
21110 G=T0*SQR(VA2(J*2,2)^2+VA2(J*2+1,2)^2)/S0/SQR(VA2(J*2,1)^2+VA2(J*2+1,2)^2)
21120 PLOT(A2,J/N1/T1,G)
21130 NEXT J
21140 PHYL(A2,0,100,55,90)
21150 SCALE(A2,1,0,40*F1,-2,2)
21160 LABEL(A2,'FREQUENCY','TAN DELTA',1/10/T1,10,1)
21170 FOR J=0 TO N1/2
21180 A=ATN(VA2(2*J+1,2)/VA2(2*J,2))-ATN(VA2(2*J+1,1)/VA2(2*J,1))
21190 PLOT(A2,J/T1/N1,A)
21200 NEXT J
21210 GO TO 4140
21220 FGSTOP \ END
21230 REM
21240 REM ***** MATCH TEST & DAP FREQUENCIES FOR FFT *****
21250 REM
21260 PRINT "NUMBER OF CYCLES"; \ INPUT C
21270 T1=(C/F1)/N1 \ REM DT.
21330 RETURN
21340 REM
21350 REM ***** SELECT FREQUENCY *****
21360 REM
21370 VTMODE \ PRINT "FREQUENCY, HZ"; \ INPUT F1
21380 RETURN
21390 REM
21400 REM ***** SIMULATE DATA IN VA1 *****
21410 REM
21420 Y8$="" \ PRINT "SKIP SIMULATION"; \ INPUT Y8$ \ IF Y8$="Y" THEN RETURN
21440 FOR I=0 TO N1
21450 VA1(I,5)=I*C/F1/INT(N1*N2) \ REM TIME
21455 IF I>N1*N2 THEN 21500 \ REM ZERO AFTER C CYCLES.
21460 VA1(I,4)=G1*COS(2*PI*F1*VA1(I,5)) \ REM STRAIN.
21470 VA1(I,4)=L1(1)*COS(2*PI*F1*VA1(I,5)+D1(1)) \ REM STRESS FUNDAMENTAL.
21475 VA1(I,4)=VA1(I,4)+L1(2)*COS(2*2*PI*F1*VA1(I,5)+D1(2)) \ REM STRESS, 2ND.
21480 VA1(I,4)=VA1(I,4)+L1(3)*COS(3*2*PI*F1*VA1(I,5)+D1(3)) \ REM STRESS, 3RD.
21490 VA1(I,4)=VA1(I,4)+(B1/2)*(2*RND-1)
21495 VA1(I,4)=VA1(I,4)+L1(0) \ REM DC OFFSET STRESS.
21500 NEXT I
21510 RETURN
22000 REM
22010 REM ***** SELECT WINDOW PLOT *****
22020 REM
22030 Y8$="" \ PRINT "SKIP WINDOW PLOTS"; \ INPUT Y8$ \ IF Y8$="Y" THEN RETURN
22045 GOSUB 360 \ REM START A GRAPH   \ GOSUB 8000 \ REM COMMENT.
22048 PHYL(A2,0,F9*100,0,F9*70)
22050 IF Y8$="STRESS" THEN GOSUB 22100
22090 REM
22100 REM ***** PLOT RECTANGULARLY WINDOWED STRESS WAVE *****
22110 REM
22120 X1=VA1(0,5) \ X2=VA1(N1-1,5) \ Y1=M8(1) \ Y2=M8(2) \ GOSUB 1500 \ REM INT
22130 GOSUB 470 \ REM AXES
22140 LABEL(A2,"TIME, SEC","SHEAR STRAIN",X5,Y5,1)
22150 FOR I=0 TO N1-1 \ PLOT(A2,VA1(I,5),VA1(I,4)) \ REM SIMUL(T,SST)   \ NEXTI
22155 REM
22160 REM ***** PLOT HANNING WINDOWED STRESS WAVE *****
22170 INVEC(A2)
22180 FOR I=0 TO N1-1 \ PLOT(A2,VA1(I,5),X(I)) \ REM SIMUL(T,HAN-SST)     \ NEXTI
22190 RETURN
22500 REM
```

```
22510 REM ***** FIND STRESS & STRAIN EXTREMA *****
22520 REM
22530 DIM M8(2),M9(2)
22540 FOR I=1 TO 2 \ REM MIN, MAX.
22550 M8(I)=VA1(0,3) \ M9(I)=VA1(0,4) \ REM STRESS & STRAIN.
22560 NEXT I
22570 FOR I=0 TO N1
22580 IF VA1(I,4)<M8(1) THEN M8(1)=VA1(I,4) \ REM STRESS MIN.
22590 IF VA1(I,4)>M8(2) THEN M8(2)=VA1(I,4) \ REM STRESS MAX.
22600 IF VA1(I,4)<M9(1) THEN M9(1)=VA1(I,4) \ REM STRAIN MIN.
22610 IF VA1(I,4)>M9(2) THEN M9(2)=VA1(I,4) \ REM STRAIN MAX.
22620 NEXT I
22630 RETURN
22700 REM
22710 REM ***** CONV TO BIN, INTEGERIZE *****
22720 REM
22770 FOR I=0 TO N1-1
22800 X(I)=INT(32767*X(I)) \ REM CONV TO BIN, INTEGERIZE.
22810 NEXT I
22820 RETURN
22900 REM
22910 REM ***** CONVERT BACK TO ENGG UNITS *****
22920 REM
22924 PRINT "SCALE=";X \ REM TROUBLESHOOTER.
22925 FOR I=0 TO N1-1 \ X(I)=2^X*X(I) \ NEXT I \ REM RESCALE AFTER FFT.
22926 FOR I=0 TO N1-1 \ X(I)=X(I)*V9 \ NEXT I \ REM UNNORMALIZE.
22930 FOR I=0 TO N1-1 \ X(I)=X(I)/32767 \ NEXT I \ REM BIN/ENGG CONV.
22950 Y8$="" \ PRINT "RESTORE OFFSET"; \ INPUT Y8$
22975 IF Y8$="Y" THEN X(0)=X(0)+M(0) \ REM RESTORES OFFSET
22980 RETURN
23000 REM
23010 REM ***** PREPARE FOR PHASE SPECTRUM *****
23020 REM
23030 PRINT "S/N ESTIMATE FROM AMP SPECTRUM"; \ INPUT N0
23160 RETURN
23200 REM
23210 REM ***** PLOT PHASE SPECTRUM *****
23220 REM
23230 TEKMODE \ ERASE
23240 GOSUB 360 \ REM START A GRAPH  \ GOSUB 8000 \ REM COMMENT.
23250 PHYL(A2,0,100*F9,0,70*F9)
23252 GOSUB 31300 \ REM MAX AMP.
23255 GOSUB 27000 \ REM S/N COMMENT.
23260 GOSUB 470 \ REM AXES
23262 SCALE(A2,0,0,1/(2*T1),0,2*PI)
23264 LABEL(A2,"FREQUENCY, HZ","PHASE-RAD",1/10/T1,PI,1)
23270 FOR I=0 TO N1-1 STEP 2
23275 GOSUB 26710 \ REM PHASE CALCULATIONS.
23320 PLOT(A2,I/N1/(2*T1),P) \ REM (FREQ,PHASE)
23325 NEXT I
23326 INVEC(A2) \ PLOT(A2,1/3/T1,0) \ PLOT(A2,1/3/T1,2*PI)
23330 RETURN
23500 REM
23510 REM ***** ARCTANGENT FOR CONTINUOUS PHASE *****
23520 REM
23525 P=0
23530 S=SGN(X(I))*SGN(X(I+1)) \ REM >0 FOR 1ST/3RD, <0 FOR 2ND/4TH.
23540 IF S<>0 THEN 23600
23550 IF X(I+1)>0 THEN P=PI/2 \ IF X(I+1)<0 THEN P=-PI/2 \ REM IM(X)=0
23555 IF X(I)=0 THEN P=0 \ REM RE(X)=0
23560 RETURN
23600 IF S>0 THEN 23700
23610 IF X(I)<0 THEN P=ATN(X(I+1)/X(I))+PI \ REM 2ND QUADRANT.
23620 IF X(I)>0 THEN P=ATN(X(I+1)/X(I))+2*PI \ REM 4TH QUADRANT.
23630 RETURN
23700 IF X(I+1)>0 THEN P=ATN(X(I+1)/X(I)) \ REM 1ST QUADRANT.
```

```
23710 IF X(I+1)<0 THEN P=ATN(X(I+1)/X(I))+PI \ REM 3RD QUADRANT.
23720 RETURN
24000 REM
24010 REM ***** REMOVE DC OFFSET *****
24020 REM
24500 DIM M(2)
24510 M(0)=0
24520 FOR I=0 TO N1-1 \ M(0)=M(0)+X(I) \ NEXT I \ M(0)=M(0)/N1
24530 FOR I=0 TO N1-1 \ X(I)=X(I)-M(0) \ NEXT I \ REM SUBTRACT OFFSET.
24535 PRINT M(0)
24540 RETURN
24600 REM
24610 REM ***** NORMALIZE X(I) *****
24620 REM
24625 V9=X(0)
24630 FOR I=0 TO N1-1 \ IF ABS(X(I))>ABS(V9) THEN V9=ABS(X(I))
24632 NEXT I
24635 FOR I=0 TO N1-1 \ X(I)=X(I)/V9 \ NEXT I \ REM NORMALIZES.
24640 RETURN
24700 REM
24710 REM ***** PLOT SPECTRUM IN RECT COORDS *****
24720 REM
24730 TEKMODE \ ERASE
24740 GOSUB 360 \ REM START A GRAPH   \ GOSUB 8000 \ REM COMMENT.
24744 GOSUB 25000 \ REM RECT EXTREMA.
24765 PHYL(A2,0,40*F9,0,70*F9)
24766 X1=0 \ X2=1/2/T1 \ Y1=H9(2) \ Y2=H9(1)
24768 GOSUB 1500 \ REM INT.
24770 SCALE(A2,0,0,1/2/T1,Y3,Y4) \ REM OVERRIDES PREVIOUS GOSUB.
24775 LABEL(A2,"FREQ, HZ","RE-STR",1/2/T1/5,Y5,1)
24780 GOSUB 470 \ REM AXES.
24790 FOR I=0 TO N1-1 STEP 2 \ REM STEP 2 IMPORTANT.
24800 PLOT(A2,I/(N1-1)/2/T1,X(I)) \ REM (FREQ,REAL)
24810 NEXT I
24820 INVEC(A2) \ PLOT(A2,1/3/T1,Y3) \ PLOT(A2,1/3/T1,Y4) \ REM SAFELINE.
24830 PHYL(A2,60*F9,100*F9,0,70*F9)
24840 SCALE(A2,0,0,1/2/T1,Y3,Y4) \ REM OVERRIDES PREVIOUS GOSUB.
24850 LABEL(A2,"FREQ, HZ","IM-STR",1/2/T1/5,Y5,1)
24860 GOSUB 470 \ REM AXES
24870 FOR I=0 TO N1-1 STEP 2 \ REM STEP 2 IMPORTANT.
24880 PLOT(A2,I/N1/2/T1,X(I+1)) \ REM (FREQ,IMAG)
24885 NEXT I
24886 INVEC(A2) \ PLOT(A2,1/3/T1,Y3) \ PLOT(A2,1/3/T1,Y4) \ REM SAFELINE.
24900 GOSUB 3800 \ REM WAIT THEN CLS  \ RETURN
25000 REM
25010 REM ***** FIND RECTANGULAR EXTREMA *****
25020 REM
25025 SETDIM H8(2),H9(2)
25026 FOR I=1 TO 2 \ H8(I)=X(1) \ H9(I)=X(0) \ NEXT I
25030 FOR I=0 TO N1-1 STEP 2
25040 IF X(I)>H9(1) THEN H9(1)=X(I) \ REM REAL MAX.
25050 IF X(I+1)>H8(1) THEN H8(1)=X(I+1) \ REM IMAG MAX.
25060 IF X(I)<H9(2) THEN H9(2)=X(I) \ REM REAL MIN.
25070 IF X(I+1)<H8(2) THEN H8(2)=X(I+1) \ REM IMAG MIN.
25080 NEXT I
25082 IF H8(1)>H9(1) THEN H9(1)=H8(1) \ REM COMMON MAX.
25084 IF H8(2)<H9(2) THEN H9(2)=H8(2) \ REM COMMON MIN.
25090 RETURN
25200 REM
25210 REM ***** COMMENTS *****
25220 REM
25230 PRINT "TITLE"; \ INPUT X1$
25235 PRINT "MATERIAL"; \ INPUT X2$
25240 X2$=X2$+", SOURCE FILE: "+C1$
25256 X3$=STR$(N1)+" POINTS, FREQ = "+STR$(F1)+" HZ, "+STR$(C)+" CYCLES."
25257 X4$="N.F.= "+STR$(1/2/T1)+" HZ, DF="+STR$(1/T1/N1)+" HZ."
```

```
25270 WHOAMI(A$) \ X6$="PGM: "+A$+" BY A.J.GIACOMIN, P.ENG."
25300 GDATE(Y9,M9,D9) \ X7$="DATE: "+STR$(Y9)+"-"+STR$(M9)+"-"+STR$(D9)
25310 GTIME(S9,M9,H9) \ X7$=X7$+", TIME. "+STR$(H9)+":"+STR$(M9)+":"+STR$(S9)
25330 RETURN
26000 REM
26010 REM ***** PLOT FILTERED AMP SPECTRUM *****
26020 REM
26030 TEKMODE \ ERASE
26040 GOSUB 360 \ REM START A GRAPH  \ GOSUB 8000 \ REM COMMENT.
26050 PHYL(A2,0,100*F9,0,70*F9)
26055 GOSUB 27000 \ REM S/N COMMENT.
26060 GOSUB 31300 \ REM MAX AMP.
26110 SCALE(A2,0,0,1/(2*T1),0,1.1*H9)
26120 LABEL(A2,'FREQUENCY, HZ','STRAIN AMP',1/10/T1,1.1*H9/5,1)
26130 GOSUB 470 \ REM AXES
26145 FOR I=0 TO N1-1 STEP 2
26150 A=2*SQR(X(I)^2+X(I+1)^2)
26152 IF A<H9/N0 THEN A=0
26153 PLOT(A2,I/N1/2/T1,A) \ REM (FREQ,AMP)
26154 NEXT I
26180 INVEC(A2) \ PLOT(A2,1/(3*T1),0) \ PLOT(A2,1/(3*T1),1.1*H9)
26190 RETURN
26700 REM
26710 REM ***** PHASE CALCULATION *****
26720 REM
26800 GOSUB 23500 \ REM  ARCTANGENT FOR CONTINUOUS PHASE.
26810 REM SETS PHASE TO ZERO WHEN AMPLITUDE INSIGNIFICANT.
26820 A=2*SQR(X(I)^2+X(I+1)^2)
26822 IF N5<>0 THEN 26840
26824 IF A<H9/N0 THEN P=0
26830 REM P=P+PI/2 \ REM CHANGES FROM COS BASED TO SIN BASED FFT.
26840 IF P>=2*PI THEN P=P-2*PI
26850 RETURN
27000 REM
27010 REM ***** S/N COMMENT *****
27020 REM
2[illegible] X8$="S/N = "+STR$(N0)
2[illegible] COMM(A2,X8$,75,90)
2[illegible] RETURN
30000 REM
30010 REM ***** LOADS FILE *****
30020 REM
30030 PRINT "FILENAME"; \ INPUT C1$
30040 OPEN C1$ FOR INPUT AS FILE #1
30050 FOR I=0 TO N1
30060 INPUT #1,A1,A6,A3,A4,A5
30080 VA1(I,1)=A1 \ VA1(I,2)=A6 \ VA1(I,3)=A3 \ VA1(I,4)=A4 \ VA1(I,5)=A5
30085 IF END #1 THEN 30100
30090 NEXT I
30100 CLOSE #1
30110 RETURN
30120 REM
31000 REM
31010 REM ****** PLOT LOG-AMP SPECTRUM *****
31020 REM
31030 TEKMODE \ ERASE
31040 GOSUB 360 \ REM START A GRAPH  \ GOSUB 8000 \ REM COMMENT
31050 PHYL(A2,0,100*F9,0,70*F9)
31075 GOSUB 31300 \ REM MAX AMP.
31105 Y1=10^(INT(LOG10(H9))+1) \ Y2=Y1/100000
31110 SCALE(A2,1,0,1/2/T1,Y2,Y1)
31120 LABEL(A2,"FREQUENCY, HZ","STRAIN AMP",1/10/T1,2,1)
31130 GOSUB 540 \ REM AXES
31140 FOR I=0 TO N1-1 STEP 2
31150 A=2*SQR(X(I)^2+X(I+1)^2) \ REM BY DEFN.
31160 IF A<=0 THEN A=Y2 \ REM FOR ZEROES.
```

```
31170 PLOT(A2,I/N1/2/T1,A)
31180 NEXT I
31190 INVEC(A2) \ PLOT(A2,1/3/T1,1.00000E-08) \ PLOT(A2,1/3/T1,1.00000E+08)
31200 GOSUB 3800 \ REM WAIT  \ RETURN
31300 REM
31310 REM ***** FINDS MAX AMP *****
31320 REM
31322 H9=X(0) \ REM STARTING VALUE.
31325 FOR I=0 TO N1-1 STEP 2
31340 A=2*SQR(X(I)^2+X(I+1)^2)
31350 IF A>H9 THEN H9=A \ REM MAX AMP.
31360 NEXT I \ RETURN
31500 REM
31510 REM ***** PRINTED REPORT ON FFT *****
31520 REM
31530 PRINT "REPORT FORTHCOMING: CTRL PRT-SCR TO PRINT"
31540 GOSUB 3800 \ REM WAIT
31570 PRINT  \ PRINT  \ PRINT
31580 PRINT "REPORT ON ";X1$
31590 PRINT
31600 PRINT X2$ \ PRINT X3$ \ PRINT X4$
31610 PRINT X6$ \ PRINT X7$
31620 PRINT "S/N= ";N0
31630 PRINT
31640 PRINT
31650 GOSUB 31300 \ REM MAX AMP.
31660 PRINT "FREQ,HZ","REAL,STR","IMAG,STR","AMP,STR","PHASE,RAD"
31670 PRINT
31680 FOR I=0 TO N1-1 STEP 2
31690 A=2*SQR(X(I)^2+X(I+1)^2) \ REM AMPLITUDE.
31700 IF A<H9/N0 THEN 31730
31710 GOSUB 26710 \ REM PHASE CALCULATIONS.
31720 PRINT I/N1/2/T1,X(I),X(I+1),2*SQR(X(I)^2+X(I+1)^2),P
31730 NEXT I
31740 PRINT  \ PRINT  \ PRINT
31750 GOSUB 3800 \ REM WAIT
31760 PRINT "TOGGLE CTRL-PRT OFF" \ GOSUB 3800 \ REM WAIT
31770 RETURN
32000 REM
32010 REM ***** STATS: MEAN & STD DEV OF NOISE *****
32020 REM
32030 N4=0 \ N8=0 \ N5=0 \ K4=0 \ REM INIT VALUES.
32050 FOR I=0 TO N1-1 STEP 2
32055 A=2*SQR(X(I)^2+X(I+1)^2)
32060 IF A>H9/N0 THEN 32078
32065 N8=N8+X(I)+X(I+1) \ REM FOR RECT MEAN.
32070 N4=N4+2*SQR(X(I)^2+X(I+1)^2) \ REM FOR POLAR MEAN.
32074 K4=K4+1 \ REM COUNTER.
32078 NEXT I
32080 N4=N4/K4 \ REM POLAR STAT MEAN.
32081 N8=N8/2/K4 \ REM RECT STAT MEAN.
32082 FOR I=0 TO N1-1 STEP 2
32086 N5=N5+(X(I)-N8)^2+(X(I+1)-N8)^2 \ REM SUM SQRS RECT. RESIDS.
32090 NEXT I
32098 N5=N5/2/K4 \ REM VARIANCE OF NOISE IN RECT.
32100 N5=SQR(N5/(K4-1)) \ REM STD. DEV. IN RECT. COORDS.
32130 PRINT "POLAR MEAN: ";N4;", RECT STD DEV: ";N5
32140 GOSUB 3800 \ REM WAIT.
32150 RETURN
32200 REM
32210 REM ***** PLOT NOISE SUBTRACTED AMP SPECTRUM *****
32211 REM          WITH CONFIDENCE INTERVALS
32220 REM
32230 TEKMODE \ ERASE
32240 GOSUB 360 \ REM START GRAPH  \ GOSUB 8000   REM COMMENT
32250 PHYL(A2,0,100*F9,0,70*F9)
```

```
32260 GOSUB 27000 \ REM S/N COMMENT.
32275 GOSUB 31300 \ REM MAX AMP.
32276 H9=H9/40 \ REM MAGNIFY TRUNKS.
32280 SCALE(A2,0,0,1/2/T1,-N4-2*N5,1.1*H9)
32290 LABEL(A2,'FREQUENCY, HZ','STRAIN',1/10/T1,1.1*H9/5,1)
32300 GOSUB 470 \ REM AXES.
32360 INVEC(A2) \ PLOT(A2,1/3/T1,0) \ PLOT(A2,1/3/T1,1.1*H9)
32365 REM UPPER CONF LIMIT.
32370 INVEC(A2) \ FOR I=0 TO N1-1 STEP 2
32380 A=2*SQR(X(I)^2+X(I+1)^2)-N4+SQR(2*2*N5^2) \ REM 95% CONF.
32390 PLOT(A2,I/N1/2/T1,A) \ REM (FREQ, UPPER LIM)
32400 NEXT I
32410 REM LOWER CONF LIMIT.
32420 INVEC(A2) \ FOR I=0 TO N1-1 STEP 2
32430 A=2*SQR(X(I)^2+X(I+1)^2)-N4-N5*SQR(2) \ REM 95% CONF.
32440 PLOT(A2,I/N1/2/T1,A) \ REM (FREQ, LOWER LIM)
32450 NEXT I
32480 GOSUB 3800 \ REM WAIT
32490 RETURN
32500 REM
32510 REM ***** PRINT REPORT ON NOISE SUBTRACTED SPECTRUM *****
32520 REM
32530 PRINT "STAT REPORT FORTHCOMING: CTRL PRT-SCR TO PRINT"
32540 GOSUB 3800 \ REM WAIT
32570 PRINT \ PRINT \ PRINT
32580 PRINT "REPORT ON ";X1$
32585 PRINT "COMPONENTS KNOWN WITH AT LEAST 95% CONFIDENCE"
32590 PRINT
32595 PRINT "POLAR MEAN: ";N4;", RECT STD DEV: ";N5
32600 PRINT X2$ \ PRINT X3$ \ PRINT X4$
32610 PRINT "S/N= ";N0
32620 PRINT X6$ \ PRINT X7$
32630 PRINT \ PRINT
32650 GOSUB 31300 \ REM MAX AMP.
32660 PRINT "FREQ,HZ","REAL,STR","IMAG,STR","AMP,STR","PHASE,RAD"
32680 FOR I=0 TO N1-1 STEP 2
32690 A=2*SQR(X(I)^2+X(I+1)^2)-N4 \ REM NOISE SUBTRACTED AMP.
32700 IF A<N5*SQR(2) THEN 32730
32710 GOSUB 26710 \ REM PHASE CALCULATIONS.
32720 PRINT I/N1/2/T1,X(I),X(I+1),A,P
3[illegible]0 NEXT I
3[illegible] PRINT \ PRINT \ PRINT
3[illegible] GOSUB 3800 \ REM WAIT
32[illegible] PRINT "TOGGLE CTRL-PRT OFF" \ GOSUB 3800 \ REM WAIT
32765 RETURN
```

```
10 REM     SPECTRAL ANALYSIS OF TOTAL FORCE FOR OSCILLATORY SHEAR
20 REM
30 REM                          BY
40 REM
50 REM                  A. JEFFREY GIACOMIN
60 REM
70 REM ACKNOWLEDGEMENTS: DR. P. CAIN, S. DOSHI.
90 REM
95 GRATTACH(2,2,Y9)
100 TEKMODE \ VTMODE
102 PRINT  \ PRINT "TOTAL POINTS (<1024)"; \ INPUT N1
105 SETDIM S(N1),X(N1+2)
106 DIM R(2),I(2)
108 SETDIM VA1(N1,5)
110 SETDIM VA2(N1+2,2)
120 GOSUB 21340 \ REM SELECT FREQUENCY.
125 GOSUB 21230 \ REM NUMBER OF CYCLES & T1.
128 GOSUB 30000 \ REM READ DATA FILE.
135 REM
140 REM ***** POST TEST PROCESSING *****
145 REM
146 GOSUB 25200 \ REM PREPARE COMMENTS.
155 GOSUB 24000 \ REM REMOVE DC OFFSET.
160 GOSUB 20430 \ REM USE HANNING WINDOW.
165 GOSUB 22500 \ REM FIND  EXTREMA.
170 GOSUB 22000 \ REM PLOT WINDOWED DATA    \ GOSUB 3800 \ REM WAIT THEN CLS.
172 GOSUB 24600 \ REM NORMALIZE X(I)
174 GOSUB 22700 \ REM CONV TO BIN, INTEGERIZE.
180 GOSUB 20530 \ REM PERFORM FFT.
185 GOSUB 22900 \ REM SCALE, CONVERT BACK TO ENGG UNITS.
187 GOSUB 24700 \ REM PLOT SPECTRUM IN RECT COORDS.
190 GOSUB 20640 \ REM PLOT AMP SPECTRUM   \ GOSUB 3800 \ REM WAIT THEN CLS.
195 GOSUB 31000 \ REM PLOT LOG-AMP SPECTRUM
200 GOSUB 23000 \ REM PREPARE FOR PHASE SPECTRUM
210 GOSUB 23200 \ REM PLOT CUT-OFF PHASE SPECTRUM  \ GOSUB 3800
220 GOSUB 26000 \ REM PLOT CUT-OFF AMP SPECTRUM    \ GOSUB 3800
230 GOSUB 31500 \ REM PRINT FFT REPORT ON CUT-OFF SPECTRUM.
240 GOSUB 32000 \ REM STATISTICAL NOISE ANALYSIS.
250 GOSUB 32200 \ REM PLOT AMP SPECTRUM WITH CONF LIMS.
260 GOSUB 32500 \ REM PRINT REPORT ON NOISE SUBTRACTED SPECTRUM.
330 STOP
340 END
350 REM
360 REM ***** START A GRAPH *****
370 REM
380 TEKMODE \ VTMODE \ PRINT "VT-240 (1) OR PLOTTER (2)"; \ INPUT A2
390 F9=1 \ IF A2=2 THEN PRINT "FRACTION OF FULLSIZE (.75)"; \ INPUT F9
400 Y8$="" \ IF A2=1 THEN 430
410 IF A2=2 THEN PRINT "PAPER INSERTED AND PEN READY"; \ INPUT Y8$
420 IF Y8$<>"Y" THEN 410 \ REM GOES TO PREV LINE.
430 IF A2=1 THEN TEKMODE(1,1)
440 IF A2=2 THEN GRON(2) \ IF A2=2 THEN SIZE(A2,108*F9,216*F9)
450 INVEC(A2) \ RETURN
470 REM
480 REM ***** AXES *****
490 REM
500 AXES(A2,0,0) \ AXES(A2,1.00000E+08,1.00000E+08)
510 AXES(A2,-1.00000E+08,-1.00000E+08)
520 RETURN
530 REM
540 REM ***** LOG-AXES *****
550 REM
555 AXES(A2,0,1)
560 AXES(A2,1.00000E+08,1.00000E+08) \ AXES(A2,1.00000E-08,1.00000E-08)
570 RETURN
```

```
700 REM
701 REM ***** STARTING SCREEN *****
702 REM
709 TEKMODE \ VTMODE \ WHOAMI(A$) \ PRINT "PROGRAM: ";A$ \ PRINT
710 GDATE(Y9,M9,D9) \ PRINT "DATE: ";Y9;"-";M9;"-";D9
720 GTIME(S9,M9,H9) \ PRINT "TIME: ";H9;":";M9;":";S9 \ PRINT
730 PRINT "ZERO LOAD, STROKE AND SST"
740 PRINT "SET SPANS 1 & 2 AT 0 & 1." \ PRINT
750 RETURN
1500 REM
1502 REM ***** INTEGERS FOR SCALES *****
1504 REM
1506 REM ***** AUGMENT SCALING LIMITS ****
1508 REM
1510 IF X2=1/2/T1 THEN 1514 \ REM SKIP AUGMENT FOR FREQ AXIS.
1512 X1=X1-ABS(X1-X2)/10 \ X2=X2+ABS(X1-X2)/10
1514 Y1=Y1-ABS(Y1-Y2)/10 \ Y2=Y2+ABS(Y1-Y2)
1559 REM
1560 REM ***** ABSCISSA MIN *****
1561 REM
1562 IF X1=0 THEN 1566 \ IF X1>0 THEN 1565
1563 X3=10^INT(LOG10(ABS(X1))-1)*INT((ABS(X1)/(10^INT(LOG10(ABS(X1))-1)))+1)
1564 X3=-X3 \ GO TO 1568
1565 X3=10^INT(LOG10(ABS(X1))-1)*INT((ABS(X1)/(10^INT(LOG10(ABS(X1))-1)))-1)
1566 IF X1=0 THEN X3=0
1567 REM
1568 REM ***** ABSCISSA MAX *****
1569 REM
1570 IF X2=0 THEN 1574 \ IF X2>0 THEN 1573
1571 X4=10^INT(LOG10(ABS(X2))-1)*INT((ABS(X2)/(10^INT(LOG10(ABS(X2))-1)))-1)
1572 X4=-X4 \ GO TO 1575
1573 X4=10^INT(LOG10(ABS(X2))-1)*INT((ABS(X2)/(10^INT(LOG10(ABS(X2))-1)))+1)
1574 IF X2=0 THEN X4=0
1575 REM
1576 REM ***** ORDINATE MIN *****
1577 REM
1578 IF Y1=0 THEN 1582 \ IF Y1>0 THEN 1581
1579 Y3=10^INT(LOG10(ABS(Y1))-1)*INT((ABS(Y1)/(10^INT(LOG10(ABS(Y1))-1)))+1)
1580 Y3=-Y3 \ GO TO 1582
1581 Y3=10^INT(LOG10(ABS(Y1))-1)*INT((ABS(Y1)/(10^INT(LOG10(ABS(Y1))-1)))-1)
1582 IF Y1=0 THEN Y3=0
1583 REM
1584 REM ***** ORDINATE MAX *****
1585 REM
1586 IF Y2=0 THEN 1590 \ IF Y2>0 THEN 1589
1587 Y4=10^INT(LOG10(ABS(Y2))-1)*INT((ABS(Y2)/(10^INT(LOG10(ABS(Y2))-1)))-1)
1588 Y4=-Y4 \ GO TO 1590
1589 Y4=10^INT(LOG10(ABS(Y2))-1)*INT((ABS(Y2)/(10^INT(LOG10(ABS(Y2))-1)))+1)
1590 IF Y2=0 THEN Y4=0
1591 REM
1592 X5=ABS(X4-X3)/5 \ Y5=ABS(Y4-Y3)/5
1593 IF X2=1/2/T1 THEN RETURN \ REM DO NOT SCALE FOR FREQ DOMAIN.
1594 SCALE(A2,0,X3,X4,Y3,Y4) \ X5=(X4-X3)/5 \ Y5=(Y4-Y3)/5
1597 RETURN
3800 REM
3810 REM ***** WAIT THEN CLS *****
3820 REM
3830 Y8$="" \ INPUT Y8$ \ Y8$="" \ TEKMODE \ VTMODE \ IF A2=2 THEN GROFF(2)
3840 RETURN
4500 REM
6000 REM
6010 REM ***** BUSY PLOT COMMENTS *****
6020 REM
6025 INVEC(A2) \ PHYL(A2,0,100*F9,0,100*F9) \ SCALE(A2,0,0,100,0,100)
6030 COMM(A2,X1$,1,100) \ REM METHOD & MODE.
6035 COMM(A2,X2$,1,96) \ REM MATERIAL NAME & TEMP.
6040 COMM(A2,X3$,1,92) \ REM BEAM & PROGRAM NUMBERS.
6045 COMM(A2,X4$,1,88) \ REM SHIM THICKNESS
6050 COMM(A2,X5$,1,84) \ REM OPERATOR.
6060 COMM(A2,X6$,1,80) \ REM EXPONENT & FORCE AMP-N.
6070 COMM(A2,X7$,1,76) \ REM HALFCYCLE TIME.
6080 COMM(A2,X8$,1,72) \ REM WHICH CYCLES & PTS/CYCLE.
6085 COMM(A2,X9$,1,68) \ REM LOAD-SST-STRAIN RS.
6090 COMM(A2,Y5$,1,64) \ REM LOAD NOISE.
6095 COMM(A2,Y4$,1,60) \ REM SST,STR NOISE.
7010 COMM(A2,Y7$,1,56) \ REM DATE.
7015 COMM(A2,Y6$,1,52) \ REM TIME.
7020 RETURN
```

```
8000 REM
8010 REM ***** ENLARGED PLOT COMMENTS *****
8020 REM
8030 INVEC(A2) \ PHYL(A2,0,100*F9,0,100*F9) \ SCALE(A2,0,0,100,0,100)
8040 COMM(A2,X1$,1,100) \ REM METHOD & MODE
8050 COMM(A2,X2$,1,96) \ REM MATERIAL NAME & TEMP.
8051 COMM(A2,X3$,1,92) \ REM BEAM & PROGRAM NUMBERS.
8052 COMM(A2,X4$,1,88) \ REM SHIM THICKNESS.
8060 COMM(A2.X6$.1.80) \ REM EXPONENT & FORCE AMP-N.
8070 COMM(A2,X7$,1,76) \ REM HALFCYCLE TIME.
8120 RETURN
8500 REM
8510 REM ***** SAVE TO FLOPPY *****
8520 REM
8530 TEKMODE \ VTMODE
8540 Y8$="" \ PRINT N1;"DATA PTS. SAVE"; \ INPUT Y8$
8550 IF Y8$="N" THEN 8650
8560 PRINT "TEST FILENAME"; \ INPUT F1$
8570 F2$="DU1:"+F1$
8580 A$=F2$ \ GOSUB 9000 \ REM CHECKS FOR PRIORS.
8650 Y8$="" \ PRINT "SAVE 1ST CYCLE"; \ INPUT Y8$
8660 IF Y8$="N" THEN RETURN
8670 PRINT "1ST CYCLE FILENAME"; \ INPUT F3$
8680 F4$="DU1:"+F3$
8690 A$=F4$ \ GOSUB 9000 \ REM CHECKS FOR PRIORS.
8700 RETURN
9000 REM
9010 REM ***** CHECKS FOR PRIORS *****
9020 REM
9030 FINDFILE(A$,S9) \ REM CHECKS FOR EXISTENCE.
9040 Y8$="" \ IF S9<>-8 THEN PRINT A$;" MAY EXIST, OVERWRITE"; \ INPUT Y8$
9050 IF Y8$<>"Y" THEN GOSUB 9200
9060 RETURN \ REM DEFAULTS WITH RETURN.
9070 REM
9200 REM
9210 REM ***** SAVE A FILE TO FLOPPY *****
9220 REM
9230 OPEN A$ FOR OUTPUT AS FILE #1 DOUBLE BUF
9240 FOR I=0 TO N1-1 \ PRINT #1,VA1(I,1),VA1(I,2),VA1(I,2),VA1(I,2),VA1(I,5)
9250 NEXT I
9260 CLOSE
9270 RETURN
9500 REM
9510 REM ***** PRINT REPORT FOR FILE ON FLOPPY *****
9520 REM
9530 PRINT  \ PRINT  \ PRINT  \ PRINT  \ PRINT "REPORT ON ";F2$;" & ";F4$
9540 PRINT
9550 PRINT X2$,X3$
9560 PRINT X4$,X5$
9570 PRINT X6$,X7$
9580 PRINT X8$,X9$
9590 PRINT Y5$,Y4$
9600 PRINT Y7$,Y6$
9610 PRINT "LVDT CAL= ";K1;" IN @ 10 V."
9620 PRINT "LOAD CAL= ";K2;" V/KG HUNG MASS @ RS 100%"
9630 PRINT "SST CAL= ";K3;" V/KG HUNG MASS @ RS=100%"
9640 PRINT "BEAM DEFLECTION CONST=";K5;" MPA/KG"
9650 PRINT "CAPACITANCE PROBE"; \ INPUT Y8$
9660 PRINT "ATTENUATION METHOD"; \ INPUT Y8$
9670 PRINT  \ PRINT  \ PRINT  \ PRINT
9680 CLOSE  \ RETURN
20000 REM
20430 REM
20440 REM ***** HANNING WINDOW  (REF. 14,8) *****
20450 REM
20451 Y8$="" \ PRINT "WINDOW: HANNING (1) OR RECT (2)"; \ INPUT Y8$
20455 FOR I=0 TO N1-1
20490 IF Y8$="1" THEN X(I)=VA1(I,2)*.5*(1-COS(2*PI*I/(N1-1))) \ REM HANNING WIN.
20491 IF Y8$="2" THEN X(I)=VA1(I,2) \ REM RECT WINDOW.
20496 NEXT I
20500 RETURN
20530 REM
20540 REM ***** FORWARD FFT *****
20550 REM
20560 PRINT "FORWARD FFT IN PROGRESS"
```

```
20570 X=0
20575 SINS(S,N1) \ REM PRECALCULATES SIRE-COSINE TABLE.
20580 PACK(X(0),N1)
20590 FFTI(0,X(0),X(0))
20600 UNPK(X(0),N1)
20620 R(2)=2*2^X*X(2*Z)/32767 \ I(2)=2*2^X*X(2*Z+1)/32767
20630 RETURN
20640 REM
20650 REM ***** PLOT AMPLITUDE SPECTRUM *****
20660 REM
20670 TEKMODE \ ERASE
20680 GOSUB 360 \ REM START A GRAPH  \ GOSUB 8000 \ REM COMMENT.
20684 PHYL(A2,0,100*F9,0,70*F9)
20685 GOSUB 31300 \ REM MAX AMP.
20686 REM H9=H9/40  \ REM BLOW UP CRESTS.
20688 SCALE(A2,0,0,1/(2*T1),0,1.1*H9)
20692 LABEL(A2,'FREQUENCY, HZ','FORCE AMP-N',1/10/T1,1.1*H9/5,1)
20696 GOSUB 470 \ REM AXES
20704 FOR I=0 TO N1-1 STEP 2
20708 A=2*SQR(X(I)^2+X(I+1)^2)
20712 PLOT(A2,I/N1/2/T1,A) \ REM (FREQ,AMP)
20713 NEXT I
20716 INVEC(A2) \ PLOT(A2,1/(3*T1),0) \ PLOT(A2,1/(3*T1),1.1*H9)
20720 RETURN
20820 REM
20830 REM ***** REAL/IMAG. GRAPHICS ****
20840 REM
20850 INVEC(A2)
20860 TEKMODE(1,1) \ ERASE
20870 PHYL(A2,0,100,0,90)
20880 SCALE(A2,1,-.2,.2,-.2,.2)
20890 LABEL(A2,"REAL","IMAGINARY",1/5,1/5,1)
20900 GOSUB 20380 \ REM AXES
20910 FOR I=1 TO 2
20920 PLOT(A2,0,0) \ PLOT(A2,R(I),I(I))
20930 MARK(1,I,R(I),I(I))
20940 NEXT I
20950 INPUT A9$
20960 VTMODE
20970 A1=ATN(I(1)/R(1)) \ A2=ATN(I(2)/R(2))
20980 S=SQR(R(1)^2+I(1)^2) \ T=SQR(R(2)^2+I(2)^2)
21000 REM T0 IS SCALE FACTOR
21010 T0=1
21020 REM S0 IS SCALE FACTOR FOR FORCE
21030 S0=1
21040 PRINT "G'=";T*T0*COS(A2-A1)/S/S0,'G"=';T*T0*SIN(A2-A1)/S/S0
21050 PRINT '<CR> TO CONTINUE'; \ INPUT A$
21060 TEKMODE \ ERASE
21070 PHYL(A2,0,100,0,45)
21080 SCALE(A2,1,0,40*F1,.01,10)
21090 LABEL(A2,'FREQUENCY','G*',1/10/T1,10,1)
21100 FOR J=1 TO N1/2
21110 G=T0*SQR(VA2(J*2,2)^2+VA2(J*2+1,2)^2)/S0/SQR(VA2(J*2,1)^2+VA2(J*2+1,2)^2)
21120 PLOT(A2,J/N1/T1,G)
21130 NEXT J
21140 PHYL(A2,0,100,55,90)
21150 SCALE(A2,1,0,40*F1,-2,2)
21160 LABEL(A2,'FREQUENCY','TAN DELTA',1/10/T1,10,1)
21170 FOR J=0 TO N1/2
21180 A=ATN(VA2(2*J+1,2)/VA2(2*J,2))-ATN(VA2(2*J+1,1)/VA2(2*J,1))
21190 PLOT(A2,J/T1/N1,A)
21200 NEXT J
21210 GO TO 4140
21220 FGSTOP \ END
21230 REM
21240 REM ***** MATCH TEST & DAP FREQUENCIES FOR FFT *****
```

```
22950 Y8$="" \ PRINT "RESTORE OFFSET"; \ INPUT Y8$
22975 IF Y8$="Y" THEN X(0)=X(0)+M(0) \ REM RESTORES OFFSET
22980 RETURN
23000 REM
23010 REM ***** PREPARE FOR PHASE SPECTRUM *****
23020 REM
23030 PRINT "S/N ESTIMATE FROM AMP SPECTRUM"; \ INPUT N0
23160 RETURN
23200 REM
23210 REM ***** PLOT PHASE SPECTRUM *****
23220 REM
23230 TEKMODE \ ERASE
23240 GOSUB 360 \ REM START A GRAPH  \ GOSUB 8000 \ REM COMMENT.
23250 PHYL(A2,0,100*F9,0,70*F9)
23252 GOSUB 31300 \ REM MAX AMP.
23255 GOSUB 27000 \ REM S/N COMMENT.
23260 GOSUB 470 \ REM AXES
23262 SCALE(A2,0,0,1/(2*T1),0,2*PI)
23264 LABEL(A2,"FREQUENCY, HZ","PHASE-RAD",1/10/T1,PI,1)
23270 FOR I=0 TO N1-1 STEP 2
23275 GOSUB 26710 \ REM PHASE CALCULATIONS.
23320 PLOT(A2,I/N1/(2*T1),P) \ REM (FREQ,PHASE)
23325 NEXT I
23326 INVEC(A2) \ PLOT(A2,1/3/T1,0) \ PLOT(A2,1/3/T1,2*PI)
23330 RETURN
23500 REM
23510 REM ***** ARCTANGENT FOR CONTINUOUS PHASE *****
23520 REM
23525 P=0
23530 S=SGN(X(I))*SGN(X(I+1)) \ REM >0 FOR 1ST/3RD, <0 FOR 2ND/4TH.
23540 IF S<>0 THEN 23600
23550 IF X(I+1)>0 THEN P=PI/2 \ IF X(I+1)<0 THEN P=-PI/2 \ REM IM(X)=0
23555 IF X(I)=0 THEN P=0 \ REM RE(X)=0
23560 RETURN
23600 IF S>0 THEN 23700
23610 IF X(I)<0 THEN P=ATN(X(I+1)/X(I))+PI \ REM 2ND QUADRANT.
23620 IF X(I)>0 THEN P=ATN(X(I+1)/X(I))+2*PI \ REM 4TH QUADRANT.
23630 RETURN
23700 IF X(I+1)>0 THEN P=ATN(X(I+1)/X(I)) \ REM 1ST QUADRANT.
23710 IF X(I+1)<0 THEN P=ATN(X(I+1)/X(I))+PI \ REM 3RD QUADRANT.
23720 RETURN
24000 REM
24010 REM ***** REMOVE DC OFFSET *****
24020 REM
24500 DIM M(2)
24510 M(0)=0
24520 FOR I=0 TO N1-1 \ M(0)=M(0)+X(I) \ NEXT I \ M(0)=M(0)/N1
24530 FOR I=0 TO N1-1 \ X(I)=X(I)-M(0) \ NEXT I \ REM SUBTRACT OFFSET.
24535 PRINT M(0)
24540 RETURN
24600 REM
24610 REM ***** NORMALIZE X(I) *****
24620 REM
24625 V9=X(0)
24630 FOR I=0 TO N1-1 \ IF ABS(X(I))>ABS(V9) THEN V9=ABS(X(I))
24632 NEXT I
24635 FOR I=0 TO N1-1 \ X(I)=X(I)/V9 \ NEXT I \ REM NORMALIZES.
24640 RETURN
24700 REM
24710 REM ***** PLOT SPECTRUM IN RECT COORDS *****
24720 REM
24730 TEKMODE \ ERASE
24740 GOSUB 360 \ REM START A GRAPH  \ GOSUB 8000 \ REM COMMENT.
24744 GOSUB 25000 \ REM RECT EXTREMA.
24765 PHYL(A2,0,40*F9,0,70*F9)
24766 X1=0 \ X2=1/2/T1 \ Y1=H9(2) \ Y2=H9(1)
```

```
22950 Y8$="" \ PRINT "RESTORE OFFSET"; \ INPUT Y8$
22975 IF Y8$="Y" THEN X(0)=X(0)+M(0) \ REM RESTORES OFFSET
22980 RETURN
23000 REM
23010 REM ***** PREPARE FOR PHASE SPECTRUM *****
23020 REM
23030 PRINT "S/N ESTIMATE FROM AMP SPECTRUM"; \ INPUT N0
23160 RETURN
23200 REM
23210 REM ***** PLOT PHASE SPECTRUM *****
23220 REM
23230 TEKMODE \ ERASE
23240 GOSUB 360 \ REM START A GRAPH  \ GOSUB 8000 \ REM COMMENT.
23250 PHYL(A2,0,100*F9,0,70*F9)
23252 GOSUB 31300 \ REM MAX AMP.
23255 GOSUB 27000 \ REM S/N COMMENT.
23260 GOSUB 470 \ REM AXES
23262 SCALE(A2,0,0,1/(2*T1),0,2*PI)
23264 LABEL(A2,"FREQUENCY, HZ","PHASE-RAD",1/10/T1,PI,1)
23270 FOR I=0 TO N1-1 STEP 2
23275 GOSUB 26710 \ REM PHASE CALCULATIONS.
23320 PLOT(A2,I/N1/(2*T1),P) \ REM (FREQ,PHASE)
23325 NEXT I
23326 INVEC(A2) \ PLOT(A2,1/3/T1,0) \ PLOT(A2,1/3/T1,2*PI)
23330 RETURN
23500 REM
23510 REM ***** ARCTANGENT FOR CONTINUOUS PHASE *****
23520 REM
23525 P=0
23530 S=SGN(X(I))*SGN(X(I+1)) \ REM >0 FOR 1ST/3RD, <0 FOR 2ND/4TH.
23540 IF S<>0 THEN 23600
23550 IF X(I+1)>0 THEN P=PI/2 \ IF X(I+1)<0 THEN P=-PI/2 \ REM IM(X)=0
23555 IF X(I)=0 THEN P=0 \ REM RE(X)=0
23560 RETURN
23600 IF S>0 THEN 23700
23610 IF X(I)<0 THEN P=ATN(X(I+1)/X(I))+PI \ REM 2ND QUADRANT.
23620 IF X(I)>0 THEN P=ATN(X(I+1)/X(I))+2*PI \ REM 4TH QUADRANT.
23630 RETURN
23700 IF X(I+1)>0 THEN P=ATN(X(I+1)/X(I)) \ REM 1ST QUADRANT.
23710 IF X(I+1)<0 THEN P=ATN(X(I+1)/X(I))+PI \ REM 3RD QUADRANT.
23720 RETURN
24000 REM
24010 REM ***** REMOVE DC OFFSET *****
24020 REM
24500 DIM M(2)
24510 M(0)=0
24520 FOR I=0 TO N1-1 \ M(0)=M(0)+X(I) \ NEXT I \ M(0)=M(0)/N1
24530 FOR I=0 TO N1-1 \ X(I)=X(I)-M(0) \ NEXT I \ REM SUBTRACT OFFSET.
24535 PRINT M(0)
24540 RETURN
24600 REM
24610 REM ***** NORMALIZE X(I) *****
24620 REM
24625 V9=X(0)
24630 FOR I=0 TO N1-1 \ IF ABS(X(I))>ABS(V9) THEN V9=ABS(X(I))
24632 NEXT I
24635 FOR I=0 TO N1-1 \ X(I)=X(I)/V9 \ NEXT I \ REM NORMALIZES.
24640 RETURN
24700 REM
24710 REM ***** PLOT SPECTRUM IN RECT COORDS *****
24720 REM
24730 TEKMODE \ ERASE
24740 GOSUB 360 \ REM START A GRAPH  \ GOSUB 8000 \ REM COMMENT.
24744 GOSUB 25000 \ REM RECT EXTREMA.
24765 PHYL(A2,0,40*F9,0,70*F9)
24766 X1=0 \ X2=1/2/T1 \ Y1=H9(2) \ Y2=H9(1)
```

```
24768 GOSUB 1500 \ REM INT.
24770 SCALE(A2,0,0,1/2/T1,Y3,Y4) \ REM OVERRIDES PREVIOUS GOSUB.
24775 LABEL(A2,"FREQ, HZ","RE-N",1/2/T1/5,Y5,1)
24780 GOSUB 470 \ REM AXES.
24790 FOR I=0 TO N1-1 STEP 2 \ REM STEP 2 IMPORTANT.
24800 PLOT(A2,I/(N1-1)/2/T1,X(I)) \ REM (FREQ,REAL)
24810 NEXT I
24820 INVEC(A2) \ PLOT(A2,1/3/T1,Y3) \ PLOT(A2,1/3/T1,Y4) \ REM SAFELINE.
24830 PHYL(A2,60*F9,100*F9,0,70*F9)
24840 SCALE(A2,0,0,1/2/T1,Y3,Y4) \ REM OVERRIDES PREVIOUS GOSUB.
24850 LABEL(A2,"FREQ, HZ","IM-N",1/2/T1/5,Y5,1)
24860 GOSUB 470 \ REM AXES
24870 FOR I=0 TO N1-1 STEP 2 \ REM STEP 2 IMPORTANT.
24880 PLOT(A2,I/N1/2/T1,X(I+1)) \ REM (FREQ,IMAG)
24885 NEXT I
24886 INVEC(A2) \ PLOT(A2,1/3/T1,Y3) \ PLOT(A2,1/3/T1,Y4) \ REM SAFELINE.
24900 GOSUB 3800 \ REM WAIT THEN CLS  \ RETURN
25000 REM
25010 REM ***** FIND RECTANGULAR EXTREMA *****
25020 REM
25025 SETDIM H8(2),H9(2)
25026 FOR I=1 TO 2 \ H8(I)=X(1) \ H9(I)=X(0) \ NEXT I
25030 FOR I=0 TO N1-1 STEP 2
25040 IF X(I)>H9(1) THEN H9(1)=X(I) \ REM REAL MAX.
25050 IF X(I+1)>H8(1) THEN H8(1)=X(I+1) \ REM IMAG MAX.
25060 IF X(I)<H9(2) THEN H9(2)=X(I) \ REM REAL MIN.
25070 IF X(I+1)<H8(2) THEN H8(2)=X(I+1) \ REM IMAG MIN.
25080 NEXT I
25082 IF H8(1)>H9(1) THEN H9(1)=H8(1) \ REM COMMON MAX.
25084 IF H8(2)<H9(2) THEN H9(2)=H8(2) \ REM COMMON MIN.
25090 RETURN
25200 REM
25210 REM ***** COMMENTS *****
25220 REM
25230 PRINT "TITLE"; \ INPUT X1$
25235 PRINT "MATERIAL"; \ INPUT X2$
25240 X2$=X2$+", SOURCE FILE: "+C1$
25256 X3$=STR$(N1)+" POINTS, FREQ = "+STR$(F1)+" HZ, "+STR$(C)+" CYCLES."
25257 X4$="N.F.= "+STR$(1/2/T1)+" HZ, DF="+STR$(1/T1/N1)+" HZ."
25270 WHOAMI(A$) \ X6$="PGM: "+A$+" BY A.J.GIACOMIN, P.ENG."
25300 GDATE(Y9,M9,D9) \ X7$="DATE: "+STR$(Y9)+"-"+STR$(M9)+"-"+STR$(D9)
25310 GTIME(S9,M9,H9) \ X7$=X7$+", TIME: "+STR$(H9)+":"+STR$(M9)+":"+STR$(S9)
25330 RETURN
26000 REM
26010 REM ***** PLOT FILTERED AMP SPECTRUM *****
26020 REM
26030 TEKMODE \ ERASE
26040 GOSUB 360 \ REM START A GRAPH  \ GOSUB 8000 \ REM COMMENT.
26050 PHYL(A2,0,100*F9,0,70*F9)
26055 GOSUB 27000 \ REM S/N COMMENT.
26060 GOSUB 31300 \ REM MAX AMP.
26110 SCALE(A2,0,0,1/(2*T1),0,1.1*H9)
26120 LABEL(A2,'FREQUENCY, HZ','FORCE AMP-N',1/10/T1,1.1*H9/5,1)
26130 GOSUB 470 \ REM AXES
26145 FOR I=0 TO N1-1 STEP 2
26150 A=2*SQR(X(I)^2+X(I+1)^2)
26152 IF A<H9/N0 THEN A=0
26153 PLOT(A2,I/N1/2/T1,A) \ REM (FREQ,AMP)
26154 NEXT I
26180 INVEC(A2) \ PLOT(A2,1/(3*T1),0) \ PLOT(A2,1/(3*T1),1.1*H9)
26190 RETURN
26700 REM
26710 REM ***** PHASE CALCULATION *****
26720 REM
26800 GOSUB 23500 \ REM  ARCTANGENT FOR CONTINUOUS PHASE.
26810 REM SETS PHASE TO ZERO WHEN AMPLITUDE INSIGNIFICANT.
```

```
26820 A=2*SQR(X(I)^2+X(I+1)^2)
26822 IF N5<>0 THEN 26840
26824 IF A<H9/N0 THEN P=0
26830 REM P=P+PI/2 \ REM CHANGES FROM COS BASED TO SIN BASED FFT.
26840 IF P>=2*PI THEN P=P-2*PI
26850 RETURN
27000 REM
27010 REM ***** S/N COMMENT *****
27020 REM
27030 X8$="S/N = "+STR$(N0)
27040 COMM(A2,X8$,75,90)
27050 RETURN
30000 REM
30010 REM ***** LOADS FILE *****
30020 REM
30030 PRINT "FILENAME"; \ INPUT C1$
30040 OPEN C1$ FOR INPUT AS FILE #1
30050 FOR I=0 TO N1
30060 INPUT #1,A1,A6,A3,A4,A5
30080 VA1(I,1)=A1 \ VA1(I,2)=A6 \ VA1(I,3)=A3 \ VA1(I,4)=A4 \ VA1(I,5)=A5
30085 IF END #1 THEN 30100
30090 NEXT I
30100 CLOSE #1
30110 RETURN
30120 REM
31000 REM
31010 REM ****** PLOT LOG-AMP SPECTRUM *****
31020 REM
31030 TEKMODE \ ERASE
31040 GOSUB 360 \ REM START A GRAPH  \ GOSUB 8000 \ REM COMMENT
31050 PHYL(A2,0,100*F9,0,70*F9)
31075 GOSUB 31300 \ REM MAX AMP.
31105 Y1=10^(INT(LOG10(H9))+1) \ Y2=Y1/100000
31110 SCALE(A2,1,0,1/2/T1,Y2,Y1)
31120 LABEL(A2,"FREQUENCY, HZ","FORCE AMP-N",1/10/T1,2,1)
31130 GOSUB 540 \ REM AXES
31140 FOR I=0 TO N1-1 STEP 2
31150 A=2*SQR(X(I)^2+X(I+1)^2) \ REM BY DEFN.
31160 IF A<=0 THEN A=Y2 \ REM FOR ZEROES.
31170 PLOT(A2,I/N1/2/T1,A)
31180 NEXT I
31190 INVEC(A2) \ PLOT(A2,1/3/T1,1.00000E-08) \ PLOT(A2,1/3/T1,1.00000E+08)
31200 GOSUB 3800 \ REM WAIT  \ RETURN
31300 REM
31310 REM ***** FINDS MAX AMP *****
31320 REM
31322 H9=X(0) \ REM STARTING VALUE.
31325 FOR I=0 TO N1-1 STEP 2
31340 A=2*SQR(X(I)^2+X(I+1)^2)
31350 IF A>H9 THEN H9=A \ REM MAX AMP.
31360 NEXT I \ RETURN
31500 REM
31510 REM ***** PRINTED REPORT ON FFT *****
31520 REM
31530 PRINT "REPORT FORTHCOMING: CTRL PRT-SCR TO PRINT"
31540 GOSUB 3800 \ REM WAIT
31570 PRINT  \ PRINT  \ PRINT
31580 PRINT "REPORT ON ";X1$
31590 PRINT
31600 PRINT X2$ \ PRINT X3$ \ PRINT X4$
31610 PRINT X6$ \ PRINT X7$
31620 PRINT "S/N= ";N0
31630 PRINT
31640 PRINT
31650 GOSUB 31300 \ REM MAX AMP.
31660 PRINT "FREQ.HZ","REAL.N","IMAG.N","AMP.N","PHASE.RAD"
```

```
31670 PRINT
31680 FOR I=0 TO N1-1 STEP 2
31690 A=2*SQR(X(I)^2+X(I+1)^2) \ REM AMPLITUDE.
31700 IF A<H9/N0 THEN 31730
31710 GOSUB 26710 \ REM PHASE CALCULATIONS.
31720 PRINT I/N1/2/T1,X(I),X(I+1),2*SQR(X(I)^2+X(I+1)^2),P
31730 NEXT I
31740 PRINT  \ PRINT  \ PRINT
31750 GOSUB 3800 \ REM WAIT
31760 PRINT "TOGGLE CTRL-PRT OFF" \ GOSUB 3800 \ REM WAIT
31770 RETURN
32000 REM
32010 REM ***** STATS: MEAN & STD DEV OF NOISE *****
32020 REM
32030 N4=0 \ N8=0 \ N5=0 \ K4=0 \ REM INIT VALUES.
32050 FOR I=0 TO N1-1 STEP 2
32055 A=2*SQR(X(I)^2+X(I+1)^2)
32060 IF A>H9/N0 THEN 32078
32065 N8=N8+X(I)+X(I+1) \ REM FOR RECT MEAN.
32070 N4=N4+2*SQR(X(I)^2+X(I+1)^2) \ REM FOR POLAR MEAN.
32074 K4=K4+1 \ REM COUNTER.
32078 NEXT I
32080 N4=N4/K4 \ REM POLAR STAT MEAN.
32081 N8=N8/2/K4 \ REM RECT STAT MEAN.
32082 FOR I=0 TO N1-1 STEP 2
32086 N5=N5+(X(I)-N8)^2+(X(I+1)-N8)^2 \ REM SUM SQRS RECT. RESIDS.
32090 NEXT I
32098 N5=N5/2/K4 \ REM VARIANCE OF NOISE IN RECT.
32100 N5=SQR(N5/(K4-1)) \ REM STD. DEV. IN RECT. COORDS.
32130 PRINT "POLAR MEAN: ";N4;", RECT STD DEV: ";N5
32140 GOSUB 3800 \ REM WAIT.
32150 RETURN
32200 REM
32210 REM ***** PLOT NOISE SUBTRACTED AMP SPECTRUM *****
32211 REM            WITH CONFIDENCE INTERVALS
32220 REM
32230 TEKMODE \ ERASE
32240 GOSUB 360 \ REM START GRAPH \ GOSUB 8000 \ REM COMMENT
32250 PHYL(A2,0,-100*F9,0,70*F9)
32260 GOSUB 27000 \ REM S/N COMMENT.
32275 GOSUB 31300 \ REM MAX AMP.
32276 H9=H9/40 \ REM MAGNIFY TRUNKS.
32280 SCALE(A2,0,0,1/2/T1,-N4-2*N5,1.1*H9)
32290 LABEL(A2,'FREQUENCY, HZ','FORCE-N',1/10/T1,1.1*H9/5,1)
32300 GOSUB 470 \ REM AXES.
32360 INVEC(A2) \ PLOT(A2,1/3/T1,0) \ PLOT(A2,1/3/T1,1.1*H9)
32365 REM UPPER CONF LIMIT.
32370 INVEC(A2) \ FOR I=0 TO N1-1 STEP 2
32380 A=2*SQR(X(I)^2+X(I+1)^2)-N4+SQR(2*2*N5^2) \ REM 95% CONF.
32390 PLOT(A2,I/N1/2/T1,A) \ REM (FREQ, UPPER LIM)
32400 NEXT I
32410 REM LOWER CONF LIMIT.
32420 INVEC(A2) \ FOR I=0 TO N1-1 STEP 2
32430 A=2*SQR(X(I)^2+X(I+1)^2)-N4-N5*SQR(2) \ REM 95% CONF..
32440 PLOT(A2,I/N1/2/T1,A) \ REM (FREQ, LOWER LIM)
32450 NEXT I
32480 GOSUB 3800 \ REM WAIT
32490 RETURN
32500 REM
32510 REM ***** PRINT REPORT ON NOISE SUBTRACTED SPECTRUM *****
32520 REM
32530 PRINT "STAT REPORT FORTHCOMING: CTRL PRT-SCR TO PRINT"
32540 GOSUB 3800 \ REM WAIT
32570 PRINT  \ PRINT  \ PRINT
32580 PRINT "REPORT ON ";X1$
32585 PRINT "COMPONENTS KNOWN WITH AT LEAST 95% CONFIDENCE"
```

```
32590 PRINT
32595 PRINT "POLAR MEAN: ";N4;", RECT STD DEV: ";N5
32600 PRINT X2$ \ PRINT X3$ \ PRINT X4$
32610 PRINT "S/N= ";N0
32620 PRINT X6$ \ PRINT X7$
32630 PRINT  \ PRINT
32650 GOSUB 31300 \ REM MAX AMP.
32660 PRINT "FREQ,HZ","REAL,N","IMAG,N","AMP,N","PHASE,RAD"
32680 FOR I=0 TO N1-1 STEP 2
32690 A=2*SQR(X(I)^2+X(I+1)^2)-N4 \ REM NOISE SUBTRACTED AMP.
32700 IF A<N5*SQR(2) THEN 32730
32710 GOSUB 26710 \ REM PHASE CALCULATIONS.
32720 PRINT I/N1/2/T1,X(I),X(I+1),A,P
32730 NEXT I
32740 PRINT  \ PRINT  \ PRINT
32750 GOSUB 3800 \ REM WAIT
32760 PRINT "TOGGLE CTRL-PRT OFF" \ GOSUB 3800 \ REM WAIT
32765 RETURN
```

APPENDIX 4: Program for Static Calibration

```
LIST

CAL17   5-Aug-86  MTS 773 MU BASIC V02.08

10 REM          TRANSDUCER CALIBRATION PROGRAM
20 REM
30 REM          BY T. SAMURKAS & A.J. GIACOMIN
40 REM
50 C1=1
60 DIM N(1,1)
70 FGSTOP \ ADSTOP \ REM A GOOD IDEA
80 TEKMODE \ VTMODE \ REM CLEARS SCREEN
90 WHOAMI(A$) \ PRINT "PROGRAM: ";A$ \ PRINT
95 GOSUB 1500 \ REM GENERAL INFORMATION.
100 PRINT "HOW MANY TESTS"; \ INPUT N1
110 PRINT "HOW MANY POINTS PER TEST"; \ INPUT N2
120 N3=(N2*N1)-1 \ SETDIM A(N3,3) \ REM DYNAMIC DIMENSIONING
130 N4=N2-1 \ SETDIM D(N4,2) \ REM BABY DATA ARRAY.
140 REM
150 REM ***** CALIBRATION MEASUREMENTS *****
160 REM
170 PRINT "READY FOR TEST #";C1; \ INPUT Y1$
180 REM
190 PRINT \ PRINT "TOTAL WEIGHT, KG"; \ INPUT W1
200 CKTIME(1,.5,Z1)
210 ADTIMED(1,D,,2,2,1,1)
220 ADINIT \ ADGO
230 IF D=N2-1 THEN 250
240 IF D<N2-1 THEN 240
250 C1=C1+1
260 ADSTOP \ CKSTOP
270 FOR I=0 TO N4
280 PRINT D(I,1),D(I,2)
290 A((C1-2)*N2+I,1)=ELEVEL(D(I,1)) \ REM STORES SST.
300 A((C1-2)*N2+I,2)=ELEVEL(D(I,2)) \ REM STORES LOAD.
310 A((C1-2)*N2+I,3)=W1
320 NEXT I
330 PRINT
340 FOR I=0 TO N3
350 PRINT A(I,1),A(I,2),A(I,3)
360 NEXT I
370 IF C1=N1+1 THEN PRINT "CALIBRATION COMPLETE"
380 IF C1=N1+1 THEN 420
390 PRINT "READY FOR TEST #";C1; \ INPUT Y1$
400 GO TO 190
410 REM
420 REM ***** FIND WMAX, LDMIN, LDMAX, SSTMIN, SSTMAX *****
430 REM
440 W2=A(1,3) \ V1=A(1,1) \ V2=A(1,1) \ P1=A(1,2) \ P2=A(1,2)
450 PRINT W2,V1,V2,P1,P2 \ REM STARTING VALUES
460 REM
470 REM DO LOOP
480 REM
490 J=0
500 IF A(J,1)<V1 THEN V1=A(J,1)
510 IF A(J,1)>V2 THEN V2=A(J,1)
520 IF A(J,2)<P1 THEN P1=A(J,2)
530 IF A(J,2)>P2 THEN P2=A(J,2)
540 IF A(J,3)>W2 THEN W2=A(J,3)
550 J=J+1
560 IF J<=N3 THEN 500 \ REM ENDS DO LOOP
```

```
570 REM
580 REM ***** LINEAR REGRESSION OF CALIBRATION MEASTS. *****
590 REM
600 REM N2*N1 IS THE NUMBER OF DATA POINTS.
610 REM SCHEME: COMPUTE Y(J),X,S1,S2 THEN GET B0 AND B1.
620 REM
630 DIM Y(2),X(2),S1(2),S2(2),B0(2),B1(2)
640 FOR J=1 TO 2
650 FOR I=0 TO N3
660 S1(J)=S1(J)+A(I,3)*A(I,J)
670 S2(J)=S2(J)+A(I,3)^2
680 X(J)=X(J)+A(I,3)
690 Y(J)=Y(J)+A(I,J)
700 NEXT I
710 X(J)=X(J)/(N2*N1) \ Y(J)=Y(J)/(N2*N1)
720 B1(J)=(S1(J)-N2*N1*X(J)*Y(J))/(S2(J)-N2*N1*X(J)^2) \ REM B1(J) IS LS SLOPE .
730 B0(J)=Y(J)-B1(J)*X(J) \ REM B0(J) IS LS ESTIMATE OF Y(J)-INTERCEPT.
740 VTMODE
750 PRINT "B0(";J;")=";B0(J);"V,","B1(";J;")=";B1(J);"V/KG."
760 NEXT J
840 N8=(V2-V1)
850 N9=(P2-P1)
860 REM
870 GRATTACH(2,2,Y9)
880 PRINT "VT-240 (1) OR PLOTTER (2)"; \ INPUT A2
890 IF A2=2 THEN GRON(A2)
900 IF A2=2 THEN PRINT "FRACTION OF FULLSIZE (.75)"; \ INPUT F9
905 IF A2=2 THEN GRON(2) \ IF A2=2 THEN SIZE(A2,108*F9,216*F9)
910 IF A2=1 THEN F9=1
920 REM
930 REM
940 REM ***** SST CALIBRATION GRAPHICS *****
950 REM
960 IF A2=1 THEN TEKMODE(1,1)
970 PHYL(A2,0,F9*40,0,F9*70)
980 SCALE(A2,0,-.1*W2,1.1*W2,V1-.1*(V2-V1),V2+.1*(V2-V1))
990 LABEL(A2,"WEIGHT, KG","SST-DV",W2/4,N8/8,1)
1000 AXES(A2,0,0) \ AXES(A2,100,100) \ AXES(A2,-100,-100)
1010 FOR I=0 TO N3
1020 MARK(A2,1,A(I,3),A(I,1))
1030 PLOT(A2,A(I,3),B0(1)+B1(1)*A(I,3))
1040 NEXT I
1050 INVEC
1060 REM
1070 REM ***** LOAD CELL CALIBRATION GRAPHICS *****
1080 REM
1090 IF A2=1 THEN TEKMODE(1,1)
1100 PHYL(A2,55*F9,95*F9,0,70*F9)
1110 SCALE(A2,0,-.1*W2,1.1*W2,P1-.1*(P2-P1),P2+.1*(P2-P1))
1120 LABEL(A2,"WEIGHT, KG","LOAD-DV",W2/4,N9/8,1)
1130 AXES(A2,0,0) \ AXES(A2,100,100) \ AXES(A2,-100,-100)
1140 FOR I=0 TO N3
1150 MARK(A2,1,A(I,3),A(I,2))
1160 PLOT(A2,A(I,3),B0(2)+A(I,3)*B1(2))
1170 NEXT I
1180 INVEC
1190 REM
1200 REM ***** GRAPHICS COMMENTS *****
1210 REM
1220 INVEC
1230 IF A2=1 THEN TEKMODE(1,1)
1240 PHYL(A2,0,95*F9,80*F9,100*F9)
1250 AXES(A2,100,100) \ AXES(A2,-100,-100) \ REM DRAWS BOX.
1260 SCALE(A2,0,0,100,0,10)
1270 GDATE(Y9,M9,D9) \ D$=STR$(Y9)+"-"+STR$(M9)+"-"+STR$(D9)
1280 GTIME(S9,M9,H9) \ T$=STR$(H9)+":"+STR$(M9)+":"+STR$(S9)
```

```
1290 C9$="DATE: "+D$+", TIME: "+T$+".  BY: "+N9$
1300 C8$="BEAM NO. "+B9$+", PROBE NO. "+P9$+", T= "+T9$+" C."
1310 COMM(A2,C9$,1,8) \ COMM(A2,C8$,1,5)
1320 A9$="PROGRAM: "+A$+", "+STR$(N1)+" TESTS, "+STR$(N2)+" PTS/TEST."
1330 COMM(A2,A9$,1,2)
1340 INVEC
1350 PHYL(A2,0,F9*100,0,F9*100)
1360 SCALE(A2,0,0,100,0,100)
1370 B1$=STR$(B1(2)*10*100/VAL(R6$)) \ V$=" V/KG" \ C2$=B1$+V$
1375 REM CONVERTS DV TO V AT RS=100%.
1380 COMM(A2,C2$,60,65)
1385 L5$="RS= "+R5$+" %" \ COMM(A2,L5$,5,60)
1390 B1$=STR$(B1(1)*10*100/VAL(R5$)) \ C1$=B1$+V$
1395 REM CONVERTS DV TO V AT RS=100%.
1400 COMM(A2,C1$,5,65)
1410 L6$="RS= "+R6$+" %" \ COMM(A2,L6$,60,60)
1420 INPUT T1$ \ IF T1$<>"" THEN 1420
1425 IF A2=2 THEN GROFF(2)
1430 TEKMODE(1,1) \ VTMODE \ GO TO 880
1440 END
1500 REM
1510 REM ***** GENERAL INFO.& GRAPHICS PREP *****
1520 REM
1530 PRINT "NAME"; \ INPUT N9$
1540 PRINT "BEAM NUMBER"; \ INPUT B9$
1550 PRINT "CAPACITANCE PROBE"; \ INPUT P9$
1560 PRINT "TEMPERATURE, C"; \ INPUT T9$
1570 PRINT "SST RANGE SETTING, %"; \ INPUT R5$
1580 PRINT "LOAD RANGE SETTING, %"; \ INPUT R6$
1590 RETURN
1600 REM
1610 REM ***** PRINTS LIST OF HANGING WEIGHTS *****
1620 REM
1630 PRINT  \ PRINT  \ PRINT
1640 PRINT "MEAST NO","MASS, KG"
1650 PRINT 1,0
1660 PRINT 2,.5001
1670 PRINT 3,.9979
1680 PRINT 4,.5001+.9979
1690 PRINT 5,.9979+.9989
1700 PRINT 6,.9979+.9989+.5001
1710 PRINT 7,.9979+.9989+.9989
1720 PRINT 8,.9979+.9989+.9989+.5001
1730 PRINT  \ PRINT  \ PRINT
1740 REM

Ready
```

AUTHOR INDEX

REFERENCES

1. Dealy, J.M., "Official nomenclature for material functions describing the response of a viscoelastic fluid to various shearing and extensional deformations", J. Rheol., 28,(3), 181-195 (1984).

2. Sieglaff, C.L., Trans. Soc. Rheol., 20, 311 (1976).

3. Leaderman, H., "Proposed nomenclature for linear viscoelastic behavior", Trans. Soc. Rheol., I, 313-222 (1957).

4 Dealy, J.M , Rheometers for Molten Plastics, Van Nostrand Reinhold Co., New York (1982).

5. Bruker, I. and A.S. Lodge, "A rheodilatometer for molten polymers", J. Rheol., 29(5), 557-577 (1985).

6 McMillan, F M , The Chain Straighteners, Fruitful Innovation , the Discovery of Linear and Stereoregular Synthetic Polymers, 82ff, Publ The MacMillan Press Ltd, London, 1979.

7. Lank, H H. and E.L. Williams, The DU PONT CANADA History, 211ff, Publ. DU PONT CANADA INC., 1982.

8 Dealy, J M , Rheometers for Molten Plastics, A Practical Guide to Testing and Property Measurement, Van Nostrand Reinhold, New York, 1982.

9. Dealy, J.M., "Melt rheometers as sensors for quality and process control", Proc. 45th Ann. Tech. Cong. & Exhibit, SPE ANTEC '87, Los Angeles (May, 1987), p. 926.

10. Wu, S., "Polymer molecular-weight distribution from dynamic melt viscoelasticity", Pol. Eng. Sci., 25(2), 122-128 ~~(Mid-February~~, 1985).

11 Wu, S., "Characterization of polymer molecular weight distribution from transient melt viscoelasticity", Advances in Rheology, Vol. 3, Polymers, (Proc. IX Intl. Congr. on Rheol., Mexico, 1984), B. Mena, A. Garcia-Rejon and C. Rangel-Nafaile, eds., pp. 359-366, Univ. Nacional Autonoma de Mexico, Mexico, 1984.

12. Tuminello, W.H., "Molecular weight and molecular weight distribution from dynamic measurements of polymer melts", Presented at Soc. Rheol. Ann. Mtg., Ann Arbor (October 14-17, 1985).

13. Montfort, J.P., G. Marin, J. Arman and Ph. Monge, "Viscoelastic properties of high molecular weight polymers in the molten state II. Influence of the molecular weight distribution on linear viscoelastic properties", Rheol. Acta, 18, 623-628 (1979).

14. Letton, A. and W.H. Tuminello, "A method for calculating the molecular weight distribution from the storage modulus master curve", Proc. 45th Ann. Tech. Conf. & Exhibit, SPE ANTEC '87, Los Angeles (May, 1987), p.997-1001.

15 Shah, B.H. and R. Darby, "Prediction of polyethylene melt rheological properties from molecular weight distribution data obtained by gel permeation chromatography", Pol. Eng. Sci., 16(8), 579 (August, 1976).

16 Shah, B.H. and R. Darby, "A note on the prediction of polyethylene melt rheological properties from molecular weight distribution data obtained by gel permeation chromatography", Pol. Eng. Sci., 22(1), 53 (January, 1982).

17 Tuminello, W H , "Determination of molecular weight distribution (MWD) from melt rheology. A review", Proc. 45 th Ann. Tech. Conf. & Exhibit, SPE ANTEC '87, Los Angeles (May, 1987).

18. Menezes, E V and W W Graessley, "Nonlinear rheological behavior of polymer systems for several shear-flow histories", J. Pol. Sci.. Pol. Phys. Ed., 20, 1817-1833 (1982).

19. Raju, V.R., E V. Menezes, G. Marin, W.W. Graessley and L.J. Fetters, "Concentration and molecular weight dependence of viscoelastic properties in linear and star polymers", Macromolecules, 14, 1668-1676 (1981).

20. Letton, A and W H Tuminello, "A method for calculating the molecular weight distribution from the storage modulus master curve", Proc. 45th Ann. Tech Conf. & Exhibit, SPE ANTEC '87, Los Angeles (May, 1987), p 997-1001.

21. Isayev, A.I. and C.A. Hieber, Rheol. Acta, 19, 168 (1980).

22 Letter, Giacomin, A.J. to G.E. Hibberd, BREAD RESEARCH INSTITUTE OF AUSTRALIA, 1984 May 8.

23 Letter, Hibberd, G.E. of the BREAD RESEARCH INSTITUTE OF AUSTRALIA to A.J. Giacomin, 1984 June 4.

24. Hibberd, G.E. and N.S. Parker, "Measurement of the Fundamental Rheological Properties of Wheat-Flour Doughs", Cereal Chem., 52(3-II), 1r-23r (1975).

25. Hibberd, G.E. and W.J. Wallace, "Requirements of Modern Dough Rheology", Cereal Sci. Today, 11(10), 434-455 (1966).

26. Davis, S.S., "Viscoelastic Properties of Pharmaceutical Semisolids IV: Destructive Oscillatory Testing", J. Pharm. Sci., 60(9), 1356-1360 (September, 1971).

27. Thurston, G.B., "Rheological Parameters for the Viscosity, Viscoelasticity and Thixotropy of Blood", Biorheology, 16, 149-162, Proc. Third Int. Congr. of Biorheol.: Symp. on Recent Adv. in Hemorheol. I,

Pergamon Press Ltd., 1979.

28. Letter, A.J. Giacomin to G.B. Thurston, Univ. of Texas at Austin, 1984 May 20.

29. Letter, G.B. Thurston of Univ. of Texas at Austin to Giacomin, A.J., 1984 May 30.

30. Sullivan, J.L. and V.C. Demery, "The Nonlinear Viscoelastic Behavior of a Carbon-Black-Filled Elastomer", J. Pol. Sci.: Pol. Phys. Ed., 20, 2083-2101 (1982).

31 Dealy, J M , Rheometers for Molten Plastics. A Practical Guide to Testing and Property Measurement, Van Nostrand Reinhold, New York, 1982.

32. Dealy, J.M., "Melt Rheometer Update", Plastics Engineering, 57-61 (March, 1983).

33 Dealy, J M , Rheometers for Molten Plastics. A Practical Guide to Testing and Property Measurement, Van Nostrand Reinhold, New York, 1982, p 107-110.

34 Dealy, J M , Rheometers for Molten Plastics. A Practical Guide to Testing and Property Measurement, Van Nostrand Reinhold, New York, 1982, p. 107-110.

35 Dealy, J M , Rheometers for Molten Plastics; A Practical Guide to Testing and Property Measurement, Van Nostrand Reinhold, New York, 1982.

36 Dealy, J M , Rheometers for Molten Plastics. A Practical Guide to Testing and Property Measurement. Van Nostrand Reinhold, New York (1982), pp. 144-145.

37. Macosko, C.W. and W.M. Davis, Rheol. Acta 13:814 (1974).

38. Gross, L.H and B. Maxwell, Trans. Soc. Rheol. 16:577 (1972).

39. Jongschaap, J.J., K.H. Knapper and J.S. Lopulissa, "On the limit of linear viscoelastic response in the flow between eccentric rotating disks", Pol. Eng. Sci., 18(10), 788-792 (1978).

40. Parker, N.S. and G.E. Hibberd, "The interpretation of dynamic measurements on non-linear viscoelastic materials", Rheol. Acta, 13, 910-915 (1974).

41. MacSporran, W.C. and R.P. Spiers, "The dynamic performance of the Weissenberg Rheogoniometer I. Small amplitude oscillatory shearing", Rheol. Acta, 21, 184-192 (1982).

42. MacSporran, W.C. and R.P. Spiers, "The dynamic performance of the Weissenberg Rheogoniometer II. Large amplitude oscillatory shearing - fundamental response", Rheol. Acta, 21, 193-200 (1982).

43. MacSporran, W.C. and R.P. Spiers, "The dynamic performance of the Weissenberg Rheogoniometer III. Large amplitude oscillatory shearing-harmonic analysis", Rheol. Acta, 23, 90-96 (1984).

44. Ganani, E. and R.L. Powell, "Transient Flow Viscometry", J. Rheol., 29(6), 931-941 (1985).

45. Walters, K., Rheometry, Chapman & Hall, London (1975).

46 Walters, K , Rheometry, Industrial Applications, John Wiley & Sons, New York (1980).

47 Walters, K., "BOOK REVIEW. Rheometers for Molten Plastics by J.M. Dealy", Rheol. Abs., 26(3) (1983).

48 Walters, K., "BOOK REVIEW. Rheometers for Molten Plastics by J.M. Dealy", J. Non-Newt. Fluid Mech., 12, 253 (1983).

49 Mewis, J , "Thixotropy-A General Review", J. Non-Newt. Fluid Mech., 6, 1-20 (1979).

50 Dealy, J M , Rheometers for Molten Plastics, A Practical Guide to Testing and Property Measurement, an SPE book, Van Nostrand Reinhold, 1982.

51. Hibberd, G.E. and N.S. Parker, "A Parallel Plate Rheometer for Measuring the Viscoelastic Properties of Wheat Flour Doughs", Cereal Chem., 55(1), 102-110 (1978).

52. Hibberd, G.E. and N.S. Parker, "Measurement of the Fundamental Rheological Properties of Wheat-Flour Doughs", Cereal Chem., 52(3-II), (May-June, 1975).

53 Hibberd, G E and N.S. Parker, "Nonlinear Creep and Creep Recovery of Wheat-Flour Doughs", Cereal Chem., 56(4), 232-236 (1979).

54. Jhon, M.S., "Polymer migration in newtonian fluids", J. Pol. Sci.: Pol. Phys. Ed., 23, 955 (1985).

55. MacSporran, W.C. and R.P. Spiers, "The dynamic performance of the Weissenberg Rheogoniometer II. Large amplitude oscillatory shearing - Fundamental response", Rheol. Acta, 21, 193-200 (1982).

56. MacSporran, W.C. and R.P. Spiers, "The dynamic performance of the Weissenberg Rheogoniometer III. Large amplitude oscillatory shearing-harmonic analysis", Rheol. Acta, 23, 90-96 (1984).

57 Dealy, J M , Rheometers for Molten Plastics, A Practical Guide to Testing and Property Measurement, Van Nostrand Reinhold, New York, 1982.

58. Walters, K., Rheometry, Chapman & Hall, London (1975).

59. Walters, K., "Basic Concepts and Formulae for the Rheogoniometer", Sangamo Controls Ltd., Bognor Regis (1968).

60. Meissner, J., "Polymer melt rheology - A challenge for the polymer scientist and engineer", Pure & Appl. Chem., 56(3), 369-384 (1984).

61 Gleissle, W., Ph.D. Dissertation, University of Karlsruhe (1978).

62. Pearson, D.S. and W.E. Rochefort, "Behaviour of Concentrated Polystyrene Solutions in Large Amplitude Oscillatory Shear Fields", J. Pol. Sci.: Pol. Phys. Ed , 20, 83-98 (1982).

63 Hoffman, R , United States Steel Corp., personal communication, March 21, 1985.

64 Boni, S., C. G'Sell, E. Weynant and J.M. Haudin, "Microscopie in situ observation of the plastic deformation of polybutene-1 films under simple shear", Pol. Testing, 3, 3-24 (1982).

65 Laun, H.M , "Elastic properties of polymer melts at high deformation rates with respect to extrusion", Proc. 2nd World Cong Chem. Eng., Montréal, Canada VI, 411-415 (1981 October 4-9).

66. Davis, S.S., "Viscoelastic Properties of Pharmaceutical Semisolids IV. Destructive Oscillatory Testing", J. Pharm. Sci., 60(9), 1356-1360 (September, 1971).

67 MacSporran, W.C. and R.P. Spiers, "The dynamic performance of the Weissenberg Rheogoniometer II. Large amplitude oscillatory shearing - Fundamental response", Rheol. Acta, 21, 193-200 (1982).

68. MacSporran, W.C. and R.P. Spiers, "The dynamic performance of the Weissenberg Rheogoniometer III. Large amplitude oscillatory shearing-harmonic analysis", Rheol. Acta, 23, 90-96 (1984).

69. Powell, R.L. and W.H. Schwarz, "Geometrical Effects in the Measurements of Mechanical Properties in Parallel Superposed Flows", J. Pol. Sci.: Pol. Phys. Ed., 17, 969-985 (1979).

70. Powell, R.L. and W.H. Schwarz, J. Rheol., 23(3), 323 (1979).

71. Ganani, E. and R.L. Powell, "Geometrical Effects in Transient Flow Stress Measurements", Abs. 55th Ann. Mtg. Soc. Rheol., Knoxville, Tenn. (October 17-20, 1983), J. Rheol., 28(4), 479 (1984).

72. Ganani, E. and R.L. Powell, "Transient Flow Viscometry", J. Rheol., 29(6), 931-941 (1985).

73. Dealy, J.M., "Method and apparatus for measuring rheological properties of fluid", U.S. Patent, #4,571,989 (Feb. 25, 1986).

74 Cusson, D., "Development and evaluation of an in-line rheometer for molten plastics", M.Eng. Proposal Presentation, McGill University, Dept. Chemical Engineering, Montreal, Canada (December 13, 1985).

75. Nelson, B.I., "The design of an improved in-line rheometer for use as an extruder process control sensor", M.Eng. Research Proposal, Dept. Chem. Eng., McGill Univ., Montreal, Canada (August, 1986).

76 Tee, T.-T. and J.M. Dealy, "Nonlinear Viscoelasticity of Polymer Melts", Trans. Soc. Rheol., 19(4), 595-615 (1975).

77 Dealy, J.M., J.F. Petersen and T.-T. Tee, "A concentric-cylinder rheometer for polymer melts", Rheol. Acta, 12, 550-558 (1973).

78 Tee, T -T., "Large Amplitude Oscillatory Shearing of Polymer Melts", Ph D. Thesis, Dept. Chem. Eng., McGill Univ., Montreal, Canada, 1974.

79 Maxwell, B and M Nguyen, "Measurement of the Elastic Properties of Polymer Melts", Pol Eng. Sci., 19(16), 1140-1150 (1979).

80 Maxwell, B., "The application of melt elasticity measurements to polymer processing", SPE Tech. Paper, Proc. ANTEC '85, 653 (1985).

81. Rheomax General Purpose Rheometer, Model CS-213, CSI, Custom Scientific Instruments, Inc., Cedar Knolls, NJ 07927.

82. Onogi, S., T. Masuda and T. Matsumoto, "Non-Linear Behavior of Viscoelastic materials I. Disperse Systems of Polystyrene Solution and Carbon Black", Trans. Soc. Rheol., 14(2), 275 (1970).

83. Matsumoto, T., Y. Segawa, Y. Warashina and S. Onogi, "Nonlinear Behavior of Viscoelastic Materials II. The Method of Analysis and Temperature Dependence of Nonlinear Viscoelastic Functions", Trans. Soc. Rheol., 17(1), 47 (1973).

84. Onogi, S. and T. Matsumoto, "Rheological Properties of Polymer Solutions and Melts Containing Suspended Particles", Pol. Eng. Revs., 1(1), 45-87 (1981).

85. McCarthy, R.V., "An Improved Rheometer Design Used to Measure Viscoelastic Properties of Polymer Melts", J. Rheol., 22(6), 623-641 (1978).

86. Hibberd, G.E., W.J. Wallace and K.A. Wyatt, "A rheometer for measuring the dynamic mechanical properties of soft solids", J. Sci. Instrum., 43, 84-87, (February, 1966)

87. Hibberd, G.E. and N.S. Parker, "Measurement of the Fundamental Rheological Properties of Wheat-Flour Doughs", Cereal Chem., 52(3-II), 1r-23r (1975).

88. Hibberd, G.E. and W.J. Wallace, Dynamic Viscoelastic Behaviour of Wheat Flour Doughs, Part 1. Linear Aspects", Rheol. Acta, 5(3), 193-198 (1966).

89. Hibberd, G.E., "Dynamic viscoelastic behaviour of wheat flour doughs, Part II: Effects of water content in the linear region", Rheol. Acta, 9, 497-500 (1970).

90. Hibberd, G E., "Dynamic viscoelastic behaviour of wheat flour doughs, Part III. The influence of the starch granules", Rheol. Acta, 9, 501-505 (1970).

91. Hibberd, G E., "Dynamic viscoelastic behavior of wheat flour doughs, Part IV: Non-linear behaviour", Rheol. Acta, 14, 151-157 (1975).

92. Hibberd, G.E., "Dynamic viscoelastic behavior of wheat flour doughs, Part IV: Non-linear behaviour", Rheol. Acta, 14, 151-157 (1975).

93. Letter, Giacomin, A.J. to G.E. Hibberd, BREAD RESEARCH INSTITUTE OF AUSTRALIA, 1984 May 8.

94. Hibberd, G.E. and N.S. Parker, "A parallel plate rheometer for measuring the viscoelastic properties of wheat flour doughs", Cereal Chem., 55(1), 102-110 (1978).

95. Hibberd, G.E., W.J. Wallace and K.A. Wyatt, "A rheometer for measuring the dynamic mechanical properties of soft solids", J Sci. Instrum., 43, 84-87 (1966).

96. Tsai, A.T. and D.S. Soong, "Measurement of Fast Transient and Steady State Responses of Viscoelastic Fluids with a Sliding Cylinder Rheometer Executing Coaxial Displacements", J. Rheol., 29(1), 1-18 (1985).

97. Tsai, A.T. and D.S. Soong, "Measurement of Fast Transient and Steady State Responses of Viscoelastic Fluids with a Sliding Cylinder Rheometer Executing Coaxial Displacements", Abs. from the 55th Ann. Mtg. of the Soc. Rheol., Knoxville, Tenn., (October 17-20, 1983), J. Rheol., 28(4), 480, (1984).

98 Soong, D.S., "A new tool for measuring polymeric fluid responses ... The sliding cylinder rheometer", Closed Loop, Publ. MTS SYSTEMS CORP., 13 (3), 14-19 (Summer, 1984).

99. Liu, T.Y., D.W. Mead, D.S. Soong and M.C. Williams, "A parallel-plate rheometer for the measurement of steady-state and transient rheological properties", Rheol. Acta, 22, 81-89 (1983).

100. Maxwell, B., "Stress Relaxation and Strain Recovery in the Tll Region", Abs. from the 55th Ann. Mtg. of the Soc. Rheol., Knoxville, Tenn., (October 17-20, 1983), J. Rheol., 28(4), 480, (1984).

101. Maxwell, B. and K.S. Cook, J. Pol. Sci., Pol. Symp., 72, 343 (1985).

102. Maxwell, B., "Order in the amorphous state of polymers", ed. by S.E. Keinath, R.L. Miller and Rieke, J.K., Plenum Publ. Corp., N.Y. (1986).

103. Hibberd, G.E. and W.J. Wallace, Dynamic Viscoelastic Behaviour of Wheat Flour Doughs, Part 1. Linear Aspects", Rheol. Acta, 5(3), 193-198 (1966).

104. Hibberd, G.E., "Dynamic viscoelastic behaviour of wheat flour doughs, Part II: Effects of water content in the linear region", Rheol. Acta, 9, 497-500 (1970).

105 Hibberd, G E , "Dynamic viscoelastic behaviour of wheat flour doughs, Part III. The influence of the starch granules", Rheol. Acta, 9, 501-505 (1970).

106. Hibberd, G.E., "Dynamic viscoelastic behavior of wheat flour doughs, Part IV: Non-linear behaviour", Rheol. Acta, 14, 151-157 (1975).

107 Hibberd, G E., "Dynamic viscoelastic behavior of wheat flour doughs, Part IV: Non-linear behaviour", Rheol. Acta, 14, 151-157 (1975).

108 Dealy, J.M. and A.J. Giacomin, "Sliding plate and sliding cylinder rheometers", in Collyer, A. and D. Clegg, eds., Physical Principles of Rheological Measurement, Elsevier Applied Science Publishers, Ltd. (1987).

109. Dealy, J M., "Rheological Characterization of Molten Polymers", Presented to CSChE, Toronto, Canada (Oct. 5, 1983).

110 Shah, B H. and R. Darby, "Rheovibron determination of the dynamic moduli of polymer melts", Pol. Eng. Sci., 16(1), 46 (January, 1976).

111 Fujiyama, M. and M. Takayanagi, Kogyo Kagaku Zasshi, 72, 1163-1168 (1969).

112. Laun, H.M. and J. Meissner, "A Sandwich-Type Creep Rheometer for the measurement of rheological properties of polymer melts at low shear stresses", Rheol. Acta, 19, 60-67 (1980).

113 Laun, H M., "Elastic Properties of Polymer Melts at High Deformation Rates with Respect to Extrusion", Proc. 2nd World Congr. Chem. Eng., 6, 411 (1981).

114 Laun, H.M., "Elastic properties of polyethylene melts at high shear rates with respect to extrusion", Rheol. Acta, 21, 464-469 (1982).

115. Meissner, J., "Polymer melt rheology - A challenge for the polymer scientist and engineer", Pure & Appl. Chem., 56(3), 369-384 (1984).

116. Huerlimann, H.P. and J. Meissner, "Multidirectional shear rheometer for polymer melt", Int. Conf. on Viscoelasticity of Polymeric Liquids, Grenoble, January 1986.

117. Meissner, J., "Forschung, Wissenschaft: Alte und neue Wege in der Rheometrie der Polymer-Schmelzen", Chimia 38(2), 35-45 (Februar, 1984).

118. Schrag, J.L., "Deviation of velocity gradient profiles from the "gap loading" and "surface loading" limits in dynamic simple shear experiments", Trans. Soc. Rheol., 21(3), 399-413 (1977).

119 Schrag, J.L , J.F. Guess and G.B. Thurston, "Shear-wave interference observed by optical birefringence induced in a viscoelastic liquid", J. Appl. Phys., 36(6), 1996-2000 (June, 1965).

120. Thurston, G.B. and J.L. Schrag, "Shear wave propagation in a birefringent viscoelastic medium", J. Appl. Phys., 35(1), 144-151 (January, 1964).

121. Thurston, G.B. and J.L. Schrag, "Measurement of dynamic birefringence of a thin fluid layer in oscillatory shear", Trans. Soc. Rheol., VI, 325-348 (1962).

122. Lodge, T.P., J.W. Miller and J.L. Schrag, "Infinite-dilution oscillatory flow birefringence properties of polystyrene and poly(α-methylstyrene) solutions", J. Pol. Sci.. Pol. Phys. ed., 20, 1409-1425 (1982).

123. Osaki, K. and M. Kurata, "Stress relaxation of a polymer solution in double-step shear deformations, a separate evaluation of the stress components due to entangled segments of different orientations", J. Pol. Sci.: Pol. Phys. Ed., 20, 623-632 (1982).

124. Kimura, S., K. Osaki and M. Kurata, "Stress relaxation of polybutadiene at large deformation. Measurements of stress and birefringence in shear and elongation", J. Pol. Sci.: Pol. Phys. Ed., 19, 151-163 (1981).

125. Dexter, F.D., J.C. Miller and W. Philippoff, "Flow Birefringence of molten polyethylene", Trans. Soc. Rheol., V, 193-204 (1961).

126. Kimura, S., K. Osaki and M. Kurata, "Stress relaxation of polybutadiene at large deformation. Measurements of stress and birefringence in shear and elongation", J. Pol. Sci.: Pol. Phys. Ed., 19, 151-163 (1981).

127. Osaki, K. and M. Kurata, "Stress relaxation of a polymer solution in double-step shear deformations. A separate evaluation of the stress components due to entangled segments of different orientations", J. Pol.

Sci.: Pol. Phys. Ed., 20, 623-632 (1982).

128. Lodge, A.S., "A network theory of flow birefringence and stress in concentrated polymer solutions", Trans. Faraday Soc., 52, 120-130 (1956).

129. Middleman, S., "Transient Response of an Elastomer to Large Shearing and Stretching Deformations", Trans. Soc. Rheol., 13, 123 (1969).

130. LaMantia, F.P., B. de Cindio, E. Sorta, and D. Acierno, "Shear behaviour of undiluted polyisobutylenes", Rheol. Acta, 18, 369 (1979).

131. Acierno, D., F.P. LaMantia, et al., "Transient shear and elongational data for polyisobutylene melts", Trans. Soc. Rheol., 21(2), 261-271 (1977).

132 Fruh, S.M. and F. Rodriguez, "Recoverable Shear Measurements in a Parallel Plate Rheometer", AIChEJ, 16(6), 907-910 (1970).

133 Bujake, J.E., "Creep Properties of Sodium Stearate", J. Colloid and Interface Sci., 27(2), 229-234 (June, 1968).

134 Nazem, F and Y Hill, "Bead Filled Thermoplastics, Elongation and Shear Viscosity of ...", Trans. Soc. Rheol., 18(1), 87-101 (1974).

135 Montes, S and J.L. White, "A comparative rheological investigation of natural and synthetic cis-1,4-polyisoprenes and their carbon black compounds", Rubber Chem. Technol., 55, 1354-1369 (1982).

136. Furuta, I., V.M. Lobe and J.L. White, "Experimental Study of the Rheological Properties of Butadiene-Styrene Gum Elastomers and Compounds", J. Non-Newt. Fluid Mechanics, 1, 207-222 (1976).

137 Goldstein, C., "Transient and Steady Shear Behavior of SBR Polymers", Trans. Soc. Rheol., 18(3), 357-369 (1974).

138 Toki, S. and J.L. White, "Rheological and Solid Wall Boundary Condition Characterization of Unvulcanized Elastomers and Their Compounds", J. Appl. Pol. Sci., 27, 3171-3184 (1982).

139 Toki, S., "Rheological and Boundary Characterization of Unvulcanized Rubbers and their Compounds", Ph.D. Thesis, U. Tenn., Knoxville (Dec., 1981).

140. Shama, F. and P. Sherman, "The Texture of Ice Cream 2. Rheological Properties of Frozen Ice Cream", J. Food Sci., 31, 699-706 (1966).

141. Shaw, D.J., "The Physical Structure of Ice Cream", Rheology of Emulsions, Sherman, P., ed., Proc. of Symp. British Soc. Rheol., Harrogate (October, 1962), pp. 125ff.

142. Fukushima, M., S. Taneya and T. Sone, "Viscoelasticity of Cheese", J. Soc. Mat. Sci. Japan, 13, 331-335 (1964).

143. Hibberd, G.E. and N.S. Parker, "A Parallel Plate Rheometer for Measuring the Viscoelastic Properties of Wheat Flour Doughs", Cereal Chem., 55(1), 102-110 (1978).

144. Hibberd, G.E. and N.S. Parker, "Measurement of the Fundamental Rheological Properties of Wheat-Flour Doughs", Cereal Chem., 52(3-II), (May-June, 1975).

145. Hibberd, G.E. and N.S. Parker, "Nonlinear Creep and Creep Recovery of Wheat-Flour Doughs", Cereal Chem., 56(4), 232-236 (1979).

146. Liu, T.Y., D.W. Mead, D.S. Soong and M.C. Williams, "A parallel-plate rheometer for the measurement of steady-state and transient rheological properties", Rheol. Acta, 22, 81-89 (1983).

147. Sivashinsky, N., A T. Tsai, T.J. Moon and D.S. Soong, "Some New Transient Test Results from a Parallel-Plate Rheometer", J. Rheol., 28(3), 287-301 (1984).

148 Liu, Y T., "Rheological Transients in Entangled Polymeric Fluids", Ph.D. Thesis, U. of California, (September, 1982).

149. Liu, T.Y., D.S. Soong and M C. Williams, "Transient and steady rheology of polydisperse entangled melts. Predictions of a kinetic network model and data comparisons", J. Pol. Sci., Pol. Phys. Ed., 22, 1561-1587 (1984)

150. Philippoff, W., "Relaxations in Polymer Solutions", in Mason, W P., ed., Physical Acoustics, II-B, Academic Press, N.Y , 1965, p 44.

151 Langlois, W.E., "A recursive approach to the theory of slow, steady-state viscoelastic flow", Trans. Soc. Rheol., VII, 75-99 (1963).

152 Tanner, R I , Engineering Rheology, Clarendon Press, Oxford (1985), p. 241.

153. Tanner, R.I., N. Phan-Thien and J. Dudek, "Boundary conditions in viscoelastic lubrication" in Mena, B., A. Garcia-Rejon and C. Rangel-Nafaile, eds , Advances in Rheology, Proc. IXth Int. Congr. Rheol., Mexico, 4, 501 (1984).

154. Miller, M.J., "The complete stress state of five viscoelastic fluids in viscometric flow", Ph.D. thesis, Univ. Utah, Chem. Eng. (1968).

155. Miller, M.J. and E.B. Christiansen, "The stress state of elastic fluids in viscometric flow", AIChE J., 18(3), 600-608 (May, 1972).

156. Pollett, W.F.O., "Rheological behaviour of continuously sheared polythene", Brit. J. Appl. Phys., 6, 199-206 (June, 1955).

157. Christiansen, E.B. and M.J. Miller, "Note. measurement of normal stresses", Trans. Soc. Rheol., 15, 189 (1971).

158 Dealy, J.M., Rheometers for Molten Plastics, Van Nostrand Reinhold Company, New York (1982).

159. Collyer, A.A. and D.W. Clegg, eds., The Physical Principles of Rheological Measurement, in chapter entitled "Sliding plate and sliding cylinder rheometers" by Dealy, J.M. and A.J. Giacomin, Elsevier Applied Science Publishers Ltd., U.K., (1988).

160. Read, W.T., "Effect of Stress-Free Edges in Plane Shear of a Flat Body", J. Appl. Mech., 17, 349-352 (1950).

161 Read, W.T., M.Sc. Thesis, Graduate Div. Appl. Math., Brown Univ., Providence, R.I., (1950).

162. Letter, Giacomin, A. J. to Dept. Appl. Math., Grad. Div., Brown Univ., (1984 Jan. 12).

163 Letter, Giacomin, A.J. to BELL LABORATORIES, (1984 Jan. 19).

164 Letter, Purzycki, M. of AT&T BELL LABORATORIES to A.J. Giacomin, (1984 Jan. 31).

165. Rivlin, R.S. and D.W. Saunders, I.R.I. Trans., 24, 296 (1949).

166 Gent, A.N and E.A. Meinecke, "Compression, bending, and shear of bonded rubber blocks", Pol Eng. Sci., 10(1), (January, 1970).

167. Payne, A.R., "Effect of compression on the shear modulus of rubber", I&EC Product Research and Development, 1(2), 86-88 (June, 1962).

168. Gent, A.N., R.L. Henry and M.L. Roxbury, "Interfacial Stresses for bonded Rubber Blocks in Compression and Shear", J. Appl. Mech., 41(4), 855-859 (December, 1974).

169. Prevost, J.-H. and K. Hoeg, "Reanalysis of simple shear soil testing", Can. Geotech. J., 13, 418-429 (1976).

170. Wood, D.M, A. Drescher and M. Budhu, "On the determination of stress state in the simple shear apparatus", Gèotechnical Testing Journal, 2(4), 211-221 (December, 1979).

171. Roscoe, K.H., "The influence of strains in soil mechanics", Géotechnique, 20(2), 129-170 (1970).

172. Arthur, J.R.F., R.G. James and K.H. Roscoe, "The determination of stress fields during plane strain of a sand mass", 14(4), 283-308 (1964).

173. Prevost, J.-H. and K. Hoeg, "Reanalysis of simple shear soil testing", Can. Geotech. J. 13, 418-429 (1976).

174. Duncan, J.M. and P. Dunlop, "Behavior of soils in simple shear tests", Proc. 7th Int. Conf. on Soil Mech. and Foundation Eng., Mexico (1969), p. 101-109.

175. Lucks, S.A., J.T. Christian, G.E. Brandow and K. Hoeg, "Stress conditions in NGI simple shear test", Tech. Note, ASCE, J. Soil Mech. Found. Div., 100(GT10), 1180-1184 (1974).

176. Roscoe, K.H., "An apparatus for the Application of simple shear to soil samples", Proc. 3rd Int. Conf. on Soil Mech. and Foundation Eng., Zurich, Session 2, 186-191 (1953).

177. Wood, D.M., A. Drescher and M. Budhu, "On the determination of stress state in the simple shear apparatus", Geotechnical Testing J., 2(4), 211-221 (December, 1979).

178. Pande, G.N. and O.C. Zienkiewicz, eds., Soil Mechanics-Transient and Cyclic Loads, Chpt. 20 by D.M. Wood, "Laboratory investigations of the behaviour of soils under cyclic loading. A review", John Wiley & Sons Ltd., New York (1982), p. 513-582.

179. Kjellman, W., "Testing the shear strength of clay in Sweden", Géotechnique, 2(3), 225-235 (1951).

180 Andrade, E.N.da C., "The Distribution of Slide in a Right Six-face subject to Pure Shear", Proc. Royal Soc. London, LXXXV, 448-461 (1911).

181 Pande, G.N and O C Zienkiewicz, eds., Soil Mechanics-Transient and Cyclic Loads, Chpt. 21 by Finn, W.D.L., S.K. Bhatia and D.J. Pickering, "The cyclic simple shear test", John Wiley & Sons Ltd., New York (1982), p. 513-582.

182. Toki, S. and J.L. White, "Rheological and Solid Wall Boundary Condition Characterization of Unvulcanized Elastomers and Their Compounds", J. Appl. Pol. Sci., 27, 3171-3184 (1982).

183. Toki, S., "Rheological and Boundary Characterization of Unvulcanized Rubbers and their Compounds", Ph.D. Thesis, U. Tenn., Knoxville (Dec., 1981).

184. Montes, S. and J.L. White, "A comparative rheological investigation of natural and synthetic cis-1,4-polyisoprenes and their carbon black compounds", Rubber Chem. Technol., 55, 1354-1369 (1982).

185. Furuta, I., V.M. Lobe and J.L. White, "Experimental Study of the Rheological Properties of Butadiene-Styrene Gum Elastomers and Compounds", J. Non-Newt. Fluid Mechanics, 1, 207-222 (1976).

186. Liu, T.Y., D.W. Mead, D.S. Soong and M.C. Williams, "A parallel-plate rheometer for the measurement of steady-state and transient rheological properties", Rheol. Acta, 22, 81-89 (1983).

187. Tanner, R I., Engineering Rheology, Clarendon Press, Oxford (1985), p. 230.

188. Tanner, R.I., Engineering Rheology, Clarendon Press, Oxford (1985), p. 241.

189. Tanner, R.I., N. Phan-Thien and J. Dudek, "Boundary conditions in viscoelastic lubrication" in Mena, B., A. Garcia-Rejon and C. Rangel-Nafaile, eds., Advances in Rheology, Proc. IXth Int. Congr. Rheol., Mexico, 4, 501 (1984).

190. Tanner, R.I., N. Phan-Thien and J. Dudek, "Boundary conditions in viscoelastic lubrication" in Mena, B., A. Garcia-Rejon and C. Rangel-Nafaile, eds., Advances in Rheology, Proc. IXth Int. Congr. Rheol., Mexico, 4, 501 (1984).

191 Dealy, J.M. and A.J. Giacomin, "Sliding plate and sliding cylinder rheometers" in Collyer, A.A. and D.W. Clegg, eds., The Physical Principles of Rheological Measurement, Elsevier Applied Science Publishers Ltd., U.K. (1988).

192 Dealy, J M , Rheometers for Molten Plastics, Van Nostrand Reinhold Co , New York (1982).

193. Williams, M.C. and R.B. Bird, "Oscillatory behavior of normal stresses in viscoelastic fluids", I&EC Fund., 3(1), 42-49 (February, 1964).

194. Laun, H.M and J. Meissner, "A sandwich-type creep rheometer for the measurement of rheological properties of polymer melts at low shear stresses", Rheol. Acta, 19,(1) 62 (1980).

195. Joseph, D.D. and G S. Beavers, "The free surface on a simple fluid between cylinders undergoing torsional oscillations - Parts I and II", Arch. Rat. Mech. Anal., 62, 323-352 (1976).

196 Sturges, L.D. and D.D. Joseph, "The free surface on a simple fluid between cylinders undergoing torsional oscillations - Part III: Oscillating Planes", Arch. Rat. Mech. Anal., 63, 246-267 (1977).

197. Dealy, J.M. and A.J. Giacomin, "Sliding plate and sliding cylinder rheometers" in Clegg, D.W. and A.A. Collyer, eds., The Physical Principles of Rheological Measurement, Elsevier Applied Science Publ. Ltd., in press.

198 Dealy, J.M , Rheometers for Molten Plastics, Van Nostrand Reinhold Co., New York (1982).

199. Dealy, J.M., "Method of measuring shear stress", U.S. Patent No. 4,464,928 (Aug. 14, 1984).

200. Dealy, J.M , "A shear stress transducer for molten polymers", Rheol. Acta, 21, 475-477 (1982).

201. Pierce, F.J., "Keynote address. shear and drag", Symposium on Fluid Dynamic Measurements, ASME Collected Papers, W.A. Spraker and H.E. Weber, eds., ASME (1971).

202 Doebelin, E O , Measurement Systems, Application and Design, McGraw-Hill Book Co., New York (1979), p. 17.

203. Dhawan, S., "Direct measurement of skin friction", NACA Report 1121, (1953).

204. Kempf, von G., "Wietere Reibungsergebnisse an ebenen glatten und rauhen Flächen", Hydrodynamische Probleme des Schiffsantriebs, Vol 1, 74-82 (1932).

205. Kempf, G., "Nene ergebnisse der widerstandsforschung", Werft, Reederie Hafen, 10, 234, 247 (1932).

206. Schultz-Grunow, F., "New frictional resistance law for smooth plates", NACA TM 986 (1941). Also Luftfahrtforschung, "Neues reibungswiderstandsgesetz für glatte platten", 17(8), 239-246 (Aug. 20, 1940).

207. Smith, D.W. and J.H. Walker, "Skin friction measurements in incompressible flow", NASA Technical Report R-26 (1959). Supercedes NACA Technical Note 4231 by same authors.

208. Naleid, J.F. and M.J. Thompson, "Pressure gradient effects an the Preston tube in supersonic flow", J. Aero/space Sci., 28, 940 (1961).

209. White, J.K. and R.E. Franklin, "Measurements of skin-friction in an annulus by the floating element technique", Current Paper No 814, Ministry of Aviation, Aeronautical Research Council, Her Majesty's Stationery Office, London (1965).

210. Padera, C.J , "Control surface having flexure areas for force measurements", U.S. Patent No. 3,460,383 (Aug. 12, 1969).

211. Fenter, F.W. and W.C. Lyons Jr., "The direct measurement of local skin friction on Viking No. 13 during ascending flight", Report No. DRL-414, CH-917, Defense Research Laboratory, The Univ. of Texas, Austin (Jan., 1958).

212. Weiler, J.E., "The design of an acceleration insensitive skin friction balance for flight testing, Report No. DRL-342, CF-2094, Defense Research Laboratory, The Univ. of Texas, Austin (Aug., 1955).

213. Dickinson, J. and N.D. Vinh, Proc. 5th Canadian Congr. Appl. Mech, p. 515 (1975).

214. Dealy, J.M., "A shear stress transducer for molten polymers", Rheol. Acta, 21, 475-477 (1982).

215. Reiss, J.H., "Method and force determining apparatus for ice breaking vessels", U.S. Patent No. 4,059,011 (Nov. 22, 1977).

216. Brown, K.C. and P.N. Joubert, "The measurement of skin friction in turbulent boundary layers with adverse pressure gradients", J. Fluid Mech., 35(4), 737-757 (1969).

217. Dhawan, S., "Direct measurement of skin friction", NACA Report 1121 (1953). Supercedes NACA Technical Note 2567 (1952) by same author.

218. Harris, C.J., "Biaxial shear force gauge", U.S. Patent No. 4,290,302 (September 22, 1981).

219 Dickinson, J., "Turbulent skin friction techniques", Laboratoire de mécanique des fluides course notes, Université Laval, Département de Génie Mécanique.

220. Brown, K C. and P.N. Joubert, "The measurement of skin friction in turbulent boundary layers with adverse pressure gradients", J. Fluid Mech., 35(4), 737-757 (1969).

221 Dhawan, S., "Direct measurement of skin friction", NACA Report 1121 (1953) Supercedes NACA Technical Note 2567 (1952) by same author.

222. Bransby, P.L., "Cambridge Contact Stress Transducers", CUED/C•SOILS/LN2 (1973), Lecture notes for course entitled "Research Techniques and Equipment in Soil Mechanics", University of Cambridge.

223. Arthur, J.R.F. and K.H. Roscoe, "An Earth Pressure Cell for the Measurement of Normal and Shear Stresses", Civ. Eng. and Public Works Eng. Rev., 56, 659 (June, 1961).

224. Arthur, J.R.F., "Strains and lateral force in sand", Ph.D. Thesis, Cambridge University (1962).

225. Blair-Fish, P.M. and P.L. Bransby, "Flow Patterns and Wall Stresses in a Mass-Flow Bunker", J. Eng. Ind., Trans. ASME, 17 (February, 1973).

226. Hancock, A.W., "Stresses on Bunker Walls", Ph.D. Thesis, Cambridge University, 1970.

227. Tüzün, U. and R.M. Nedderman, "Gravity flow of granular materials round obstacles-II", Chem. Eng. Sci., 40(3), 337 (1985).

228. Smith, I.A.A., "Stress and Strain in a Sand Mass Adjacent to a Model Wall", Ph.D. Thesis, Cambridge University, 1972.

229. Lord, J.A., "Stress and Strain in Earth Pressure Problem", Ph.D. Thesis, Cambridge University, 1969.

230. Roscoe, K.H., "The influence of strains in soil mechanics", Géotechnique, 20(2), 129-170 (1970).

231. Letter, Giacomin, A.J. to P.L. Bransby, University of Cambridge (1984 June 13).

232. Hambly, E.C., "A waterproof earth pressure cell for the measurement of normal effective stress and shear stress", Internal report, Dept. Engineering, University of Cambridge (1967).

233. Stroud, M.A., "The behavior of sand at low stress levels in the simple shear apparatus", Ph.D. Thesis, Cambridge University, 1971.

234. Roscoe, K.H., "The influence of strains in soil mechanics", Géotechnique, 20(2), 129-170 (1970).

235 Pande, G N and O.C Zienkiewicz, eds , Soil Mechanics-Transient and Cyclic Loads, Chpt. 20 by D.M. Wood, "Laboratory investigations of the behaviour of soils under cyclic loading A review", John Wiley & Sons Ltd , New York (1982), p. 513-582.

236. Hambly, E.C., "Plane Strain Behaviour Of Soft Clay", Ph.D. Thesis, Cambridge University, 1969.

237. Roscoe, K.H., "The influence of strains in soil mechanics", Géotechnique, 20(2), 129-170 (1970).

238 Delaplaine, J.W., "Forces Acting in Flowing Beds of Solids", AIChEJ, 2(1), 127-138, (1956)

239. Delaplaine, J.W , "Errata", AIChEJ, 2(3), 371 (1956).

240. Pickett, S.F., "Interface shear transducer", U.S. Patent No. 4,155,265 (May 22, 1979).

241. Gent, A.N., R.L. Henry and M.L. Roxbury, "Interfacial stresses for bonded rubber blocks in compression and shear", J. Appl. Mech., 41(4), 855-859 (December, 1974).

242. Agarwal, S.L. and S. Venkatesan, "An Instrument to Measure Skin Friction and Normal Earth Pressure on Deep Foundations", Instruments and Apparatus for Soil and Rock Mechanics, ASTM STP 392, 1965, pp. 152-169.

243. Letter, Giacomin, A.J. to S.L. Agarwal, UNIVERSITY OF ROORKEE, 1984 June 13.

244 Cusson, D., "Development and Evaluation of an In-Line Rheometer for Molten Plastics", M.Sc. Proposal Report, 1984 October 29.

245. Dealy, J.M., "Method and apparatus for measuring rheological properties of fluid", U.S. Patent # 4,571,989 (Feb. 25, 1986).

246. Broersma, G., Behaviour of granular materials, Stam Technical Publications, Culemborg, The Netherlands, 49-72 (1972).

247. Broersma, G., "Combined shear stress/pressure meter for dry granular materials", THTR Symposium, March 6-7, Jülich (Germany), 356-362 (1968).

248. Letter, Giacomin, A.J. to J. Smid, Czechoslovak Academy of Science, 1984 June 12.

249 Letter, Smid, J., CZECHOSLOVAK ACADEMY OF SCIENCE to A.J. Giacomin, 1984 August 15.

250. Smid, J. and J. Novosad, "Pressure Cell for Measuring Normal and Shear Stresses", Powder Technol., 4, 322-327 (1970/71).

251 Smid, J. and J. Novosad, "Contribution to the measurement of normal and shear stresses in walls of bunkers", Collection Czechoslov. Chem. Commun., 37, 3568-3578 (1972).

252 Smid, J , "Pressure of Granular Material on Wall of Model Silo", Collection Czechoslov. Chem. Commun., 40, 2424-2436 (1975).

253 Smid, Von J , "Druckverteilung unter einem Schüttguthaufen", Grundl. Landtechnic Bd 33(3), 72-75 (1983)

254. Smid, J., "Wandspannung in Schüttgut bei einem Bunker mit Umfangsaustrag", TIZ-Fachberichte Rohstoff-Engineering, 4(104), 238-240 (1980).

255. Pennywitt, K.E., "Robotic tactile sensing", BYTE, 11(1), 177-200 (January, 1986).

256. Dario, P. and D. De Rossi, "Tactile sensors and the gripping challenge", IEEE Spectrum, 46-52 (August, 1985).

257 Soong, S S , "A parallel plate viscoelastometer for molten polymers", Ph D Thesis, Dept. Chem. Eng., McGill Univ., Montreal, Canada (June, 1983).

258 Dealy, J.M., "A shear stress transducer for molten polymers", Rheol. Acta, 21, 475-477 (1982).

259 Dealy, J M. and S.S. Soong, "A Rheometer for the Study of Nonlinear Viscoelasticity in Molten Polymers", Abs. from the 55th Ann. Mtg. Soc. Rheol., Knoxville, Tenn., (Oct., 17-20, 1983), J. Rheol., 28(4), 482 (1984).

260. Dealy, J.M. and S.S. Soong, "A shear stress transducer for molten plastics", SPE Tech. Papers, ANTEC 1982, pp. 76-78.

261. Dealy, J.M., "Method of measuring shear stress", U.S. Patent No. 4,464,928 (August 14, 1984).

262. Dealy, J.M., "A shear stress transducer for molten polymers", Rheol. Acta, 21, 475-477 (1982).

263. Dealy, J.M., "Method of measuring shear stress", U.S. Patent No. 4,464,928 (August 14, 1984).

264. Soong, S.S., "A parallel plate viscoelastometer for molten polymers", Ph.D. Thesis, Dept. Chem. Eng., McGill University, Montreal, Canada (June, 1983).

265. Product literature, KISTLER INSTRUMENTS, Winterthur, Switzerland.

266. Dealy, J.M., "Method of measuring shear stress", U.S. Patent No. 4,464,928 (August 14, 1984).

267. Dealy, J.M. and S.S. Soong, "A Parallel Plate Melt Rheometer Incorporating a Shear Stress Transducer", J. Rheol., 28(4), 355-365 (1984).

268 Discussions, Kissinger, C.D., MTI Instruments Division, Mechanical Technology Inc , Latham, N.Y., 1983 October

269. Isayev, A I. and C.A. Hieber, Rheol. Acta, 19, 168 (1980).

270 Tanner, R I., Engineering Rheology, Clarendon Press, Oxford (1985).

271 Mase, G.E., Continuum Mechanics, Schaum's Outline Series in Engineering, McGraw-Hill Book Company, (1970).

272 Truesdell, C and W Noll, The nonlinear field theories of mechanics, Springer-Verlag, Berlin (1965).

273 Tanner, R.I , Engineering rheology, Clarendon Press, Oxford (1985).

274. Akbay, U., E. Becker and S. Sponagel, "Instability of plane Couette flow of viscoelastic liquids", J Non-Newt. Fluid Mech., 18, 123-141 (1985).

275 Lodge, A S , Elastic Liquids. An introductory vector treatment of finite-strain polymer rheology, Academic Press, London (1964), p. 10.

276. Mutel, A.T. and M.R. Kamal, "The effect of glass fibers on the rheological behavior of polypropylene melts between rotating parallel plates", Pol. Comp., 5(1), (January, 1984).

277. Markovitz, H., "Boltzmann and the beginnings of linear viscoelasticity", Trans. Soc. Rheol., 21(3), 381-398 (1977).

278. Dealy, J.M., "Rheology of Liquids: Course Notes", Dept. Chem. Eng., McGill University, Montreal, Canada (1983).

279. Jongschaap, R.J.J., K.H. Knapper and J.S. Lopulissa, "On the limit of linear viscoelastic response in the flow between eccentric rotating disks", Pol. Eng. Sci., 18(10), 788-792 (1978).

280. Parker, N.S. and G.E. Hibberd, "The interpretation of dynamic measurements on non-linear viscoelastic materials", Rheol. Acta, 13, 910-915 (1974).

281. Ferry, J.D., Viscoelastic Properties of Polymers, 3rd ed., John Wiley, New York, 1980.

282 Lodge, A S, Elastic liquids. An introductory vector treatment of finite-strain polymer rheology. Academic Press, London (1964), p.78.

283. Booij, H.C., "Influence of superimposed steady shear flow on the dynamic properties of non-Newtonian fluids. I. Measurements on non-Newtonian solutions", Rheol. Acta, 5(3), 215-221 (1966).

284 Pollett, W.F.O., "Rheological behaviour of continuously sheared polythene", Brit. J. Appl. Phys., 6, 199-206 (June, 1955).

285. Pollett, W.F.O. and A.H. Cross, "A continuous-shear rheometer for measuring total stress in rubber-like materials", J. Sci. Instrum., 27, 209-212 (August, 1950).

286. Williams, M.C. and R.B. Bird, "Oscillatory behavior of normal stresses in viscoelastic fluids", I&EC Fund., 3(1), 42-49 (February, 1964).

287 Williams, M.C. and R.B. Bird, "Three-constant Oldroyd model for viscoelastic fluids", Phys. Fluids, 5, 1126-1128 (1962).

288 Dexter, F D., J.C. Miller and W. Philippoff, "Flow birefringence of molten polyethylene", Trans. Soc. Rheol., V, 193-204 (1961).

289 Ferry, J.D, Viscoelastic Properties of Polymers, 3rd ed., John Wiley, New York, 1980.

290 ASTM D4065-82 "Standard practice for determining and reporting dynamic mechanical properties of plastics", 1986 Annual book of ASTM standards, Section 8, Vol. 08.03.

291. Mewis, J., "Thixotropy - A general review", J. Non-Newt. Fluid Mech., 6, 1-20 (1979).

292 Broch, J T, Mechanical Vibration and Shock Measurements, 2nd ed., Bruehl & Kjaer, Denmark (April, 1984), p. 52.

293. Weissenberg, K., "The testing of materials by means of the rheogoniometer", Sangamo Controls Ltd. (1964).

294. Ramirez, R.W., The FFT: Fundamentals and Concepts, Prentice-Hall, Inc., Englewoods Cliffs (1985).

295. Vinogradov, G.V. and A. Ya. Malkin, Rheology of Polymers, Mir Publishers, Moscow (1980).

296. Freeman, S.M. and K. Weissenberg, "Some new anisotropic time effects in rheology", Nature, 161(4087), 324-325 (Feb. 28, 1948).

297. Tanaka, A. and S. Onogi, "Nonlinear viscoelastic properties of crystalline polymers", Pol. Eng. Rev., 3(2-4), 235-275 (1983).

298 Schmidt, E , "Experimentelle untersuchung von schwingungsdampfenden unterlagen fur maschinen", Gesundheits-Ing., 6(46), 61-71 (1923).

299. Harris, J. and K. Bogie, "The experimental analysis of non-linear waves in mechanical systems", Rheol. Acta, 6(1), 3 (1967).

300. Harris, J., "Response of time-dependent materials to oscillatory motion", Nature, 207, 744 (August 14, 1965).

301. Harris, J., "A continuum theory of time-dependent inelastic flow", Rheol. Acta, 6(1), 6 (1967).

302. Onogi, S , T. Masuda and T. Matsumoto, "Non-linear behavior of viscoelastic materials. I. Disperse systems of polystyrene solution and carbon black", Trans. Soc. Rheol., 14(2), 275-294 (1976).

303. Isayev, A I. and C.A. Hieber, "Oscillatory shear flow of polymeric systems", J Pol. Sci. Pol. Phys. Ed., 20, 423-440 (1982).

304 Soong, S S., "A parallel plate viscoelastometer for molten polymers", doctoral dissertation, Dept. Chemical Engineering, McGill University, Montréal, Canada (June, 1983).

305 Tee, T.-T , "Large amplitude oscillatory shearing of polymer melts", doctoral dissertation, Dept. Chemical Engineering, McGill University, Montréal, Canada (1974).

306. Tsang, W.K W., "The use of large transient deformations to elucidate structural phenomena and evaluate network models for molten polymers", doctoral dissertation, Dept. Chemical Engineering, McGill University, Montréal, Canada (1980).

307. Liu, Y.-H.T., "Rheological transients in entangled polymeric fluids", doctoral dissertation, Chemical Engineering, Univ. of California, Berkeley (1976).

308. Booij, H.C., "Influence of superimposed steady shear flow on the dynamic properties of non-Newtonian fluids. II. Theoretical approach based on the Oldroyd theory", Rheol. Acta, 5(3), 222-227 (1966).

309. Harris, J., "A continuum theory of time-dependent inelastic flow", Rheol. Acta, 6(1), 6 (1967).

310. Davis, W.M and C.W. Macosko, "Nonlinear dynamic mechanical moduli for polycarbonate and PMMA", J. Rheol., 22(1), 53-71 (1978).

311. Dealy, J.M., J.F. Petersen and T.-T. Tee, "A concentric-cylinder rheometer for polymer melts", Rheol. Acta, 12, 550-558 (1973).

312. Krieger, I.M. and T.-F. Niu, "A rheometer for oscillatory studies of nonlinear fluids", Rheol. Acta, 12, 567-571 (1973).

313. MacSporran, W.C. and R.P. Spiers, "The dynamic performance of the Weissenberg rheogoniometer. III. Large amplitude oscillatory shearing - harmonic analysis", Rheol. Acta, 23, 90-96 (1984).

314. Matsumoto, T., Y. Segawa, Y. Warashina and S. Onogi, "Nonlinear behavior of viscoelastic materials.: II. The method of analysis and temperature dependence of nonlinear viscoelastic functions", Trans. Soc. Rheol., 17(1), 47-62 (1973).

315 Onogi, S. and T. Matsumoto, "Rheological properties of polymer solutions and melts containing suspended particles", Pol. Eng. Rev., 1(1), 45-87 (1981).

316 Philippoff, W., "Vibrational measurements with large amplitudes", Trans. Soc. Rheol., 10(1), 317-334 (1966).

317 Tee, T.-T. and J.M. Dealy, "Nonlinear viscoelasticity of polymer melts", Trans. Soc. Rheol., 19(4), 595-615 (1975).

318 Booij, H.C., "Influence of superimposed steady shear flow on the dynamic properties of non-Newtonian fluids: I. Measurements on non-Newtonian solutions", Rheol. Acta, 5(3), 215-221 (1966).

319. Dodge, J.S. and I.M. Krieger, "Oscillatory shear of nonlinear fluids: I Preliminary Investigation", Trans. Soc. Rheol., 15(4), 589-601 (1971).

320. Onogi, S., T. Masuda and T. Matsumoto, "Non-linear behavior of viscoelastic materials. I. Disperse systems of polystyrene solution and carbon black", Trans. Soc. Rheol, 14(2), 275-294 (1970).

321. Onogi, S. and T. Matsumoto, "Rheological properties of polymer solutions and melts containing suspended particles", Pol. Eng. Rev., 1(1), 45-87 (1981).

322. Powell, R.L. and W.H. Schwarz, "Nonlinear dynamic viscoelasticity", J. Rheol., 23(3), 323-352 (1979).

323 Isayev, A.I. and C.A. Hieber, "Oscillatory shear flow of polymeric systems", J. Pol. Sci.: Pol. Phys. Ed., 20, 423-440 (1982).

324. Davis, W.M. and C.W. Macosko, "Nonlinear dynamic mechanical moduli for polycarbonate and PMMA", J. Rheol., 22(1), 53-71 (1978).

325. Weissenberg, K., "The testing of materials by means of the rheogoniometer", Sangamo Controls, Ltd. (1964).

326. Isayev, A.I. and C.A. Hieber, "Oscillatory shear flow of polymeric systems", J. Pol. Sci.: Pol. Phys. Ed., 20, 423-440 (1982).

327. Weissenberg, K., "Rheology of hydrocarbon gels", Proc. Royal Soc. (London), A200, 183 (1950).

328. Weissenberg, K., Nature, Lond., 159, 310 (1947).

329. Akers, L.C. and M.C. Williams, "Oscillatory normal stresses in dilute polymer solutions", J. Chem. Phys., 51(9), 3834 (November, 1969).

330. Kajiura, H., H. Endo and M. Nagasawa, "Sinusoidal normal stress measurements with the Weissenberg rheogoniometer", J. Pol. Sci.. Pol. Phys. Ed., 11, 2371-2376 (1973).

331. Endo, H. and M. Nagasawa, "Normal stress and shear stress in a viscoelastic liquid under oscillatory shear flow", J. Pol. Sci.. Part A-2, 8, 371-381 (1970).

332. Booij, H.C., "Influence of superimposed steady shear flow on the dynamic properties of non-Newtonian fluids. III. Measurements on oscillatory normal stress components", Rheol. Acta, 7(3), 202 (1968).

333. Booij, H C., "Influence of superimposed steady shear flow on the dynamic properties of non-Newtonian fluids. I. Measurements on non-Newtonian solutions", Rheol Acta, 5(3), 215-221 (1966).

334. Ward, A.F.H. and G.M. Jenkins, "Normal thrust in dynamic torsion for rubber-like materials", Rheol. Acta, 1(2-3), 110-114 (1958).

335 Christiansen, E.B. and M.J. Miller, "Note: Measurement of normal stresses", Trans. Soc. Rheol., 15, 189 (1971).

336. Miller, M.J., Ph.D. Thesis, Univ. of Utah, Salt Lake City (1968).

337 Hull, D , Introduction to Dislocations, Pergamon Press Ltd., Oxford (1965

338 Billmeyer, F W. Jr., Textbook of Polymer Science, 2nd ed., Wiley-Interscience, New York (1971).

339 Treloar, L R G., The Physics of Rubber Elasticity, 2nd ed., Oxford University Press, London (1958).

340. Treloar, L R G., The Physics of Rubber Elasticity, 2nd ed., Oxford University Press, London (1958).

341. Vinogradov, G.V., Yu. Yanovsky and A.I. Isayev, "Viscoelastic behavior of an amorphous polymer under oscillations of large amplitude", J. Pol. Sci.: Part A-2, 8, 1239-1259 (1970).

342 Hoffman, R , United States Steel Corp., personal communication, March 21, 1985.

343. Kausch, H.H., Polymer Fracture, Springer-Verlag, New York (1978), p. 42.

344. Kausch, H.H., "The role of network orientation in fracture", H.H. Kausch, ed., Molecular order-molecular motion: Their response to macroscopic stresses, J. Pol. Sci., Part C, Pol. Symp., Interscience Publ., New York (1971), p. 3.

345. Dealy, J.M. and S.S. Soong, "A parallel plate melt rheometer incorporating a shear stress transducer", J. Rheol., 28(4), 355-365 (1984)

346 Laun, H M , "Elastic properties of polymer melts at high deformation rates with respect to extrusion", Proc. 2nd World Cong. Chem. Eng., (Montréal, 1981), Vol. VI, p. 411-415.

347 Boni, S., C. G'Sell, E. Weynant and J.M. Haudin, "Microscopic in situ observation of the plastic deformation of polybutene-1 films under simple shear", Pol. Testing, 3, 3-24 (1982).

348. Boni, S , Mémoire dipl. ing., Conservatoir National des Arts et Métiers de Paris, 1981.

349 Gopez, A J R , Thèse doctorale, Institut National Polytechnique de Lorraine, 1983.

350 Eringen, A.C., "Simple microfluids", Int. J. Engng. Sci., 2, 205-217 (1964).

351 Eringen, A.C. and E.S. Suhubi, "Nonlinear theory of simple micro-elastic solids-I.", Int. J. Engng. Sci., 2, 189-203 (1964).

352. Suhubi, E.S. and A.C. Eringen, "nonlinear theory of micro-elastic solids-II.", Int. J. Engng. Sci., 2, 389-404 (1964).

353. Truesdell, C. and W. Noll, The nonlinear field theories of mechanics, Springer-Verlag, Berlin, (1965), pp. 389-401.

354. Ericksen, J., Trans. Soc. Rheol., 5, 23 (1961).

355 Tanner, R I , Engineering Rheology, Clarendon Press, Oxford (1985), p. 32.

356. Agarwal, S.L. and S. Venkatesan, "An instrument to measure skin friction and normal earth pressure on deep foundations", Instruments and Apparatus for Soil and Rock Mechanics, ASTM STP 392, 152-169 (1965).

357. Arthur, J.R.F. and K.H. Roscoe, "An earth pressure cell for the measurement of normal and shear stresses", Civil Eng. Public Works Rev., 56(659), 766-770 (June, 1961).

358. Bruker, I. and A.S. Lodge, "A rheodilatometer for molten polymers", J. Rheol., 29(5), 557-577 (1985).

359. Martin, B., "Some analytical solutions for viscometric flows of power-law fluids with heat generation and temperature dependent viscosity", Int. J. Non-Linear Mechanics, 2, 285-301 (1967).

360. Joseph, D.D., "Variable viscosity effects on the flow and stability of flow in channels and pipes", Phys. Fluids, 7(11), 1761-1771 (November, 1964)

361. Joseph, D.D., "Stability of frictionally-heated flow", Phys Fluids, 8(12), 2195-2200 (December, 1965).

362. Regirer, S.A , Prikl. Math. Mekh , 22, 414 (1958).

363. Hausenblas, H., Ing-Arch , 18, 151 (1950).

364. Nahme, R., Ing-Arch., 11, 191 (1940).

365. Kingsbury, A., "Heat effects in lubricating films", Mech Eng., 55, 685 (1933).

366. Duncan, J A , "Heat effects in lubricating films", Mech Eng , 56, 120 (1934)

367. Sukanek, P.C., C.A. Goldstein and R.L. Laurence, "The stability of plane Couette flow with viscous heating", J. Fluid Mech., 57, part 4, 651-670 (1973).

368. Gavis, J and R.L. Laurence, "Viscous heating in plane and circular flow between moving surfaces", I&EC Fund., 7(2), 232-239 (May, 1968).

369. Nihoul, J.C., "Nonlinear Couette flows with temperature-dependent viscosity", Phys. Fluids, 13(1), 203-204 (January, 1970).

370. Sukanek, P.C. and R.L. Lawrence, "An experimental investigation of viscous heating in some simple shear flows", AIChEJ, 20, 474 (1974).

371. Nahme, Von R., "Beiträge zur hydrodynamischen theorie der lagerreibung", Trans. Soc. Rheol., 7, 195-207 (1963).

372. Hartnett, J.P. and T.F. Irvine, Jr., eds., Advances in Heat Transfer, Vol. 13, Academic Press, New York, Winter, H.H., "Viscous dissipation in shear flows of molten polymers", pp. 205-267.

373. Martin, B., "Some analytical solutions for viscometric flows of power-law fluids with heat generation and temperature dependent viscosity", Int. J. Non-Linear Mech., 2, 285-301 (1967).

374 Gavis, J. and R.L. Laurence, "Viscous heating of a power-law liquid in plane flow", I&EC Fund., 7(3), 525-527 (August, 1968).

375 Turian, R.M., "The critical stress in frictionally heated non-Newtonian plane Couette flow", Chem. Eng. Sci., 24, 1581-1587 (1969).

376. Kingsbury, A , "Heat effects in lubricating films", Mech. Eng., 55, 685-688 (1933).

377 Martin, B., "Some analytical solutions for viscometric flows of power-law fluids with heat generation and temperature dependent viscosity", Int. J. Non-Linear Mechanics, 2, 285-301 (1967).

378 Tanner, R I , Engineering Rheology, Clarendon Press, Oxford (1985), pp. 371-373

379 Nahme, Von R , "Beiträge zur hydrodynamischen theorie der lagerreibung", Trans. Soc Rheol., 7, 195-207 (1963).

380 Hausenblas, Von H., "Die nichtisotherme laminare strömung einer zähen flüssigkeit durch enge spalte,und kapillarröhren", Ing.-Arch., 18, 151-166 (1950).

381 Nihoul, J C J., "Nonlinear Couette flows with temperature-dependent viscosity", Phys. Fluids, 13(1), 203-204 (January, 1970).

382 Joseph, D.D , "Stability of frictionally-heated flow", Phys. Fluids, 8(12), 2195-2200 (December, 1965).

383. Joseph, D D., "Variable viscosity effects on the flow and stability of flow in channels and pipes", Phys. Fluids, 7(11), 1761-1771 (November 1964).

384. Turian, R.M., "The critical stress in frictionally heated non-Newtonian plane Couette flow", Chem. Eng. Sci., 24, 1581-1587 (1969).

385. Gavis, J. and R.L. Laurence, "Viscous heating of a power-law liquid in plane flow", I&EC Fund., 7(3), 525-527 (August, 1968).

386 Martin, B., "Some analytical solutions for viscometric flows of power-law fluids with heat generation and temperature dependent viscosity", Int. J. Non-Linear Mech., 2, 285-301 (1967).

387. Bird, R.B., W.E. Stewart and E.N. Lightfoot, Transport Phenomena, John Wiley & Sons, Inc., New York (1960), pp. 306-307.

388. Sukanek, P.C. and R.L. Lawrence, "An experimental investigation of viscous heating in some simple shear flows", AIChEJ, 20, 474 (1974).

389. Gruntfest, I.J., "Thermal feedback in liquid flow, plane shear at constant stress", Trans. Soc. Rheol., VII, 195-207 (1963).

390. Kingsbury, A., "Heat effects in lubricating films", Mech. Eng., 55, 687 (November, 1933).

391. Gruntfest, I.J., "Thermal feedback in liquid flow, plane shear at constant stress", Trans. Soc. Rheol., VII, 195-207 (1963).

392 Carslaw, H S and J.C Jaeger, Conduction of Heat in Solids, Oxford Univ. Press, London, 1959.

393 Welty, J R., C.E. Wicks and R.E. Wilson, Fundamentals of Momentum Heat and Mass Transfer, 2nd ed., John Wiley & Sons, New York (1976), p. 318

394. Powell, R.L. and S. Middleman, "Transient thermal response of plane couette flow with viscous heat generation-effect of a solid conducting boundary", Int. J. Eng Sci., 6, 49-57 (1968).

395 Powell, R L. and S. Middleman, "Transient thermal response of plane couette flow with viscous heat generation-effect of a solid conducting boundary", Int J Eng. Sci , 6, 49-57 (1968).

396 Powell, R L. and S. Middleman, "Transient thermal response of plane couette flow with viscous heat generation-effect of a solid conducting boundary", Int J. Eng. Sci., 6, 49-57 (1968).

397. Gruntfest, I J., "Thermal feedback in liquid flow, plane shear at constant stress", Trans. Soc. Rheol., VII, 195-207 (1963).

398 Hartnett, J.P. and T.F Irvine, Jr., eds , Advances in Heat Transfer, Vol. 13, Academic Press, New York, Winter, H.H., "Viscous dissipation in shear flows of molten polymers", pp. 205-267.

399 Schapery, R.A. and D.E. Cantey, "Thermomechanical response studies of solid propellants subjected to cyclic and random loading", AIAA J., 4(2), 255-261 (February, 1966).

400. Schapery, R.A., "Effect of cyclic loading on the temperature in viscoelastic media with variable properties", 2(5), 827-835 (May, 1964).

401. Schapery, R.A., "Thermomechanical behavior of viscoelastic media with variable properties subjected to cyclic loading", J. Appl. Mech., 611-619 (September, 1965).

402. Pipkin, A.C , Lectures on Viscoelasticity Theory, 2nd ed., Vol. 7 in "Applied Mathematical Sciences", (Springer-Verlag, New York), 1986, pp. 102-106.

403 Pipkin, A C , Lectures on Viscoelasticity Theory, 1st ed., Vol. 7 in "Applied Mathematical Sciences", (Springer-Verlag, New York), 1972, pp. 100-104.

404 Tanner, R I , Engineering Rheology, Clarendon Press, Oxford (1985), pp. 371-373.

405 Schapery, R A. and D.E. Cantey, "Thermomechanical response studies of solid propellants subjected to cyclic and random loading", AIAA J., 4(2), (February 1966).

406 Tanner, R.I , Engineering Rheology, Clarendon Press, Oxford (1985), pp. 373-374.

407 Schapery, R A and D E Cantey, "Thermomechanical response studies of solid propellants subjected to cyclic and random loading", AIAA J., 4(2), (February 1966)

408 Schapery, R A , "Effect of cyclic loading on the temperature in viscoelastic media with variable properties", 2(5), 827-835 (May, 1964).

409 Schapery, R A , "Thermomechanical behavior of viscoelastic media with variable properties subjected to cyclic loading", J. Appl. Mech., 611-619 (September, 1965).

410 Pipkin, A C , Lectures on Viscoelasticity Theory, 2nd ed., Vol. 7 in "Applied Mathematical Sciences", (Springer-Verlag, New York), 1986, pp. 102-106.

411 Tanner, R I , Engineering Rheology, Clarendon Press, Oxford (1985), pp. 371-373.

412 Schapery, R A and D.E. Cantey, "Thermomechanical response studies of solid propellants subjected to cyclic and random loading", AIAA J., 4(2), (February 1966).

413. Narain, A. and D.D. Joseph, "Remarks about the interpretation of impulse experiments in shear flows of viscoelastic liquids", Rheol. Acta, 22, 528-538 (1983).

414 Batchelor, G K., An Introduction to Fluid Dynamics, Cambridge University Press, 1967.

415 Soong, S S., "A parallel plate viscoelastometer for molten polymers", Dept. Chem. Eng., McGill University, Montreal (June, 1983).

416. Schlichting, H., Boundary Layer Theory, 4th ed., McGraw-Hill Book Co., Inc., New York (1960), pp. 73-74.

417 Joseph, D , "Remarks about the interpretation of impulse experiments in shear flows of viscoelastic liquids", Rheol. Acta, 22, 528-538 (1983).

418 Christensen, R N., Theory of Viscoelasticity - An Introduction, Academic Press, New York (1971).

419. Denn, M.M. and K.C. Porteous, Chem. Eng. J., 2, 280-286 (1971).

420 Kazakia, J.Y. and R.S. Rivlin, Rheol. Acta, 20, 111-127 (1981).

421 Moshimaru, Y., "Unsteady-state development of plane Couette flow for viscoelastic fluids". J. Non-Newt. Fluid Mech , 12, 135-152 (1983)

422. Narain, A. and D.D Joseph, Rheol. Acta, 21, 228-250 (1982).

423 Chow, A.W and G G. Fuller, "Some experimental results on the development of Couette flow for non-Newtonian fluids", J. Non-Newt. Fluid Mech , 17, 233-243 (1985).

424 Schlichting, H., Boundary Layer Theory, 4th ed , McGraw-Hill Book Co., Inc., New York (1960), pp. 75-77.

425 Batchelor, G K., An Introduction to Fluid Dynamics, Cambridge University Press, (1967), pp. 191-193.

426 Darby, R , Viscoelastic Fluids, An Introduction to their Properties and Behavior, Marcel Dekker, Inc., New York (1976), pp. 251-253.

427 Schrag, J L , "Deviation of velocity gradient profiles from the "gap loading" and "surface loading" limits in dynamic simple shear experiments", Trans. Soc. Rheol., 21(3), 399-413 (1977).

428 Schrag, J.L., J.F. Guess and G.B. Thurston, "Shear-wave interference observed by optical birefringence induced in a viscoelastic liquid", J. Appl. Phys., 36(6), 1996-2000 (June, 1965).

429. Thurston, G.B. and J.L. Schrag, "Shear wave propagation in a birefringent viscoelastic medium", J. Appl. Phys., 35(1) 144-151 (January, 1964).

430. Thurston, G.B. and J.L. Schrag, "Measurement of dynamic birefringence of a thin fluid layer in oscillatory shear", Trans. Soc. Rheol., VI, 325-348 (1962).

431. Shah, B.H. and R. Darby, "Rheovibron determination of the dynamic moduli of polymer melts", Pol. Eng. Sci., 16(1), 46 (January, 1976).

432. Schrag, J.L., "Deviation of velocity gradient profiles from the 'gap loading' and 'surface loading' limits in dynamic simple shear experiments", Trans. Soc. Rheol., 21(3), 399-413 (1977).

433 Darby, R , Viscoelastic Fluids, An Introduction to their Properties and Behavior, Marcel Dekker, Inc., New York (1976), pp. 251-253.

434. Shah, B.H. and R. Darby, "Rheovibron determination of the dynamic moduli of polymer melts", Pol. Eng. Sci., 16(1), 46 (January, 1976).

435 Yong, R.N., Dutertre, J.C. and R.J. Krizek, "Stress propagation in a frequency-dependent clay soil", Trans. Soc. Rheol., 18(3), 411-420 (1974).

436 Bottom, V.E., Introduction to Quartz Crystal Unit Design, Van Nostrand Reinhold Co., New York (1982), p.10.

437 Bird, R B , W E Stewart and E.N. Lightfoot, Transport Phenomena, John Wiley & Sons, Inc., New York (1960).

438 Weinberg, B., "Some results of experimental study of substances having considerable internal friction", Indian J. Phys., 1, 279-310 (1926-7)

439 Liu, Y -H T , "Rheological transients in entangled polymeric fluids", Ph.D. thesis, Chem. Eng., Univ Calif. at Berkeley (1976).

440 Liu, T Y , D W. Mead, D S. Soong and M.C. Williams, "A parallel-plate rheometer for the measurement of steady-state and transient rheological properties", Rheol. Acta, 22, 81-89 (1983)

441 Burton, R.H., M.J. Folkes, K.A. Narh and A. Keller, "Spatial variation in viscosity in sheared polymer melts", J. Mat. Sci., 18, 315-320 (1983).

442 Collyer, A and D. Clegg, eds., Physical Principles of Rheological Measurement, Elsevier Applied Science Publishers, Ltd., "Sliding plate and sliding cylinder rheometers" by J.M. Dealy and A.J. Giacomin, in press.

443 Israelachvili, J.N., "Measurements of the viscosity of thin fluid films between two surfaces with and without adsorbed polymers", Colloid & Pol. Sci., 264, 1060-1065 (1986).

444 Schlichting, H , Boundary Layer Theory, McGraw-Hill, New York (1955), p. 357.

445 Dealy, J M , Rheometers for Molten Plastics, A Practical Guide to Testing and Property Measurement, Van Nostrand Reinhold Company, New York (1982), p. 122.

446. Gill, A.E., J. Fluid Mech., 21, 503 (1965).

447. Sukanek, P.C., C.A. Goldstein and R.L. Laurence, "The stability of plane Couette flow with viscous heating", J. Fluid Mech., 57, Part 4, 651-670 (1973).

448. Gallagher, A.P. and A. Mercer, J. Fluid. Mech., 13, 91 (1962).

449. Gallagher, A.P. and A. Mercer, J. Fluid. Mech., 15, 350 (1964).

450. Southwell, R.V. and L. Chitty, Phil. Trans., 229, Part A, 205 (1930).

451. Deardorff, J.W., J. Fluid Mech., 15, 623 (1963).

452. Ponomarenko, Iu.B., J. Appl. Math. Mech., 32, 627 (1968).

453. Gallagher, A.P., SIAM J Appl. Math., 4, 3 (1969).

454. Petrov, G'I , Prikl Math. Mech , 4, 3 (1940)

455. Joseph, D.D., "Variable viscosity effects on the flow and stability of flow in channels and pipes", Phys Fluids, 7(11), 1761-1771 (November, 1964)

456 Joseph, D.D., "Stability of frictionally-heated flow", Phys Fluids, 8(12), 2195-2200 (1965)

457 Sukanek, P C., C.A. Goldstein and R.L. Laurence, "The stability of plane Couette flow with viscous heating", J. Fluid Mech , 57, Part 4, 651-670 (1973).

458 Rivlin, R S , "The propagation of vorticity in a viscoelastic fluid", J. Non-Newt. Fluid Mech , 17, 313-329 (1985)

459 Huilgol, R R., "Propagation of a vortex sheet in viscoelastic liquids - the Rayleigh problem", J. Non-Newt. Fluid Mech., 8, 337-347 (1981).

460 Huilgol, R.R., "Corrections and extensions to 'Propagation of a vortex sheet in viscoelastic liquids - the Rayleigh problem'", J. Non-Newt. Fluid Mech., 8, 337-347 (1981).

461 Akbay, U , E. Becker and S. Sponagel, "Instability of plane Couette flow of viscoelastic liquids", J. Non-Newt. Fluid Mech., 18, 123-141 (1985).

462 Kausch, H H , Polymer Fracture, Springer-Verlag, New York (1978), p. 42.

463. Tanner, R.I. and M. Keentok, "Shear fracture in cone-plate rheometry", J. Rheol. 27(1), 47-57 (1983).

464 . Laun, H M , "Elastic properties of polymer melts at high deformation rates with respect to extrusion", Proc. 2nd World Cong. Chem. Eng., (Montréal, 1981), Vol. VI, p. 411-415.

465. Grubb, D.T. and A. Keller, J. Pol. Sci., Pol. Lett. Ed., 12, 419 (1974).

466. Burton, R.H., M.J. Folkes, K.A. Narh and A. Keller, "Spatial variation in viscosity in sheared polymer melts", J. Mat. Sci., 18, 315-320 (1983).

467 Doebelin, E O , Measurement Systems: Application and Design, McGraw-Hill Book Company, New York, revised ed. (1975).

468. Macosko, C.W. and D.J. Morse, "Transient shear testing with the mechanical spectrometer", Proc. VIIth Int. Congr. Rheol., Gothenburg, Sweden (1976), pp. 376-377.

469 Doebelin, E O , Measurement Systems, 3rd ed., McGraw-Hill Book Co., New York (1983).

470 User Manual for Rheometrics Mechanical Spectrometer, Model RMS-605, Rheometrics, Inc., One Possumtown road, Piscataway, NJ 08854.

471 Doebel~~in, E O ,~~ Measurement Systems, Application and Design, McGraw-Hill Book Company, New York, revised ed. (1975).

472 Doebelin, E O , Measurement Systems, Application and Design, McGraw-Hill Book Company, New York, revised ed. (1975).

473 Hoerner, G M Jr , "Finding system characteristics from initial step response", Control Eng., 103-104 (May, 1962).

474 Anderson, N A., "Step-analysis method of finding time constant", Instruments & Control Systems, 36, 130-135 (November, 1963).

475 Doebelin, E O , Measurement Systems, Application and Design, McGraw-Hill Book Company, New York, revised ed. (1975).

476 Hoerner, G.M.Jr , "Second order system characteristics from initial step response", Control Eng., 93-95 (December, 1962).

477 Ramirez, R W , The FFT Fundamentals and Concepts, Prentice-Hall, Inc., Englewood Cliffs (1985).

478. Dealy, J.M. and S.S. Soong, "A parallel plate melt rheometer incorporating a shear stress transducer", J. Rheol., 28(4), 355-365 (1984).

479. Dealy, J.M. and S.S. Soong, SPE Tech. Paper., 28, 76 (1982).

480 Soong, S S , Doctoral Dissertation, Dept. of Chemical Engineering, McGill University, 1983.

481 Tee, T.-T. and J.M. Dealy, "Nonlinear viscoelasticity of polymer melts", Trans. Soc. Rheol., 19(4), 595-615 (1975).

482. Tee, T.-T., "Large amplitude oscillatory shearing of polymer melts", doctoral dissertation, Dept. of Chemical Engineering, McGill University, Montreal, Canada (1974).

483. Giacomin, A.J., "The development and evaluation of a melt rheometer incorporating a shear stress transducer", Ph.D. Thesis Proposal, Dept. Chemical Engineering, McGill University, Montreal, Canada (1984 September 17).

484. Giacomin, A.J. and J.M. Dealy, "A new rheometer for molten plastics", ANTEC '86 Proc., 711-714 (1986).

485 Giacomin, A.J. and J.M. Dealy, "A new rheometer for molten plastics", SPE Tech. Paper, ANTEC '86, pp. 711-714.

486 Soong, S.S., "A parallel plate viscoelastometer for molten polymers", Ph.D Thesis, McGill University, Dept. Chem. Eng., Montreal (June, 1983).

487. Zell, K.D., "A review of advanced electrohydraulic systems for fatigue testing", MTS Systems Corp., Tech. Bull. 160-02-01, 12/71

488 Woo, C.W., "Computer aided material testing", Hong Kong Engineer, 15-19 (August, 1982).

489 Cain, P.J., "Application of MTS BASIC-11 to material testing", MTS Systems Corp., Tech Bull 300013-15 160.16-02 279.

490 Navickis, L.L. and E.B. Bagley, "Yield Stresses in Concentrated Dispersions of Closely Packed, Deformable Gel Particles", J. Rheol., 27(6), 519-536 (1983).

491. Kjellman, W., "Testing the shear strength of clay in Sweden", Géotechnique, 2(3), 225 (1951).

492 SCHNEEBERGER product literature, "Linear Bearings and Frictionless Tables", Bull. No. 100f/02, p. 73.

493 Laun, H.M., "Elastic properties of polyethylene melts at high shear rates with respect to extrusion", Rheol. Acta, 21, 464-469 (1982).

494 Laun, H.M., "Elastic Properties of Polymer Melts at High Deformation Rates with Respect to Extrusion", Proc. 2nd World Congr. Chem. Eng., 6, 411 (1981).

495. Navickis, L.L. and E.B. Bagley, "Yield Stresses in Concentrated Dispersions of Closely Packed, Deformable Gel Particles", J. Rheol., 27(6), 519-536 (1983).

496. Gibbs, D.A., Proc. 4th Cong. on Rheol., Part 2, Interscience NY, 1965, p. 183.

497 Goldstein, C., "Transient and Steady Shear Behavior of SBR Polymers", Trans. Soc. Rheol., 18(3), 357-369 (1974).

498. Zakharenko, N.V., F.S. Tolstukhina and G.M. Bartenev, Rubber Chem. Technol., 35, 326 (1962).

499. Letter, Lapointe, R., MTS (CANADA) LTD, to A.J. Giacomin, 1984 February 16.

500 Boni, S., Mémoire dipl. ing., Conservatoire national des arts et métier de Paris, 1981.

501 Gopez, A J.R., Thèse doctorale, Institut National Polytechnique de Lorraine, 1983.

502 SCHNEEBERGER product literature, "Linear Bearings and Frictionless Tables", Bull. No. 100f/02, p. 73.

503 Gyalokay, M , MIKON ENGINEERING LTD., personal communication, 1984 February 2.

504 Gyalokay, M., MIKON ENGINEERING LTD., personal communication, 1984 February 2.

505 SCHNEEBERGER Catalog, "Anti-friction Guideways", ed. 100g/03, p. 93.

506 Laun, H.M. and J. Meissner, "A Sandwich-Type Creep Rheometer for the measurement of rheological properties of polymer melts at low shear stresses", Rheol. Acta, 19, 60-67 (1980).

507 McCarthy, R.V., "An improved rheometer design used to measure viscoelastic properties of polymer melts", J. Rheol., 22(6), 623-641 (1978)

508 Faridi, H , ed , Rheology of Wheat Products, "Dynamic rheological testing of wheat flour doughs" by Faubion, J.M., P.C. Dreese and K.C. Diehl, The American Association of Cereal Chemists, Inc., St. Paul, MN (1985), p. 91.

509. Szczesniak, A.A., J. Loh and W.R. Manell, "Effect of moisture transfer on dynamic viscoelastic properties of wheat flour/water systems", 27, 523 (1983).

510 "Oven cleaners. Some excellent cleaners. But only one contains no lye", Consumer Reports, 140-141 (March, 1987).

511. A product of the NEVER-SEEZ COMPOUND Corp., 2910 S. 18th Ave., Broadview, IL.

512. Labout, J.W.A. and W.P. van Oort, "Micromethod for determining Viscosity of High Viscosity Materials", Anal. Chem., 28(7), 1147 (1956).

513. Laun, H.M., "Elastic properties of polyethylene melts at high shear rates with respect to extrusion", Rheol. Acta, 21, 464-469 (1982).

514. Laun, H.M., "Elastic Properties of Polymer Melts at High Deformation Rates with Respect to Extrusion", Proc. 2nd World Congr. Chem. Eng., 6, 411 (1981).

515. Dexter, F.D., J.C. Miller and W. Philippoff, "Flow birefringence of molten polyethylene", Trans. Soc. Rheol., 5, 193-204 (1961).

516. Zakharenko, N.V., F.S. Tolstukhina and G.M. Bartenev, Rubber Chem. Technol., 35, 326 (1962).

517. Toki, S. and J.L. White, "Rheological and Solid Wall Boundary Condition Characterization of Unvulcanized Elastomers and their Compounds", J. Appl. Pol. Sci., 27, 3171-3184 (1982).

518. Toki, S., "Rheological and Boundary Characterization of Unvulcanized Rubbers and their Compounds", Ph D. Thesis, U. Tenn , Knoxville (Dec., 1981)

519. Montes, S. and J.L. White, "A comparative rheological investigation of natural and synthetic cis-1,4-polyisoprenes and their carbon black compounds", Rubber Chem. Technol., 55, 1354-1369 (1982).

520. Bujake, J.E., "Creep Properties of Sodium Stearate", J Colloid and Interface Sci., 27(2), 229-234 (June, 1968)

521. Fruh, S.M. and F. Rodriguez, "Recoverable Shear Measurements in a Parallel Plate Rheometer", AIChEJ, 16(6), 907-910 (1970).

522. Van Holde, K.E. and J W. Williams, "Study of the Viscoelastic Behavior and Molecular Weight Distribution of Polyisobutylene", J. Pol. Sci., XI(3), 243-268 (1953).

523. Shama, F. and P. Sherman, "The Texture of Ice Cream 2. Rheological Properties of Frozen Ice Cream", J. Food Sci., 31, 699-706 (1966).

524 Griffin, R.L. Miles, C.J. Penther and W.C. Simpson, Road and Paving Materials, ASTM STP 212, 36-50 (1957).

525. Griffin, R.L., T.K. Miles and C.J. Penther, Assn. Asphalt Paving Technologists, 24, 31 (1955).

526. ASTM D3570-77, "Standard Test Method for Viscosity of Materials with a Sliding Plate Microviscometer".

527. "RHEOMETRICS Dynamic Spectrometer Model LA", 1981 RHEOMETRICS, INC., product literature, Bulletin No. PL-02 3.0M 0982.

528. Shah, B.H. and R. Darby, "Rheovibron determination of the dynamic moduli of polymer melts", Pol. Eng. Sci., 16(1), 46 (January, 1976).

529. Fitzgerald, E.R. and J.D. Ferry, "Method for determining the dynamic mechanical behavior of gels and solids at audio-frequencies; comparison of mechanical and electrical properties", J. Coll. Sci., 8, 1-34 (1953).

530 Fitzgerald, E.R., "Dynamic electrical and mechanical behavior of polymeric systems", Ph.D. Thesis, U. of Wisconsin, 1951.

531. Hull, H., J. Coll. Sci., 7, 316 (1952).

532. Taylor, J.H. and S.E. Cozzens, Amer. Ink Maker, 62ff (May 1961).

533 Laun, H M. and J. Meissner, "A Sandwich-Type Creep-Rheometer for the measurement of rheological properties of polymer melts at low shear stresses", Rheol. Acta, 19, 60-67 (1980).

534. Dealy, J.M , personal communication.

535 McCarthy, R.V., "An improved rheometer design used to measure viscoelastic properties of polymer melts", J. Rheol., 22(6), 623-641 (1978)

536 Humphreys, F.E. and N. Stone, "Measurement of high viscosities by shearing between parallel plates", J. Sci. Instr., 34, 26-27 (1957).

537. Mutel, A.T., McGill University, Dept. Chem. Eng., Montreal, Canada, personal communication, 1987, September.

538. Spiegel, M R , Applied Differential Equations, 2nd ed., Prentice-Hall, Englewood Cliffs, N.J., (1967), pp. 99ff.

539. Whitaker, S. and R.L. Pigford, "An approach to numerical differentiation of experimental data", I&EC, 52(2), 185-187 (February, 1960)

540. Alexander, H., McGill University, Dept. Chem. Eng., Machine Shop, personal communication, 1984 June.

541 Hurley, R., Firth Brown Stainless Steel, Toronto, Canada, personal communication, 1983 July 3.

542. Perry, R.H. and C.H. Chilton, Chemical Engineers' Handbook, 5th ed., McGraw-Hill Book Co., New York, (1973), pp. 23-40.

543 Soong, S.S , "A parallel plate viscoelastometer for molten polymers", doctoral dissertation, McGill University, Dept. Chemical Engineering, Montréal, Canada (June, 1983).

544. Liu, T Y., D.W. Mead, D.S. Soong and M.C. Williams, "A parallel-plate rheometer for the measurement of steady-state and transient rheological properties", Rheol. Acta, 22, 81-89 (1983).

545. McCarthy, R.V., "An improved rheometer design used to measure viscoelastic properties of polymer melts", J. Rheol., 22(6), 623-641 (1978).

546. Sivashinsky, N., A.T. Tsai, T.J. Moon and D.S. Soong, "Some New Transient Test Results from a Parallel-Plate Rheometer", To be published, J. Rheol. (1984).

547. Liu, T.Y., D.W. Mead, D.S. Soong and M.C. Williams, "A parallel-plate rheometer for the measurement of steady-state and transient rheological properties", Rheol. Acta, 22, 81-89 (1983).

548. Tsai, A.T. and D.S. Soong, Measurement of Fast Transient and Steady State Responses of Viscoelastic Fluids with a Sliding Cylinder Rheometer Executing Coaxial Displacements", Submitted to J. Rheol., 1984.

549. Liu, Y.T., "Rheological Transients in Entangled Polymeric Fluids", Ph.D. Thesis, U. of California, (September, 1982).

550 Cain, P.J., MTS Systems Corp., personal communication, 1985 August.

551. Tee, T.-T., "Large amplitude oscillatory shearing of polymer melts", Ph D Thesis, Dept. of Chemical Engineering, McGill University, Montreal, Canada (1974)

552 Patel, N., M.Eng. Thesis, Dept of Chemical Engineering, McGill University, Montreal, Canada (1985).

553 Woo, C.W., "Computer aided material testing", Hong Kong Engineer, 15-19 (August 1982).

554. Cain, P.J., "Application of MTS BASIC-11 to material testing", MTS Systems Corp., Prod. Bull. No. 300013-15, 160 16-02 279.

555. Dealy, J.M., "Method of measuring shear stress", U.S. Patent No. 4,464,928 (Aug. 14, 1984).

556 Broch, J T , Mechanical Vibration and Shock Measurements, 2nd ed., Bruehl & Kjehr, Denmark (April, 1984).

557. Lagace, L.J. and C.D. Kissinger, "Non-Contact Displacement and Vibration Measurement Systems Employing Fiber Optic and Capacitance Transducers", Proc. 23rd Int. Instrumentation Symp., 1977.

558. Hohenberg, R., "Sensing Shaft Position Without Contact", SAE Automotive Engineering Congress and Exp., Detroit, Michigan (1976 February 23-27).

559. Soong, S.S., "A parallel plate viscoelastometer for molten polymers", Ph.D. Thesis, Dept. Chem. Eng., McGill Univ., Montreal, Canada, (June, 1983).

560 Broch, J T , Mechanical Vibration and Shock Measurements, 2nd ed., Bruehl & Kjehr, Denmark (April, 1984).

561. Zygo Interferometer Systems Product Bulletin No. SB-0110A, Zygo Corp., Laurel Brook Road, Middlefield, CT 06455 (1986).

562. Keusseyan, R.L. and C.-Y. Li, "Precision strain measurement at elevated temperatures using a capacitance probe", J. Testing and Eval., 9(3), 214-217 (May, 1981).

563. Cook, R.O. and, C.W. Hamm, "Fiber optic lever displacement transducer", Applied Optics, 18, 3230 (1979 October 1).

564 Kissinger, C., "Fiber Optic Lever Displacement Sensors and Automated Reflectance Compensation Improvements", Paper presented at FOC/LAN 83, 7th Int Fiber Optics & Communications Exp., Atlantic City, NJ (1983 October 10-14)

565. Kissinger, C.D. and R.L. Smith, "Improved Noncontact Fiber Optics/Lens Displacement Measuring System", Proc. Technical Program, Electro-Optical Systems Design Conf., 372-377 (1973).

566 Porter, J H , "Differential fiber optic differential pressure sensor", U.S. Patent #4,210,029 (Jul. 1, 1980).

567. Kissinger, C D., MECHANICAL TECHNOLOGY INC., Latham, N.Y., personal communications, 1983 December.

568. Keusseyan, R.L. and C.-Y. Li, "Precision Strain Measurement at Elevated Temperatures Using a Capacitance Probe", J. Testing and Evaluation, JTEVA, 9(3), 214-217 (1981 May).

569 Bell, D.A., "Temperature coefficient of capacitance and of inductance", Electron. Techn., 37, 342-345 (1960)

570. DANTEC ELECTRONICS Ltd., Scarborough, Canada M1S 3S6, "Modules which complete your 56C00 system", Publication No. 4201 E (April, 1984).

571 DANTEC ELEKTRONIK Ltd., Denmark, "Instruction and service manual: 56E01 Reactance converter", Product Bull. 9150A0431 (June, 1984).

572 Bruehl & Kjaer Instruments, "Capacitive Transducer", Product Bulletin #11 MM 0004.

573. Konigsberg, R.L., "Operational bridge gages high capacitance", Electronics, 175-177 (January 1, 1957).

574 Doebelin, E.O., Measurement Systems, Application and Design, rev. ed., McGraw-Hill Book Co., New York (1975), pp. 250ff.

575. Doebelin, E.O., Measurement Systems, Application and Design, 3rd. ed., McGraw-Hill Book Co., New York (1983).

576. Dorman, R.A., C.D. Kissinger and L.J. Lagace, Jr., "Capacitance type non-contact displacement and vibration measuring device and method of maintaining calibration", U.S. Patent No. 4,067,225, Mechanical Technology Inc., Latham, N.Y. (January 10, 1978).

577. Dorman, R.A., "Signal amplifier system for controlled carrier signal measuring sensor/transducer of the variable impedance type", U.S. Patent No. 4,176,555, Mechanical Technology Inc., Latham, N.Y. (December 4, 1979).

578. Dorman, R.A., "Signal amplifier system for controlled carrier signal measuring sensor/transducer fo the variable impedance type", U.S. Patent No. 4,176,555 (Dec. 4, 1979).

579. Dorman, R.A., C.D. Kissinger and L.J. Lagace, "Capacitance type non-contact displacement and vibration measuring device and method of maintaining calibration", U.S. Patent No. 4,067,225 (Jan. 10, 1978).

580. Lagace, L.J. and C.D. Kissinger, "Noncontact displacement & vibration measurement systems employing fiber optic and capacitance transducers", Proc. 23rd Int. Instr Symp., Las Vegas, Nevada (1977 May 1-5).

581. Hooke, C.J. and Y.P. Kakoullis, "On-line measurement of film thickness", I. Mech. E., Paper No. C128/79, 51-59 (1979).

582. Hohenberg, R., "Sensing shaft position without contact", S.A.E. Paper No. 760313, Proc. Automotive Eng. Congr. and Exp., Detroit (February 23-27, 1976).

583. Calvert, R., "Apparatus for measuring small distances", U.S. Patent #3,048,775 (Aug. 7, 1962).

584. Hugill, A.L., "Displacement transducers based on reactive sensors in transformer ratio bridge circuits", Chapter 3 in Instrument Science and Technology, vol. 2, Jones, B.E., ed., Adam Hilger Ltd., Bristol, pp. 21-32 (1983).

585. Dorman, R.A., "Signal amplifier system for controlled carrier signal measuring sensor/transducer fo the variable impedance type", U.S. Patent No. 4,176,555 (Dec. 4, 1979).

586. Doebelin, E O., Measurement Systems, Application and Design, rev. ed., McGraw-Hill Book Co., New York (1975), pp. 250ff.

587 Doebelin, E O., Measurement Systems, Application and Design, 3rd. ed., McGraw-Hill Book Co., New York (1983).

588. Khan, A.R., I.J. Brown and M.A. Brown, "The behaviour of capacitance displacement transducers using epoxy resin as an electrode-guard ring spacer", J. Phys. E.: Sci. Instrum., 13, 1280-1281 (1980).

589. Brown, M.A. and C.E. Bulleid, "The effect of tilt and surface damage on practical capacitance displacement transducers", J. Phys. E.: Sci. Instrum., 11, 429-432 (1978).

590 Griffel, W., Beam Formulas, Frederick Ungar Publ. Co., New York (1970).

591. Carnahan, B., H.A. Luther and J.O. Wilkes, Applied Numerical Methods, John Wiley & Sons, Inc., (New York, 1969).

592. Griffel, W., "Beams under combined axial and transverse loads", Machine Design, 34(17), 185-189 (july 19, 1962).

593 Griffel, W, Handbook of Formulas for Stress and Strain, Frederick Ungar Publishing Co., New York (1966).

594. Griffel, W, "Unsymmetrical bending of beams", Prod. Eng., 106-108 (July 22, 1963).

595 Mase, G.E, Continuum Mechanics, Schaum's Outline Series in Engineering, McGraw-Hill Book Company, (1970).

596. Griffel, W, Handbook of Formulas for Stress and Strain, Frederick Ungar Publishing Co., New York (1966).

597. Carnahan, B H., H.A. Luther and J.O. Wilkes, Applied Numerical Methods, John Wiley & Sons, Inc., New York (1969), p. 203 and prob. 3.27.

598 Wylie, C R, Advanced Engineering Mathematics,, McGraw-Hill, New York (1951).

599 Leonard, R.W., "On solutions for the transient response of beams", NASA Tech. Report R-21 (1959).

600. Jacobsen, L.S. and R.S. Ayre, Engineering Vibrations with Applications to Structures and Machinery, McGraw-Hill Book Co., Inc., New York (1958).

601 Soong, S.S, "A parallel plate viscoelastometer for molten polymers", doctoral dissertation, Dept. of Chemical Engineering, McGill University, Montreal (1983).

602. Pilkey, W.D. and O.H. Pilkey, Mechanics of Solids, Quantum Publ. Inc., New York, 389 (1974).

603. Letter, Giacomin, A.J. to J. Smid, CZECHOSLOVAK ACADEMY OF SCIENCE, 1984 June 12.

604. Smid, J., CZECHOSLOVAK ACADEMY OF SCIENCE, personal communication, 1984 August 15.

605. Smid, J. and J. Novosad, "Pressure Cell for Measuring Normal and Shear Stresses", Powder Technol., 4, 322-327 (1970/71).

606. Soong, S.S., "A parallel plate viscoelastometer for molten polymers", doctoral dissertation, Dept. of Chemical Engineering, McGill University, Montreal (1983).

607. MTS Systems Corp., Product Bulletin 0285, 661.19A-1 (1985).

608. Darby, R. Viscoelastic Fluids. An Introduction to Their Properties and Behavior, Chem. Proc. and Eng., vol. 9, Marcel Dekker, Inc., New York (1976), pp. 370-371.

609. Randall, R.B., Application of B&K Equipment to Frequency Analysis, 2nd ed., Bruehl & Kjaer, Denmark (September, 1977).

610. Broch, J.T., Mechanical Vibration and Shock Measurements, 2nd ed., Bruehl & Kjaer, Denmark (April, 1984).

611. Ramirez, R.W., The FFT. Fundamentals and Concepts, Prentice-Hall, Inc., Englewoods Cliffs (1985).

612. Clune, T.R., "Book Review. 'The FFT: Fundamentals and Concepts'", BYTE, 11(4), 57-67 (April, 1986).

613. Ramirez, R.W., The FFT. Fundamentals and Concepts, Prentice-Hall, Inc., Englewoods Cliffs (1985).

614. Ramirez, R.W., The FFT. Fundamentals and Concepts, Prentice-Hall, Inc., Englewoods Cliffs (1985).

615. Ramirez, R.W., The FFT. Fundamentals and Concepts, Prentice-Hall, Inc., Englewoods Cliffs (1985).

616. Ramirez, R.W., The FFT. Fundamentals and Concepts, Prentice-Hall, Inc., Englewoods Cliffs (1985).

617. Ramirez, R.W., The FFT. Fundamentals and Concepts, Prentice-Hall, Inc., Englewoods Cliffs (1985).

618. Cooley, P.M. and J.W. Tukey, "An algorithm for the machine computation of complex Fourier series", Mathematics of Computation, 19, 297-301 (April, 1965).

619. Krieger, I.M. and T.-F. Niu, "A rheometer for oscillatory studies of nonlinear fluids", Rheol. Acta, 12, 567-571 (1973).

620. MacSporran, W.C. and R.P. Spiers, "The dynamic performance of the Weissenberg rheogoniometer. III. Large amplitude oscillatory shearing - harmonic analysis", Rheol. Acta, 23, 90-96 (1984).

621 Ramirez, R W., The FFT: Fundamentals and Concepts, Prentice-Hall, Inc., Englewoods Cliffs (1985).

622. Ramirez, R.W., The FFT: Fundamentals and Concepts, Prentice-Hall, Inc., Englewoods Cliffs (1985).

623 Brigham, E O., The Fast Fourier Transform, Prentice-Hall, Inc., N.J. (1974).

624 Ramirez, R W, The FFT: Fundamentals and Concepts, Prentice-Hall, Inc., Englewoods Cliffs (1985).

625. Schapery, R.A. and D.E. Cantey, ""Thermomechanical response studies of solid propellants subjected to cyclic and random loading", AIAA J., 4(2), 255-264 (February, 1966).

626 Walters, K. and T.E.R. Jones, "Further studies on the usefulness of the Weissenberg rheogoniometer", in Onogi, S., ed., Proc. 5th Int. Cong. Rheol, Univ. Tokyo Press, 4, 337-350 (1970).

627 Powell, R.L. and W.H. Schwarz, "Geometrical effects in the measurements of mechanical properties in parallel superposed flows", J. Pol. Sci.: Pol. Phys. Ed., 17, 969-985 (1979).

628 Yen, H.-C. and L.V. McIntire, "Finite amplitude dynamic motion of viscoelastic materials", Trans. Soc. Rheol., 16(4), 711-726 (1972).

629 Powell, R L. and W.H. Schwarz, "Nonlinear dynamic viscoelasticity", J. Rheol., 23(3), 323-352 (1979).

630. Personal Communication, R.L. Powell to J.M. Dealy, August 12, 1986.

631 Birnboim, M.H., J.S. Burke and R.L. Anderson, "A computer approach to instrumentation in viscoelasticity", Proc. 5th Int. Congr. Rheol., Kyoto, 1968, 1, 409 (1969).

632. Weihart, D.F., N.M. Davis and C.W. Macosko, Symp. Non-Linear Viscoelastic Behavior of Molten and Solid Polymers, Div. Organic Coatings and Plastics Chem., A.C.S., Chicago, 1977.

633. Davis, W.M. and C.W. Macosko, "Nonlinear dynamic mechanical moduli for polycarbonate and PMMA", J. Rheol., 22, 53 (1978).

634 Ramirez, R.W., The FFT: Fundamentals and Concepts, Prentice-Hall, Inc., Englewoods Cliffs (1985).

635. Imass, Inc., Hingham, MA, "New product news: Rheophaser for the Rheometrics mechanical spectrometer".

636. Philippoff, W., "Vibrational measurements with large amplitudes", Trans. Soc. Rheol., 10(1), 317-334 (1966).

637. Walters, K. and T.E.R. Jones, "Further studies on the usefulness of the Weissenberg rheogoniometer", in Onogi, S., ed., Proc. 5th Int. Cong. Rheol., Univ. Tokyo Press, 4, 337 (1970).

638. Harris, J. and K. Bogie, "The experimental analysis of non-linear waves in mechanical systems", Rheol. Acta, 6(1), 3 (1967).

639. Bogie, K. and J. Harris, "An experimental analysis of the Weissenberg rheogoniometer", Rheol. Acta, 5(3), 212-215 (1966).

640. Bogie, K. and J. Harris, Rheol. Acta, 5(3), 212-215 (1966).

641. Philippoff, W., "Vibrational measurements with large amplitudes", Trans. Soc. Rheol., 10(1), 317-334 (1966).

642. Philippoff, W., "Vibrational measurements with large amplitudes", Trans. Soc. Rheol., 10(1), 317-334 (1966).

643. Booij, H.C., "Influence of superimposed steady shear flow on the dynamic properties of non-Newtonian fluids", Rheol. Acta, 5(3), 215 (1966).

644. Personal Communication, R.L. Powell to J.M. Dealy, August 12, 1986.

645. Fuller, M., "Numerical Differentiation", Colloquium, McGill Univ., Dept. Chem. Eng., Montreal, Canada (1984 March 23).

646. Whitaker, S. and R.L. Pigford, "An approach to numerical differentiation of experimental data", Ind. Eng. Chem., 52(2), 185-187 (February, 1960).

647 Tee, T.-T. and J.M. Dealy, "Nonlinear viscoelasticity of polymer melts", Trans. Soc. Rheol., 19(4), 595-615 (1975).

648 Soong, S S., "A parallel plate viscoelastometer for molten polymers", doctoral dissertation, Dept. Chem. Eng., McGill Univ., Montreal, Canada (June, 1983).

649. Tee, T.-T., "Large amplitude oscillatory shearing of polymer melts", doctoral dissertation, Dept. Chem. Eng., McGill Univ., Montreal, Canada (1974).

650. Dealy, J.M., J.F. Petersen and T.-T. Tee, "A concentric-cylinder rheometer for polymer melts", Rheol. Acta, 12, 550-558 (1973).

651 Peterson, A.P.G. and E.E. Gross, Jr., Handbook of Noise Measurement, 8th ed., Genrad Publ., Concord, MA (1978).

652 Personal communication, H.C. Booij, Dutch State Mines (Netherlands) to J.M. Dealy (1987).

653. Harris, J., "Response of time-dependent materials to oscillatory motion", Nature, 207, 744 (August 14, 1965).

654. Matsumoto, T., Y. Segawa, Y. Warashina and S. Onogi, "Nonlinear behavior of viscoelastic materials. II. The method of analysis and temperature dependence of nonlinear viscoelastic functions", Trans. Soc. Rheol., 17(1), 47-62 (1973).

655 Doebelin, E.O., Measurement Systems, revised ed., McGraw-Hill Book Company, New York (1975).

656. Astbury, N.F. and F. Moore, "Torsional hysteresis in plastic clay", Rheol. Acta, 9(1), 124-129 (1970).

657. Matsumoto, T., Y. Segawa, Y. Warashina and S. Onogi, "Nonlinear behavior of viscoelastic materials. II. The method of analysis and temperature dependence of nonlinear viscoelastic functions", Trans. Soc. Rheol., 17(1), 47-62 (1973).

658 Lammiman, K.A. and J.E. Roberts, "Notes on the measurement of viscoelasticity in materials of high viscosity", Laboratory Practice, 816-824 (november, 1961).

659 Manley, R G , Waveform Analysis, John Wiley & Sons, Inc., New York (1945)

660. Tee, T -T. and J.M. Dealy, "Nonlinear viscoelasticity of polymer melts", Trans. Soc. Rheol., 19(4), 595-615 (1975).

661 Tee, T -T., "Large amplitude oscillatory shearing of polymer melts", Ph D. Thesis, Chem. Eng. Dept., McGill Univ., Montreal, Canada (1974).

662. Dealy, J.M., J.F. Petersen and T.-T. Tee, "A concentric-cylinder rheometer for polymer melts", Rheol. Acta, 12, 550-558 (1973).

663 Prentiss, S , The Complete Book of Oscilloscopes, Tab Books Inc., Blue Ridge Summit, Pa. (1983).

664 Bapton, D , Modern Oscilloscope Handbook, Reston Publishing Company, Reston, VA (1979).

665 Manley, R G , Waveform Analysis, John Wiley & Sons, Inc., New York (1945)

666. French, A.P., Vibrations and Waves, W.W. Norton & Company Inc., New York (1971).

667. Cain, P.J., "Measurement of dynamic mechanical properties of elastomers and elastomeric devices", MTS Systems Corp., Bull. No. 300014-56 170.70-02 (1986).

668. Stalnaker, D.O. and T.S. Fleischman, "Frequency effects on rubber moduli", Closed Loop, 14(2), 4-11, MTS Systems Corp. (Fall 1985).

669. Macdonald, I.F., B.D. Marsh and E. Ashare, "Rheological behavior for large amplitude oscillatory motion", Chem. Eng. Sci., 24, 1615-1625 (1969).

670. McCarthy, R.V., "An improved rheometer design used to measure viscoelastic properties of polymer melts", J. Rheol., 22(6), 623-641 (1978).

671. Vinogradov, G.V. and A. Ya. Malkin, Rheology of Polymers, Mir Publishers, Moscow (1980).

672. Vinogradov, G.V., Yu. Yanovsky and A.I. Isayev, "Viscoelastic behavior of an amorphous polymer under oscillations of large amplitude", J. Pol. Sci.: Part A-2, 8, 1239-1259 (1970).

673. Philippoff, W., "Vibrational measurements with large amplitudes", Trans. Soc. Rheol., 10(1), 317-334 (1966).

674. Thurston, G.B., "Shear rate dependence of the viscoelasticity of polymer solutions. I. Theoretical Model", J. Non-Newt. Fluid Mech., 9, 57-68 (1981).

675. Thurston, G.B. and G.A. Pope, "Shear rate dependence of the viscoelasticity of polymer solutions. II. Xanthan gum", J. Non-Newt. Fluid Mech., 9, 69-78 (1981).

676. Imass Inc., Hingham, MA, "Product Bulletin. Model MER-1000", Bull. MER 1081.

677 Johnson, D.E., J.L. Hilburn and J.R. Johnson, Basic Electric Circuit Analysis, Prentice-Hall, Inc., Englewood Cliffs, N.J. (1978).

678 Tee, T.-T , "Large amplitude oscillatory shearing of polymer melts", Ph.D. Thesis, Chem. Eng. Dept., McGill Univ., Montreal, Canada (1974).

679 Soong, S.S., "A parallel plate viscoelastometer for molten polymers", Ph D. thesis, Dept. Chem. Eng., McGill Univ., Montreal, Canada (June, 1983).

680 Tsang, W.K.W., "The use of large transient deformations to elucidate structural phenomena and evaluate network models for molten polymers", PH.D. thesis, Ch.E., McGill Univ., Montreal, Canada (1980).

681 Macdonald, I.F., B.D. Marsh and E. Ashare, "Rheological behavior for large amplitude oscillatory motion", Chem. Eng. Sci., 24, 1615-1625 (1969).

682. Harris, J., "A continuum theory of time-dependent inelastic flow", Rheol. Acta, 6(1), 6-12 (1967).

683. Isayev, A.I. and C.A. Hieber, "Oscillatory shear flow of polymeric systems", J. Pol. Sci.: Pol. Phys. Ed., 20, 423-440 (1982).

684. Liu, T.Y., D.S. Soong and M.C. Williams, "Transient and steady rheology of polydisperse entangled melts. Predictions of a kinetic network model and data comparisons", J. Pol. Sci.. Pol. Phys. Ed., 22, 1561-1587 (1984)

685. Pearson, D.S. and W.E. Rochefort, "Behavior of concentrated polystyrene solutions in large-amplitude oscillating shear fields", J. Pol. Sci.: Pol. Phys. Ed., 20, 83-98 (1982).

686. Thurston, G.B., "Shear rate dependence of the viscoelasticity of polymer solutions. I. Theoretical Model", J. Non-Newt. Fluid Mech., 9, 57-68 (1981).

687. Thurston, G.B. and G.A. Pope, "Shear rate dependence of the viscoelasticity of polymer solutions. II. Xanthan gum", J. Non-Newt. Fluid Mech., 9, 69-78 (1981).

688 Liu, Y -H T , "Rheological transients in entangled polymeric fluids", Ph.D. thesis, Dept. Chem. Eng., Univ. California at Berkeley (1982).

689. Williams, M.C. and R.B. Bird, "Oscillatory behavior of normal stresses in viscoelastic fluids", I&EC Fund., 3(1), 42-49 (February, 1964).

690 Yen, H -C. and L.V McIntire, "Finite amplitude dynamic motion of viscoelastic materials", Trans. Soc. Rheol., 16(4), 711-726 (1972).

691 Soong, S S , "A parallel plate viscoelastometer for molten polymers", Ph D thesis, Dept. Chem. Eng., McGill Univ., Montreal, Canada (June, 1983).

692 Tsang, W.K W., "The use of large transient deformations to elucidate structural phenomena and evaluate network models for molten polymers", Ph.D. thesis, Ch.E., McGill Univ., Montreal, Canada (1980).

693. Vinogradov, G.V. and A. Ya. Malkin, Rheology of Polymers, Mir Publishers, Moscow (1980).

694. Vinogradov, G.V., Yu. Yanovsky and A.I. Isayev, "Viscoelastic behavior of an amorphous polymer under oscillations of large amplitude", J. Pol. Sci.: Part A-2, 8, 1239-1259 (1970).

695 Soong, S S. , "A parallel plate viscoelastometer for molten doctoral dissertation, polymers", Dept. Chem. Eng., McGill Univ., Montreal, Canada (June, 1983).

696 Ramirez, R.W , The FFT, Fundamentals and Concepts, Prentice-Hall, Inc., Englewoods Cliffs (1985).

697 Ramirez, R.W., The FFT, Fundamentals and Concepts, Prentice-Hall, Inc., Englewoods Cliffs (1985).

698. Product Literature No. 82M56, "Instruction Manual: Accumeasure System 1000, Capacitive displacement vibration measurement instrument", MTI Intruments, Div. Mechanical Technology Inc., 968 Albany-Shaker Road, Latham, New York 12110.

699. Dorman, R.A., "Signal amplifier system for controlled carrier signal measuring sensor/transducer of the variable impedance type", U.S. Patent No. 4,176,555, Mechanical Technology Inc., Latham, N.Y. (December 4, 1979).

700. Dorman, R.A., C.D. Kissinger and L.J. Lagace, "Capacitance type non-contact displacement and vibration measuring device and method of maintaining calibration", U.S. Patent No. 4,067,225 (Jan. 10, 1978).

701. Calvert, R., "Apparatus for measuring small distances", U.S. Patent #3,048,775 (Aug. 7, 1962).

702. Product Bulletin No. INS101, "Accumeasure System 1000. Accuracy without contact", MTI Instruments, Mechanical Technology Inc., 968 Albany-Shaker Road, Latham, NY.

703. Tee, T.-T. and J.M. Dealy, "Nonlinear viscoelasticity of polymer melts", Trans. Soc. Rheol., 19(4), 595-615 (1975).

704. Tee, T.-T., "Large amplitude oscillatory shearing of polymer melts", Ph.D. Thesis, Chem. Eng. Dept., McGill Univ., Montreal, Canada (1974).

705. Maerker, J.M. and W.R. Schowalter, Rheol. Acta, 13, 627-638 (1974).

706. Soong, S.S., "A parallel plate viscoelastometer for molten polymers", Dept. Chem. Eng., McGill Univ., Montreal, Canada (June, 1983).

707. Dealy, J.M. and S.S. Soong, "A parallel plate melt rheometer incorporating a shear stress transducer", J. Rheol., 28(4), 355-365 (1984).

708. Van Holde, K.E. and J.W. Williams, "Study of the ~~viscoelastic~~ behavior and molecular weight distribution of polyisobutylene", J. Pol. Sci., XI(3), 243-268 (1953).

709. Fruh, S.M. and F. Rodriguez, "Recoverable shear measurements in a parallel plate rheometer", AIChE J., 16(6), 907-910 (November, 1970).

710. Philippoff, W., F.H. Gaskins and J.G. Brodnyan, J. Appl. Pol. Sci., 28, 1118 (1957).

711. Soong, S.S., "A parallel plate viscoelastometer for molten polymers", Dept. Chem. Eng., McGill Univ., Montreal, Canada (June, 1983).

712. Eichinger, B.E. and P.J. Flory, Macromolecules, 1(3), 285-286 (1968).

713 Ramirez, R W , The FFT: Fundamentals and Concepts, Prentice-Hall, Inc., Englewoods Cliffs (1985).

714. Whitaker, S. and R.L. Pigford, "An approach to numerical differentiation of experimental data", I&EC, 52(2), 185-187 (February, 1960).

715 Soong, S.S , "A parallel plate viscoelastometer for molten polymers", doctoral dissertation, Dept. Chem. Eng., McGill Univ., Montreal, Canada (June, 1983).

716. Mewis, J. and G. De Cleyn, "Shear history effects in the spinning of polymers", A.I.Ch.E.J., 28(6), 900-907 (November, 1982)

717. De Cleyn, G. and J. Mewis, "A constitutive equation for polymer liquids. application to shear flow", J. Non-Newt. Fluid Mech., 9, 91-105 (1981)

718 Lamontagne, R., "Mewis model predictions in oscillatory shear", research report submitted to J.M. Dealy, Dept. Chem. Eng., McGill Univ., Montreal (22/4/85).

719 Soong, S.S , "A parallel plate viscoelastometer for molten polymers", doctoral dissertation, Dept. Chem. Eng., McGill Univ., Montreal, Canada (June, 1983).

720 Giacomin, A.J and J.M. Dealy, "A new rheometer for molten plastics", S P E Tech. Papers, XXXII, Proc. 44th Annual Tech. Conf., Boston (May, 1986).

721. Dealy, J.M., "Method of measuring shear stress", U.S. Patent No. 4,464,928 (Aug. 14, 1984).

722 Dealy, J.M., "A shear stress transducer for molten polymers", Rheol. Acta, 21, 475-477 (1982).

723. Garritano, R.F., "Compensated rheometer", U.S. Patent No. 4,501,155 (Feb. 26, 1985).

724 Personal communication, Dr. Patrick J. Cain, MTS Systems Corp., Minneapolis, Minnesota.

725. Locati, G., "The operation of the Rheovibron in the shear mode", Pol. Eng. Sci., 18(10), 793-798 (Mid-August, 1978).

726. Tee, T.-T. and J.M. Dealy, "Nonlinear viscoelasticity of polymer melts", Trans. Soc. Rheol., 19(4), 595-615 (1975).

727 Tee, T.-T., "Large amplitude oscillatory shearing of polymer melts", Ph.D. Thesis, Chem. Eng. Dept., McGill Univ., Montreal, Canada (1974).

728. Meissner, J., "Polymer melt rheology - A challenge for the polymer scientist and engineer", Pure & Appl. Chem., 56(3), 369-384 (1984).

729. Meissner, J., Chimia, 38(2), 35-75 (1984).

730. Dealy, J.M., Dept. Chem. Eng., McGill Univ., Montreal, Canada, personal communication, (1983).

731 Ramirez, R W., The FFT: Fundamentals and Concepts, Prentice-Hall, Inc., Englewoods Cliffs (1985).

732 Randall, R B, Application of B&K Equipment to Frequency Analysis, 2nd ed., Bruehl & Kjaer, Denmark (September, 1977).

733. Personal communication, T. Samurkas, Dept. Chem. Eng., McGill Univ., Montreal, Canada (January, 1987).

734 Broch, J T., Mechanical Vibration and Shock Measurements, 2nd ed., Bruehl & Kjaer, Denmark (April, 1984).

735. Stastna, J., D. De Kee and M.B. Powley, "Complex viscosity as a generalized response function", J. Rheol., 29(4), 457-469 (1985).